ISSN 1580-3155

Pages 295–466 ■ Year 2023, Vol. 70, No. 3

Slovensko kemijsko društvo
Slovenian Chemical Society

Acta Chimica Slovenica

3

70/2023

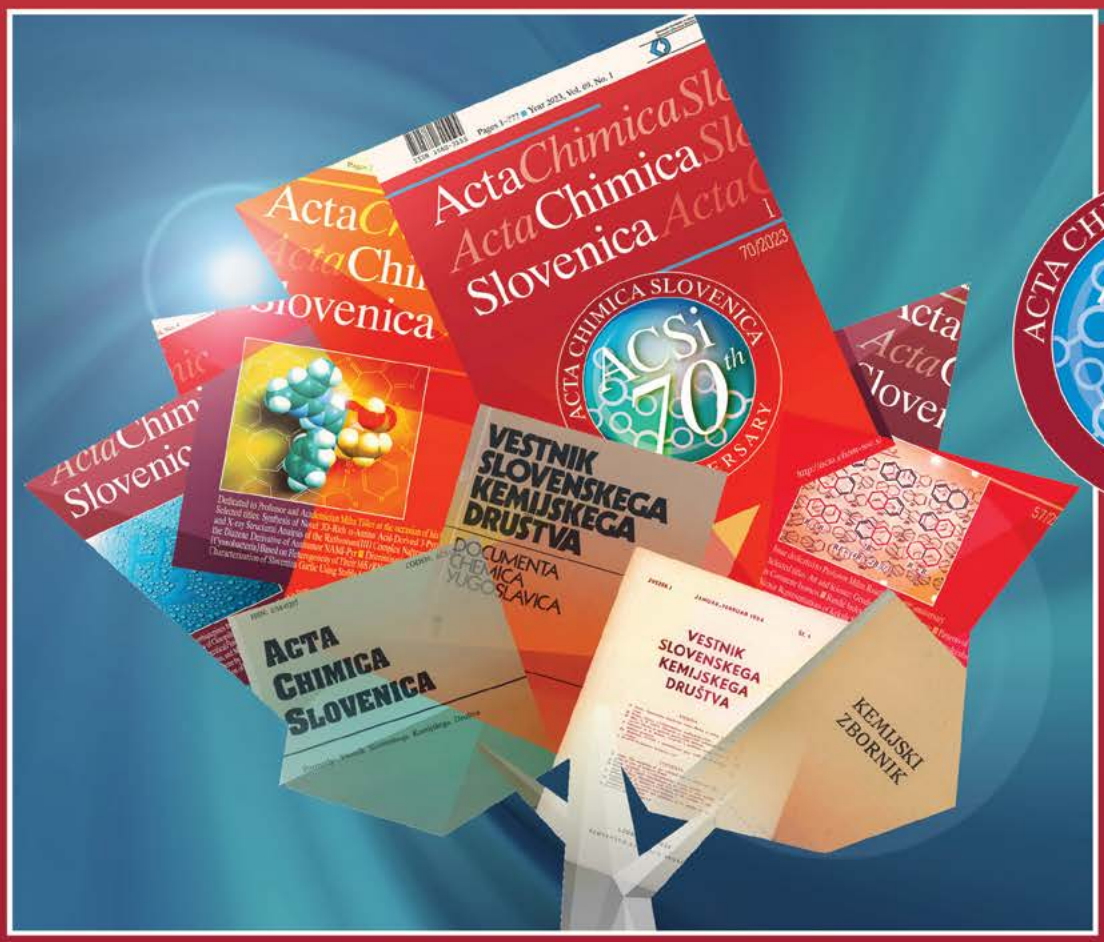

http://acta.chem-soc.si

Acta Chimica Slovenica is indexed in: *Academic Search Complete, Central & Eastern European Academic Source, Chemical Abstracts Plus, Chemical Engineering Collection (India), Chemistry Citation Index Expanded, Current Contents (Physical, Chemical and Earth Sciences), Digitalna knjižnica Slovenije (dLib.si), DOAJ, ISI Alerting Services, PubMed, Science Citation Index Expanded, SciFinder (CAS), Scopus, Web of Science and Portico.* Impact factor for 2021 is IF = 1.524.

Izdaja – Published by:
SLOVENSKO KEMIJSKO DRUŠTVO – SLOVENIAN CHEMICAL SOCIETY
Naslov redakcije in uprave – Address of the Editorial Board and Administration
Hajdrihova 19, SI-1000 Ljubljana, Slovenija
Tel.: (+386)-1-476-0252; Fax: (+386)-1-476-0300; E-mail: chem.soc@ki.si

Izdajanje sofinancirajo – Financially supported by:
National Institute of Chemistry, Ljubljana, Slovenia
Jožef Stefan Institute, Ljubljana, Slovenia
Faculty of Chemistry and Chemical Technology, University of Ljubljana, Slovenia
Faculty of Chemistry and Chemical Engineering, University of Maribor, Slovenia
University of Nova Gorica, Slovenia

Acta Chimica Slovenica izhaja štirikrat letno v elektronski obliki na spletni strani http://*acta.chem-soc.si*. V primeru posvečenih številk izhaja revija tudi v tiskani obliki v omejenem številu izvodov.

Acta Chimica Slovenica appears quarterly in electronic form on the web site *http://acta.chem-soc.si*. In case of dedicated issues, a limited number of printed copies are issued as well.

Transakcijski račun: 02053-0013322846 Bank Account No.: SI56020530013322846-Nova Ljubljanska banka d. d., Trg republike 2, SI-1520 Ljubljana, Slovenia, SWIFT Code: LJBA SI 2X

Oblikovanje ovitka – Design cover: KULT, oblikovalski studio, Simon KAJTNA, s. p. Grafična priprava za tisk: OSITO, Laura Jankovič, s.p.

Graphical Contents

Acta Chimica Slovenica

Year 2023, Vol. 70, No. 3

SCIENTIFIC PAPER

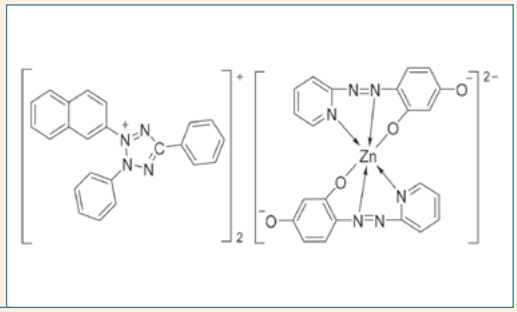

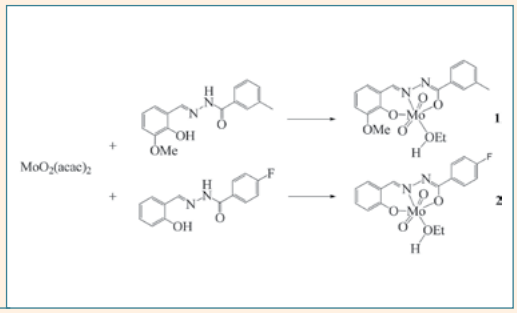

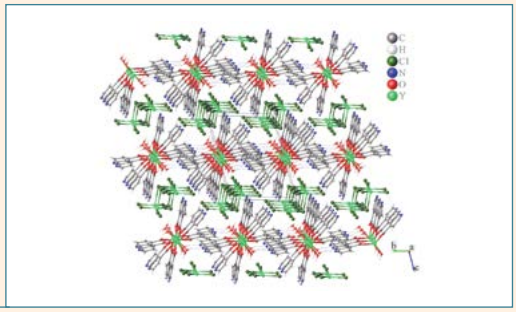

Scientific paper

Study on the Equilibria of the Complex Formation of Anionic Chelate of Zn(II) with Tridentate Ligand and the Cation of 3-(2-naphtyl)-2,5-diphenyl-2*H*-tetrazolium chloride

Kirila Stojnova, Pavel Yanev and Vanya Lekova*

Department of General and Inorganic Chemistry with Methodology of Chemistry Education, Faculty of Chemistry, University of Plovdiv "Paisii Hilendarski", 24 Tzar Assen Street, Plovdiv 4000, Bulgaria

** Corresponding author: E-mail: vanlek@uni-plovdiv.bg; tel.:+35932261420*

Received: 04-18-2023

Abstract

The equilibria of the complex formation between the anionic chelate of zinc(II) with the tridentate ligand of 4-(2-pyridylazo)-resorcinol (PAR) and the bulky organic tetrazolium cation of 3-(2-naphtyl)-2,5-diphenyl-2*H*-tetrazolium chloride (TV) in the liquid-liquid extraction system Zn(II)–PAR–TV–H_2O–2-methyl-1-propanol was studied by spectrophotometric method. The molar ratio of the reagents was determined by independent methods under the optimum condition for ion-association and for extraction. The validity of Beer's law was checked and some analytical characteristics were calculated. The constants, describing the association process in aqueous phase and the extraction equilibria, were calculated. Based on this, a reaction scheme, a general formula and a structural formula of the complex were suggested. The zinc(II) cation is six coordinated with the tridentate ligand through the following atoms: the azo nitrogen, the pyridine nitrogen and the oxygen atom from the phenolic group, which is in *ortho* position relative to the azo group, each of them forming two five-membered chelate rings.

Keywords: zinc(II); tridentate ligand; chelate formation; extraction equilibria

1. Introduction

The zinc is a typical transition, complex forming metal essential from biochemical point of view. It is an important trace element needed by plants,[1] animals,[2] and microorganisms.[3] In the human body the zinc content amounts to 2–4 g.[4] Zinc is the second most abundant metal in the human body[5] and is a cofactor for more than 300 enzymes involved in many processes, including the cellular respiration, immunity, DNA and protein synthesis, metabolism, cell division, etc.[6–10] It is known that zinc can be toxic when exposures exceed physiological needs. Negative health effects have been documented after short-term exposure to concentrations of zinc in water and beverages between 1.0 and 2.5 mg L^{-1}, e.g. poisoning incidents with symptoms of gastrointestinal distress, nausea and diarrhea.[11]

The zinc forms metal complexes with potential application in the fields of medicine, pharmacy, catalysis, photoluminescence, or as semiconductor materials.[12–16] Zinc(II) complexes with ligands, containing [S,S], [O,O], [N,O], [N,N] donor atoms, like 1,10-phenantroline, 2,2´-bipyridene,[17] 2-(2´-aminophenyl)benzothiazole,[18] *N*-benzoyl-glycine, *N*-acetyl amino acids and their amine adducts,[19] *N*-ethyl-3-carbazolecarboxaldehyde-3-thiosemicarbazone,[20] tetraphenylporphyrin, *meso*-tetrakis(4-sulfophenyl)porphyrin,[21] 1-[(5-benzyl-1,3-thiazol-2-yl) diazenyl]naphthalene-2-ol,[22] 1-(2-pyridylazo)-2-naphthol,[23] Schiff bases[24], were synthesized and structurally characterized. Zinc(II) gives colored chelates with polyphenols and their functional derivatives, containing azo groups and two or more hydroxyl groups in *ortho* position relative to each other, such as 2-(*N*-acetylamino)-6-methylpyridine,[25] 8-hydroxyquinoline and its derivatives,[26] xylenol orange[27], methylthymol blue, 1-(2-pyridilazo)-2-naphtol, 2-(4,6-dimethyl-2-pyrimidylazo)-1-naphthol-4sulphonate sodium salt.[28]

Colored anionic chelates of zinc(II) can form ion-associated complexes with bulky organic cations, like tetra-

zolium salts. The structure and properties of tetrazolium salts determine their ability to form ion-associated complexes.[29,30] The bulky hydrophobic organic substituents in the molecules of the tetrazolium salts increase the extractability of the ion-associated complexes. The presence of a quaternary nitrogen atom in the molecules of the tetrazolium salts determines the ability to form ionic associates with chelates of metals in aqueous phase without protonation, as opposed to the amines. Tetrazolium salts are used as reagents for the preparation of various ion-associated complexes of metals, e.g. Ga(III), Co(II), Ge(IV), Mo(-VI).[29, 31–39]

The liquid-liquid extraction is a part of the chemistry of the solutions and the coordination compounds. It is applied to study the processes of complex formation and the extraction equilibria.[40–43] The extraction spectrophotometry is a relatively simple, convenient, sensitive, selective, rapid to perform and inexpensive method for preparation and characterization of new complex compounds as well as for their application in the chemical analysis.[44–49]

This present work aims to study the extraction equilibria for complex formation between the anionic chelate of Zn(II) with the tridentate ligand of 4-(2-pyridylazo)-resorcinol (PAR) and the cation of 3-(2-naphthyl)-2,5-diphenyl-2*H*-tetrazolium chloride (TV) in the liquid-liquid system Zn(II)–PAR–TV–H_2O–*i*-BuOH by spectrophotometric method. The selected organic solvent *i*-BuOH is characterized by a low volatility and toxicity, it is readily biodegradable and non-bioaccumulative, and can be produced from renewable resources.[50,51] The final goal was to evaluate the possible applications of the system for the determination of the traces of zinc(II) in biological, medical, and pharmaceutical samples.

2. Experimental

2. 1. Reagents and Apparatus

Zinc(II) chloride, anhydrous ($ZnCl_2$) (Alfa Aesar, 98%): an aqueous 1.53×10^{-2} mol L^{-1} solution was prepared. 4-(2-Pyridyazo)-resorcinol (PAR) (Sigma–Aldrich, 96%): PAR was dissolved in slightly alkaline distilled water to give a 2.0×10^{-3} mol L^{-1} solution. 3-(2-Naphtyl)-2,5-diphenyl-2*H*-tetrazolium chloride (Tetrazolium Violet, TV) (Loba Feinchemie, p. a.): an aqueous 3.0×10^{-3} mol L^{-1} solution was prepared. The alkalinity of the aqueous medium was determined using an aqueous sodium hydroxide solution. As organic solvent 2-methyl-1-propanol (isobutyl alcohol, i-BuOH) (Chempur, p.a.) was used. The pH was checked by HI 83140 pH meter (Romania). A Camspes M 508 spectrophotometer (United Kingdom), equipped with 10 mm path length cells, was employed for reading of the absorbance.

2. 2. Procedure for Establishment of the Optimum Conditions for Chelate Formation and Ion-association

Aliquots of the solutions of Zn(II), PAR, TV and sodium hydroxide (pH = 7.0–10.0) were filled into 100 mL separatory funnels. The resulting solutions were diluted with distilled water to a total volume of 10 mL. Then 10 mL of isobutyl alcohol was added and the funnels were shaken for a fixed time (up 180 s). A portion of the organic extract was filtered through a filter paper into a cell. The absorbance was read against a blank sample, which was prepared in the same manner, but in the absence of zinc(II).[39]

3. Results and Discussion

3. 1. Optimum Conditions for Chelate Formation and Ion-association

The absorption spectra of the extract of ion-associated complex, formed between the orange-colored anionic chelate of zinc(II) with 4-(2-pyridyazo)-resorcinol and the cation of the tetrazolium salt, and the blank sample, containing 4-(2-pyridyazo)-resorcinol and 3-(2-naphtyl)-2,5-diphenyl-2*H*-tetrazolium chloride, are shown in Figure 1. The absorption maximum of the complex appears in the visible range at 510 nm, where the blank sample absorbs insignificantly. The maximum and constant extraction of the ion-associated complex is achieved in the pH range from 7.0 to 10.0 and aqueous sodium hydroxide solution was used in all further experiments. The extraction equilibrium of the ion-associated complex is established for shaking time not less than 90 s and for this reason the experiments were performed for 2 min. To

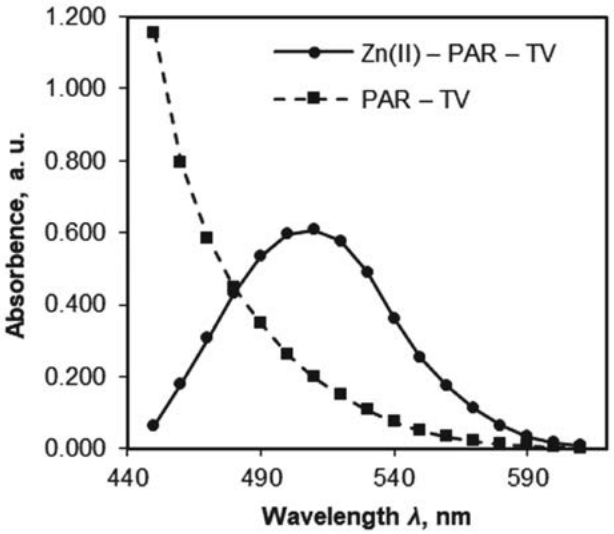

Figure 1. Absorption spectra of the complex of Zn-PAR-TV and the bank sample PAR-TV in *i*-BuOH; $C_{Zn(II)} = 1.53\times10^{-5}$ mol L^{-1}; $C_{PAR} = 2.0\times10^{-4}$ mol L^{-1}; $C_{TV} = 3.0\times10^{-4}$ mol L^{-1}, $\tau = 2$ min

determine the influence of the concentration of reagents on the extraction equilibrium, the fold excess of the reagents was calculated. The chelate formation of Zn(II)-PAR requires 13.7-fold excess of PAR ($C_{PAR} \geq 1.8 \times 10^{-4}$ mol L^{-1}) and 19.61-fold excess of TV ($C_{TV} \geq 2.7 \times 10^{-4}$ mol L^{-1}) for maximum association and extraction.

The optimum experimental conditions for the chelate formation and extraction of the ion-associated complex are summarized in Table 1, column 1.

3. 2. Beer's Law, Molar Absorptivity and Other Analytical Characteristics

The linear relationship between the zinc(II) concentration ($C_{Zn(II)}$, μg mL^{-1}) in the aqueous phase and the absorbance of the ion-associated complex in the organic phase after extraction was studied using regression analysis under the optimum conditions for complex formation. The range of obedience to Beer's Law, i.e. the linearity, is observed for concentration up to 2.80 μg mL^{-1} Zn(II). The equation of a straight line was found to be Y = 0.6102 X + 0.0013 with a correlation coefficient squared 0.9999. Further analytical characteristics, such as apparent molar absorptivity ε´, Sandell's sensitivity, limit of detection and limit of quantification, are shown in Table 1, column 2.

On the basis of the analytical characteristics of the extraction system Zn(II)–PAR–H_2O–*i*-BuOH, it can be concluded that the ion-associate formed between the anionic chelate of Zn(II)-PAR and the tetrazolium cation allows determination of Zn(II) with a high sensitivity.

3. 3. Molar Ratios of the Ion-associated Complex, Reaction Scheme and Suggested General Formula

The molar ratios of the components of the ion-associated complex were determined by three independent methods: the mobile equilibrium method, the straight-line method of Asmus and the method of continuous variations.[52] The results from the application of the mobile equilibrium method to prove the molar ratios Zn(II):PAR and Zn(II):TV are presented in Figure 2.

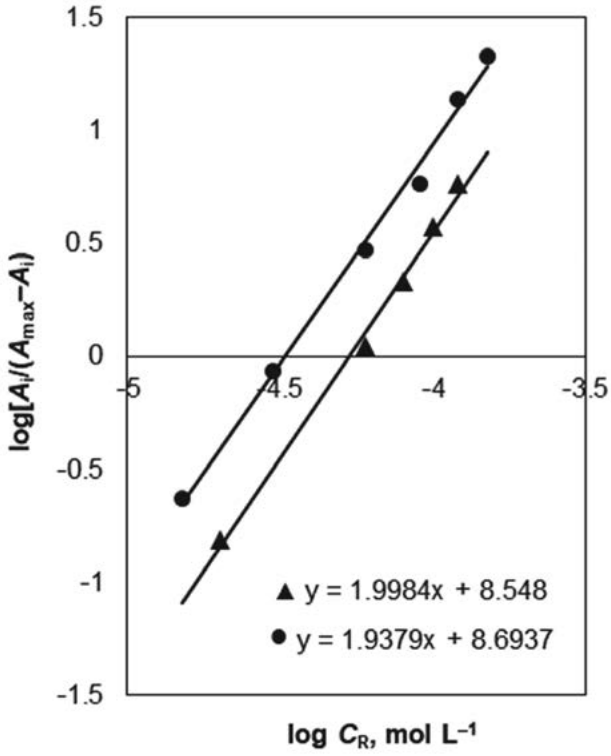

Figures 2. Straight line by the mobile equilibrium method for determination of the molar ratio Zn(II):PAR and Zn(II):TV; $C_{Zn(II)} = 1.53 \times 10^{-5}$ mol L^{-1}; λ = 510 nm; τ = 2 min; ▲ Zn(II):PAR; $C_{TV} = 3.0 \times 10^{-4}$ mol L^{-1}; • Zn(II):TV; $C_{PAR} = 2.0 \times 10^{-4}$ mol L^{-1}

The results from the application of the straight-line method of Asmus to prove the molar ratios Zn(II):PAR and Zn(II):TV are shown in Figure 3 and Figure 4, respectively.

The results from the application of the mobile equilibrium method and the straight-line method of Asmus reveal that the molar ratio for chelate formation between

Table 1. Optimum extraction-spectrophotometric conditions and analytical characteristics of the system Zn(II)–PAR–H_2O–*i*-BuOH

Optimum Conditions	Analytical Characteristic
Absorption maximum (λ_{max}) 510 nm	Apparent molar absorptivity (ε´) $(3.94 \pm 0.06) \times 10^4$ L $mol^{-1}cm^{-1}$
Volume of the aqueous phase 10 cm^3	True molar absorptivity (ε) $(3.86 \pm 0.06) \times 10^4$ L $mol^{-1}cm^{-1}$
Volume of the organic phase 10 cm^3	Sandell's sensitivity (SS) 1.66 ng cm^{-2}
pH of the aqueous phase 7.0 ÷10.0	Adherence to Beer's law up to 2.80 μg cm^{-3}
Shaking time (τ) 2 min	Relative standard deviation (RSD) 1.66%
Concentration of PAR $\geq 1.8 \times 10^{-4}$ mol L^{-1}	Limit of detection (LOD) 0.04 μg cm^{-3}
Concentration of TV $\geq 2.7 \times 10^{-5}$ mol L^{-1}	Limit of quantification (LOQ) 0.13 μg cm^{-3}

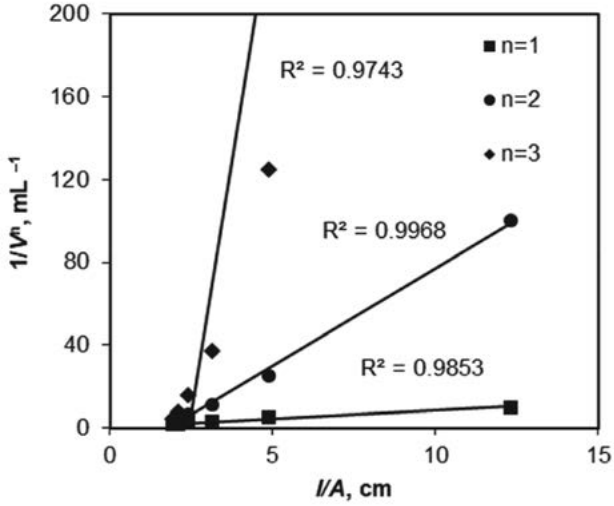

Figures 3. Determination of molar ratio (n) Zn(II):PAR by the method of Asmus; $C_{Zn(II)} = 1.53 \times 10^{-5}$ mol L^{-1}; $C_{TV} = 3.0 \times 10^{-4}$ mol L^{-1}; λ = 510 nm; τ = 2 min

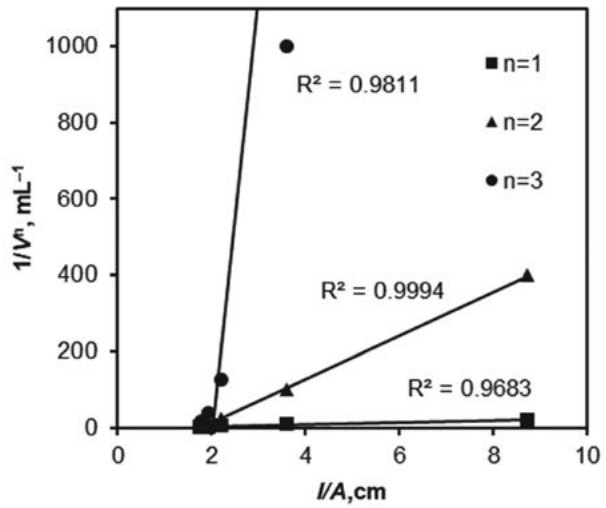

Figures 4. Determination of molar ratio (n) Zn(II):TV by the method of Asmus; $C_{Zn(II)} = 1.53 \times 10^{-5}$ mol L^{-1}; $C_{PAR} = 2.0 \times 10^{-4}$ mol L^{-1}; λ = 510 nm; τ = 2 min

Zn(II) and PAR is 1:2 and the ion-associated complex Zn(II)–PAR–TV is formed in the molar ratio 1:2:2, respectively.

The application of the method of continuous variations confirmed the molar ratio Zn(II):TV = 1:2 (Figure 5).

Zincates containing $[Zn(OH)_3]^-$, $[Zn(OH)_4]^{2-}$, $[Zn(OH)_3(H_2O)]^-$, $[Zn(OH)_6]^{4-}$ $[Zn(OH)_4(H_2O)_2]^{2-}$ in alkaline solutions are already described in the literature.[53,54] In the pH range from 1.5 to 6.5, functional azo derivatives of polyphenols, such as TAR or PAR are presented in a molecular form (H_2R). The deprotonation (HR^-) starts at pH = 4.0, while a complete deprotonation (R^{2-}) is achieved in the alkaline range (pH >11).[33]

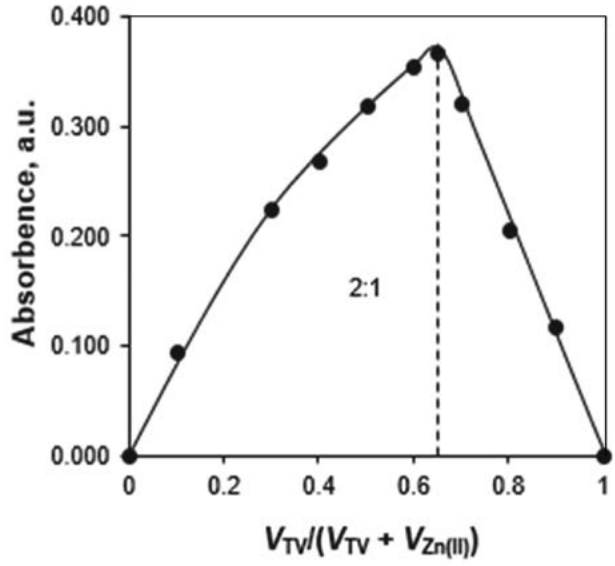

Figure 5. Determination of the molar ratio (*n*) Zn(II):TV by the method of continuous variations $C_{Zn(II)} + C_{TV} = 3.06 \times 10^{-5}$ mol L^{-1}; $C_{PAR} = 2.0 \times 10^{-4}$ mol L^{-1}; λ = 510 nm; τ = 2 min

The carried out experiments showed that the complex formation and the extraction of the ion-associated complex have occurred in the pH range from 7.0 to 10.0. Under these conditions, an equilibrium between the monoprotonated form (HR^-) and the deprotonated form (R^{2-}) exists in the solution. Therefore, the complex formation of anionic chelate of zinc(II) with 4-(2-pyridyazo)-resorcinol ($C_{11}H_9N_3O_2$) can be given by equation (1):

$$[Zn(OH)_4(H_2O)_2]^{2-}(aq) + [C_{11}H_7N_3(OH)O]^-(aq) + [C_{11}H_7N_3O_2]^{2-}(aq) \rightarrow [Zn(C_{11}H_7N_3O_2)_2]^{2-}(aq) + 3OH^- + 3H_2O \quad (1)$$

The formation of the ion-associate in aqueous phase, its distribution between the aqueous and the organic phases and its extraction in *i*-BuOH can be given the following equations (2–4):

$$[Zn(C_{11}H_7N_3O_2)_2]^{2-}(aq) + 2(TV^+)(aq) \leftrightharpoons \{(TV)_2[Zn(C_{11}H_7N_3O_2)_2]\}(aq) \quad (2)$$

$$\{(TV)_2[Zn(C_{11}H_7N_3O_2)_2]\}(aq) \leftrightharpoons \{(TV)_2[Zn(C_{11}H_7N_3O_2)_2]\}(org) \quad (3)$$

$$2(TV)^+(aq) + [Zn(C_{11}H_7N_3O_2)_2]^{2-}(aq) \leftrightharpoons \{(TV)_2[Zn(C_{11}H_7N_3O_2)_2]\}(org) \quad (4)$$

Therefore, the ion-associated complex formed between the anionic chelate $[Zn(C_{11}H_7N_3O_2)_2]^{2-}$ and the cation of monotetrazolium salt can be represented by the general formula $(TV)_2[Zn(C_{11}H_7N_3O_2)_2]$.

3. 4. Equilibrium Constants, True Molar Absorptivity, Recovery Factor and Suggested Structural Formula of the Ion-associated Complex

The association process in aqueous phase and the extraction equilibria were investigated and quantitatively characterized with respect to the following key constants: association constant β, distribution constant K_D and extraction constant K_{ex}, as well as the recovery factor *R*%.

The ion-association in the aqueous phase between the anionic chelate $[Zn(C_{11}H_7N_3O_2)_2]^{2-}$ and the tetrazolium cation $(TV)^+$ is given with the association constant (β) by the equation (5):

$$\beta = \{(TV)_2[Zn(C_{11}H_7N_3O_2)_2]\}(aq) / \{\{TV^+\}^2(aq) \times \{[Zn(C_{11}H_7N_3O_2)_2]^{2-}\}(aq)\} \quad (5)$$

The association constant β was determined by two independent methods: Komar–Tolmachev method[52] and Holme–Langmyhr method[55] and the obtained values (logβ) are given in Table 2, column 2.

The association constant β was calculated by the equation (6)[52]:

$$\beta = (l/n)^n / [\varepsilon (tg\ \alpha)^{n+1}] \quad (6)$$

where l *is* the cuvette thickness (l = 1 cm); n is the molar ratio between the components independently determined (e.g. by the mobile equilibrium method, the straight-line method of Asmus or the method of continuous variations) (n = 2); ε is the true molar absorptivity.

The true molar absorptivity ε was determined by the method of Komar-Tolmachev from the equation of a straight line Y = 0.3879 X + 2.5940; $\varepsilon = 1/(2.594\times10^{-5})$ L mol^{-1} cm^{-1} (Figure 6).

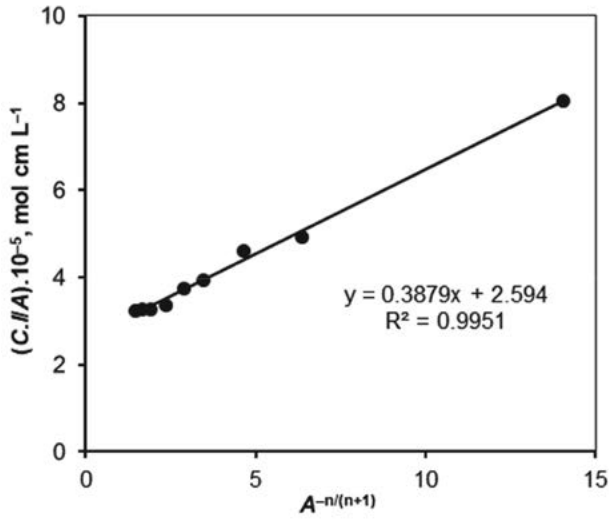

Figure 6. Dependency of $(C\times l / A)$ on $A^{-n/(n+1)}$ (method of Komar–Tolmachev); $C_{Zn(II)} = 2C_{TV} = C$, mol L^{-1}; $C_{PAR} = 2.0\times10^{-4}$ mol L^{-1}; *A* – absorbance; *l* – cell thickness, *l* = 1 cm; *n* = 2; λ = 510 nm; τ = 2 min

The distribution of the ion-associated complex between the aqueous and the organic phase is given by the distribution constant K_D of the equation (7):

$$K_D = \{(TV)_2[Zn(C_{11}H_7N_3O_2)_2]\}(org) / \{(TV)_2[Zn(C_{11}H_7N_3O_2)_2]\}(aq) \quad (7)$$

The distribution constant K_D was calculated by the equation (8):

$$K_D = A_1/(A_3 - A_1) \quad (8)$$

where A_1 is the light absorbance obtained after a single extraction at the optimum conditions; A_3 is the absorbance obtained after a triple extraction under the same conditions.[56]

The recovery factor was determined by the equation (9):

$$R\% = 100\ K_D / (K_D + 1) \quad (9)$$

The extraction equilibrium of the ion-associate between the aqueous and the organic phases is given by the extraction constant K_D for the equation (10)

$$K_{ex} = \{(TV)_2[Zn(C_{11}H_7N_3O_2)_2]\}(org) / \{\{TV^+\}^2(aq)\times\{[Zn(C_{11}H_7N_3O_2)_2]^{2-}\}(aq)\} \quad (10)$$

The extraction constant K_{ex} was calculated by two independent methods:

(i) from the equation $\log K_{ex} = \log K_D + \log \beta$ (11)

where β was calculated by the method of Komar–Tolmachev.[52]

(ii) by the method of Likussar-Boltz:[57]

The method of Likussar-Boltz uses the data from the method of continuous variations (Figure 5). The extraction constant K_{ex} was calculated by the equation of Likussar-Boltz for molar ratio 1:2 (equation 12):

$$\log K_{ex} = 0.3522 - 2 \log K + \log Y_{max} - 3 \log (1 - Y_{max}) \quad (12)$$

where K is the total concentration of reagents ($K = C_{Zn(II)} + C_{TV} = 3.06 \times 10^{-5}$ mol L^{-1}); Y_{max} and $(1–Y_{max})$ are determined from the additionally plotted normalized absorption curve (Y_{max} = 0.8852; $(1 - Y_{max}) = 0.1148$).

The values of the equilibrium constants and the recovery factor, obtained by the independent methods, are statistically similar (Table 2). They indicate that the ion-associated complex, formed between the anionic chelate Zn(II) and the tridentate ligand (PAR) in the presence of the bulky organic cation of the tetrazolium salt, is characterized by sufficiently high stability and good extractability. Therefore, the ion-associated complex Zn(II)–PAR–TV

Table 2. Values of the equilibrium constants and the recovery factor

Equilibrium Constant and Recovery Factor	Value
Equilibrium (equation 2)-Association constant β	
$\beta = \{(TV)_2[Zn(C_{11}H_7N_3O_2)_2]\}(aq) / \{\{TV^+\}^2(aq) \times \{[Zn(C_{11}H_7N_3O_2)_2]^{2-}\}(aq)\}$	$\log\beta = (11.05 \pm 1.08)$[a]
	$\log\beta = (11.04 \pm 0.95)$[b]
Equilibrium (equation 3) - Distribution constant K_D	
$K_D = \{(TV)_2[Zn(C_{11}H_7N_3O_2)_2]\}(org) / \{(TV)_2[Zn(C_{11}H_7N_3O_2)_2]\}(aq)$	$\log K_D = (1.32 \pm 0.01)$[c]
Equilibrium (equation 4)-Extraction constant K_{ex}	
$K_{ex} = \{(TV)_2[Zn(C_{11}H_7N_3O_2)_2]\}(org) /\{\{TV^+\}^2(aq) \times \{[Zn(C_{11}H_7N_3O_2)_2]^{2-}\}(aq)\}$	$\log K_{ex} = (12.37 \pm 1.09)$[d]
	$\log K_{ex} = (12.15 \pm 0.10)$[e]
Recovery factor, R%	$R = (95.48 \pm 0.01)\%$[f]

[a] Calculated by Komar-Tolmachev method (equation 6); [b] Calculated by Holme-Langmyhr method;[55] [c] Calculated by equation 8; [d] Calculated by equation 11, where β is determined by the Komar-Tolmachev method; [e] Calculated by Likussar-Boltz method (equation 12); [f] Calculated by equation 9.

can be successfully applied for determination of zinc(II) in alloys, medical, biological and pharmaceutical samples.

The results obtained by the independent methods, confirm the proposed reaction scheme of the process of chelate formation of the ion-associate in the aqueous phase, its distribution between the aqueous and the organic phases and its extraction into *i*-BuOH (equations 1-4). Based on this, the proposed structural formula of the ion-associated complex is represented in Figure 7. The zinc(II) cation is six coordinated with the tridentate ligand through the following atoms: the azo nitrogen, the pyridine nitrogen and the oxygen atom from the phenolic group, which is in *ortho* position relative to the azo group, each of them forming two five-membered chelate rings.

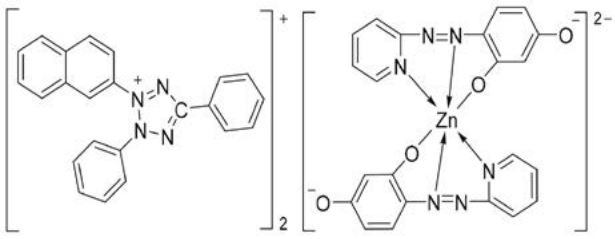

Figure 7. Structural formula of the ion-associated complex Zn(II)-PAR-TV

4. Conclusion

The equilibria of the complex formation between the orange-colored anionic chelate of zinc(II) with the tridentate ligand of 4-(2-pyridylazo)resorcinol (PAR) and the bulky organic tetrazolium cation of 3-(2-naphtyl)-2,5-diphenyl-2H-tetrazolium chloride (TV) in the liquid-liquid extraction system Zn(II)-PAR-TV-H_2O-*i*-BuOH was studied by spectrophotometric method. The optimum conditions for the ion-association in aqueous phase and for the extraction of the ion-associated complex Zn(II)-PAR-TV into *i*-BuOH were established. The validity of Beer's law was checked and some analytical characteristics were calculated: the apparent molar absorptivity (ε′), the true molar absorptivity (ε), the limit of detection (LOD), the limit of quantification (LOQ) and the Sandell's sensitivity (SS). From the analytical characteristics of the extraction system Zn(II)-PAR-TV-H_2O-*i*-BuOH, it can be concluded that the ion-associate, formed between the anionic chelate of Zn(II)-PAR and the tetrazolium cation, allows determinations of Zn(II) with a high sensitivity. The following key constants, needed for the quantitative assessment of the association process in aqueous phase and the extraction equilibria, were also calculated: the association constant (β), the distribution constant (K_D), the extraction constant (*Kex*), as well as the recovery factor (*R*). The molar ration of the reagents, determined by independent methods, showed that the ion-associated complex can be represented with the general formula $(TV)_2[Zn(C_{11}H_7N_3O_2)_2]$, which corresponds to the suggested reaction scheme. A structural formula of the complex also was proposed. The zinc(II) cation is six coordinated with the tridentate ligand through the following atoms: the azo nitrogen, the pyridine nitrogen and the oxygen atom from the phenolic group, which is in *ortho* position relative to the azo group, each of them forming two five-membered chelate rings.

5. References

1. M. R. Broadley, P. J. White, J. P. Hammond, I. Zelko, A. Lux, *New Phytol.* **2007**, *173*, 677–702. **DOI:**10.1111/j.1469-8137.2007.01996.x
2. A. S. Prasad, *Mol. Med.* **2008**, *14*, 353–357. **DOI:**10.2119/2008-00033.Prasad
3. B. Sugarman, *Rev. Infect. Dis.* **1983**, *5*, 137–147. **DOI:**10.1093/clinids/5.1.137
4. L. Rink, Ph. Gabriel, *P. Nutr. Soc.* **2000**, *59*, 541–552. **DOI:**10.1017/S0029665100000781
5. K. A. Mccall, C. Huang, C. A. Fierke, *J. Nutr.* **2000**, *130*, 1437S–1446S. **DOI:**10.1093/jn/130.5.1437S

6. M. Jarosz, M. Olbert, G. Wyszogrodzka, K. Młyniec, T. Librowski, *Inflammopharmacol* **2017**, *25*, 11–24. **DOI:**10.1007/s10787-017-0309-4
7. P. Bonaventura, G. Benedetti, F. Albarède, P. Miossec, *Autoimmun. Rev*. **2015**, *14*, 277–285. **DOI:**10.1016/j.autrev.2014.11.008
8. P.-H. Lin, M. Sermersheim, H. Li, P. H. U. Lee, S. M. Steinberg, J. Ma, *Nutrients* **2018**, *10*, 16. **DOI:**10.3390/nu10010016
9. L. Rochette, S. Ghibu, *J. Mol. Sci*. **2021**, *22*, 7979. **DOI:**10.3390/ijms22157979
10. L. L. Rus, A. M. Juncan, V. I. Craciun, A. Frum, S.-C. Heghes, A. Butuca, C. M. Dobrea, A. A. Chis, A. C. Muntean, A. L. Vonica-Tincu, C. Morgovan, *Appl. Sci*. **2022**, *12*, 4476. **DOI:**10.3390/app12094476
11. M. Hernick, C. A. Fierke, *Arch. Biochem. Biophys*. **2005**, *443*, 71–84. **DOI:**10.1016/j.abb.2004.08.006
12. W. H. Zhao, V. Ferro, M. V. Baker, *Coord. Chem. Rev.* **2017**, *339*, 1–16. **DOI:**10.1016/j.ccr.2017.03.005
13. M. Hu, X. Z. Ai, Z. M. Wang, Z. J. Zhang, H. L. Chong, W. M. Zhang, J. Lin, H. H. Yang, B. G. Xing, *Nano Res.* **2018**, *11*, 5474–5498. **DOI:**10.1007/s12274-018-2138-1
14. H. J. Chen, G. Y. Lyu, Y. F. Yue, T. W. Wang, D. P. Li, H. Shi, J. N. Xing, J. Y. Shao, R. Zhang, J. Liu, *J. Mater. Chem. C*. **2019**, *7*, 7249–7258. **DOI:**10.1039/C9TC01520E
15. L. H. Abdel-Rahman, A. M. Abu-Dief, R. M. Shehata, F. M. Atlam, *Appl. Organomet. Chem.* **2019**, *33*, E4699–4700. **DOI:**10.1002/aoc.4699
16. X.-G. Yi, X.-N. Fang, J. Guo, J. Li, Z.-P. Xie, *Acta Chim. Slov.* **2020**, *67*, 507–515. **DOI:**10.17344/acsi.2019.5532
17. E. A. Ermakova, J. A. Golubeva, K. S. Smirnova, L. S. Klyushova, I. V. Eltsov, A. A. Zubenko, L. N. Fetisov, A. E. Svyatogorova, E. V. Lider, *Polyhedron* **2023**, *230*, 116213. **DOI:**10.1016/j.poly.2022.116213
18. T. S. Sukhikh, D. S. Kolybalov, E. K. Pylova, S. N. Konchenko, *Inorganics* **2022**, *10*, 138. **DOI:**10.3390/inorganics10090138
19. A. B. Corradi, *Coord. Chem. Rev.* **1992**, *117*, 45–98. **DOI:**10.1016/0010-8545(92)80020-R
20. K. J. Reddy, J. R. Kumar, C. Ramachandraiah, T. Thriveni, A. V. Reddy, *Food Chem*. **2007**, *101*, 585–591. **DOI:**10.1016/j.foodchem.2006.02.018
21. M. Biesaga, K. Pyrzynska, M. Trojanowicz, *Talanta* **2000**, *51*, 209–224. **DOI:**10.1016/S0039-9140(99)00291-X
22. M. Fizer, V. Sidey, A. Tupys, Y. Ostapiuk, O. Tymoshuk, Y. Bazel, *J. Mol. Struct*. **2017**, *1149*, 669e682. **DOI:**10.1016/j.molstruc.2017.08.037
23. G. Supriyanto, J. Simon, *Talanta* **2005**, *68*, 318–322. **DOI:**10.1016/j.talanta.2005.08.052
24. H. Keypour, F. Forouzandeh, S. Salehzadeh, F. Hajibabaei, S. Feizi, R. Karamian, N. Ghiasi, R. W. Gable, *Polyhedron* **2019**, *170*, 584–592. **DOI:**10.1016/j.poly.2019.06.023
25. A. S. Berezin, O. V. Antonova, E. V. Lider, A. I. Smolentsev, V. A. Nadolinny, M. S. Mel'gunov, *J. Lumin*. **2017**, *190*, 261–266. **DOI:**10.1016/j.jlumin.2017.05.024
26. D. N. Konshina, I. A. Lupanova, S. E. Efimenko, V. V. Konshin, *Solvent Extr. Ion Exch*. **2022**, *40*, 236–250. **DOI:**10.1080/07366299.2021.1910271
27. M. Benamor, K. Belhamel, M. T. Draa, *J. Pharmaceut. Biomed*. **2000**, *23*, 1033–1038. **DOI:**10.1016/S0731-7085(00)00366-6
28. I. Singh, *Indian J. Chem*. **2000**, *39A*, 545–547. http://nopr.niscpr.res.in/handle/123456789/21128
29. K. Gavazov, A. Dimitrov, V. Lekova, *Russ. Chem. Rev*. **2007**, *76*, 169–179. **DOI:**10.1070/RC2007v076n02ABEH003655
30. H. Şenöz, *Hacettepe J. Biol. & Chem*. **2012**, *40*, 293–301.
31. K. Stojnova, K. Gavazov, V. Lekova, *Acta Chim. Slov.* **2013**, *60*, 390–396.
32. K. T. Stojnova, V. V. Divarova, P. V. Racheva, V. D. Lekova, *J. Appl. Spectrosc.* **2015**, *82*, 853–856. **DOI:**10.1007/s10812-015-0193-x
33. V. Divarova, K. Stojnova, P. Racheva, V. Lekova, *Acta Chim. Slov.* **2016**, *63*, 97–103 **DOI:**10.17344/acsi.2015.1987
34. V. Divarova, K. Stojnova, P. Racheva, V. Lekova, *Russ. J. Inorg. Chem*. **2018,** *63,* 974–977. **DOI:**10.1134/S0036023618070057
35. P. Racheva, K. Stojnova, V. Divarova, V. Lekova, *Acta Chim. Slov.* **2017**, *64*, 365–372. **DOI:**10.17344/acsi.2017.3214
36. K. Stojnova, V. Lekova, *Acta Chim. Slov.* **2019**, *66*, 360–366. **DOI:**10.17344/acsi.2018.4862
37. K. Stojnova, V. Divarova, P. Racheva, K. Bozhinova, V. Lekova, *Acta Chim. Slov.* **2016**, *63*, 654–660. **DOI:**10.17344/acsi.2016.2513
38. K. Stojnova, V. Divarova, P. Racheva, K. Bozhinova, V. Lekova, *Acta Chim. Slov.* **2018**, *65*, 213–220. **DOI:**10.17344/acsi.2017.3860
39. K. Stojnova, P. Racheva, V. Divarova, P. Yanev, V. Lekova, *Acta Chim. Slov.* **2020**, *67*, 594–601. **DOI:**10.17344/acsi.2019.5612
40. A. N. Turanov, V. K. Karandashev, O. I. Artyushin, E. V. Sharova, *Solvent Extr. Ion Exch*. **2015**, *33*, 540–553. **DOI:**10.1080/07366299.2015.1067052
41. A. N. Turanov, V. K. Karandashev, V. E. Baulin, E. V. Kirillov, S. V. Kirillov, V. N. Rychkov, A. Yu. Tsivadze, *Russ. J. Inorg. Chem*. **2016**, *61*, 1335–1338. **DOI:**10.1134/S0036023616100211
42. G. Kristian: Analytical Chemistry, BINOM, Moscow, Russia, **2009,** pp. 113–121.
43. A. N. Turanov, V. K. Karandashev, V. E. Baulin, D. V. Baulin, A. Y. Tsivadze, *Acta Chim. Slov*. **2020**, *67*, 246–252. **DOI:**10.17344/acsi.2019.5380
44. A. K. Babko, A. T. Pilipenko: Photometric Analysis, Khimiya, Moscow, Russia, **1968,** pp. 159–164.
45. V. V. Divarova, K. T. Stojnova P. V. Racheva, V. D. Lekova, *J. Appl. Spectrosc.* **2017,** *84,* 231–236. **DOI:**10.1007/s10812-017-0456-9
46. P. V. Racheva, D. G. Hristov, K. B. Gavazov, *Russ. J. Gen. Chem*. **2020**, *90*, 1351–1356. **DOI:**10.1134/S1070363220070245
47. D. Tomov, G. Bocheva, V. Divarova, L. Kasabova, D. Svinarov, *J. Med. Biochem*. **2021**, *40*, 10–16. **DOI:**10.5937/jomb0-24746
48. P. V. Racheva, N. P. Milcheva, F. Genc, K. B. Gavazov, *Spectrochim. Acta A* **2021**, *262*, 120106. **DOI:**10.1016/j.saa.2021.120106
49. D. G. Hristov, V. V. Divarova, R. D. Mancheva, K. B. Gavazov, *Russ. J. Gen. Chem*. **2019**, *89*, 2136–2142.

DOI:10.1134/S1070363219100232
50. A. Pal, V. Manish, S. Gupta, N. Kumar, *SAE Tech. Pap*. **2013**, *2013-24-0151*. **DOI:**10.4271/2013-24-0151
51. G. K. Toncheva, D. G. Hristov, N. P. Milcheva, K. B. Gavazov, *Acta Chim. Slov.* **2020,** *67,* 151–158. **DOI:**10.17344/acsi.2019.5299
52. M. I. Bulatov, I. P. Kalinkin: Practical Handbook on Photometric Methods of Analysis, Khimiya, Leningrad, Russia, **1986**, pp. 174–264.
53. F. A. Cotton, G. Wilkinson, C. A. Murillo, M. Bochmann: Advanced Inorganic Chemistry, Wiley Publishers, New Jersey, **1999**, pp. 599–606.
54. H. Remy: Inorganic chemistry, Mir, Moscow, Russia, **1966**, pp. 464–476.
55. A. Holme, F. J. Langmyhr, *Anal. Chim. Acta* **1966**, *36*, 383–391. **DOI:**10.1016/0003-2670(66)80066-1
56. K. T. Stojnova, V. D. Lekova, *Russ. J. Inorg. Chem*. **2019**, *64*, 1235–1241. **DOI:**10.1134/S0036023619100152
57. W. Likussar, D. F. Boltz, *Anal. Chem.* **1971**, *43*, 1265–1272. **DOI:**10.1021/ac60304a006

Povzetek

S spektrofotometričnimi metodami smo raziskali ravnotežno reakcijo tvorbe kompleksa med anionskim kelatom zgrajen iz cinka(II) in tridentatnega liganda 4-(2-piridilazo)-resorcinolom (PAR) in organskim tetrazolijevim kationom 3-(2-naftil)-2,5-difenil-2H-tetrazolijevim kloridom (TV) v tekoče-tekoče ekstrakcijskem sistemu Zn(II)-PAR-TV-H_2O-2-metil-1-propanol. Molsko razmerje reagentov je bilo določeno z neodvisnimi metodami pri optimalnih pogojih za ionsko asociacijo in ekstrakcijo. Preverili smo veljavnost Beerovega zakona in izračunali nekatere analizne značilnosti. Izračunane so bile konstante, ki opisujejo proces asociacije v vodni fazi in ekstrakcijsko ravnotežje. Na podlagi tega so bili predlagani reakcijska shema, splošna formula in strukturna formula kompleksa. Cinkov(II) kation je šestvezno koordiniran s tridentatnim ligandom prek naslednjih atomov: azo dušik, piridinski dušik in kisikov atom iz fenolne skupine, ki je v orto položaju glede na azo skupino, vsak od njih pa tvori dva petčlenska kelatna obroča.

Scientific paper

Ethanol-Coordinated Dioxidomolybdenum(VI) Complexes with Aroylhyrazone Ligands: Synthesis, Spectroscopic Characterization, Crystal structures and Catalytic Oxidation Property

Zheng Zhou*, Cheng Qiu, Xiuchan Xiao and Yan Lei

School of Materials and Environmental Engineering, Chengdu Technological University, Chengdu 611730, P.R. China

** Corresponding author: E-mail: lswtqzz@163.com*

Received: 04-17-2023

Abstract

Two new dioxidomolybdenum(VI) complexes, $[MoO_2L^1(EtOH)]$ (**1**) and $[MoO_2L^2(EtOH)]$ (**2**), derived from the aroylhydrazone ligands *N*'-(2-hydroxyl-3-methoxybenzylidene)-3-methylbenzohydrazide (H_2L^1) and 4-fluoro-*N*'-(2-hydroxylbenzylidene)benzohydrazide (H_2L^2), respectively, were prepared in ethanol under ambient temperature. Both complexes were characterized by elemental analysis, IR and UV-Vis spectroscopy, as well as single crystal X-ray determination. The Mo atoms in the complexes are in octahedral coordination. Crystal structures of the complexes are stabilized by hydrogen bonds. The catalytic property for epoxidation of styrene by both complexes was studied.

Keywords: Molybdenum complex; aroylhydrazone; crystal structure; catalytic property

1. Introduction

The petrochemical and pharmaceutical industries are inevitably causing serious environmental problems followed by the organic synthesis. To solve this problem, the application of catalysts is an efficient way to reduce the energy consumption. Schiff bases and their complexes with various metal atoms have received particular attention in many aspects like catalysts,[1] magnetism[2] and biological applications.[3] Aroylhydrazones bearing the functional group –CH=N–NH–C(O)– are a kind of special Schiff bases having donor atoms around the metal ions that can adopt both keto and enol forms during coordination.[4] Complexes with aroyhydrazone ligands have wide applications as catalysts for the oxidation of sulfides, polymerization and asymmetric epoxidation.[5] The oxidation of alkenes to their corresponding epoxides is of great industrial and academic interest. Among the epoxides, cyclooctene and cyclohexene oxides are the most important intermediates used in the preparation of a great number of organic products. Molybdenum complexes are reported to have fascinating catalytic properties on epoxidation reactions.[6] Tridentate dianionic Schiff base complexes such as *cis*-MoO_2LL' (L' = solvent) are good substrates for redox reactions because of the ability of L' replacement with other solvents.[7] There are several crystal structures of molybdenum(VI) complexes with methanol acting as L'. However, those with ethanol as co-ligands are rare. The reason might be that the size of methanol molecule is smaller than ethanol, which leads to easier coordination of methanol to Mo in respect with ethanol. In pursuit of new catalysts for epoxidation reactions, we report herein two new ethanol-coordinated dioxidomolybdenum(VI) complexes, $MoO_2L^1(EtOH)]$ (**1**) and $MoO_2L^2(EtOH)]$ (**2**), where L^1 and L^2 are the dianionic form of *N*'-(2-hydroxyl-3-methoxybenzylidene)-3-methylbenzohydrazide (H_2L^1) and 4-fluoro-*N*'-(2-hydroxylbenzylidene)benzohydrazide (H_2L^2), respectively (Scheme 1).

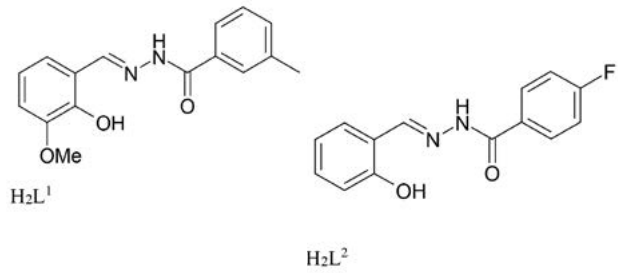

Scheme 1. The aroylhydrazone ligands.

2. Experimental

2. 1. Reagents

$MoO_2(acac)_2$, 3-methoxysalicylaldehyde, salicylaldehyde, 3-methylbenzohydrazide and 4-fluorobenzohydrazide were purchased from Aldrich. All other reagents with AR grade were used as received without further purification.

2. 2. Instruments

Elemental analyses were carried out on a Perkin-Elmer 2400 CHN elemental analyzer. Infrared spectra (4000–400 cm^{-1}) were recorded as KBr discs with a FTS-40 BioRad FT-IR spectrophotometer. Electronic spectra were recorded on a Lambda 35 spectrometer. Solution electrical conductivity was measured at 298 K using a DDS-11 conductivity meter. GC analyses were performed on a Shimadzu GC-2010 gas chromatograph.

2. 3. Syntheses

2. 3. 1. Synthesis of $[MoO_2L^1(EtOH)]$ (1)

H_2L^1 (1.0 mmol, 0.28 g) and $[MoO_2(acac)_2]$ (1.0 mmol, 0.33 g) were mixed and stirred in ethanol (40 mL) for 30 min at room temperature. The yellow solution was evaporated to remove three quarters of the solvents under reduced pressure, yielding orange solid product. Yield: 87%. Well-shaped single crystals suitable for X-ray diffraction were obtained by re-crystallization of the solid from ethanol. Analysis calculated for $C_{18}H_{20}MoN_2O_6$: C, 47.38; H, 4.42; N, 6.14%; found: C, 47.23; H, 4.51; N, 6.08%. IR data (KBr, cm^{-1}): 3420 (w, ν_{OH}), 1605 (s, $\nu_{C=N}$), 945 (m, $\nu_{Mo=O}$). UV-Vis data (λ_{max}, nm): 220, 303, 370.

2. 3. 2. Synthesis of $MoO_2L^1(EtOH)]$ (2)

H_2L^2 (1.0 mmol, 0.26 g) and $[MoO_2(acac)_2]$ (1.0 mmol, 0.33 g) were mixed and stirred in ethanol (40 mL) for 30 min at room temperature. The yellow solution was evaporated to remove three quarters of the solvents under reduced pressure, yielding orange solid product. Yield: 83%. Well-shaped single crystals suitable for X-ray diffraction were obtained by re-crystallization of the solid from ethanol. Analysis calculated for $C_{16}H_{15}FMoN_2O_5$: C, 44.67; H, 3.51; N, 6.51%; found: C, 44.53; H, 3.45; N, 6.60%. IR data (KBr, cm^{-1}): 3407 (w, ν_{OH}), 1608 (s, $\nu_{C=N}$), 945 (m, $\nu_{Mo=O}$). UV-Vis data (λ_{max}, nm): 230, 305, 400.

2. 4. X-ray Crystallography

Crystallographic data of the complexes were collected on a Bruker SMART CCD area diffractometer with graphite monochromated Mo-Kα radiation (λ = 0.71073 Å) at 298(2) K. Absorption corrections were applied by using the multi-scan program.[8] Structures of the two complexes were solved by direct methods and successive Fourier difference syntheses, and anisotropic thermal parameters for all non-hydrogen atoms were refined by full-matrix least-squares procedure against F^2.[9] All non-hydrogen atoms were refined anisotropically. The ethanol H atoms of both complexes were located from difference Fourier maps and refined isotropically, with O–H distances restrained to 0.85(1) Å. The remaining hydrogen atoms were located at calculated positions, and refined isotropically with U_{iso}(H) values constrained to 1.2 U_{iso}(C) and 1.5 $U_{iso}(C_{methyl})$. The crystallographic data and experimental details for the complexes are listed in Table 1.

Table 1. Crystallographic data for the complexes

	1	2
Empirical formula	$C_{18}H_{20}MoN_2O_6$	$C_{16}H_{15}FMoN_2O_5$
Formula weight	456.30	430.24
Temperature (K)	298(2)	298(2)
Crystal system	Triclinic	Monoclinic
Space group	*P*–1	$P2_1/c$
a (Å)	7.993(2)	7.987(2)
b (Å)	10.371(2)	16.023(2)
c (Å)	11.475(2)	15.515(2)
α (°)	95.413(2)	90
β (°)	94.189(2)	120.973(2)
γ (°)	101.323(2)	90
V (Å^3)	924.5(3)	1702.4(5)
Z	2	4
F(000)	464	864
M (mm^{-1})	0.747	0.810
R_{int}	0.0297	0.0374
Collected data	5511	7165
Unique data	3433	2351
Observed data [$I > 2\sigma(I)$]	3118	1830
Restraints	1	1
Parameters	250	230
Goodness-of-fit on F^2	1.054	0.935
R_1, wR_2 indices [$I > 2\sigma(I)$]	0.0385, 0.1020	0.0333, 0.0846
R_1, wR_2 indices (all data)	0.0428, 0.1061	0.0456, 0.0883
Large diff. peak and hole, *e* Å^{-3}	0.880, –0.790	0.409, –0.354

2. 5. General Procedure for Catalytic Epoxidation of Styrene

The epoxidation reaction was carried out at room temperature in acetonitrile under N_2 atmosphere with constant stirring. The composition of the reaction mixture was 2.00 mmol of styrene, 2.00 mmol of chlorobenzene (internal standard), 0.10 mmol of the complexes (catalyst) and 2.00 mmol iodosylbenzene or sodium hypochlorite (oxidant) in 5.00 mL freshly distilled acetonitrile. When the oxidant was sodium hypochlorite, the solution was buffered to pH = 11.2 with NaH_2PO_4 and NaOH. The composition of reaction medium was determined by GC

with styrene and styrene epoxide quantified by the internal standard method (chlorobenzene). All other products detected by GC were mentioned as others. For each complex the reaction time for maximum epoxide yield was determined by withdrawing periodically 0.1 mL aliquots from the reaction mixture and this time was used to monitor the efficiency of the catalyst on performing at least two independent experiments. Blank experiments with each oxidant and using the same experimental conditions except catalyst were also performed.

3. Results and Discussion

3. 1. Chemistry

By using the aroylhydrazone compounds H_2L^1 and H_2L^2 as ligands to react with dioxomolybdenum(VI) acetylacetonate in ethanol, two new dioxidomolybdenum complexes were obtained (Scheme 2). The progress of the reaction was accompanied by an immediate color change of the solution from colorless to yellow. The hydrazones were deprotonated during the coordination. The hydrazones are in dianionic form with no base used during the synthesis. This is not uncommon for the preparation of such type complexes. The two H atoms of the hydrazone ligands may transfer to acetylacetone. The analytical data are in good agreement with the proposed molecular formulae. Both complexes are insoluble in water but soluble in CH_2Cl_2, $CHCl_3$, CH_3CN, MeOH, EtOH, DMF and DMSO. The molar conductivity of the complexes at concentration of 1.0×10^{-3} M in DMSO and water solution (Λ_M = 23 Ω^{-1} cm^2 mol^{-1} for **1** and 31 Ω^{-1} cm^2 mol^{-1} for **2**) is in agreement with non-electrolyte behavior.[10]

and angles are given in Table 2. Single crystal X-ray analysis indicates that the complexes are mononuclear dioxidomolybdenum(VI) compounds. The Mo atoms in the complexes are in octahedral geometry, with the equatorial plane defined by the enolate oxygen (O1), phenolate oxygen (O2), imino nitrogen (N2) of the aroylhydrazone ligand, and one oxido oxygen (O3). The axial positions are occupied by the other oxido oxygen (O4) and ethanol oxygen (O5). The Mo atoms displaced toward the axial oxido O4 atoms by 0.322(1) Å for **1**, and 0.338(1) Å for **2**, from the equatorial planes of the octahedral coordination. The distortion of the coordination of both complexes can be observed from the bond angles related to the Mo atoms. The *cis*- and *trans*-angles at the equatorial planes are in the ranges of 71.18(9)–103.97(11)° and 149.69(10)–156.72(11)° for **1** and 71.29(10)–102.55(14)° and 149.74(13)–156.38(16)° for **2**. The angles among the axial and basal bonds are in the ranges of 75.94(9)–105.30(13)° for **1** and 75.31(11)–105.57(18)° for **2**. The bond lengths of Mo–O and Mo–N of both complexes are similar to each other, and comparable to those in other Mo complexes reported in literature.[11] The terminal Mo=O [1.68–1.70 Å] bond distances of both complexes agree well with the corresponding values reported for related systems.[11] Because of the *trans* influence of the oxido groups (O4), the bond distances of Mo1–O5 (2.36 Å) are considerably elongated, making the O5 atoms weakly coordinated to the Mo atoms. Such elongation has previously been observed in other complexes with similar structures. The aroylhydrazone ligands coordinate to the Mo atoms through dianionic form, which can be observed from the bond lengths of C7–O1 and C7–N1. The bonds C7–O1 are obviously longer than typical double bonds, while the bonds C7–N1

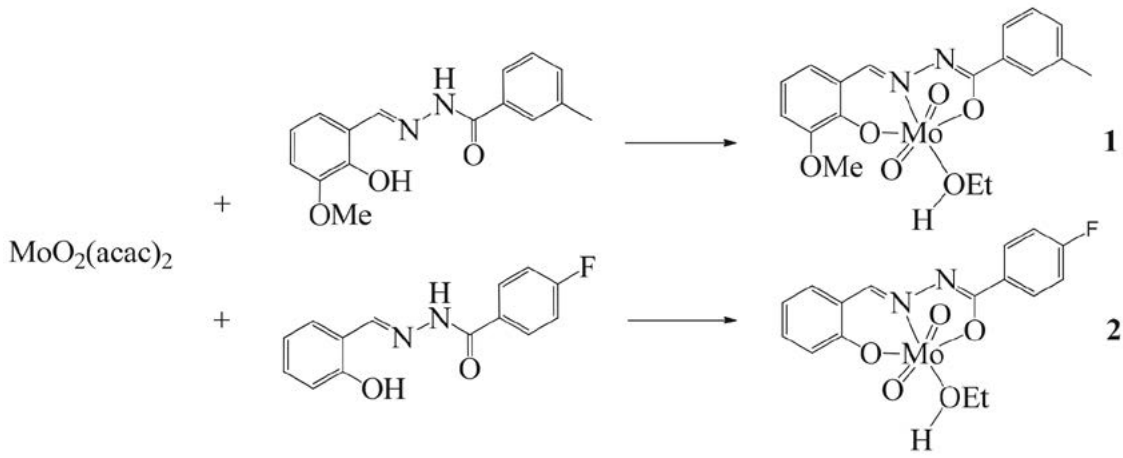

Scheme 2. The synthesis of the dioxidomolybdenum(VI) complexes.

3. 2. Crystal Structure Description of the Complexes

The ORTEP plots of the complexes **1** and **2** are shown in Figs. 1 and 2, respectively. Selected bond lengths

are shorter than typical single bonds. This phenomenon is not uncommon for metal complexes with hydrazone ligands.

In the crystal structure of complex **1** (Fig. 3), the molecules are linked by C15–H15B···O4 hydrogen

bonds (Table 3) to form chains along the *a* axis. The chains are linked through C16-H16B···O6 and O5-H5···N1 hydrogen bonds along the *c* axis, to generate a two dimensional network parallel to the *ac* plane. In the crystal structure of complex **2** (Fig. 4), the molecules are linked by C5-H5A···O3 and C12-H12···O3 hydrogen bonds (Table 3) to form two dimensional network along parallel to the *bc* plane. The layers are further linked through C10-H10···O4 and O5-H5···N1 hydrogen bonds along the *a* axis, to generate a three dimensional network.

Table 2. Selected bond distances (Å) and bond angles (°) for the complexes

	1	**2**
Mo1-O1	2.018(2)	2.019(3)
Mo1-O2	1.924(2)	1.923(3)
Mo1-O3	1.700(2)	1.694(3)
Mo1-O4	1.686(3)	1.683(4)
Mo1-O5	2.360(2)	2.362(4)
Mo1-N2	2.249(3)	2.243(3)
O4-Mo1-O3	105.30(13)	105.57(18)
O4-Mo1-O2	98.57(13)	99.27(17)
O3-Mo1-O2	103.97(11)	102.55(14)
O4-Mo1-O1	96.34(12)	97.17(16)
O3-Mo1-O1	97.28(11)	97.23(13)
O2-Mo1-O1	149.69(10)	149.74(13)
O4-Mo1-N2	96.22(12)	96.48(14)
O3-Mo1-N2	156.72(11)	156.38(16)
O2-Mo1-N2	81.06(9)	81.72(11)
O1-Mo1-N2	71.18(9)	71.29(10)
O4-Mo1-O5	171.75(11)	171.56(13)
O3-Mo1-O5	82.09(11)	82.29(15)
O2-Mo1-O5	82.90(10)	81.69(15)
O1-Mo1-O5	78.84(9)	78.51(13)
N2-Mo1-O5	75.94(9)	75.31(11)

Table 3. Hydrogen bond distances (Å) and bond angles (°) for the complexes

D*–H···*A	***d*(*D*–H)**	***d*(H···*A*)**	***d*(*D*···*A*)**	***Angle* (*D*–H···*A*)**
1				
O5–H5···N1$^{\#1}$	0.85	2.04(3)	2.885(4)	176(5)
C15–H15B···O4$^{\#2}$	0.97	2.50(3)	3.441(5)	163(5)
C16–H16B···O6$^{\#3}$	0.96	2.56(3)	3.456(5)	156(5)
2				
O5–H5···N1$^{\#4}$	0.85	2.01(3)	2.847(5)	167(4)
C5–H5A···O3$^{\#5}$	0.93	2.48(4)	3.404(5)	171(5)
C10–H10···O4$^{\#6}$	0.93	2.55(4)	3.283(5)	136(5)
C12–H12···O3$^{\#7}$	0.93	2.39(4)	3.176(5)	142(5)

Symmetry codes: #1: 1 – *x*, 1 – *y*, 1 – *z*; #2: 1 + *x*, *y*, *z*; #3: 1 – *x*, 1 – *y*, 2 – *z*; #4: – *x*, – *y*, – *z*; #5: –1 + *x*, ½ – *y*, –½ + *z*. #6: 1 – *x*, – *y*, 1 – *z*; #7: 1 + *x*, ½ – *y*, ½ + *z*.

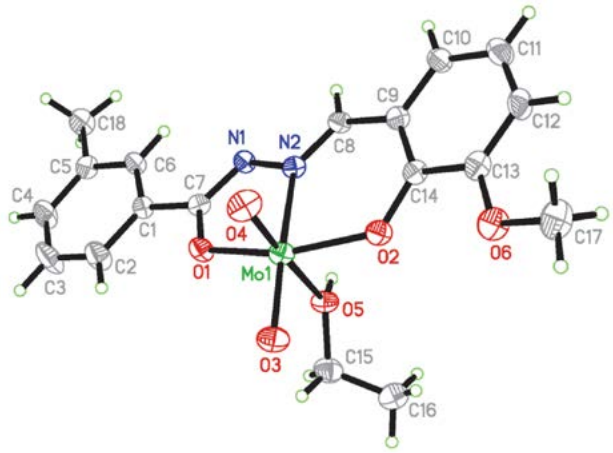

Fig. 1. ORTEP diagram of complex **1** with 30% thermal ellipsoid.

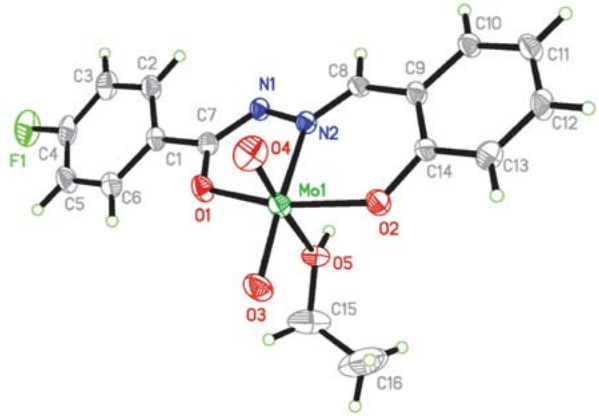

Fig. 2. ORTEP diagram of complex **2** with 30% thermal ellipsoid.

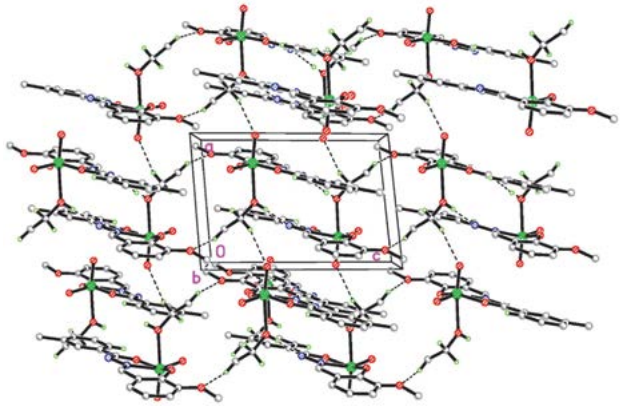

Fig. 3. Molecular packing structure of complex **1** linked by hydrogen bonds (dashed lines).

3. 3. IR Spectra of the Complexes

The weak and broad absorptions centered at 3420 cm^{-1} for complex **1** and 3407 cm^{-1} for complex **2** are attributed to the O-H bonds of the ethanol ligands. The in-

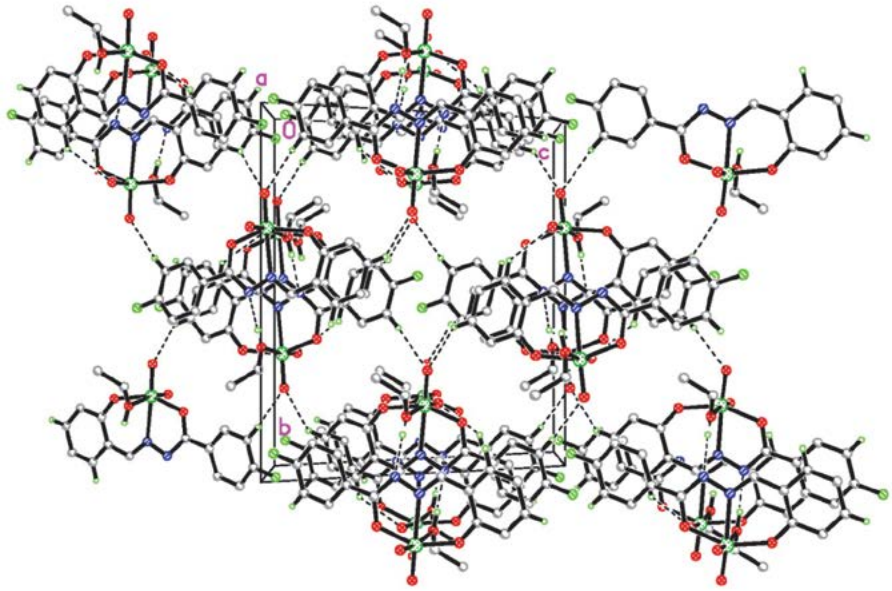

Fig. 4. Molecular packing structure of complex **2** linked by hydrogen bonds (dashed lines).

tense bands at 1605 cm^{-1} for complex **1** and 1608 cm^{-1} for complex **2** are assigned to the vibrations of the azomethine groups, ν(C=N).[12] The characteristic of the spectra of both complexes is the exhibition of sharp bands at 945 cm^{-1}, corresponding to the Mo=O stretching vibration.[13] Further evidence of the bonding is also shown by the observation that new bands in the IR spectra of the metal complexes appear at 450–470 cm^{-1} and 520–550 cm^{-1} assigned to M–N and M–O stretching vibrations.

3. 4. Catalytic Properties of the Complexes

The percentage of conversion of styrene, selectivity for styrene oxide, yield of styrene oxide and reaction time to obtain maximum yield using both the oxidants are presented in Table 4. The data reveals that both complexes as catalysts convert styrene most efficiently in the presence of the oxidants. Nevertheless, the catalysts are selective towards the formation of styrene epoxides despite of the formation of by-products which have been identified by GC-MS as benzaldehyde, phenylacetaldehyde, styrene epoxides derivative, alcohols *etc.* From the data it is also clear that the complexes exhibit excellent efficiency for styrene epoxide yield. When the reactions are carried out with PhIO and NaOCl, styrene conversions of complexes **1** and **2** were about 89% and 85%, and 91% and 86%, respectively. It is evident that between PhIO and NaOCl, the former acts as a better oxidant with respect to both styrene conversion and styrene epoxide selectivity. The epoxide yields for the complexes **1** and **2** using PhIO and NaOCl as oxidants are 79% and 88%, and 80% and 91%, respectively. The two complexes have similar catalytic oxidation behavior with the molybdenum(VI) complex with 2-bromo-*N*'-(3,5-dichloro-2-hydroxybenzylidene)benzohydrazide as ligand,[14] and better activity than the copper(II) and manganese(II) complexes with hydrazones.[15]

Table 4. Catalytic epoxidation results of complexes **1** and **2**[a]

	1		**2**	
Oxidant	PhIO	NaOCl	PhIO	NaOCl
Conversion (%)	89	85	91	86
Epoxide yield (%)	79	88	80	91
Selectivity (%)	95	93	92	88

[a] The time is 2 h for PhIO, and 3 h for NaOCl.

4. Conclusion

We have successful synthesized two new mononuclear dioxidomolybdenum(VI) complexes with the aroylhydrazone ligands *N*'-(2-hydroxyl-3-methoxybenzylidene)-3-methylbenzohydrazide and 4-fluoro-*N*'-(2-hydroxylbenzylidene)benzohydrazide. Single crystal X-ray analysis indicates that the Mo atoms in both complexes are in distorted octahedral coordination. The aroylhydrazone ligands are in dianionic chelate form and coordinate to the metal through the enolate oxygen, phenolate oxygen and imino nitrogen. Two oxo ligands and an ethanol furnish the remaining coordination sites. The complexes have effective catalytic property for the epoxidation of styrene, with conversions over 85% and selectivity over 88%. The resulting epoxides are both of academic and industrial interest.

Supplementary Material

CCDC 2256616 for **1** and 2256617 for **2** contain the supplementary crystallographic data for this paper. These

data can be obtained free of charge *via* http://www.ccdc.cam.ac.uk/conts/retrieving.html, or from the Cambridge Crystallographic Data Centre, 12 Union Road, Cambridge CB2 1EZ, UK; fax: (+44) 1223-336-033; or e-mail: deposit@ccdc.cam.ac.uk.

5. References

1. (a) K. Kim, S. Nayab, Y. Cho, H. Jung, H. Yeo, H. Lee, S.H. Lee, *RSC Advances* **2022**, *12*, 35896–35904; **DOI:**10.1039/D2RA07241F
   (b) K. Mondal, S. Mistri, *Comm. Inorg. Chem.* **2022**, *43*, 77–105; **DOI:**10.1080/02603594.2022.2094919
   (c) H. Kargar, M. Fallah-Mehrjardi, R. Behjatmanesh-Ardakani, M. Bahadori, M. Moghadam, M. Ashfaq, K.S. Munawar, M.N. Tahir, *J. Coord. Chem.* **2022**, *75*, 972–993; **DOI:**10.1080/00958972.2022.2092846
   (d) Q.-B. Li, Y.-J. Han, G.-Q. Zhao, L.-W. Xue, *Acta Chim. Slov.* **2017**, *64*, 500–505. **DOI:**10.17344/acsi.2017.3416
2. P. Middya, D. Roy, S. Chattopadhyay, *Inorg. Chim. Acta* **2023**, *548*, 121377; **DOI:**10.1016/j.ica.2023.121377
   (b) V. Muraskova, V. Eigner, M. Dusek, J. Poplstein, J. Sturala, D. Sedmidubsky, *Polyhedron* **2022**, *228*, 116156. **DOI:**10.1016/j.poly.2022.116156
3. (a) A. S. Hassan, N. M. Morsy, W. M. Aboulthana, A. Ragab, *RSC Advances* **2023**, *13*, 9281–9303; **DOI:**10.1039/D3RA00297G
   (b) N. A. A. Elkanzi, H. Hrichi, H. Salah, M. Albqmi, A. M. Ali, A. Abdou, *Polyhedron* **2023**, *230*, 116219; **DOI:**10.1016/j.poly.2022.116219
   (b) N. Ranjitha, G. Krishnamurthy, H. S. B. Naik, M. Pari, L. Afroz, K. R. Sumadevi, M. N. Manjunatha, *Inorg. Chim. Acta* **2022**, *543*, 121191; **DOI:**10.1016/j.ica.2022.121191
   (c) L.-W. Xue, X. Fu, G.-Q. Zhao, Q.-B. Li, *Acta Chim. Slov.* **2021**, *68*, 17–24; **DOI:**10.17344/acsi.2020.5817
   (d) S. Esmaielzadeh, E. Zarenezhad, *Acta Chim. Slov.* **2018**, *65*, 416–428. **DOI:**10.17344/acsi.2018.4159
4. (a) L. Nishana, A. Sakthivel, M. R. P. Kurup, *J. Mol. Struct.* **2023**, *1281*, 135128; **DOI:**10.1016/j.molstruc.2023.135128
   (b) M. S. S. Adam, S. Shaaban, M. E. Khalifa, M. Alhasani, N. El-Metwaly, *J. Mol. Liquids* **2021**, *335*, 116554; **DOI:**10.1016/j.molliq.2021.116554
   (c) G. S. Hegde, S. S. Bhat, S. P. Netalkar, P. L. Hegde, A. Kotian, R. J. Butcher, V. K. Revankar, *Inorg. Chim. Acta* **2021**, *522*, 120352; **DOI:**10.1016/j.ica.2021.120352
   (d) Y.-Q. Li, C.H. Qian, Y. Li, Y. Yang, D. Lin, X.H. Liu, C. Chen, *J. Inorg. Biochem.* **2021**, *218*, 111405; **DOI:**10.1016/j.jinorgbio.2021.111405
   (e) D.-H. Zou, M. Liang, W. Chen, *Acta Chim. Slov.* **2021**, *68*, 441–446. **DOI:**10.17344/acsi.2020.6553
5. (a) M. Sutradhar, T. R. Barman, A. J. L. Pombeiro, L. M. D. R. S. Martins, *Inter. J. Mol. Sci.* **2020**, *21*, 2832; **DOI:**10.3390/ijms21082832
   (b) M. Sutradhar, T. R. Barman, E. C. B. A. Alegria, M. F. C. G. da Silva, C.-M. Liu, H.-Z. Kou, A. J. L. Pombeiro, *Dalton Trans.* **2019**, *48*, 12839–12849; **DOI:**10.1039/C9DT02196E
   (c) M. S. S. Adam, S. Shaaban, N. M. El-Metwaly, *Appl. Organomet. Chem.* **2022**, *36*, e6763;
   (d) I. Yadav, V. Prakash, M. R. Maurya, M. Sankar, *Inorg. Chem.* **2023**. **DOI:**10.1021/acs.inorgchem.3c00504
6. (a) D. C. Martinez, C. A. Trujillo, J. G. Carriazo, N. J. Castellanos, *Catal. Lett.* **2022**, *153*, 1756–1772 **DOI:**10.1007/s10562-022-04096-y
   (b) M. S. Nunes, D. M. Gomes, A. C. Gomes, P. Neves, R. F. Mendes, F. A. A. Paz, A. D. Lopes, A. A. Valente, I. S. Goncalves, M. Pillinger, *Catalysts* **2021**, *11*, 1407; **DOI:**10.3390/catal11111407
   (c) D. Martinez-Martinez, M. L. Santiago, R. A. Toscano, M. Amezquita-Valencia, *Eur. J. Inorg. Chem.* **2021**, *2021*, 243–251; **DOI:**10.1002/ejic.202000790
   (d) Q. Liu, J.H. Lin, J. Liu, W. Chen, Y.M. Cui, *Acta Chim. Slov.* **2016**, *63*, 279–286.
7. (a) Y. Sui, X. Zeng, X. Fang, X. Fu, Y. Xiao, L. Chen, M. Li, S. Cheng, *J. Mol. Catal. A: Chem.* **2007**, *270*, 61–67; **DOI:**10.1016/j.molcata.2007.01.032
   (b) N. K. Ngan, K. M. Lo, C. S. R. Wong, *Polyhedron* **2012**, *33*, 235–251; **DOI:**10.1016/j.poly.2011.11.057
   (c) V. W. L. Ng, M. K. Taylor, C. G. Young, *Inorg. Chem.* **2012**, *51*, 3202–3211; **DOI:**10.1021/ic2026686
   (d) R. Takjoo, J. T. Mague, A. Akbari, M. Ahmadi, *J. Coord. Chem.* **2013**, *66*, 1854–1865. **DOI:**10.1080/00958972.2013.791922
8. G.M. Sheldrick. SAINT (version 6.02), SADABS (version 2.03), Madison (WI, USA): Bruker AXS Inc, **2002**.
9. G.M. Sheldrick. SHELXL-97, A Program for Crystal Structure Solution, Göttingen (Germany): University of Göttingen, **1997**.
10. W. J. Geary, *Coord. Chem. Rev.* **1971**, *7*, 81–122. **DOI:**10.1016/S0010-8545(00)80009-0
11. (a) S. Y. Ebrahimipour, H. Khabazadeh, J. Castro, I. Sheikhshoaie, A. Crochet, K. M. Fromm, *Inorg. Chim. Acta* **2015**, *427*, 52–61; **DOI:**10.1016/j.ica.2014.11.023
    (b) R. X. Hu, H. Liang, Q. Yu, G. Y. Yang, L. Chen, Z. Y. Zhou, X. G. Zhou, *Acta Chim. Slov.* **2001**, *59*, 972–975;
    (c) I. Sheikhsoaie, A. Rezaeffard, N. Monadi, S. Kaafi, *Polyhedron* **2009**, *28*, 733–738; **DOI:**10.1016/j.poly.2008.12.044
    (d) T. M. Asha, M. R. P. Kurup, *Inorg. Chim. Acta* **2018**, *483*, 44–52. **DOI:**10.1016/j.ica.2018.07.041
12. M. Ghorbanloo, R. Bikas, G. Malecki, *Inorg. Chim. Acta* **2016**, *445*, 8–16. **DOI:**10.1016/j.ica.2016.02.018
13. Z. Moradi-Shoeili, M. Zare, M. Bagherzadeh, M. Kubicki, D.M. Boghaei, *J. Coord. Chem.* **2015**, *68*, 548–559. **DOI:**10.1080/00958972.2014.993321
14. Y. Lei, Q. Yang, Y. Bai, Y. Tan, *J. Coord. Chem.* **2022**, *75*, 1147–1158. **DOI:**10.1080/00958972.2022.2095907
15. (a) Y. Tan, Y. Lei, *Acta Chim. Slov.* **2021**, *68*, 44–50; **DOI:**10.17344/acsi.2020.6044
    (b) Y. Tan, *Acta Chim. Slov.* **2020**, *67*, 1233–1238. **DOI:**10.17344/acsi.2020.6136

Povzetek

Sintetizirali smo dva nova dioksidomolibdenova(VI) kompleksa, $[MoO_2L^1(EtOH)]$ (**1**) in $[MoO_2L^2(EtOH)]$ (**2**), pridobljena iz aroilhidrazonskih ligandov *N*'-(2-hidroksil-3-metoksibenziliden)-3-metilbenzohidrazida (H_2L^1) oziroma 4-fluoro-*N*'-(2-hidroksilbenziliden)benzohidrazida (H_2L^2), v etanolu pri sobni temperaturi. Oba kompleksa smo okarakterizirali z elementno analizo, IR in UV-Vis spektroskopijo ter z rentgensko monokristalno analizo. Mo atomi v kompleksih so koordinirani oktaedrično. Kristalne strukture kompleksov so stabilizirane z vodikovimi vezmi. Preučevali smo katalitične lastnosti obeh kompleksov pri epoksidaciji stirena.

DOI: 10.17344/acsi.2023.8005 *Acta Chim. Slov.* **2023,** *70,* 310–317

Scientific paper

Preparation, Structure, Characterization and Properties of a Novel $[Y(HIA)_3(H_2O)2]n \cdot nYCl_3$ (HIA = Isonicotinic Acid)

Kun-Zhong Yang,[1,3] Rong Zou,[1] Wen-Ming Liao,[1] Xiu-Guang Yi[1,*] and Jin-Bing Zhang[2,*]

[1] *School of Chemistry and Chemical Engineering, Jinggangshan University, Ji'an, 343009, China*

[2] *School of Materials Science and Engineering, NingboTech University, Ningbo, 315100, China*

[3] *Experimental Testing Team of Jiangxi Geological Bureau, Nanchang, 330009, China*

** Corresponding author: E-mail: jayxgggchem@163.com & zhangjb@nbt.edu.cn*

Received: 01-08-2023

Abstract

A novel yttrium complex $[Y(HIA)_3(H_2O)_2]_n \cdot nYCl_3$ (HIA = isonicotinic acid) has been synthesized via a hydrothermal reaction and characterized by single crystal X-ray diffraction technique. The title complex features a one-dimensional (1-*D*) chain-like structure. A solid state photoluminescence measurement revealed that there is one strong emission peak at 487 nm. These peak can be assigned to the characteristic electronic transition and stacking effect inside the ligand. The title complex shows CIE (Commission Internationale de I' Éclairage) chromaticity coordinates in the blue region (0.1049, 0.1221). At the same time, the title complex has a wide band gap of 2.03 eV, which was revealed by a solid-state UV/Vis diffuse reflection experiment.

Keywords: Yttrium, Crystal structure, Photoluminescence, Band gap

1. Introduction

In recent decades, lanthanide coordination complexes have attracted more and more interest, due to their excellent photoluminescence properties, magnetic and other properties. [1–5] At present, lanthanide coordination complexes have been found to be widely used in luminescent probes, electroluminescent devices, luminescent materials, magnetic materials, cell imaging and sensors.[6–10] It is well known that the chemical and physical properties of lanthanide coordination complexes are mainly related to the 4*f* electronic configuration of rare earth ions. For example, if 4*f* electrons in lanthanide coordination complexes are effectively transferred, photoluminescence may occur. However, in many cases, due to the low absorption coefficient of rare earth ions, the conversion between 4*f* election orbitals is impossible to form, so lanthanide coordination complexes usually cannot show ideal photoluminescence. In order to increase the absorption coefficient of rare earth ions and promote the conversion between 4*f* electron orbitals, scientists usually a strategy called "antenna effect". In order to achieve this strategy, scientists usually use organic molecular ligands with conjugated structure as "antenna" effect to bind rare earth ions.[11–13]

Aromatic carboxylic acid is a good organic ligand, and its carboxylate ion has a variety of ligand modes, such as monodentate coordination, symmetrical chelation coordination, asymmetrical chelation coordination, monooxy bridging coordination, dioxygen bridging coordination and so on.[14–16] Isonicotinic acid (HIA) is a very good organic ligand, because both ends of its structure contain a carboxyl group and a nitrogen atom respectively, which can make it achieve different coordination geometry and extended structure with metal ions.

Based on the interest in this aromatic carboxylic acid ligand and the author's region is rich in yttrium element. In order to better develop the use of yttrium element, our research group prepared a novel dual-core type of yttrium-isonicotinic acid coordination complexes $[Y(HIA)_3(H_2O)_2]_n \cdot nYCl_3$ (HIA = isonicotinic acid).

2. Experimental

2. 1. Materials and Physical Measurements

All chemicals are analytical reagent grade, commercially obtained and used without further purification. Photoluminescence experiment was carried out on a F97XP photoluminescence spectrometer. The solid-state UV/Vis measurements were conducted on TU1901 UV/Vis spectrometer with the wavelength range of 200–900 nm. The infrared spectra was obtained from the PE Spectrum-One Fourier transform infrared (FT-IR) with the wavelength range of 4000–500 nm.

2. 2. Preparation of the Title Complex $[Y(HIA)_3(H_2O)_2]_n \cdot nYCl_3$

$YCl_3 \cdot 6H_2O$ (1 mmol, 304 mg), isonicotinic acid (1 mmol, 123 mg) and 15 mL distilled water were loaded into a 25 mL Teflon-lined stainless steel vessel, then heated to 453 K and kept there for seven days in an oven, and finally cooled down to room temperature. Yellow block-like crystals were collected manually and washed with distilled water. Yield = 56% (based on $YCl_3 \cdot 6H_2O$). IR (KBr, cm^{-1}): 3451 (vs), 2924 (w), 2855 (w), 1620 (vs), 1546 (w), 1413 (m), 766 (w), 530 (w), as shown in Figure 1.

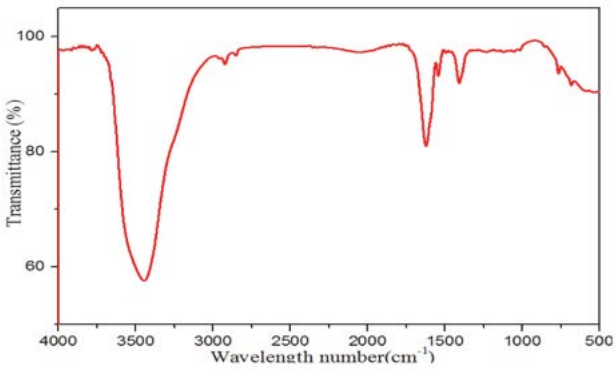

Figure 1. FTIR spectra of the title complex $[Y(HIA)_3(H_2O)_2]_n \cdot nYCl_3$

2. 3. Crystallographic Data Collection and Refinement

The single crystal data of the title complex were collected with a suitable single crystal (size 0.03 mm, 0.05 mm, 0.16 mm) on a SuperNova charge-coupled device (CCD) X-ray diffractometer. During the data acquisition, the crystal temperature was kept at 293(2) K. Using Olex2, the structure was solved with the SIR2004 structure solution program using Direct Methods and refined with the ShelXL refinement package using Least Squares minimisation.[17–19] All of the non hydrogen atoms were generated based on the subsequent Fourier difference diagram and were refined anisotropically. The hydrogen atoms were located theoretically and ride on their parent atoms. Table 1 provides a summary of the crystallographic data and refinement results. Table 2 lists selected bond lengths and angles for the title complex.

Table 1. Crystallographic data and structure analysis for the title complex

Empirical formula	$C_{18}H_{16}Cl_3N_3O_8Y_2$
Formula weight	686.51
Temperature/K	293(2)
Crystal system	triclinic
Space group	*P*-1
a/Å	9.6260(3)
b/Å	11.8097(4)
c/Å	14.6020(5)
α/°	101.772(3)
β/°	95.383(3)
γ/°	113.606(3)
V/Å^3	1460.28(9)
Z	2
ρ_{calc}g/cm^3	1.561
μ/mm^{-1}	4.269
F(000)	676.0
Crystal size/mm^3	0.16 × 0.05 × 0.03
Radiation	MoKα (λ = 0.71073)
2θ range for data collection/°	7.53 to 50.048
Index ranges	$-11 \le h \le 11$, $-13 \le k \le 14$, $-17 \le l \le 11$
Reflections collected	11237
Independent reflections	3901 (R_{int} = 0.0346)
Data/restraints/parameters	3901/273/318
Goodness-of-fit on F^2	1.011
Final R indexes [$I>=2\sigma(I)$]	R_1 = 0.0692, wR_2 = 0.1735
Final R indexes [all data]	R_1 = 0.0771, wR_2 = 0.1831
Largest diff. peak/hole / e Å^{-3}	1.03/–0.60

3. Results and Discussion

3. 1. Crystal Structure

The title complex crystallizes in the triclinic *P*-1. The asymmetric unit contains two neutral molecules $Y(HIA)_3 \cdot (H_2O)_2$ and YCl_3, as shown in Figure 2. The yttrium ions have two different coordination environments. The Y(1) ion is coordinated with three oxygen of three isonicotinic acid and two oxygen of two water, forming a slightly distorted tetragonal antiprism configuration, the Y(2) ion is surrounded by three chloride ions. The 1-*D* chains are interconnected through Y(1) bridges running along the *a* axis, as shown in Figure 3. In the title complex, the following bond distances were observed: Y(1)-O(1W) / O(2W) / O(1)^2 / O(2) / O(3) / O(4)^3 / O(5)^3 / O(6) 2.609(8) / 2.625(7) / 2.510(6) / 2.444(7) / 2.522(7) / 2.449(7) / 2.842(8) / 2.452(7) Å; Y(2)-Cl(1A)^1 / Cl(2) / Cl(3) 3.153(4) / 2.780(3) / 2.716(3) Å; Cl(1A)-Y(2)

2.776(5) Å; Cl(1A)-Y(2)[1] 3.153(4) Å; Cl(1B)-Y(2) 2.748(5) Å, as shown in Table 2. These are comparable with those reported in the literature for similar or related compounds.[20–22]

In the title complex, there are 5 groups of intermolecular hydrogen bonds and one group of intramolecular hydrogen bonds in the crystal structure of the form O-H···O / N and C-H···O, as shown in Table 3 and Figure 4 for details. In the crystal structure, the nitrogen atom does not directly participate in coordination, but undergoes intermolecular hydrogen bonding with O-H. There is no π···π interaction, but it has a large number of intermolecular hydrogen bonds and van de Waals attraction yielding the 3-*D* supramolecular structure running parallel to the *bc* plane, and the crystal packing is presented in Figure 5.

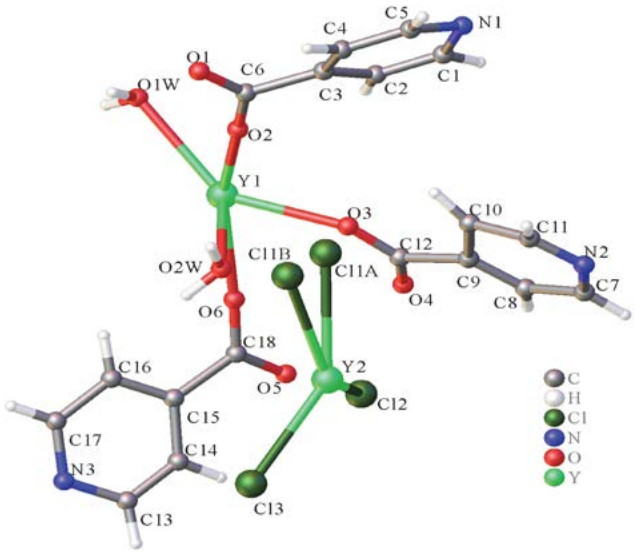

Figure 2. The asymmetric unit molecular diagram of the title complex

3. 2. Hirshfeld Surface analysis

In order to further analyze various weak intermolecular forces, the Hirshfeld surface analysis method was

Table 2. Selected bond lengths (Å) and bond angles (°) for the title complex

Atom-Atom	Lengths(Å)	Atom-Atom	Lengths(Å)
Cl(1A)-Y(2)	2.776(5)	Y(1)-O(3)	2.522(7)
Cl(1A)-Y(2)[1]	3.153(4)	Y(1)-O(4)[3]	2.449(7)
Cl(1B)-Y(2)	2.748(5)	Y(1)-O(5)[3]	2.482(8)
Y(1)-O(1W)	2.609(8)	Y(1)-O(6)	2.452(7)
Y(1)-O(2W)	2.625(7)	Y(2)-Cl(1A)[1]	3.153(4)
Y(1)-O(1)[2]	2.510(6)	Y(2)-Cl(2)	2.716(3)
Y(1)-O(2)	2.444(7)	Y(2)-Cl(3)	2.780(3)
Atom-Atom-Atom	Angle (°)	Atom-Atom-Atom	Angle (°)
Y(2)-Cl(1A)-Y(2)[1]	94.26(13)	O(4)3-Y(1)-O(6)	69.7(3)
O(1W)-Y(1)-O(2W)	123.5(2)	O(5)3-Y(1)-O(1W)	70.8(3)
O(1)2-Y(1)-O(1W)	72.1(3)	O(5)3-Y(1)-O(2W)	137.5(3)
O(1)2-Y(1)-O(2W)	72.1(3)	O(5)3-Y(1)-O(1)[2]	142.1(3)
O(1)2-Y(1)-O(3)	138.0(3)	O(5)3-Y(1)-O(3)	79.0(3)
O(2)-Y(1)-O(1W)	72.6(3)	O(6)-Y(1)-O(1W)	136.9(3)
O(2)-Y(1)-O(2W)	72.0(2)	O(6)-Y(1)-O(2W)	77.6(2)
O(2)-Y(1)-O(1)[2]	99.5(2)	O(6)-Y(1)-O(1)[2]	82.3(2)
O(2)-Y(1)-O(3)	79.1(2)	O(6)-Y(1)-O(3)	78.3(2)
O(2)-Y(1)-O(4)[3]	143.0(3)	O(6)-Y(1)-O(5)[3]	121.3(2)
O(2)-Y(1)-O(5)[3]	76.5(2)	Cl(1A)-Y(2)-Cl(1A)[1]	85.74913)
O(2)-Y(1)-O(6)	147.3(2)	Cl(1A)-Y(2)-Cl(3)	133.2(2)
O(3)-Y(1)-O(1W)	142.4(3)	Cl(1B)-Y(2)-Cl(3)	109.3(3)
O(3)-Y(1)-O(2W)	67.6(2)	Cl(2)-Y(2)-Cl(1A)[1]	112.79(18)
O(4)3-Y(1)-O(1W)	71.9(3)	Cl(2)-Y(2)-Cl(1A)	110.7(2)
O(4)3-Y(1)-O(2W)	138.9(3)	Cl(2)-Y(2)-Cl(1B)	131.9(2)
O(4)3-Y(1)-O(1)[2]	79.4(3)	Cl(2)-Y(2)-Cl(3)	110.12(6)
O(4)3-Y(1)-O(3)	126.1(2)	Cl(3)-Y(2)-Cl(1A)[1]	98.8(2)
O(4)3-Y(1)-O(5)[3]	82.2(3)		

Symmetry codes: 1 = 3 – *x*, 2 – *y*, – *z*; 2 = 3 – *x*, 2 – *y*, 1 – *z*; 3 = 4 – *x*, 2 – *y*, 1 – *z*.

Table 3. Hydrogen bond lengths (Å) and bond angles (°)

D-H···A	[ARU]	D-A(Å)	H···A(Å)	D···A(Å)	D-H···A(°)
O(1W)-H(1WA)···O(2)	[2876]	0.86	2.55	3.195(12)	132
O(1W)-H(1WA)···O(2W)	[2876]	0.86	2.10	2.862(13)	148
O(2W)-H(2WA)···N(3)	[2986]	0.86	1.99	2.775(12)	152
O(2W)-H(2WB)···O(1W)	[2876]	0.85	2.03	2.862(13)	165
C(14)-H(14)···O(5)		0.93	2.57	2.875(15)	100
C(16)-H(16)···O(1)	[2876]	0.93	2.43	3.338(15)	164

Symmetry codes: [2876] = 3 – *x*, 2 – *y*, 1 – *z*; [2986] = 4 – *x*, 3 – *y*, 1 – *z*.

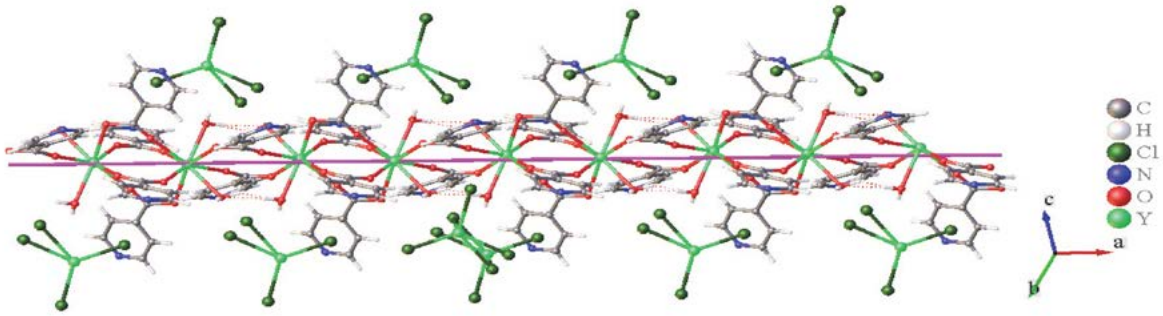

Figure 3. The 1-D chain-like structure of the title complex viewed along the *a* axis.

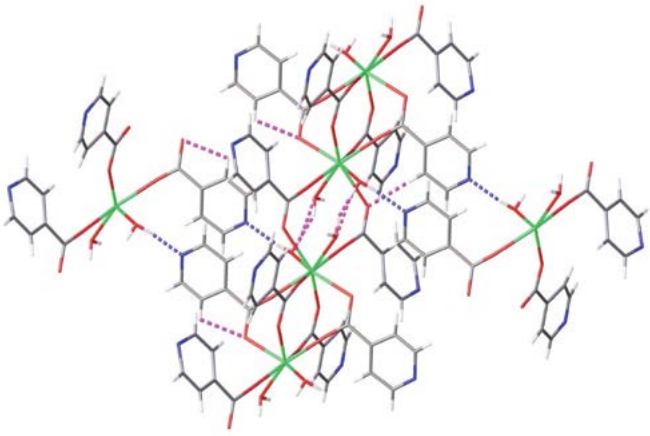

Figure 4. The hydrogen bond diagram of the title complex. n[YCl_3] molecules not involved in the motif show were removed for clarity.

used to quantitatively analyze the weak intermolecular forces of the title complex. Through Crystal Explorer 3.1 program calculation of the Hirshfeld Surface of the complex molecules distribution of force, obtaining dnorm, shape index, and curvature figure. Hirshfeld analysis was performed on the title complex, as shown in the Figure 6. The range of dnorm, shape index and curednes is –1.0523 ~ 1.9122, –1.0000 ~ 1.0000, –4.0000 ~ 4.0000.

The Hirshfeld surface of the title complex and the contribution percentage of various mode of action to the Hirshfeld surface are shown in Figure 7. The four main mode of action are H···H, C···H, O···H and H···Cl connections. Among them, the effect of H···H is distributed in the middle area of the fingerprint, which contributes the most to the Hirshfeld surface, reaching 25.7%, and is the most important mode of action. Next are the action of C···H,

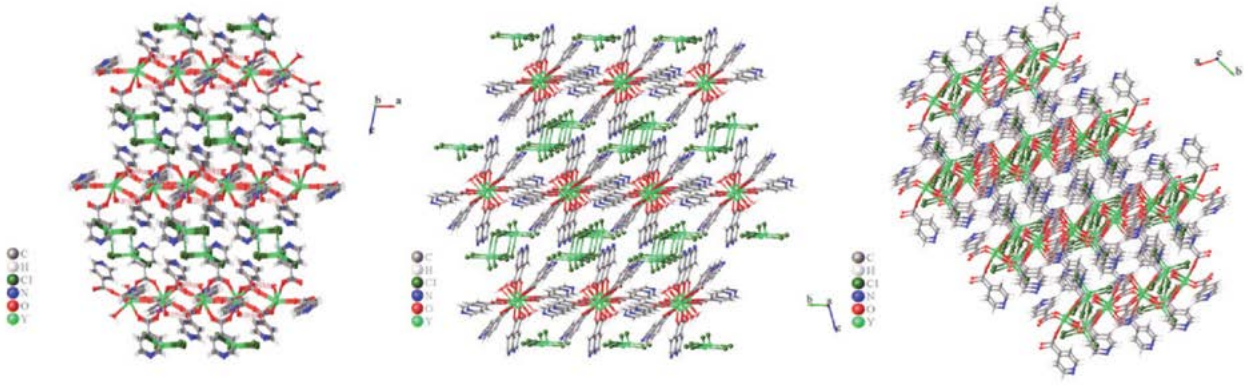

Figure 5. The packing diagram of the title complex viewed along the *ab,bc, bc.*

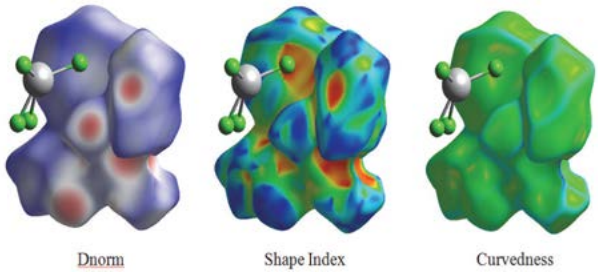

Figure 6. The Hirshfeld surface picture of the title complex

H···Cl and O···H, with a contribution ratio of 14.1%, 14.1% and 13.6%, respectively.

3. 3. Solid-State Photoluminescence Spectra

In order to investigate the photoluminescence characteristics of the title complex, the photoluminescence spectra of the solid state samples were measured at room temperature, and the results are shown in Figure 8. It is obvious that the photoluminescent spectrum of the title complex displayed an effective energy absorption in a

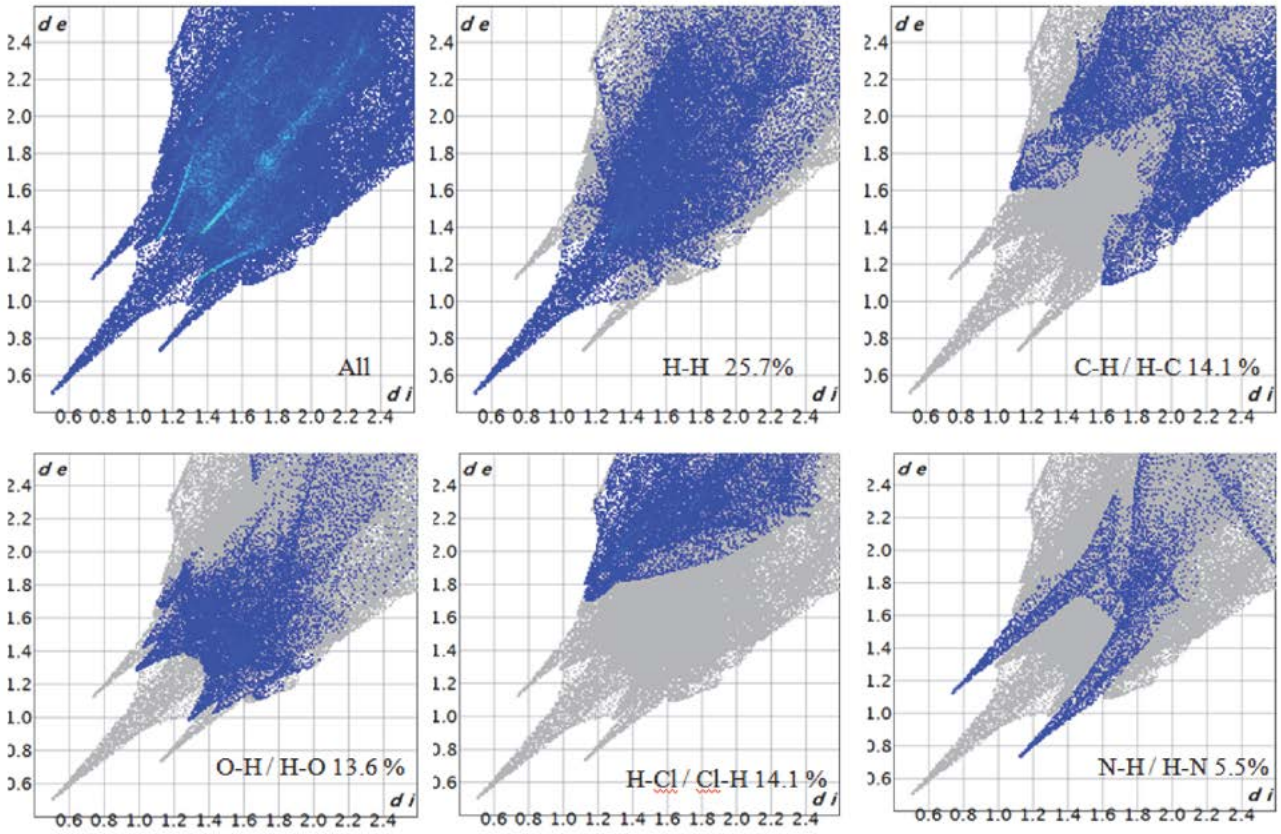

Figure 7. 2D fingerprint of the title complex (global 2D fingerprint & fingerprint of different molecular connections)

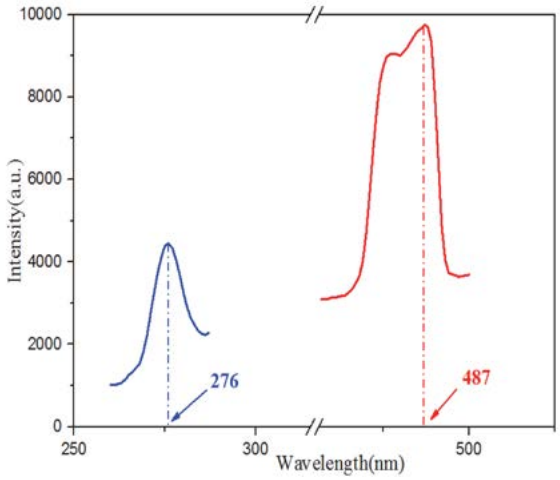

wavelength rang of 350–500 nm. Upon the emission of 487 nm, the excitation spectrum showed a band at 276 nm. Upon excitation at 276 nm, the emission spectrum was characterized by a sharp band at 487 nm in the blue region. The emission band of the title complex located in the blue violet light region with the CIE1931 chromaticity coordinate (0.1049, 0.1221), as shown in Figure 8. As the result, the title complex is a potential blue photoluminescent material.

Figure 8. Solid-state photoluminescence of the title complex (blue line: emission; red line: excitation).

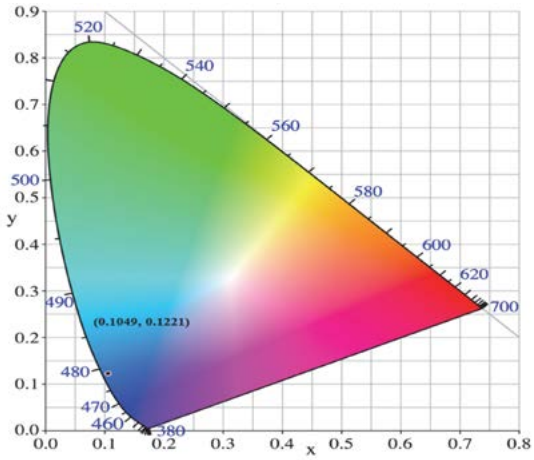

Figure 9. The CIE chromaticity diagram and chromaticity coordinate of the emission spectrum of the title complex

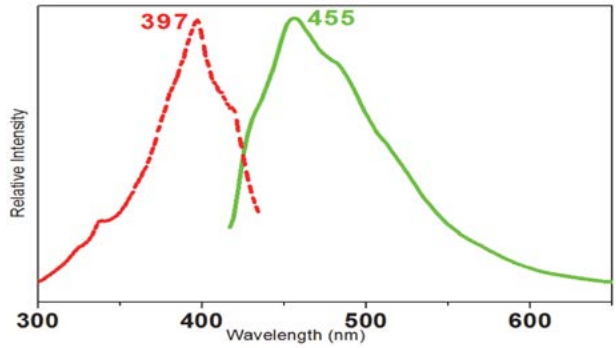

Figure 10. Solid-state photoluminescence of the title HIA ligand (red line: emission; green line: excitation).

It can be seen from the solid-state fluorescence spectra of Figure 8 and Figure 10 that the emission peak of the ligand HIA is 455 nm under the excitation peak of 397 nm. However, under the excitation peak of 276 nm, the emission peak of the title yttrium complex is a single peak of 487 nm, with a red shift of 32 nm relative to the HIA ligand. This is mainly due to the electronic transition and stacking effect inside the ligand.

3. 4. Solid-State UV-Vis Diffuse Reflectance Spectra of the Title Complex

Based on barium sulfate as the reference for 100% reflectivity, the UV-Vis diffuse reflectance spectra of the title complex was measured at room temperature, using the solid-state compound. The Kuberka-Monk function $\alpha/S = (1\text{-}R)^2/2R$ is used to process the solid diffuse reflection spectral data, where the parameter α refers to the absorption coefficient, *S* is the scattering coefficient which is actually independent of the wavelength when the particle size is larger than 5 μm, and *R* is the reflectivity. By extrapolating the linear part of the α/*S* absorption edge with the energy graph, the value of the optical band gap can be determined.[23,24] Solid UV-Vis diffuse reflection spectrum shows that the title complex possesses a wide optical band gap of 2.03 eV, as shown in Figure 11. Therefore, this may be a good candidate material for broad band gap semiconductors, which is obviously larger than those of GaAs (1.4 eV), CdTe (1.5 eV), and $CuInS_2$ (1.55 eV), which are called efficient band gap photovoltaic materials.[25,26]

4. Conclusions

In summary, a novel yttrium complex with isonicotinic acid (HIA) ligand including lattice water and yttrium chloride molecule has been synthesized and characterized by single-crystal X-ray diffraction. The title yttrium complex is characterized by a one-dimensional chain-like structure by metal ion bridge chain bond, the title yttrium complex packs for form a layer structure including weak interactions containing hydrogen bonding and van de Waals attraction. Based on the solid-state photoluminescent spectrum and the solid-state diffuse reflectance spectrum experiment, we believe that the title complex may be a good blue photoluminescent material (CIE chromaticity coordinates 0.1049, 0.1221) and a candidate material for wide band gap semiconductor (2.03 eV).

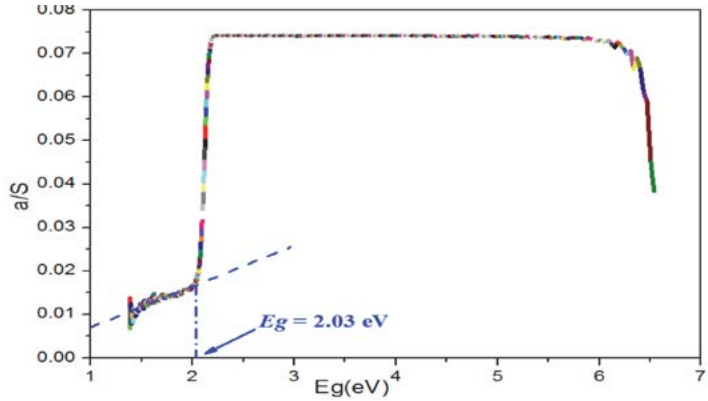

Figure 11. Solid-state UV/Vis diffuse reflectance spectrum of the title complex.

Supplementary Materials

Crystallographic data for the structural analysis have been deposited with the Cambridge Crystallographic Data Center, CCDC **No. 2190846**. Copies of this information can be obtained free of charge from the Director, CCDC, 12 Union Road, Cambridge, CBZ, 1 EZ, UK (fax: +44-1223-336033); email: deposit@ccdc.cam.ac.uk or online at http://www.ccdc.cam.ac.uk.

Acknowledgements

The National Natural Science Foundation of China (22168018), the Natural Science Foundation of Jiangxi Province of China (20232BAB203048, 20202BABL203003), the Science and Technology Plan Project of Ji'an (20211-025317).

Data Availability

Data Availability CCDC **2190846** contain the supplementary crystallographic data for the title complex. The data can be obtained free of charge from the Cambridge Crystallographic Data Centre via www.ccdc.com.ac.uk/structures.

Declarations

Conflict of interest on behalf of all authors, the corresponding author states that there is no conflict of interest.

5. References

1. P. Xu, J. Li, J. H. Huang, F. Yu, C. H. Li, Y. X. Zheng, *New J. Chem.* **2021**, *45*, 13168-13174. **DOI:**10.1039/D1NJ02454J
2. S. Chorazy, M. Wyczesany, Sieklucka, *Molecules* **2017**, *22*, 1902. **DOI:**10.3390/molecules22111902
3. Y. Abbas, S. N. Yun, M. S. Javed, J. G. Chen, M. F. Tahir, Z. Q. Wang, et al., *Ceram. Inter.* **2020**, *46*, 4470-4476. **DOI:**10.1016/j.ceramint.2019.10.173
4. A. Quader, G. M. Mustafa, S. K. Abbas, H. Ahmad, S. Atiq, *Chem. Eng. J.* **2020**, *396*, 125198. **DOI:**10.1016/j.cej.2020.125198
5. D. Mahmoud, M. S. EI-Deab, M. E. Elshakre, N. K. Allam, *J. Phys. Chem. C* **2020**, *124*, 7007-7015. **DOI:**10.1021/acs.jpcc.9b12045
6. J. N. Xing, M. Shu, W. Y. Wang, R. Zhang, J. Liu. *Chin. J. Inorg. Chem.* **2021**, *37*, 1847-1852.
7. W. T. Chen. *J. Mol. Struct.* **2020**, *1219*, 128580/1-128580/6. **DOI:**10.1016/j.molstruc.2020.128580
8. W. A. Fu, H. J. Chen, Y. Y. Han, W. Y. Wang, R. Zhang, J. Liu. *New J. Chem.* **2021**, *45*, 19082-19087. **DOI:**10.1039/D1NJ04074J
9. H. Shi, F. F. Zhao, X. H. Chen, S. L. Yang, J. N. Xing, H. J. Chen, et al. *Tetrahedron Lett.* **2019**, *60*, 151330-151334. **DOI:**10.1016/j.tetlet.2019.151330
10. H. J. Chen, G. Y. Lyu, Y. F. Yue, T. W. Wang, D. P. Li, H. Shi, et al. *J. Mat. Chem. C* **2019**, *7*, 7249-7259. **DOI:**10.1039/C9TC01520E
11. J. H. Wei, J. W. Yi, M. L. Han, B. Li, S. Liu, Y. P. Wu, et al. *Chem - Asian J.* **2019**, 14, 3694-3701. **DOI:**10.1002/asia.201900706
12. X. W. Li, N. Ma, G. T. Xu, R. Zhang, J. Liu. *Sol. Energy Mater. Sol. Cells* **2022**, *234*, 111449. **DOI:**10.1016/j.solmat.2021.111449
13. C. Jeffrey, R. B. David, L. Li, L. M. David. *J. Biomed. Opt.* **2019**, *24*, 051409-051420.
14. H. H. Chen, X. G. Yi, C. W. Pan, J. W. Wen, C. Zhang. *Chin. J. Struct. Chem.* **2021**, *4*, 501-506.
15. X. G. Yi, Y. Z. Liu, X. N. Fang, X. Y. Zhou, Y. X. Li. *Chin. J. Struct. Chem.*, **2019**, *38*, 325-330.
16. W. Y. Wang, H. J. Chen, Y. F. Yue, R. Zhang, J. Liu. *Dyes Pigm.* **2021**, *194*, 109615. **DOI:**10.1016/j.dyepig.2021.109615
17. O. V. Dolomanov, L. J. Bourhis, R. J. Gildea. *J. Appl. Crystallogr.* **2009**, *42*, 339-341. **DOI:**10.1107/S0021889808042726
18. G. M. Sheldick. *Acta Crystallogr. A,* **2008**, *64*, 112-122. **DOI:**10.1107/S0108767307043930
19. G. M. Sheldrick. *Acta Crystallogr C,* **2015**, *71*, 3-8. **DOI:**10.1107/S2053273314026370
16. H. R. Rong, X. M. Wang, Y. W. Ma, G. X. Gao, H. Q. Su, L. F. Lai, Q. Liu. *Chin. J. Inorg. Chem.* **2021**, *37*, 206-212.
17. X. G. Yi, F. P. Lai, Y. Y. Yan, C. Zhang, W. P. Li. *J. Chem. Res.* **2021**, *45*, 295-304. **DOI:**10.1177/1747519820948363
18. Y. N. Wang, S. D. Wang, K. Z. Cao, G. D. Zou. *J. Photochem. Photobiol., A* **2021**, *411*, 113204. **DOI:**10.1016/j.jphotochem.2021.113204
19. X. N. Fang, X. G. Yi, Z. Q. Yi, J. Y. Chen, Y. X. Li. *Chin. J. Inorg. Chem.* **2019**, *35*, 930-936.
20. K. Lou, F. H. Zu, J. J. Yi, C. M. Cui. *Organometallics* **2021**, 40, 4092-4097. **DOI:**10.1021/acs.organomet.1c00501
21. T. F. Jenkins, S. Bekoe, J. W. Ziller, F. Furche, W. J. Evans. *Organometallics* 2021, 40, 3917-3925. **DOI:**10.1021/acs.organomet.1c00482
22. C. H. Li, Y. F. Kuang, W. Li, Y. L. Li. *Chin. J. Struct. Chem.* 2020, *39*, 2016-2020.
23. W. B. Fan, Y. R. Jiang, T. Xu, Z. Li, L. J. Chen. *Mater. Rep. B* **2015**, 29, 15-20.
24. Y. Zhu, H. F. Jiu, B. J. Gao, H. L. Zuo. *J. North Univ. China, Nat. Sci. Ed.* **2008**, 29, 347-351. **DOI:**10.1007/s11741-008-0412-4
25. W. S. Lin, H. M. Kuang, H. Luo, W. T. Chen. *Chin. J. Struct. Chem.* **2019**, 38, 1012-1020.
26. S. K. Loyalka, C. A. Riggs. *Appl. Spectrosc.* **1995**, *49*, 1107-1110. **DOI:**10.1366/0003702953964976
27. C. Lee, W. Yang, R. G. Parr. *Phys. Rev. B* **1988**, *37*, 785-789. **DOI:**10.1103/PhysRevB.37.785

28. W. Bensch, P. Dürichen, O. Helmer, A. Reller, U. Sazama. *Inorg. Chim. Acta* **1996**, *252*, 47-53.
DOI:10.1016/S0020-1693(96)05297-8

Povzetek

S hidrotermalno reakcijo smo sintetizirali nov itrijev kompleks $[Y(HIA)_3(H_2O)_2]_n \cdot nYCl_3$ (HIA = izonikotinska kislina) in ga karakterizirali z monokristalno rentgensko difrakcijo. Spojina ima enodimenzionalno (1-*D*) verižno strukturo. Fotoluminiscenčne meritve v trdnem stanju kažejo na močan emisijski vrh pri 487 nm, ki ga lahko pripišemo karakterističnemu elektronskemu prehodu v ligandu. Spojina kaže CIE (Commission Internationale de I' Éclairage) kromatske koordinate v modrem področju (0.1049, 0.1221). Meritve UV/Vis v trdnem stanju so pokazale na širino prepovedanega 2.03 eV.

DOI: 10.17344/acsi.2023.8081 *Acta Chim. Slov.* **2023,** *70,* 318–326

Scientific paper

Monte Carlo Optimization Based QSAR Modeling of Angiotensin II Receptor Antagonists

Nemanja Nikolić,[1] Tomislav Kostić,[2,3] Mlađan Golubović,[3,4] Tamara Nikolić,[1] Marija Marinković,[5] Velimir Perić,[4] Sara Mladenović[3] and Aleksandar M. Veselinović[6,*]

[1] *Policlinic "Dr Nikolić", Niš, Serbia.*

[2] *Clinic for Cardiology, Clinical Center Niš, Niš, Serbia.*

[3] *Faculty of Medicine, University of Niš, Niš, Serbia.*

[4] *Department for Cardiac Surgery, Clinic for Anaesthesiology and Intensive Therapy, Clinical Center Niš, Niš, Serbia.*

[5] *Clinic for Pulmology, Clinical Center Niš, Niš, Serbia*

[6] *Departmant of Chemistry, Faculty of Medicine, University of Nis, Nis, Serbia*

* *Corresponding author: E-mail: aveselinovic@medfak.ni.ac.rs*
Fax: +381 18 4238770; Phone: +381 18 4570029

Received: 02-16-2023

Abstract

The pathogenesis of essential hypertension, congestive heart failure, and reno-vascular hypertension is related to angiotensin II. This study presents QSAR modeling for a set of compounds acting as angiotensin II receptor antagonists based on the Monte Carlo optimization with molecular graph-based and SMILES notation based descriptors. Conformation independent QSAR models were developed for three random splits. Various statistical approaches were used to assess the statistical quality of the developed models, and the obtained results were very good. This study used a novel statistical metric known as the index of ideality of correlation for the final assessment of the model, and the results that were obtained suggested that the model was good. Also, molecular fragments which account for the increases and/or decreases of a studied activity were defined and then used for the computer-aided design of new compounds as potential angiotensin II receptor antagonists. The final assessment of the designed inhibitors, was performed with the use of molecular docking studies, highlighting exceptional correlation with the QSAR modeling results. The methodology which is presented in this research can be applied for seeking new agents for cardiovascular disorders treatment by angiotensin II receptor antagonism.

Keywords: Angiotensin II receptor antagonists; hypertension; QSAR; Molecular modeling; Drug design

1. Introduction

The pathogenesis of essential hypertension, congestive heart failure, and reno-vascular hypertension is related to angiotensin II associated with renin-angiotensin system (RAS), because (RAS) has important role in the regulation of cardiovascular homeostasis and electrolyte/fluid balance in both normotensive and hypertensive subjects.[1–3] This effect of angiotensin II could be associated with the mediation through selective membrane bound angiotensin II receptors type 1 (AT1) and type 2 (AT2) and this feature can be used for the treatment of above stated conditions with the application of of angiotensin-converting enzyme (ACE) inhibitors. RAS a major target for drug discovery programs in the pharmaceutical industry was established after clinical success of ACE inhibitors as therapeutics used for the treatment of hypertension and congestive heart failure.[4–6] Unfortunately the application of ACE inhibitors leads to occasional side effects, like angioneurotic edema and dry cough.[7–9] These side effects are related to the increase of bradykinin and substance P concentration, caused by the inhibition of

these peptides degradation.[10,11] To overcome this issue the alternative route has been suggested that will have the direct mode of intervening in the RAS with minimal potential side effect based on inhibition of the interactions of the primary effector hormone angiotensin II at the receptor level.[12–14] In light of the given facts, there is still a need to develop a reliable QSAR model for angiotensin II receptor antagonism that can be used to develop therapeutics for the treatment of hypertension and congestive heart failure.

A Monte Carlo optimization method in which the studied activity is treated as a random event has emerged as a promising approach in QSAR modeling in recent years. This method is based on the conformation-independent approach with optimal descriptors based on topological molecular features and molecules in the Simplified Molecular Input Line Entry System (SMILES) notation.[15–17] One of the primary advantages of the described method over more commonly used ones is its simplicity and efficiency. Also, this method can determine molecular fragments (calculated as SMILES notation descriptors) that have an influence on studied activity and that can be associated with the chemical structures of studied compounds. The main aim of this research is the development of a conformation-independent QSAR model based on the Monte Carlo optimization method for the angiotensin II receptor antagonism. Further, one of the main aims of this research was to define SMILES notation descriptors associated with molecular fragments that have both positive and negative influences on angiotensin II receptor antagonism. Molecular docking studies were used as the "final validator" of the established QSAR models and designed molecules antagonism potential

2. Materials and Methods

2. 1. Development and Validation of QSAR Models

As the first step in developing appropriate QSAR models, molecules obtained from literaturewere drawn using ACD/ChemSketch software v.11.0 and converted into the SMILES notation using the same software.[18,19] Chemical structures of compounds used for QSAR modeling with their SMILES notation are presented in Supporting Information and their general structures in Figure 1.

As the dependent variable for the development of the QSAR model, we used the inhibitor activities rabbit uterine membrane AT1 (IC_{50}) converted to -log10(IC_{50}) and given as pIC_{50} and this numerical values are presented in Table S1, Supplementary material. After we finished constructing the appropriate database, we made three different random splits of the main molecule database into two sets-the training set, which included 56 compounds (75%), and the test set with 19 compounds (25%), and we checked the normality of the activity distribution according to published method.[20] To establish conformation-independent QSAR models we applied software called CORAL (CORrelation and Logic, http://www.insilico.eu/coral) based on the Monte Carlo method and its algorithm, which treats the pertinent activity as a random event. We took into consideration two types of molecular descriptors based on the molecular graph and SMILES notation. Based on molecular graphs, invariants were defined as local graph invariants: Morgan extended connectivity index of increasing order (EC0), path numbers of length 2 and 3 (p2, p3), valence shells of range 2 and 3 (s2, s3), and the Code of Nearest Neighbors (NNCk). In recent years, Simplified Molecular Input-Line Entry System (SMILES) notation has become one of the most convenient representations, especially used in chemoinformatics because SMILES notation is considered as a very convenient alternative to the molecular graph. This fact is very appealing for medicinal chemistry since correlating molecular fragments with molecular graph-based descriptors can be quite challenging. For QSAR modeling, SMILES notation can be used to define molecular optimal descriptors (DCW), where DCW can be calculated as a function of SMILES notation according to Equation 1.

$$DCW(T,N_{epoch}) = \Sigma CW(S_k) + \Sigma CW(SS_k) + \Sigma CW(SSS_k) + \Sigma CW(EC0_k) + \Sigma CW(PT2_k) + \Sigma CW(PT3_k) + \Sigma CW(VS2_k) + \Sigma CW(VS3_k) + \Sigma CW(NNC_k) \quad (1)$$

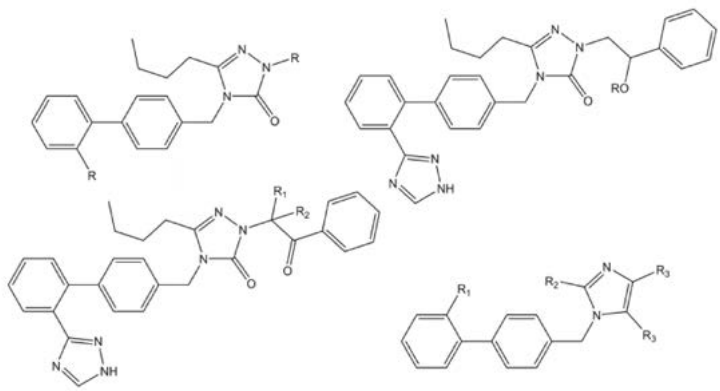

Figure 1. General chemical structures of molecules used for QSAR models development.

In this research, we used all SMILES notation based descriptors: local, global, and HARD-index. One of the main features of the developed QSAR model with the application of the Monte Carlo method is that we calculate correlation weight (CW), a numerical value for each used optimal descriptor.[17] The manner in which this process is achieved is based on generating suitable random numbers and observing how that fraction of numbers obeys some property or properties, in which CW values are randomly assigned to all used optimal descriptors, both molecular graph and SMILES notation based descriptors, in each independent Monte Carlo run. The Monte Carlo optimization process is applied further to calculate the numerical data for the correlation weights, which give the maximal value of the correlation coefficient between studied activity and used optimal descriptors. For this purpose, the Monte Carlo method uses two parameters: threshold (T) and the number of epochs (N_{epoch}). For the development of QSAR models, we used values of 0–10 for T and 0–70 for Nepoch, from which the search for the most predictive combination of T and N_{epoch} was concluded according to published methodology.[15–27] The development of a robust model capable of predicting the properties of new molecules in an objective, reliable, and precise manner is the main goal of any QSAR modeling process. We used the following methods to determine the goodness of the established QSAR models: internal validation using the training set, external validation using the validation set, and data randomization (Y-scrambling test). This was done by using statistical parameters such as the correlation coefficient (r^2), cross-validated correlation coefficient (q^2), standard error of estimation (s), mean absolute error (MAE), Fischer ratio (F), root-mean-square error (RMSE), R_m^2, and MAE-based metrics.[20–25] Recently, the so-called Index of Ideality of Correlation (IIC) has been suggested as a novel criterion for the estimation of the predictive potential of QSAR models, considering not only the correlation coefficient but also the arrangement of the cluster of dots-images relative to the diagonal, in coordinates observed-calculated values of the studied endpoint, and we calculated IIC according to Equations 2–5 as the QSAR model final estimator.[25–27]

$$\Delta_k = observed_k - calculated_k \quad (2)$$

Having data on all Δ_k for the test set, one can calculate sum of negative and positive values of Δ_k similar to mean absolute error (MAE):

$$^{-}MAE_{test} = \frac{1}{^{-}N}\sum_{k=1}^{^{-}N}|\Delta_k| \quad \Delta_k < 0,\ ^{-}N \text{ is the number of } \Delta_k < 0 \quad (3)$$

$$^{+}MAE_{test} = \frac{1}{^{+}N}\sum_{k=1}^{^{+}N}|\Delta_k| \quad \Delta_k \geq 0,\ ^{+}N \text{ is the number of } \Delta_k \geq 0 \quad (4)$$

$$IIC_{test} = r_{test} \times \frac{min(^{-}MAE_{test}, ^{+}MAE_{test})}{max(^{-}MAE_{test}, ^{+}MAE_{test})} \quad (5)$$

2. 2. Molecular Docking Studies

Molegro Virtual Docker (MVD) software was used for docking studies with geometrically optimized ligands using MMFF94 force field implemented in Marvin sketch (Marvin 6.1.0, 2013, ChemAxon) software. As the target for docking studies crystal structure of the angiotensin II type 2 receptoror (AT2R) (PDB: 7jni) was used. For, MVD rigid receptor structure and flexible structure for ligands was used for prerfoming docking studies. MVD yields both hydrophobic (mostly related to steric and Van der Waals interactions) and hydrophilic interactions, including identification of hydrogen bonds between amino acids from the active site and studied ligands. These interactions can be quantified through "scoring" functions, calculated numerical values related to relevant binding energies.[28] For most enzymes there is rule of thumb, the higher the interaction between receptor and ligand is the higher inhibition is achieved, so for this reason obtained numerical values for "scoring" functions could be used to assess the potential inhibition effect of studied ligands[29]. In this research following "scoring" functions were calculated and used further for inhibitory potential estimation: VdW, Steric, Hbond, NoHbond, Pose energy, Electro, ElectroLong, MolDock, and Rerank Score, and complete molecular docking protocol was validated according to published methodology.[31,32] Maestro Version 11.1.012, release 2017-1 was used for showing two-dimensional representations of the interactions between the studied molecules and the amino acids angiotensin II type 2 receptoror active site.

3. Results and Discussion

The applicability domain (AD) is a fundamental characteristic based on which the selection of molecules is done.[32–34] For defining AD we apply published methodology and we determined that all molecules in this study were within the range of AD defined and we did not identify any outliers[17]. Using the Least Squares method, the best developed QSAR models for the studied activity, regarding T and N_{epoch} values, are presented in the form of Eq. 6–8.

$$\text{Split 1: } pIC_{50} = 1.9668(\pm 0.0410) + 0.0580(\pm 0.0004)\times DCW(4,11) \quad (6)$$

$$\text{Split 2: } pIC_{50} = 2.0290(\pm 0.0447) + 0.1134(\pm 0.0009)\times DCW(4,12) \quad (7)$$

Table 1. The statistical quality of the developed QSAR models for angiotensin II receptor antagonism

		Training set						Test set					
		r^2	q^2	CCC	IIC	s	MAE	F	r^2	q^2	CCC	IIC	s	MAE	F
Split 1	1 run	0.8046	0.8917	0.7774	0.7902	0.388	0.294	222	0.8421	0.9104	0.9175	0.7842	0.402	0.315	91
	2 run	0.8145	0.8978	0.7278	0.8012	0.378	0.284	237	0.8755	0.9176	0.9347	0.8292	0.375	0.281	119
	3 run	0.8234	0.9032	0.8449	0.8119	0.368	0.288	252	0.8909	0.9217	0.9438	0.8551	0.362	0.268	139
	Av	0.8142	0.8976	0.7834	0.8011	0.378	0.289	237	0.8695	0.9166	0.9320	0.8228	0.380	0.288	116
Split 2	1 run	0.8878	0.9406	0.8773	0.8775	0.292	0.230	427	0.8029	0.8940	0.8960	0.7551	0.450	0.352	69
	2 run	0.8688	0.9298	0.8678	0.8593	0.315	0.239	358	0.8200	0.9036	0.9055	0.7752	0.450	0.362	77
	3 run	0.8951	0.9446	0.9461	0.8852	0.282	0.216	461	0.8231	0.9020	0.9072	0.7742	0.424	0.359	79
	Av	0.8839	0.9383	0.8971	0.8740	0.296	0.228	415	0.8153	0.9000	0.9029	0.7682	0.441	0.358	75
Split 3	1 run	0.8485	0.9180	0.8576	0.8353	0.360	0.297	302	0.8813	0.9046	0.9382	0.8558	0.335	0.283	126
	2 run	0.8814	0.9369	0.8136	0.8712	0.319	0.259	401	0.8465	0.8784	0.9189	0.8158	0.375	0.290	94
	3 run	0.8417	0.9140	0.9174	0.8290	0.368	0.300	287	0.8578	0.8896	0.9254	0.8297	0.360	0.288	103
	Av	0.8572	0.9230	0.8629	0.8452	0.349	0.285	330	0.8620	0.8909	0.9275	0.8338	0.357	0.287	108

r^2 – Correlation coefficient q^2 – Cross-validated correlation coefficient CCC – Concordance correlation coefficient IIC – Index of ideality of correlation s – Standard error of estimation
MAE – Mean absolute error F – Fischer ratio Av – Average value for statistical parameters obtained from three independent Monte Carlo optimization runs

Split 3: $pIC_{50} = 2.1274(\pm 0.0486) + 0.0659(\pm 0.0006) \times DCW(1,7)$ (8)

The values of the statistical metrics that helped us to determine the quality of the developed QSAR models for angiotensin II antagonism are available in Table 1. They indicate that the applied method was capable of establishing a QSAR model with good reproducibility, which we tested using the concordance correlation coefficient. We evaluated the predictability of the developed QSAR model using values presented in Table 1, and the developed model was proved valid. In addition, the model was classified as valid using MAE-based metrics. We performed the final evaluation of the developed QSAR models both for the training and the test set using the index of ideality of correlation and obtained values that suggest that developed QSAR models have a high predictive potential. Further, we applied Y-randomization, which implied scrambling of Y values in 1000 trials in ten separate runs, to assess the sturdiness of the developed QSAR models.[20] The obtained values presented in Table 2 indicate that there was no correlation by chance among the developed models. In regards to obtained values for statistical methods, we obtained the best QSAR model from the first split.

Table 2. Y-randomization of the best QSAR models (best optimization run) for three independent splits

	Split 1		Split 2		Split 3	
	Training	Test	Training	Test	Training	Test
0	0.8234	0.8909	0.8951	0.8231	0.8485	0.8813
1	0.0054	0.0403	0.0025	0.06	0.0822	0.0027
2	0.0849	0	0.0002	0.0066	0.0027	0.0496
3	0.0005	0.0001	0.0027	0.0009	0.0054	0
4	0.0004	0.0031	0.0681	0.0193	0.0054	0.0725
5	0.0059	0.0299	0.0146	0.081	0.0424	0.0866
6	0.0347	0.0086	0.0013	0.099	0.0027	0.0041
7	0.0068	0.013	0.0065	0.1115	0.0033	0.0056
8	0.0145	0.0756	0.0076	0.0792	0.0596	0.0048
9	0.0002	0.0128	0.0048	0.1635	0.0213	0.0021
10	0.0003	0.0141	0.0182	0.0039	0.0004	0.0255
R_r^2	0.0154	0.0198	0.0127	0.0625	0.0225	0.0254
$^{C}R_p^2$	0.8157	0.881	0.8887	0.7912	0.8371	0.8685

$^{C}R_p^2 = R \times (R^2 - R_r^2)^{1/2}$ should be > 0.5

Also, we observed that the best model was obtained with a T value of 4, whereas the best N_{epoch} value amounted to 11. The best Monte Carlo optimization runs (the highest value for r^2) for the developed QSAR models for all splits are shown in Figure 2 in the form of graphical representations.

Determining molecular fragments, defined as the SMILES notation optimal descriptors having a positive and negative influence on the examined activity, was

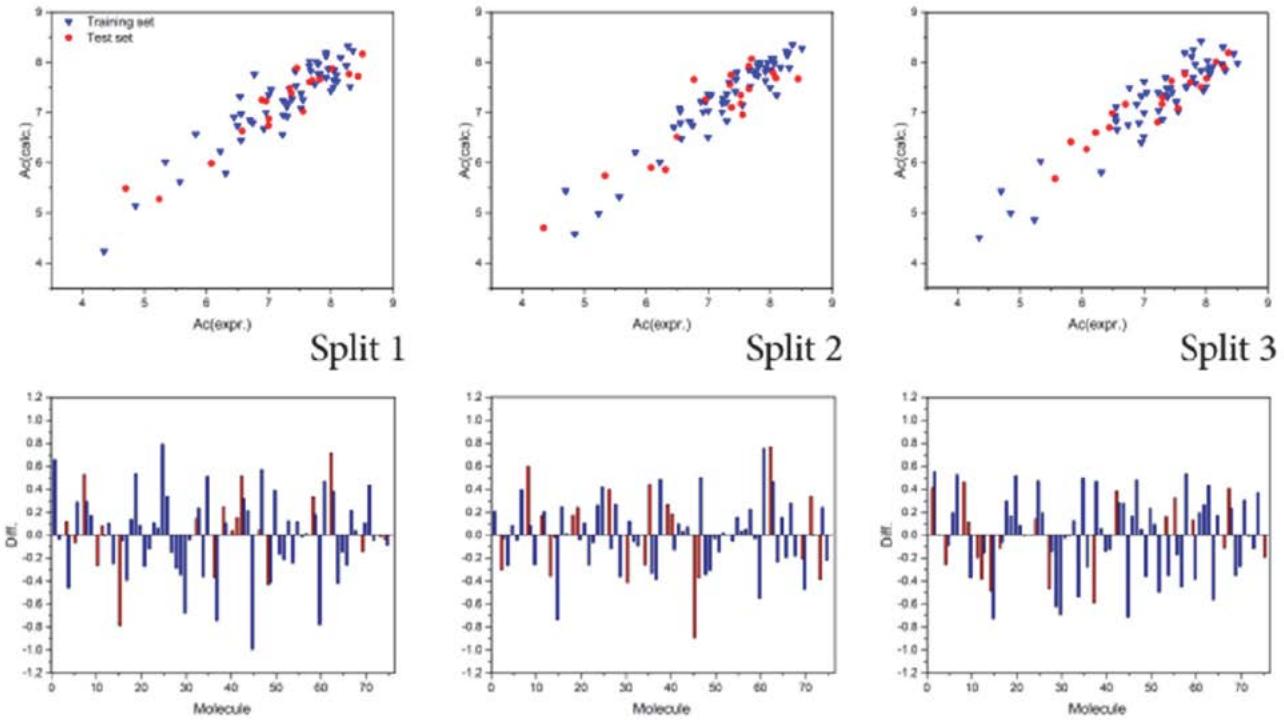

Figure 2. Graphical presentation of the best Monte Carlo optimization runs (the highest value for r^2) for the developed QSAR models.

among the main goals of this research.[17,29,35–38] Table S2 (Supplementary Material) contains the full list of molecular descriptors, which are based both on the SMILES notation and the molecular graph. The calculation example of molecule's both summarized correlation weight (DCW) and studied activity (pED_{50}) is presented in Table 3, where molecular graph-based descriptors were omitted with the aim of achieving an easier interpretation.

According to the published methodology we classified obtained SA_Ks as promoters of angiotensin II receptor antagonism.[17,31,32–35] In Table 4 we enlisted selected SA_Ks with their mechanistic interpretation while the complete list is given in Table S2 (Supporting Information). We presented the analysis of molecular fragments' contribution to angiotensin II receptor antagonism in Figure 3. In presented Figure, green color indicate groups that have positive, while red color indicate groups that have negative influence on corneal permeability. As already stated each SA_K contributes with its CW value.

The computer-aided design of five new potential antagonists whose structures presented in Figure 4 was generated from the conformational-independent results obtained from developed QSAR models. The template molecule was molecule **A**, a molecule taken from initial data base, since it is one of the least chemically exploited molecules. Table 4 contains the list of all the designed molecules, as well as their calculated values for the pIC_{50}.

Based on the obtained results from QSAR modelling, the SMILES notation descriptors associated with molecular fragments with a positive impact on pIC_{50} for angiotensin II receptor antagonism activity and that yield increase in its activity are: "C....." – carbon atom or a methyl group, and "O....." – oxygen atom or a hydroxyl group, where both fragments with positive impact on pIC_{50} numerical value and whose addition lead to the increase of calculated pIC_{50} values for molecule **A1** in comparison to calculated pEC_{50} values for template molecule **A**; also molecule **A1** had additional fragments related to molecular branching – "(....." and "(...C....." both promoters of pIC_{50} increase; further molecular branching was obtained with molecule **A2** with further addition of "C.....", "(....." and "(...C....." fragments that lead to further increase of pIC_{50} numerical value. In molecules **A3** and **A4** oxygen atom was changed with nitrogen atom

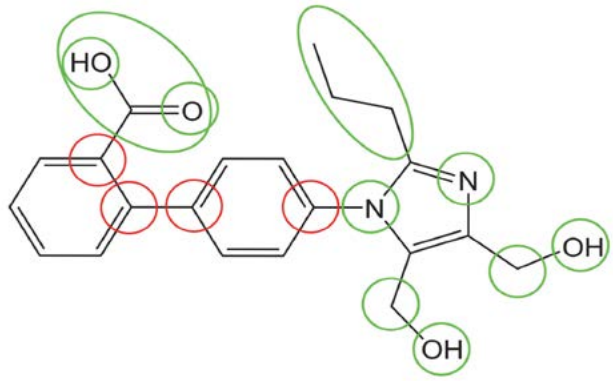

Figure 3. Molecular fragments contribution to angiotensin II receptor antagonism (green – increase, red – decrease).

Table 3. Example of DCW calculation

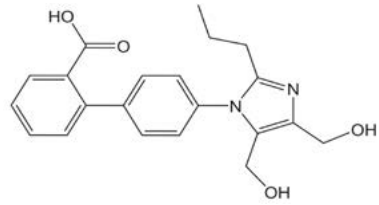

SMILES notation: O=C(O)c1ccccc1c1ccc(cc1)n1c(CO)c(nc1CCC)CO
DCW: 63.10893
Ac(calc.): 5.6237

O.....	0.3453	c.....	−0.0995	c...(.....	0.3361	c...c...(...	−0.8827
=.....	0.1241	1.....	0.2002	C...(.....	2.0522	c...c...1...	0.1897
C.....	0.905	C.....	0.905	O...C.....	−0.6716	c...1...(...	0.1978
(.....	−0.9914	C.....	0.905	O...(.....	1.0042	n...(...1...	0.4829
O.....	0.3453	C.....	0.905	c...(.....	0.3361	1...n...(...	0.9117
(.....	−0.9914	(.....	−0.9914	c...(.....	0.3361	n...1...c...	0.2376
c.....	−0.0995	C.....	0.905	n...(.....	0.1064	1...c...(...	−1.0596
1.....	0.2002	O.....	0.3453	n...c.....	0.2222	c...(...C...	0.6814
c.....	−0.0995	O...=.....	−0.2385	c...1.....	−0.927	O...C...(...	0.3324
c.....	−0.0995	C...=.....	−1.4962	C...1.....	0.4536	C...O...(...	−0.5291
c.....	−0.0995	C...(.....	2.0522	C...C.....	0.2526	c...(...O...	−0.2309
c.....	−0.0995	O...(.....	1.0042	C...C.....	0.2526	(...c...(...	0.3821
c.....	−0.0995	O...(.....	1.0042	C...(.....	2.0522	n...(...c...	−6.9698
1.....	0.2002	c...(.....	0.3361	C...(.....	2.0522	c...n...(...	1.5402
c.....	−0.0995	c...1.....	−0.927	O...C.....	−0.6716	n...c...1...	−0.0889
1.....	0.2002	c...1.....	−0.927	O...=...C...	0.4779	c...1...C...	0.1189
c.....	−0.0995	c...c.....	−0.2115	=...C...(...	−0.5437	C...C...1...	−0.6848
c.....	−0.0995	c...c.....	−0.2115	O...(...C...	0.4236	C...C...C...	−0.5269
c.....	−0.0995	c...c.....	−0.2115	(...O...(...	0.1847	C...C...(...	0.3714
(.....	−0.9914	c...c.....	−0.2115	c...(...O...	−0.2309	C...(...C...	0.3742
c.....	−0.0995	c...1.....	−0.927	1...c...(...	−1.0596	O...C...(...	0.3324
c.....	−0.0995	c...1.....	−0.927	c...1...c...	0.1224	Cmax.1.....	−0.4456
1.....	0.2002	c...1.....	−0.927	c...c...1...	0.1897	Nmax.0.....	0.3887
(.....	−0.9914	c...1.....	−0.927	c...c...c...	−0.5425	Omax.4.....	−0.2055
n.....	0.171	c...c.....	−0.2115	c...c...c...	−0.5425	Smax.0.....	2.5295
1.....	0.2002	c...c.....	−0.2115	c...c...c...	−0.5425	NOSP01000000	0.3921
c.....	−0.0995	c...(.....	0.3361	c...c...1...	0.1897	HALO00000000	−5.5836
(.....	−0.9914	c...(.....	0.3361	c...1...c...	0.1224	BOND10000000	1.7716
C.....	0.905	c...c.....	−0.2115	1...c...1...	0.0916	++++N---O===	9.883
O.....	0.3453	c...1.....	−0.927	c...1...c...	0.1224	++++O---B2==	1.4457
(.....	−0.9914	1...(.....	−1.147	c...c...1...	0.1897	++++N---B2==	1.2326
c.....	−0.0995	n...(.....	0.1064	c...c...c...	−0.5425	10001000000	0.2082
(.....	−0.9914	n...1.....	−0.0595	c...c...(...	−0.8827		
n.....	0.171	c...1.....	−0.927	c...(...c...	1.4185		

leading to switching of "O....." and "(...O....." fragments with "N....." and "(...N....." both with pIC_{50} numerical value increase feature. Both molecules **A3** and **A4** have higher value for pIC_{50} in comparison to molecule A pIC_{50} numerical value. Since fragments "O....." and "(...O....." have higher numerical values for CW in comparison to "N....." and "(...N....." CW numerical values, calculated values for molecules **A1** and **A2** pIC_{50} were higher in comparison to molecules **A3** and **A4** pIC50 values. Molecule **A5** has additional "O...C...(...", "O...=...C...", "O...C....." fragments, all promoters of pIC_{50} increase, in comparison to molecule **A**, leading to pIC_{50} numerical value increase.

To assess the developed QSAR models' predictability and to validate them further, all designed molecules and template molecule A were subjected to molecular docking studies with angiotensin II type 2 receptoror. Numerical values for all calculated "scoring" functions are presented in Table 6. When the assessment of the inhibitory potency is made different scoring functions should be taken into consideration, since they are related to different ligand-amino acids interactions. According to obtained re-

Table 4. Mechanistic interpretation of selected SA_Ks

SA_k	Increase
C.....	Carbon atom
N.....	Nitrogen atom
O.....	Oxygen atom
(...(..... (..... (...C...(... (...N...(... N...(..... (...O...(... C...(...C...	Branching in molecule as such, branching in molecule on either carbon, nitrogen or oxygen atom
O...C...(... O...=...C... O...C.....	Fragments associated with carboxyl group
	Decrease
1..... 2..... C...(...1...	Presence of one or two rings in molecule
O...=.....	Oxygen atom with double bond
c...(.....	Branching on benzyl group

sults for MolDock and ReRank "score" functions molecule with the potentially highest inhibitory activity is molecule A2 and this result is in correlation with the results from QSAR modeling. The molecule with the lowest values for MolDock and ReRank "score" functions was template molecule A, which is also in good correlation with the results obtained from QSAR modeling. The detailed definitions of other "scoring" functions and their potential impact on inhibitory activity can be found in the literature[27].

Highest energy related to close electrostatic interactions, calculated with Electro "scoring" function, is indentified for molecules M2 and lowest for molecule M5. Further, both highest and lowest energies related to long electrostatic interactions, calculated with ElectroLong "scoring" function, were identified for same molecules as for Electro "scoring" function. Highest energy related to hydrogen bonds is indentified for molecules A4 and lowest for molecule A5. Also same molecules had the highest and lowest energy related to the hydrogen bonding energy (protein-ligand) as calculated if the directionality of the hydrogen bond was not taken into account calculated with NoHBond90 "scoring" function. Highest energy related to steric interactions, calculated with Steric "scoring" function, is indentified for molecules A1 and lowest for molecule A. For Van der Walls energies the highest values was calculated, with application of VdW "scoring" function, for molecule A4, and lowest for molecule A4. Highest energy from overall interactions between ligand and receptor, calculated with Energy "scoring" function, was obtained for molecule A2 and lowest for molecule A.

All interactions between the selected molecules and amino acids from angiotensin II type 2 receptoror active site are identified and 2D representation of hydrogen bonds, hydrophobic, and hydrophilic interactions inside the binding pocket are presented in Figures in the Supplementary Information section, while the best-calculated poses for all designed molecules inside the active site of angiotensin II type 2 receptoror are presented in Figure 5. According to obtained results there are two clusters of molecules inside angiotensin II type 2 receptoror active site. Molecules A, A2, A4 and A5 (cluster 1) were docked in one part of active site, while molecules A1 and A3 (cluster 2) in other. Molecules from cluster 1 had hydrogen bonds with amino acids ARG182, LYS215

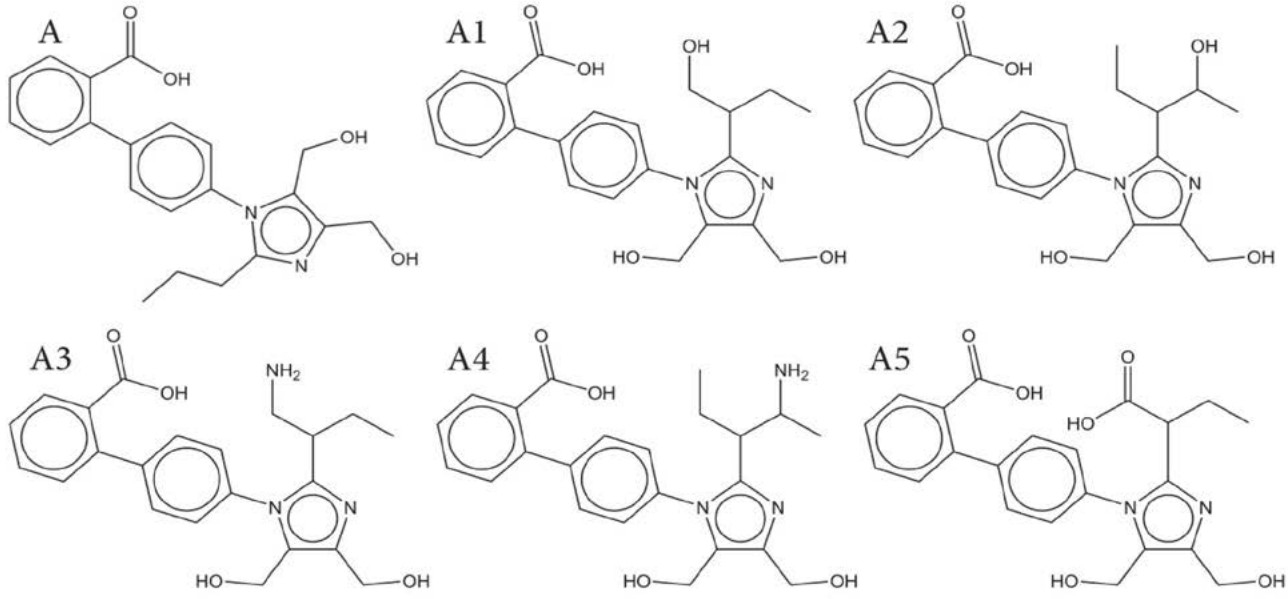

Figure 4. Chemical structures of designed molecules.

Table 5. The list of all designed molecules with their SMILES notation and calculated activities

Molecule	SMILES Notation	Ac(calc.)
A	O=C(O)c1ccccc1c1ccc(cc1)n1c(CO)c(nc1CCC)CO	5.6237
A1	O=C(O)c1ccccc1c1ccc(cc1)n1c(CO)c(nc1C(CC)CO)CO	6.2100
A2	O=C(O)c1ccccc1c1ccc(cc1)n1c(CO)c(nc1C(CC)C(C)O)CO	6.7472
A3	O=C(O)c1ccccc1c1ccc(cc1)n1c(CO)c(nc1C(CC)CN)CO	6.1397
A4	O=C(O)c1ccccc1c1ccc(cc1)n1c(CO)c(nc1C(CC)C(C)N)CO	6.5279
A5	O=C(O)c1ccccc1c1ccc(cc1)n1c(CO)c(nc1C(CC)C(=O)O)CO	6.4697

Table 6. Score values (kcal/mol) for all computer-aided designed compounds

Molecule	Electro	ElectroLong	Steric	VdW	HBond	NoHBond90	Energy	PoseEnergy	RerankScore
A	−8.03766	−2.77855	−139.592	−45.6996	−9.69917	−9.71146	−151.25	−145.534	−112.478
A1	−1.31333	−1.95883	−154.897	−46.1529	−5	−5.38596	−158.14	−150.184	−123.34
A2	−10.8113	−5.73813	−148.83	−42.3753	−9.10444	−10.3858	−167.669	−157.889	−125.207
A3	−8.75907	−2.86037	−152.509	−41.8093	−7.5	−8.39838	−156.857	−150.872	−121.193
A4	−8.3428	−2.78078	−153.414	−26.587	−11.4747	−11.5507	−157.525	−155.959	−121.392
A5	−1.29674	−1.9214	−152.925	−44.0886	−2.5	−2.5	−156.511	−147.798	−120.706

and ILE304, while molecules from cluster 1 had hydrogen bonds with amino acid PRO301. Also molecules from cluster 2 shown π-π interactions with amino acid TRP100.

4. Conclusion

Developing robust QSAR models for angiotensin II receptor antagonism that possess good predictability, which is determined by utilizing various statistical parameters, represents the main aim of this research. Calculations of the conformation independent models, which were developed in accordance with the optimal descriptors and derived from a local graph and the SMILES notation invariants, were performed by employing the Monte Carlo optimization method. Applying a range of statistical techniques yielded the evaluation of the developed QSAR models' predictive potential and robustness. The high applicability of the developed QSAR models is displayed by the realized numerical values applied to validate the mentioned. The Monte Carlo optimization method successfully determined molecular fragments, used in QSAR modeling as the SMILES notation fragments with a positive and negative effect on angiotensin II receptor antagonism and the mentioned were used for the computer-aided design of novel compounds with higher pIC_{50} values. The final validator of the developed QSAR model and the designed molecules' potential inhibitory effect were the molecular docking studies, and the obtained results show good inter-correlation. In summary, new therapeutics for the treatment of hypertension and congestive heart failure can be sought by applying the methodology presented in this research.

We have no conflict of interest to disclose.

Acknowledgments

This work is supported by the Ministry of Education and Science, the Republic of Serbia and the Faculty of Medicine, University of Niš, Republic of Serbia (Internal project No. 70). The authors would like to thank the Ministry of Education, Science and Technological Development of Republic of Serbia (Grant No: 451-03-68/2022-14/200113) for financial support.

5. References

1. C. M. Ferrario, *J. Cardiovasc. Pharmacol.* **1990**, *15*, 51–55 **DOI:**10.1097/00005344-199000153-00001
2. M. Burnier, *Circulation* **2001**, *103*, 904–912 **DOI:**10.1161/01.CIR.103.6.904
3. M. Burnier, H.R. Brunner, *Lancet* **2003**, *355*, 637–645 **DOI:**10.1016/S0140-6736(99)10365-9
4. V. Agrawal, J. K. Gupta, S.S. Qureshi, V. K. Vishwakarma, *Indian Heart J.* **2016**, *68*, 856–861. **DOI:**10.1016/j.ihj.2016.06.010
5. B. Raymer, D. Ebner, *Expert Opin Ther Pat.* **2015**, *25*, 1175–1190. **DOI:**10.1517/13543776.2015.1061997
6. M. A. Zaman, S. Oparil, D. A. Calhoun, *Nat. Rev. Drug Discov.* **2002**,*1*, 621–636. **DOI:**10.1038/nrd873
7. C. M. Ferrario, A. E. Mullick, *Pharmacol. Res.* **2017,** *125*, 57–71. **DOI:**10.1016/j.phrs.2017.05.020
8. A. Nehme, K. Zibara, *Hypertens. Res.* **2017**, *40*, 903–909. **DOI:**10.1038/hr.2017.65
9. H. Cheng, R.C. Harris, *Expert Opin. Drug Saf.* **2006**, *5*, 631–641. **DOI:**10.1517/14740338.5.5.631

10. R. Igic, R. Behnia, *Curr. Pharm. Des.* **2007**, *13*, 1199–1214. **DOI:**10.2174/138161207780618876
11. D. Regoli, G. E. Plante, F. Gobeil Jr, *Pharmacol. Therapeut.* **2012**, *135*, 94–111. **DOI:**10.1016/j.pharmthera.2012.04.002
12. C. Guang, R. D. Phillips, B. Jiang, F. Milani, *Arch. Cardiovasc. Dis.* **2012**, *105*, 373–385. **DOI:**10.1016/j.acvd.2012.02.010
13. K. Hanif, H. K. Bid, R. Konwar, *Hypertens. Res.* **2010**, *33*, 11–21. **DOI:**10.1038/hr.2009.184
14. J. Kućmierz, W. Frąk, E. Młynarska, B. Franczyk, J. Rysz, *Int. J. Mol. Sci.* **2021**, *22*, 9669. **DOI:**10.3390/ijms22189669
15. M. A. Toropova, I. Jr. Raška, A. A. Toropov, M. Raškova, *Comb. Chem. High T. Scr.* **2016**, *19*, 676–687. **DOI:**10.2174/1386207319666160725145852
16. A. P. Toropova, A. A. Toropov, *Mini-Rev. Med. Chem.* **2018**, *18*, 382–391. **DOI:**10.2174/1389557517666170927154931
17. A. M. Veselinović, J. B. Veselinović, J. V. Živković, G. M. Nikolić, *Curr. Top. Med. Chem.* **2015**, *15*, 1768–1779.
18. M. C. Sharma, *Interdiscip. Sci.* **2016**, *8*, 1–0. **DOI:**10.1007/s12539-016-0176-5
19. A. Parate, S. C. Chaturvedi, *Med. Chem. Res.* **2012**, *21*, 1166–1178. **DOI:**10.1007/s00044-011-9622-4
20. P. K. Ojha, K. Roy, *Chemometr. Intell. Lab.* **2011**, *109*, 146–161. **DOI:**10.1016/j.chemolab.2011.08.007
21. P. K. Ojha, I. Mitra, R. N. Das, K. Roy, *Chemometr. Intell. Lab.* **2011**, *107*, 194–205. **DOI:**10.1016/j.chemolab.2011.03.011
22. P. P. Roy, J. T. Leonard, K. Roy, *Chemometr. Intell. Lab.* **2008**, *90*, 31–42. **DOI:**10.1016/j.chemolab.2007.07.004
23. K. Roy, R. N. Das, P. Ambure, R. B. Aher, *Chemometr. Intell. Lab.* **2016**, *152*, 18–33. **DOI:**10.1016/j.chemolab.2016.01.008
24. L. I. Lin, *Biometrics*, **1989**, *45*, 255–268. **DOI:**10.2307/2532051
25. V. Stoičkov, D. Stojanović, I. Tasić, S. Šarić, D. Radenković, P. Babović, D. Sokolović, A. M. Veselinović, *Struct. Chem.* **2018**, *29*, 441–449. **DOI:**10.1007/s11224-017-1041-9
26. A. A. Toropov, A. P. Toropova, *Mutat. Res.- Gen. Tox. En.* **2017**, *819*, 31–37. **DOI:**10.1016/j.mrgentox.2017.05.008
27. A. M. Veselinović, A. Toropov, A. Toropova, D. Stanković-Đorđević, J. B. Veselinović, *New J. Chem.* **2018**, *42*, 10976–10982. **DOI:**10.1039/C8NJ01034J
28. R. Thomsen, M. H. Christensen, *J. Med. Chem.* 2006, 499, 3315–3321. **DOI:**10.1021/jm051197e
29. M. Zivkovic, M. Zlatanovic, N. Zlatanovic, M. Golubović, A. M. Veselinović, Mini-Rev. *Med. Chem.* 2020, 20, 1389–1402. **DOI:**10.2174/1389557520666200212111428
30. S. A. Amin, N. Adhikari, S. Gayen, T. Jha, *J. Biomol. Struct. Dyn.* 2017, 36, 590–608. **DOI:**10.1080/07391102.2017.1288659
31. S. A. Amin, N. Adhikari, S. Gayen, T. Jha, *J. Biomol. Struct. Dyn.* 2019, 37, 4528–4541. **DOI:**10.1080/07391102.2018.1552895
32. D. Gadaleta, G.F. Mangiatordi, M. Catto, A. Carotti, O. Nicolotti, *IJQSPR*, **2016**, *1*, 45–63. **DOI:**10.4018/IJQSPR.2016010102
33. P. Gramatica, *QSAR Comb. Sci.* **2007**, *26*, 694–701. **DOI:**10.1002/qsar.200610151
34. P. Gramatica, A. Sangion, *J. Chem. Inf. Model.* **2016**, *56*, 1127–1131. **DOI:**10.1021/acs.jcim.6b00088
35. P. Kumar, A. Kumar, J. Sindhu *SAR QSAR Environ. Res.* **2019**, *30*, 525–541. **DOI:**10.1080/1062936X.2019.1629998
36. S. Ahmadi, S. Lotfi, S. Afshari, P. Kumar, E. Ghasemi, *SAR QSAR Environ. Res.* **2021**, *32*, 1013–1031. **DOI:**10.1080/1062936X.2021.2003429
37. S. Ahmadi, S. Lotfi, P. Kumar, *Toxicol. Mech. Methods* **2022**, *32*, 302–312. **DOI:**10.1080/15376516.2021.2000686
38. S. Lotfi, S. Ahmadi, P. Kumar, *RSC Adv.* **2021**, *11*, 33849–33857. **DOI:**10.1039/D1RA06861J

Povzetek

Patogeneza esencialne hipertenzije, kongestivnega srčnega popuščanja in renovaskularne hipertenzije je povezana z angiotenzinom II. Ta študija predstavlja modeliranje QSAR za nabor spojin, ki delujejo kot antagonisti receptorjev angiotenzina II, na podlagi optimizacije Monte Carlo z deskriptorji na osnovi molekularnih grafov in zapisov SMILES. Konformacijsko neodvisni modeli QSAR so bili razviti za tri naključne razdelitve. Za oceno statistične kakovosti razvitih modelov smo uporabili različne statistične pristope, dobljeni rezultati pa so bili zelo dobri. Za končno oceno modela smo uporabili novo statistično metriko, znano kot indeks idealnosti korelacije, in dobljeni rezultati kažejo, da je bil model dober. Prav tako so bili definirani molekularni fragmenti, ki so odgovorni za povečanja in/ali zmanjšanja proučevane aktivnosti, in nato uporabljeni za računalniško podprto načrtovanje novih spojin kot potencialnih antagonistov receptorjev angiotenzina II. Končna ocena načrtovanih zaviralcev je bila izvedena z uporabo študij molekularnega sidranja, ki poudarjajo izjemno visoko stopnjo korelacije z rezultati modeliranja QSAR. Metodologijo, ki je predstavljena v tej raziskavi, je mogoče uporabiti pri iskanju novih učinkovin za zdravljenje srčno-žilnih obolenj z antagonizmom receptorjev angiotenzina II.

Scientific paper

Syntheses, Crystal Structures and Antimicrobial Activity of Copper(II) Complexes with the Ligand *N,N'*-Bis(4-bromosalicylidene)propane-1,2-diamine

Yu-Mei Hao

Department of Chemistry, Baicheng Normal University, Baicheng 137000, P.R. China

** Corresponding author: E-mail: jyxygzb@163.com*

Received: 02-27-2023

Abstract

Two new copper(II) complexes, [CuL] (**1**) and $[Cu_4Cl_2L_2(N_3)_2]\cdot CH_3OH$ (**2**), derived from the bis-Schiff base *N,N'*-bis(4-bromosalicylidene)propane-1,2-diamine (H_2L) have been prepared and characterized by spectroscopy methods, as well as single crystal X-ray determination. The Cu atom in the mononuclear complex **1** is in square planar coordination. The outer and inner Cu atoms in the phenolate and azide co-bridged tetranuclear complex **2** are in square planar and square pyramidal coordination, respectively. The antibacterial activities of the Schiff base and the two copper complexes have been assayed on the bacteria *Staphylococcus aureus* and *Escherichia coli*, and the yeast *Candida parapsilosis*.

Keywords: Schiff base; Copper complex; Crystal structure; Antibacterial

1. Introduction

Schiff bases due to their easy preparation and good metal-binding ability have been widely used as preferred ligands in the construction of complexes with various metal salts.[1] The compounds with N, O, S donor atoms have structure similarities with some natural biological enzymes. Schiff bases and their metal complexes have a broad range of applications in pharmaceutical and biological fields.[2] In the last few years, Schiff bases have been widely known for their remarkable biological activities, such as antifungal, antibacterial, anti-proliferative, antimalarial, antiviral, antipyretic, and anti-inflammatory activities.[3] Copper complexes with Schiff bases have been extensive studied and are considered as excellent alternatives for classic organic antibacterial agents.[4] Despite the presence of considerable research on the antibacterial activities of Schiff base complexes, it is still necessary to search for new samples to find more effective agents as well as to better understand the biological mechanisms of this type of compounds. With an interest in the chemistry of biologically active compounds, this study aimed to synthesize Schiff base and its copper(II) complexes. The newly synthesized complexes, [CuL] (**1**) and $[Cu_4Cl_2L_2(N_3)_2]\cdot CH_3OH$ (**2**), where L is the deprotonated form of *N,N'*-bis(4-bromosalicylidene)propane-1,2-diamine (H_2L; Scheme 1), are presented and examined for their antimicrobial activities.

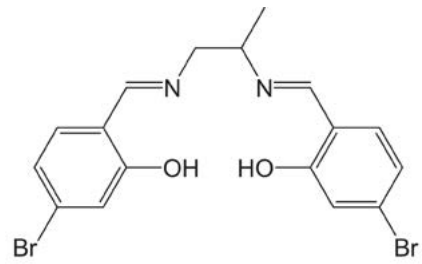

Scheme 1. The Schiff base H_2L

2. Experimental

2. 1. Materials and Methods

4-Bromosalicylaldehyde and 1,2-diaminopropane were purchased from TCI Chemical Reagent Co. Ltd. $CuCl_2\cdot 2H_2O$ and NaN_3 were purchased from Aladdin Chemical Reagent Co. Ltd. The methanol was purchased from Kemiou Chemical Reagent Co. Ltd. IR spectra were recorded on a Jasco FT/IR-4000 spectrometer as KBr pellets in the 4000–400 cm^{-1} region. Elemental analyses were performed on a Perkin-Elmer 240C elemental analyzer. UV-Vis spectra were recorded on a Lambda 900 spectrometer. Single crystal X-ray diffraction was carried out on a Bruker SMART 1000 CCD diffractometer.

Caution! The azide complexes are potentially explosive. Although no problem was encountered in the present study, only small amounts of the materials should be prepared and they must be handled with care.

2. 2. Syntheis of H_2L

4-Bromosalicylaldehyde (0.84 g, 4.0 mmol) was dissolved by methanol (20 mL). Then, it was added dropwise to the methanol solution (30 mL) of 1,2-diaminopropane (0.15 g, 2.0 mmol). The reaction mixture was stirred and heated to reflux for 30 min. The solvent was removed by evaporation under reduced pressure. The yellow solid was recrystallized from ethanol to give yellowish crystalline product. Yield: 0.77 g (87%). IR data (KBr, cm^{-1}): 3434, 1623, 1489, 1374, 1243, 1200, 1133, 1040, 985, 905, 853, 798, 587. UV-Vis λ_{max}/nm (1.2×10^{-5} mol L^{-1}, MeOH; ε, L mol^{-1} cm^{-1}): 225 (25,600), 262 (19,750), 315 (7,150), 400 (2,900). Anal. Calcd. (%) for $C_{17}H_{16}Br_2N_2O_2$: C, 46.39; H, 3.66; N, 6.36. Found (%): C, 46.25; H, 3.73; N, 6.45.

2. 3. Synthesis of [CuL] (1)

H_2L (44 mg, 0.10 mmol) and $CuCl_2{\cdot}2H_2O$ (34 mg, 0.20 mmol) were mixed in methanol (30 mL). The mixture was stirred at room temperature for 30 min to give a brown solution. Single crystals of the complex, suitable for X-ray diffraction, were obtained after 5 days. Yield: 27 mg (54%). IR data (cm^{-1}): 1610, 1512, 1407, 1285, 1190, 1132, 1053, 972, 913, 855, 772, 523, 471. UV-Vis (1.3×10^{-5} mol L^{-1}, MeOH; ε, L mol^{-1} cm^{-1}): 232 (21,780), 250 (20,910), 275 (14,810), 357 (6,100). Anal. Calcd. (%) for $C_{17}H_{14}Br_2CuN_2O_2$: C, 40.70; H, 2.81; N, 5.58. Found (%): C, 40.55; H, 2.87; N, 5.66.

2. 4. Synthesis of $[Cu_4Cl_2L_2(N_3)_2]{\cdot}CH_3OH$ (2)

H_2L (44 mg, 0.10 mmol), $CuCl_2{\cdot}2H_2O$ (34 mg, 0.20 mmol) and NaN_3 (13 mg, 0.20 mmol) were mixed in methanol (30 mL). The mixture was stirred at room temperature for 30 min to give a deep brown solution. Single crystals of the complex, suitable for X-ray diffraction, were obtained after 5 days. Yield: 32 mg (48%). IR data (cm^{-1}): 3421, 2072, 1635, 1585, 1534, 1517, 1470, 1415, 1383, 1282, 1265, 1203, 1133, 1067, 1009, 913, 838, 791, 620, 590, 532, 458. UV-Vis (1.3×10^{-5} mol L^{-1}, MeOH; ε, L mol^{-1} cm^{-1}): 230 (20,540), 250 (18,500), 276 (12,610), 355 (5,050). Anal. Calcd. (%) for $C_{35}H_{33}Br_4Cl_2Cu_4N_{10}O_5$: C, 31.88; H, 2.52; N, 10.62. Found (%): C, 31.72; H, 2.43; N, 10.75.

2. 5. X-ray Crystallography

Single crystal X-ray data for the complexes were collected on a Bruker SMART 1000 CCD diffractometer using the SMART/SAINT software.[5] Intensity data were collected using graphite-monochromatized MoK_α radia-

Table 1. Crystallographic data and refinement parameters for the complexes

	1	**2**
Chemical Formula	$C_{17}H_{14}Br_2CuN_2O_2$	$C_{35}H_{33}Br_4Cl_2Cu_4N_{10}O_5$
Fw	501.66	1318.41
T (K)	298(2)	298(2)
Crystal system	Monoclinic	Orthorhombic
Space group	$P2_1/c$	$Pbca$
a (Å)	11.6858(18)	12.3951(11)
b (Å)	11.4195(17)	16.5472(13)
c (Å)	13.0760(18)	22.3770(15)
α (°)	90	90
β (°)	100.562(2)	90
γ (°)	90	90
V (Å^3)	1715.4(4)	4589.6(6)
Z	4	4
m (Mo Kα) (cm^{-1})	5.944	5.478
D_c (g cm^{-3})	1.942	1.908
Reflections collected	8892	23307
Unique reflections	3181	4256
Observed reflections [I ≥ 2σ(I)]	1964	2466
Parameters	218	283
Restraints	0	0
Goodness of fit on F^2	1.047	1.090
R_{int}	0.0458	0.0782
R_1, wR_2 [$I \geq 2\sigma(I)$]	0.0519, 0.1221	0.0698, 0.1757
R_1, wR_2 (all data)	0.0953, 0.1396	0.1270, 0.2058

tion (0.71073 Å) at 298(2) K. The structures were solved by direct methods using SHELX.[6] Multi-scan absorption corrections were applied with SADABS.[7] All non-hydrogen atoms were refined with anisotropic displacement coefficients. The hydrogen atoms bonded to carbon were included in geometric positions and given thermal parameters equivalent to 1.2 and 1.5 times those of the atom to which they were attached. The anisotropic displacement parameters for atoms C8, C9 and C10 in complex **2** are a little larger than usual, which is caused by the slight disorder of the group. Crystallographic data and refinement parameters are given in Table 1, and important interatomic distances and angles are given in Table 2.

Table 2. Selected bond distances (Å) and angles (°) for the complexes

	1		
C7–N1	1.289(10)	C11–N2	1.279(10)
C8–N1	1.461(10)	C9–N2	1.477(10)
Cu1–O1	1.894(4)	Cu1–O2	1.887(5)
Cu1–N1	1.924(6)	Cu1–N2	1.933(6)
O2–Cu1–O1	88.82(18)	O2–Cu1–N1	174.4(2)
O1–Cu1–N1	93.4(2)	O2–Cu1–N2	93.8(2)
O1–Cu1–N2	176.0(2)	N1–Cu1–N2	84.2(3)
	2		
C7–N1	1.221(14)	C11–N2	1.287(15)
C8–N1	1.531(15)	C9–N2	1.487(16)
Cu1–O1	1.946(6)	Cu1–O2	1.893(6)
Cu1–N1	1.935(9)	Cu1–N2	1.911(10)
Cu2–O1	1.982(5)	Cu2–O2	2.375(6)
Cu2–N3	1.962(7)	Cu2–N3A	2.013(8)
Cu2–Cl1	2.240(3)		
O2–Cu1–N2	95.3(4)	O2–Cu1–N1	175.6(4)
N2–Cu1–N1	85.4(4)	O2–Cu1–O1	85.9(2)
N2–Cu1–O1	172.7(4)	N1–Cu1–O1	92.8(3)
N3–Cu2–O1	165.9(3)	N3–Cu2–N3A	76.5(3)
O1–Cu2–N3A	91.0(3)	N3–Cu2–Cl1	98.1(3)
O1–Cu2–Cl1	95.9(2)	N3A–Cu2–Cl1	155.8(2)
N3–Cu2–O2	104.7(3)	O1–Cu2–O2	73.2(2)
N3A–Cu2–O2	109.7(3)	Cl1–Cu2–O2	94.55(19)

Symmetry code for A: *–x*, 1 – *y*, *–z*.

2. 6. Biological Assay

The antibacterial property of the compounds was evaluated by a macro-dilution method using *Staphylococcus aureus*, *Escherichia coli*, and the yeast *Candida parapsilosis*. The cultures of bacteria and yeasts were incubated under vigorous shaking. The compounds were dissolved in small amount of DMSO. Concentration of the tested compounds ranging from 0.010 to 2.5 mmol L^{-1} for the bacteria and yeasts was used in all experiments. The antibacterial activity was characterized by IC_{50} and MIC values. MIC experiments on subculture dishes were used to assess the minimal microbicidal concentration (MMC). Subcultures were prepared separately in Petri dishes containing competent agar medium and incubated at 30 °C for 48 h. The MMC value was taken as the lowest concentration, which showed no visible growth of microbial colonies in the subculture dishes.

3. Results and Discussion

3. 1. Chemistry

The Schiff base *N,N'*-bis(4-bromosalicylidene)propane-1,2-diamine was prepared by the reaction of 2:1 molar ratio of 4-bromosalicylaldehyde and 1,2-diaminopropane in methanol (Scheme 2). Complex **1** was facile synthesized by the reaction of the Schiff base H_2L with copper chloride in methanol (Scheme 3). Complex **2** was obtained by the reaction of the Schiff base H_2L with copper chloride and sodium azide in methanol (Scheme 3). Single crystals of the complexes were formed by slow evaporation of the solvent at room temperature.

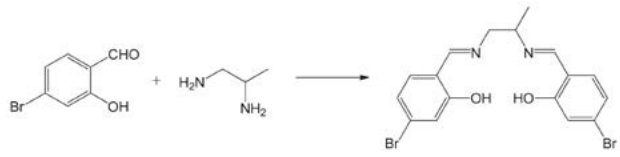

Scheme 2. The synthetic procedure of the Schiff base H_2L

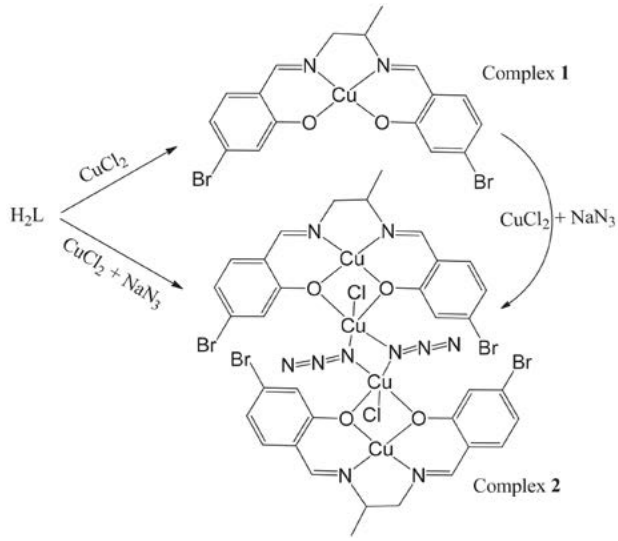

Scheme 3. The synthetic procedure of the complexes

3. 2. Crystal Structure Description of Complex 1

The molecular structure of complex **1** is shown in Fig. 1. The complex is a mononuclear copper(II) species. The Cu atom is coordinated by two imine nitrogen and two phenolate oxygen of the Schiff base ligand, forming

a square planar geometry. The *trans* and *cis* bond angles are 174.4(2)–176.0(2)° and 84.2(3)–93.8(2)°, respectively. Thus, the square planar coordination is slightly distorted, which is mainly caused by the five-membered chelate ring Cu1–N1–C8–C9–N2. The Cu–O and Cu–N bonds are 1.887(5)–1.894(4) Å and 1.924(6)–1.933(6) Å, respectively, which are comparable to those observed in Schiff base copper(II) complexes.[8] The two benzene rings form a dihedral angle of 5.2(5)°.

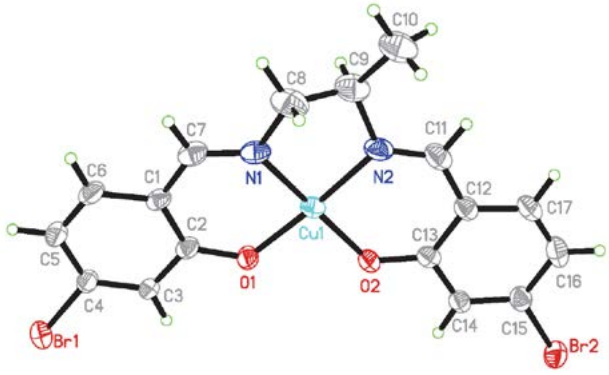

Fig. 1. A perspective view of the molecular structure of complex **1** with the atom labeling scheme. Thermal ellipsoids are drawn at the 30% probability level.

3. 3. Crystal Structure Description of Complex 2

The molecular structure of complex **2** is shown in Fig. 2. The complex is a phenolate and end-on azide co-bridged tetranuclear copper(II) species, with the two [Cu_2ClL] units connected by two bridging azide ligands. Molecule of the complex possesses a crystallographic inversion center symmetry. The phenolate bridged Cu···Cu distance is 3.148(2) Å, and the azide bridged Cu···Cu distance is 3.122(2) Å. The outer Cu atom (Cu1) is coordinated by two imine nitrogen and two phenolate oxygen of the Schiff base ligand, forming a square planar geometry. The *trans* and *cis* bond angles are 172.7(4)–175.6(4)° and 85.4(4)–95.3(4)°, respectively. Thus, the square planar coordination is slightly distorted, which is mainly caused by the strain created by the five-membered chelate ring Cu1–N1–C8–C9–N2. The Cu–O and Cu–N bonds are 1.893(6)–1.946(6) Å and 1.911(10)–1.935(9) Å, respectively, which are comparable to those observed in complex **1** and other Schiff base copper(II) complexes.[9] The inner Cu atom (Cu2) is in a distorted square pyramidal coordination geometry, with the phenolate oxygen (O1), two azide nitrogen (N3 and N3A, symmetry code for A: $-x$, 1 $-y$, $-z$), and one Cl ligand, define the basal plane, and with the other phenolate oxygen (O2) occupies the apical position. The Cu2 atom deviates from the best coordination plane defined by the four basal donor atoms by 0.242(3) Å in direction of the apical donor atom. The *cis* and *trans* bond angles in the basal plane are in the ranges of 76.5(3)–98.1(3)° and 155.8(2)–165.9(3)°, and those among the apical and basal donor atoms are in the range of 73.2(2)–109.7(3)°. Thus, the coordination is distorted from the ideal geometry of a square pyramid. The distortion is mainly caused by the strain created by the four-membered chelate rings Cu1–O1–O2–Cu2 and Cu2–N3–Cu2A–N3A. The bond lengths related to Cu2 atom are 1.982(5)–2.375(6) Å for Cu–O, 1.962(7)–2.013(8) Å for Cu–N and 2.240(3) Å for Cu–Cl, which are comparable to those observed in Schiff base copper(II) complexes with bridging azide ligands.[10] The two benzene rings of the Schiff base ligand form a dihedral angle of 10.4(5)°. The dihedral angle between the two planes formed by the four-membered chelate rings is 69.7(3)°. In the crystal structure, the molecules are linked through intermolecular hydrogen bonds of O–H···Br and intramolecular hydrogen bonds of O–H···Cl, to form a three-dimensional network (Fig. 3).

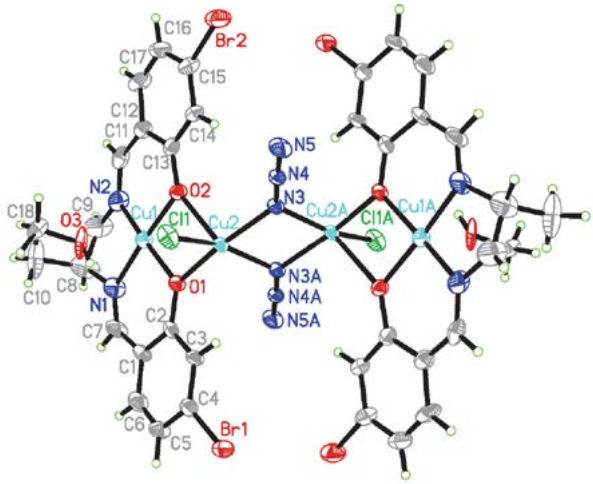

Fig. 2. A perspective view of the molecular structure of complex **2** with the atom labeling scheme. Thermal ellipsoids are drawn at the 30% probability level. Atoms labelled with the suffix A or unlabelled are at the symmetry position $-x$, 1 $-y$, $-z$.

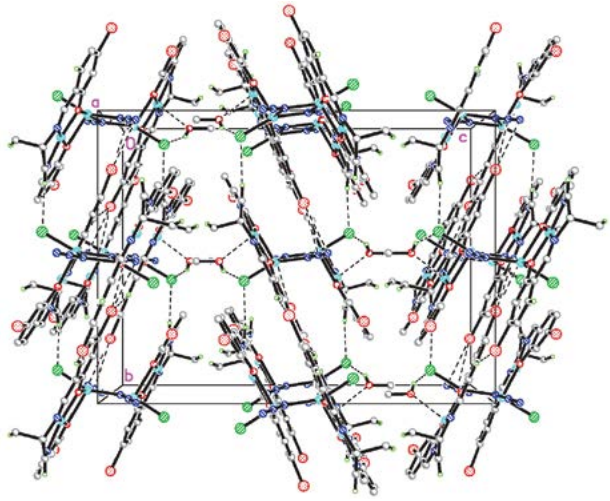

Fig. 3. Molecular packing diagram of complex **2**, viewed along the *a* axis. Hydrogen bonds are shown as dashed lines.

Table 3. Geometrical parameters for hydrogen bonds for complex **2**

D–H···A	Distance, Å		Angle, °	
	D–H	H···A	D···A	D–H···A
O3–H3···Cl1	0.82	2.72	3.208(4)	120(4)
C6–H6···Br1^{i}	0.93	2.87	3.707(4)	150(5)
C10–H10C···N2	0.96	2.61	3.001(4)	105(4)

Symmetry transformation used to generate the symmetry related atoms: ^{i} 1/2 + *x*, 3/2 – *y*, –*z*.

3. 4. IR and UV-Vis Spectra

The weak and broad absorptions centered at 3434 and 3421 cm^{-1} in the spectra of H_2L and complex **2** substantiate the presence of O–H groups. The strong absorption band at 1623 cm^{-1} for H_2L is assigned to the azomethine groups, ν(C=N),[10] which is shifted to lower wave number 1610 cm^{-1} for complex **1** and higher wave number 1635 cm^{-1} for complex **2**. This is in accordance with the variation of the bond lengths of C=N in the compounds. The intense band at 2072 cm^{-1} for complex **2** can be assigned to the stretching vibration of azide ligands.[11] The weak bands in the low wave numbers 450–540 cm^{-1} are due to the vibration of the Cu–O and Cu–N bonds.[12]

In the electronic spectra of H_2L and the complexes, the intense bands observed at about 230–280 nm for the compounds are assigned to intra-ligand π–π^* transitions. The copper complexes displayed bands centered at about 275 nm, which can be assigned to the n–π^* transition.[13] The charge transfer LMCT bands are located at about 355 nm.[14]

3. 5. Antibacterial Activity

The antimicrobial results are summarized in Table 4. The free Schiff base H_2L showed medium activity against *E. coli*, while no activity on *S. aureus* and *C. parapsilosis*. Obviously, the two copper complexes have higher activities than H_2L. The mononuclear copper complex (**1**) showed strong activity against *S. aureus* and *E. coli*, and weak activity against *C. parapsilosis*. The tetranuclear copper complex (**2**) showed strong activity against *S. aureus*, medium activity against *E. coli* and weak activity against *C. parapsilosis*. Interestingly, complex **2** has the most activity against *S. aureus*, with IC_{50} and MIC values of 0.17 and 0.13 mmol L^{-1}, which deserves further study. As a comparison, the copper complexes have similar antibacterial activities against *S. aureus* and *E. coli* to the Schiff base manganese(III) complex[15] and the Schiff base copper(II) complexes.[16]

Table 4. Antibacterial activity of H_2L and the copper complexes

Compound	*S. aureus*		*E. coli*		*C. parapsilosis*	
	IC_{50}*	MIC*	IC_{50}	MIC	IC_{50}	MIC
H_2L	>2.50	>2.50	1.45	2.50	>2.50	>2.50
1	0.38	0.23	0.75	0.42	2.03	1.70
2	0.17	0.13	1.16	0.95	2.27	1.89

* mmol L^{-1}

4. Conclusion

In summary, *N,N'*-bis(4-bromosalicylidene)propane-1,2-diamine was prepared. With the bis-Schiff base, a mononuclear copper(II) complex and a phenolate and azide co-bridged tetranuclear copper(II) complex were obtained. The Schiff base and the two complexes were characterized by physico-chemical methods. Structures of the complexes were confirmed by single crystal X-ray determination. The Schiff base ligand coordinates to the metal atoms through the phenolate oxygen and imine nitrogen. The complexes have effective antibacterial activities on the bacteria *Staphylococcus aureus* and *Escherichia coli*, and the yeast *Candida parapsilosis*.

Supplementary Material

CCDC 2244579 (**1**) and 2244580 (**2**) contain the supplementary crystallographic data for this paper. These data can be obtained free of charge at http://www.ccdc.cam.ac.uk/const/retrieving.html or from the Cambridge Crystallographic Data Centre, 12 Union Road, Cambridge CB2 1EZ, UK; fax: +44(0)1223-336033 or email: deposit@ccdc.cam.ac.uk.

5. References

1. (a) P. Bhunia, S. Dutta, S. Maity, J. Mayans, A. Escuer, A. Ghosh, *Inorg. Chim. Acta* **2023**, *545*, 121264 **DOI:**10.1016/j.ica.2022.121264
(b) A. Ajaz, M. A. Shaheen, M. Ahmed, K. S. Munawar, A. Siddique, A. Karim, N. Ahmad, M. F. U. Rehman, *RSC Advances* **2023**, *13*, 2756–2767; **DOI:**10.1039/D2RA07051K
(c) P. Middya, D. Roy, S. Chattopadhyay, *Inorg. Chim. Acta* **2023**, *548*, 121377; **DOI:**10.1016/j.ica.2023.121377
(d) M. Abdi, A. F. Shojaei, M. Ghadermazi, Z. Moradi-Shoeili, *Acta Chim. Slov.* **2020**, *67*, 476–486; **DOI:**10.17344/acsi.2019.5466
(e) L.-W. Xue, Q.-L. Peng, P.-P. Wang, H.-J. Zhang, *Acta Chim. Slov.* **2019**, *66*, 694–700; **DOI:**10.17344/acsi.2019.5151
(f) C.-L. Zhang, X.-Y. Qiu, S.-J. Liu, *Acta Chim. Slov.* **2019**, *66*, 484–489. **DOI:**10.17344/acsi.2019.5019
2. (a) N. A. A. Elkanzi, H. Hrichi, H. Salah, M. Albqmi, A. M. Ali, A. Abdou, *Polyhedron* **2023**, *230*, 116219; **DOI:**10.1016/j.poly.2022.116219
(b) S. K. Patel, K. Kolte, C. J. Savani, P. Raghavaiah, D. Dave, A. A. Isab, D. Mistry, D. Suthar, V. K. Singh, *Inorg. Chim. Acta* **2022**, *543*, 121139; **DOI:**10.1016/j.ica.2022.121139
(c) A. Ali, M. Pervaiz, Z. Saeed, U. Younas, R. Bashir, S. Ullah, S. M. Bukhari, F. Ali, S. Jelani, A. Rashid, A. Adnan, *Inorg. Chem. Commun.* **2022**, *145*, 109903; **DOI:**10.1016/j.inoche.2022.109903
(d) D.-L. Peng, N. Sun, *Acta Chim. Slov.* **2018**, *65*, 895–901; **DOI:**10.17344/acsi.2018.4543
(e) G.-X. He, L.-W. Xue, Q.-L. Peng, P.-P. Wang, H.-J. Zhang,

Acta Chim. Slov. **2019**, *66*, 570–575. **DOI:**10.17344/acsi.2018.4868
3. (a) S. Mandal, T. Sen, U. Mandal, D. Bhunia, C. Rizzoli, D. Bandyopadhyay, *J. Coord. Chem.* **2019**, *72*, 3614–3624; **DOI:**10.1080/00958972.2019.1704275
(b) H. Keypour, F. Forouzandeh, S. Salehzadeh, F. Hajibabaei, S. Feizi, R. Karamian, N. Ghiasi, R. W. Gable, *Polyhedron* **2019**, *170*, 584–592; **DOI:**10.1016/j.poly.2019.06.023
(c) H. Y. Qian, N. Sun, *Transition Met. Chem.* **2019**, *44*, 501–506; **DOI:**10.1007/s11243-018-00296-x
(d) M. H. Esfahani, H. Iranmanesh, J. E. Beves, M. Kaur, J. P. Jasinski, M. Behzad, *J. Coord. Chem.* **2019**, *72*, 2326–2336. **DOI:**10.1080/00958972.2019.1643846
4. (a) L. Saghatforoush, K. Moeini, S. A. Hosseini-Yazdi, Z. Mardani, A. Bakhtiari, A. Hajabbas-Farshchi, S. Honarvar, M. S. M. Abdelbaky, *Polyhedron* **2019**, *170*, 312–324; **DOI:**10.1016/j.poly.2019.05.057
(b) Y. Yuan, X.-K. Lu, G.-Q. Zhou, X.-Y. Qiu, *Acta Chim. Slov.* **2021**, *68*, 1008–1015; **DOI:**10.17344/acsi.2021.7070
(c) K. Dankhoff, M. Gold, L. Kober, F. Schmitt, L. Pfeifer, A. Durrmann, H. Kostrhunova, M. Rothemund, V. Brabec, R. Schobert, B. Weber, *Dalton Trans.* **2019**, *48*, 15220–15230; **DOI:**10.1039/C9DT02571E
(d) S.-F. Yu, X.-Y. Qiu, S.-J. Liu, *Acta Chim. Slov.* **2020**, *67*, 1301–1308. **DOI:**10.17344/acsi.2020.6321
5. *SMART/SAINT*, Madison (WI, USA): Bruker AXS, Inc., **2004**.
6. G. M. Sheldrick, *Acta Crystallogr.* **2015**, *C71*, 3–11.
7. G. M. Sheldrick, *SADABS*, Göttingen (Germany): Univ. of Göttingen, **1999**.
8. (a) E. C. Constable, G. Q. Zhang, C. E. Housecroft, M. Neuburger, J. A. Zampese, *CrystEngComm* **2010**, *12*, 1764–1773; **DOI:**10.1039/b922929a
(b) G. Margraf, T. Kretz, F. F. de Biani, F. Laschi, S. Losi, P. Zanello, J. W. Bats, B. Wolf, K. Removic-Langer, M. Lang, A. Prokofiev, W. Assmus, H.-W. Lerner, M. Wagner, *Inorg. Chem.* **2006**, *45*, 1277–1288; **DOI:**10.1021/ic051016z
(c) H.-H. Yao, W.-T. Huang, J.-M. Lo, F.-L. Liao, P. Chattopadhyay, *J. Coord. Chem.* **2005**, *58*, 975–984. **DOI:**10.1080/00958970500111006
9. (a) S. Koner, S. Saha, K.-I. Okamoto, J.-P. Tuchagues, *Inorg. Chem.* **2003**, *42*, 4668–4672; **DOI:**10.1021/ic020526f
(b) A. D. Khalaji, H. Stoekli-Evans, *Polyhedron* **2009**, *28*, 3769–3773; **DOI:**10.1016/j.poly.2009.07.068
(c) A. Ray, S. Mitra, A. D. Khalaji, C. Atmani, N. Cosquer, S. Triki, J. M. Clemente-Juan, S. Cardona-Serra, C. J. Gomez-Garcia, R. J. Butcher, E. Garribba, D. J. Xu, *Inorg. Chim. Acta* **2010**, *363*, 3580–3588. **DOI:**10.1016/j.ica.2010.07.014
10. (a) K. R. S. Gowda, H. S. B. Naik, B. V. Kumar, C. N. Sudhamani, H. V. Sudeep, T. R. R. Naik, G. Krishnamurthy, *Spectrochim. Acta A* **2013**, *105*, 229–237; **DOI:**10.1016/j.saa.2012.12.011
(b) B. Sarkar, M. G. B. Drew, M. Estrader, C. Diaz, A. Ghosh, *Polyhedron* **2008**, *27*, 2625–2633; **DOI:**10.1016/j.poly.2008.05.004
(c) A. Jayamani, M. Sethrupathi, S. O. Ojwach, N. Sengottuvelan, *Inorg. Chem. Commun.* **2017**, *84*, 144–149. **DOI:**10.1016/j.inoche.2017.08.013
11. (a) A. D. Khalaji, S. Triki, J. M. Clemente-Juan, C. J. Gomez-Garcia, *Polyhedron* **2013**, *50*, 45–50; **DOI:**10.1016/j.poly.2012.10.031
(b) S. Naiya, C. Biswas, M. G. B. Drew, C. J. Gomez-Garcia, J. M. Clemente-Juan, A. Ghosh, *Inorg. Chem.* **2010**, *49*, 6616–6627. **DOI:**10.1021/ic1005456
12. A. Ray, D. Sadhukhan, G. Rosair, C. J. Gomez-Garcia, S. Mitra, *Polyhedron* **2009**, *28*, 3542–3550. **DOI:**10.1016/j.poly.2009.07.017
13. A. Jayamani, M. Sethupathi, S. O. Ojwach, N. Sengottuvelan, *Inorg. Chem. Commun.* **2017**, *84*, 144–149. **DOI:**10.1016/j.inoche.2017.08.013
14. B. Sarkar, M. G. B. Drew, M. Estrader, C. Diaz, A. Ghosh, *Polyhedron* **2008**, *27*, 2625–2633. **DOI:**10.1016/j.poly.2008.05.004
15. Y.-M. Hao, *Russ. J. Coord. Chem.* **2015**, *41*, 25–30. **DOI:**10.1134/S1070328415010030
16. (a) A. Valent, M. Melnik, D. Hudecova, B. Dudova, R. Kivekas, M. R. Sundberg, *Inorg. Chim. Acta* **2002**, *340*, 15–20; **DOI:**10.1016/S0020-1693(02)01062-9
(b) Y.-M. Hao, *Acta Chim. Slov.* **2021**, *68*, 102–108. **DOI:**10.17344/acsi.2020.6205

Povzetek

Sintetizirali smo dva nova kompleksa bakra(II), [CuL] (**1**) in $[Cu_4Cl_2L_2(N_3)_2]\cdot CH_3OH$ (**2**), z ligandom *N,N'*-bis(4-bromosaliciliden)propan-1,2-diamin (H_2L). Spojini smo karakterizirali s spektroskopskimi metodami in monokristalno rentgensko difrakcijo. Bakrov atom v enojedrnem kompleksu **1** je kvadratno planarno koordiniran. Zunanji in notranji bakrovi atomi v štirijedrnem kompleksu **2**, ki jih povezujejo mostovni fenolatni in azidni ligandi, so kvadratno planarno in kvadratno piramidalno koordinirani. Protibakterijsko učinkovitost liganda in obeh kompleksov smo preizkusili na bakterijah *Staphylococcus aureus* in *Escherichia coli* ter na glivi *Candida parapsilosis*.

Scientific paper

Comparative Molecular Field Analysis (CoMFA), Molecular Docking and ADMET Study on Thiazolidine-4-carboxylic acid Derivatives as New Neuraminidase Inhibitors

Lotfi Bourougaa,[1] Mebarka Ouassaf[1,*] and Shafi Ullah Khan[2]

[1] *Group of Computational and Medicinal Chemistry, LMCE Laboratory, University of Biskra, BP 145 Biskra 707000, Algeria*

[2] *Product and Process Innovation Department, Qarshi Brands Pvt. Ltd., Hattar Industrial Estate-22610, Haripur, KPK Pakistan*

** Corresponding author: E-mail: nouassaf@univ-biskra.dz*

Received: 03-04-2023

Abstract

The objective of this research was to create a 3D-QSAR CoMFA model for a set of twenty-five neuraminidase inhibitors containing thiazolidine-4-carboxylic acid derivatives and to identify a new potent neuraminidase inhibitor for the treatment of influenza. The statistical parameters of the generated model are excellent: $Q^2 = 0.708$, $R^2 = 0.997$. The external validation results were ($r^2_0 = 0.922$, K= 1.016, $R^2_{pred} = 0.674$, $r^2_m = 0.778$) indicating that the constructed model has good predictive power. Based on the contour map of the CoMFA model, we were able to propose six novel compounds with higher neuraminidase inhibitory activity than the most active compound. The six proposed molecules were submitted to molecular docking to analyse the bindings formed between the newly designed molecules and the neuraminidase. All of the proposed molecules were found to be more stable on the active site of neuraminidase than the reference molecule (1SJ). SwissADME was used to estimate the pharmacokinetic properties of each proposed molecule, while ProToxII and VEGA QSAR were used to investigate any potential toxicity. Finally, a reaction mechanism for synthesizing the six proposed compounds was described, which could potentially be explored further in the search for novel neuraminidase inhibitors. In conclusion, this study has identified potential candidates for the development of more effective neuraminidase inhibitors for the treatment of influenza.

Keywords: thiazolidine-4-carboxylic acid, Neuraminidase, influenza, 3D-QSAR, CoMFA, Molecular Docking, ADMET study.

1. Introduction

Influenza is a respiratory disease caused by the *Orthomyxoviridae* virus family. Every year, influenza viruses generate seasonal epidemics that mostly affect the adult population. 10–30% of sick people are hospitalized, and 3–15% die.[1] Influenza symptoms include a sudden onset of high temperature, aching muscles, headache, severe exhaustion, a nonproductive cough, a sore throat, and a runny nose.[2] The variation of influenza viruses can develop in a pandemic, posing a major danger to public health.[3] Neuraminidase (NA) is a glycoprotein located in the envelope of the influenza virus that plays a critical role in the process of infecting and spreading amongst human host cells.[4] Neuraminidase is an important target of drug design for the treatment of influenza infections because to its involvement in viral propagation and it's largely preserved active site.[5] Neuraminidase inhibitors (NAI) represent the only extensively approved class of antiviral medications used for the treatment and prevention of seasonal influenza.[6] *Oseltamivir* is widely utilized, whereas *Zanamivir*, *Peramivir*, and *Laninamivir* are used in fewer nations concurrently.[7] NAIs are the most often given anti-influenza medications nowadays, they have been shown to be beneficial in speeding viral clearance, lowering clinical disease duration, and decreasing hospital stay and death.[8]

Computer-Aided Drug Design (CADD) is the process of using computer methods and resources to design and identify novel potential pharmaceutical drugs.[9] A QSAR is simply a mathematical equation that is derived from a set of molecules with a known activity using computational techniques. A variety of statistical approaches and computed molecular descriptors may be employed to

identify the exact form of the relationship between structure and activity, and this relationship is subsequently employed to predict the activity of new compounds.[10,11] QSAR investigations are based on the notion that changes in bioactivity are related with structural and molecular variation in a group of molecules.[12] The three-dimensional quantitative structure-activity relationship is one of the most successful and valuable strategies for the development and design of potent medications(3D-QSAR).[13]

The goals of this research are to develop new neuraminidase inhibitors for the treatment of influenza. In a 3D-QSAR study based on a series of biologically active thiazolidine-4-carboxylic acid derivatives, we used comparative molecular field analysis (CoMFA) to find a statistically significant relationship between the three-dimensional structure of the molecules and their biological activity. After designing these molecules, we performed a docking study to arrange them in the active site of neuraminidase based on their stability. To identify the molecules with the best pharmacological properties, the compounds identified were also subjected to in silico absorption, distribution, metabolism, elimination, and toxicity (ADMET) property testing. We used ProToxII to assess the potential toxicity of all proposed molecules. Finally, we provided a reaction mechanism for the synthesis of each of these proposed compounds for future research into neuraminidase inhibitors.

2. Materials and Methods

2. 1. Experimental Databases

A set of twenty-five thiazolidine-4-carboxylic acid derivatives reported by Asadollah, M et al and Yu. L et al were chosen for molecular modelling studies.[14,15] Thiazolidine-4-carboxylic acid is a cyclic sulfur amino acid with a molecular structure similar to proline, hence the name thioproline. The thiazolidine-4-carboxylic acid sulfhydryl group is essential in metabolism as an antioxidant protector and in detoxification processes.[16] Inhibitory activity was provided as IC50 values, which were then converted to pIC50 values [pIC50 = –log (IC50)] and used in 3D-QSAR experiments. All experimental data were divided into two categories: a training set for model generation and a test set for external evaluation of model accuracy, the training set contains twenty molecules and the test set contains five molecules. The variability of bioactivity rates and biological properties was also taken into account when randomly partitioning the training and test sets.[17] (Table 1).

2. 2. Structure Preparation and Alignment

The SYBYL-X 2.0 software suite (Certara Enhances SYBYL-X Drug Design and Discovery Software Suite) was used to construct and optimise the structures of the twenty-five compounds with energy minimization.[18] The tripos standard force field was used, and a condition of 0.01 kcal/(mol) in Gasteiger-Hückel charge atomic partial was established. The tripos standard force field was used, and a condition of 0.01 kcal/(mol) in Gasteiger-Hückel charge atomic partial was established.[19,20] Molecular alignment is the most sensitive component, and it has a significant impact on 3D-QSAR models.[21] The structures that have been minimised and aligned are used to create the 3D-QSAR model.

2. 3. Generation of 3D-QSAR by CoMFA

Our goal was to develop a predictive 3D-QSAR model using comparative molecular field analysis (CoMFA). The CoMFA method is a useful 3D-QSAR tool that has been used successfully in several medicinal chemistry studies. One of the significant advantages of this approach is its immediate application in the examination of any structure-dependent biological characteristics.[22] The CoMFA theory states that differences in a target property between chemicals are frequently associated with changes in the noncovalent fields that surround those structures. These fields, which are the electrostatic (Coulombic) and steric (Lennard-Jones) fields, are computed at regular intervals within a predetermined area.[23] Steric and electrostatic descriptors were generated using a tripos force field and an ordered divergence grid of 2 Å with a cutoff energy value of 30 kcal/mol.[24] All other parameters have been reset to their default settings.

2. 4. PLS analysis and Validations

PLS regression is a well-established multivariate method that has been widely used in a variety of chemical fields.[25] A PLS model was built for the training set, and the model was validated using the remaining test set. To be trustworthy and predictive, 3D-QSAR models should be validated by producing correct predictions for external data sets that were not used in the model's development.[10] PLS can assess complex structure-activity data more realistically and efficiently determine how molecular structure affects biological activity.[26] As a result, we estimate the mode's predictive power using external validation. A QSAR model is predictive, according to Golbraikh and Tropsha, if the following conditions are met.[27]

$$R^2_{pred} > 0.6, \quad [r^2 - r^2_0] / r^2 < 0.1, \quad [r^2 - r'^2_0] / r^2 < 0,$$
and
$$0.85 < k < 1.15 \text{ or } 0.85 < k' < 1.15$$

Roy and Paul developed the term r^2_m to verify the external predictability of the chosen model.[27] An r^2_m value greater than 0.5 may be interpreted as indicating good external predictability.

The 3D-QSAR model was also validated using a Y-randomization test, which eliminates chance correlations between dependent and independent variables.[28] If the randomised models' correlation coefficient values R2

and Q2 are less than the original non-randomized model's R2 and Q2, we can be confident that the QSAR models are robust and not the result of random correlation.[29]

2. 5. Molecular Docking

Molecular docking is a computational tool for determining the structure of a protein-ligand interaction automatically.[30] The true docking process, on the other hand, is so adaptable that receptors and ligands must adjust their conformation to match each other well.[31] This technique has been widely used in the drug design research sector in recent years, and it also significantly increases efficiency and lowers research costs.[32] One of the most famous molecular docking software packages, AutoDock Vina, combines a fast stochastic conformational search method with accurate and well-rated force-field-based and empirical scoring systems.[33,34] The structure of neuraminidase was obtained from the RCSB database (PDB Id: 4ks2) Influenza neuraminidase in complex with an antiviral compound (1SJ)[35] as shown in the figure 1. In 1999, the Food and Drug Administration (FDA) approved Oseltamivir (italique) as a neuraminidase inhibitor.[36] As a second reference ligand, we docked Oseltamivir into the neuraminidase protein pocket. The receptors were then processed with UCSF Chimera 1.16 to remove non-standard residues before being docked using AutoDock Vina 1.1.2.[37] The AUTOGRID system, which calculates ligand binding energy with their receptor, was used to define the three-dimensional grid.[38] The active site is located at coordinates (x = –23.4893 Å, y = 20.7720 Å, and z = –9.6124 Å), and the grid size is x = 26.4819, y = 25.6602, and z = 24.2547. The docking results were visualised using the Biovia discovery studio visualizer.[39]

Table 1. A Tabular analysis of relationship between structures of compounds and experimental Activity.

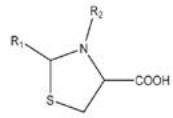

Compound	R_1	R_2	pIC_{50}
01	C_6H_5–	H	4.672
02	(2-OH)C_6H_5–	H	4.695
03	(2-COOH)C_6H_5–	H	4.742
04	(4-CN)C_6H_5–	H	4.631
05	(2-NO2)C_6H_5–	H	4.648
06	(2-OH, 3-CH3O)C_6H_5–	H	4.91
07	C_4H_3O–	H	4.366
08	C_6H_5–	$ClCH_2CO$–	5.123
09	(2-OH)C_6H_5–	$ClCH_2CO$–	5.234
10	(2-COOH)C_6H_5–	$ClCH_2CO$–	4.971
11	(4-CN)C_6H_5–	$ClCH_2CO$–	5.063
12	(2-NO2)C_6H_5–	$ClCH_2CO$–	5.116
13	(2-OH, 3-CH3O)C_6H_5–	$ClCH_2CO$–	5.101
14	C_4H_3O–	$ClCH_2CO$–	4.889
15	C_6H_5–	$PhCH_2CO$–	5.917
16	(2-OH)C_6H_5–	$PhCH_2CO$–	6.187
17	(2-COOH)C_6H_5–	$PhCH_2CO$–	5.717
18	(4-CN)C_6H_5–	$PhCH_2CO$–	5.607
19	(2-OH, 3-CH3O)C_6H_5–	$PhCH_2CO$–	5.79
20	C_4H_3O–	$PhCH_2CO$–	5.539
21	C_6H_5–	NH_2CH_2CO–	6.276
22	(2-OH)C_6H_5–	NH_2CH_2CO–	6.678
23	(2-COOH)C_6H_5–	NH_2CH_2CO–	6.553
24	(2-OH, 3-CH3O)C_6H_5–	NH_2CH_2CO–	6.854
25	C_4H_3O–	NH_2CH_2CO–	6.009

2. 6. Prediction of ADMET Properties

Following the molecular docking of the designed compounds for influenza neuraminidase inhibition, the absorption, distribution, metabolism, and elimination are estimated using the SwissADME web server.[40] Furthermore, the ProToxII-II and VEGA QSAR platforms were used to assess potential toxicity.[41,42]

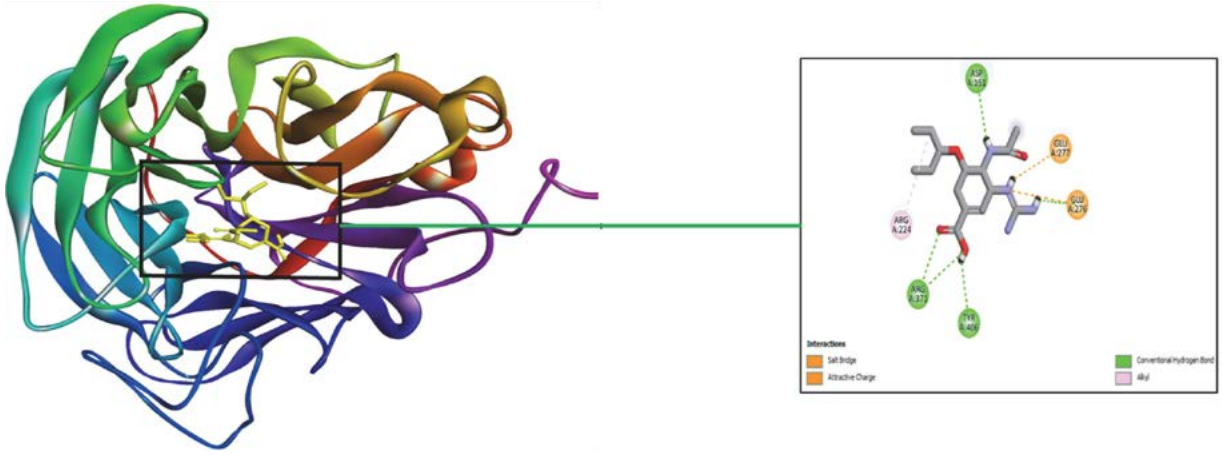

Fig. 1. Binding interaction illustration of Neuraminidase in complex with 1SJ.

3. Results and Discussions

3. 1. Molecular Alignment of Dataset

Molecular alignment is one of the most important factors influencing the performance of 3D-QSAR approaches.[43] The database was aligned for this phase using SYBYL-X 2.0 software, with the most active compound (compound 24, pIC50 = 6.780) serving as the structural template for the other compounds' alignment. Figure 2 shows the alignment of all molecules in the database (training and test set).

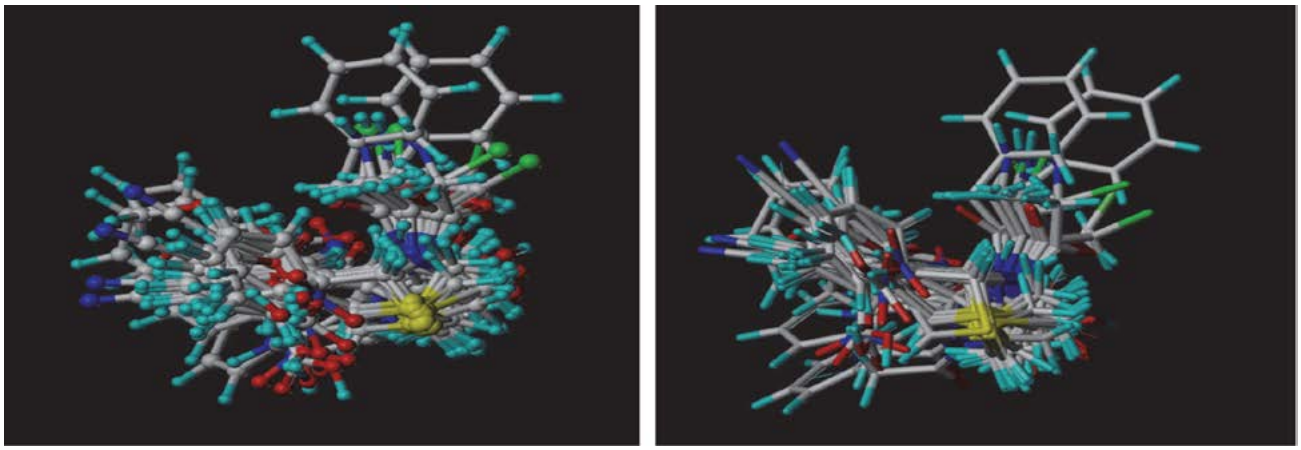

Fig. 2. The alignment of all molecules in the database (left: training set; right: test set).

3. 2. 3D-QSAR Model and Validations

The comparative molecular field method is used to establish a quantifiable link between the 3D structure of the compounds and their biological activity. Table 2 shows the statistical results of the PLS analysis for the CoMFA model. This CoMFA model has an extremely high R2 value of 0.997, the optimal number of components of 5, and an F-value of 883.433. Furthermore, the built model had a cross validated coefficient of Q2 of 0.708, with a very small standard error of estimation (SEE) of 0.050. The significant R2 and Q2 values, as well as the low SEE value, suggest that the CoMFA model developed is stable and has excellent predictive power.

Second, Table 3 shows the results of the CoMFA model's external validation. A high R2pred value greater than 0.6 indicates that the CoMFA model has good predictive power, and an R2m value of 0.778 indicates that the model has good predictive ability. Also, all values of r^2_0 and r'^2_0 are close to r^2, $[r^2–r^2_0]/r^2$ and $[r^2–r'^2_0]/r^2$ have values much less than 0.1.

The Y-randomization test was performed fifty times to confirm the robustness of the CoMFA model. Table S1, shows the results of the Y-randomization test. The results show that the Q2 and R2 values obtained by the fifty random variations are lower than the values obtained by the original models. These findings show that the built model is reliable and did not result from random correlation of the training set.

TThe PLS results and the external validation show that the CoMFA model is reliable and statistically significant. The actual and predicted pIC50 values, as well as the residual values determined by the CoMFA model, are shown in Table S2. Figure 3 depicts the excellent correlation between actual and predicted activity, demonstrating the 3D-QSAR model's superior predictive ability.

Table 2. Statistical parameters of partial Least Squares (PLS) analysis on the comparative molecular field analysis (CoMFA) model.

Model	Q^2	R^2	SEE	F	N	Fraction	
						Steric	Electrostatic
CoMFA	0.708	0.997	0.050	883.433	5	0.412	0.588

Table 3. Assessing the predictive performance by statistical parameters of external validation for the comparative molecular field analysis (CoMFA) model.

R^2_{pred}	r^2	r^2_0	r'^2_0	K	K'	$[r^2–r^2_0]/r^2$	$[r^2–r'^2_0]/r^2$	r^2_m
0.674	0.957	0.922	0.955	1.016	0.982	0.036	0.001	0.778

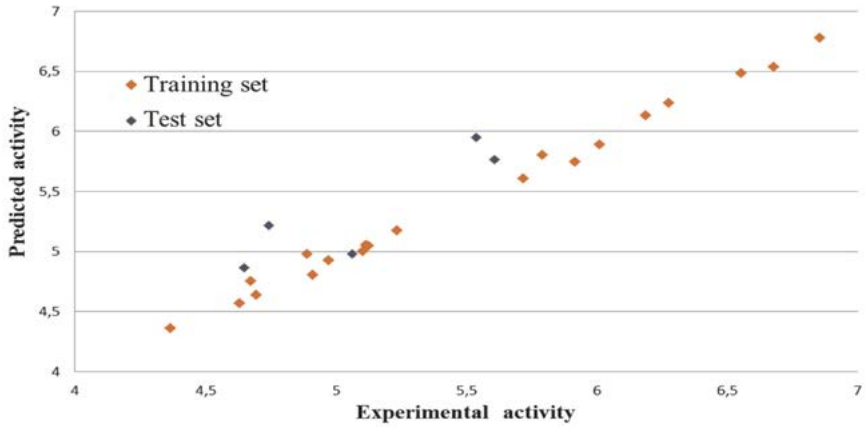

Fig. 3. The plot of the correlation between the experimental and predicted activity using 3D-QSAR model of training and test set.

3. 3. CoMFA Contour Map

The collected data were used to illustrate the favourable and unfavourable regions during which the structural changes of the compound result in an increase or decrease in biological activity for this critical phase. The steric and electrostatic contour maps generated by CoMFA modelling for the most active compound are shown in Figure 4. The green contours represent areas where bulky groups have a positive influence on neuraminidase inhibitory activity, whereas the yellow contours represent areas where bulky groups have a negative influence on inhibitory activity. Steric contour maps show the spatial volume of substituted groups in a variety of locations. Because of the presence of bulky groups in advantageous locations, it is possible that the steric effect influences the inhibitory activity of compounds 22, 23, and 24.

Blue and green regions are favorable for inhibitory activity, red and yellow green regions are unfavorable for inhibitory activity.

The blue contours indicate locations where electronegative groups positively influence neuraminidase inhibitory activity, whereas the red contours indicate locations where electronegative groups negatively influence inhibitory activity. The contour map shows the presence of two large blue contour maps located between the nitrogen and sulfur atoms of the thiazolidine ring, as well as medium-sized contours near the aromatic ring. This helps to explain the higher activity of compound 24 with a methoxy group near the aromatic ring and the thiazolidine's NH2CH2CO- radical. This demonstrates that electronegative groups in these zones enhance the inhibitory activity of influenza virus. From these observations, it can be explained why the inhibitory activity of the best compounds to inhibit the vital function of neuraminidase.

3. 4. Design for New Neuraminidase Inhibitors

This study's primary goal is to develop new anti-influenza thiazolidine inhibitors. The CoMFA model contour map analysis provides useful information on structural properties for improving neuraminidase inhibitory

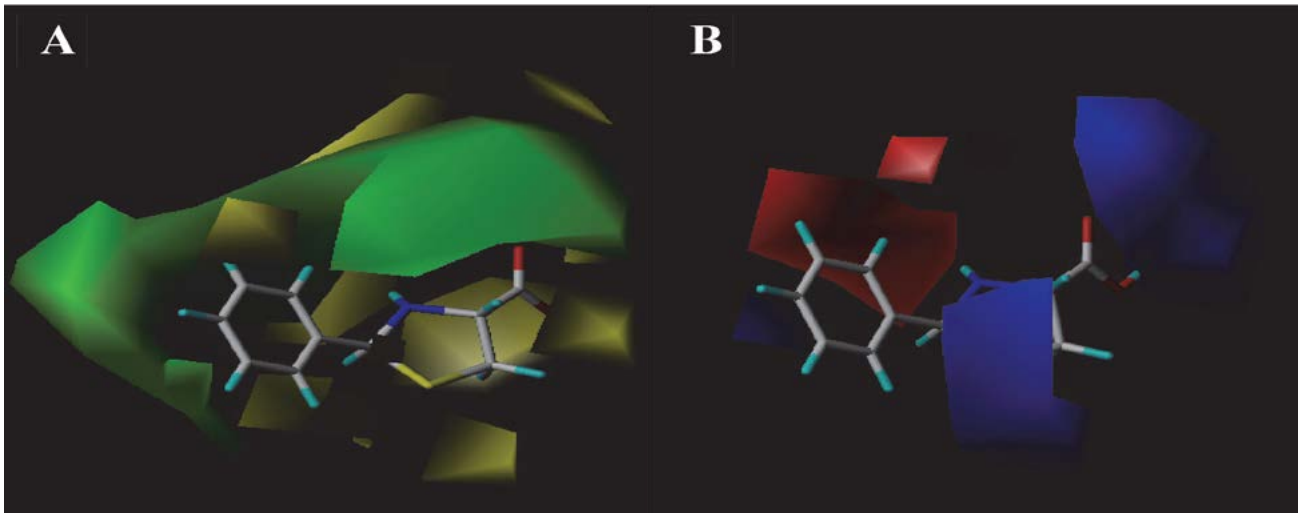

Fig. 4. CoMFA contour plot of compound binding to target: Visualization of (**A**) Steric and (**B**) Electrostatic Fields.

activity. Figure 5 depicts the collection of all orientations obtained from the CoMFA contour map, which proved to be a dependable and effective optimization strategy for the design of novel thiazolidines with high predicted inhibitory activity. Using a comparative molecular field, we created six (Th1-Th6) novel anti-influenza thiazolidine derivatives. Six molecules were optimised and aligned, with the most active compound acting as a structural template. Table 5 summarises the chemical structures and predicted pIC50 values of the novel compounds proposed. All six proposed compounds have higher predictive pIC50 values than the most active molecule (predictive pIC50 = 6,780 for the most active compound). These molecules can be thoroughly investigated. Finally, as shown in figures 6 and 7, we proposed a reaction mechanism for synthesising these new molecules.

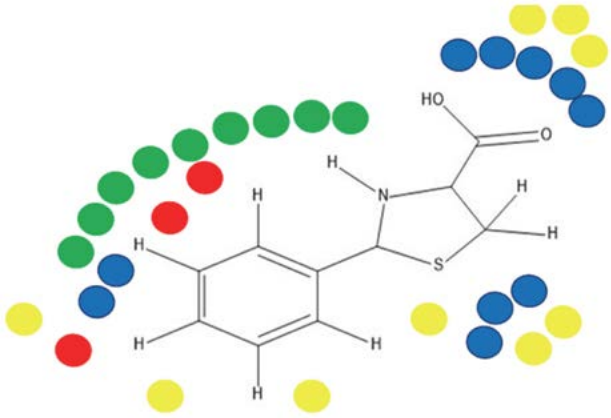

Fig. 5. Structural characteristics derived from CoMFA contour Map: Analysis of favorable and unfavorable regions for inhibitory activity. Blue and green regions are favorable for inhibitory activity, red and yellow green regions are unfavorable for inhibitory activity.

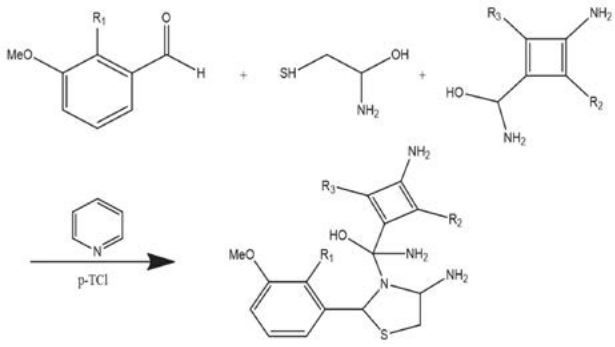

Fig. 6. Proposed reaction: General form and chemical equations.

3. 5. Molecular Docking

We performed molecular docking for the six designated molecules (Th1-Th6) to gain a better understanding of how the molecules obtained by 3D-QSAR inhibit the vital function of influenza virus neuraminidase, as well as the binding energy and types of interactions. Furthermore, we

Table 4. Structures and pIC_{50} values of novel molecules predicted by the CoMFA model.

Compound	Chemical structures	pIC_{50} predictive CoMFA
Th1	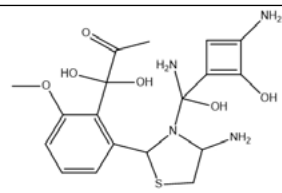	7.036
Th2	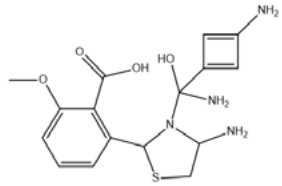	7.638
Th3	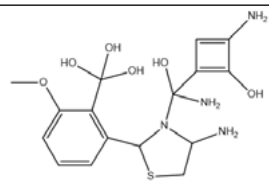	7.090
Th4	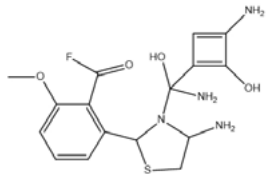	7.211
Th5	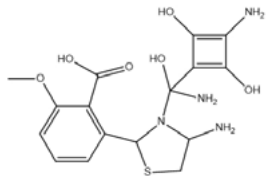	7.347
Th6	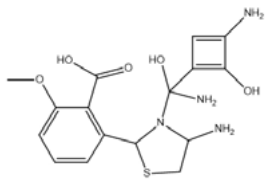	7.223

docked Oseltamivir (italique) with neuraminidase to get a better estimate of the inhibitory efficacy of the proposed compounds (as another reference molecule). The docking modelling results for all proposed molecules and the neuraminidase inhibitor are presented in Table 7, and their types of interactions with the neuraminidase active site are shown in Figure 8. The results show that the designed compounds have binding affinity values ranging from –6.6 to –7.5 kcal/mol, while the binding affinity value of the reference compound (1SJ) is –6.6 kcal/mol, and the binding affinity value of Oseltamivir into neuraminidase is –6.6 kcal/mol. The interaction of the reference molecule (1SJ) and Oseltamivir with the active site of neuraminidase is depicted in Figure 9.

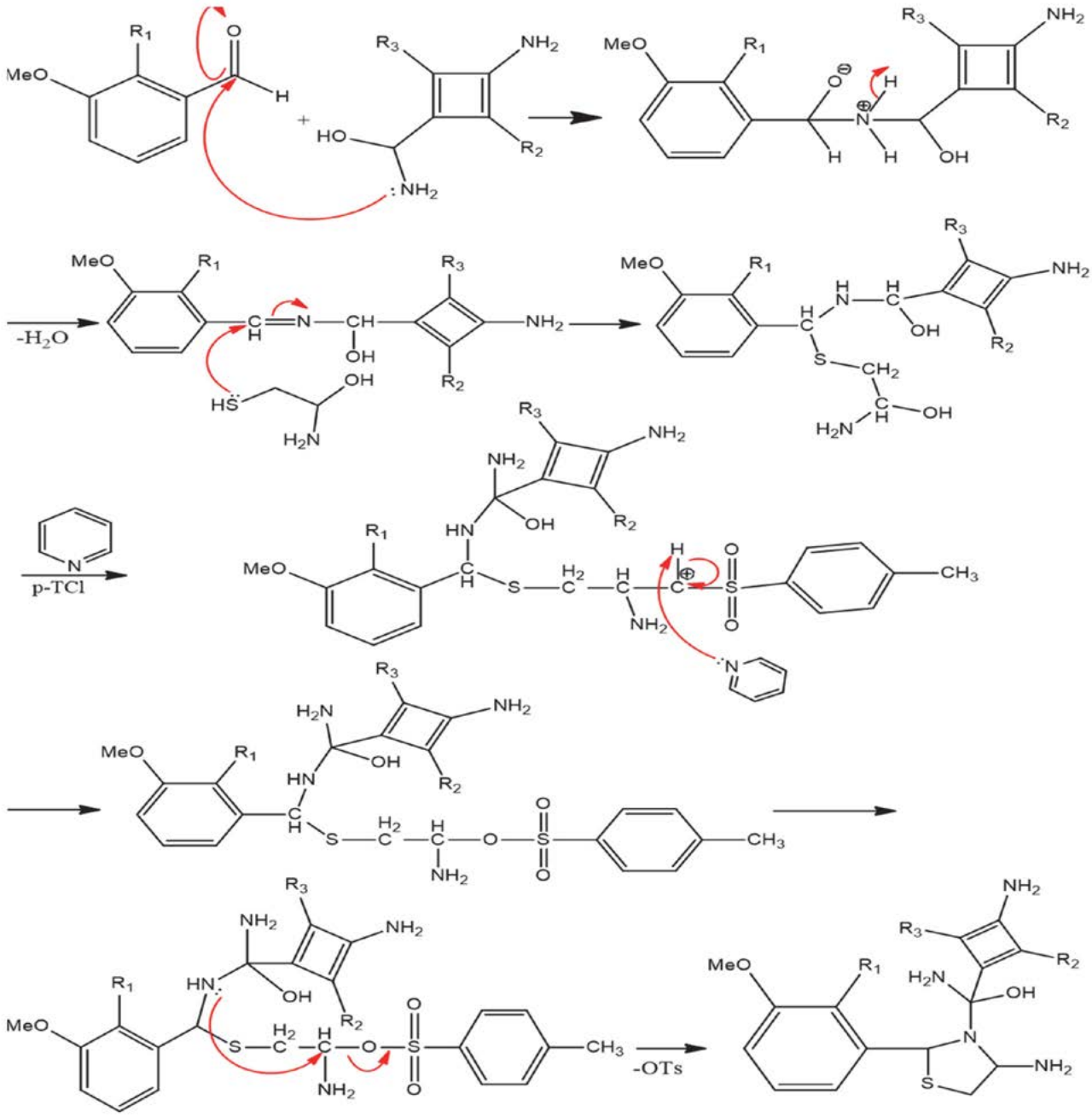

Fig. 7. Proposed general mechanism for synthesizing the six compounds: Insights into reaction pathways and synthetic strategies.

Th1, Th2, Th4, Th5, and Th6 have lower binding affinities than the reference molecule, indicating that this molecule is significantly more stable in the active site of neuraminidase. All of the molecules, including the reference compound, interacted with the amino acids Glu119, Asp151, Glu276 and Glu277 via Salt Bridge and Attractive Charge interactions.

We observed a similarity of interaction for the two molecules with the highest binding affinity (Th2 and Th6), which interact with the amino acids Glu119, Trp178, Asp227, Glu277, and Tyr406. The reference molecule only interacts with the active site via a conventional hydrogen bond formed by the amino acids Asp151, Glu276 and Tyr406. It should be noted that conventional hydrogen bond interaction with the amino acids Glu119, Trp178, and Asp227 is critical for inhibiting the vital function of neuraminidase. The designed molecules Th1, Th2, Th4, Th5, and Th6 demonstrate significant binding to the active site of neuraminidase, confirming the 3D-QSAR model's good predictive power. Finally, our findings regarding the interactions between the six proposed molecules and the active site of neuraminidase agree with the findings of Gracy Fathima Selvaraj et al.[44]

Table 5. Binding interactions and affinity values of six neuraminidase inhibitors within the active site.

Ligand	Binding affinity (Kcal/mol)	Conventional Hydrogen Bond	Salt Bridge	Attractive Charge
Th1	–7.1	Asp151	Glu277	Asp151, Glu276, Glu277
Th2	–7.5	Asp277, Trp178, Glu277, Tyr406	Glu277	Asp151, Glu276, Glu277
Th3	–6.6	Glu276, Glu277, Tyr347, Tyr406	Asp151, Glu277	Glu119, Asp151, Glu277
Th4	–7.0	Asp151, Glu277, Tyr406	–	–
Th5	–6.9	Ala246, Tyr406	Asp151, Glu119, Glu277	Asp151, Glu119, Glu277
Th6	–7.5	Glu119, Trp178,Tyr406	Glu277	Asp151, Glu277
1SJ [ref]	–6.6	Asp151, Glu276, Tyr406	Glu277	Glu277
Oseltamivir	–6.6	Tyr406	–	Asp151, Glu119, Glu277

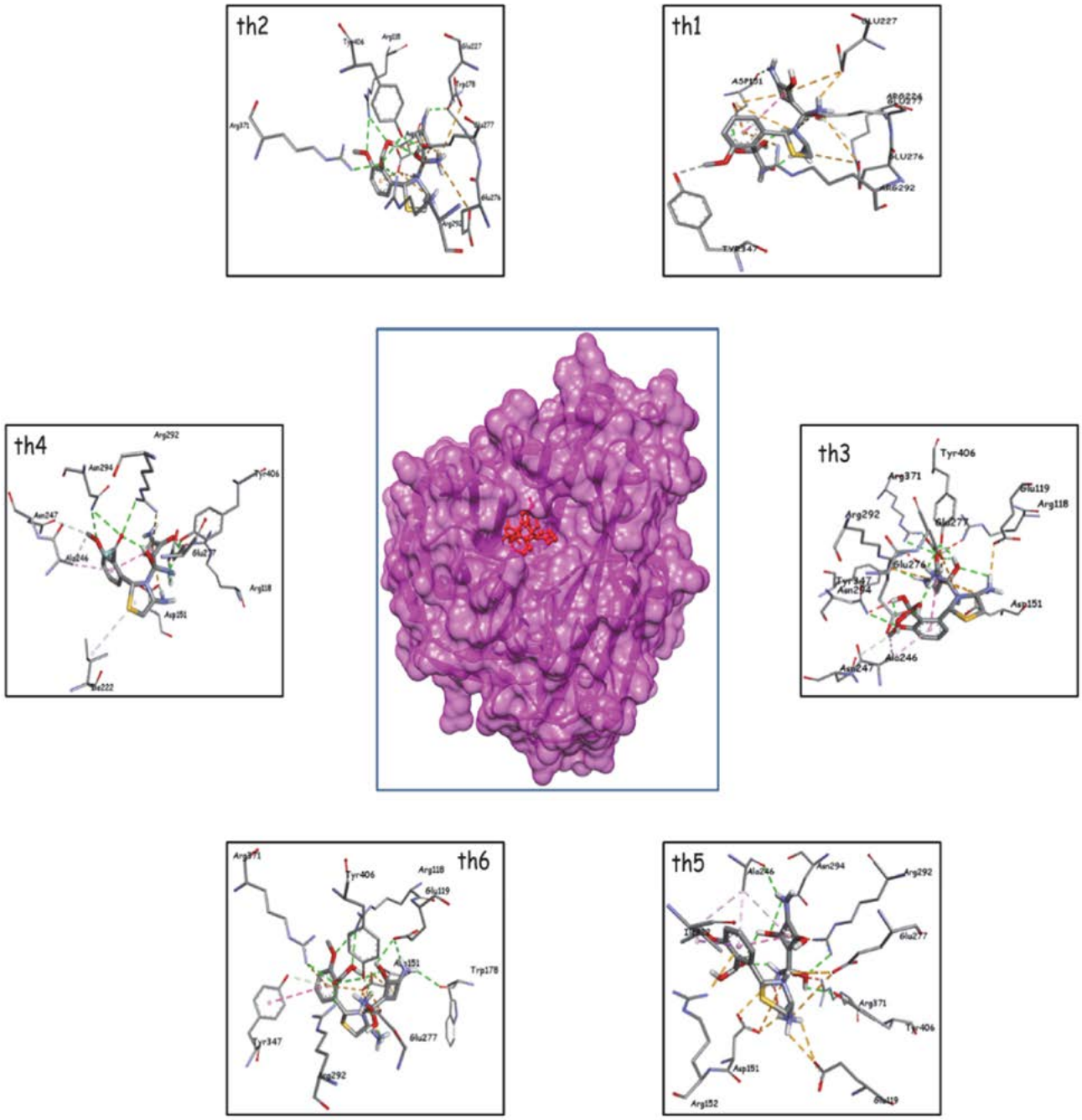

Fig. 8. Insights into ligand binding modes: Interactions of six designed compounds with neuraminidase active site.

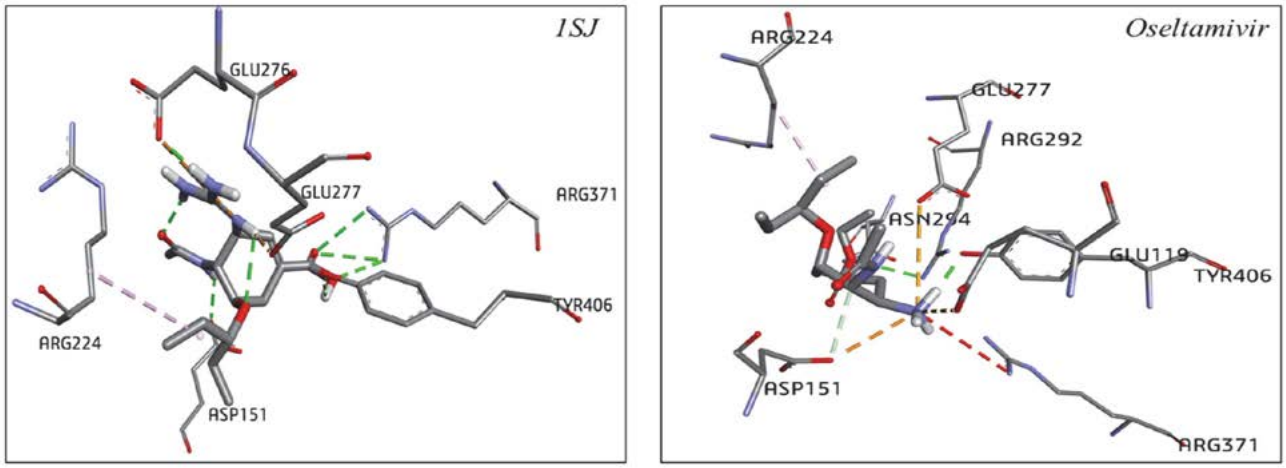

Fig. 9. Comparative analysis of ligand binding modes: Interactions of *1SJ* (left) and *Oseltamivir* (right) with neuraminidase

3.6 ADMET and Bioavailability Prediction

This study was conducted to determine the critical pharmacokinetic parameters for the six designated molecules. The results obtained by SwissADME are shown in Table S3. All the molecules have LogP values between –1.30 and 0.06, these values indicate that all the molecules designed have good permeability towards biological membranes. For aqueous solubility, the six molecules have Log S values between –1 and 0, which means that all the molecules are easily soluble in aqueous media, according to these two parameters all the compounds have a good distribution. The six designed molecules (Th1–Th6) were estimated in silico using the five rules of Lipinski. It was that all molecules follows the Lipinski's rule. For the interactions with hepatic cytochrome P450, we did not record any interaction with them, which means that both molecules have a good metabolism. Another important parameter to quantify the pharmacokinetics of these designated molecules is the bioavailability score, the six molecules have the same bioavailability score (0.55), this value indicates that all the molecules will reach the blood circulation by the oral route (That is, both molecules are well absorbed.). For elimination, due to the aqueous solubility of six proposed compounds, they are readily eliminated renally. Also good LogKp (skin permeation) values between –10.94 and –8.55. Finally, all the proposed molecules are moderately easy to synthesize (the six molecules have synthetic accessibility values lower than 4.75).

For a quick assessment of drug-likeness, a bioavailability radar is provided. The Bioavailability radar takes into account six physicochemical properties. Lipophilicity, size, polarity, solubility, flexibility, and saturation are the parameters involved. For all molecules to be drug-like compounds, the bioavailability radar graph must be contained within a pink area. If the graph is in this pink area, the molecule has a drug-like compound. The bioavailability radar plots of the six compounds are shown in Figure 10. Th2 and Th4 are pharmaceutical candidates. Although there is a small deviation from area at the point of polar feature, Th1, Th3, Th5, and Th6 molecules are on the verge of being considered as drug candidates. These findings indicate that all molecules have very good bioavailability profiles.

We calculated the potential toxicity of these new molecules. Table S4, displays the ProToxII results. We found no evidence of toxicity caused by the designed compounds, whether it was Hepatotoxicity, Carcinogenicity, Immunotoxicity, Mutagenicity, or Cytotoxicity. With LD50 predictive values ranging from 230 to 8000 mg/kg and toxicity classes ranging from 2 to 4. We conclude that the molecules proposed using 3D QSAR are both safe and pharmacologically active.

We estimated Mutagenicity (Ames test) model (CAESAR) 2.1.14, Developmental Toxicity (CAESAR) 2.1.8, Skin Irritation (CONCERT/Kode) 1.0.0, Plasma Protein Binding (– LogK, IRFMN) 1.0.0, P-Glycoprotein activity model (NIC) 1.0.1, and finally total body elimination half-life (QSARINS) 1.0.1 using VEGA QSAR. All of the obtained results are shown in Table S5. All predictions show that the six designed compounds are not mutagenic or toxic to development. Aside from that, none of these molecules cause skin irritation or infection. All molecules had plasma protein binding values ranging from –0.3285 to –0.0484. Furthermore, none of the six proposed compounds interact with P-Glycoprotein, which is found on the surface of biological cells. Furthermore, because their total body elimination half-life ranges between 1.533 and 2.837 hours, renal elimination of these molecules will be simple. The predicted toxicity study results show that all six proposed compounds are both safe and pharmacologically active.

4. Conclusion

A 3D-QSAR analysis of 25 thiazolidine-4-carboxylic acid derivatives was constructed in this study. This analysis was carried out by creating a 3D-QSAR model using the

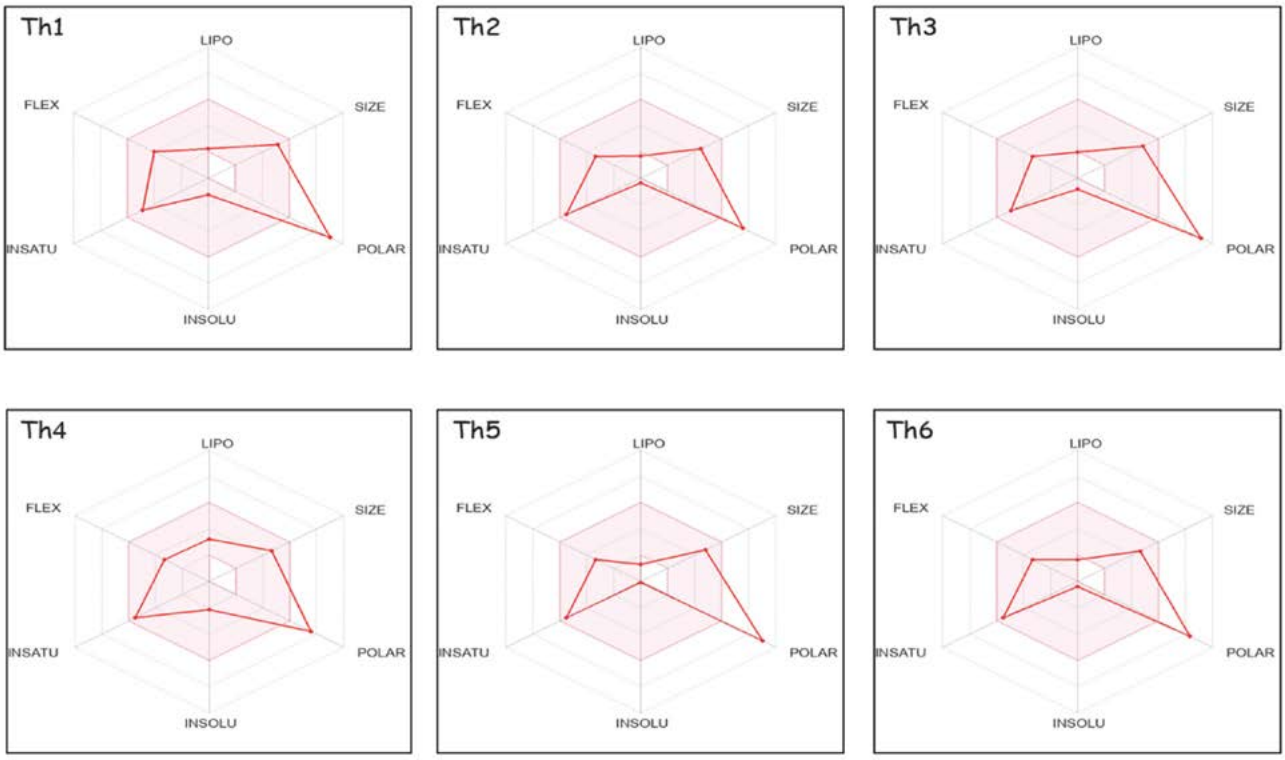

Fig. 10. Assessing Drug-like properties: Bioavailability radar graphs of six designed molecules.

CoMFA methodology. The derived 3D-QSAR models were validated using an external validation technique. We proposed six novel compounds with predicted inhibitory activity (pIC50) greater than the most active compound based on the information provided by the contour maps. All of the proposed compounds are more stable in the active site of neuraminidase than the reference molecule. however, Oseltamivir (italique) is more stable in the active site of neuraminidase (as second reference molecule). The molecular docking analysis confirms the 3D QSAR model's excellent prediction ability. Furthermore, we investigated the pharmacokinetic profile and potential toxicity of the six proposed compounds, and the results showed that each molecule follows Lipinski's rule and can be considered pharmacologically active and safe. We also presented a reaction mechanism for synthesizing these chemicals in order to conduct experimental research on their ability to suppress the critical function of neuraminidase and assess their efficacy in vitro and in vivo.

5. References

1. S. Lipničanová, B. Legerská, D. Chmelová, M. Ondrejovič, S, Miertuš, *Biomolecules* **2022**, *2,* 331–343. **DOI:**10.3390/biom12020331
2. J. Mauskopf, M. Klesse, S. Lee, G. Herrera-Taracena, *Med. Econ.* **2013**, *2,* 264–277. **DOI:**10.3111/13696998.2012.752376
3. R. Yoshida, M. Igarashi, H. Ozaki, N. Kishida, D. Tomabechi, H. Kida, K. Ito, A. Takada, *PLoS Pathog.* **2009**, *3,* 1000350–1000359. **DOI:**10.1371/journal.ppat.1000350
4. G. J. D. Smith, D. Vijaykrishna, J. Bahl, S. J. Lycett, M. Worobey, O. G. Pybus, S. K. Ma, C. L. Cheung, J. Raghwani, S. Bhatt, J. S. M. Peiris, Y. Guan, A. Rambaut, *Nature* **2009**, *459,* 2605–2615. **DOI:**10.1038/nature08182
5. C. Seniya, G. J. Khan, R. Misra, V. Vyas, S. Kaushik, *Asian Pac. J. Trop. Dis.* **2014**, *4, 1,* 467–476. **DOI:**10.1016/S2222-1808(14)60492-8
6. A. Lackenby, T. G. Besselaar, R. S. Daniels, A. Fry, V. Gregory, L. V. Gubareva, W. Huang, A. C. Hurt, S. Leang, R. T.C. Lee, J. Lo, L. Lollis, S. Maurer-Stroh, T. Odagiri, D. Pereyaslov, E. Takashita, D. Wang, W. Zhang, A.Meijer, *Antivir. Res.* **2018**, *157,* 38–46. **DOI:**10.1016/j.antiviral.2018.07.001
7. M. G. Ison, *Clin. Chest. Med.* **2017**, *1,* 139–153. **DOI:**10.1016/j.ccm.2016.11.008
8. T. Jefferson, V. Demicheli, C. D. Pietrantonj, D. Rivetti, *Cochrane Database Syst. Rev.* **2006**. **DOI:**10.1002/14651858.CD001169.pub3
9. A. V. Veselovsky, A.S. Ivanov, *Curr. Drug Targets Infect. Disord.* **2003**. *3,* 33–40. **DOI:**10.2174/1568005033342145
10. J. Verma, V. M. Khedkar, E. C. Coutinho, *Curr. Top. Med. Chem.* **2010**, *10,* 95–115. **DOI:**10.2174/156802610790232260
11. S. Weaver, M. P. Gleeson, *Mol. Graph. Model.* **2008**, *26,* 1315–1326. **DOI:**10.1016/j.jmgm.2008.01.002
12. A. Lavecchia, C. D. Giovanni, *Curr. Med. Chem.* **2013**, *20,* 2839–2860. **DOI:**10.2174/09298673113209990001
13. K. Nikolic, L. Mavridis, T. Djikic, J. Vucicevic, D. Agbaba, K.

Yelekci, J. B. O. Mitchell, *Front. Neurosci*. **2016**, *10,* 265–296. **DOI:**10.3389/fnins.2016.00265
14. M. Asadollahi-Baboli, A. Mani-Varnosfaderani, *Med. Chem. Res*. **2013**, *22,* 1700–1710. **DOI:**10.1007/s00044-012-0175-y
15. Y. Liu, F. Jing, Y. Xu, Y. Xie, F. Shi, H. Fang, M. Li, W. Xu, *Bioorg. Med. Chem*. **2011**, *7,* 2342–2348. **DOI:**10.1016/j.bmc.2011.02.019
16. H. U. Weber, J. F. Fleming, J. Miquel, *Arch. Gerontol. Geriatr*. **1982**, *4,* 299–310. **DOI:**10.1016/0167-4943(82)90030-9
17. A. D. Beirami, Z. Hajimahdi, A. Zarghi, *Biomol. Struct. Dyn*. **2018**, *11,* 2999–3006. **DOI:**10.1080/07391102.2018.1502687
18. TRIPOS Associates, Inc. **2012**, Sybyl-X molecular modeling software packages, version 2.1.1. https://www.certara.com/pressreleases/certaraenhances-sybyl-x-drug-designand-discovery-software-suite/
19. H. Yuan, J. Zhuang, S. Hu, H. Li, J. Xu, Y. Hu, X. Xiong, Y. Chen, T. Lu, *Chem. Inf. Model* . **2014**, *9,* 2544–2554. **DOI:**10.1021/ci500268s
20. M. Clark, R. D. Cramer, N. V. Opdenbosch, *Comput. Chem*. **1989**, *8,* 982–1012. **DOI:**10.1002/jcc.540100804
21. H. Hong, H. Fang, Q. Xie, R. Perkins, D. M. Sheehan, W. Tong, *SAR QSAR Environ Res*. **2003**, *18,* 373–388 **DOI:**10.1080/1062936031000162396
22. A. Zieba, T. Laitinen, J. Z. Patel, A. Poso, A. A. Kaczor, *Int. J. Mol. Sci*. **2021**, *22,* 6108–6124. **DOI:**10.3390/ijms22116108
23. L. STAHLE, S. WOLD, *Prog. Med. Chem*. **1988**, *25,* 291–338. **DOI:**10.1016/S0079-6468(08)70281-9
24. M. Baroni, G. Costantino, G. Cruciani, D. Riganelli, R. Valigi, S. Clementi, *Quant. Struct.-Act. Rel.* **1993**, *12,* 9–20. **DOI:**10.1002/qsar.19930120103
25. L. El Mchichi, A. El Aissouq, R. Kasmi, A. Belhassan, R. El-Mernissi, A. Ouammou, T. Lakhlifi, M. Bouachrine, *Mater. Today: Proc*. **2021**, *45,* 7661–7674. **DOI:**10.1016/j.matpr.2021.03.152
26. A. Golbraikh, A. Tropsha, *Mol. Graph. Model.* **2002**, *20,* 269–276. **DOI:**10.1016/S1093-3263(01)00123-1
27. R. Veerasamy, H. Rajak, A. Jain, S. Sivadasan, C. P. Varghese, R. K. Agrawal, *Int. J. Drug Discov*. **2011**, *3,* 511–519.
28. K. Roy, *Expert. Opin. Drug. Deliv.* **2007**, *2,* 1567–1577. **DOI:**10.1517/17460441.2.12.1567
29. C. Rucker, G. Rucker, M. Meringer, *Chem. Inf. Model*. **2007**, *47,* 2345–2357. **DOI:**10.1021/ci700157b
30. R. Dias, W. F. D. Azevedo Jr, *Curr. Drug. Targets*, **2008**, *9,* 1040–1047. **DOI:**10.2174/138945008786949432
31. J. Fan, A. Fu, L. Zhang, *Quant. Biol*. **2019**, *2,* 83–89. **DOI:**10.1007/s40484-019-0172-y
32. F. D. Prieto-Martínez, E. L. Lopez, K. E. J. Mercado, J. L. Medina-Franco, *In Silico Drug Des.* **2019**, *20,* 19–44. **DOI:**10.1016/B978-0-12-816125-8.00002-X
33. O. Trott, A. J. Olson, *Comput. Chem.* **2009**, *31,* 455–466. **DOI:**10.1002/jcc.21334
34. V. Temml, Z. Kutil, *Comput. Struct. Biotechnol. J*. **2021**, *19,* 1431–1444. **DOI:**10.1016/j.csbj.2021.02.018
35. B. Acharya, S. Ghosh, H. K. Manikyam, *Pharm. Sci. Res*, **2016**, *6,* 2699–2719. **DOI:**10.13040/IJPSR.0975-8232.7(6).2699-19
36. Q. Tan, L. Duan, Y. Ma, F. Wu, Q. Huang, K. Mao, W. Xiao, H. Xia, S Zhang, E. Zhou, P. Ma, S. Song, Y. Li, Z. Zhao, Y. Sun, Z. Li, W. Geng, Z. Yin, Y. Jin, *Bioorg. Chem*. **2020**, *104,* 104257–104257. **DOI:**10.1016/j.bioorg.2020.104257
37. D. Seeliger, B. L. G. Groot, *J. Comput. Aided. Mol. Des*. **2010**, 24, 417–422. **DOI:**10.1007/s10822-010-9352-6
38. G. M. Morris, D. S. Goodsell, R. S. Halliday, R. Huey, W. E. Hart, R. K. Belew, A. J. Olson, *Comput. Chem*. **1998**, *14,* 1639–1662. **DOI:**10.1002/(SICI)1096-987X(19981115)19:14<1639::AID-JCC10>3.0.CO;2-B
39. S. Sharma, P. Kumar, R. Chandra: Molecular Dynamics Simulation of Nanocomposites Using BIOVIA Materials Studio, Lammps and Gromacs, **2019**, 39–100. **DOI:**10.1016/B978-0-12-816954-4.00007-3
40. A. Daina, O. Michielin, V. Zoete, *Nature* **2017**, *7,* 42717–42720. **DOI:**10.1038/srep42717
41. P. Banerjee, A. O. Eckert, A. K. Schrey, R. Preissner, *Nucleic Acids Res.* **2018**, *46,* 257–263. **DOI:**10.1093/nar/gky318
42. Benfenati E, Manganaro A, Gini G. **2013**, *1107,* 21–28. http://www.vegahub.eu/portfolio-item/vega-qsar/. Accessed 12 April 2019
43. A. Zieba, T. Laitinen, J. Z. Patel, A. Poso, A. A. Kaczor, *Int. J. Mol. Sci.* **2021**, *22,* 6108–6114. **DOI:**10.3390/ijms22116108
44. G. F. Selvaraj, S. Piramanayagam, V. Devadasan, S. Hassan, K. Krishnasamy, S. Srinivasan, *Inform. Med. Unlocked* **2020,** *18,* 100284–10095. **DOI:**10.1016/j.imu.2019.100284

Povzetek

Cilj te raziskave je bil ustvariti model 3D-QSAR CoMFA za nabor petindvajsetih zaviralcev nevraminidaze, ki vsebujejo derivate tiazolidin-4-karboksilne kisline, in identificirati nov močan zaviralec nevraminidaze za zdravljenje gripe. Statistični parametri generiranega modela so odlični: Q2 = 0,708, R2 = 0,997. Rezultati zunanje validacije so bili (r^2_0 = 0.922, K = 1.016, R^2_{pred} = 0.674, r^2_m = 0.778), kar kaže, da ima izdelani model dobro napovedno vrednost. Na podlagi konturne karte modela CoMFA smo predlagali šest novih spojin z večjo inhibitorno aktivnostjo za nevraminidazo kot najbolj aktivna spojina. Te spojine smo s tehniko molekulskega sidranja ugnezdili v nevraminidazo, da bi analizirali interakcije z aktivnim mestom encima. Ugotovili smo, da so vse predlagane molekule bolj stabilno ugnezdene v aktivno mesto nevraminidaze kot referenčna molekula (1SJ). Uporabili pa smo tudi tehniko SwissADME za oceno farmakokinetičnih lastnosti vsake predlagane molekule, medtem ko smo za raziskovanje morebitne toksičnosti uporabili tehniki ProToxII in VEGA QSAR. Na koncu opisujemo reakcijski mehanizem za sintezo šestih predlaganih spojin, ki bi ga lahko še dodatno proučili pri iskanju novih inhibitorjev nevraminidaze. Ta študija je identificirala potencialne kandidate za razvoj učinkovitejših zaviralcev nevraminidaze za zdravljenje gripe.

Scientific paper

Investigating the Polyphenolic Profile and the Antioxidant and Antibacterial Activity of Tarragon (*Artemisia Dracunculus L*) Cultivated in Central Romania

Ramona Maria (Iancu) Cristea[1] and Daniela Maria Șandru[2]

[1] *Department of Agricultural Sciences and Food Engineering, Lucian Blaga University of Sibiu, Doctor Ion Rațiu 7, 550012 Sibiu, Romania*

[2] *Department of Agricultural Sciences and Food Engineering, Lucian Blaga University of Sibiu, Doctor Ion Rațiu 7, 550012 Sibiu, Romania*

* *Corresponding author: E-mail: daniela.sandru@ulbsibiu.ro, ramona.cristea@ulbsibiu.ro Tel.: +40 743 915 240, +40 755 108 317*

Received: 05-04-2023

Abstract

The chemical composition, the antioxidant and antibacterial properties of *Artemisia dracunculus* L. leaves were examined through the utilization of four solvents for extraction. These solvents included ultrapure water, ethanol, methanol and acetic acid. The values reached for total polyphenols were between 77.2 mg gallic acid equivalent (GAE)/g for the acetic acid extracts and 192.1 mg GAE/g for the methanolic extracts. The total flavonoids were identified at 46.4 mg quercetin equivalent (QE)/g for the acetic acid extracts and 126.4 mg QE/g for the methanolic extracts. The IC50 antioxidant capacity values determined by the 2,2-diphenyl-2-picrylhydrazyl (DPPH) method were between 14.66 μg/mL (acetic acid extracts) and 20.33 μg/mL (methanolic extracts). 23 phenolic compounds were identified using the High Performance Liquid Chromatography (HPLC) method. The methanolic and the aqueous extracts have on very good antibacterial activity on the *Staphylococcus aureus 231* and *Enterococcus faecalis 428* strains. *A. dracunculus* L. leaf extracts are rich in a diverse range of valuable active chemical and biological compounds.

Keywords: polyphenols, antioxidant, antibacterial, phenolic compounds, tarragon.

1. Introduction

Tarragon (*Artemisia dracunculus* L.) is a perennial herbaceous plant that originated from the Nordic hemisphere and has spread across Europe, Central and Eastern Asia, India, Western North America and Southern to Northern Mexico.[1,2] It belongs to the *Artemisia* genus, which encompasses 500 species, each with distinct aromas and unique biological properties. With a height that can reach up to 150 cm, tarragon has a tall, branching stem adorned with lanceolate leaves that emit a delightful fragrance. The plant also produces whitish flowers. In Europe, tarragon is primarily cultivated and utilized either in its fresh or dried form for its aromatic qualities in culinary applications and traditional or complementary medicine.[4–6] When grown to maturity and during inflorescence periods, tarragon thrives and can yield significant harvests.

Artemisia species are rich in compounds with therapeutic properties against diseases such as malaria, hepatitis, cancer, diabetes, depression, seizures, inflammation, and fungal, bacterial, or viral infections.[7–13] The stems and leaves of *A. dracunculus* L. are used in international and traditional cuisine, while the flowers and other parts of the plant are used in alternative medicine.[14–17] Plant-based derivatives used as alternative medicines are in high demand, as these are considered safe and reliable compared to expensive synthetic drugs that come with secondary effects.

Herbs and spices contain many phytonutrients, viable sources of natural immunity-simulating antioxidants.[18–21] Of these, phenols are one of the countless general classes of naturally occurring vegetal metabolites; we presently know over 8,000 phenolic forms.[22–26]

A. dracunculus L. is rich in essential oils rich in flavonoids, phenolic acids, coumarins, sterols, fatty acids, alkamides and other valuable compounds that make tarra-

gon a useful plant.[7,27–35] The volatile compounds found in the plant are monoterpenoids, diterpenoids, triterpenoids, sesquiterpenoids, derivatives of phenylpropanes, polyacetylenes and others elements.[7,27,31,33,34,36–46] These compounds participate to the bioactive qualities of the different parts of the tarragon.

Thanks to this variety of volatile and phenolic compounds, tarragon has antioxidant[30,38,47], anticancer [45], hepatoprotective [47], immunomodulating[48] and antineoplastic properties, and can be used to treat gastritis, dermatitis, epilepsy, or various forms of allergies.[27,42,49–51]

Tarragon shows broad-spectrum antibacterial activity, including against human pathogens, such as *Pseudomonas aeruginosa, E. coli, S. aureus, Salmonella typhimurium, and S. epidermidis,* as well as *Proteus vulgaris*.[29,30,33,38,43.52–58] More than that, *A. dracunculus* L. has shown antifungal activity against certain fungal species, such as *Candida albicans, Cryptococcus neoformans, Aspergillus niger, Microsporum canis, Trichophyton rubrum, Microsporum gypseum,* and *Fonsecaea pedrosol*.[59–61]

2. Experimental

2. 1. *A. dracunculus* L. samples

This paper aims at showing the qualities of tarragon cultivated in the sub-mountainous area of the Sibiu depression in Central Romania, with a relief characterized by hills, river valleys, and terraces.

A. dracunculus L. plants were collected from the commune of Răşinari, with GPS coordinates of latitude: 45°42′0.00"N and longitude: 24°04′0.01"E at a 573 m altitude, the plantation having an area of 1 hectare. The samples were registered with voucher number 366 of the Microbiology Laboratory of the Research Centre in Biotechnology and Food Engineering (CCBIA) within the Faculty of Agricultural Sciences, Food Industry and Environmental Protection, "Lucian Blaga" University of Sibiu, Romania. The climate in the area is humid and cool, with more rainfall in June, which is favourable to rich, varied vegetation. The average annual temperature is 9.5 °C, with big variations throughout the day, with winds dominantly blowing from the South-Southwest, which makes snow melt faster thus influencing drought periods. Soils here are typical for premontane areas, varying from cambic chernozems to alluvial, clay-sandy soils.

The harvesting area exhibits a naturally low degree of fertility, with alluvial soils in various stages of evolution, slightly acidic. Improvement and fertilization work has been carried out, including the temporary removal of excess water. The predominant climate is characterized by a high frequency of temperate oceanic air coming from the west, especially during the warm season, and a low frequency of temperate continental air from the northeast and east. *A. dracunculus* L. is not a very demanding plant, so it develops well in these conditions, generating small, valuable, useful crops. The tarragon culture was founded with rooted cuttings, planted at 25 cm between them in parallel rows, at the end of April. Fertilization of the land was carried out in autumn with semi-fermented manure (40t/ha), no irrigation operations being necessary. Periodically the weeds were weeded, and the flower stalks were removed. The whole plants (stem with leaves) were collected on June 10, 2022, in the afternoon, stored in crates in a thin layer and transported to the laboratory on the same day. The leaves were separated from the stem and prepared for drying.

2. 2. Chemicals, Reagents, Bacterial Strains and Culture Media

We have used analytically pure reagents from Sigma-Aldrich GmbH, Steinheim, Germany: absolute ethanol 99.8%, methanol 99.9%, acetic acid 99.8%, Folin-Ciocalteu reagent, sodium carbonate 7.5%, sodium nitrite 5%, aluminum chloride 10%, sodium hydroxide 1M, DPPH/2,2,-difenil-2-picrilhidrazil, Trolox (6-hydroxy-2,5,7,8-tetramethylchroman-2- carboxylic acid), gallic acid (≥99%), quercetin (≥95%) , kaempferol (≥97%), luteolin (≥98%), apigenin (≥99%), davidigenin (≥99%), rutoside (≥94%), aridiodiol (≥98.5%), artemidine (≥98%), artidin (≥95%), coumarin (≥99%), herniarin (≥98%), scopoletin (≥97%), caffeic acid (≥98%), chicory acid (≥95%), chlorogenic acid (≥95%), p-coumaric acid (≥98%), ferulic acid (≥99%), syringic acid (≥95%), vanillic acid (≥97%), 2-methoxicinnamic acid (≥97%), 4,5-di-o-caffeoylquinic acid (≥90%), sakuranetin (≥95%).

We analysed the antibacterial activity of *A. dracunculus* L. extracts on six bacterial strains isolated in the Microbiology Laboratory (CCBIA/ULBS), of which three Gram-positive: *Clostridium perfringens 211, Enterococcus faecalis 428, Staphylococcus aureus 231,* and three Gram-negative: *Escherichia coli 29, Pseudomonas aeruginosa 323, Salmonella typhimurium 14*. We used specific growth media: Mueller Hinton agar, Mueller Hinton broth (Sigma-Aldrich GmbH, Steinheim, Germany), Cefoxitin Antimicrobial Susceptibility discs, 30 µg (Thermo Fisher Scientific™ Oxoid™)

2. 3. Methods

2. 3. 1. Extract Preparation

500g of *A. dracunculus* L. leaves are dried for three days in the Memmert incubator at 40 °C (until reaching a constant mass).

After drying, the leaves are ground to a particle size of 100–500 microns, resulting in a fine powder. Each 10g of powder is homogenized with 100 mL of the following solvents: ultrapure water, ethyl alcohol, and distilled water (in a 1:2 ratio), methanol and distilled water (in a 1:2 ratio), 9% v/v acetic acid. The extraction takes place in covered recipients, in the dark, at room temperature.

Periodically, the samples are homogenized on a magnetic stirrer, and after 24 hours, they are filtered using Whatman filter paper no. 54. The extraction process is repeated three times, and the resulting extracts are concentrated using the IKA RV 3 rotary evaporator at a rotation speed of 300 rpm, and finally weighed.

The dried powders are stored at 3 °C for analysis. The dry powders were resuspended in distilled water in a 1:1 ratio and methanol in a 1:1 ratio for the determinations.

2. 3. 2. Determining Total Polyphenol Contents (TPC)

To determine the total polyphenol contents, we used a slightly modified Folin-Ciocâlteu spectrophotometric method, i.e. homogenized 100 µL aqueous extract (1mg/mL concentration) with 2.5 mL ultrapure water, 100 µL Folin-Ciocâlteu reagent, and incubated for 10 minutes at room temperature. Then, we added 250 µL of 20% sodium carbonate, and incubated the samples again for 30 minutes at room temperature in the dark. We used a UV-1900 SHIMADZU spectrophotometer (Shimadzu Corporation, Kyoto, Japan) to read the samples at a wavelength of 760 nm and compared them to the control samples containing the same reagents, while the extract was replaced with distilled water. We used gallic acid for the calibration curve and expressed total polyphenol values in mg equivalent to gallic acid/g of dry extract. All determinations were performed in triplicate.[62]

2. 3. 3. Antioxidant Activity Assessment

The antioxidant activity involved testing compounds that have the ability to donate hydrogen or eliminate free radicals in the presence of DPPH (2,2-diphenyl-2-picrylhydrazyl) using a slightly modified spectroscopic method.[62] A stock methanolic solution of DPPH (25:100) is prepared by dissolving 25g of DPPH in 100 mL of methanol and stored at a temperature of –20 °C in the dark. From the stock solution, a working solution is prepared in a ratio of 10:90. The working solution is obtained by homogenizing 10mL of the stock solution with 90mL of methanol. The samples are prepared in a ratio of 1:1 (dry extract:methanol). 20 µL of the sample is weighed and homogenized with 180µL of the working solution.

The mixture is left to react in the dark at a temperature of 20 °C. After 30 minutes, the absorbance is read using a UV-1900 SHIMADZU spectrophotometer at a wavelength of 515 nm. The control sample is obtained following the same procedure, with the extract replaced by methanol. A calibration curve is constructed using Trolox (6-hydroxy-2,5,7,8-tetramethylchroman-2- carboxylic acid), and the results are expressed in milligrams of Trolox equivalent per gram of dry substance (mg TE/g). The inhibition percentage (I) is calculated according to the equation:

$$\% I = \frac{Ab - Aa}{Ab} \times 100,$$

where Ab is the absorbance of the control, and Aa is the absorbance of the reaction between the sample and the radicals.

2. 3. 4. Determining Total Flavonoid Contents (TFC)

To determine total flavonoid contents, we used an adapted colorimetric method[63] by homogenizing 1 mL extract (1mg/mL concentration) with 0.5 mL of 5% $NaNO_2$. The samples were incubated at room temperature for 5 minutes, then we added 0.5 mL of 10% $AlCl_3 \cdot 6H_2O$. They were incubated again in the dark for 15 minutes, as we then added 2 ml of 1M NaOH. We used distilled water to dilute the samples to 10 mL, then read them at a wavelength of 510 nm using a UV-1900 SHIMADZU spectrophotometer. We used quercetin for the calibration curve and expressed the results in mg equivalent to quercetin/g of dry extract (QE/g). All determinations were performed in triplicate.

2. 3. 5. Quantifying Phenolic Compounds Through HPLC

We used a slightly modified HPLC method[63] to identify valuable phenolic compounds in tarragon extracts with an Agilent 1200 device (Agilent Technologies, Santa Clara, CA, USA) equipped with a quaternary pump, automatic injector, and PDS (photo diode system) detector. We set the device to read at the wavelengths: λ = 280 nm, 320 nm, 360 nm. We used a 250 mm × 4.6 mm i.d. and 5.0 µm p.s. C18 Zorbax chromatography column, with a sample injection volume of 20 µL. We used 95/5 v/v water/acetic acid solution as eluent A, and a 100/5/95 v/v/v acetonitrile/water/acetic acid solution as eluent B. The mobile phase was degassed at 22°C for 15 minutes as we established an extraction scheme with the following gradient profile: 0–15 min, 20% B; 15–30 min, 30% B; 30–45 min, 40% B; 40–70 min, 50% B; 70–75 min, 55% B; 75–80 min, 95% B; 80–85 min, 100% B; 85–90 min, 10% B. The resulting values were expressed in µg/g dry extract, as determinations were made on triplicate. To identify and quantify phenolic compounds, we compared the results obtained to the corresponding calibration curves (quercetin, kaempferol, luteolin, apigenin, davidigenin, rutoside, aridiodiol, artemidine, artidin, coumarin, herniarin, scopoletin, caffeic acid, chicory acid, chlorogenic acid, p-coumaric acid, ferulic acid, gallic acid, syringic acid, vanillic acid, 2-methoxicinnamic acid, 4,5-di-o-caffeoylquinic acid, sakuranetin).

2. 3. 6. Determining Antibacterial Activity (MIC) / Disk Diffusion and Serial Dilution Test

Minimum inhibitory concentration (MIC) is frequently used in microbiology to test whether certain ex-

tracts or compounds can halt the development of microorganisms and to use this information in the field. We activated the bacteria in Mueller Hinton media at 37 °C for 24 hours and brought the inoculum to a density of 0.5 McFarland = 1.5×10^8 Colony Forming Units (CFU)/mL. To do so, we obtained serial dilutions of the extract under analysis, from 2000 µg/mL, 1000 µg/mL, 500 µg/mL, 250 µg/mL, 125 µg/mL, 62.5 µg/mL, to 31.25 µg/mL. Using a pipette, we dropped 10 µL of diluted extract to a disk placed in the Petri dished containing Mueller Hinton solidified culture media covered with the microorganism under analysis (*Clostridium perfringens 211, Enterococcus faecalis 428, S. aureus 231, E. coli 29, Pseudomonas aeruginosa 323, Salmonella typhimurium 14*). The plates were incubated at 37°C for 24 hours, then we analysed the antibacterial activity of the extracts. The lowest extract concentration that inhibited bacteria growth was considered the minimum inhibitory concentration (MIC). We used cefoxitin disks (30 µg) as a positive control.

2. 3. 7. Statistical Analysis

The results obtained are the mean of three determinations, including the standard deviation of the measurements (± standard deviation/SD). We used a one-way analysis of variance (ANOVA), with a statistical significance of $p \leq 0.05$.

3. Results and Discussion

3. 1. Total Phenolic, Antioxidant Activity and Flavonoid Content

The findings presented in Table 1 demonstrate variations in the polyphenol concentrations of tarragon leaf extracts based on the solvent used for extraction. Water, being a polar solvent, has a limited ability to extract compounds with high polarity. Conversely, the inclusion of solvents like methanol or ethanol enhances the extraction process, resulting in a noteworthy increase in the concentration of measurable phenolic compounds.

Polyphenols can be extracted using various methods, and the efficiency of these processes or the solvents used can be correlated with the plant material and the structure of phenolic compounds. They are abundantly present in the natural environment, comprising different parts of plants, as is the case with samples of *A. dracunculus* L. Polyphenols determined in the methanolic extracts obtained from the leaves of *A. dracunculus* L. showed values of 192.1 ± 5.3 mg GAE/g dry weight (d.w.), which were the most significant in terms of quantity. In the aqueous extracts, 168.3 ± 2.7 mg GAE/g d.w were identified and quantified, while the alcoholic extracts were, on average, 48% lower. The lowest values were observed in the case of acetic acid extracts, where they did not exceed an average of 77.2 ± 1.4 mg GAE/g d.w. The polyphenol values of tarragon were also found in methanolic extracts (2681 ± 0.12 mg GAE/g d.w.)[26] as well in ethanolic extracts (167.20 ± 21.32 µg rutin/mg extract).[28] The antioxidant activity characterizes an extract by looking at how its bioactive components can impact various medical.[30,65] In the case of the extracts in this research, the highest values were identified in methanolic extracts, with a mean DPPH of 76.4 ± 0.4 % and an IC_{50} of 20.3 ± 0.2 µg/ml. The lower the IC_{50}, the higher the extract's antioxidant capacity.

Many studies described the antioxidant potential of *A. dracunculus* L, as they all reached the same conclusion that this is a direct result of the concentration of polyphenols extracted.[30,65] Other studies found a connection between total polyphenol contents (24.10 mg GAE/g d.w.), total flavonoid contents (20 mg QE/g), and the DPPH test with IC_{50} levels of 65.50 µg/mL[38]. Significant levels of polyphenols were also found in hydroethanolic extracts (197.22 mg GAE/g d.w.), as their antioxidant activity determined using DPPH and ABTS tests was high. The antioxidant activity of tarragon reached IC_{50} levels of 1.15 mg/mL for DPPH and 0.17 mg/mL for ABTS, while in the case of ascorbic acid, used as a control sample, the values determined were 0.002 mg/mL for DPPH and 0.005 mg/mL for ABTS.[42,47,66] Flavonoids are a major component found in *A. dracunculus* L. extracts, playing a significant role as the configuration of natural antioxidants in plants.[65,67,68]

As per Table 1, flavonoid contents found in *A. dracunculus* L. extracts fall between 46.4 ± 0.1 mg QE/g d.w. and 126.4 ± 0.3 mg QE/g d.w. The type of solvent used for extraction influences the level of flavonoids. The methanolic extracts were found to contain the highest amounts

Table 1. Total polyphenol contents, antioxidant activity and flavonoid contents identified in *A. dracunculus* L. leaf extracts.

	Aqueous extract	Ethanolic extract	Methanolic extract	Acetic acid extract
Total phenolic content (mg GAE/g d.w.) ± SD[a]	168.3 ± 2.7	113.9 ± 1.9	192.1 ± 5.3	77.2 ± 1.4
DPPH scavenging activity (%) ± SD[b]	51.1 ± 0.6	44.2 ± 0.4	76.4 ± 0.4	41.9 ± 0.3
IC_{50} µg/mL ± SD[c]	17.4 ± 0.2	16.1 ± 0.3	20.3 ± 0.2	14.6 ± 0.3
TE (mg/g dry extract) ± SD[d]	683 ± 29	667 ± 31	761 ± 45	567 ± 31
Total flavonoid content (mg QE/g d.w.) ± SD[e]	92.1 ± 0.2	88.4 ± 0.2	126.4 ± 0.3	46.4 ± 0.1

GAE-gallic acid equivalent; [b]DPPH-2,2-diphenyl-2-picrylhydrazyl; [c]IC_{50} -the concentration at which a substance exerts half of its maximal inhibitory effect; [d]TE-Trolox equivalent; [e]QE -quercetin equivalent, SD-standard deviation, $p \leq 0.05$.

of flavonoids (126.4 ± 0.3 mg QE/g d.w), followed by water-based extracts (92.1 ± 0.2 mg QE/g d.w.). Ethanolic extracts showed 88.4 ± 0.2 mg QE/g d.w, while acetic acid extracts have significantly lower flavonoid contents (46.4 ± 0.1 mg QE/g d.w).

Through the ANOVA test it was established that there are differences in the case of the independent variable, the post hoc test demonstrating that they vary depending on the solvent used.

The scientific literature confirms the fact that *A. dracunculus* L. contains flavonoids, as these were determined at levels of 50.40 ± 1.60 mg RE/g d.w.[65], 48.84 ± 2.04 μg rutin/mg extract[28], 31.90 ± 0.03 mg/g.[30]

3. 2. Quantifying Phenolic Compounds Through HPLC Analysis

A. dracunculus L. leaf extracts contain valuable phenolic compounds in amounts that vary depending on the solvent used. The extracts are rich in luteolin (116.20 ± 5.55 μg/g d.w. –342.19 ± 7.78 μg/g d.w.). The methanolic extracts presents the highest concentrations. We have also identified and quantified herniarin and chlorogenic acid, at levels between 41.20 ± 0.77 μg/g d.w. and 66.81 ± 0.91 μg/g d.w., as well as 25.21 ± 0.98 μg/g d.w. and 34.14 ± 0.77 μg/g d.w. respectively. Water-based extracts were found to contain the highest amount of chlorogenic acid, followed by ethanolic extracts. Furthermore, Table 2 shows that the extracts contain significant amounts of quercetin (6.11 ± 0.15 μg/g d.w. –18.22 ± 0.26 μg/g d.w.), as well as kaemferol, with recorded values between 1.03 ± 0.07 μg/g d.w. and 5.22 ± 0.27 μg/g d.w. Phenolics acids were found at levels over 10 μg/g d.w. in close values for water-based, ethanolic and methanolic extracts to caffeic acid, gallic acid, and vanillic acid. Ferulic acid was determined at a maximum level of 5.12 ± 0.16 μg/g d.w. in methanolic extracts, while syringic acid in water-based extracts (13.20 ± 0.45 μg/g d.w.).

Scopoletin and 2-methoxicinnamic acid were found in all types of extracts, with highest levels in methanolic ones. Subunit values were determined in the case of compounds like apigenin, artemidine, aridiodiol present in water-based, ethanolic, and methanolic extracts.

These compounds were only found in acetic acid extracts. Traces of davidigenin and rutoside were determined in water-based extracts, while artidin and sakuranetin were not found in any of the samples under analysis. In scientific literature, flavonoids and coumarins were found by more studies, while phenolic acids were determined in various amounts, depending on the area where the plant originated, the extraction method, or the equipment used to investigate the compounds.[65,27–31]

Through the ANOVA test it was established that there are differences in the case of the independent variable, the post hoc test demonstrating that they vary depending on the solvent used.

Table 2. Phenolic compounds identified and quantified in *A. dracunculus* L. leaf.

Compound	Aqueous extract μg/g d.w.[a]	Ethanolic extract μg/g d.w.[a]	Methanolic extract μg/g d.w.[a]	Acetic acid extract μg/g d.w.[a]
apigenin	0.15 ± 0.01	0.21 ± 0.03	0.25 ± 0.02	n.d.
artemidine	0.06 ± 0.01	0.07 ± 0.01	0.07 ± 0.01	n.d.
davidigenin	tr	0.04 ± 0.01	0.05 ± 0.01	n.d.
kaempherol	2.28 ± 0.16	5.14 ± 0.21	5.22 ± 0.27	1.03 ± 0.07
luteolin	278.11 ± 6.24	302.20 ± 7.21	342.19 ± 7.78	116.20 ± 5.55
rutoside	tr	0.02 ± 0.01	0.02 ± 0.01	n.d.
quercetin	18.22 ± 0.26	12.33 ± 0.51	15.81 ± 0.66	6.11 ± 0.15
artidin	n.d	n.d	n.d	n.d
aridiodiol	0.04 ± 0.01	0.05 ± 0.01	0.07 ± 0.01	n.d.
coumarin	24.23 ± 0.34	29.00 ± 0.61	32.77 ± 0.65	20.23 ± 0.34
herniarin	45.45 ± 1.01	59.37 ± 0.87	66.81 ± 0.91	41.20 ± 0.77
scopoletin	3.05 ± 0.44	1.21 ± 0.43	3.44 ± 0.56	1.40 ± 0.22
caffeic acid	19.23 ± 1.12	19.21 ± 1.05	18.99 ± 1.02	10.21 ± 1.01
2-methoxicinnamic acid	1.29 ± 0.14	1.98 ± 0.28	2.99 ± 0.26	0.79 ± 0.06
4,5-di-o-caffeoylquinic acid	0.01 ± 0.12	0.17 ± 0.01	0.27 ± 0.01	n.d.
chicory acid	1.62 ± 0.08	0.98 ± 0.12	2.99 ± 0.15	n.d.
chlorogenic acid	34.14 ± 0.77	31.44 ± 0.75	27.26 ± 0.78	25.21 ± 0.98
p-coumaric acid	4.88 ± 0.25	3.56 ± 0.21	4.78 ± 0.28	3.84 ± 0.32
gallic acid	14.11 ± 0.32	12.00 ± 0.24	12.04 ± 0.16	10.07 ± 0.25
ferulic acid	4.99 ± 0.26	4.72 ± 0.22	5.12 ± 0.16	3.45 ± 0.29
syringic acid	13.20 ± 0.45	13.11 ± 0.54	11.21 ± 0.47	7.77 ± 0.23
sacuranetin	n.d.	n.d.	n.d.	n.d.
vanillic acid	14.22 ± 0.46	15.98 ± 0.65	16.12 ± 0.31	10.56 ± 0.11

[a] data expressed as mean ± standard deviation of triplicate, tr.-trace, n.d.-not detected, $p \leq 0.05$

3. 3. Determining Antibacterial Activity (MIC)

The antimicrobial activity of *A. dracunculus* L. extracts differ depending on how it is extracted, and the type of strain tested. As per Table 3, Gram-positive bacteria are more sensitive to the active biological compounds in the extracts, showing lower MIC values than Gram-negative strains. In the case of the *Clostridium perfringens 211* strains, MIC values fell between 62.5 μg/mL for methanolic extracts, which are richer in phenolic compounds, and 250 μg/mL in the case of acetic acid extracts. *Enterococcus faecalis 428* reacts with a MIC value of 31.25 μg/mL to methanolic extracts, 62.5 μg/mL to aqueous extracts and with a MIC value of 125 μg/mL to ethanolic and acetic acid extracts. The *S. aureus 231* strains is the most sensitive to the antibacterial action of *A. dracunculus* L. extracts, with MIC values of 31.25 μg/mL for water-based and methanolic extracts, and 62.5 μg/mL to ethanolic ones. Gram-negative bacteria are more resistant to the antibacterial action of these extracts, recording values between ≥1000 μg/mL and ≥2000 μg/mL in the case of *E. coli 29* and *Pseudomonas aeruginosa 323,* and 250 μg/mL and ≥1000 μg/mL in the case of *Salmonella typhimurium 14.* We benchmarked these strains with cefoxitin, which showed MIC values between 31.25 μg/mL and 125 μg/mL. anolic extracts exhibited higher levels of polyphenols and flavonoids, despite water-based extracts being more commonly employed in traditional medicine. On the other hand, acetic acid extracts yielded the lowest results, making it an unfavorable solvent choice. These compounds contribute to the extracts' notable antioxidant activity, suggesting that tarragon could serve as a valuable source of metabolites.

Furthermore, the study demonstrated that extracts of *A. dracunculus* L. possess potent antimicrobial properties, particularly towards Gram-positive bacteria. However, their efficacy against Gram-negative bacteria was comparatively weaker. This disparity can be attributed to the structural differences in the cellular composition of these bacteria. The presence of a lipopolysaccharide layer, varying in proportions between Gram-positive and Gram-negative bacteria, likely affects the absorption of vital elements, thereby influencing the antimicrobial activity observed. LPS is the major component of the outer membrane of Gram-negative bacteria, contributing greatly to the structural integrity of the bacteria and protecting the membrane from certain types of chemical attack. Showing the above characteristics tarragon plants can be useful as a food/condiment or as an ingredient in natural supplements.

Table 3. Antimicrobial activity of four different *A. dracunculus* L. extracts (MIC, μg/mL).

Strains	Aqueous extract	Ethanolic extract	Methanolic extract	Acetic acid extract	Cefoxitin
Clostridium perfringens 211	125	125	62.5	250	31.25
Enterococcus faecalis 428	62.5	125	31.25	125	31.25
Staphylococcus aureus 231	31.25	62.5	31.25	125	31.25
Escherichia coli 29	≥2000	≥2000	≥1000	≥2000	62.5
Pseudomonas aeruginosa 323	≥1000	≥1000	≥1000	≥2000	125
Salmonella typhimurium 14	500	250	250	≥1000	62.5

The antibacterial and antifungal action of *A. dracunculus* L. extracts were analysed in more studies. These looked at the plant's activity in both solvent-based extracts and essential oils, and their results confirmed the antibacterial properties of tarragon.[25,33,43,54] Not all bacterial strains showed sensitivity to the compounds of *A. dracunculus* L., for some studies proved lack of reactivity in the case of *E. coli* or *Yersinia enterocolitica*. MIC values were determined from 1 mg/mL to 32 mg/mL for *S. pyogenes, S. aureus, B. subtilis, B. cereus, E. coli P. vulgaris, P. aeruginosa,* getting the best results in the case of *S. pyogenes, S. aureus, B. subtilis,* (1 mg/mL, 2 mg/mL) and lowest values for *P. aeruginosa* (32 mg/mL).[38]

4. Conclusions

The findings of this study reveal that tarragon extracts contain beneficial phenolic compounds; however, it is important to consider the extraction solvent used. Meth-

5. References

1. J. C. Fernández-Lizarazo, T. Mosquera-Vásquez, C. Bernardo, F. Sarmiento, *Agron. Colomb.* **2011**, *29,* 387–397.
2. R. S. Chauhan, S. Kitchlu, G. Ram, M. K. Kaul, A. Tava, *Ind. Crops Prod.* **2010**, *31*, 546–549. **DOI:**10.1016/j.indcrop.2010.02.005
3. R. N. Ĕ. Wierdak, G. ZawiĞlak, *Acta Sci Pol* **2014**, *13*, 207–221.
4. D. Jadczak, M. Grzeszczuk, *J. Elementol.* **2008**, *13,* 221–226.
5. G. Zawislak, K. Dzida, *J. Elementol.* **2012**, *17,* 721–729. **DOI:**10.5601/jelem.2012.17.4.14
6. N. S. Alzoreky, K. Nakahara, *IntJ Food Microbiol* **2003**, *80,* 223–230. **DOI:**10.1016/S0168-1605(02)00169-1
7. H. Ekiert, J. Świątkowska, E. Knut, P. Klin, A. Rzepiela, M. Tomczyk, A. Szopa, *Frontiers in Pharmacology* **2021**, *12*, 1–18. **DOI:**10.3389/fphar.2021.653993
8. M. Willcox, *J. Altern. Complement. Med.* **2009**, *15*, 101–109. **DOI**:10. 1089/act.2009.1530910.1089/acm.2008.0327
9. J. Wang, A. E. Fernández, S. Tiano, J. Huang, E. Floyd, A. Poulev, et al., *Oxidative Med. Cell Longevity* **2018**, 1–9.

DOI:10.1155/2018/7418681
10. K. S. Bora, A. Sharma, *Pharm. Biol.* **2011**, *49*, 101–109. **DOI:**10.3109/13880209.2010.497815
11. A. Eidi, S. Oryan, J. Zaringhalam, M. Rad, *Pharm. Biol.* **2016**, *54*, 549–554. **DOI:**10.3109/13880209.2015.1056312
12. S. W. Eisenman, A. Poulev, L. Struwe, I. Raskin, D. M. Ribnicky, *Fitoterapia* **2011**, *82*, 1062–1074. **DOI:**10.1016/j.fitote.2011.07.003
13. M. Sayyah, L. Nadjafnia, M. Kamalinejad, *J. Ethnopharmacol.* **2004**, *94*, 283–287. **DOI:**10.1016/j.jep.2004.05.021
14. R. S. Chaleshtori, N. Roknib, M. Rafieian-Kopaeic, M., Dreesd, F., Sharafati-Chaleshtoric, E. Salehic, *Italian Journal of Food Science* **2014**, *26*, 427–432.
15. B. Çorapcı, B. Köstekli, A. Eyüboglu, D. Kocatepe, *J. Food Process. Preserv.* **2020**, *44*, e14751. **DOI:**10.1111/jfpp.14751
16. M. Méndez-del Villar, A. M. Puebla-Pérez, M. J. Sánchez-Peña, L. J. González-Ortiz, E. Martínez-Abundis, M. González-Ortiz, *J. Med. Food* **2016**, *19*, 481–485. **DOI:**10.1089/jmf.2016.0005
17. D. M. Ribnicky, A. Poulev, J. O'Neal, G. Wnorowski, D. E. Malek, R. Jäger, R., et al., (2004). *Food Chem. Toxicol.* **2004**, *42*, 585–598. **DOI:**10.1016/j.fct.2003.11.002
18. N. Erkan, G. Ayranci, E. Ayranci, *Food Chem.* **2008**, *110*, 76–82. **DOI:**10.1016/j.foodchem.2008.01.058
19. H. Safari, G. Anani Sarab, M. Naseri, *Nutr. Neurosci.* **2019**, *24*, 1–7. **DOI:**10.1080/1028415X.2019.1681742
20. S. Kordali, R. Kotan, A. Mavi, A. Cakir, A. Ala, A. Yildirim, *J. Agric. Food Chem.* **2005**, *53*, 9452–9458. **DOI:**10.1021/jf0516538
21. B. Koul, P. Taak, *J. Glycomics Lipidomics* **2017**, *07*, 142. **DOI:**10.4172/2153-0637
22. D. M. Pereira, P. Valentao, J. A. Pereira, P. B. Andrade, *Molecules* **2009**, *14,* 2202–2211. **DOI:**10.3390/molecules14062202
23. J. Dai, R. J. Mumper, *Molecules* **2010**, *15,* 7313–7352. **DOI:**10.3390/molecules15107313
24. I. U. R. Tak, D. Mohiuddin, B. A. Ganai, M. Z. Chishti, F. Ahmad, J. S. Dar, *Afr. J. Plant Sci.* **2014**, *8*, 72–75. **DOI**:10.5897/AJPS2013. 1145
25. O. Sagdic, A. Karahan, M. Ozcan, G. Ozkan, *Food Sci. Technol. Int.* **2003**, *9*, 353–358. **DOI:**10.1177/1082013203038976
26. S. Ceylan, B. Harsit, O. Saral, M. Ozcan, E. Sonmez, *Medical Science and Discovery* **2018**, *5*, 245–252. **DOI:**10.17546/msd.419536
27. D. Obolskiy, I. Pischel, B. Feistel, N. Glotov, M. Heinrich, *J. Agric. Food Chem.* **2011**, *59*, 11367–11384. **DOI:**10.1021/jf202277w
28. R. Jahani, D. Khaledyan, A. Jahani, E. Jamshidi, M. Kamalinejad, M. Khoramjouy, et al., *Res. Pharm. Sci.* **2019**, *14*, 544–553. **DOI:**10.4103/1735-5362.272563
29. M. Majdan, A. K. Kiss, R. Hałasa, S. Granica, E. Osinska, M. E. Czerwińska, (2020). *Front. Pharmacol.* **2020**, *11*, 947. **DOI:**10.3389/fphar.2020.00947
30. A. Ribeiro, L. Barros, R. C. Calhelh, M. Carocho, A. Ćirić, M. Sokovic, M. M. Dias, C. Santos-Buelga, M. F. Barreiro, I. C. F. R. Ferreira, *Journal of Functional Foods* **2016**, *26*, 268–278. **DOI:**10.1016/j.jff.2016.08.019
31. A. M. Aglarova, I. N. Zilfikarov, O. V. Severtseva, *Pharm. Chem. J.* **2008**, *42*, 81–86. **DOI:**10.1007/s11094-008-0064-3
32. T. Aydin, H. Akincioglu, M. Gumustas, I. Gulcin, C. Kazaz, A. Cakir, (2020). *Z. Naturforsch. – Sect. C J. Biosci.* **2020**, *75*, 459–466. **DOI:**10.1515/znc-2019-0227
33. F. Abdollahnejad, F. Kobarfard, M. Kamalinejad, H. Mehrgan, M. Babaeian, *J. Essent. Oil Bearing Plants* **2016**, *19*, 574–581. **DOI:**10.1080/0972060X.2014.963167
34. A. Karimi, J. Hadian, M. Farzaneh, A. Khadivi-Khub, *Ind. Crops Prod.* **2015**, *65*, 315–323. **DOI:**10.1016/j.indcrop.2014.12.003
35. E. Mateusz, F. S. Senderski, P. Leśna, A. Salimov, S. Numonov, M. Bakri, Z. Sangov, M. Habasi, *Nat. Prod. Comm.* **2020**, *15*, 1–7. **DOI**:10.1177/ 1934578X20977394
36. F. Ayoughi, M. Barzegar, M. A. Sahari, H. Naghdibadi, *J. Agric. Sci. Technol.* **2011**, *13*, 79–88.
37. S. Bedini, G. Flamini, F. Cosci, R. Ascrizzi, M. C. Echeverria, L. Guidi, et al., *Parasites Vectors* **2017**, *10*, 1–10. **DOI:**10.1186/s13071-017-2006-y
38. B. A. Behbahani, F. Shahidi, F. T. Yazdi, S. A. Mortazavi, M. Mohebbi, *Food Measure* **2017**, *11*, 847–863. **DOI:**10.1007/s11694-016-9456-3
39. M. Osanloo, A. Amani, H. Sereshti, M. R. Abai, F. Esmaeili, M. M. Sedaghat, *Ind. Crops Prod.* **2017**, *109*, 214–219. **DOI:**10.1016/j.indcrop.2017.08.037
40. M. Szczepanik, M. Walczak, B. Zawitowska, M. Michalska-Sionkowska, A. Szumny, C. Wawrzenczyk, et al., *J. Sci. Food Agric.* **2018**, *98*, 767–774. **DOI:**10.1002/jsfa.8524
41. R. W. Bussmann, K. Batsatsashvili, Z. Kikvidze, F. Khajoei Nasab, A. Ghorbani, N. Y. Paniagua-Zambrana, et al., in: K. Batsatsashvili, Z. Kikvidze, R. Bussmann (Eds.) Catalogue of Life, Cham, Switzerland, **2020**, pp. 131–146. **DOI:**10.1007/978-3-030-28940-9_16
42. F. S. Sharopov, A. Salimov, S. Numonov, et al., *Nat. Prod. Commun.* **2020**, *15*, 1–7. **DOI:**10.1177/1934578X20927814
43. M. I. Socaciu, M. Fogarasi, C. A. Semeniuc, S. A. Socaci, M. A. Rotar, V. Muresan, et al., *Polymers* **2020**, *12*, 1748. **DOI:**10.3390/polym12081748
44. R. Joshi, P. Satyal, W. Setzer, *Medicines* **2016**, *3*, 6. **DOI:**10.3390/medicines3010006
45. M. H. Navarro-Salcedo, J. I. Delgado-Saucedo, V. H. Siordia-Sánchez, L. J. GonzálezOrtiz, G. A. Castillo-Herrera, A. M. Puebla-Pérez, *J. Med. Food* **2017**, *20*, 1076–1082. **DOI:**10.1089/jmf.2017.0044
46. T. D. Bhutia, K. M. Valant-Vetschera, *Nat. Prod. Commun.* **2008**, *3*, 1289–1292. **DOI:**10.1177/1934578X0800300811
47. V. Zarezade, J. Moludi, M. Mostafazadeh, M. Mohammadi, A. Veisi, *Avicenna J. Phytomedicine* **2018**, *8*, 51–62. **DOI**:10.22038/ajp.2017.19137.1738
48. S. M. Abtahi Froushani, L. Zarei, H. Esmaeili Gouvarchin Ghaleh, B. Mansori Motlagh, *Avicenna J. Phytomedicine* **2016**, *6*, 526–534. **DOI**:10.22038/ajp.2016.6479
49. N. Mamedov, Z. Grdner, L. E. Craker, *J. Herbs Spices Med. Plants* **2004**, *11*, 191–222. **DOI:**10.1300/J044v11n01_07
50. M. Mohammadi, M. Saeb, S. Nazifi, *Comp. Clin. Pathol.* **2020**, *29*, 485–494. **DOI:**10.1007/s00580-019-03080-0

51. F. U. Alakbarov, *J. Herbal Pharmacother* **2001**, *1*, 35–49. **DOI:**10.1080/J157v01n03_04
52. T. Aydın, B. Yurtvermez, M., S¸entürk, C. Kazaz, A. Çakır, *Rec. Nat. Prod.* **2019***, 13*, 216–225. **DOI:**10.25135/rnp.102.18.07.329
53. J. Sharifi-Rad, J. Herrera-Bravo, P. Semwal, S. Painuli, H. Badoni, S.M. Ezzat, M.M. Farid, R.M. Merghany, N.M. Aborehab, M.A. Salem, S. Sen, K. Acharya, N. Lapava, M. Martorell, B. Tynybekov, D. Calina, W.C. Cho, *Oxid Med Cell Longev*, **2022. DOI:**10.1155/2022/5628601
54. M. Benli, I. Kaya, N. Yigit, *Cell Biochem. Funct.* **2007**, *25*, 681–686. **DOI:**10.1002/cbf.1373
55. D. Lopes-Lutz, D. S. Alviano, C. S., Alviano, P. P. Kolodziejczyk, *Phytochemistry* **2008**, *69,* 1732–1738. **DOI:**10.1016/j.phytochem.2008.02.014
56. M. Tajbakhsh, N. Soleimani, *Jorjani Biomed. J.* **2018**, *6*, 22–32. **DOI:**10.29252/jorjanibiomedj.6.1.22
57. S. G. Deans, K. P. Svoboda, *Horti. Sci. J.* **2015**, *63*, 503–508. **DOI:**10.1080/14620316.1988.11515884
58. R. S. Chaleshtori, N. Rokni, V. Razavilar, M. R. Kopaei, *Jundishapur J. Microbiol.* **2013**, *6*, 1–35. **DOI:**10.5812/jjm.7877
59. B. Teixeira, A. Marques, C. Ramos, N. R. Neng, J. M. F. Nogueira, J. A. Saraiva, M. L. Nunes, *Ind Crops Prod* **2013**, *43,* 587–595. **DOI:**10.1016/j.indcrop.2012.07.069
60. M. A. Zarasvand, M. Madani, M. Modaresi, *Jundishapur J. Nat. Pharm. Prod.* **2016**, *11*, 2–5. **DOI:**10.17795/jjnpp-29911
61. D. Obistioiu, R. T. Cristina, I. Schmerold, R. Chizzola, K. Stolze, I. Nichita, et al., *Chem. Cent. J.* **2014**, *8*, 6. **DOI:**10.1186/1752-153X-8-6
62. D. I. Stegarus, E. Lengyel, G. F. Apostolescu, O. R. Botoran, C. Tanase, *Plants* **2021**, *10*, 2710. **DOI:**10.3390/plants10122710
63. D. I. Popescu, E. Lengyel, F. G. Apostolescu, L. C. Soare, O. R. Botoran, N. A. Şuţan, *Horticulturae* **2022**, *8*, 952. **DOI:**10.3390/horticulturae8100952
64. D. I. Popescu, O. R. Botoran, R. Cristea, C. Mihaescu, N. A. Sutan, *Horticulturae* **2023**, *9*, 325. **DOI:**10.3390/horticulturae9030325
65. H. Mumivand, M. Babalar, L. Tabrizi, L. E. Craker, M. Shokrpour, J. Hadian, *Hortic. Environ. Biotechnol.* **2017**, *58*, 414–422. **DOI:**10.1007/s13580-017-0121-5
66. A. Rajabian, K. M. Hassanzadeh, S. A. Emami, N. Z. Tayarani, O. R. Rahimzadeh, J. Asili, *Jundishapur J Nat Pharm Prod.* **2017**, *12*, 323–325. **DOI:**10.5812/jjnpp.32325
67. R. A. Mustafa A. A. Hamid S. Mohamed F. A. Baka, *J Food Sci* **2010**, *75*, 28–35. **DOI:**10.1111/j.1750-3841.2009.01401.x
68. C. Proestos, I. S. Boziaris, G. J. E. Nychas, M. Komaitis, *Food Chem* **2006**, *95*, 664–671. **DOI:**10.1016/j.foodchem.2005.01.049

Povzetek

Kemijsko sestavo, antioksidativne in antibakterijske lastnosti listov *Artemisia dracunculus* L. so v raziskavi proučili z uporabo štirih topil za ekstrakcijo. Ta topila so vključevala ultra čisto vodo, etanol, metanol in ocetno kislino. Dosežene vrednosti skupnih polifenolov so bile med 77,2 mg ekvivalenta galne kisline (GAE)/g za ekstrakte z ocetno kislino in 192,1 mg GAE/g za metanolne ekstrakte. Skupni flavonoidi so znašali 46,4 mg ekvivalenta kvercetina (QE)/g za ekstrakte ocetne kisline in 126,4 mg QE/g za metanolne ekstrakte. Vrednosti IC50 antioksidativne zmogljivosti, določene z metodo 2,2-difenil-2-pikrilhidrazil (DPPH), so bile med 14,66 μg/ml (izvlečki ocetne kisline) in 20,33 μg/ml (metanolni izvlečki). Z metodo tekočinske kromatografije visoke ločljivosti (HPLC) je bilo identificiranih 23 fenolnih spojin. Metanolni in vodni izvleček sta imela zelo dobro antibakterijsko delovanje na seva *Staphylococcus aureus* 231 in *Enterococcus faecalis* 428. Ekstrakti listov *A. dracunculus* L. so bogati z raznolikim naborom dragocenih aktivnih kemičnih in bioloških spojin.

Scientific paper

Synthesis, Crystal Structures and Urease Inhibition of Copper(II) and Cobalt(III) Complexes Derived from (((2-(Pyrrolidin-1-yl)ethyl)imino)methyl)naphthalen-2-ol

Jian Jiang,[1,*] Peng Liang,[2] Yuxin Han,[1] Hui Zhang[1] and Zhonglu You[3]

[1] *College of Chemical Engineering and Machinery, Eastern Liaoning University, Dandong 118003, P. R. China*

[2] *School of Engineering and Technology, Eastern Liaoning University, Dandong 118003, P. R. China*

[3] *Department of Chemistry and Chemical Engineering, Liaoning Normal University, Dalian 116029, P. R. China*

* *Corresponding author: E-mail: jiangjiandd2012@126.com*

Received: 05-31-2023

Abstract

Three copper(II) and cobalt(III) complexes, $[CuL(dca)]_n$ (**1**), $[CuL(N_3)]_n$ (**2**) and $[CoL(N_3)_2(DMF)]$ (**3**), where L is the monoanionic form of the Schiff base (((2-(pyrrolidin-1-yl)ethyl)imino)methyl)naphthalen-2-ol (HL), and dca is dicyanamide, have been prepared and characterized by elemental analyses, IR and UV-Vis spectroscopy, as well as single crystal X-ray diffraction. The Cu atoms in complexes **1** and **2** are in square pyramidal coordination, and the Co atom in complex **3** is in octahedral one. Complexes **1** and **2** inhibit the *Jack bean* urease with IC_{50} values of 0.25 ± 0.14 and 0.32 ± 0.15 μmol L^{-1}, respectively. Complex **3** show weak activity on *Jack bean* urease with percentage inhibition of 37%.

Keywords: Schiff base; Copper complex; Cobalt complex; Crystal structure; Urease inhibition

1. Introduction

Urease exists in nature, animals and even our human beings, which efficiently catalyzes the hydrolysis reaction of urea to ammonia. This process has negative effects to soil, plants, animals,[1] and related to many diseases of human beings.[2] It showed a major role in urinary catheter incrustation, peptic ulceration, pyelonephritis, kidney stone, hepatic encephalopathy, urolithiasis, and arthritis.[3] So, it is important to decrease the activity of urease. In the last few years, a number of urease inhibitors have been reported including inorganic metal salts like silver, copper, mercury,[4] and organic compounds like hydroxamic acids, triazoles, semicarbazones, Schiff bases, urea derivatives, oxadiazoles, *etc.*[5] However, most of the above mentioned urease inhibitors are not applicable for their low efficiency and side effect like cytotoxicity.[6] The copper nitrate and copper chloride have effective activities on urease, yet, they are harmful to both soil and living organisms. A search of literature indicated that some Schiff base copper and cobalt complexes have good urease inhibitory activities.[7] Considering that copper and cobalt complexes with Schiff bases have a wide range of biological applications,[8] and their application on urease inhibition is rare, in the present work, three new copper(II) and cobalt(III) complexes, $[CuL(dca)]_n$ (**1**), $[CuL(N_3)]_n$ (**2**) and $[CoL(N_3)_2(DMF)]$ (**3**), where L is the monoanionic form of the Schiff base (((2-(pyrrolidin-1-yl)ethyl)imino)methyl)naphthalen-2-ol (HL, Scheme 1), dca is dicyanamide, and N_3 is azide, are presented.

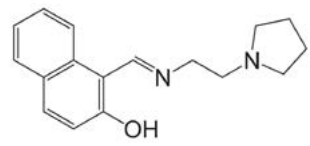

Scheme 1. The Schiff base HL.

2. Experimental

2. 1. Materials and Measurements

2-Hydroxy-1-naphthaldehyde, *N*-(2-aminoethyl) pyrrolidine, sodium dicyanamide, sodium azide, copper nitrate, cobalt nitrate, and solvents with AR grade were pur-

chased from Xiya Chemicals Co. Ltd. (China). Elemental analyses for C, H and N were performed on a Perkin-Elmer 240C elemental analyzer. IR spectra were recorded on a Jasco FT/IR-4000 spectrometer as KBr pellets in the 4000–400 cm^{-1} region. Electronic spectra were recorded on a Lambda 35 spectrophotometer. Single crystal X-ray diffraction was carried out on a Bruker SMART 1000 CCD diffractometer.

2. 2. Synthesis of (((2-(pyrrolidin-1-yl)ethyl) imino)methyl)naphthalen-2-ol (HL)

2-Hydroxy-1-naphthaldehyde (0.17 g, 1.0 mmol) and *N*-(2-aminoethyl)pyrrolidine (0.11 g, 1.0 mmol) were mixed in 30 mL methanol. The mixture was stirred at ambient temperature for 20 min to give slight yellow solution. The solvent was evaporated to give solid product, which was re-crystallized from methanol. Yield: 0.23 g (85%). Anal. Calc. for $C_{17}H_{20}N_2O$ (%): C, 76.09; H, 7.51; N, 10.44. Found (%): C, 75.87; H, 7.46; N, 10.55. IR data (cm^{-1}): 3412w (OH), 1632s (C=N), 1543m, 1524m, 1492w, 1446w, 1402w, 1356s, 1212m, 1185m, 1141m, 836m, 749m, 640w, 504w. UV-Vis data (methanol, λ/nm (ε/M^{-1} cm^{-1})): 230 (21,530), 305 (4,700), 410 (4,730). ^{1}H NMR (500 MHz, d_6-DMSO) δ 13.91 (s, 1H, OH), 9.07 (s, 1H, CH=N), 8.04 (d, 1H, ArH), 7.69 (d, 1H, ArH), 7.62 (d, 1H, ArH), 7.43 (t, 1H, ArH), 7.17 (t, 1H, ArH), 6.69 (d, 1H, ArH), 3.76 (t, 2H, CH_2), 2.73 (t, 2H, CH_2), 2.52 (m, 4H, CH_2), 1.69 (m, 4H, CH_2). ^{13}C NMR (126 MHz, d_6-DMSO) δ 177.88, 158.84, 137.02, 134.42, 128.78, 127.77, 125.83, 124.98, 121.91, 118.22, 105.44, 55.52, 53.51, 49.44, 23.16.

2. 3. Synthesis of $[CuL(dca)]_n$ (1)

The Schiff base HL (0.027 g, 0.10 mmol), copper nitrate trihydrate (0.024 g, 0.10 mmol) and sodium dicyanamide (0.018 g, 0.20 mmol) were mixed in methanol (30 mL). The mixture was stirred at ambient temperature for 30 min to give brown solution. Half of the solvent was slowly evaporated at room temperature for 5 days to give single crystals. Yield: 0.022 g (55%). Anal. Calc. for $C_{19}H_{19}CuN_5O$ (%): C, 57.49; H, 4.82; N, 17.64. Found (%): C, 57.27; H, 4.91; N, 17.53. IR data (cm^{-1}): 2282s, 2221w, 2152vs (dca), 1621s (C=N), 1542s, 1510 w, 1457m, 1432m, 1417w, 1397w, 1362m, 1347s, 1182m, 1141w, 1041w, 940w, 828m, 743m, 569w, 518w, 483w, 456w. UV-Vis data (methanol, λ/nm (ε/M^{-1} cm^{-1})): 238 (18,310), 250 (16,273), 305 (8,750), 390 (4,135).

2. 4. Synthesis of $[CuL(N_3)]_n$ (2)

This complex was prepared by the similar method as described for complex **1**, with sodium dicyanamide

Table 1. Crystal data for the complexes

	1	**2**	**3**
Chemical Formula	$C_{19}H_{19}CuN_5O$	$C_{17}H_{19}CuN_5O$	$C_{20}H_{26}CoN_9O_2$
Fw	396.93	372.91	483.43
T (K)	298(2)	298(2)	298(2)
λ (Mo Kα) (Å)	0.71073	0.71073	0.71073
Crystal system	Monoclinic	Monoclinic	Monoclinic
Space group	$P2_1/c$	Cc	$P2_1/n$
a (Å)	17.4581(15)	9.3323(12)	14.0242(9)
b (Å)	7.5382(11)	23.6903(15)	11.0415(7)
c (Å)	13.5353(13)	7.7450(11)	14.5537(9)
α (°)	90	90	90
β (°)	94.485(2)	108.0630(10)	100.2960(10)
γ (°)	90	90	90
V (Å^3)	1776.0(3)	1627.9(3)	2217.3(2)
Z	4	4	4
μ (Mo Kα) (cm^{-1})	1.248	1.356	0.811
D_c (g cm^{-3})	1.485	1.522	1.448
Reflections	17656	4469	23648
Unique reflections	3304	2813	4131
Observed reflections [$I \geq 2\sigma(I)$]	2929	2606	3410
Parameters	235	218	291
Restraints	0	0	0
Goodness of fit on F^2	1.067	1.028	1.020
R_{int}	0.0273	0.0174	0.0283
R_1 [$I \geq 2\sigma(I)$]	0.0341	0.0278	0.0367
wR_2 [$I \geq 2\sigma(I)$]	0.1097	0.0633	0.0921
R_1 (all data)	0.0390	0.0317	0.0478
wR_2 (all data)	0.1146	0.0649	0.1004
$\Delta\rho_{max}/\Delta\rho_{min}$, e Å^{-3}	0.483/–0.393	0.395/–0.324	0.751/–0.275

replaced by sodium azide (0.013 g, 0.20 mmol). Half of the solvent was slowly evaporated at room temperature for 5 days to give single crystals. Yield: 0.024 g (65%). Anal. Calc. for $C_{17}H_{19}CuN_5O$ (%): C, 54.75; H, 5.14; N, 18.78. Found (%): C, 54.54; H, 5.23; N, 18.61. IR data (cm^{-1}): 2051vs (N_3), 1623s (C=N), 1536m, 1506 w, 1457m, 1439m, 1413m, 1385m, 1361m, 1343m, 1181m, 1167w, 1037w, 973w, 827m, 749m, 649w, 518w, 476w, 456w. UV-Vis data (methanol, λ/nm (ε/M^{-1} cm^{-1})): 240 (17,590), 250 (16,132), 261 (12,350), 290 (7,853), 315 (5,430), 385 (4,550).

2. 5. Synthesis of $[CoL(N_3)_2(DMF)]$ (3)

The Schiff base HL (0.027 g, 0.10 mmol), cobalt nitrate hexahydrate (0.029 g, 0.10 mmol) and sodium azide (0.013 g, 0.20 mmol) were mixed in methanol (30 mL). The mixture was stirred at ambient temperature for 30 min to give deep brown suspension. Then, 5 mL DMF was added to dissolve the precipitation. Half of the solvent was slowly evaporated at room temperature for 12 days to give single crystals. Yield: 0.031 g (64%). Anal. Calc. for $C_{20}H_{26}CoN_9O_2$ (%): C, 49.69; H, 5.42; N, 26.08. Found (%): C, 49.81; H, 5.50; N, 25.89. IR data (cm^{-1}): 2014vs (N_3), 1640s (C=O), 1620s (C=N), 1538m, 1505w, 1440m, 1414w, 1417w, 1356s, 1287m, 1256w, 1188w, 1120m, 1099w, 1036w, 982w, 929w, 868w, 835m, 761m, 708m, 619w, 593w, 528w, 510w, 454w. UV-Vis data (methanol, λ/nm (ε/M^{-1} cm^{-1})): 230 (16,720), 262 (18,630), 320 (8,317), 400 (3,220).

2. 6. X-ray Diffraction

The diffraction intensities for crystals of the copper and cobalt complexes were collected at room temperature using Bruker SMART 1000 CCD area-detector diffractometer with MoKα radiation (λ = 0.71073 Å). The data were reduced with SAINT program,[9] and multi-scan absorption correction was performed with SADABS program.[10] Structures of the three complexes were solved by direct method and refined against F^2 by full-matrix least-squares method with SHELXL.[11] All non-hydrogen atoms were refined anisotropically. Hydrogen atoms were placed in calculated positions and constrained to ride on their parent atoms. The crystallographic data for the complexes are summarized in Table 1.

Table 1. Crystal data for the complexes

	1	2	3
Chemical Formula	$C_{19}H_{19}CuN_5O$	$C_{17}H_{19}CuN_5O$	$C_{20}H_{26}CoN_9O_2$
Fw	396.93	372.91	483.43
T (K)	298(2)	298(2)	298(2)
λ (Mo Kα) (Å)	0.71073	0.71073	0.71073
Crystal system	Monoclinic	Monoclinic	Monoclinic
Space group	$P2_1/c$	Cc	$P2_1/n$
a (Å)	17.4581(15)	9.3323(12)	14.0242(9)
b (Å)	7.5382(11)	23.6903(15)	11.0415(7)
c (Å)	13.5353(13)	7.7450(11)	14.5537(9)
α (°)	90	90	90
β (°)	94.485(2)	108.0630(10)	100.2960(10)
γ (°)	90	90	90
V (Å^3)	1776.0(3)	1627.9(3)	2217.3(2)
Z	4	4	4
μ (Mo Kα) (cm^{-1})	1.248	1.356	0.811
D_c (g cm^{-3})	1.485	1.522	1.448
Reflections	17656	4469	23648
Unique reflections	3304	2813	4131
Observed reflections [$I \geq 2\sigma(I)$]	2929	2606	3410
Parameters	235	218	291
Restraints	0	0	0
Goodness of fit on F2	1.067	1.028	1.020
R_{int}	0.0273	0.0174	0.0283
R_1 [$I \geq 2\sigma(I)$]	0.0341	0.0278	0.0367
wR_2 [$I \geq 2\sigma(I)$]	0.1097	0.0633	0.0921
R_1 (all data)	0.0390	0.0317	0.0478
wR_2 (all data)	0.1146	0.0649	0.1004
$\Delta\rho_{max}/\Delta\rho_{min}$, e Å–3	0.483/–0.393	0.395/–0.324	0.751/–0.275

2. 7. Urease Inhibitory Activity Assay

The measurement of urease inhibitory activity was carried out according to the literature method.[12] The assay mixture containing 75 μL of *Jack bean* urease (EC 3.5.1.5, Canavalia ensiformis) and 75 μL of tested compounds with various concentrations (100 μmol L^{-1}, 50 μmol L^{-1}, 25 μmol L^{-1}, 12.5 μmol L^{-1}, 6.25 μmol L^{-1}, 3.12 μmol L^{-1}, 1.56 μmol L^{-1}, 0.78 μmol L^{-1}, 0.39 μmol L^{-1}, 0.20 μmol L^{-1}, 0.10 μmol L^{-1}, 0.05 μmol L^{-1}; dissolved in 1 mL DMSO) was preincubated for 15 min on a 96-well assay plate. Acetohydroxamic acid was used as a reference, and copper nitrate was assayed as comparison. Then 75 μL of phosphate buffer at pH 6.8 containing phenol red (0.18 mmol L^{-1}) and urea (400 mmol L^{-1}) were added and incubated at 25 °C. The reaction time required for enough ammonium carbonate to form to raise the pH of the phosphate buffer from 6.8 to 7.7 was measured by a micro-plate reader (560 nm) with the end-point being determined by the color change of phenol-red indicator.

3. Results and Discussion

3. 1. Chemistry

The copper complexes were prepared by the reaction of 1:1:2 molar ratio of HL, copper nitrate and sodium dicyanamide or sodium azide in methanol. The cobalt

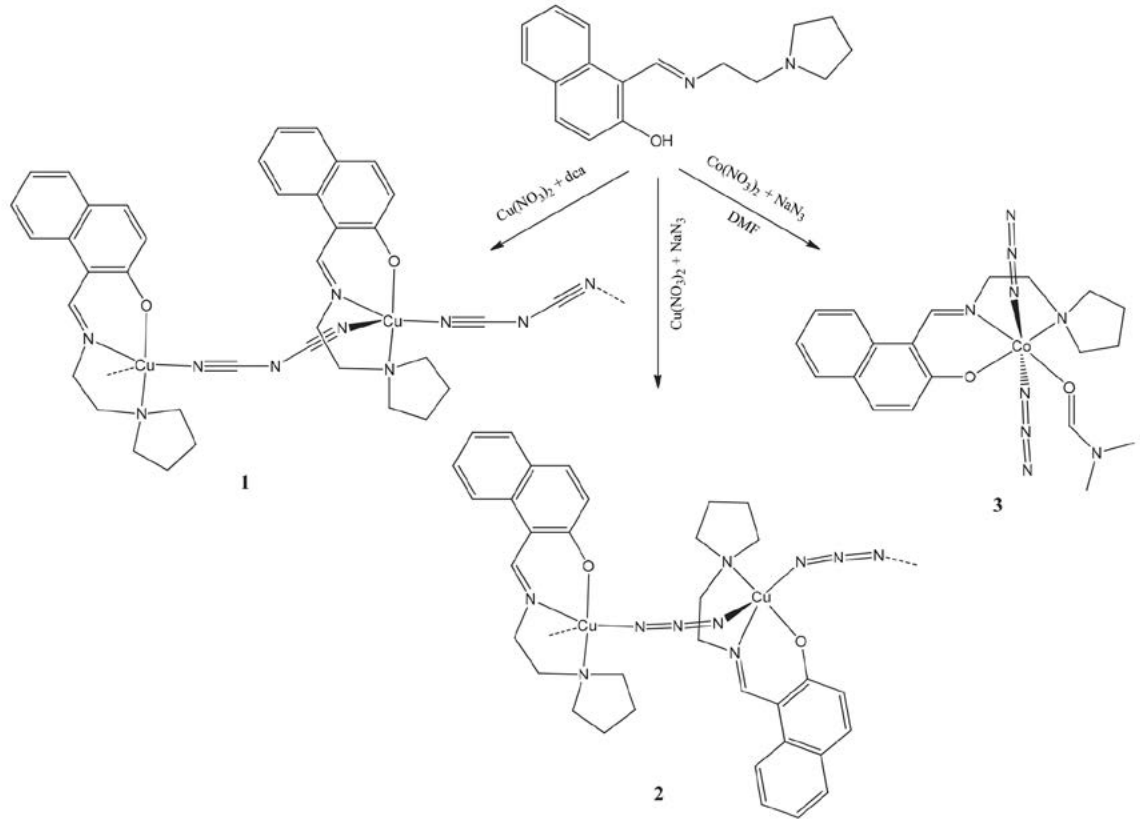

Scheme 2. The synthetic procedures for the three complexes.

complex was prepared by the reaction of 1:1:2 molar ratio of HL, cobalt nitrate and sodium azide in methanol and DMF (Scheme 2). Single crystals of the complexes were obtained by slow evaporation of the solvents of their synthetic solutions. The crystals are stable in air at room temperature.

3. 2. Structure Description of Complexes 1 and 2

The molecular structures of complexes **1** and **2** are shown in Figs. 1 and 2, respectively. Selected bond lengths and angles are given in Table 2. The Cu atoms in both complexes are five-coordinated in square pyramidal geometry, as evidenced by the τ parameters (0.23 for **1**, 0.15 for **2**).[13] The basal plane of the square pyramidal coordination is defined by the phenolate oxygen (O1), imino nitrogen (N1) and pyrrolidine nitrogen (N2) of the Schiff base ligand L and the terminal nitrogen (N3) of the dca ligand for **1** or azide ligand for **2**. The apical position of the square pyramidal coordination is occupied by the other terminal nitrogen (N5) of the second dca or azide ligand. The distortion of the square pyramidal coordination can be observed by the bond angles around the Cu center. The *cis* and *trans* angles in the basal plane are 84.60(9)–92.24(9)° and 158.09(9)–171.97(8)° for **1**, and 84.82(16)–94.42(15)° and 166.3(2)–175.54(14)° for **2**, respectively. The bond angles among the apical and basal donor atoms are 90.08(9)–102.22(9)° for **1** and 86.16(14)–99.7(2)° for **2**. The Cu–O bond lengths are 1.9016(18) Å in **1** and 1.922(3) Å in **2**, which are comparable to each other. The Cu–N bond

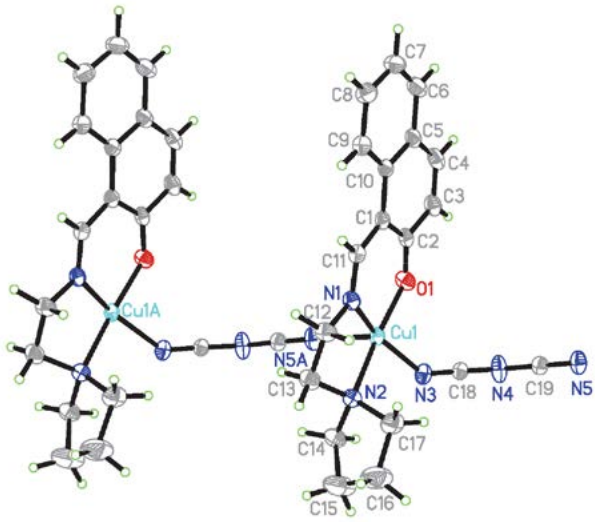

Fig. 1. A perspective view of the molecular structure of complex **1** with the atom labeling scheme. Thermal ellipsoids are drawn at the 30% probability level. Atoms labeled with the suffix A are related to the symmetry operation $x, -1 + y, z$.

lengths in the basal plane of 1.933(2)–2.065(2) Å in **1** and 1.941(5)–2.077(4) Å in **2** are also comparable to each other. The coordinate bond lengths are within normal values for similar Schiff base copper(II) complexes.[14] The apical bond lengths of Cu1–N5 are longer than the basal bonds, which is not uncommon for such complexes.

In the crystal structure of complex **1**, the [CuL] units are linked by $\mu_{1,5}$-dca ligands, to form one dimensional chain running along the *b* axis (Fig. 3). In the crystal structure of complex **2**, the [CuL] units are linked by $\mu_{1,3}$-N_3 ligands, to form one dimensional chain running along the *a* axis (Fig. 4). In addition, there are π···π interactions among the C1–C10 and C5–C10 planes in complex **1** (Cg···Cg = 3.7–4.4 Å, Table 3).

Fig. 2. A perspective view of the molecular structure of complex **2** with the atom labeling scheme. Thermal ellipsoids are drawn at the 30% probability level. Atoms labeled with the suffix A are related to the symmetry operation ½ + *x*, ½ – *y*, ½ + *z*.

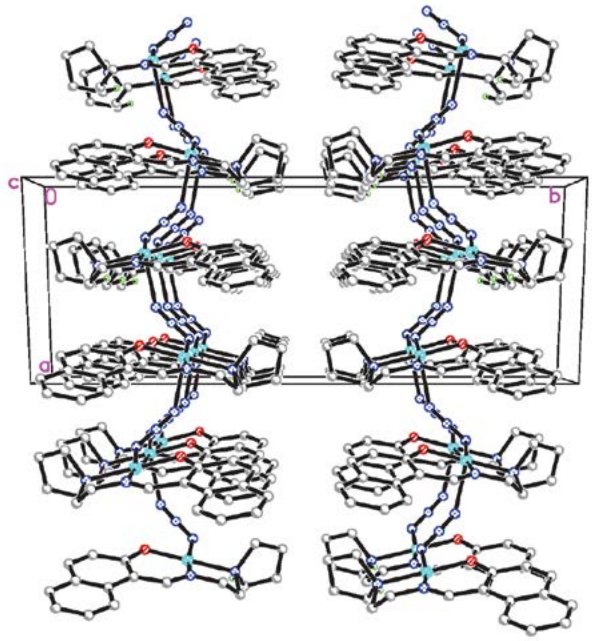

Fig. 4. Molecular packing diagram of complex **2**, viewed along the *c* axis. Hydrogen atoms are omitted for clarity.

octahedral geometry. The basal plane of the octahedral coordination is defined by the phenolate oxygen (O1), imino nitrogen (N1) and pyrrolidine nitrogen (N2) of the Schiff base ligand L and the carbonyl oxygen (O2) of the DMF ligand. The axial positions of the octahedral coordination are occupied by two terminal nitrogen atoms (N3 and N6) of two azide ligands. The distortion of the octahedral coordination can be observed by the bond angles around the Co center. The *cis* and *trans* angles in the basal plane are 86.79(8)–94.31(8)° and 176.07(8)–177.86(8)°, respectively. The bond angles among the axial and basal donor atoms are 87.11(9)–91.79(9)°. The Co–O and Co–N bond lengths are 1.8726(16)–1.9521(17) Å and 1.8622(19)–2.023(2) Å, respectively, which are with-

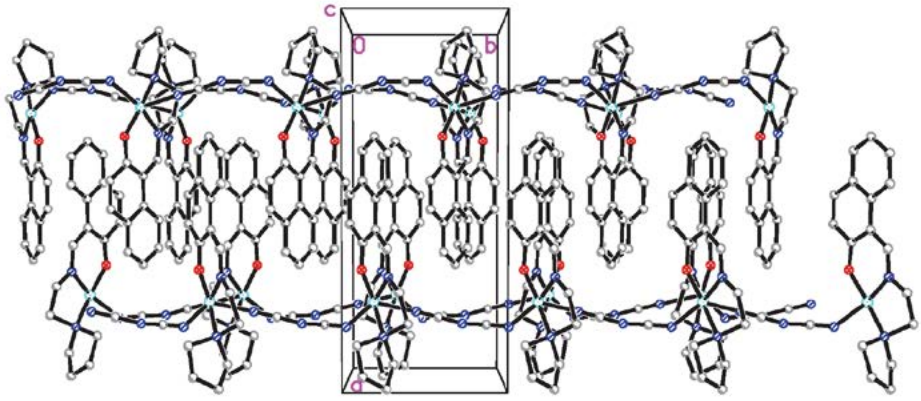

Fig. 3. Molecular packing diagram of complex **1**, viewed along the *c* axis. Hydrogen atoms are omitted for clarity.

3. 3. Structure Description of Complex 3

The molecular structure of complex **3** is shown in Fig. 5. Selected bond lengths and angles are given in Table 2. The Co atom in the complex is six-coordinated in

in normal values for similar Schiff base cobalt(III) complexes.[15]

In the crystal structure of the complex, the complex molecules are linked through intermolecular non-classical hydrogen bonds of C19–H19C···N5 (C19–H19C = 0.96 Å, H19C···N5 = 2.52 Å, C19···N5 = 3.4454(2) Å, C19–H19C···N5 = 162(3)°, symmetry code for i: ½ – *x*, –½ + *y*, ½ – *z*), to form one dimensional chains running along the *a* axis (Fig. 6). In addition, there are π···π interactions among the C1–C10 and C5–C10 planes in the complex (Cg···Cg = 3.9–4.2 Å, Table 3).

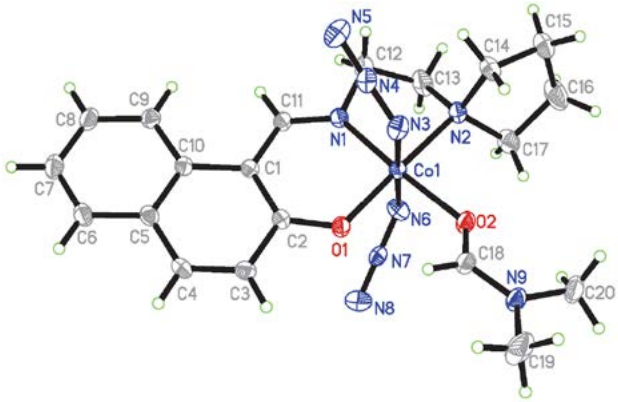

Fig. 5. A perspective view of the molecular structure of complex **3** with the atom labeling scheme. Thermal ellipsoids are drawn at the 30% probability level.

Table 2. Selected bond lengths (Å) and angles (°) for the complexes

1			
Cu1–O1	1.9016(18)	Cu1–N1	1.933(2)
Cu1–N2	2.065(2)	Cu1–N3	2.026(2)
Cu1–N5A	2.320(2)		
O1–Cu1–N1	92.03(8)	O1–Cu1–N3	88.18(9)
N1–Cu1–N3	158.09(9)	O1–Cu1–N2	171.97(8)
N1–Cu1–N2	84.60(9)	N3–Cu1–N2	92.24(9)
O1–Cu1–N5A	97.77(9)	N1–Cu1–N5A	102.22(9)
N3–Cu1–N5A	99.46(9)	N2–Cu1–N5A	90.08(9)
Symmetry code for A: *x*, –1 + *y*, *z*.			
2			
Cu1–O1	1.922(3)	Cu1–N1	1.941(5)
Cu1–N2	2.077(4)	Cu1–N3	1.966(5)
Cu1–N5A	2.415(4)		
O1–Cu1–N1	91.06(15)	O1–Cu1–N3	94.42(15)
N1–Cu1–N3	166.3(2)	O1–Cu1–N2	175.54(14)
N1–Cu1–N2	84.82(16)	N3–Cu1–N2	89.23(16)
O1–Cu1–N5A	95.72(14)	N1–Cu1–N5	92.22(18)
N3–Cu1–N5A	99.7(2)	N2–Cu1–N5A	86.16(14)
Symmetry code for A: ½ + *x*, ½ – *y*, ½ + *z*.			
3			
Co1–O1	1.8726(16)	Co1–O2	1.9521(17)
Co1–N1	1.862(2)	Co1–N2	2.023(2)
Co1–N3	1.976(2)	Co1–N6	1.956(2)
N1–Co1–O1	94.31(8)	N1–Co1–O2	176.07(8)
O1–Co1–O2	89.59(7)	N1–Co1–N6	90.39(10)
O1–Co1–N6	91.04(9)	O2–Co1–N6	89.03(9)
N1–Co1–N3	91.79(9)	O1–Co1–N3	87.85(9)
O2–Co1–N3	88.85(9)	N6–Co1–N3	177.62(10)
N1–Co1–N2	86.79(8)	O1–Co1–N2	177.86(8)
O2–Co1–N2	89.30(8)	N6–Co1–N2	87.11(9)
N3–Co1–N2	93.96(9)		

Table 3. *π*···*π* interactions of the complexes

Cg···*Cg*	distance (Å)	*Cg*···*Cg*	distance (Å)
1			
*Cg*1···*Cg*1^{i}	4.4043(6)	*Cg*1···*Cg*2^{i}	3.7814(6)
3			
*Cg*3···*Cg*4^{ii}	4.1682(3)	*Cg*4···*Cg*4^{ii}	3.9317(3)

Symmetry codes: (i): 1 – *x*, 2 – *y*, –*z*; (ii): –*x*, 1 – *y*, –*z*. *Cg*1 and *Cg*2 are the centroids of C1–C10 and C5–C10 in complex **1**, respectively. *Cg*3 and *Cg*4 are the centroids of C1–C10 and C5–C10 in complex **3**, respectively.

3. 4. IR Spectra

In the infrared spectra of the complexes, there are no typical bands at 3200–3500 cm^{-1}, indicating the coordination of the Schiff bases through deprotonated form. The strong bands at 1621 cm^{-1} for **1**, 1623 cm^{-1} for **2**, and 1620 cm^{-1} for **3** are due to the azomethine groups, μ(C=N).[16] The strong band for the C=O group of the DMF ligand is observed at 1640 cm^{-1} for **3**. The typical absorptions for the dicyanamide ligand in complex **1** are observed at 2282, 2221 and 2152 cm^{-1}.[17] The intense absorptions for the azide ligands in complexes **2** and **3** are observed at 2051 and 2014 cm^{-1}, respectively.[18]

3. 5. Urease Inhibitory Activity

The two copper complexes **1** and **2** have effective inhibitory activity on *Jack bean* urease, with IC_{50} values of 0.43 ± 0.26 and 0.34 ± 0.15 μmol L^{-1}, respectively, whereas the free Schiff base HL and the cobalt complex **3** have weak activity (> 50 μmol L^{-1}). The reported copper complexes have shown better activity than the reference drug acetohydroxamic acid (IC_{50} = 28.5 ± 2.7 μmol L^{-1}) and the copper nitrate (IC_{50} = 8.6 ± 1.5 μmol L^{-1}). The two copper complexes have better activity against urease than the copper(II) complex with the Schiff base ligand *N*,*N*'-bis(4-fluorosalicylidene)-1,2-diaminopropane (IC_{50} = 2.1–3.4 μmol L^{-1}),[19] and the copper(II) complex with the reduced Schiff base ligand 2,2'-((propane-1,3-diylbis(azanediyl))bis(methylene)diphenol (IC_{50} = 1.6 μmol L^{-1}),[20] and have similar activity when compared with the copper complexes derived from *N*'-(pyridin-2-ylmethylene)picolinohydrazide and 4-methyl-2-(((pyridin-2-ylmethyl)imino)methyl)phenol.[21] The cobalt complex has weaker activities than the cobalt complexes with the Schiff

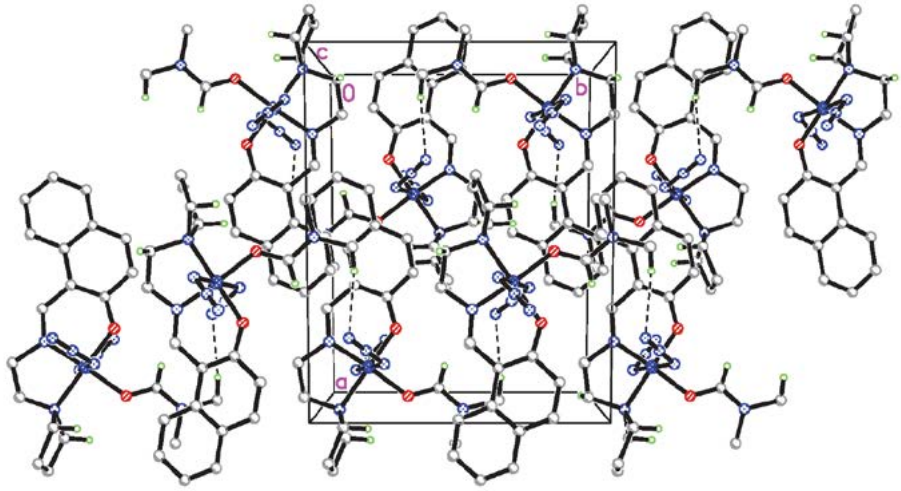

Fig. 6. Molecular packing diagram of complex **3**, viewed along the *c* axis. Hydrogen atoms are omitted for clarity.

base ligands 5-((benzylamino)methylene)-1,3-dimethylpyrimidine-2,4,6(1*H*,3*H*,5*H*)-trione (IC_{50} = 16 μmol L^{-1}),[22] *N,N*'-bis(5-chlorosalicylidene)-1,3-propanediamine (IC_{50} = 45 μmol L^{-1}),[23] *N*'-(2-hydroxy-5-methoxybenzylidene)-3-methylbenzohydrazide and 2-[(2-dimethylaminoethylimino)methyl]-4-methylphenol (IC_{50} = 0.3-4.3 μmol L^{-1}).[24]

4. Conclusion

The present paper intends to report the syntheses, crystal structures and urease inhibition activity of three copper(II) and cobalt(III) complexes with the tridentate Schiff base ligand (((2-(pyrrolidin-1-yl)ethyl)imino)methyl)naphthalen-2-ol. The dicyanamide ligand in **1** and the azide ligand in **2** act as bridging groups, while the azide ligands in **3** act as terminal ligands. The two copper complexes have remarkable inhibitory activity on *Jack bean* urease, with IC_{50} values lower than 1.0 μmol L^{-1}.

Appendix A. Supplementary material

CCDC 2266362 (**1**), 2266363 (**2**) and 2266364 (**3**) contain the supplementary crystallographic data for this article. These data can be obtained free of charge at http://www.ccdc.cam.ac.uk/const/retrieving.html or from the Cambridge Crystallographic Data Centre (CCDC), 12 Union Road, Cambridge CB2 1EZ, UK; Fax: +44(0)1223-336033 or E-mail: deposit@ccdc.cam.ac.uk.

5. References

1. (a) A. M. Duff, P. Forrestal, I. Ikoyi, F. Brennan, *Soil Biol. Biochem.* **2022**, *170*, 108709; **DOI:**10.1016/j.soilbio.2022.108709
(b) T. Lan, Y. X. Huang, X. Song, O. P. Deng, W. Zhou, L. Luo, X. Y. Tang, J. Zeng, G. D. Chen, X. S. Gao, *Environ. Pollut.* **2021**, *293*, 118499; **DOI:**10.1016/j.envpol.2021.118499
(c) M. P. Byrne, J. T. Tobin, P. J. Forrestal, M. Danaher, C. G. Nkwonta, K. Richards, E. Cummins, S. A. Hogan, T. F. O'Callaghan, *Sustainability* **2020**, *12*, 6018. **DOI:**10.3390/su12156018
2. (a) A. T. Fiori-Duarte, R. P. Rodrigues, R. R. Kitagawa, D. F. Kawano, *Curr. Med. Chem.* **2020**, *27*, 3967–3982; **DOI:**10.2174/0929867326666190301143549
(b) M. Taha, N. H. Ismail, S. Imran, A. Wadood, F. Rahim, M. Riaz, *J. Bioorg. Med. Chem.* **2015**, *23*, 7211–7218. **DOI:**10.1016/j.bmc.2015.10.017
3. (a) C. Montecucco, R. Rappuoli, *Nat. Rev. Mol. Cell Biol.* **2001**, *2*, 457–466; **DOI:**10.1038/35073084
(b) H. Mobley, R. P. Hausinger, *Microbiol. Rev.* **1989**, *53*, 85–108. **DOI:**10.1128/mr.53.1.85-108.1989
4. G. I. Perez-Perez, C. B. Gower, M. J. Blaser, *Infect. Immun.* **1994**, *62*, 299–302. **DOI:**10.1128/iai.62.1.299-302.1994
5. (a) W. Q. Song, M. L. Liu, L. C. Yuan, S. Y. Li, Y. N. Wang, Z. P. Xiao, H. L. Zhu, *Bioorg. Med. Chem. Lett.* **2022**, *78*, 129043; **DOI:**10.1016/j.bmcl.2022.129043
(b) S. Iqbal, A. Khan, R. Nazir, S. Kiran, S. Perveen, K. M. Khan, M. I. Choudhary, *Med. Chem.* **2020**, *16*, 244–255; **DOI:**10.2174/1573406415666190415163309
(c) S. Daud, O. U. R. Abid, A. Sardar, B. A. Shah, M. Rafiq, A. Wadood, M. Ghufran, W. Rehman, Zain-ul-Wahab, F. Iftikhar, R. Sultana, H. Daud, B. Niaz, *Med. Chem. Res.* **2022**, *31*, 316–336; **DOI:**10.1007/s00044-021-02814-6
(d) M. Talebi, E. Hamidian, F. Niasari-Naslaji, S. Rahmani, F. S. Hosseini, S. Boumi, M. N. Montazer, M. Asadi, M. Amanlou, *Med. Chem. Res.* **2021**, *30*, 1220–1229; **DOI:**10.1007/s00044-021-02727-4
(e) M. A. S. Aslam, S. Mahmood, M. Shahid, A. Saeed, J. Iqbal, *Eur. J. Med. Chem.* **2011**, *46*, 5473–5479; **DOI:**10.1016/j.ejmech.2011.09.009
(f) E. Menteşe, M. Emirik, B. B. Sökmen, *Bioorg. Chem.* **2019**, *86*, 151–158. **DOI:**10.1016/j.bioorg.2019.01.061

6. (a) Z.-J. Chen, Y.-N. Chen, C.-N. Xu, S.-S. Zhao, Q.-Y. Cao, S.-S. Qian, J. Qin, H.-L. Zhu, *J. Mol. Struct.* **2016**, *1117*, 293–299; **DOI:**10.1016/j.molstruc.2016.03.084
(b) Z.-P. Xiao, Z.-Y. Peng, J.-J. Dong, R.-C. Deng, X.-D. Wang, H. Ouyang, P. Yang, J. He, Y.-F. Wang, M. Zhu, X.-C. Peng, W.-X. Peng, H.-L. Zhu, *Eur. J. Med. Chem.* **2013**, *68*, 212–221. **DOI:**10.1016/j.ejmech.2013.07.047
7. (a) W. Yang, Z. Y. Peng, G. C. Wang, *J. Enzyme Inhib. Med. Chem.* **2023**, *38*, 361–375; **DOI:**10.1080/14756366.2022.2150182
(b) A. Barakat, S. M. Soliman, M. Ali, A. Elmarghany, A. M. Al-Majid, S. Yousuf, Z. Ul-Haq, M. I. Choudhary, A. El-Faham, *Inorg. Chim. Acta* **2020**, *503*, 119405; **DOI:**10.1016/j.ica.2019.119405
(c) H. Y. Yu, S. H. Guo, J. Y. Cheng, G. F. Jiang, Z. W. Li, W. Q. Zhai, A. Li, Y. M. Jiang, Z. L. You, *J. Coord. Chem.* **2018**, *71*, 4164–4179; **DOI:**10.1080/00958972.2018.1533959
(d) C. L. Jing, C. F. Wang, K. Yan, K. D. Zhao, G. H. Sheng, D. Qu, F. Niu, H. L. Zhu, Z. L. You, *Bioorg. Med. Chem.* **2016**, *24*, 270–276; **DOI:**10.1016/j.bmc.2015.12.013
(e) L. Habala, A. Roller, M. Matuska, J. Valentova, A. Rompel, F. Devinsky, *Inorg. Chim. Acta* **2014**, *421*, 423–426. **DOI:**10.1016/j.ica.2014.06.035
8. (a) S. Dasgupta, K. Kar, A. Barua, D. Ghosh, B. Kabi, K. Dewan, A. Chandra, *Life Sci.* **2022**, *308*, 120963; **DOI:**10.1016/j.lfs.2022.120963
(b) H. Pervez, N. Khan, J. Iqbal, S. Zaib, M. Yaqub, M. M. Naseer, *Acta Chim. Slov.* **2018**, *65*, 108–118; **DOI:**10.17344/acsi.2017.3649
(c) H. Zhao, X.-R. Liu, X. Wang, J. Hu, Y.-J. Cai, Q.-A. Peng, *Acta Chim. Slov.* **2021**, *68*, 804–810; **DOI:**10.17344/acsi.2021.6781
(d) M. Wozniczka, M. Lichawska, M. Sutradhar, M. Chmiela, W. Gonciarz, M. Pajak, *Pharmaceuticals* **2021**, *14*, 1254. **DOI:**10.3390/ph14121254
9. Bruker, SMART and SAINT, Bruker AXS Inc., Madison, **2002**.
10. G. M. Sheldrick. SADABS, University of Göttingen, Germany, **1996**.
11. G. M. Sheldrick, *Acta Crystallogr.* **2015**, *C71*, 3–8.
12. W.-J. Mao, P.-C. Lv, L. Shi, H.-Q. Li, H.-L. Zhu, *Bioorg. Med. Chem.* **2009**, *17*, 7531–7536. **DOI:**10.1016/j.bmc.2009.09.018
13. A. W. Addison, T. N. Rao, J. Reedijk, J. van Rijn, G. C. Verschoor, *J. Chem. Soc., Dalton Trans.* **1984**, 1349–1356. **DOI:**10.1039/DT9840001349
14. (a) S.-F. Yu, X.-Y. Qiu, S.-J. Liu, *Acta Chim. Slov.* **2020**, *67*, 1301–1308; **DOI:**10.17344/acsi.2020.6321
(b) J. Q. Wang, Y. Y. Luo, Y. X. Zhang, Y. Chen, F. Gao, Y. Ma, D. M. Xian, Z. L. You, *J. Coord. Chem.* **2021**, *74*, 1028–1038. **DOI:**10.1080/00958972.2020.1861603
15. (a) D. Bandyopadhyay, M. Layek, M. Fleck, R. Saha, C. Rizzoli, *Inorg. Chim. Acta* **2017**, *461*, 174–182; **DOI:**10.1016/j.ica.2017.02.018
(b) X. Q. Luo, Q. R. Liu, Y. J. Han, L. W. Xue, *Acta Chim. Slov.* **2020**, *67*, 159–166; **DOI:**10.17344/acsi.2019.5303
(c) H. Y. Qian, *Acta Chim. Slov.* **2021**, *68*, 700–708. **DOI:**10.17344/acsi.2021.6721
16. (a) Y. Y. Luo, J. Q. Wang, B. T. Zhang, Y. X. Guan, T. Yang, X. Y. Li, L. Y. Xu, J. Wang, Z. L. You, *J. Coord. Chem.* **2020**, *73*, 1765–1777; **DOI:**10.1080/00958972.2020.1795645
(b) M. M. Duan, Y. M. Li, L. Y. Xu, H. L. Yang, F. W. Luo, Y. X. Guan, B. T. Zhang, C. L. Jing, Z. L. You, *Inorg. Chem. Commun.* **2019**, *100*, 27–31. **DOI:**10.1016/j.inoche.2018.12.009
17. (a) A. Ray, G. Pilet, C. J. Gomez-Garcia, S. Mitra, *Polyhedron* **2009**, *28*, 511–520; **DOI:**10.1016/j.poly.2008.11.054
(b) P. Talukder, S. Shit, A. Sasmal, S. R. Batten, B. Moubaraki, K. S. Murray, S. Mitra, *Polyhedron* **2011**, *30*, 1767–1773. **DOI:**10.1016/j.poly.2011.03.049
18. (a) S.-F. Yu, X.-Y. Qiu, S.-J. Liu, *Acta Chim. Slov.* **2020**, *67*, 1301–1308; **DOI:**10.17344/acsi.2020.6321
(b) G.-P. Cheng, L.-W. Xue, C.-X. Zhang, *Acta Chim. Slov.* **2017**, *64*, 261–265. **DOI:**10.17344/acsi.2016.3036
19. Y. Y. Luo, J. Q. Wang, B. T. Zhang, Y. X. Guan, T. Yang, X. Y. Li, L. Y. Xu, J. Wang, Z. L. You, *J. Coord. Chem.* **2020**, *73*, 1765–1777. **DOI:**10.1080/00958972.2020.1795645
20. M. M. Duan, Y. M. Li, L. Y. Xu, H. L. Yang, F. W. Luo, Y. X. Guan, B. T. Zhang, C. L. Jing, Z. L. You, *Inorg. Chem. Commun.* **2019**, *100*, 27–31. **DOI:**10.1016/j.inoche.2018.12.009
21. J. Jiang, P. Liang, H. Yu, Z. You, *Acta Chim. Slov.* **2022**, *69*, 629–637. **DOI:**10.17344/acsi.2022.7513
22. A. Barakat, S. M. Soliman, M. Ali, A. Elmarghany, A. Mohammed Al-Majid, S. Yousuf, Z. Ul-Haq, M.I. Choudhary, A. El-Faham, *Acta Chim. Slov.* **2022**, *69*, 629–637.
23. Z.-L. You, P. Zhou, *Inorg. Chem. Commun.* **2007**, *10*, 1273–1275. **DOI:**10.1016/j.inoche.2007.08.007
24. C. Jing, C. Wang, K. Yan, K. Zhao, G. Sheng, D. Qu, F. Niu, H. Zhu, Z. You, *Bioorg. Med. Chem.* **2016**, *24*, 270–276. **DOI:**10.1016/j.bmc.2015.12.013

Povzetek

Sintetizirali smo tri bakrove(II) in kobaltove(III) komplekse $[CuL(dca)]_n$ (**1**), $[CuL(N_3)]_n$ (**2**) in $[CoL(N_3)_2(DMF)]$ (**3**), kjer je L monoanionska oblika Schiffove baze (((2-(pirolidin-1-il)etil)imino)metil)naftalen-2-ol (HL) in dca je dicianamid, ter jih okarakterizirali z elementno analizo, IR in UV-Vis spektroskopijo ter monokristalno rentgensko difrakcijo. Cu atomi v kompleksih **1** in **2** so v kvadratno piramidalni koordinaciji, Co atom v kompleksu **3** pa v oktaedrični. Kompleksa **1** in **2** zavirata ureazo stročnice *Canavalia ensiformis* z vrednostmi IC_{50} 0,25 ± 0,14 oziroma 0,32 ± 0,15 μmol L^{-1}. Kompleks **3** ima šibko delovanje na ureazo stročnice *Canavalia ensiformis* s 37 % inhibicije.

Scientific paper

Co(II) and Ni(II) Removal from Aqueous Solutions by Polymer and Polymer/Silica Adsorbents with Sulfo and Carboxyl groups

Mariia Zhyhailo,[1] Oksana Demchyna,[1,*] Iryna Yevchuk[1] and Oksana Makota[2]

[1] *Department of Physical Chemistry of Fossil Fuels of the Institute of Physical-Organic Chemistry and Coal Chemistry named after L. M. Lytvynenko of the National Academy of Sciences of Ukraine, 79060, Lviv, Naukova Str., 3a, Ukraine*

[2] *Lviv Polytechnic National University, Lviv, Bandery Str., 12, Ukraine*

* *Corresponding author: E-mail: demchynaoksana@ukr.net*
Phone: (+38) (032) 263 51 74

Received: 09-12-2022

Abstract

Sulfo and carboxyl group-containing polymers and polymer/silica adsorbents poly(acrylonitrile-*co*-2-acrylamido-2-methylpropane-1-sulfonic acid-*co*-acrylic acid-*co*-*N,N'*-methylene-bis-acrylamide) [poly(AN-*co*-AMPS-*co*-AA-*co*-MBA)] and poly(AN-*co*-AMPS-*co*-AA-*co*-MBA)/SiO_2 were synthesized by a UV-initiated polymerization or simultaneous UV-initiated polymerization and *in situ* sol-gel process and used as adsorbents for removal of Co(II) and Ni(II) ions from aqueous solutions. The adsorption capacity and the effect of the pH in the removal process have been studied. The poly(AN-*co*-AMPS-*co*-AA-*co*-MBA) adsorbent exhibited high efficiency: up to 91.8 % removal of Co(II) and 89.7 % removal of Ni(II). Polymer/silica adsorbents showed higher removal capacity as compared to pure polymer. The adsorption kinetics of Co(II) and Ni(II) ions were found to be satisfactorily described by the pseudo-second-order reaction equation of the Lagergren kinetic model, suggesting the ion-exchange nature of the process.

Keywords: polymer/silica membrane; adsorbent; wastewater treatment; heavy metal ion; kinetic model

1. Introduction

Membrane technologies successfully compete with other methods of wastewater treatment. Contaminants discharged into water without prior treatment can be inorganic and organic substrates, pesticides, radioactive elements, surfactants, detergents and others. Most of the pollutants, especially in hydrometallurgical wastewater, are heavy metal salts.[1] Among the various water treatment techniques, adsorption and ion exchange are of great importance.[2] For the removal of metal ions by these methods, polymer and composite materials are most widely used nowadays.

Numerous ion adsorption and ion exchange polymers have been presented in the scientific literature in recent years.[3-4] The polymers are insoluble and include various functional groups, such as amino, amide, ammonium, carboxyl, *etc*. A large number of research papers are devoted to the development of ion exchange polymers containing sulfo groups. Cavus C. and coauthors[5] studied the removal of heavy metal ions Cu(II), Cd(II) and Pb(II) from aqueous solutions by poly(2-acrylamido-2-methyl-1-propane-sulfonic acid-*co*-itaconic acid). Yiqi Wang and coauthors reported a successful synthesis of a phosphazene-based amine-functionalized porous polymer, which demonstrated an excellent adsorption ability for Hg(II) ions.[6] A significant amount of research in this area was carried out by Rivas B.L. and coauthors. The adsorption of Cu(II), Cd(II), Co(II), Hg(II), Ni(II), Zn(II), Cr(III) and Ag(I) ions by polymers such as poly(2-acrylamido-2-methyl-1-propane-sulfonic acid), poly(methacrylic acid), poly(2-acrylamido-2-methyl-1-propane-sulfonic acid-*co*-methacrylic acid), and cross-linked copolymer poly(4-styrene sodium sulfonate-*co*-acrylic acid) was investigated.[7–8] Recent studies by this research team include the synthesis of cation-exchange resins based on water-soluble copolymers: poly(acrylamide-*co*-styrene sodium sulfonate), poly(2-acrylamido-2-methyl-1-propanesulfonic acid-*co*-acrylic acid), poly(2-acrylamidoglycolic acid-*co*-2-acrylamido-2-methyl-1-propanesulfonic ac-

id).[9–11] The developed ion-exchange copolymers demonstrated the ability to remove Cr(III) ions from aqueous solutions. Synthetic polymer materials for ion exchange adsorbents consisting of 4-styrene sodium sulfonate, methacrylic acid and methyl methacrylate at different ratios were prepared by polymerization in solution.[12] Adsorbents were prepared by cross-linking at heating and esterification reactions. The ion-exchange capacity of the materials was 0.51–0.99 meq/g. The material for the manufacture of the ion-exchange membrane described in[13] is terpolymer of acrylonitrile (AN), styrene sodium sulfonate and *N*-butyl acrylate. The required properties of the material were achieved by selecting the feed composition of monomers: AN : SGS : BA = 75 : 15: 10 wt. %. The process of free radical polymerization took place for 4 h at the temperature of 358 K with 80 % yield. The resulting membrane has an ion exchange capacity of 1.50 meq/g.

It should be noted that polymer adsorbents used for water purification have several limitations, such as the trade-off between water permeability and selectivity for dissolved compounds, low fouling resistance, and others.[14] To improve the performance of the adsorbents, their modification with inorganic fillers are often used. Urbano B. F. and Rivas B. L.[15] investigated the sorption properties of composites based on 2-acrylamido-2-methyl-1-propanesulfonic acid for Pb(II), Cu(II), Cd(II). It was found that the addition of montmorillonite to the polymer increased the mechanical properties of the ion exchange membrane.

A series of new hybrid copolymers was obtained by free radical polymerization and sol-gel process using 3-methacryloxypropyl trimethoxysilane (MAPTMS) and acrylic acid (AA).[16] The obtained copolymers maintain thermal stability up to 693 K. In addition, a more stable molecular structure and desired properties can be obtained by adjusting silica and AA content, respectively. The copolymer showed high adsorption capacity in aqueous solutions containing Cu(II) and Pb(II) ions.

Co(II) and Ni(II) are one of the most common heavy metals in wastewater.[17] Co(II) high concentration in water solution can cause a number of unwanted effects, including low blood pressure, heart failure, thyroid and liver damage in humans. The Contact Dermatitis Society of America named Ni(II) the Allergen of 2008 Year, and its role and impact on breast cancer was also noted.[18] Therefore, the purification of wastewater from Co(II) and Ni(II) salts is extremely necessary. In this study we synthesized new polymer adsorbents based on AN, AA and 2-acrylamido-2-methylpropane-1-sulfonic acid (AMPS) cross-linked with *N,N'*-methylene-bis-acrylamide (MBA) by UV-initiated copolymerization and investigated their adsorption capacity on the removal of heavy metal ions (Co(II) and Ni(II)) from aqueous solutions. In order to improve the efficiency of membrane adsorption, the adsorbents were modified with the precursors tetraethoxysilane (TEOS) and MAPTMS using the sol-gel method.

2. Experiment

2. 1. Materials

The reagents for adsorbent preparation: AN (99%), AMPS (99%), AA (99%), MBA (99%), 2,2-dimethoxy-2-phenylacetophenone (DMPA) (99%), TEOS (99%), MAPTMS (99%), phosphoric acid (PhA) (99%) were purchased from Sigma-Aldrich. Milli-Q® water and ethanol (VWR) were used as solvents. The reagents to study the removal process: nickel (II) nitrate hexahydrate ($Ni(NO_3)_2 \times 6H_2O$) and cobalt (II) nitrate hexahydrate ($Co(NO_3)_2 \times 6H_2O$) were purchased from LLC Sfera Sim.

2. 2. Synthesis of adsorbents

The polymer adsorbents were prepared by UV-initiated polymerization of a mixture of acrylic monomers in the presence of photoinitiator DMPA and cross-linking agent MBA. Water soluble reagents (AA, AMPS) were mixed with the appropriate amount of previously dissolved AN and DMPA and stirred for 35 min (500 rpm) at room temperature to obtain a homogeneous mixture.

The resulting mixture was placed in a handmade glass mold (50 × 20 × 0.15 mm) and covered with thin glass to prevent the inhibitory effect of oxygen. The samples were irradiated with UV light (365 nm, radiation power 15 J/cm^2) using a multi-lamp BIO-LINK® cross-linker (BLX-365, Witec AG, Switzerland) equipped with 5 UV lamps (8 W, output 0.8 W).

In the case of organic/inorganic adsorbent preparation, a sol-gel system (SGS) was prepared according to the appropriate procedure.[19] Sol-gel precursors MAPTMS and

Table 1. Feed composition for adsorbents synthesis.

Sample /Content (mass %)	NSA-613	NSA-613-SGS	NSA-612	NSA-612-SGS
AN	60	60	60	60
AMPS	30	30	25	25
AA	10	10	15	15
MBA*	3	3	3	3
DMPA*	2	2	2	2
SGS*	/	20	/	20

* – from mass of monomers

TEOS are insoluble in water, hence, ethanol-water solvent was used for their dissolution. PhA was used as a sol-gel process catalyst. The components were mixed in a following ratio: MAPTMS : TEOS : C_2H_5OH : H_2O : H_3PO_4 = 0.75 : 0.25 : 4 : 2 : 1.8 (mol) and stirred for 30 min (500 rpm) at 323 K. As a result of hydrolysis of the precursors a silica sol was formed. An appropriate amount of the sol shortly before gelation was added to the monomer mixture under stirring. Further steps of the organic/inorganic adsorbent preparation were the same as for the synthesis of pure polymer adsorbents. The feed compositions for the synthesis of polymer and nanocomposite adsorbents are given in Table 1.

The resulting films were separated from the mold, washed thoroughly to remove the unreacted compounds, and finally dried at 323 K until constant weight.

2. 3. Characterization

IR spectroscopy

The FTIR/ATR spectra were examined in 4000-600 cm^{-1} using FTIR Microscope Hyperion 2000 (Bruker, Germany) equipped with MCT detector and ATR objective connected to spectrometer Vertex 70 (Bruker, Germany). The base lines were corrected and the spectra were normalized with respect to the band of stretching vibration of nitrile group (2243 cm^{-1}).

Morphology

Morphology of polymer and polymer/silica adsorbents were determined by scanning electron microscopy using NEON 40 FIB-SEM (Carl Zeiss Microscopy GmbH, Germany). To visualize the cross section, the samples were fractionated and then immersed in liquid nitrogen. Prior to imaging, all test samples were coated with a layer of carbon ~20 nm thick to avoid accumulation of charge in the electron beam.

Degree of swelling

The degree of swelling of the prepared materials was determined gravimetrically by measuring the difference in dimensions of the samples before and after immersion in Milli-Q® water. Before measurement, the samples were dried at 323 K in a vacuum to obtain a constant mass. The dried and weighed adsorbents were placed and kept in deionized water at different temperatures for 24 h.

Degree of swelling (*DS*) was calculated using the following equation:

$$DS = \frac{d_w - d_d}{d_d} \times 100\%, \quad (1)$$

wher.e d_w and d_d – the dimension (length, width or thickness) of wet and dry samples, respectively.

Adsorption capacity

A batch equilibrium procedure was applied to determine the adsorption capacity of the synthesized materials. Co(II) and Ni(II) solutions were prepared with the initial concentration of 50 mg/L. 150 mg of the synthesized membrane was introduced to 50 mL of metal ion solution. All experiments were performed under ambient conditions without forced stirring. The pH values of the solutions (5, 6) were adjusted with 0.1N NaOH. Metal ions were determined by measuring the optical density of the solution at a wavelength of 516 nm for Co and 395 nm for Ni using a spectrophotometer Spekol 11 (Carl Zeiss Jena, Germany).

The amount of metal ions absorbed by the adsorbent (mol/g) was calculated by the formula:

$$q = \frac{C_0 - C_{eq}}{m} \times V, \quad (2)$$

where C_o is the initial metal ion concentration in mol/L; C_{eq} is the equilibrium metal ion concentration in mol/L; V is the volume of the solution in L; m is the dry adsorbent mass in g.

The adsorption efficiency, $A_{eff,}$ was calculated as:

$$A_{eff} = \frac{C_0 - C_{eq}}{C_0} \times 100\ \%, \quad (3)$$

3. Results and Discussion

Two series of cross-linked polymer adsorbents were synthesized by photoinitiated radical copolymerization of acrylic monomers – AA, AN, AMPS and *N,N*'-ethylene-bis-acrylamide in the appropriate ratio in the presence of photoinitiator (see Table 1). AMPS and AA include functional sulfo and carboxyl groups which are necessary for metal ion sorption. The AN was chosen to provide mechanical, thermal and film-forming properties. MBA served as a cross-linker providing the cross-linked structure of the material. Fig. 1, 2 illustrate the structure of the synthesized polymer adsorbents.

To compare the adsorption capacity of polymer and polymer/inorganic adsorbents a series of hybrid organic/inorganic adsorbents were synthesized. The preparation of hybrid materials involves two simultaneous processes: radical UV-initiated copolymerization of the monomers and a sol-gel process of silica precursors. We used a mixture of TEOS and MAPTMS as silica precursors. As a result of the sol-gel process silica network is formed in the polymer matrix. The hydrolysis of precursors forms silanol groups, the condensation between silanol groups or between silanol and alkoxy groups creates siloxane bridges (Si-O-Si) that form the entire silica structure (Fig. 3.).[20]

It should be noted that MAPTMS acts as a coupling agent between organic and inorganic phases, hence, the incorporation of the sol-gel precursor into the organic phase leads to the formation of a cross-linked structure.[21–22] As a result, the interpenetrating networks of organic and inorganic phases are covalently linked with each other.

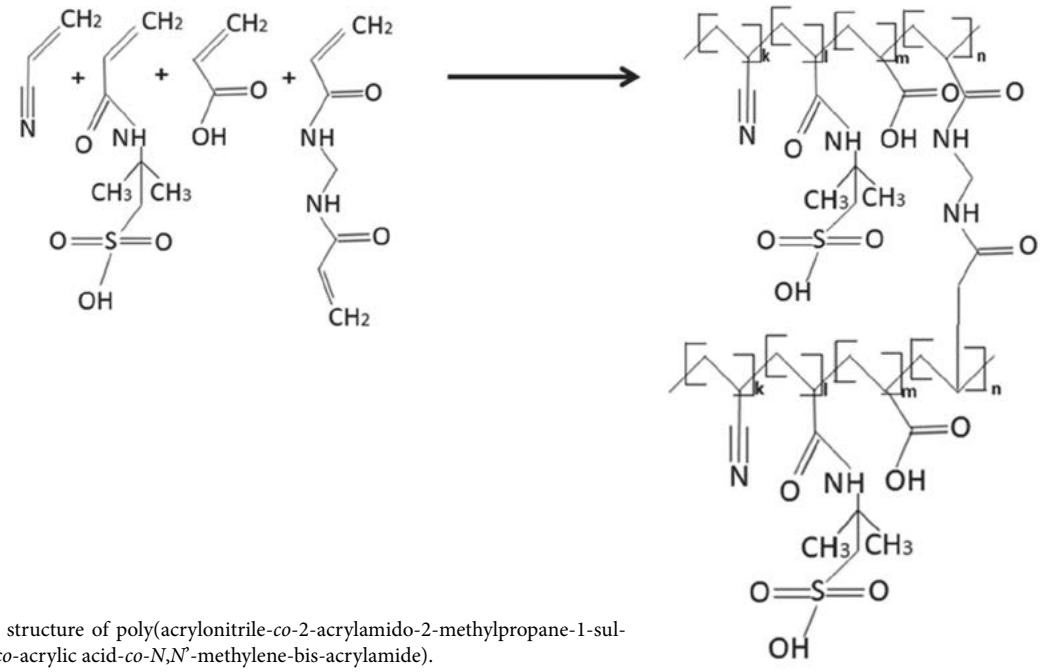

Fig. 1. The structure of poly(acrylonitrile-*co*-2-acrylamido-2-methylpropane-1-sulfonic acid-*co*-acrylic acid-*co*-*N*,*N*'-methylene-bis-acrylamide).

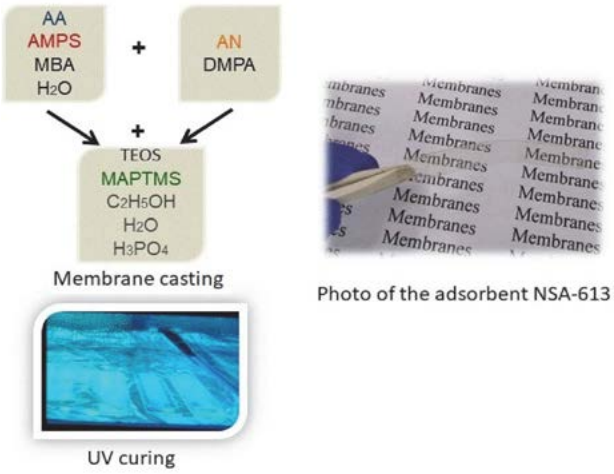

Fig. 2. Scheme of the preparation process polymer/silica materials

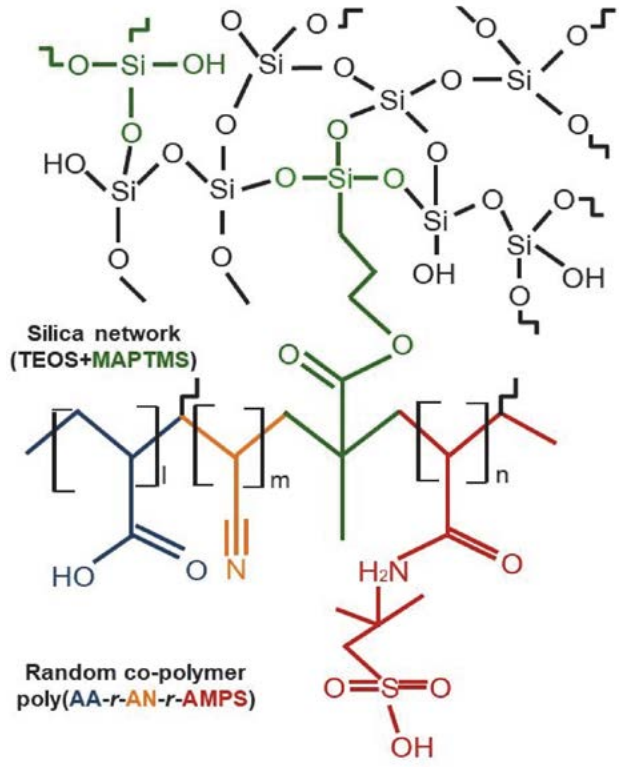

Fig. 3. Chemical structure of polymer/silica adsorbent poly(AN-*co*-AMPS-*co*-AA)

The polymerization yields were estimated by determining the gel fractions of the synthesized materials (Table 2). The gel fractions of the adsorbents were found as the difference in the sample weight before and after keeping them in Soxhlet apparatus for 24 hours. The content of the gel fraction was high in all cases, which indicates the successful completion of the UV polymerization process.

The obtained polymer and organic/inorganic adsorbents were characterized by FTIR spectroscopy to identify the typical absorption signals of the exchange groups. Table 3 summarizes the most important signals in the corresponding spectra of the characteristic functional groups.

The obtained polymer and polymer/silica adsorbents are thin (150–200 μm), transparent, tack-free films evidencing successful synthesis of the materials with homogeneous structure.

Fig. 4 shows SEM photographs of the cross-sectional views of the adsorbents. The adsorbents exhibited a uni-

Table 2. The gel fractions of the adsorbents

Sample	NSA-613	NSA-613-SGS	NSA-612	NSA-612-SGS
GF, mass %	97.1 ± 0.1	96.4 ± 0.1	97.8 ± 0.2	97.5 ± 0.2

Table 3. FTIR absorption signals

Signal, cm^{-1}					
$-SO_3H$	–OH	C=O	NH–C=O	C≡N	Si–O–Si
1214	3100–3500	1724	1646	2242	1000

form and compact morphology without any visible phase separation and inclusions revealing the structural homogeneity.

Moreover, the degree of swelling (*DS*) is one of the important characteristics for the use of the adsorbents as adsorbents. *DS* value must be sufficient to ensure metal ion diffusion inside the adsorbent, at the same time a significant change in the adsorbent size leads to mechanical fragility.

The synthesized adsorbents contain hydrophilic carboxyl and sulfonic acid groups and therefore they have a high affinity for water. Table 4 presents the results of measured changes in the dimensions of the obtained adsorbents (length (*l*), width (*w*), thickness (*t*)) after swelling in Milli-Q® water for 24 hours at two temperatures.

According to the obtained results, the synthesized polymers and polymer/silica nanocomposites are hydrogel-type materials.[23]

The capacity of the adsorbents depends on pH value of the solutions. With an increase in pH, the protonation of electrically charged functional groups decreases, which leads to the fact that the active centers become increasingly ionized and the competition between hydrogen ions and metal ions decreases, so metal ions are adsorbed to higher values. The highest adsorption capacity of sulfo-containing polyacrylate adsorbents for Cu(II), Ni(II), Co(II), and Zn(II) was observed at pH values of 4-7.[24] Habis Al-Zoubi et al.[18] reported that the ability to remove Ni(II) ions by nanocomposite adsorbents increases with an increase in pH from 3 to 7, low values of Ni(II) adsorption capacity at lower pH values they attributed to the partial protonation of sulfo groups, which prevents the interaction between the adsorbent and metal ions. MAPTMS-based membrane was used as an adsorbent for Ni(II),[25] in the range of pH > 7 a precipitate was observed in the solution. Based on the literature data, the appropriate pH values of the solutions were selected.

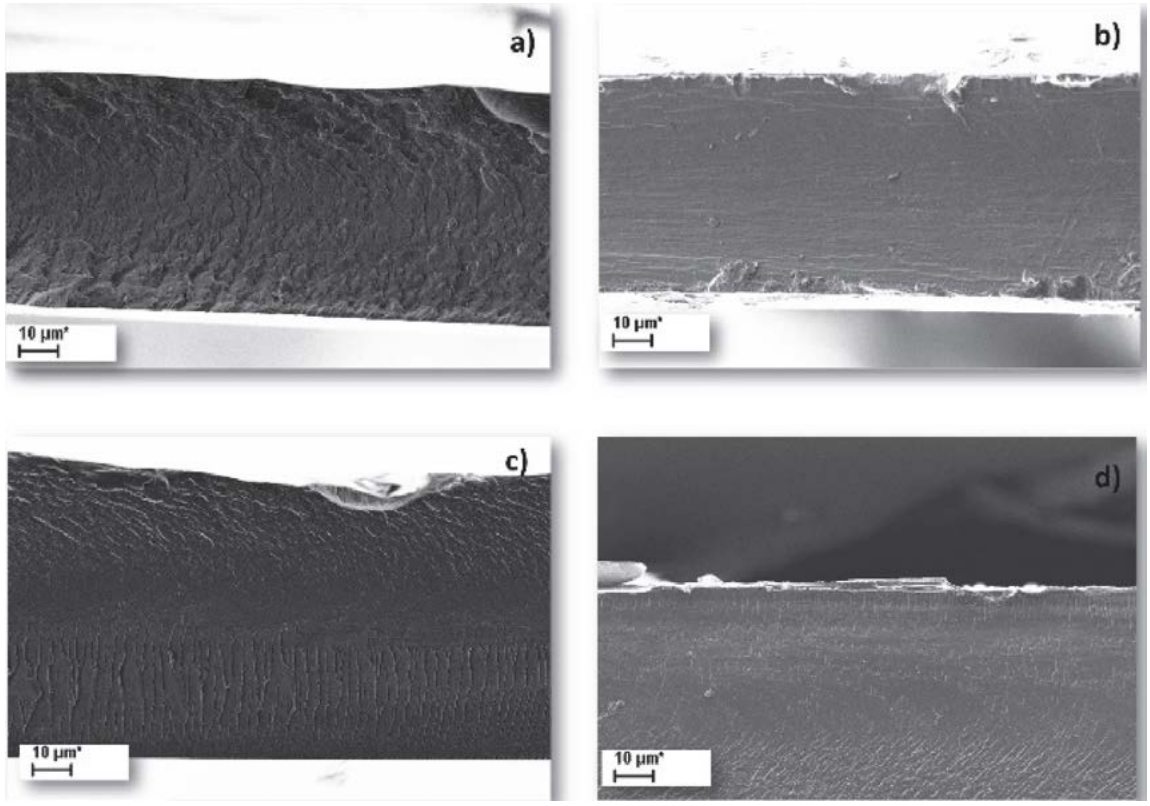

Fig. 4. SEM images of polymer and polymer/silica adsorbents: a) HSA-612; b) HSA-613; c) HSA-612-SGS; d) HSA-613-SGS

Table 4. Adsorbent size changes at swelling

T, °C	*l*, cm	Δl, %	*w*, cm	Δw, %	*t*, μm	Δt, %
			NSA-612			
25	2.8–3.4	21.4 ± 1.9	1.8–2.2	22.4 ± 2.4	130–160	23.0 ± 2.2
50	2.7–3.4	25.7 ± 2.5	1.9–2.4	26.3 ± 2.1	120–150	24.8 ± 3.0
			NSA-612-SGS			
25	2.7–3.3	22.4 ± 2.2	1.6–2.0	25.1 ± 1.8	130–160	25.0 ± 1.6
50	2.6–3.4	26.9 ± 2.0	1.8–2.3	27.7 ± 2.3	150–180	26.7 ± 2.3
			NSA-613			
25	2.7–3.4	25.9 ± 2.0	1.7–2.2	29.4 ± 2.5	130–170	30.7 ± 2.1
50	2.8–3.6	28.6 ± 2.4	1.6–2.1	31.8 ± 2.9	120–160	33.3 ± 2.9
			NSA-613-SGS			
25	2.7–3.4	26.3 ± 2.1	1.7–2.2	30.4 ± 2.3	130–150	31.7 ± 2.3
50	2.7–3.5	29.8 ± 2.1	1.8–2.1	32.7 ± 2.2	150–170	34.3 ± 2.7

The results of the experimental study of the removal capacity of the adsorbents NSA-613, NSA-613-SGS, NSA-612 and NSA-612-SGS for Co(II) and Ni(II) ions are presented in Fig. 5.

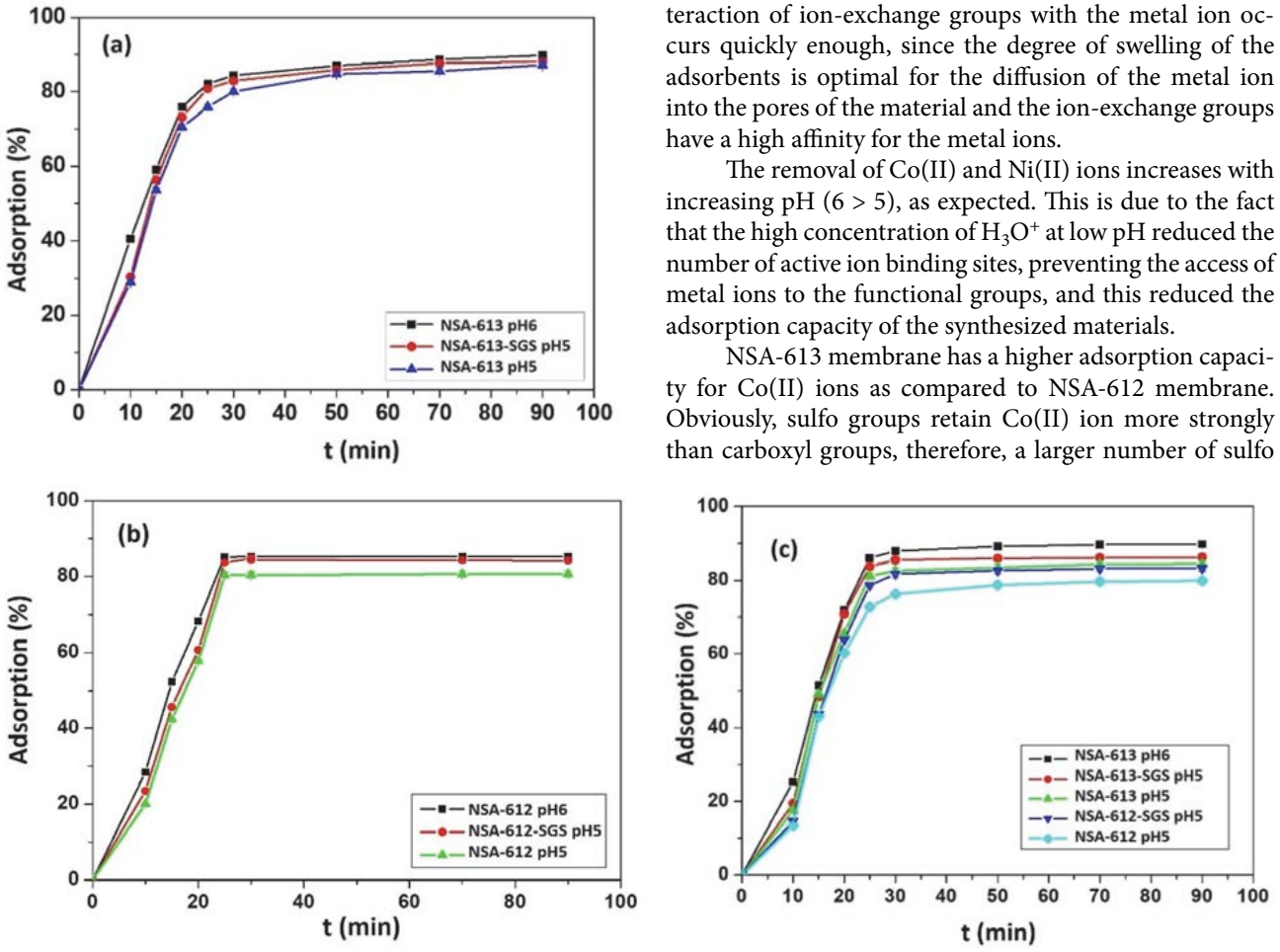

Fig. 5. Co(II) (a, b) and Ni(II) (c) adsorption *vs* time, pH and adsorbent composition

As can be seen from the data in Fig. 5, in all cases adsorption proceeds to an equilibrium state. It was found that the studied polymer and polymer/silica adsorbents have a sufficiently high adsorption rate. The maximum values of adsorption are reached during the first 25-30 min contact of the membrane with metal ion solution. The interaction of ion-exchange groups with the metal ion occurs quickly enough, since the degree of swelling of the adsorbents is optimal for the diffusion of the metal ion into the pores of the material and the ion-exchange groups have a high affinity for the metal ions.

The removal of Co(II) and Ni(II) ions increases with increasing pH (6 > 5), as expected. This is due to the fact that the high concentration of H_3O^+ at low pH reduced the number of active ion binding sites, preventing the access of metal ions to the functional groups, and this reduced the adsorption capacity of the synthesized materials.

NSA-613 membrane has a higher adsorption capacity for Co(II) ions as compared to NSA-612 membrane. Obviously, sulfo groups retain Co(II) ion more strongly than carboxyl groups, therefore, a larger number of sulfo

groups in the copolymer leads to an increase in the adsorption value. These results correlated with the data obtained by.[11] The results of the adsorption study are presented in Table 5.

Table 5. Parameters of Co(II) and Ni(II) adsorption

Sample	pH	Co(II)		Ni(II)	
		$C_o \times 10^{-3}$, g/L	A_{eff}, %	$C_o \times 10^{-3}$, g/L	A_{eff}, %
NSA-613	6	2.5	91.80	2.5	89.68
NSA-613-SGS	5	2.5	90.20	2.5	86.18
NSA-613	5	2.5	87.20	2.5	8436
NSA-612	6	2.5	85.40	2.5	83.26
NSA-612-SGS	5	2.5	84.40	2.5	79.87
NSA-612	5	2.5	80.80		

An SEM study of the adsorbents was carried out after their saturation with Co(II) and Ni(II) ions. The results are presented in Fig. 6.

Analysis of the SEM images of the surface and cross-section of the NSA-612 membrane at pH 5 revealed that during the experiment Co(II) ions seeped and "entered" along the entire cross-section of the membrane (a top, middle and bottom) and are available on the surface of the sample. The distribution of the adsorbed elements was also determined (Table 6).

The adsorbed Co(II) and Ni(II) ions are almost uniformly distributed both across the cross-section of the membrane sample and on its surface. It should be noted that according to both to the adsorption isotherms and the results of the SEM analysis, the polymer/silica adsorbents show higher adsorption capacity compared to the polymer ones. For example, the adsorption capacity of the NSA-613 membrane is 85%, while the same characteristic of the NSA-613-SGS adsorbent is 90%. This can be caused by another morphology of the hybrid organic/inorganic adsorbents: they have a branched system of nanopores formed as a result of a sol-gel process of the precursors, which occurs *in situ* in the polymer matrix during UV-initiated polymerization.

Kinetics of the adsorption process

To determine the mechanism of Co(II) and Ni(II) ions adsorption by polymer and polymer/silica adsor-

Table 6. Distribution of adsorbed Co(II) and Ni (II) in the adsorbents

Element, mass. %	Adsorbent	Cross-section part			Sample surface
		Top	middle	Bottom	
Co	NSA-612	1.81 ± 0.12	1.97 ± 0.14	1.99 ± 0.13	1.91 ± 0.12
Ni	NSA-612	2.02 ± 0.17	1.96 ± 0.19	1.94 ± 0.21	2.00 ± 0.24
Ni	NSA-613-SGS	2.30 ± 0.14	2.25 ± 0.19	2.21 ± 0.18	2.14 ± 0.16

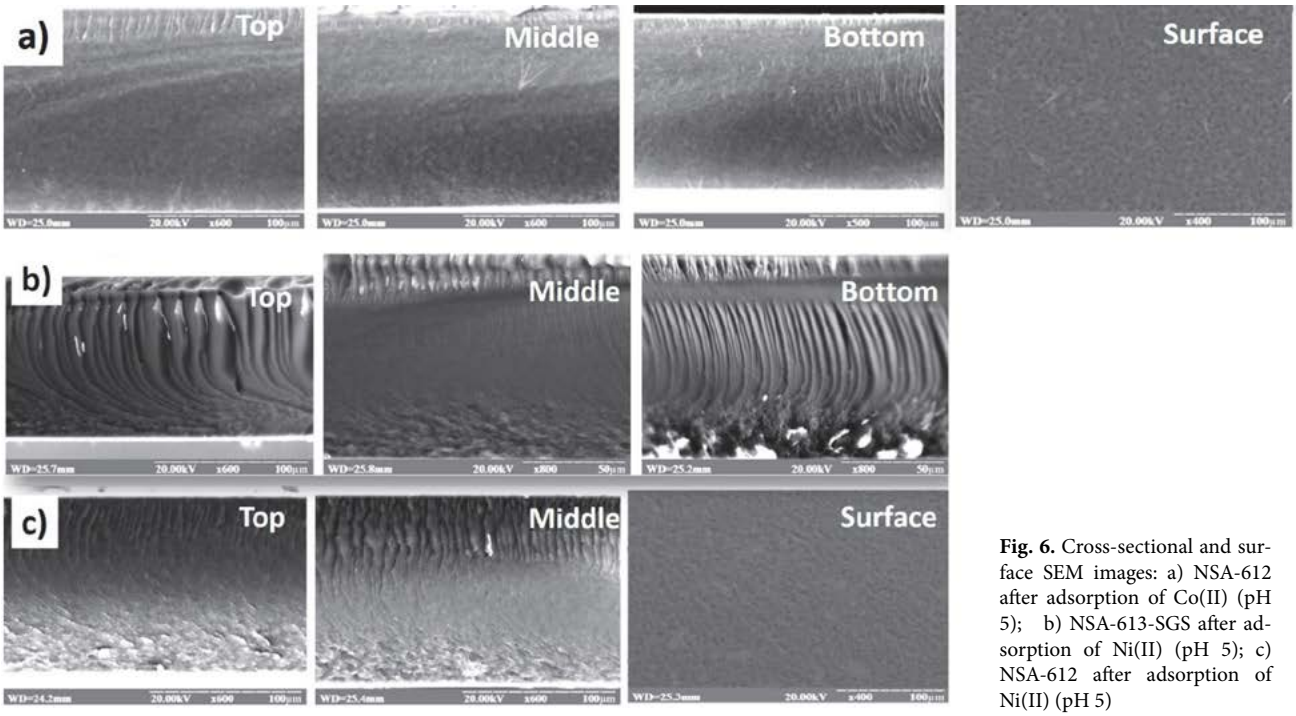

Fig. 6. Cross-sectional and surface SEM images: a) NSA-612 after adsorption of Co(II) (pH 5); b) NSA-613-SGS after adsorption of Ni(II) (pH 5); c) NSA-612 after adsorption of Ni(II) (pH 5)

bents, the kinetics of the process was studied using Lagergren models, similar to the determination of the rate of pseudo-first and pseudo-second order reactions, which are used in modeling sorption processes in the systems solid/liquid.[26]

A pseudo-first-order kinetic model is proposed to describe processes in which the rate of occupation of active centers (binding centers) is proportional to the number of unoccupied sorbent centers, and is represented by the equation:

$$log(qe - qt) = logqe - \frac{k1}{2.303}t \quad (4)$$

where q_t and q_e are the amount of metal ions adsorbed at this moment in time and in a state of equilibrium (mg/g); k_1 is the rate constant of the first-order adsorption process (min^{-1}). It can be determined from the tangent of the slope angle of the direct dependence $log(q_e - q_t) - t$.

The kinetics of the process of adsorption of Co(II) and Ni(II) ions from aqueous solutions with different pH by the investigated adsorbents in the coordinates of the pseudo-first-order equation is shown in Fig. 7. The rate constants of the adsorption process were calculated from the tangent of the angle of the straight lines inclination.

However, the pseudo-first-order equation does not adequately describe the process, as we obtained low determination coefficients ($R^2 \approx 0.9577$). Therefore, the kinetics of adsorption of metal ions was estimated using the pseudo-second-order model, which is described by the equation:

$$\frac{t}{qt} = \frac{1}{k2qe^2} + \left(\frac{1}{qe}\right)t \quad (5)$$

where k_2 is the rate constant of the second-order adsorption process (g/mg min). The initial rate of adsorption h (at $t = 0$) is found from the dependence:

$$h = k_2 \cdot {q_e}^2 \quad (6)$$

Fig. 8 presents the kinetics of the adsorption process of Co(II) and Ni(II) ions in the coordinates of the pseudo-second order equation. The kinetic parameters of the equation were found from the values of the segment cut off on the ordinate axis of the direct dependence $t/q_t - t$.

Table 7 shows the kinetic parameters of the process of metal ion adsorption from aqueous solutions at different pH by the synthesized adsorbents.

Table 7. Kinetic parameters of the adsorption of Co(II) and Ni(II) ions

Parameter		k_1	R^2	k_2	R^2	h	pH
NSA-613	Co(II)	0.0160	0.9715	0.5116	0.9974	5.4525	6
NSA-613-SGS		0.0161	0.9466	0.3236	0.9981	2.5145	5
NSA-613		0.0165	0.9578	0.7617	0.9930	6.9440	5
NSA-612		0.0161	0.9281	0.4422	0.9975	4.3859	6
NSA-612-SGS		0.0161	0.9417	0.6107	0.9964	5.8892	5
NSA-612		0.0162	0.9311	0.8131	0.9969	6.9442	5
NSA-613	Ni(II)	0.0172	0.9577	1.0031	0.9986	10.6750	6
NSA-613-SGS		0.0165	0.8796	0.8272	0.9982	9.6834	5
NSA-613		0.0162	0.9306	0.5706	0.9983	5.4377	5
NSA-612-SGS		0.0161	0.9244	0.8576	0.9982	7.8678	5

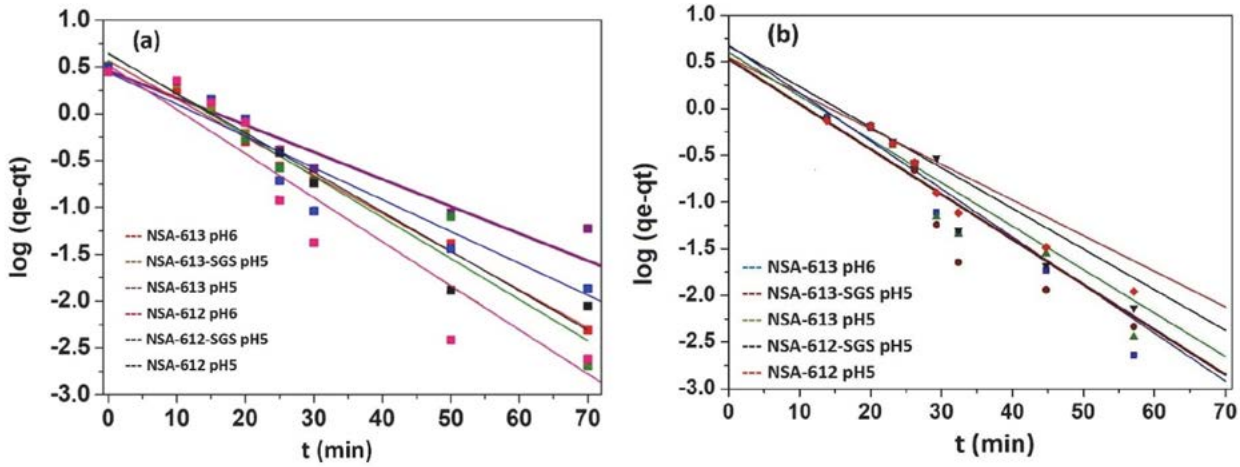

Fig. 7. The adsorption kinetics of a) Co(II) and b) Ni(II) ions in the coordinates of the pseudo-first-order equation

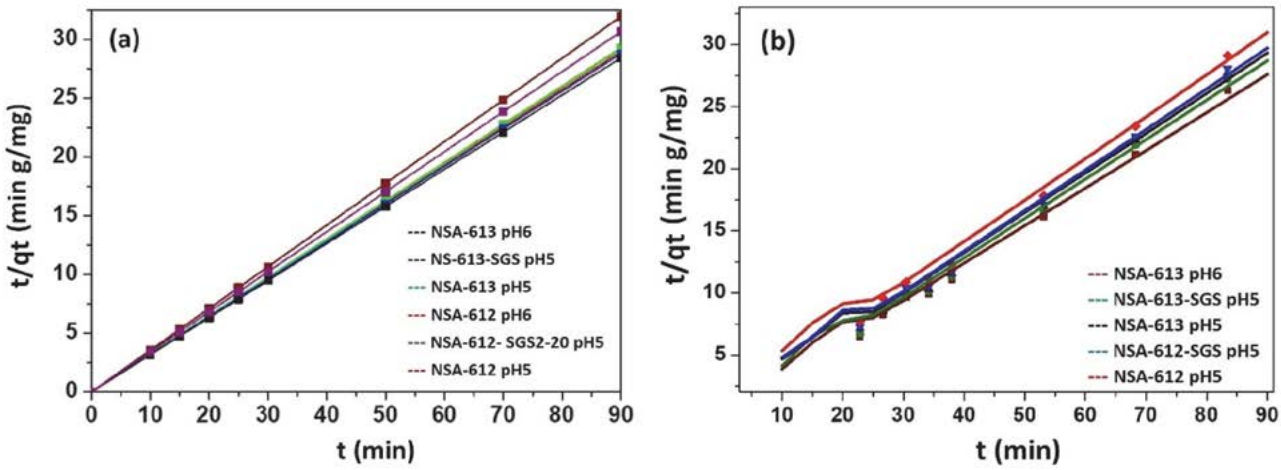

Fig. 8. The adsorption kinetics of a) Co(II) and b) Ni(II) ions in the coordinates of the pseudo-second-order equation

The process of adsorption of metal ions by polymer and polymer/silica adsorbents is better described by the second-order kinetic model, since the values of determination coefficients for the pseudo-second-order model are significantly higher than for the pseudo-first-order model. This can be explained by the fact that the kinetics of metal ion adsorption by adsorbents is influenced not only by the concentration of ions, but also by the concentration of sulfo groups and carboxyl groups in the copolymer. This confirms the mechanism of the electrostatic interaction of metal ions with polymers.

4. Conclusions

The adsorption capacity of the poly(AN-*co*-AMPS-*co*-AA-*co*-MBA) and poly(AN-*co*-AMPS-*co*-AA-*co*-MBA)/SiO_2 adsorbents synthesized in this study for the removal of heavy metal ions from solutions reached 87% for Co(II) ions and 90 % for Ni(II) ions. Due to the formation of a nanoporous structure in the polymer/silica adsorbents, they demonstrate a higher adsorption capacity compared to the polymer adsorbents. A fast rate to the equilibrium state in the adsorption process was revealed for all types of the adsorbents. The effect of pH of metal salt solutions on the adsorption efficiency for Co(II) and Ni(II) ions by the studied adsorbents was found - when pH increases from 5 to 6, the adsorption capacity of the proposed adsorbents increases. The results of the SEM analysis of adsorbents reveal the uniform distribution of Co(II) and Ni(II) on the surface and throughout the adsorbents. The kinetics of adsorption of Co(II) and Ni(II) ions from aqueous solutions by synthesized adsorbents at different the pH was studied. The obtained results were analyzed within the framework of the pseudo-first and pseudo-second order Lagergren kinetic model.

5. References

1. F. Bucatariu, C. Teodosiu, I. Morosanu, D. Fighir, R. Ciobanu, L.-M. Petrila, M. Mihai, *Polymers*, **2021**, *13*, 3963. **DOI:**10.3390/polym13223963.
2. T. A. Saleh, *Environ. Technol. & Innov.,* **2021**, *24*, 101821. **DOI:**10.1016/j.eti.2021.101821
3. Z.-Q. Huang, Z.-Fa Cheng, *J. Appl. Polym. Sci.*, **2019**, *137*, 48579. **DOI:**10.1002/app.48579
4. M. Z. A. Zaimee, M. S. Sarjadi, M. L. Rahman, *Water*, **2021**, *13*, 2659. **DOI:**10.3390/w13192659
5. S. Cavus, G. Gurdag, *Polym. Adv. Technol.*, **2008**, *19*, 1209–1217. **DOI:**10.1002/pat.1113.
6. Y. Wang, N. Yang, M. Soldatov, H. Liu, *React. Funct. Polym.,* **2022,** 173, 105235. **DOI:**10.1016/j.reactfunctpolym.2022.105235
7. B. L. Rivas, C. Muñoz, *J. Appl. Polym. Sci.* **2009**, *114*, 1587–1592. DOI:10.1002/app.30722
8. B. L. Rivas, C. Muñoz, L. Leiton, S. A. Pooley, *J. Appl. Polym. Sci.*, **2011**, *120*, 586–591. **DOI:**10.1002/app.33194
9. B. L. Rivas, I. M. Peric, C. Muñoz, R. Alvear, *Polym. Bull.*, **2012**, *68*, 391–403. **DOI:**10.1007/s00289-011-0551-7
10. B. L. Rivas, C. Muñoz, *J. Appl. Polym. Sci.*, **2007**, *104*, 1769–1774. DOI:10.1002/app.25825
11. B. L. Rivas, D. V. Morales, N. Kabay, M. Bryjak, *J. Chil. Chem. Soc.*, **2018**, *63*, 4012–4018. **DOI:**10.4067/s0717-97072018000204012. **DOI:**10.4067/s0717-97072018000204012
12. N.-S. Kwak, J. S. Koo, T. S. Hwang, E. M. Choi, *Desalination*, **2012**, *285*, 138–146. **DOI:**10.1016/j.desal.2011.09.046
13. V. Bhadja, U. Chatterjee, S. K. Jewrajka, *RSC Adv.*, **2015**, *5*, 40026–40035. **DOI:**10.1039/C5RA07191G
14. J. Yin, B. Deng, *J. Membr. Sci.*, **2015**, *479*, 256–275. **DOI:**10.1016/j.memsci.2014.11.019
15. B. F. Urbano, B. L. Rivas, *Polym. Bull.*, **2013**, *70*, 1143–1162. **DOI:**10.1007/s00289-012-0894-8
16. J. Liu, X. Wang, T. Xu, G. Shao, *Sep. Purif. Technol.,* **2009**, *66*, 135–142. **DOI:**10.1016/j.seppur.2008.11.005

17. J. Kabuba, M. Banza, *Results Eng.*, **2020**, *8*, 100189. **DOI:**10.1016/j.rineng.2020.100189
18. H. Al-Zoubi, K. A. Ibrahim, K. A. Abu-Sbeih, *J. Water Process Eng.*, **2015**, *8*, 19–27. **DOI:**10.1016/j.jwpe.2015.08.002
19. M. M. Zhyhailo, I. Yu. Yevchuk, O. I. Demchyna, V. V. Kochubei, O. I. Makota, *Phys. Chem. Solid St.,* 2021, 22, 775–780. **DOI:**10.15330/pcss.22.4.775-780
20. I. Ab Rahman, V. Padavettan, *J. Nanomater.*, **2012**, article ID 132424,. **DOI:**10.1155/2012/132424
21. P. Kapoor, S. T. Mhaske, K. Joshi, *Prog. Org. Coat.*, **2016**, 94, 124–130. **DOI:**10.1016/j.porgcoat.2015.11.021
22. M. Hwang, J. S. Jeong, J. C. Lee, S. Yu, H. S. Jung, B.-S. Cho, K.-Y. Kim, *Korean J. Chem. Eng.*, **2021**, 38, 454–460. **DOI:**10.1007/s11814-020-0695-y
23. D. Morales, B. L. Rivas, *J. Chil. Chem. Soc.*, **2014**, *59*, 2420–2426. **DOI:**10.4067/S0717-97072014000200005
24. B. L. Rivas, E. Pereira, R. Cid, K. E. Geckeler, *J. Appl. Polym. Sci.,* **2005**, *95*, 1091–1099. **DOI:**10.1002/app.21424
25. B. L. Rivas, E. Pereira, A. Maureira, *Polym. Int.*, **2009**, *58*, 1093–1114. **DOI:**10.1002/pi.2632
26. A. Mittal, M. Teotia, R. K. Soni, J. Mittal, *J. Mol. Liq.*, **2016**, *223*, 376–387. **DOI:**10.1016/j.molliq.2016.08.065

Povzetek

Z namenom uporabe kot adsorbenta za odstranjevanje Co(II) in Ni(II) ionov iz vodnih raztopin sta bila sintetizirana dva polimerna adsorbenta s sulfonskimi in karboksilnimi skupinami, poli(akrilonitril-*ko*-2-akrilamido-2-metilpropan-1-sulfonska kislina-*ko*-akrilna kislina-*ko*-*N*,*N*'-metilen-bis-akrilamid) [poli(AN-*ko*-AMPS-*ko*-AA-*ko*-MBA)], pri čemer je drugi adsorbent polimer, kombiniran s silicijevim dioksidom, [poli(AN-*ko*-AMPS-*ko*-AA-*ko*-MBA)]/SiO_2. Sintetizirana sta bila z UV-iniciirano polimerizacijo ali kombinacijo hkratne UV-iniciirane polimerizacije in *in situ* sol-gel postopka. Proučevani sta bili adsorpcijska sposobnost in vpliv pH v procesu odstranjevanja Co(II) in Ni(II) ionov. Poli(AN-*ko*-AMPS-*ko*-AA-*ko*-MBA) adsorbent je pokazal visoko učinkovitost odstranjevanja ionov, do 91,8 % Co(II) in 89,7 % Ni(II) ionov. Poli(AN-*ko*-AMPS-*ko*-AA-*ko*-MBA)/SiO_2 adsorbenti so pokazali večjo učinkovitost odstranjevanja ionov v primerjavi s polimernim adsorbentom. Ugotovljeno je bilo, da je adsorpcijska kinetika ionov Co(II) in Ni(II) zadovoljivo opisana z reakcijsko enačbo psevdodrugega reda Lagergrenovega kinetičnega modela, kar kaže na ionsko-izmenjevalno naravo procesa.

Scientific paper

Formation and Evolution of the Hydrotalcite-Like Phase During Ageing of Dolomite-Cement Mortars under Various Conditions

Elena Sutormina, Marjan Marinšek and Anton Meden*

University of Ljubljana, Faculty of Chemistry and Chemical Technology, Večna pot 113, 1000 Ljubljana, Slovenia

** Corresponding author: E-mail: Anton.Meden@fkkt.uni-lj.si*

Received: 11-30-2022

Abstract

This work considers the reactions of dolomite powder mixed with Portland cement during ageing under accelerating conditions (60 °C, water or alkaline medium). The phase composition and microstructure of cement-dolomite mortars were studied using X-ray diffraction (XRD), thermogravimetric analysis (TGA), and scanning electron microscopy with X-ray microanalysis (SEM-EDS). The results showed that the alkalinity of the medium increased the dolomite reaction degree but did not affect the reaction products' composition. The formation of the hydrotalcite-like phase with the general formula $Mg_4Al_2(CO_3)_{1-x}(OH)_{12+2x}{\cdot}nH_2O$ proved to be the predominant route of dolomite consumption in the presence of available aluminium in the hardened cement paste. Then, after three months of ageing, an interlayer anions replacement became noticeable: carbonate anions in the structure of hydrotalcite are gradually replaced by hydroxide ones.

Keywords: dolomite-cement mortars, accelerating ageing conditions, dedolomitisation, hydrotalcite-like phase, interlayer anions replacement

1. Introduction

Concrete is the most widely used building material and is characterised by high compressive strength, availability, durability, low price, easy preparation and possibility of casting in desired shapes and sizes.[1] It is a composite material consisting essentially of cement paste in which particles or fragments of aggregates are embedded. Due to their abundance, dolomitic aggregates are the most commonly used for concrete preparation in the Alpine region.[2]

Dolomitic aggregates in concrete can undergo chemical reactions when exposed to the alkaline environment of the cement paste: this is the so-called dedolomitisation reaction with the formation of calcite and poorly soluble brucite: [3–5]

$$CaMg(CO_3)_2 + 2OH^- \rightarrow CaCO_3 + Mg(OH)_2 + CO_3^{2-} \quad (1)$$

Dolomite powder, which releases carbonate ions, may be involved in the hydration reaction of cement, forming calcite and carbonate-AFm (calcium aluminate) phases, thereby affecting the mechanical strength of concrete. It has also been shown that dolomite can react with alumina sources and portlandite to form hydrotalcite (HT) and calcite: [3,5,6]

$$6CaMg(CO_3)_2 + 2Al(OH)_4^- + 8OH^- + 5H_2O \rightarrow Mg_6Al_2(CO_3)(OH)_{16}{\cdot}5H_2O + 6CaCO_3 + 5CO_3^{2-} \quad (2)$$

Aluminate ions $Al(OH)_4^-$ originate from soluble nature of alumina in cement minerals (tricalcium aluminate $3CaO{\cdot}Al_2O_3$ and tetracalcium aluminoferrite $4CaO{\cdot}Al_2O_3{\cdot}Fe_2O_3$) under alkaline conditions. Subsequently, they migrate to the aggregate-cement paste interface. At the interface, dolomite dissolves, liberating Ca^{2+} and CO_3^{2-} ions into the cement paste and absorbing aluminate ions from the cement paste in accordance to equation (2). This reaction was proposed to be a typical metasomatism caused by the replacement of mobile components between dolomite and cement paste, keeping the texture of the original outlines of dolomite aggregate.[3] As a result, a narrow rim composed of hydrotalcite is formed on the dolomite aggregate.

It has been suggested that this route is preferable for Mg^{2+} released from dolomite because the resulting hydrotalcite is thermodynamically more stable than equivalent amounts of brucite, boehmite (AlOOH), magnesite ($MgCO_3$), and water. According to the thermodynamic data,[7] the $\Delta G°_f$ of hydrotalcite is about 10 kJ/mol lower than that

of the separated phases listed above.

The hydrotalcite structure can be described as brucite-like layers in which some of the Mg^{2+} cations are replaced by Al^{3+} cations.[8] Between the structural layers there are weakly bound charge-balancing anions (CO_3^{2-}, SO_4^{2-}, Cl^-, OH^-, etc.), which can enter into anion-exchange reactions,[9] and water molecules. Natural hydrotalcite has the formula $Mg_6Al_2(CO_3)(OH)_{16}{\cdot}4H_2O$ with an Mg/Al ratio of 3. However, studies of synthetic HT show that this ratio can vary in the range of 0.5–3.2 depending on the pH of the medium.[10] For cement-dolomite systems, the Mg/Al ratio of hydrotalcite has been reported to be 1.9–3.2 in various works.[6,11,12] It was found that the formation of hydrotalcite in the dolomite reaction was strongly limited by the alkalinity of the pore solution and the portlandite content of the cement paste.

The formation of Mg-Al hydrotalcite in dolomite-cement mortars has been shown to contribute to strength development and durability properties (resistance to leaching and carbonation), as well as an efficient binding capacity of chloride ions.[13] However, there is insufficient information on the stability of hydrotalcite and the kinetics of its formation under various ageing conditions. The anionic composition of the hydrotalcite-like phase and its possible evolution during ageing has yet to be studied.

The present work aims to study the reaction products of dolomite during the ageing of dolomite-cement mortars, in particular, the hydrotalcite phase formed during the reaction of dolomite with Al-containing compounds from the cement paste, its composition, the kinetics of its occurrence and possible transformation depending on the ageing conditions. Various techniques (XRD, TGA, SEM-EDS) were used to study the phase composition and microstructure of the mortars. Since the dedolomitisation reaction is rather slow at room temperature, the accelerated conditions (de-ionised water or 1M NaOH at 60 °C), are suggested. In this way, the influence of the alkalinity of the medium on the dolomite reaction degree and the properties of the resulting products could also be determined. Dolomite powder with fine particles was used to increase the surface-to-volume ratio, since the reactions occur mainly on or near the interface of the dolomitic aggregates and the cement paste binder.

2. Materials and Methods

2. 1. Raw Materials and Samples Preparation

A dolomite-cement mortar mixture was prepared from dolomite aggregate from the southern part of Slovenia and Portland cement CEMI 42.5 N supplied by Salonit Anhovo. A crushed sand (fraction 0–2 mm) was used, characterised by water absorption of 0.14% and density of 1470 kg/m^3. The chemical compositions of the cement and dolomite aggregate determined by ICP-OES analysis (Agilent 5100) are given in Table 1. The results of quantitative X-ray analysis (QXRD) show that dolomite accounts for 93.6 % of the mineral content of the aggregate, while the minor phases are calcite (4.5%), lime, periclase and quartz.

A total of 1093 g of Portland cement was dry mixed with 3216 g of dolomite aggregate using a RILEM-CEN mixer for 3 min at a speed of 300 rpm, providing the aggregate-to-cement mass ratio 3:1. Then 500 ml of de-ionised water was added and mixed for 1.5 min at 300 rpm to ensure good homogenisation of the pastes. To improve the rheology of concrete suspensions during mixing, 17.7 ml of superplasticizer SP-481 was added. The water-to-binder ratio of the mortars was 0.46.

Mortar tablets (25 mm in diameter and 10 mm high) were prepared from dolomite-cement mortar mixture to study phase composition and microstructure. After hardening at room temperature for 24 hours, the mortar tablets were demoulded and cured in an environment with a relative humidity of 90% and a temperature of 20 °C for 28 days. Then, the tablets were divided into two groups and placed in plastic containers filled with (a) 500 ml of de-ionized water with pH = 7.9 or (b) 500 ml of 1 M aqueous NaOH solution with pH = 14. The amount of liquid significantly exceeded the volume of cement tablets, so they were all submerged in liquid. Plastic containers, tightly closed to avoid evaporation of the solutions, were placed in a drying oven at a temperature 60 ± 2 °C for 1–12 months. The samples were submitted to analyses as prepared and after 1, 3, 6, 12 months of ageing, named M0 and M1–M12, respectively.

2. 2. Methods

X-ray powder diffraction (XRD) data of the samples were collected at room temperature with a PANalytical X'Pert PRO high-resolution diffractometer using Cu-$K_{\alpha 1}$ radiation (λ = 1.5406 Å) in the reflection geometry. Data were collected in the 2θ range from 5 to 80° in steps of 0.033° using a 128-channel linear multi-strip detector to achieve a total integration time of 500 s per step. The peak positions and relative heights of the peaks were determined based on the experimental patterns. The crystalline phases present in the samples studied were identified using the PDF-4 database (release 2021). Quantitative phase analysis was performed using the Rietveld method, which is a re-

Table 1. Chemical composition of cement and dolomite aggregates.

Oxide (wt%)	CaO	MgO	SiO_2	Al_2O_3	Fe_2O_3	K_2O	Na_2O	SO_3	LOI
cement	60.4	2.5	22.2	5.5	3.3	0.8	0.5	3.0	1.3
aggregate	33.2	18.9	1.4	0.8	0.3	0.1	<0.1	–	0.1

liable analytical approach for quantifying the amounts of different cementitious phases in multiphase mixtures containing phases with significant peak overlap and various peak widths. Topas Academic V4.1 software (Burker-AXS) and the ICSD database were used.

A scanning electron microscope, FE-SEM Zeiss Ultra Plus, equipped with EDS (Oxford X-Max SDD 50 mm^2 106 detector and INCA 4.14 X-ray microanalysis software) at 20 kV accelerating voltage, a vacuum environment of $1–2{\cdot}10^{-6}$ mbar, and a beam current of about 20 nA was used on polished sections to detect microstructural changes during the dedolomitisation process. The EDS spectra were recorded on flat areas of the C-coated samples with a process time of 5 s, a lifetime of 120 s and an accelerating voltage of 20 kV. Qualitative analysis of the X-ray spectra was performed according to the standard procedure provided by the software manufacturer. Different fields of view were analysed in different areas of interest to obtain statistically reliable data.

Thermogravimetric analysis (TG/DTG) of samples was performed using a Netzsch STA 449 F3 Jupiter instrument in conjunction with a QMS 403 C Aëolos mass spectrometer. Typically, approximately 100 mg of sample was used for each run. The sample was heated in a 30 ml/min O_2 + Ar flow from 30 to 1200 °C at a heating rate of 10 °C/min under oxidative conditions (synthetic air containing 20 vol.% O_2 and 80 vol.% Ar). QMS analysis focused on monitoring the signals characteristic of H_2O and CO_2 (m/z = 18 and m/z = 44, respectively) to describe accurately the reactions associated with H_2O and CO_2 release from the different phases. Microcal Origin 6.0 was used for deconvolution and calculating overlapping peak areas.

3. Results and discussions

3. 1. Phase Composition

XRD analysis of the initial dolomite-cement mortar before ageing (sample M0) indicates the presence of a predominant phase of dolomite and cement hydration products such as portlandite, ettringite, hemi-/monocarbonate, hydrogarnet, as well as unreacted ferrite and belite. The main difference in the phase composition of the samples in the XRD patterns during ageing is seen at low angles, where the main non-overlapping reflections of the minor phases are located.

Fig.1a–b show the XRD patterns in the range of 10–25° *2θ* for samples aged for 0–12 months at 60 °C in water and 1M NaOH. Under accelerated ageing conditions, the process of dedolomitisation begins in the dolomite grains: the dolomite content decreases significantly, and calcite and brucite are formed according to the reaction (1). Traces of brucite appear after 1 month of ageing in NaOH, while the reaction in water is much slower and shows noticeable brucite formation only after 6 months of ageing.

It is also seen that dolomite readily reacts with Al-containing compounds from cement paste to form a hydrotalcite-like phase (HT) and calcite (reaction 2). At the same time, it was observed that the monocarbonate, ferrite and ettringite peaks become smaller and almost disappear with time in NaOH. This is consistent with the results of J. Xu *et al.*, who suggested that the formation of hydrotalcite promotes the decomposition of these Al-containing compounds due to its lower solubility.[10] Meanwhile, hydrogarnet $Ca_3(Al,Fe)_2(SiO_4)(OH)_8$, which is also formed during the hydration of cement paste at elevated temperatures, remains stable in the long run, as previously reported.[14] It should be mentioned that the hydrotalcite-like phase appears earlier than brucite (especially during ageing in water, where the dedolomitisation is slower), confirming the assumption that the Mg^{2+} cations released from the dolomite prefer to form hydrotalcite rather than brucite.

The intensity of the hydrotalcite peak at 11.40° *2θ* began to increase sharply with increasing ageing time and reached the maximum after 3 months for the sample aged in NaOH. During this period, most of the available

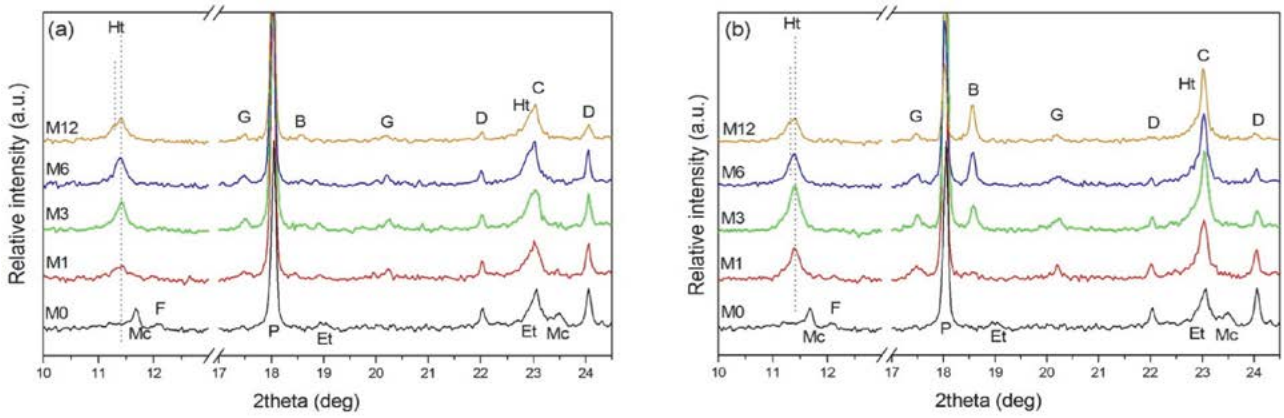

Figure 1. XRD patterns for the samples aged for 0–12 months at 60° C (a) in water and (b) in NaOH. Here and below in the figures: D – dolomite, P – portlandite, C – calcite, B – brucite, Ht –hydrotalcite, F – ferrite, Et – ettringite, Mc – monocarbonate, G – hydrogarnet.

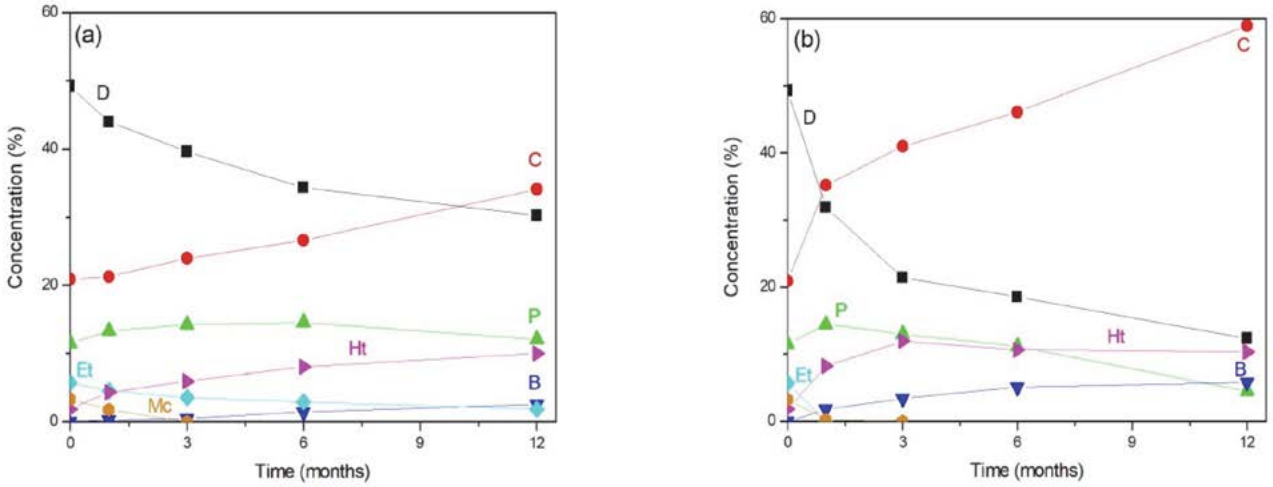

Figure 2. Phase composition of dolomite-cement mortars aged for 0–12 months at 60 °C in (a) water and (b) NaOH, according to QXRD data (crystalline phases only).

aluminium from the cement paste was likely bound in the form of hydrotalcite. Thereafter, the reflections in the XRD patterns indicate the changes in the hydrotalcite-like phase: the peak broadened, and a shoulder at 11.28° *2θ* appeared in the samples aged for 6–12 months both in water and NaOH. The detailed study of hydrotalcite-like compounds with different interlayer anions (NO_3^-, Cl^-, SO_4^{2-}, OH^- and CO_3^{2-}) showed that the basal spacing for hydrotalcite increased when CO_3^{2-} ions were replaced by OH^- ions in the interlayer region.[15] Thus, the occurrence of the shoulder could be related to the formation of the hydrotalcite-like phase in which carbonate anions are replaced with hydroxide ions (HT-OH).

QXRD was used to quantify the amount of unreacted dolomite and the products of the dedolomitisation process in the cement-containing samples. The quantitative XRD results of the main reaction products found in the samples aged in water and NaOH are presented in Fig.2a–b. Thus far, the calculations have been performed without considering the amorphous phases (the amount of which can be determined by adding an external standard). The conversion of dolomite during 12 months of ageing in water is rather low, less than 40%, and ettringite also disappears slowly during ageing. The concentration of HT increases slightly with time and reaches 10% after 12 months of ageing, while the content of brucite is rather low and is 2.5%. For the sample aged in NaOH, QXRD showed that a significant amount of dolomite reacted after 12 months of ageing: the conversion was about 75%. The fraction of the hydrotalcite-like phase is 10–11% after 3 months of ageing and then remains almost constant, while the fraction of brucite increases steadily to 5.8%.

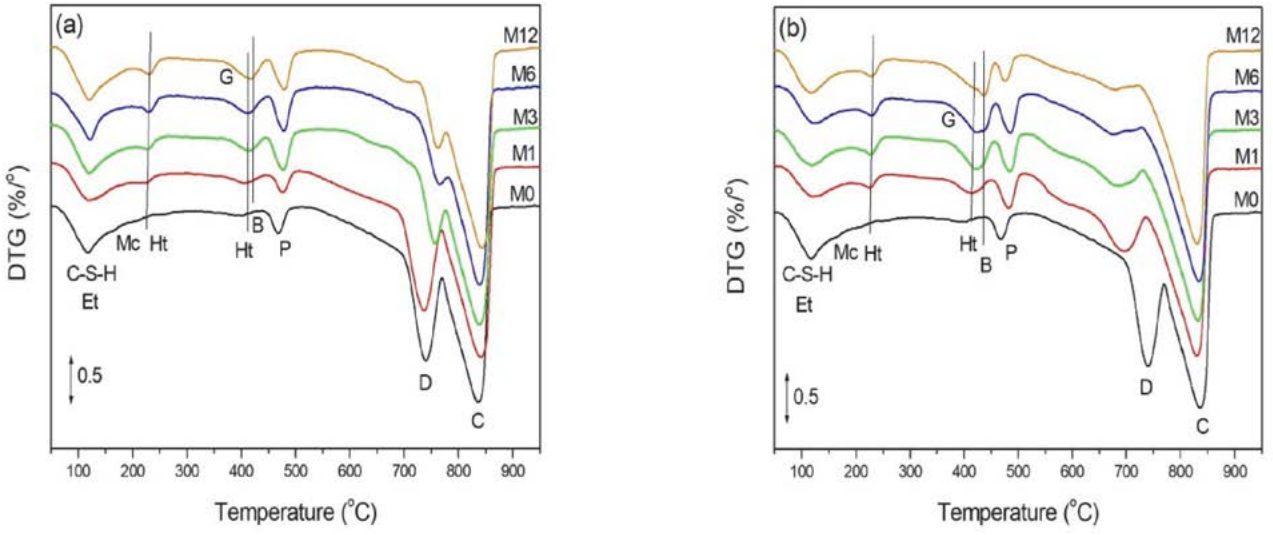

Figure 3. DTG curves for the samples aged for 0–12 months at 60 °C in (a) water and (b) NaOH. C-S-H – calcium-silicate hydrate.

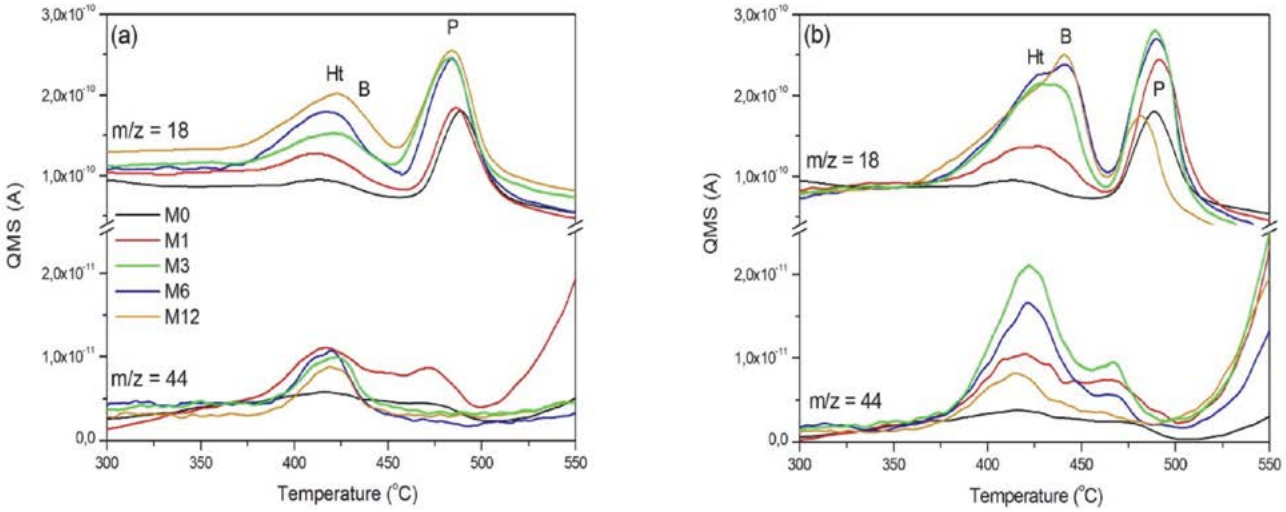

Figure 4. H_2O (m/z =18) and CO_2 (m/z=44) release in the temperature range 350–500 °C for the samples aged for 0–12 months at 60 °C in (a) water and (b) NaOH.

3. 2. Thermogravimetric Analysis

Thermal analysis was used for a more detailed study of the reaction products in aged mortars, especially for the composition of the hydrotalcite-like phase. Fig. 3a–b show the DTG curves of the samples aged at 60 °C in water and 1M NaOH for 0–12 months. Six main peaks of mass loss were found in the DTG curves. The first peak at about 120 °C corresponds to the dehydration of C-S-H and ettringite/monocarbonate.[16] The decomposition peaks of monocarbonate were found mainly in the initial unaged sample, which is consistent with the XRD observations. The second peak at about 230 °C, which appeared in aged samples, was attributed to the dehydration of hydrotalcite.[17] The third peak is due to two parallel processes: a) further decomposition of bound hydroxyl groups and removal of carbonate ions in the interlayers of hydrotalcite and b) decomposition of brucite. This peak increases with increasing duration of ageing. The fourth peak at 475–485 °C corresponds to the decomposition of portlandite. Two pronounced peaks at high-temperature ranges (550–780 °C and up to 880 °C) are due to the decomposition of dolomite and calcite, respectively.[18] The broad peaks that occurred at lower temperatures could be related to the formation of amorphous and finely divided particles of calcite (probably secondary calcite) or dolomite.

It can be seen that the general trends in phase composition established by XRD are also confirmed by thermal analysis. The reaction proceeds more slowly in water: the peaks corresponding to hydrotalcite are less intense, and brucite is practically undetectable, while the peaks of dolomite and portlandite decrease only slightly. Another difference is the absence of peaks corresponding to fine calcite/dolomite particles in the 515–725 °C temperature range, after ageing in water at 60 °C for 3–12 months. This could be due to the dissolution of calcite in water, especially in the presence of CO_2 (open system), while the dissolution of calcite in an alkaline medium is much lower.[19]

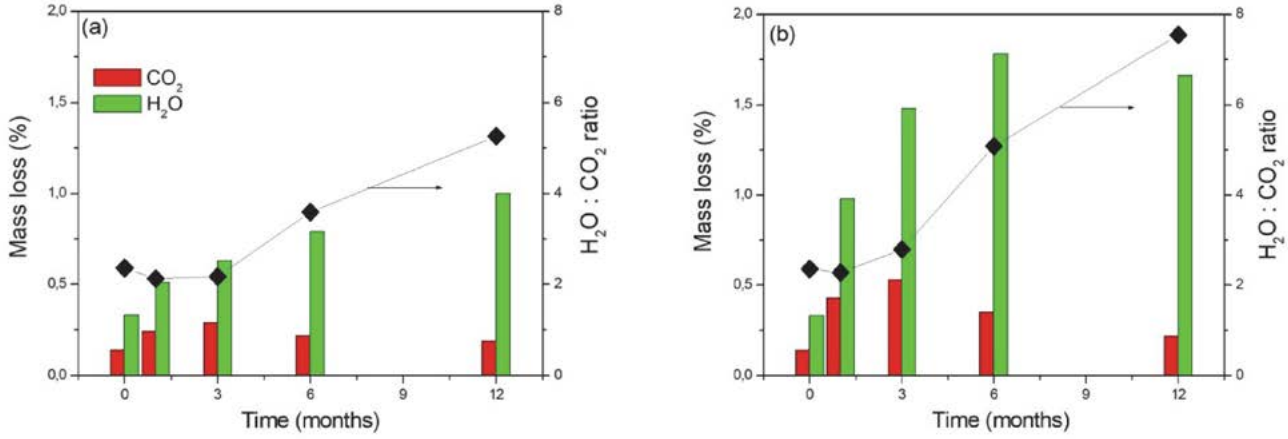

Figure 5. Comparison of H_2O release and CO_2 release due to decomposition of HT in the range 350–500 °C, and H_2O : CO_2 ratio for the samples aged for 0–12 months at 60 °C in (a) water and (b) NaOH.

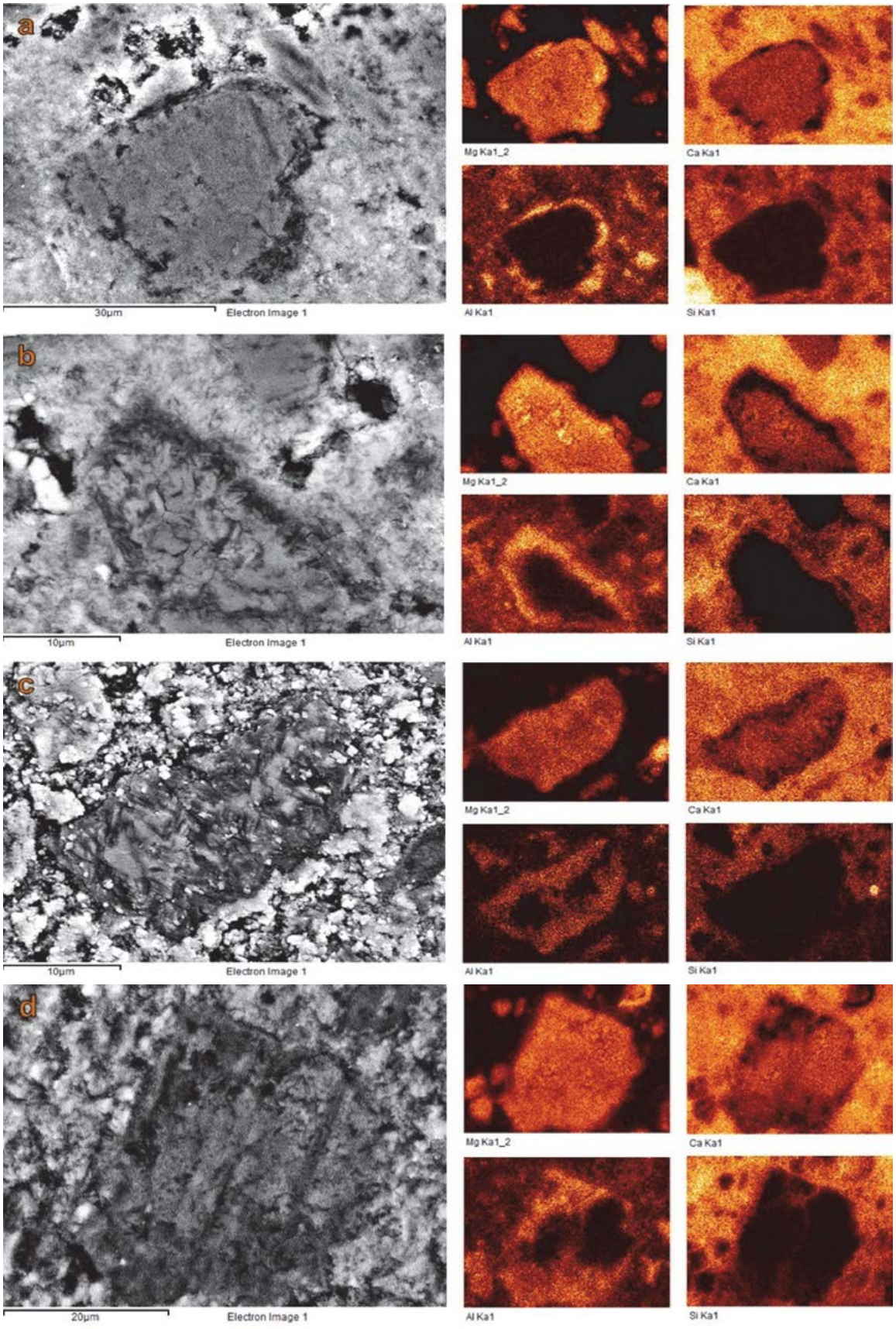

Figure 6. SEM image and elemental maps of Mg, Al, Ca and Si for the sample aged in (a) water at 60 °C for 12 months and in NaOH at 60 °C for (b) 3 months, (c) 6 months and (d) 12 months.

For further analysis of the hydrotalcite composition, the weight losses of the samples and the releases of water and CO_2 were compared in the temperature range from 300 to 550 °C (Fig.4). The peaks at about 420 °C, where the simultaneous release of H_2O and CO_2 is observed, correspond to the decomposition of hydrotalcite. The additional release of CO_2 at other temperatures could be due to the decomposition of monocarbonate or other carbonate-containing phases. The peak areas associated with the decomposition of hydrotalcite were calculated and compared with the total mass loss in this temperature range. In this way, the percentage ratio of H_2O and CO_2 released was determined, which is about 3.27 for natural hydrotalcite. In our case, the estimated H_2O : CO_2 mass ratio was 2.23 ± 0.10 for the unaged sample (M0) and the samples at an early stage of ageing (M1/M3), which is close to the ratio in hydrotalcite-like structure with lower Mg/Al ratio, e.g., quintenite $Mg_4Al_2(CO_3)(OH)_{12}{\cdot}3H_2O$, whose thermal decomposition is characterised by slightly higher reaction temperatures compared to hydrotalcite.[20]

The CO_2 and H_2O releases corresponding to the decomposition of hydrotalcite increase up to three months of ageing in both water and in NaOH. Thereafter, the amount of water released continues to increase for samples aged 6 and 12 months, consistent with XRD data on hydrotalcite phase content, while the amount of CO_2 released decreases. As a result, the H_2O : CO_2 ratio changes to 5.3 when aged in water and 7.5 when aged in NaOH for samples aged for 6 and 12 months. These data suggest a possible substitution of carbonate anions in the HT-CO_3 structure by hydroxide anions or the formation of a predominantly HT-OH phase, confirming the conclusions of the XRD study.

3. 3. Morphology

The changes in the microstructure of the mortars due to the dedolomitisation reaction and formation of new phases in the vicinity of dolomite grains were followed using SEM microscopy. Fig. 6a–d show typical SEM images of dolomitic grains and elemental maps (Mg, Al, Ca, and Si) in the samples aged at 60 °C in water for 12 months and in NaOH for 3–12 months.

It is noteworthy that during the first six months of ageing in the water environment, no significant changes were observed in the microstructure: the dolomitic aggregate grains remained almost intact. A new, well-defined Mg-Al phase has appeared as a narrow rim within a decaying dolomitic grain only after 12 months of ageing, indicating that Mg^{2+} does not move outside the grain boundary of the dolomite due to its limited mobility in water and alkali environment. The thickness of the hydrotalcite rim reaches only 3.4 ± 1.1 μm after ageing in water and does not exhibit a unique thickness that is likely sensitive to aggregate composition. When aged in NaOH, the Al-containing rim appears already after only 3 months of ageing, and its thickness increases with time from 3.3 ± 0.8 μm to about 8.9 ± 2.8 μm after 12 months of ageing. At the same time, the small dolomite grains look completely dedolomitised. Thus, the SEM data show that ageing in NaOH for 3 months results in the same changes in the dolomite grains as ageing in water for 12 months. This is also confirmed by XRD and TGA data on the amount of brucite and hydrotalcite-like phase formed.

The composition of the hydrotalcite-like phase in the samples was determined by plotting the Mg/Ca ratio *vs* the Al/Ca ratio from EDS analyses (Fig.7). A good correlation between Mg/Ca and Al/Ca indicates the presence of a hydrotalcite-like phase with a molar ratio of Mg/Al of about 2 for both water-aged and NaOH-aged samples. A similar ratio was reported for dolomite-cement systems.[11] Fig.7a indicates that the Mg/Al ratio in this phase does not change with time of ageing. Machner et al. have also shown that the Mg/Al ratio in dolomite/metakaolin-cement mortars was stable and did not change during leaching, carbonation or chloride exposure.[13]

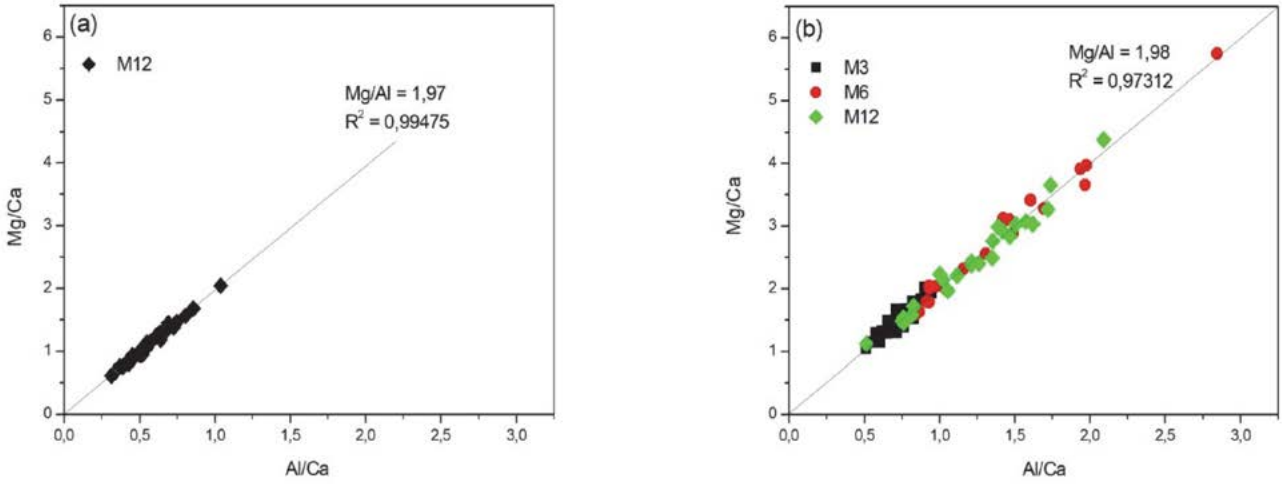

Figure 7. Results of SEM–EDS chemical analysis of hydrotalcite phase in the samples aged for 3–12 months at 60 °C in (a) water and (b) NaOH.

3. 4. Final Composition of HT-like Phase

According to XRD and TGA data, the formation of the hydrotalcite-like phase in dolomite-cement mortars starts from the very beginning of the ageing process of the samples at 60 °C both in water and in NaOH. The reaction can be written as following:

$$4CaMg(CO_3)_2 + 2Al(OH)_4^- + 4OH^- + nH_2O \rightarrow \rightarrow Mg_4Al_2(CO_3)(OH)_{12}{\cdot}nH_2O + 4CaCO_3 + + 3CO_3^{2-} \quad (3)$$

since the data from SEM give the Mg/Al ratio of 2 and, in our case, it does not depend on the alkalinity of the medium. The reaction proceeds more slowly in water, as expected from the literature data: phase composition and microstructure show that ageing in water for 12 months leads to the same changes in dolomite grains as ageing in 1M NaOH for 3 months. The amount of HT apparently increases with time as long as available aluminum cations remain in the cement paste.

The XRD and TGA data indicate that carbonate anions are replaced with hydroxide anions in the hydrotalcite-like phase during ageing:

$$Mg_4Al_2(CO_3)(OH)_{12}{\cdot}nH_2O + 2xOH^- \rightarrow \rightarrow Mg_4Al_2(CO_3)_{1-x}(OH)_{12+2x}{\cdot}nH_2O + xCO_3^{2-} \quad (4)$$

The formation of hydrotalcite containing mainly OH^- in the interlayer in carbonate-free hydrated Portland cement and of hydrotalcite containing both CO_3^{2-} and OH^- in Portland cement in the presence of carbonates was predicted.[15] Moreover, thermodynamic data showed that HT-OH is more stable than HT-CO_3 under conditions typical for Portland cement.[21] The released carbonate ions can migrate into the surrounding hydrated cement paste and assist in portlandite dissolution. This process takes place more easily when ageing occurs in water, since CO_3^{2-} ions readily migrate into solution under these conditions.

The final reaction products can therefore be identified as the hydrotalcite-like phase $Mg_4Al_2(CO_3)_{1-x}(OH)_{12+2x}{\cdot}nH_2O$, where x is the substitution degree of carbonates for hydroxides. This value was calculated from TGA data to be 0.53 and 0.64 for the hydrotalcite-like phase formed after 12 months of exposure in water and in an alkaline medium, respectively. Rietveld refinement of the HT peaks in the diffraction patterns yields close values of the substitution degrees (0.52 and 0.66 for samples aged in water and alkaline medium, respectively). The substitution degree will likely increase during the subsequent ageing of the samples.

4. Conclusion

In this work, we investigated the phase composition and microstructure of dolomite-cement mortars after ageing for 0–12 months under accelerated conditions (water or 1M NaOH, 60 °C). It was found that dolomite aggregates interact with cement paste and form the same reaction products (calcite, brucite and hydrotalcite) in alkaline environment and in water. However, the reaction in the water is much slower than in NaOH: the changes that occurred in dolomite grains during 12 months of ageing in water correspond to the changes that occurred during 3 months in 1M NaOH. The formation of the hydrotalcite-like phase rather than brucite is the predominant pathway for dolomite transformation in the presence of a large amount of available aluminium sources.

The hydrotalcite formed has the formula $Mg_4Al_2(CO_3)_{1-x}(OH)_{12+2x}{\cdot}nH_2O$, and the Mg/Al ratio does not change with ageing. No effect of the alkalinity of the medium on the composition of the hydrotalcite phase (Mg/Al ratio) was found. However, the carbonate anions in the structure of hydrotalcite are gradually replaced by hydroxide anions after three months of ageing, resulting in the formation of hydrotalcite containing mainly OH^- in the interlayer. The substitution degree x was estimated to be 0.53 or 0.64 after 12 months of ageing in water or NaOH, respectively.

Acknowledgements

The authors thank Petra Štukovnik (University of Ljubljana, Faculty of Civil and Geodetic Engineering) for her help with sample preparation and Edi Kranjc (National Institute of Chemistry, Ljubljana) for performing XRD measurements. We also thank the Slovenian Research Agency for financial support through grant P1-0175.

5. References

1. P. K. Mehta, P. J. M. Monteiro, Concrete: Microstructure, Properties, and Materials, 3rd Edition; McGraw-Hill, New York, 2006, 659 p.
2. I. Fernandes, Ö. Andiç-Çakir, C. Giebson, K. Seyfarth, in: I. Sims and A. Poole (Eds) Alkali-Aggregate Reaction in Concrete: A World Review, Taylor & Francis Group, London, UK, **2017**, pp. 321–432.
3. T. Katayama, *Cem. Concr. Res.* **2010**, *40,* 643–675. **DOI:**10.1016/j.cemconres.2009.09.020
4. X. Zhang, F. P. Glasser, K. L. Scrivener, *Cem. Concr. Res.* **2014**, *66,* 11–18. **DOI:**10.1016/j.cemconres.2014.07.017
5. P. Štukovnik, V. Bokan-Bosiljkov, M. Marinšek, *Constr. Build. Mater.* **2019**, *216*, 325–336. **DOI:**10.1016/j.conbuildmat.2019.04.260
6. A. Machner, M. Zajac, M. Ben Haha, K. O. Kjellsen, M. R. Geiker, K. De Weerdt, *Cem. Concr. Res.* **2018**, *105,* 1–17. **DOI:**10.1016/j.cemconres.2017.11.007
7. K. Rozov, U. Berner, D. Kulik, L. W. Diamond, *Clay Clay Miner.* **2011**, *59,* 215–232. **DOI:**10.1346/CCMN.2011.0590301
8. M. Bellotto, B. Rebours, O. Clause, J. Lynch, D. Bazin, E.

Elkaim, *J. Phys. Chem.* **1996**, *100*, 8527–8534. **DOI:**10.1021/jp960039j
9. S. Miyata, *Clay Clay Miner*. **1983,** *31,* 305–311. **DOI:**10.1346/CCMN.1983.0310409
10. Q. Wang, H. Huang Tay, Z. Guo, L. Chen, Y. Liu, J. Chang, Z. Zhong, J. Luo, A. Borgna, *Appl. Clay Sci.* **2012,** *55,* 18–26. **DOI:**10.1016/j.clay.2011.07.024
11. M. Zajac, S. K. Bremseth, M. Whitehead, M. Ben Haha, *Cem. Concr. Res.* **2014**, *65*, 21–29. **DOI:**10.1016/j.cemconres.2014.07.002
12. J. Xu, D. Lu, S. Zhang, Z. Xu, R. D. Hooton, *Constr. Build. Mater.* **2021**, *270*, 121375. **DOI:**10.1016/j.conbuildmat.2020.121375
13. A. Machner, M. Zajac, M. Ben Haha, K. O. Kjellsen, M. R. Geiker, K. De Weerdt, *Cem. Concr. Res.* **2018**, *89*, 89–106. **DOI:**10.1016/j.cemconcomp.2018.02.013
14. B. Z. Dilnesa, E. Wieland, B. Lothenbach, R. Dähn, K. L. Scrivener, *Cem. Concr. Res.* **2014**, *58*, 45–55. **DOI:**10.1016/j.cemconres.2013.12.012
15. E. Bernard, W. Jan Zucha, B. Lothenbach, U. Mäder, *Cem. Concr. Res.* **2022**, *152*, 106674. **DOI:**10.1016/j.cemconres.2021.106674
16. V. S. Ramachandran, R. F. Feldman, P. J. Sereda, *Highw. Res. Rec.* **1964**, 40–61.
17. R. Yahyaoui, P. E. Sanchez Jimenez, L. A. Pérez Maqueda, K. Nahdi, J. M. Criado Luque, *Thermochim. Acta* **2018**, *667*, 177–184. **DOI:**10.1016/j.tca.2018.07.025
18. R. Gabrovšek, T. Vuk, V Kaučič, *Acta Chim. Slov.* **2006**, *53*, 159–165.
19. B. Coto, C. Martos, J. L. Peña, R. Rodríguez, G. Pastor, *Fluid Phase Equilib.* 2012, *324* , 1–7. **DOI:**10.1016/j.fluid.2012.03.020
20. E. S. Zhitova , H. C. Greenwell , M. G. Krzhizhanovskaya, D. C. Apperley, I.V. Pekov, V. N. Yakovenchuk, *Minerals,* **2020**, *10*, 961. **DOI:**10.3390/min10110961
21. B. Lothenbach, F. Winnefeld, *Cem. Concr. Res.* **2006**, *36*, 209 – 226. **DOI:**10.1016/j.cemconres.2005.03.001

Povzetek

To delo obravnava reakcije dolomitnega prahu, zmešanega s portlandskim cementom, med staranjem v pogojih pospeševanja (60 °C, voda ali alkalni medij). Fazno sestavo in mikrostrukturo cementno-dolomitnih malt smo preučevali z rentgensko difrakcijo (XRD), termogravimetrično analizo (TGA) in vrstično elektronsko mikroskopijo z rentgensko mikroanalizo (SEM-EDS). Rezultati so pokazali, da je alkalnost medija povečala stopnjo reakcije dolomita, vendar ni vplivala na sestavo reakcijskih produktov. Izkazalo se je, da je tvorba hidrotalcitu podobne faze s splošno formulo $Mg_4Al_2(CO_3)_{1-x}(OH)_{12+2x}{\cdot}nH_2O$ prevladujoča pot porabe dolomita ob prisotnosti razpoložljivega aluminija v strjeni cementni pasti. Nato je po treh mesecih staranja postala opazna zamenjava vmesnih anionov (or anionov med plastmi): karbonatne anione v strukturi hidrotalcita postopoma zamenjajo hidroksidni.

DOI: 10.17344/acsi.2023.8016 *Acta Chim. Slov.* **2023,** *70,* 380–384

Scientific paper

Synthesis of New Coumarin Scaffold Bearing 2-Iminochromene Moiety

Reem A. K. Al-Harbi

Chemistry Department, Faculty of Science, Taibah University, Almadinah Almunawarrah, Saudi Arabia.

** Corresponding author: E-mail: rakharbi@taibahu.edu.sa; reemal94@hotmail.com*

Received: 01-19-2023

Abstract

Coumarin is classified as one of interesting therapeutic starting research points to obtain remarkable compounds with high efficacy. So, during this research, new 2-iminochromene derivatives bearing coumarin moiety were synthesized. At first, cyanoacetohydrazone of 3-acetylcoumarin was prepared and used as the starting material. The 2-iminochromene derivatives were synthesized through the ring closure of cyanoacetohydrazone derivative with 4-hydroxysalicylaldehyde, 5-aryldiazosalicylaldehydes, 2-hydroxynaphthaldehyde and 7-hydroxychromone-6-carboxaldehyde derivative. All of the newly synthesized coumarin derivatives were obtained in excellent yields; so, the new synthesized coumarin derivatives will participate in the enrichment of the chemical libraries.

Keywords: Coumarins; 2-Iminochromenes; Benzopyrones; Chromenes; Chromen-2-ones.

1. Introduction

Coumarins (chromen-2-one derivatives) and 2-iminochromene derivatives are classes of natural benzopyrone. They are found in different varieties of the plant species. Coumarin is classified as one of interesting therapeutic starting research points and is being studied to obtain remarkable compounds with high efficacy and low toxicity. In the field of drug development and discovery, many various coumarin derivatives of synthetic origin are being developed as important compounds because they possess a wide range of pharmacological properties.[1–5]

Chromene derivatives have antibacterial and antifungal activities. Their promising antifungal activities make them potentially useful in agri-food and as pharmaceutical agents.[4–8] Chromene derivatives have great roles in treating of various cancers such as leukemia, lymphoma and renal cell carcinoma. Moreover, they reduce the effects of radiation therapy.[9,10] Chromene derivatives have been effective against several viruses, such as HIV, influenza, hepatitis, Dengue and Chikungunya.[11,12] Chromene derivatives were reported as analgesic, anti-pyretic and anti-inflammatory agents; where they recover fluid and edema in harmful tissues.[13,14] Some chromene derivatives were marketed as drugs to inhibit blood clotting such as phenprocoumon, choleraicin A, warfarin, acenocoumarin, the antibiotic novobiocin and hymecromone (umbelliferone).[15,16]

As shown in Figure 1, beside the application of chromene derivatives in the field of medicinal chemistry, some chromene derivatives have applications in various fields such as optical brighteners, markers, photosensitizers, lasers, fluorescent dyes, cosmetics, perfumes, pigments, dyes, solar cells and optical data storage devices.[17–19]

Depend on the above facts, it was aimed to synthesizing new 2-iminochromene derivatives bearing coumarin moiety wishing to discover new chromene derivatives that may have significant activities.

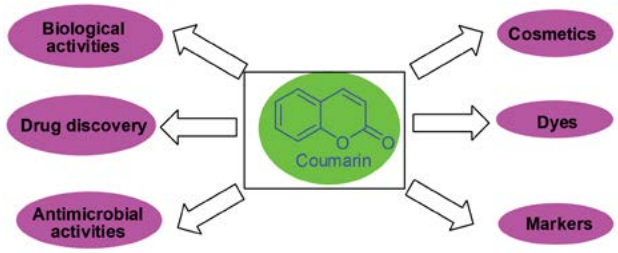

Figure 1. Applications of coumarin nucleus

2. Results and Discussion

The cyanoacetohydrazone **2** as starting material was prepared as illustrated in Scheme 1. First, 3-acetylcoumarin (**1**) was prepared *via* ring closure of salicylaldehyde

with ethyl acetoacetate. Cyanoacetohydrazone **2** of 3-acetylcoumarin was prepared through the condensation of 3-acetylcoumarin (**1**) with cyanoacetohydrazide.[20]

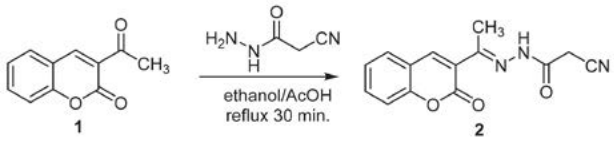

Scheme 1. Synthesis of the starting material cyanoacetohydrazone **2**

Here, the author aimed to synthesize coumarin scaffold bearing 2-iminochromene moiety hoping to obtain some significant compounds. Thus, as shown in Scheme 2, cyclocondensation of cyanoacetamide **2** with 4-hydroxysalicylaldehyde in ethanol containing piperidine gave 2-iminochromene derivative **3** in excellent yield. ^{1}H NMR spectrum of coumarin derivative **3** was characterized by the presence of one diagnostic singlet signal at δ 2.27 ppm corresponding to methyl protons. The seven protons of two benzene rings were displayed in 7.27–7.96 ppm region. Two diagnostic singlet signals of C_4-H of chromenes appeared at δ 8.29 and 8.64 ppm. Also, ^{1}H NMR spectrum showed three diagnostic singlets, broad and singlet signals at: 9.32, 10.50 and 13.69 ppm with one proton integral value for two imino and hydroxyl protons.

Several diazenyl derivatives have been synthesized for their potential activities.[21–25] Thus, the present work describes the preparation of chromene nucleus containing aryldiazo group. Thus, cyclization of cyanoacetamide **2** with 5-aryldiazosalicylaldehydes in the presence of piperidine afforded of 6-(aryldiazenyl)-2-iminochromene derivatives **4a**–**f**. ^{1}H NMR spectrum of iminochromene derivative **4d** showed two singlet signals at δ 2.29 and 2.43 ppm with three protons integral value for two methyl groups. Beside the diagnostic singlet signal for iminochromene-(H-5) at δ 8.44 ppm, the remaining ten benzopyran protons were assigned in δ 7.35–8.10 region. The two singlet signals at δ 8.30 and 8.76 were displayed for two C_4-H of chromene protons. The two imine protons signals were assigned at δ 9.52 and 13.58 ppm. Moreover, cyclocondensation reaction of **2** with 2-hydroxy-1-naphthaldehyde in ethanol containing piperidine smoothly furnished benzo[*f*]chromene derivative **5**. Finally, cyclocondensation reaction of **2** with derivative of 7-hydroxychromone-6-carboxaldehyde in ethanol containing piperidine smoothly furnished pyrano[3,2-*g*]chromene derivative **6**. ^{1}H NMR spectrum of pyrano[3,2-*g*]chromene derivative **6** was characteristic by the presence of three singlet signals at

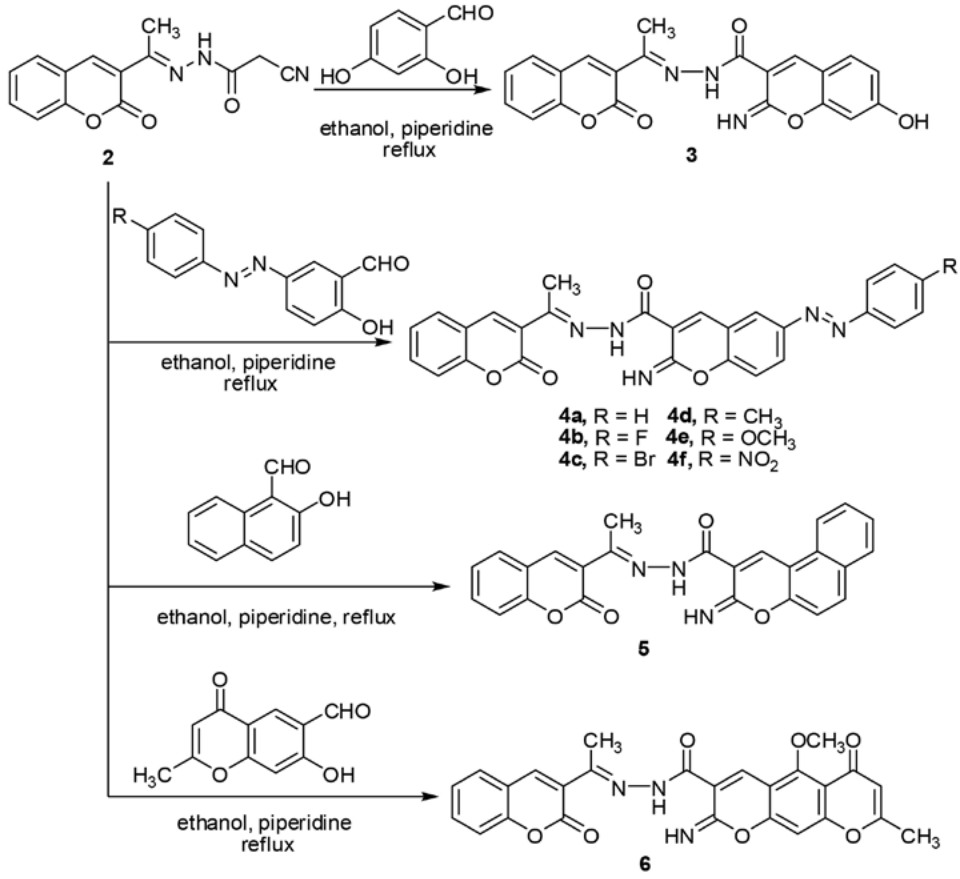

Scheme 2. Synthesis of 2-iminochromene derivatives **3**–**6**

δ 2.30, 2.36 and 3.96 ppm assignable for two methyl and one methoxy protons. The two singlet signals at δ 10.25 and 11.16 ppm were assigned to the two imino groups.

3. Conclusions

In this study, new functionalized coumarin derivatives bearing 2-iminochromene moiety were synthesized. The new coumarin derivatives were obtained in excellent yields and in high purity through ring closure of cyanoacetohydrazone derivative with 4-hydroxysalicylaldehyde, different derivatives of 5-aryldiazosalicylaldehyde, 2-hydroxy-naphthaldehyde and 7-hydroxychromone-6-carboxaldehyde derivative.

4. Experimental Section

Nuclear magnetic resonance spectra were carried out in deuterated dimethylsulfoxide (DMSO-d_6) by using Bruker spectrometers (^{1}H NMR 400 MHz) with chemical shift in δ from internal TMS. Elemental analyses were carried out on a EuroVector instrument C, H, N analyzer EA3000 Series.

Synthesis of 2-Cyano-*N*'-(1-(2-oxo-2*H*-chromen-3-yl) ethylidene)acetohydrazide (2)

The mixture of equimolar amounts of 3-acetylcoumarin (**1**) (1.88 g, 0.01 mol) and the cyanoacetic acid hydrazide (0.99 g, 0.01 mol) in the mixture of 1 mL AcOH and 50 mL ethanol was heated under reflux for 0.5 h, left to cool, the resultant solid product was collected by filtration. The solid product was crystallized from ethanol. Yield 2.152 g (80%); m.p. 175–176 °C; IR: ν/cm^{-1} 3181 (NH), 3082 (CH-arom.), 2962, 2922 (CH-aliph.), 2265 (C≡N), 1715, 1680 (C=O), 1619, 1604 (C=N); ^{1}H NMR: δ 2.26 (s, 3H, CH_3-C=N), 4.10 (s, 2H, CH_2), 7.40 (t, 1H, *J* = 7.5 Hz, C_6-H of chromene), 7.43 (d, 1H, *J* = 8.2 Hz, C_8-H of chromene), 7.65 (t, 1H, *J* = 7.8 Hz, C_7-H of chromene), 7.79 (dd, 1H, *J* = 7.7, 1.3 Hz, C_5-H of chromene), 8.36 (s, 1H, C_4-H of chromene), 11.44 (s, 1H, NH).

Synthesis of 7-Hydroxy-2-imino-*N*'-(1-(2-oxo-2*H*-chromen-3-yl)ethylidene)-2*H*-chromene-3-carbohydrazide (3)

To a hot solution of the mixture of equimolar amounts of cyanoacetamide **2** (269 mg, 1 mmol) and 4-hydroxysalicylaldehyde (138 mg, 1 mmol) in ethanol (100 mL), piperidine (8.5 mg, 0.1 mmol) was added. The reaction mixture was heated under reflux for 0.5 h. The solid product formed while hot was collected by filtration and recrystallized from dioxane to give **3**. Yield 350 mg (90%); m.p. 273–275°C; IR: ν/cm^{-1} 3327 (NH), 3070 (CH-arom.), 2957 (CH-aliph.), 1719, 1694, 1640 (C=O); ^{1}H NMR: δ 2.27 (s, 3H, CH_3), 7.27–7.52 (m, 3H, Ar-H), 7.57–7.73 (m, 2H, Ar-H), 7.80–7.96 (m, 2H, Ar-H), 8.29 (s, 1H, C_4-H of chromene), 8.64 (s, 1H, C_4-H of chromene), 9.32 (s, 1H, NH), 10.50 (br, 1H, OH), 13.69 (s, 1H, NH); MS: *m/z* (%) 389 (M^+; 52.5). Anal. calcd for $C_{21}H_{15}N_3O_5$ (389.36): C, 64.78; H, 3.88; N, 10.79. Found: C, 64.82; H, 3.86; N, 10.83%.

Synthesis of 2-Imino-*N*'-(1-(2-oxo-2*H*-chromen-3-yl) ethylidene)-6-(aryldiazenyl)-2*H*-chromene-3-carbohydrazides 4a–f

To a hot solution of the mixture of equimolar amounts of cyanoacetamide **2** (269 mg, 1 mmol) and 5-aryldiazenylsalicyaldehyde (namely, 5-((phenyl)diazenyl)salicyaldehyde (226 mg, 1 mmol), 5-((4-fluorophenyl) diazenyl)salicyaldehyde (244 mg, 1 mmol), 5-((4-bromophenyl)diazenyl)salicyaldehyde (305 mg, 1 mmol), 5-((4-methylphenyl)diazenyl)salicyaldehyde (240 mg, 1 mmol), 5-((4-methoxyphenyl)diazenyl)salicyaldehyde (256 mg, 1 mmol) and 5-((4-nitrophenyl)diazenyl)salicyaldehyde (271 mg, 1 mmol)) in ethanol (100 mL), piperidine (8.5 mg, 0.1 mmol) was added. The reaction mixture was heated under reflux for 0.5 h. The solid product formed while hot was collected by filtration and recrystallized from dioxane to give products **4a–f**.

2-Imino-*N*'-(1-(2-oxo-2*H*-chromen-3-yl)ethylidene) -6-(phenyldiazenyl)-2*H*-chromene-3-carbohydrazide (4a): Yield 453 mg (95%); m.p. 208–210 °C; IR: ν/cm^{-1} 3327 (NH), 3041 (CH-arom.), 2963 (CH-aliph.), 1694, 1641 (C=O), 1607 (C=N); ^{1}H NMR: δ 2.27 (s, 3H, CH_3), 7.33–8.46 (m, 12H, Ar-H), 8.78 (s, 1H, C_4-H of chromene), 9.10 (s, 1H, C_4-H of chromene), 9.54 (s, 1H, NH), 13.59 (s, 1H, NH); MS: *m/z* (%) 477 (M^+; 55.4). Anal. calcd for $C_{27}H_{19}N_5O_4$ (477.47): C, 67.92; H, 4.01; N, 14.67. Found: C, 67.87; H, 3.99; N, 14.72%.

6-((4-Fluorophenyl)diazenyl)-2-imino-*N*'-(1-(2-oxo-2*H*-chromen-3-yl)ethylidene)-2*H*-chromene-3-carbohydrazide (4b): Yield 446 mg (90%); m.p. 193–195 °C; IR: ν/cm^{-1} 3324 (NH), 3007 (CH-arom.), 1723, 1702 (C=O); ^{1}H NMR: δ 2.27 (s, 3H, CH_3), 7.38–8.45 (m, 11H, Ar-H), 8.78 (s, 1H, C_4-H of chromene), 9.09 (s, 1H, C_4-H of chromene), 9.54 (s, 1H, NH), 13.59 (s, 1H, NH); MS: *m/z* (%) 495 (M^+; 31.2). Anal. calcd for $C_{27}H_{18}FN_5O_4$ (495.46): C, 65.45; H, 3.66; N, 14.14. Found: C, 65.41; H, 3.65; N, 14.11%.

6-((4-Bromophenyl)diazenyl)-2-imino-*N*'-(1-(2-oxo-2*H*-chromen-3-yl)ethylidene)-2*H*-chromene-3-carbohydrazide (4c): Yield 528 mg (95%); m.p. 199–201 °C; IR: ν/cm^{-1} 3275 (NH), 3045 (CH-arom.), 1703 (C=O), 1607 (C=N); ^{1}H NMR: δ 2.26 (s, 3H, CH_3), 6.88 (t, 1H, *J* = 7.3 Hz, Ar-H), 6.97 (d, 1H, *J* = 8.1 Hz, Ar-H), 7.30–7.48 (m, 2H, Ar-H), 7.70 (d, 1H, *J* = 8.9 Hz, Ar-H), 7.74–7.94 (m, 5H, Ar-H), 8.27 (d, 1H, *J* = 8.8 Hz, Ar-H), 8.34 (s,1H, C_4-H of chromene), 9.07 (s, 1H, C_4-H of chromene), 11.16 (s,

1H, NH), 13.57 (s, 1H, NH); MS: *m/z* (%) 556.37 (M^+; 28.7). Anal. calcd for $C_{27}H_{18}BrN_5O_4$ (556.37): C, 58.29; H, 3.26; N, 12.59. Found: C, 58.32; H, 3.25; N, 12.63%.

2-Imino-*N*'-(1-(2-oxo-2*H*-chromen-3-yl)ethylidene)-6-(*para*-tolyldiazenyl)-2*H*-chromene-3-carbohydrazide (4d): Yield 441 mg (90%); m.p. 205–206 °C; IR: ν/cm^{-1} 3318 (NH), 3047 (CH-arom.), 1705 (C=O); ^{1}H NMR: δ 2.29 (s, 3H, CH_3), 2.43 (s, 3H, CH_3), 7.35–8.10 (m, 10H, Ar-H), 8.30 (s, 1H, C_4-H of chromene), 8.44 (s, 1H, Ar-H), 8.76 (s, 1H, C_4-H of chromene), 9.52 (s, 1H, NH), 13.58 (s, 1H, NH); MS: *m/z* (%) 491.50 (M^+; 42.2). Anal. calcd for $C_{28}H_{21}N_5O_4$ (491.50): C, 68.42; H, 4.31; N, 14.25. Found: C, 68.37; H, 4.30; N, 14.31%.

2-Imino-6-((4-methoxyphenyl)diazenyl)-*N*'-(1-(2-oxo-2*H*-chromen-3-yl)ethylidene)-2*H*-chromene-3-carbohydrazide (4e): Yield 464 mg (90%); m.p. 214–215 °C; IR: ν/cm^{-1} 3327 (NH), 3070, 3035 (CH-arom.), 2954 (CH-aliph.), 1719, 1693 (C=O); ^{1}H NMR: δ 2.29 (s, 3H, CH_3), 3.85 (s, 3H, OCH_3), 7.35–8.10 (m, 10H, Ar-H), 8.30 (s, 1H, Ar-H), 8.44 (s, 1H, Ar-H), 8.76 (s, 1H, C_4-H of chromene), 9.52 (s, 1H, NH), 13.58 (s, 1H, NH); MS: *m/z* (%) 507 (M^+; 33.8). Anal. calcd for $C_{28}H_{21}N_5O$ (507.50): C, 66.27; H, 4.17; N, 13.80. Found: C, 66.32; H, 4.16; N, 13.78%.

2-Imino-6-((4-nitrophenyl)diazenyl)-*N*'-(1-(2-oxo-2H-chromen-3-yl)ethylidene)-2*H*-chromene-3-carbohydrazide (4f): Yield 496 g (95%); m.p. 217–219 °C; IR: ν/cm^{-1} 3307 (NH), 3062 (CH-arom.), 1682 (C=O), 1606 (C=N); MS: *m/z* (%) 522 (M^+; 62.3). Anal. calcd for $C_{27}H_{18}N_6O_6$ (522.47): C, 62.07; H, 3.47; N, 16.09. Found: C, 62.12; H, 3.46; N, 16.11%.

Synthesis of 3-Imino-*N*'-(1-(2-oxo-2*H*-chromen-3-yl) ethylidene)-3*H*-benzo[*f*]chromene-2-carbohydrazide (5)

To a hot solution of the mixture of equimolar amounts of cyanoacetamide **2** (269 mg, 0.01 mol) and 2-hydroxy-1-naphthaldehyde (172 mg, 0.01 mol) in ethanol (100 mL), piperidine (8.5 mg, 0.1 mmol) was added. The reaction mixture was heated under reflux for 0.5 h. The solid product formed while hot was collected by filtration and recrystallized from dioxane to give **5**. Yield 402 mg (95%); m.p. 240–242 °C; IR: ν/cm^{-1} 3306 (NH), 2908 (CH-aliph.), 1713, 1687 (C=O); ^{1}H NMR: δ 2.26 (s, 3H, CH_3), 7.21–8.74 (m, 11H, Ar-H), 9.81 (s,1H, C_4-H of chromene), 11.16 (s, 1H, NH), 13.74 (s, 1H, NH); MS: *m/z* (%) 423.42 (M^+; 55.2). Anal. calcd for $C_{25}H_{17}N_3O_4$ (423.42): C, 70.91; H, 4.05; N, 9.92. Found: C, 70.87; H, 4.04; N, 9.88%.

Synthesis of 2-Imino-5-methoxy-8-methyl-6-oxo-*N*'-(1-(2-oxo-2*H*-chromen-3-yl)ethylidene)-2,6-dihydropyrano[3,2-*g*]chromene-3-carbohydrazide (6)

To a hot solution of the mixture of equimolar amounts of cyanoacetamide **2** (269 mg, 1 mmol) and 7-hydroxy-5-methoxy-2-methyl-4-oxo-4*H*-chromone-6-carboxaldehyde (204 mg, 1 mmol) in ethanol (100 mL), piperidine (8.5 mg, 0.1 mmol) was added. The reaction mixture was heated under reflux for 0.5 h. The solid product formed while hot was collected by filtration and recrystallized from dioxane to give **6**. Yield 446 mg (98%); m.p. 243–245 °C; IR: ν/cm^{-1} 3327 (NH), 3009 (CH-arom.), 1699, 1664 (C=O), 1605 (C=N); ^{1}H NMR: δ 2.30 (s, 3H, CH_3), 2.36 (s, 3H, CH_3), 3.96 (s, 3H, OCH_3), 6.22 (s, 1H, Ar-H), 6.80–7.80 (m, 6H, Ar-H), 9.02 (s, 1H, C_4-H of chromene), 10.25 (s, 1H, NH); 11.16 (s, 1H, NH); MS: *m/z* (%) 485 (M^+; 46.5). Anal. calcd for $C_{26}H_{19}N_3O_7$ (485.44): C, 64.33; H, 3.95; N, 8.66. Found: C, 64.29; H, 3.94; N, 8.62%.

5. References

1 M. A. Salem, M. H. Helal, M. A. Gouda, Y. A. Ammar, M. S. A. El-Gaby, S. Y. Abbas, *Synthetic Commun.,* **2018**, *48*, 1534–1550. **DOI:**10.1080/00397911.2018.1455873

2 M. A. Salem, S. Y. Abbas, M. H. Helal, A. Y. Alzahrani, *Polycycl. Aromat. Compd.*, **2023**, *43*, 1081–1091. **DOI:**10.1080/10406638.2021.2024583

3 M. A. Salem, S. Y. Abbas, M. H. Helal, A. Y. Alzahrani, *J. Heterocycl. Chem.,* **2021**, *58*, 2117–2123. **DOI:**10.1002/jhet.4335

4 S. A. Hessein, M. A. M. El-Sharief, S. Y. Abbas, H. K. Thabet, Y. A. Ammar, *Croat. Chem. Acta,* **2016**, *89*, 91–100. **DOI:**10.5562/cca2811

5 S. A. Fouad, S. A. Hessein, S. Y. Abbas, A. M. Farrag, Y. A. Ammar, *Croat. Chem. Acta,* **2018**, *91*, 99–107.

6 F. Annunziata, C. Pinna, S. Dallavalle, L. Tamborini, A. Pinto, *Int. J. Mol. Sci.*, **2020**, *21*, 4618. **DOI:**10.3390/ijms21134618

7 K. N. Venugopala, V. Rashmi, B. Odhav, *Bio. Med res. int.*, **2013**, *2013*, 1–14. **DOI:**10.1155/2013/963248

8 N. Hamdi, M. C. Puerta, P. Valerga, *Eur. J. Med. Chem.*, **2008**, *43*, 2541–2548. **DOI:**10.1016/j.ejmech.2008.03.038

9 E. Küpeli Akkol, Y. Genç, B. Karpuz, E. Sobarzo-Sánchez, R. Capasso, *Cancers*, **2020**, *12*, 1959. **DOI:**10.3390/cancers12071959

10 J. Ding, J. Liu, Z. Zhang, J. Guo, M. Cheng, Y. Wan, R. Wang, Y. Fang, Z. Guan, Y. Jin, S.-S. Xie, *Bioorg. Chem.,* **2020***, 101,* 104023. **DOI:**10.1016/j.bioorg.2020.104023

11 S. Mishra, A. Pandey, S. Manvati, *Heliyon*, **2020**, 6, e03217. **DOI:**10.1016/j.heliyon.2020.e03217

12 H. Zakaryan, E. Arabyan, A. Oo, K. Zandi, *Arch Virol.,* **2017,** *162*, 2539–2551. **DOI:**10.1007/s00705-017-3417-y

13 S. S. Garg, J. Gupta, S. Sharma, D. Sahu, *Eur. J. Pharm. Sci.*, **2020**, *152*, 105424. **DOI:**10.1016/j.ejps.2020.105424

14 H. M. Revankar, S. N. A. Bukhari, G. B. Kumar, H.-L. Qin, *Bioorg. Chem.*, **2017,***71*, 146–159. **DOI:**10.1016/j.bioorg.2017.02.001

15 R. Frederick, C. Charlier, S. Robert, *Bioorg. Med. Chem. Letters*, **2006,** *16*, 2017–2021.

16 O. Bruno, C. Brullo, S. Schenone, F. Bondavalli, A. Ranise, M.

Tognolini, M. Impicciatore, V. Ballabeni, E. Barocelli, *Bioorg. Med. Chem*. **2006,** 14, 121–130. **DOI:**10.1016/j.bmc.2005.07.066

17 S. Chen, M. Zhang, C. Zhu, H. Lu, M. Zhao, X. Tian, Q. Zhang, S. C. De Souza, F. Rong, H. Zhou, J. Wu, Y. Tian, *Dyes and Pigments,* **2018,** *148*, 429–436. **DOI:**10.1016/j.dyepig.2017.09.047

18 X. Wang, Z. Guo, S. Zhu, Y. Liu, P. Shi, H. Tian, W.-H. Zhu, *J. Mater. Chem. B,* **2016**, *4*, 4683e9. **DOI:**10.1039/C6TB01096B

19 I. Yahaya, N. Seferoğlu, Z. Seferoğlu, *Tetrahedron*, **2019**, *75*, 2143–2154. **DOI:**10.1016/j.tet.2019.02.034

20 R. M. Mohareb, N. Y. M. Abdo, *Chem. Pharm. Bull.* **2015**, *63*, 678–687. **DOI:**10.1248/cpb.c15-00115

21 S. Y. Abbas, W. M. Basyouni, K. A. M. El-Bayouki, R. M. Dawood, T. H. Abdelhafez, M. K. Elawady, *Synthetic Commun.,* **2019**, *49*, 2411–2416. **DOI:**10.1080/00397911.2019.1626893

22 S. Y. Abbas, W. M. Basyouni, K. A. M. El-Bayouk, *Appl. Organomet. Chem.,* **2018**, *32*, e4032. **DOI:**10.1002/aoc.4032

23 W. M. Basyouni, S. Y. Abbas, K. A. M. El-Bayouki, R. M. Dawood, M. K. Elawady, *Synthetic Commun.,* **2021**, *51*, 2168–2174. **DOI:**10.1080/00397911.2021.1925298

24 M. A. Salem, S. Y. Abbas, S. A. Darwish, M. H. Helal, E. H. Aish, *Russian J. Gen. Chem.,* **2021**, *91*, 1578–1583. **DOI:**10.1134/S1070363221080211

25 M. A. Salem, S. Y. Abbas, M. A. M. Sh. El-Sharief, A. Y. Alzahrani, M. H. Helal, H. K. Thabet, *Synthetic Commun.,* **2021**, *51*, 3325–3331. **DOI:**10.1080/00397911.2021.1968909

Povzetek

Kumarin je terapevtsko zanimiva spojina, ki predstavlja izhodišče za pripravo mnogih pomembnih spojin z opaznimi učinki. V predstavljeni raziskavi sem sintetiziral nove 2-iminokromenske derivate, ki vsebujejo kumarinski fragment. Najprej sem kot izhodno spojino pripravil cianoacetohidrazon iz 3-acetilkumarina. 2-Iminokromenske derivate sem pripravil s sintezo s pomočjo ciklizacije med cianoacetohidrazonskimi derivati in ustreznimi aldehidi (4-hidroksisalicilaldehid, 5-arildiazosalicilaldehid, 2-hidroksinaftaldehid in 7-hidroksikromon-6-karboksaldehid). Vsi novi pripravljeni kumarinski derivati so bili izolirani v visokih izkoristkih. Novi kumarini tako predstavljajo obogatitev kemijskih knjižnic.

Scientific paper

Micellar Liquid Chromatographic Method for Determination of Moxifloxacin and its Impurities

Alma Salkić,[1, 2,*] Biljana Otašević,[3] Marija Rašević[3] and Mira Zečević[3]

[1] *ZADA Pharmaceuticals d.o.o. Bistarac Donji bb, 75300 Lukavac, Bosnia and Herzegovina*

[2] *Faculty of Pharmacy, University of Tuzla, Studentska 6, 75000 Tuzla, Bosnia and Herzegovina*

[3] *Department of Drug Analysis, Faculty of Pharmacy, University of Belgrade, 450 Vojvode Stepe, 11221 Belgrade, Serbia*

* *Corresponding author: E-mail: alma.salkic@zada.ba*

Received: 01-23-2023

Abstract

A selective eco-friendly micellar HPLC method was developed for investigation of moxifloxacin and related compounds in the presence of its degradation products. Central composite design was used to optimize the experimental conditions. The proposed method is based on isocratic elution on a C18 column using 92.5% (v/v) biodegradable aqueous mobile phase containing 0.01 M sodium dihydrogen phosphate, 0.15 M sodium dodecyl sulfate (SDS) and 0.5% triethylamine (v/v) with a pH of 3.5 and 7.5% isopropanol (v/v) as eco- friendly organic solvent. The flow rate and injection volume were 0.6 ml/min and 5 µl, respectively. Experiments were performed at a temperature of 60 °C and detection was performed at 295 nm. The optimized method was validated. The method was found to be suitable for the quantification of moxifloxacin and its related compounds in moxifloxacin drug substance. The Green Analytical Procedure Index (GAPI) proves the superiority of the developed method against other reported methods.

Keywords: Moxifloxacin, Micellar, Impurities, SDS, Degradation, GAPI

Introduction

Moxifloxacin is an anti-infective from the group of fluoroquinolones. Moxifloxacin drug substance is described in the European (Ph. Eur.) and United States Pharmacopeia (USP).[1–2] High-performance liquid chromatography (HPLC) is the most commonly used analytical tool for pharmaceutical analysis. Most published HPLC methods for investigation of moxifloxacin are based on the reversed-phase (RP) mode using organic solvents such as acetonitrile and methanol in mobile phase.

These two solvents are not preferred in terms of environmental impact and health safety. Even if methanol is less toxic and more easily biodegradable than acetonitrile, it is also ranked as a hazardous solvent due to its inherent toxicity and the great requirements of its waste disposal.

The organic solvents commonly accepted as green, and which can be used in RP-HPLC, are ethanol, isopropanol, n-propanol, acetone, ethyl acetate, ethyl lactate, and propylene carbonate. [3]

The official HPLC methods for the analysis of the drug substance moxifloxacin and its impurities described in Ph. Eur. and USP are essentially similar and use a mobile phase containing methanol and aqueous solution containing 0.5 g/l tetrabutylammonium hydrogen sulfate, 1 g/l potassium dihydrogen phosphate and 3.4 g/l phosphoric acid (28:72, v/v).

Also, most reported HPLC methods for determination of moxifloxacin and its impurities use a high percentage of organic solvents (methanol or acetonitrile) in the mobile phase which cannot be considered as environmentally friendly solvents. [4–11]

Micellar liquid chromatography (MLC) method has been investigated as an interesting approach for green analytical chemistry (GAC), as it eliminates or reduces the use of organic solvents and uses mobile phases containing 90% (v/v) or more water.[12–17] MLC is attractive due to its lower cost, lower toxicity, greater stability, reduced negative impact on the environment and greater safety for laboratory use. MLC depends on using surfactants at a concentration above their critical micellar concentration (CMC).[13]

The choice of surfactant is of great importance when creating a hybrid micellar chromatography system. In previous research, sodium dodecyl sulfate (SDS) was most often examined with regard to its availability and low price.[18] The large amount of data available in the literature on mi-

cellar and hybrid micellar systems with SDS as a surfactant facilitates the setting up of chromatographic methods for specific analyses.[19–23]

Another important advantage of MLC concerns sample treatment. In fact, the great solubilizing ability of micelles allows the direct injection of drugs in complex matrices (e.g., biological fluids and dosage forms) without the need for any sample pretreatment other than filtration.[3] Moreover, MLC is compatible with existing RP-HPLC instruments. Therefore, it does not require any modification of existing RP-HPLC instrumentation.[3]

To the best of our knowledge, no method has been reported for the determination of moxifloxacin and its related substances by micellar HPLC. A few papers have been published on the topic of determination of fluoroquinolone using micellar HPLC.[24–25]

In a published study[24] a method for simultanous separation of four quinolones including moxifloxacin was developed. Also, a study was conducted on the simultaneous separation of levofloxacin and ambroxol.[25] The aim of this work was to develop an environmentally friendly MCL method for the investigation of moxifloxacin and related compounds (Figure 1) in the presence of its degradation products, using ecologically safer mobile phase composition and lower solvent consumption.

The proposed method was compared favorably with published methods using the new assessment tool, GAPI index, to provide additionally support for the environmental benefits of the proposed method.

2. Experimental

2. 1. Materials

A moxifloxacin drug substance sample was provided by the Hetero Drugs Limited, India. Moxifloxacin hydrochloride CRS (purity of 96.1%) was purchased from EDQM. Five moxifloxacin impurities namely Impurity-A, Impurity-B, Impurity-C, Impurity-D, Impurity-E (Figure 1) with stated purity of 99.94%, 100.00%, 99.72%, 99.75%, 98.82%, respectively, were purchased from Veeprho Pharmaceuticals s.r.o, Europe. All reagents used were of analytical grade.

Sodium phosphate monobasic monohydrate was purchesed from CARLO ERBA (CARLO ERBA Reagents S.A.S, France), SDS was purchased from ACROS ORGANICS (ACROS ORGANICS, Geel, Belgium), triethylamine and orthophosphoric acid were supplied by Fischer Scientific U.K. Limited.

For the mobile phase, isopropanol was HPLC grade purchased from Fischer Scientific U.K. Limited. HPLC grade water was produced using a Milli-Q purification system (Millipore Co., MA, USA) provided by ZADA Pharmaceuticals.

2. 2. Equipment and Chromatographic Conditions

Chromatographic analyses were done using a *Thermo Finigian* HPLC system (*Thermo Fisher Scientific Inc.*, Waltham, SAD) equipped with a DAD detector. Separations were achieved on a ZORBAX SB C18 150 mm x 4.6

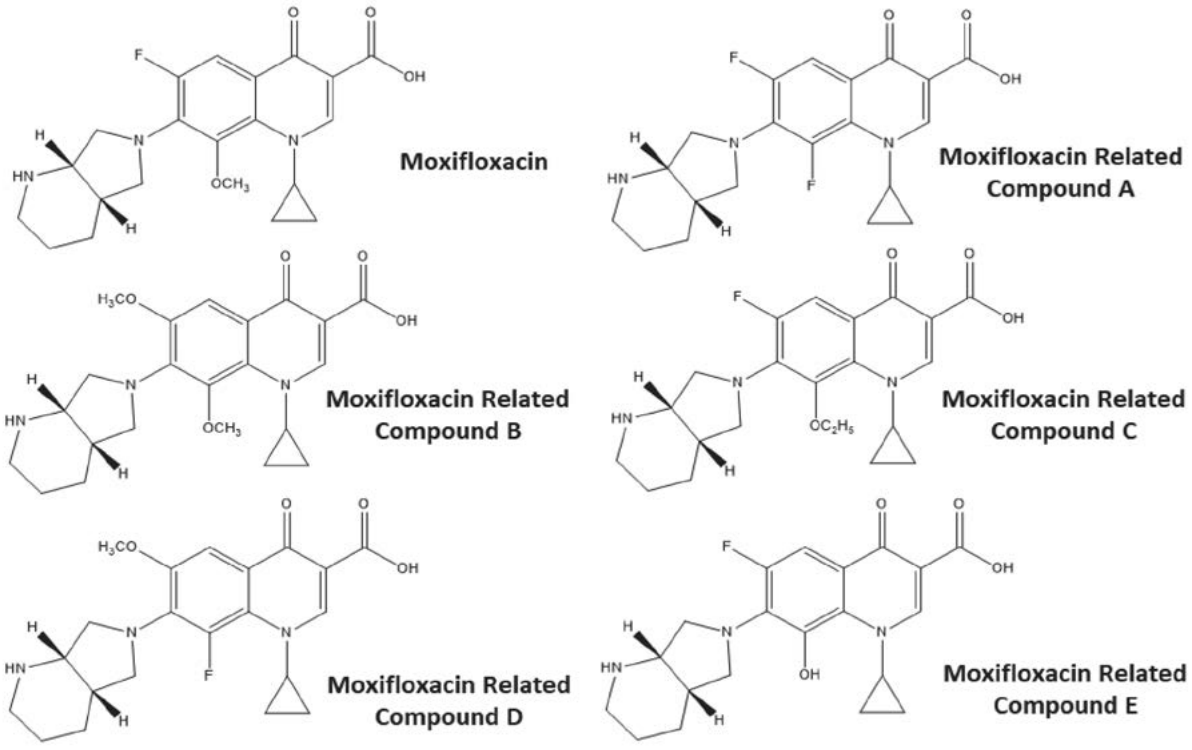

Figure 1. Structures of moxifloxacin and its known related compounds

mm; 3.5 μm particle size column. Aqueous part of the mobile phase was prepared using 0.01 M sodium dihydrogen phosphate, with added SDS (0.15 M) and triethylamine (0.5%, v/v). The pH was adjusted to 3.5 with orthophosphoric acid HPLC electrochemical grade, after adding SDS and other components. Lastly, 92.5% (v/v) of aqueous phase was mixed with 7.5% of isopropanol (v/v).

The flow rate and injection volume were 0.6 ml/min and 5 μl, respectively. Experiments were performed at a temperature of 60 °C and detection was performed at 295 nm. Before use, the mobile phase, standard and sample solutions were filtered through a 0.45 μm nylon filter (*LLG Labware*, Meckenheim, Germany).

2. 3. Standard and Samples Solution

Standard solution for determination of moxifloxacin assay was prepared using mobile phase as diluent in concentration of 0.1 mg/ml. Standard solutions for determination of moxifloxacin impurities in concentration of 0.2 μg/ml using the same solvent were also prepared. Moxifloxacin drug substance sample solution was prepared in a concentration of 0.1 mg/ml.

2. 4. Stress Samples

To conduct the forced degradation study, moxifloxacin was subjected to acidic, alkaline, oxidative, thermal, UV light, humidity and photolytic conditions. Stress samples for acid and base hydrolysis were prepared using 4 M HCl and 4 M NaOH as stress agents. Sample stock solution of moxifloxacin drug substance was prepared in concentration of 1 mg/ml using the mobile phase as a diluent. 1 ml of stock solution was transferred to 10 ml volumetric flasks, then 1 ml of each different stress agent was added to each volumetric flask containing the stock solution. The solutions containing an acidic stress agent were subjected to a temperature of 70 °C and the solutions containing the base were subjected to a temperature of 50 °C, in each case for a period of 6 days. After the stress treatment, samples were diluted up to the volume of the 10 ml flask with the same diluent (0.1 mg/ml concentration).

For degradation under oxidizing conditions, the drug was heated under reflux with 3 % H_2O_2 (v/v) at room temperature for 24 hours. For thermal degradation, the powdered drug was exposed to a temperature of 70 °C for 48 hours. With respect to photodegradation, powdered moxifloxacin was exposed to UV light for 3 days and daylight for 7 days. Within the stress studies, untreated, zero time and blank samples were prepared as controls in addition to stress samples.

2. 5. Method Optimization

Central composite design was used to optimize the experimental conditions in order to develop an appropriate method with the shortest possible run time and maximum resolution factors for the critical peaks. During the optimization, the effects of column temperature (A), amount of organic solvent (B), pH (C) and flow rate of a mobile phase (D) were studied. Resolution factors for the critical peaks and retention time of the last eluted component were selected as observed responses.

For method optimization, a sample was prepared by adding five known moxifloxacin impurities (impurities A, B, C, D and E) to the stress sample.

Central composite design was performed using *Design-Expert 7.0* (*Stat-Ease Inc*., Minneapolis, SAD). Thirty experiments were conducted with the aim of investigating the influence of four variables (A, B, C and D). The plan of the experiment and observed responses are presented in Table 3.

2. 6. Method Validation

System suitability test (SST)

SST for moxifloxacin assay determination was performed by six replicate injections of moxifloxacin standard solution in concentration of 0.1 mg/ml. The parameters evaluated included relative standard deviation (% RSD) for peak area, tailing factor, and column efficiency.

SST for determination of related substances was evaluated including resolution factors for the critical peaks and % RSD for peak area for each known moxifloxacin impurity.

To evaluate the resolution factors for the critical peaks, sample containing moxifloxacin hydrochloride in concentration of 0.1 mg/ml with added five known moxifloxacin impurities in concentration of 0.2 μg/ was injected. Six replicate injections of a sample which containing five known moxifloxacin impurities and moxifloxacin CRS in concentration of 0.2 μg/ml were injected to evaluate % RSD for peak area of impurities.

Selectivity test

The selectivity of the optimized MLC method was evaluated by comparing chromatograms obtained from the analysis of solvent, sample solution, sample solution with known impurities, stress sample solution and stress agents sample solution. The method was considered selective if the peaks observed in the chromatograms were well separated and there were no co-eluting peaks at retention time of moxifloxacin, known moxifloxacin impurities and degradation products from forced degradation studies. The acceptance criteria applied was related to the resolution factor calculated for adjacent peaks of all analytes and which had to be equal to or greater than 1.5. In addition, a diode array detector (DAD) was used to evaluate peak purity based on the peak purity index.

Linearity

The linearity of the optimized MLC method was evaluated by fitting the calibration data using least squares

regression with five different concentrations of moxifloxacin in the range of 0.05–0.15 mg/ml (50–150% of the target concentration denoted as 0.1 mg/ml) and five different concentrations for each known moxifloxacin impurity in the range of 0.1–0.3 μg/ml (50–150% of the target concentration 0.2 μg/ml, selected considering the specification limit for moxifloxacin related substances defined in Ph.Eur. and USP). Linearity was evaluated by the values of the correlation coefficient (R^2 value).

Accuracy

The accuracy of the method was determined by analyzing a solution containing moxifloxacin and all impurities at three different concentrations (80%, 100% and 120% with respect to the target value) of each in triplicate at the specified limit. The percentage of recoveries for each analyte was calculated by injecting the standard solution for each level.

Precision

The inter-day precision of the method was checked by injecting six invidual solutions containing moxifloxacin and its impurities in target concentrations of 0.1 mg/ml and 0.2 μg/ml, respectively. The % RSD for the peak area of each analyte was calculated. The intermediate precision of the method was also evaluated using different analyst and different instruments in the same laboratory using appropriate sets of solutions prepared in the same way as in case of inter-day precision.

Robustness

The robustness of the method was investigated by analysing the results of previously performed central composite design. The robustness was evaluated considering the same factors as used for method optimization: column temperature (A), amount of organic solvent (B), pH (C) and flow rate of a mobile phase (D).

Limit of detection and Limit of quantification

The limit of detection (LOD) and limit of quantification (LOQ) were determined experimentally by measuring the signal-to-noise ratio of the each substance by injecting a series of dilute solutions with known concentration. LOD and LOQ were determined with 3.3s/n and 10s/n criteria, respectively from the data from calibration curve.

3. Results and Disscusion

3. 1. Development of MLC Method

Preliminary studies were performed to select an efficient method for the analysis of moxifloxacin and related substances in the presence of its degradation products. The aim was to apply an eco-friendly MCL method with isocratic elution. In the RP-HPLC system, special attention is paid to the selection of the stationary phase. The most commonly used stationary phases are silica stationary phases modified with alkyl groups, such as C18 and C8. However, in micellar chromatography systems, in addition to the selection of a suitable stationary phase, the choice of surfactant is also very important. The presence of a surfactant significantly changes the properties of the stationary phase and opens up possibilities for numerous and varied interactions with analytes.[26]

Development began with the use of anionic SDS as one of the most commonly used surfactant in MLC. A solution of sodium dihydrogen phosphate with the addition of SDS and triethylamine was used as aqueous solvent, and isopropanol was used as organic solvent.

A C18 HPLC column was used. The preliminary tests were initially necessary to determine whether the proposed method could separate the peak of moxifloxacin and the peaks of moxifloxacin impurities defined by the pharmacopoeia (impurities A, B, C, D and E). [1,2]

Preliminary tests were based on the identification of the main factors that could affect the separation of analytes: pH of the mobile phase, possibility of using different water phases (buffer solution), concentrations of SDS and triethylamine, percentage of organic solvent and possibility of using different organic solvents, influence of column temperature and flow rate.

According to the values of pKa and log P as a function of pH, the pH of the mobile phase was selected to be pH=3.0. The pKa values and pH dependence on the ionic and non-ionic forms of the substances indicated that all analytes are present in the protonated form on the N-heterocycle of piperidine, as the NH+ and -COOH group are non-ionized, which ensures interactions with the negatively charged surface of the surfactant adsorbed on the stationary phase and the negatively charged surface of the micelle.

0.01 M sodium dihydrogen phosphate was used as a basic aqueous solution to have efficient control of the pH of the mobile phase.

Solubilizing capacity of micelles and consequently their influence on retention was analysed by varying the concentration of SDS (0.10 M and 0.15 M). It was found that there was no significant difference in the quality of chromatographic separation of all adjacent chromatographic peaks with different SDS concentration. Increased concentration of SDS (0.15 M) resulted in a shorter run compared to the lower concentration of SDS (0.10 M), which is explained by the fact that the surfactant increases the affinity and interactions with the surfactant monomers in the mobile phase, resulting in a decrease in retention. Reduction in the retention time of the analyte is usually achieved by increasing the concentration of the surfactant or the organic solvent.[27] In order to shorten the time required for the analysis, the SDS concentration of 0.15 M was chosen. Concentration of SDS (0.15 M) in our micellar system is higher than the CMC. Increasing the surfactant concentration above the CMC does not affect the critical

micelle concentration because any added monomer is incorporated into the micelles, while the concentration of free surfactant monomers does not change and remains equal to the CMC.[28]

Variations in the percentage of triethylamine (0.5%, 0.7% and 1.0%, v/v) were also investigated. This additive usually contributes to the symmetry of the chromatographic peaks by minimizing the undesirable secondary interactions of the basic analytes with free silanol groups on the surface of the stationary phase.[29] The addition of small amounts, 0.1–0.2% (v/v), of triethylamine in chromatography is typically used to reduce the effect of tailing for basic small molecule compounds.[29] In this regard, changing the peak shape may affect the base line separation of closely spaced elution peaks. When the percentage of triethylamine is increased, co-elution of the impurity A peak with the moxifloxacin peak occurs, disturbing the purity of the peak, while with 1.0% triethylamine the separation of impurity A and moxifloxacin peak is not achieved. The best conditions were achieved with 0.5% (v/v) triethylamine. This concentration of triethylamine can affect the decrease of the critical micelle concentration since the amount of triethylamine added is larger than would be added as a typical stationary phase modifier, a large portion of the triethylammonium ion remains in the mobile phase. Although the triethylammonium ion and negatively charged SDS sulfate monomers will not spontaneously form dodecyltriethylammonium sulfate, some electrostatic attraction may occur between the two which could further inhibit the monomers from adsorbing to the stationary phase.[29]

In order to increase the efficiency of the MCL method and achieve retention in a suitable time, it was necessary to add an appropriate amount of organic solvent to the aqueous mobile phase. The use of the most commonly used organic solvents in MCL, isopropanol and acetonitrile, was considered. Since it is well known that the organic solvent increases the affinity and interactions of the analyte with the mobile phase, and desorbs SDS from the stationary phase, it was necessary to determine the optimal amount of the organic solvent.[30] The addition of propanol to the aqueous micellar solution of SDS leads to a decrease in CMC. [31] The tests were based on the use of isopropanol and the variation of its percentage, but the possibility of using acetonitrile (10%, 15% and 20% (v/v) in the mobile phase) was also tested. Acetonitrile did not prove to be the solvent of choice, since its use did not separate all known impurities. It is also very important to avoid the use of acetonitrile, since the aim of the method was to use a less toxic organic solvent such as isopropanol.

The percentage of isopropanol in the mobile phase was varied between 2.5% and 8.0% (v/v). In preliminary tests, satisfactory chromatographic conditions and system responses were achieved with 5.0% (v/v) isopropanol.

The influence of column temperature was also investigated. Since the most frequently reported cases in the literature were analyzes performed at a column temperature of 25 °C, the experiments were initially performed at this temperature. An increase in temperature can affect the micellization process and increase the CMC because it destroys the ordered structure of water around the hydrophobic surfactant groups so that the micelles are broken down.[31] Unfortunately, satisfactory chromatographic separations could not be obtained at the temperature of 25 °C and the column temperature was carefully increased to 50 °C. The choice of column temperature of 50 °C showed

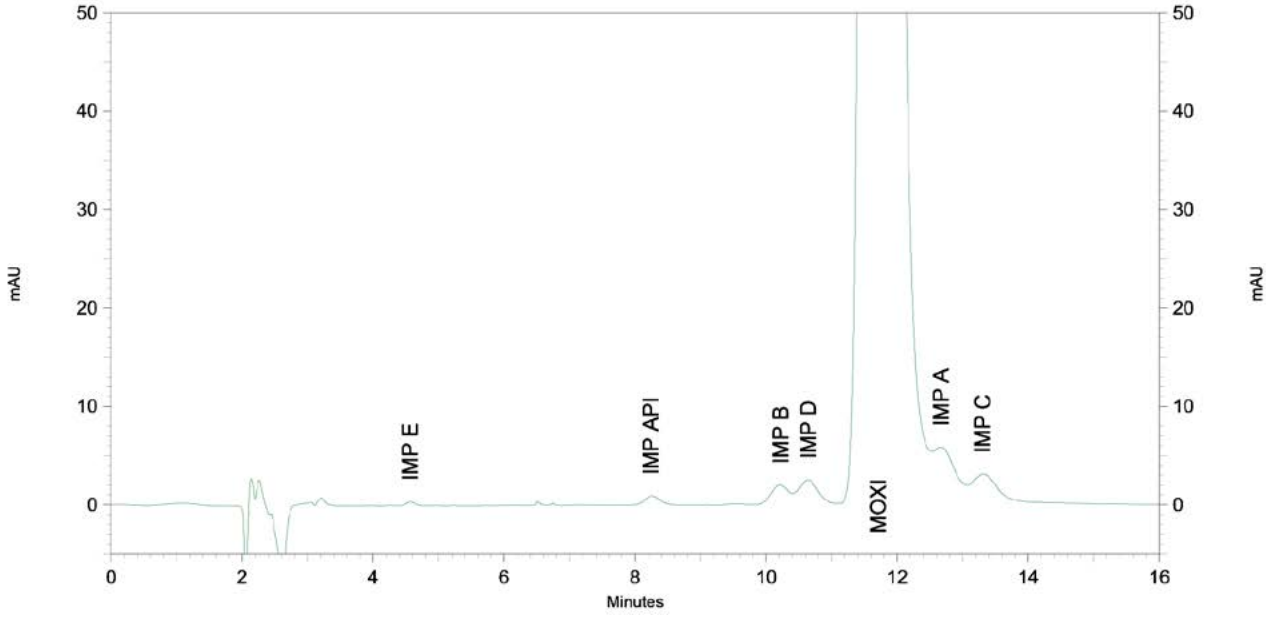

Figure 2. Sample of moxifloxacin and its known related compounds

that an unexpected phenomenon occurred, namely the increased effect of temperature on the reduction of hydration of the polar groups, which further favored.[32]

During the preliminary tests, the experiments were started with a flow rate of 1.0 ml/min. However, despite simultaneous variation of other chromatographic conditions with this flow rate, it was not possible to separate impurity A from moxifloxacin because impurity A peak eluted immediately after the moxifloxacin peak. Accordingly, the flow rates of 0.8 ml/min and 0.5 ml/min were tested. Finally, with the reduction of the flow rate to 0.5 ml/min, the separation of the critical peaks was achieved (Figure 2).

3. 2. Forced Degradation Study

In forced degradation studies, moxifloxacin drug substance was found to be extremely stable to: thermal and photodegradation, oxidative stress and base hydrolysis. Significant degradation was caused by acidic conditions, using very high concentration of acid (4M HCl) and at extremely high temperature (Figure 3, Table 1)

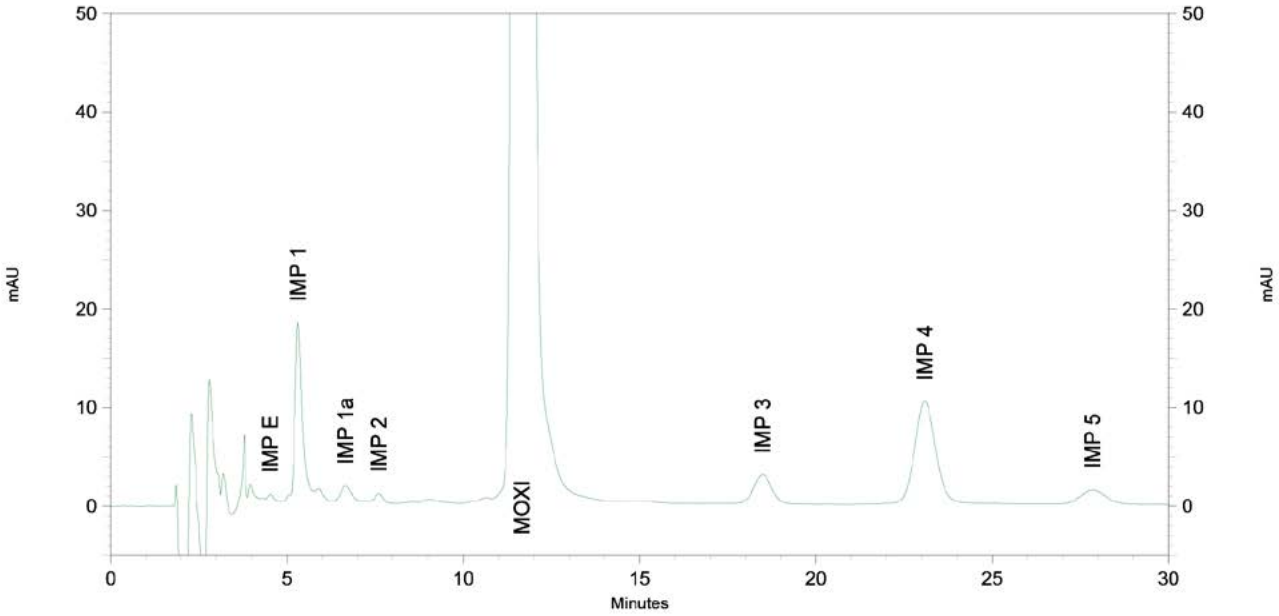

Figure 3. Stress sample of moxifloxacin subjected to acidic hydrolysis

Table 1. Results of forced degradation studies

Stress condition	Moxifloxacin	Percentage of degradation (%)	Degradation products (content %)	Moxifloxacin peak purity content (%)
Untreated sample	101.20	–	–	0.999940
Acid hydrolysis (4 mol/l HCl, 70 °C, 6 days)	85.19	16.01	IMP E (0.018%) IMP 1 (0.841%) IMP 1a (0.112%) IMP 2 (0.049%) IMP 3 (0.351%) IMP 4 (1.469%) IMP 5 (0.239%)	0.999845
Base hydrolysis (4 mol/l NaOH, 50 °C, 6 days)	100.41	–	–	0.999899
Oxidation (3 % H_2O_2, room temperature, 24 hours)	100.20	–	–	0.999887
Photodegradation (UV 254 3 days, daylight 7 days)	101.05	–	–	0.999989
Thermal degradation (70 °C, 2 days)	100.95	–	–	0.9999978

for 6 days. The strength of the stress agents was chosen in such a way that the degradation was in the range of 5–20%. Preparation of three additional control samples was mandatory for the correct determination the obtained results. The published study also demonstrated that moxifloxacin is very stable under all conditions recommended by ICH Q1A (R2) at lower concentration of acid and base.[33]

The percentage of degradation and the mass balance on all tested samples were calculated (Table 1) and the content of all degradation products formed was reported .

Forced degradation studies were performed for moxifloxacin drug substance to provide an indication of the specificity of the proposed method.

3. 3. Optimization

Central composite design was performed using 30 experimental runs. The levels of independent variables namely column temperature (A), amount of organic solvent (B), pH (C) and mobile phase flow rate (D), and the responses or dependent variables are shown in Table 3. According to the preliminary results independent variables were tested on the level presented in Table 2.

Table 2: Level of investigated variables

Variables	Level		
	(–1)	(0)	(+1)
Column temperature (°C, A)	50	55	60
Amount of isopropanol (%, B)	2.5	5.0	7.5
pH (C)	2.5	3.0	3.5
Flow rate (ml/min, D)	0.4	0.5	0.6

Optimization study was done using stress sample (acid hydrolysis) spiked with five known moxifloxacin impurities (impurities A, B, C, D and E).

Statistical parameters for the selection of the best fit model (p value <0.05; Lack of Fit >0.05, R^2 value >0.8) were achieved for all five responses (Table 4).

Table 3. Central composite design results using four independent variables

Run	Variables				Responses				
	Column temperature (°C; A)	Amount of organic solvent, isopropanol (%; B)	pH (C)	Flow rate (ml/min; D)	Resolution (IMP B / IMP D)	Resolution (IMP D/MOXI)	Resolution (MOXI /IMP A)	Resolution (IMP A/ IMP C)	Retention time $_{IMP\ 5}$
1	50	2.5	2.5	0.4	1.16	3.15	2.15	1.22	44.48
2	60	2.5	2.5	0.4	1.16	2.97	2.24	1.31	42.35
3	50	7.5	2.5	0.4	1.04	1.70	1.73	2.21	36.27
4	60	7.5	2.5	0.4	1.10	1.76	1.73	2.22	34.20
5	50	2.5	3.5	0.4	0.96	2.87	2.29	1.05	30.88
6	60	2.5	3.5	0.4	1.10	2.91	2.35	1.05	28.58
7	50	7.5	3.5	0.4	1.14	1.71	2.10	2.21	27.60
8	60	7.5	3.5	0.4	1.27	1.64	2.10	2.11	25.35
9	50	2.5	2.5	0.6	1.01	2.85	2.16	1.41	29.42
10	60	2.5	2.5	0.6	1.26	3.07	2.10	1.51	27.78
11	50	7.5	2.5	0.6	1.05	1.67	1.53	2.21	23.90
12	60	7.5	2.5	0.6	1.10	1.70	1.50	2.20	22.30
13	50	2.5	3.5	0.6	0.81	2.73	2.15	1.21	21.28
14	60	2.5	3.5	0.6	1.08	2.61	2.14	1.25	19.46
15	50	7.5	3.5	0.6	1.07	1.66	1.73	2.05	20.63
16	60	7.5	3.5	0.6	1.20	1.67	1.78	2.05	18.81
17	50	5.0	3.0	0.5	0.89	2.28	1.81	1.60	27.08
18	60	5.0	3.0	0.5	0.98	2.21	1.90	1.60	25.16
19	55	2.5	3.0	0.5	1.00	2.56	2.07	1.30	28.08
20	55	7.5	3.0	0.5	1.14	1.59	1.54	2.20	23.65
21	55	5.0	2.5	0.5	1.51	2.56	1.50	1.78	31.00
22	55	5.0	3.5	0.5	1.50	2.19	1.82	1.54	22.53
23	55	5.0	3.0	0.4	1.08	2.53	1.94	1.60	32.71
24	55	5.0	3.0	0.6	1.05	1.67	1.94	1.60	21.89
25	55	5.0	3.0	0.5	1.18	2.57	1.75	1.61	25.92
26	55	5.0	3.0	0.5	1.04	2.33	1.79	1.58	25.90
27	55	5.0	3.0	0.5	0.93	2.43	1.80	1.58	25.93
28	55	5.0	3.0	0.5	1.03	2.39	1.76	1.60	25.92
29	55	5.0	3.0	0.5	0.97	2.33	1.83	1.57	25.90
30	55	5.0	3.0	0.5	1.02	2.37	1.83	1.61	25.91

Table 4: Statistical parameters for selection of the best fit model

	$R_{s(IMP\ B\ /\ IMP\ D)}$	$R_{s\ (IMP\ D/\ MOXI)}$	$R_{s(MOXI/\ IMP\ A)}$	$R_{s(IMP\ A/\ IMP\ C)}$	Run time IMP 5
Model	**quadratic**	**linear**	**quadratic**	**quadratic**	**quadratic**
p-value	0.0005	<0.0001	<0.0001	<0.0001	<0.0001
Lack of fit	0.6316	0.0578	0.0820	0.0562	0.083
R^2	0.8547	0.8995	0.9710	0.9963	1.000
R^2adjusted	0.7191	0.8687	0.9439	0.9929	1.000

The proposed models for five observed responses were as presented in following equations (1-5):

$$Rs_{Imp\ B/Imp\ D} = 1{,}08 + 0{,}062A + 0{,}032B - 0{,}014C - 0{,}021D\ 0{,}018AB + 0{,}019AC + 0{,}023AD + 0{,}064BC + 5{,}625*10^{-3}BD - 0{,}017CD - 0{,}20A^2 - 0{,}069B^2 + 0{,}37C^2 - 0{,}074D^2 \quad (1)$$

$$Rs_{Imp\ D/Moxi} = 2{,}29 - 4{,}444*10^{-3}A - 0{,}59\ B - 0{,}080\ C - 0{,}089\ D \quad (2)$$

$$Rs_{Moxi/Imp\ A} = 1{,}78 + 0{,}011A - 0{,}22B + 0{,}10C - 0{,}089D - 3{,}750*10^{-3}AB + 6{,}250*10^{-3}AC - 0{,}013AD + 0{,}059\ BC - 0{,}040\ BD - 0{,}030\ CD + 0{,}091A^2 - 0{,}041B^2 - 0{,}10C^2 + 0{,}18D^2 \quad (3)$$

$$Rs_{Imp\ A/Imp\ C} = 1{,}61 + 7{,}222*10^{-3}A + 0{,}45B - 0{,}086C + 0{,}028D - 0{,}021AB - 0{,}016AC + 8{,}125*10^{-3}AD + 0{,}029\ BC - 0{,}062\ BD - 0{,}014\ CD - 0{,}028A^2 + 0{,}12B^2 + 0{,}032C^2 - 0{,}028D^2 \quad (4)$$

$$k_{Imp5} = 25{,}91 - 0{,}98A - 2{,}20B - 4{,}25C - 5{,}39D + 9{,}379*10^{-3}AB - 0{,}047AC + 0{,}12AD + 1{,}22BC + 0{,}66BD + 1{,}35CD + 0{,}21A^2 - 0{,}043B^2 + 0{,}86C^2 + 1{,}39D^2 \quad (5)$$

The *Desirability* function evaluation was introduced with the aim to make compromising solution that satisfies following optimisation objectives: the least possible run time and the maximum resolution factors for the critical peak pairs. The analysis of the 3D chart presented in Figure 4 enabled the definition of the experimental region for which the *Desirability* function is equal to 1 indicating the maximal fulfillment of all predefined optimization objectives. The observed responses under optimized chromatographic conditions, were as presented in Table 5.

The chromatographic conditions finally selected were pH 3.5 and 7.5% isopropanol (v/v) in the mobile phase, flow rate of 0.6 ml/min and column temperature of 60 °C. According to these optimal chromatographic conditions, representative chromatogram was recorded and presented on the Figure 5.

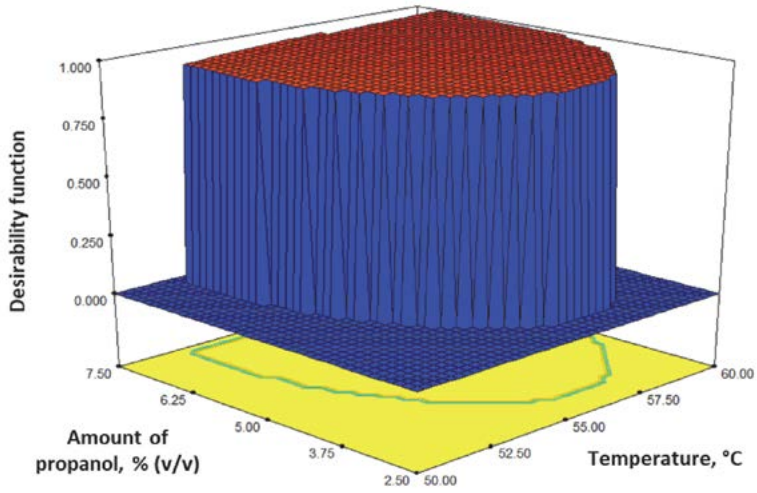

Figure 4. Response surface plot of desirability function

Table 5. Responses of the system under optimal experimental conditions

Resolution factors for critical peaks (>1.50)				Run time
$R_{s\ (IMP\ B\ /\ IMP\ D)}$	$R_{s\ (IMP\ D/\ MOXI)}$	$R_{s\ (MOXI/\ IMP\ A)}$	$R_{s\ (IMP\ A/\ IMP\ C)}$	
1.20 (p/V=5.5) RSD <5%	1.67	1.78	2.05	18.81

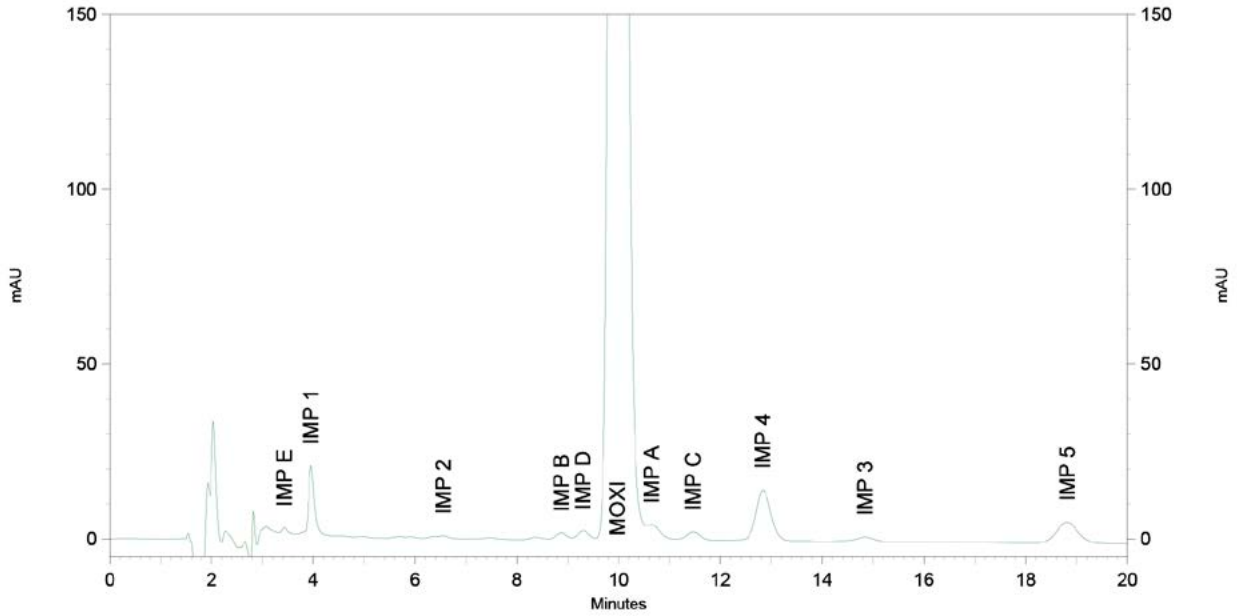

Figure 5. Stress sample of moxifloxacin under acid hydrolysis with added known moxifloxacin impurities (under optimal chromatographic conditions)

3. 4. Validation

The optimized method was validated and met all acceptance criteria required by ICH regulation.[34] Summary of the validation results is presented in Table 6. Before validation of the HPLC method, SST was performed. SST parameters evaluated for the determination of moxifloxacin assay were RSD for peak area (<1%), tailing factor (<2%), and the number of theoretical plates (>2000) while SST parameters for determination of moxifloxacin impurities were resolution between critical peaks (>1.5) and % RSD for peak area for each known impurity (<5%).

Selectivity test showed stability indicating property and specificity of the proposed method peak purity index was between 990 and 1000 showing that there were no co-eluting peaks with moxifloxacin, moxifloxacin known impurities and degradation products. In addition, resolution values of the analytes (moxifloxacin and impurities) were >1.5.

Linearity test showed that there was an excellent correlation between the peak area and concentration of moxifloxacin and all five impurities. All calibration curves were linear (R^2 >0.99) over the calibration ranges tested. The ranges were 50%–150% of the specification limit of each tested analyte (Table 6).

Accuracy of moxifloxacin and all five impurities was found to be in between the predefined acceptance criteria of 80% to 120% and the data given in Table 6.

The Precision was determined at the concentration of 0.2 µg/ml for all impurities and 0.1 mg/ml for moxifloxacin and the % RSD was found to be below 5% for all impurities and below 2% for moxifloxacin (Table 6).

The robustness of the method was investigated by experimental design methodology using the same considerations of the effects of column temperature (A), amount of organic solvent (B), pH (C) and flow rate of a mobile phase (D). Analyses of 3D response surfaces plotted using equations (1)-(5) were done taking in mind the usual variation of experimental factors in the ranges required for robustness testing which arise from analytical measurement uncertainty (e.g. column temperature in the range ± 5 °C

Table 6. Validation results summary

	Moxifloxacin	**Impurity A**	**Impurity B**	**Impurity C**	**Impurity D**	**Impurity E**
R^2 value concentration range 0.05–0.15 mg/ml (for moxifloxacin) 0.1–0.3 µg/ml (for impurities)	0.99895	0.99867	0.99669	0.99976	0.99483	0.99935
Accuracy at 80%	98.80	104.41	106.29	104.99	105.95	100.69
Accuracy at 100%	97.29	97.89	101.07	98.17	101.03	97.40
Accuracy at 120%	101.26	97.70	94.32	92.31	92.24	90.99
Precision (% RSD)	1.38	2.98	3.38	3.17	3.58	2.51
Limit of detection (ng/ml)	5.2	11.2	18.2	5.3	11.8	8.0
Limit of quantification (ng/ml)	15.8	34.2	55.3	16.2	35.7	24.3

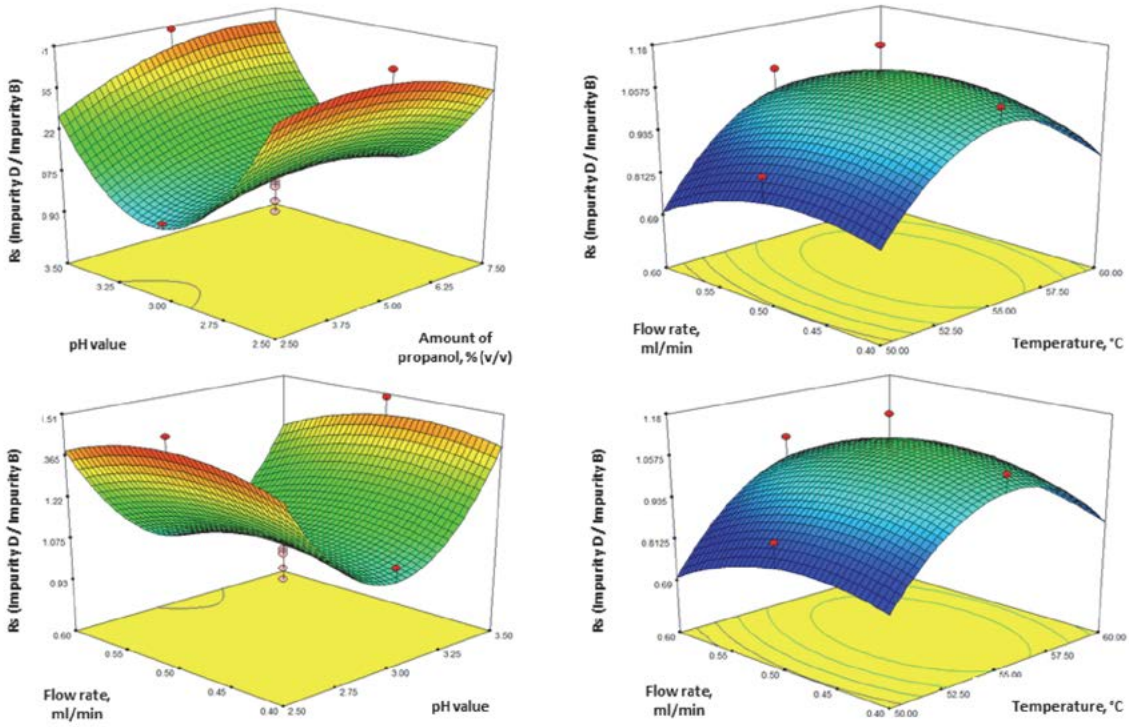

Figure 6. Response surfaces and estimated contours of the resolution of critical peak pair

from the nominal value set within method optimization). It was considered that the moderate slope of the 3D response surfaces related to the particular influence should indicate that the method is robust towards this experiment. The curvature of the 3D response surface indicates the presence of factor interactions and it was interpreted in combination with the slope. According to the representative 3D response surfaces presented in Figure 6 it can be concluded that careful maintenance of method settings is very important in order to retain the satisfactory chromatographic behavior of demanding mixture of analytes as the one used in this study. Fortunately, the common instrument qualification procedure should result in proper control of instrument as well as other experimental factor variations.

3D responses showed that the method has acceptable robustness under the given controlled conditions.

Limit of detection and Limit of quantification for known impurities were in ranges 5.3–18.2 ng/ml and 16.2–55.3 ng/ml, respectively. LOD and LOQ values for moxifloxacin were 5.2 ng/ml and 15.8 ng/ml, respectively.

3. 5. Comparison with Other Reported Methods

Most published methods for investigation of moxifloxacin and its impurities, including the official Ph. Eur. and USP methods, are based on the RP-HPLC mode using organic solvents, such as methanol and acetonitrile in the mobile phase, which cannot be considered as environmentally friendly solvents.

The proposed MCL method has advantages in term of greenness since it uses mixture of biodegradable aqueous mobile phase containing SDS and a much lower percentage of the more eco-friendly organic solvent, isopropanol, compared to the other published methods.

As for greenness, several tools are now present to assess and compare different methodologies in terms of their ecological impact. In this work GAPI index is used. GAPI index [35] has the advantage of covering the whole analytical procedure as compared to the earlier analytical eco-scale.[36]

The proposed MCL method was compared with the official pharmacopoeial methods and six other published methods. Table 7 shows the GAPI index for the proposed and previously published methods. The proposed method has similar greenness comparing to the pharmacopoeial methods and four other reported methods.[1,2,4,6,10,11] The red zones in GAPI pentograms for sampling denote mandatory offline sampling. The advantage of the proposed method is that only 7.5% (v/v) isopropanol is used in the mobile phase compared with published methods.

Compared to pharmacopoeial methods, the developed MLC method can be used for investigation of moxifloxacin and its impurities in the presence of its degradation products. The developed MLC method also achieved a shorter retention time than the pharmacopoeial methods. The use of the biodegradable anionic surfactant SDS (0.15 M) in the aqueous phase increased the surface polarity of the bound C_{18} stationary phase. This change resulted in faster separation of analytes in shorter analysis time,

Table 7. Assessment of the proposed and reported methods-GAPI pictograms

Study	Applied instruments and chromatographic conditions	GAPI
Proposed method	HPLC-DAD using RP-C18 column. Isocratic elution using 92.5% (v/v) biodegradable aqueous mobile phase containing 0.01 M sodium dihydrogen phosphate, 0.15 M sodium dodecyl sulfate (SDS) and 0.5% triethylamine (v/v) and 7.5% of isopropanol (v/v). Sample preparation: in mobile phase.	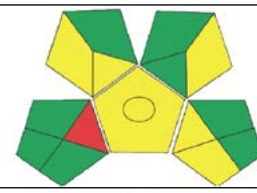
Ph. Eur./USP method for moxifloxacin related substances.[1,2]	HPLC-DAD using RP-C18 column. Isocratic elution using mobile phase containing methanol and aqueous solution containing 0.5 g/l tetrabutylammonium hydrogen sulfate, 1 g/l potassium dihydrogen phosphate i 3.4 g/l phosphoric acid (28:72, v/v). Sample preparation: aqueous solution.	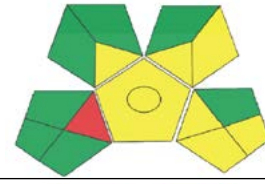
A Rapid RP-HPLC Stability Indicating Method Development and Validation of Moxifloxacin Hydrochloride Related Substances in Finished Dosage Forms.[4]	HPLC-DAD using RP-C18 column. Isocratic elution using mobile phase containing 0.01M potassium dihydrogen orthophosphate as buffer and methanol in the ratio of 70:30. Sample preparation: buffer and methanol in the ratio of 50:50 (v/v).	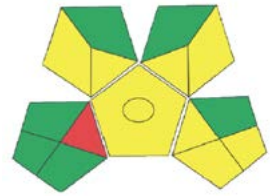
A Validated, Specific Stability-Indicating RP-LC Method for Moxifloxacin and Its Related Substances.[5]	HPLC-DAD using RP-C18 column. Gradient elution using mobile phase gradient prepared from 25 mM aqueous sodium dihydrogen orthophosphate dihydrate containing 0.2% triethylamine with orthophosphoric acid (component A) and methanol (component B). The gradient program (time (min)/% B) was: 0/20, 20/50, 30/70, 35/80, 36/20 with a post run time of 5 min. Sample preparation: degassed 60:40 (v/v) mixture of water and acetonitrile.	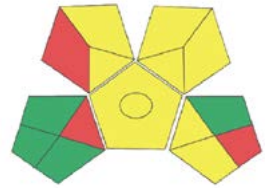
Optimization of separation and determination of moxifloxacin and its related substances by RP-HPLC.[6]	HPLC-DAD using RP-C18 column. Isocratic elution using mobile phase, water (+2% triethylamine): acetonitrile 90:10 (v/v). Sample preparation: 0.1% phosporic acid.	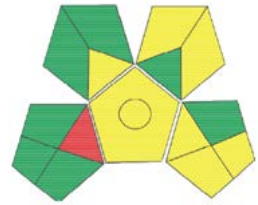
A simple and sensitive HPLC-fluorescence method for the determination of moxifloxacin in human plasma and its application in a pharmacokinetic study.[9]	HPLC-fluorescence detection using RP-C18 column. Isocratic elution using mobile phase composed of 50 mM potassium dihydrogen phosphate buffer pH 2.4 and 100% acetonitrile (77:23, v/v). Sample preparation: the samples were deproteinized by the addition of 500 µl of freshly prepared 6 % trichloroacetic acid in 20 % acetonitrile.	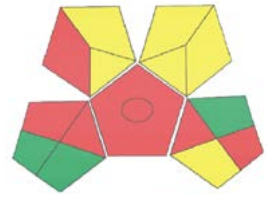
Stability indicating HPLC method for the simultaneous determination of moxifloxacin and prednisolone in pharmaceutical formulations.[10]	HPLC-DAD using RP-C8 column. Isocratic elution using mobile phase containing mixture phosphate buffer (18 mM) containing 0.1% (v/v) triethylamine, at pH 2.8 (adjusted with dilute phosphoric acid) and methanol (38:62 v/v) Sample preparation: in mobile phase.	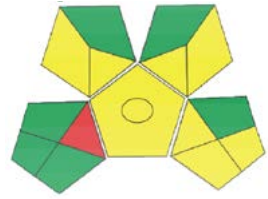
Simultaneous determination of dexamethasone and moxifloxacin in pharmaceutical formulations using stability indicating HPLC method. [11]	HPLC-DAD using RP-C8 column. Isocratic elution using mobile phase containing mixture of phosphate buffer (20 mM) containing 0.1% (v/v) triethylamine, at pH 2.8 and methanol (38.5:61.5 v/v) Sample preparation: in mobile phase.	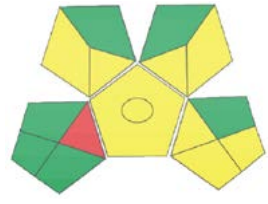

enabled the use of isopropanol instead of toxic organic solvent such as acetonitrile, which is more environmentally friendly, and also decreased the ratio required to improve elution to only 7.5% (v/v).[37]

Other reported methods have 3 and 6 red-colored pentograms.[5,9] Compared to the stability indicating method[5], our method has advantages in terms of greenness and also in terms of analysis time. The aim of this research was the same as our proposed method: to develop a method for quantitative analysis of moxifloxacin and its related substances in the presence of degradation products and process-related impurities. This method is based on a gradient mode, while our proposed method is based on an isocratic elution. This method uses acetonitrile, which is not preferred in terms of environmental impact and health safety, while our method uses isopropanol, an environmentally friendly solvent. The analysis time was longer (30 minutes) compared to our method (20 minutes). Compared the proposed method with the method for determination of moxifloxacin in human plasma,[9] the main difference is in the extraction step and sample preparation. Since a very important advantage of MLC concerns sample treatment, without the need for sample pretreatment other than filtration, the proposed MCL method can be considered for use in biological fluids. [3, 12, 38, 39]

4. Conclusions

A new, accurate and selective isocratic eco-friendly MCL method was developed for the determination of moxifloxacin and its related substances in moxifloxacin drug substance in presence of its degradation products. As a result of the central composite design adaptability, a significant acceptability score was achieved, while still obtaining acceptable resolution factors for all critical peaks. Run time was significantly decrease after optimization of the experimental conditions. GAPI was used to compare the proposed method's eco-friendliness to that or other previously reported HPLC methods. The proposed MCL method has advantages in term of greenness since it uses mixture of biodegradable aqueous mobile phase containing SDS, as one of the most researched and best understood widely used anionic surfactant with low price, and low percentage (7.5%) of the more eco-friendly organic solvent, isopropanol. Analysis time was considered as acceptable because the developed method was capable to separate complex mixture containing 11 components. Considering these facts, developed method has lower cost, lower toxicity, greater stability, less negative impact on the environment and greater safety for laboratory use. The developed method also considers the applicability in industrial facilities where selection criteria are based mainly on profit through cost and time. The mathod was found to be simple, selective, precise, accurate and robust. Therefore, this method can be used for routine testing of moxifloxacin drug substance. All statistical results were within the acceptance criteria.

Acknowledgments

This study was done with the support of the ZADA Pharmaceuticals company in practical contributions and technical support.

5. References

1. Ph. Eur. Pharmacopeia. 10th edition. Strasbourg: Council of Europe; **2022**, pp. 5067–5069.
2. The United States Pharmacopoeia. National formulary. USP43-NF38. Rockville (MD): United States Pharmacopeial Convention, 2022, pp. 3302.
3. M. Yabré, L. Feyer, I. T. Somé and K. Gaudin, *Molecules* **2018**, 23, 1065. **DOI:**10.3390/molecules23051065
4. K. R. Vankalapati, P. Algete and S. Boodida, *Biomed. Chromatogr.* **2021**, 35 (11), 5192. **DOI:**10.1002/bmc.5192
5. M. L. Devi, K. B. Chandrasekhar, *Chromatographia* **2009**, 69, 993–999. **DOI:**10.1365/s10337-009-1061-8
6. P. Djurdjevic, A. Ciric, A. Djurdjevic, M. J. Stankov, *J. Pharm. Biomed. Anal.* **2009**, 50 (2), 117–126. **DOI:**10.1016/j.jpba.2009.03.029
7. C. S. Wu, Z. X. Jia, B. M. Ning, J. L. Zhang, S. Wu,. *Chinese Chem. Lett.* **2012**, 23, 1185–1188. **DOI:**10.1016/j.cclet.2012.09.001
8. S. N. Razzaq and I. U. Khan, M. Ashfaq, I. Mariam, *Quim. Nova* **2012**, 35 (6), 1216–1221. **DOI:**10.1590/S0100-40422012000600028
9. W. Wichitnithad, T. Kiatkumjorn, P. Jithavech, P. Thanawattanawanich, P. Ratnatilaka na Bhuket, P. Rojsitthisak, *Pharmazie* **2018**, 73, 625–629. **DOI:** 10.1691/ph.2018.8148
10. S. N. Razzaq, I. U. Khan, I. Mariam, S. S. Razzaq, *Chem. Cent. J.* **2012**, 6 (1), 94. **DOI:**10.1186/1752-153X-6-94
11. S. N. Razzaq, M. Ashfaq, I. U. Khan, I. Mariam, S. S. Razzaq, W. Azeem, *Arab. J. Chem.* **2017**, 10 (3), 321–328. **DOI:**10.1016/j.arabjc.2014.11.016
12. R. N. El-Shaheny, M. H. El-Maghrabey and F. F. Belal, *Open Chem.* **2015**, 13 (1), 877–892. **DOI:**10.1515/chem-2015-0101
13. D. T. M. El-Sherbiny, S. M. El-Ashry, M. A. Mustafa, A. A. El-Emam, S. H. Hansen, *J. Sep. Sci.* **2003**, 26, 503–509. **DOI:**10.1002/jssc.200390067
14. M. J. Ruiz-Ángel, S. Carda-Broch, J. R. Torres-Lapasió, M. C. García-Álvarez-Coque, *J. Chromatogr. A*. **2009**, 1216, 1798–1814. **DOI:**10.1016/j.chroma.2008.09.053
15. A. P. Boichenkoa, A. Berthod, *J. Chromatogr. A*. **2010**, 1217, 5665–5673. **DOI:**10.1016/j.chroma.2010.07.001
16. P. Kawczak, T. Bączek, *Cent. Eur. J. Chem.* **2012**, 10(3), 570–584. **DOI:**10.2478/s11532-012-0004-7
17. D. P. Thomas, J. P. Foley, *J. Chromatogr. A*. **2007**, 1149 (2), 282–293. **DOI:**10.1016/j.chroma.2007.03.045
18. M. J. Ruiz-Ángel, M. C. García-Alvarez-Coque, A. Berthod,

Sep. Purif. Rev. **2009**, 38 (1), 45–96.
DOI:10.1080/15422110802178876
19. F. Belal, M. K. Sharaf El-Din, M. I. Eid, R. M. El-Gamal, *J. Chromatogr. Sci.* **2014**, 52 (4), 298–309.
DOI:10.1093/chromsci/bmt028
20. D. C. da Silva, C. C. Oliveira, *J. Anal. Methods Chem*. **2018**, 2018 (2), 1–12. **DOI:**10.1155/2018/9143730
21. F. Ibrahim, M. K. Sharaf El-Din, A. K. El-Deen, K. Shimizu, *J. Chromatogr. Sci*. **2017**, 55 (1), 23–29.
DOI:10.1093/chromsci/bmw143
22. Y. A. Sharaf, S. E. Deeb, A. E. Ibrahim, A. Al-Harrasi, R. A. Sayed, *Molecules*. **2022**, 27 (7), 2330.
DOI:10.3390/molecules27072330
23. F. Belal , F. Ibrahim , Z. A. Sheribah , H. Alaa, *J. Chromatogr. B. Analyt. Technol. Biomed. Life. Sci.* **2018**, 1091, 36–45.
DOI:10.1016/j.jchromb.2018.05.030
24. M. A. Collado-Sánchez, M. Rambla-Alegre, S. Carda-Broch, J. Esteve-Romero, *J. Liq. Chromatogr. R. T*. **2010**, 33, 513–525.
DOI:10.1080/10826070903574519
25. F. F. Belal, M. K. Sharaf El-Din, N. M. El-Enany, S. Saad, *Chem. Cent. J.* **2013**, 7 (81), 162. **DOI:**10.1186/1752-153X-7-162
26. M. J. Ruiz-Ángel, J. R. Torres-Lapasió, S. Carda-Broch, M. C. García-Álvarez-Coque, *J. Chromatogr. Sci,* **2003**, 41 (7), 350–8. **DOI:**10.1093/chromsci/41.7.350
27. M.C. García-Alvarez-Coque, J.R. Torres-Lapasío, J.J. Baeza-Baeza, *J. Chromatogr. A* **1997,** 780, 129–148.
DOI:10.1016/S0021-9673(97)00051-4
28. N. Pejić, M. Aleksić: Odabrana poglavlja koloidne hemije, II dopunjeno izdanje, Univerzitet u Beogradu, Farmaceutski fakultet, Beograd, **2018**, pp. 21–77.
29. D. P. Thomas, J. P. Foley, *J. Chromatogr. A*. **2008**, 1205 (1-2), 36–45. **DOI:**10.1016/j.chroma.2008.07.082
30. M. J. Ruiz-Ángel, S. Carda-Broch, J.R. Torres-Lapasío, M.C. García-Álvarez-Coque, *J. Chromatogr. A* **2009**, 1216 (10), 1798–814. **DOI:**10.1016/j.chroma.2008.09.053
31. G. Kumar, M.S. Chauhan, A. Kumar, S. Suvercha, R. Kumar, *Der Chem. Sin.* **2012**, 3(3), 628–635
32. S.K. Mehta, S. Chaudhary, K.K. Bhasin, R. Kumar, M. Aratono, *Colloids and Surfaces A: Physicochem. Eng. Aspects* **2007**, 304, 88–95. **DOI:**10.1016/j.colsurfa.2007.04.031
33. P. R. Sankar, K. D. Deepthi, P. S. Babu, G. Rachana, A. S. Geethika, J. Bhargavi, L. P. Kalyan, K. N. Poojitha, *J. Pharm*. **2019**, 9, 30–41
34. ICH, Q2 (R1); Validation of Analitical Procedures: text and metodology, International Conference on Harmonization. *Tech. Requir. Regist. Pharm. Hum.* Use, pp.1–17.
35. J. Płotka-Wasylka, *Talanta* **2018**, 181, 204–209.
DOI:10.1016/j.talanta.2018.01.013
36. A. Gałuszka, Z. M. Migaszewski, P. Konieczka, J. Namieśnik, *Trends Anal. Chem.* **2012**, 37, 61–72.
DOI:10.1016/j.trac.2012.03.013
37. M. M. Ayad, M. M. Hosny, A. E. Ibrahim, O. M. El-Abassy, F. F. Belal, *J. Iran. Chem. Soc.* **2020**, 17 (7), 1725–1730.
DOI:10.1007/s13738-020-01897-z
38. G. Sharma, P. Pahade, A. Durgbanshi, S. Carda-Broch, J. Peris-Vicente, D. Bose, *Total Environ. Res. Themes* **2022**, 2772–8099. **DOI:**10.1016/j.totert.2022.100003
39. J. Esteve-Romero, S. Carda-Broch, M. Gil-Agusti, M.E. Capella-Peiró's, *Trends Anal. Chem*. **2005,** 24(2), 75–91.
DOI:10.1016/j.trac.2004.11.003

Povzetek

Razvita je bila selektivna in okolju prijazna micelarna HPLC metoda za študije moksifloksacina in sorodnih spojin v prisotnosti njegovih razgradnih produktov. Za optimizacijo eksperimentalnih pogojev je bil uporabljen centralni kompozitni dizajn. Predlagana metoda temelji na izokratni eluciji spojin na C18 koloni z uporabo 92,5 % (v/v) biorazgradljive vodne mobilne faze, ki vsebuje 0,01 M natrijevega dihidrogenfosfata, 0,15 M natrijevega dodecil sulfata (SDS) in 0,5 % trietilamina (v/v) pH 3,5 in 7,5 % izopropanola (v/v) kot okolju prijaznega organskega topila. Hitrost pretoka in volumen injiciranja sta bila 0,6 ml/min ter 5 µl. Poskusi so bili izvedeni pri temperaturi 60 °C, detekcija spojin pa se je vršila pri 295 nm. Optimizirana metoda je bila validirana. Ugotovljeno je bilo, da je metoda primerna za kvantifikacijo moksifloksacina in njemu sorodnih spojin v zdravilni učinkovini moksifloksacin. Indeks zelenih analitičnih postopkov (GAPI) dokazuje superiornost razvite metode v primerjavi z drugimi znanimi metodami.

DOI: 10.17344/acsi.2023.8057 *Acta Chim. Slov.* **2023,** *70,* 398–420

Scientific paper

Cytotoxic Activities and Morphological Sudies of Thiophene, Thiazole and Pyridazine Derivatives Synthesized from Benzo[*d*]thiazole Derivatives

Karam Ahmed El-Sharkawy,[1] Rafat Milad Mohareb,*,[2] Sayeed Mukhtar,[3] Humaira Parveen[3] and Mahmoud Ali Abdelaziz[3]

[1] *Pharmaceutical Chemistry Department, Pharmacy College, Jazan University, P.O. Box 114, Jazan, Saudi Arabia*

[2] *Department of Chemistry, Faculty of Science, Cairo University, Giza, A. R. Egypt*

[3] *Department of Chemistry, Faculty of Science, University of Tabuk, Tabuk – 71491, Kingdom of Saudi Arabia*

* *Corresponding author: E-mail: raafat_mohareb@cu.edu.eg; raafat_mohareb@yahoo.com*

Received: 02-08-2023

Abstract

The benzo[*d*]thiazole derivatives **4a–c** were synthesized and used for the synthesis of thiophene derivatives **6a–f**. They form the arylhydrazone derivatives **8a–i** which were capable to form pyridazine derivatives **9a–i** and **10a–i**. The latter compounds reacted with thioglycolic acid to produce the thiazole derivatives **12a–i** and **13a–i**, respectively. The thiazole derivatives **15a–c** were also produced from **4a–c** through their reactions with elemental sulfur and phenylisothiocyanate. Further heterocyclization reactions of **15a** were carried out to produce thiophene derivatives. Evaluations of the synthesized products were carried out against some selected cancer cell lines and the most active compounds were further evaluated against the seventeen cancer cell lines classified according to the disease. Morphological changes of A549 cell line by the effect of compounds **13c** and **13h** were studied using microenvironment of the lung tissue where an excellent result was obtained.

Keywords: Benzo[*d*]thiazole, thiophene, thiazole, pyridazine, cytotoxicity, morphological studies

1. Introduction

In the field of synthetic and medicinal chemistry, heterocyclic compounds are important compounds that are considered not only as versatile set of scaffolds but also for being part of natural products. As a result, different substituents attached to the ring system can enhance the results of many studies of structure–activity relationship and as a result there is a possibility to tailor the physicochemical properties of the molecules. From a number of pharmacological areas benzo[*d*]thiazole is present in many bioactive compounds. Compounds containing the benzo[*d*]thiazole showed variety of biological activities these include antibacterial,[1] antifungal,[2] and anticancer agents,[3] and they have antidiabetic,[4] antidepressant,[5] anticonvulsant,[6] and radioprotective activities,[7] as well as neuroprotective properties useful for treating Alzheimer's disease[8] and Parkinson's disease.[9] Structure bottom right on the Figure 1 presents riluzole, a market drug that contains benzo[*d*]thiazole skeleton within its structure characterized by neuroprotective, anticonvulsant, and sedative properties[10,11] being very useful to treat amyotrophic lateral sclerosis.[12] Luciferin, another drug known in the market containing the benzo[*d*]thiazole moiety, extracted from firefly characterizes the bioluminescence of firefly species.[13] For that reason some of the compounds containing the benzo[*d*]thiazole nucleus can be used as fluorescent probes.[14]

Benzo[*d*]thiazole derivatives can be synthesized through cyclization or condensation reactions by the use of different catalysts like ammonium chloride, iodine, bromine, palladium acetate and copper catalysts. In addition, there are different reaction conditions that can be used for their synthesis like microwave, acidic and basic conditions and sometimes polymer-supported condensation reactions were adopted.[15–22] In recent years, our research group was concerned with the synthesis of varieties of new

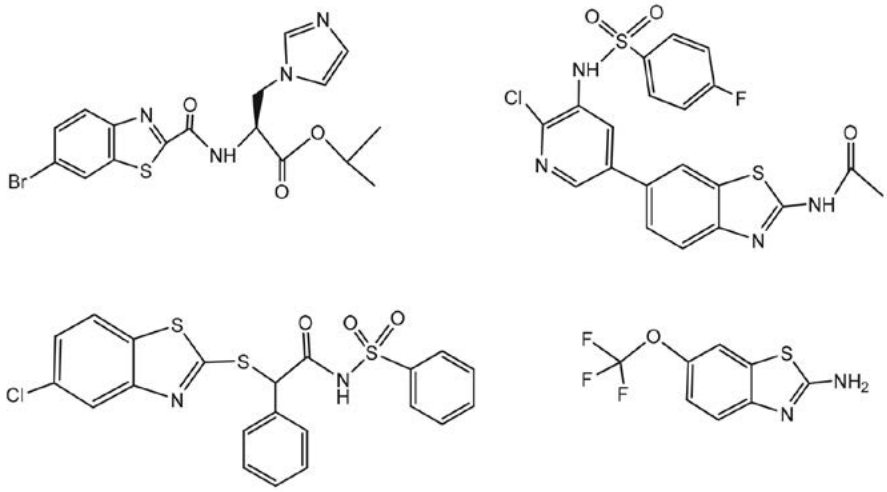

Figure 1. Representative examples of pharmacologically active benzo[*d*]thiazoles.

heterocyclic compounds followed by studying of their cytotoxicity against different cancer cell lines. Our previous work demonstrated that many of the synthesized compounds were useful in future drug designing.[23–26] In continuation of the previous work we are describing here a rapid and efficient preparation of a set of new benzo[*d*] thiazole derivatives starting from *ortho*-aminothiophenol that reacted with either ethyl cyanoacetate, diethylmalonate or ethyl acetoacetate. This new approach enables more rapid generation of a higher number of benzo[*d*]thiazole derivatives that were obtained using simple reactions using readily available reagents. The newly synthesized products were evaluated against six cancer cell lines together with studying c-Met kinase inhibitions.

2. Experimental

2. 1. General

Dry solvents were used through this work and all melting points of the synthesized compounds were recorded on Büchi melting point apparatus D-545. The IR spectra (KBr discs) were recorded on Bruker Vector 22 instrument. ^{13}C NMR and ^{1}H NMR spectra were measured on Bruker DPX300 instrument in DMSO-d_6 with TMS as the internal standard. Mass spectra were measured using EIMS (Shimadzu) and ESI-esquire 3000 Bruker Daltonics instrument. Elemental analyses were measured in the Micro-analytical Data center at Cairo University. All reactions was monitored by TLC on 2 × 5 cm pre-coated silica gel 60 F254 plates of thickness of 0.25 mm (Merck) for getting complete reactions.

2. 1. 1. General Procedure for the Synthesis of the Benzo[d]thiazol-2-yl Derivatives 4a–c

Either ethyl cyanoacetate (1.13 g, 0.01 mol), diethylmalonate (1.60 g, 0.01 mol) or ethyl 3-oxobutanoate (1.30 g, 0.01 mol) was added to *ortho*-aminothiophenol (1.25 g, 0.01 mol). The whole reaction mixture was heated in an oil bath at 120 °C for 30 min, then was left to cool. The remaining product was triturated with ethanol and the formed solid product was collected by filtration.

2-(Benzo[*d*]thiazol-2-yl)acetonitrile (4a)

Yellow crystals from 1,4-dioxane, yield (1.39 g, 80%), m.p. 191–193 °C. IR (KBr) ν_{max} (cm^{-1}): 3050 (CH-aromatic), 2951 (CH-aliphatic), 2220 (CN), 1580 (C=C). ^{1}H NMR (DMSO-d_6, 300 MHz): δ 3.80 (s, 2H, CH_2), 7.25–7.39 (m, 4H, C_6H_4). ^{13}C NMR (DMSO-d_6, 75 MHz): δ 36.3 (CH_2), 116.8 (CN), 120.4, 121.8, 122.2, 122.7, 123.3, 123.6, 123.8, 124.2 (C_6H_4), 168.3 (C=N). Anal. Calcd for: $C_9H_6N_2S$ (174.22): C, 62.05; H, 3.47; N, 16.08; S, 18.40. Found: C, 61.87; H, 3.52; N, 15.80; S, 18.26%. EIMS: *m/z* 174 [M]$^+$ (62%).

Ethyl 2-(benzo[*d*]thiazol-2-yl)acetate (4b)

Yellow crystals from ethanol, yield 1.85 g (84%), m.p. 177–179 °C. IR (KBr) ν_{max} (cm^{-1}): 3053 (CH-aromatic), 2951 (CH-aliphatic), 1688 (CO), 1585 (C=C). ^{1}H NMR (DMSO-d_6, 300 MHz): δ 1.16 (t, 3H, J = 7.25 Hz, $OCH_2\underline{CH_3}$), 3.83 (s, 2H, CH_2), 4.23 (q, 2H, J = 7.25 Hz, OCH_2CH_3), 7.26–7.43 (m, 4H, C_6H_4). ^{13}C NMR (DMSO-d_6, 75 MHz): δ 16.8 ($OCH_2\underline{CH_3}$), 36.3 (CH_2), 50.2 ($O\underline{CH_2}CH_3$), 120.1, 121.5, 121.7, 121.9, 122.8, 123.0, 123.4, 124.7 (C_6H_4), 165.2 (CO), 168.1 (C=N). Anal. Calcd for: $C_{11}H_{11}NO_2S$ (221.28): C, 59.71; H, 5.01; N, 6.33; S, 14.49. Found: C, 59.92; H, 4.83; N, 6.51; S, 14.62%. EIMS: *m/z* 221 [M]$^+$ (62%).

1-(Benzo[*d*]thiazol-2-yl)propan-2-one (4c)

Pale yellow crystals from ethanol, yield 1.43 g (75%), m.p. 210–212 °C. IR (KBr) ν_{max} (cm^{-1}): 3050 (CH-aromatic), 2954 (CH-aliphatic), 1689 (CO), 1583 (C=C). ^{1}H NMR (DMSO-d_6, 300 MHz): δ 2.28 (s, 3H, CH_3), 3.81 (s, 2H, CH_2), 7.27–7.45 (m, 4H, C_6H_4). ^{13}C

NMR (DMSO-d_6, 75 MHz): δ 24.6 (CH_3), 36.6 (CH_2), 119.8, 120.4, 120.7, 121.8, 122.3, 122.8, 123.4, 124.4 (C_6H_4), 165.8 (CO), 168.3 (C=N). Anal. Calcd for: $C_{10}H_9NOS$ (191.25): C, 62.80; H, 4.74; N, 7.32; S, 16.77. Found: C, 62.69; H, 4.81; N, 7.42; S, 16.58%. EIMS: *m/z* 191 $[M]^+$ (68%).

2. 1. 2. General Procedure for the Synthesis of the Thiophene Derivatives 6a–f

To a solution of either compound **4a** (1.74 g, 0.01 mol), **4b** (2.21 g, 0.01 mol) or **4c** (1.91 g, 0.01 mol) in absolute ethanol (60 mL) containing triethylamine (1.0 mL) either malononitrile (0.66 g, 0.01 mol) or ethyl cyanoacetate (1.07 g, 0.01 mol) was added. The whole reaction mixture was heated under the reflux conditions for 1 h then was left to cool to room temperature and the produced solid product was collected by filtration.

2,4-Diamino-5-(benzo[*d*]thiazol-2-yl)thiophene-3-carbonitrile (6a)

Yellow crystals from 1,4-dioxane, yield 1.79 g (66%), m.p. 193–195 °C. IR (KBr) ν max (cm^{-1}): 3458-3323 (NH_2), 3054 (CH-aromatic), 2954 (CH-aliphatic), 2220 (CN), 1580 (C=C). ^{1}H NMR (DMSO-d_6, 300 MHz): δ = 3.83, 4.28 (2s, 4H, D_2O exchangeable, $2NH_2$), 7.24–7.52 (m, 4H, C_6H_4). ^{13}C NMR (DMSO-d_6, 75 MHz): δ 116.7 (CN), 121.5, 122.2, 122.9, 123.5, 123.6, 123.8, 124.8 (C_6H_4), 138.3, 138.9, 140.2, 142.6 (thiophene C), 168.6 (C=N). Anal. Calcd for: $C_{12}H_8N_4S_2$ (272.35): C, 52.92; H, 2.96; N, 20.57; S, 23.55. Found: C, 52.87; H, 3.15; N, 20.72; S, 23.62%. EIMS: *m/z* 272 $[M]^+$ (68%).

2-Amino-5-(benzo[*d*]thiazol-2-yl)-4-hydroxythiophene-3-carbonitrile (6b)

Yellow crystals from 1,4-dioxane, yield 1.79 g (66%), m.p. 183–185 °C. IR (KBr) ν_{max} (cm^{-1}): 3549–3321 (OH, NH_2), 3054 (CH-aromatic), 2954 (CH-aliphatic), 2221 (CN), 1583 (C=C). ^{1}H NMR (DMSO-d_6, 300 MHz): δ 3.84 (s, 2H, D_2O exchangeable, NH_2), 7.27–7.42 (m, 4H, C_6H_4), 10.22 (s, 1H, D_2O exchangeable, OH). ^{13}C NMR (DMSO-d_6, 75 MHz): δ 116.7 (CN), 121.5, 122.2, 122.9, 123.5, 123.6, 123.8, 124.8 (C_6H_4), 138.1, 138.4, 140.1, 142.8 (thiophene C), 168.8 (C=N). Anal. Calcd for: $C_{12}H_7N_3OS_2$ (273.33): C, 52.73; H, 2.58; N, 15.37; S, 23.46. Found: C, 52.88; H, 2.67; N, 15.48; S, 23.39%. EIMS: *m/z* 273 $[M]^+$ (80%).

2-Amino-5-(benzo[*d*]thiazol-2-yl)-4-methylthiophene-3-carbonitrile (6c)

Yellow crystals from ethanol, yield 1.76 g (65%), m.p. 153–155 °C. IR (KBr) ν_{max} (cm^{-1}): 3486–3323 (NH_2), 3056 (CH-aromatic), 2953 (CH-aliphatic), 2220 (CN), 1582 (C=C). ^{1}H NMR (DMSO-d_6, 300 MHz): δ 2.89 (s, 3H, CH_3), 3.81 (s, 2H, D_2O exchangeable, NH_2), 7.24–7.46 (m, 4H, C_6H_4). ^{13}C NMR (DMSO-d_6, 75 MHz): δ 37.4 (CH_3), 116.4 (CN), 120.1, 122.5, 122.6, 123.2, 123.4, 123.7, 125.2 (C_6H_4), 138.0, 138.6, 140.1, 142.7 (thiophene C), 168.7 (C=N). Anal. Calcd for: $C_{13}H_9N_3S_2$ (271.36): C, 57.54; H, 3.34; N, 15.48; S, 23.63. Found: C, 57.72; H, 3.50; N, 15.16; S, 23.72%. EIMS: *m/z* 271 $[M]^+$ (72%).

Ethyl 2,4-Diamino-5-(benzo[*d*]thiazol-2-yl)thiophene-3-carboxylate (6d)

Orange crystals from ethanol, yield 1.91 g (60%), m.p. 203–205 °C. IR (KBr) ν_{max} (cm^{-1}): 3496–3341 (NH_2), 3055 (CH-aromatic), 2953 (CH-aliphatic), 2220 (CN), 1689 (CO), 1582 (C=C). ^{1}H NMR (DMSO-d_6, 300 MHz): δ 1.14 (t, 3H, J = 6.93 Hz, $OCH_2\underline{CH_3}$), 3.81, 4.25 (2×s, 4H, D_2O exchangeable, 2×NH_2), 4.23 (q, 2H, J = 6.93 Hz, $O\underline{CH_2}CH_3$), 7.24–7.46 (m, 4H, C_6H_4). ^{13}C NMR (DMSO-d_6, 75 MHz): δ 16.2 ($OCH_2\underline{CH_3}$), 50.2 ($O\underline{CH_2}CH_3$), 121.5, 122.7, 122.6, 123.3, 123.5, 124.1, 125.6 (C_6H_4), 138.1, 139.2, 140.5, 142.8 (thiophene C), 165.4 (CO), 168.8 (C=N). Anal. Calcd for: $C_{14}H_{13}N_3O_2S_2$ (319.40): C, 52.65; H, 4.10; N, 13.16; S, 20.08. Found: C, 52.71; H, 3.96; N, 13.42; S, 19.83%. EIMS: *m/z* 319 $[M]^+$ (68%).

Ethyl 2-Amino-5-(benzo[*d*]thiazol-2-yl)-4-hydroxythiophene-3-carboxylate (6e)

Pale brown crystals from ethanol, yield 2.17 g (68%), m.p. 165–168 °C. IR (KBr) ν_{max} (cm^{-1}): 3536–3358 (OH, NH_2), 3055 (CH-aromatic), 2952 (CH-aliphatic), 1688 (CO), 1588 (C=C). ^{1}H NMR (DMSO-d_6, 300 MHz): δ 1.13 (t, 3H, J = 6.11 Hz, $OCH_2\underline{CH_3}$), 4.28 (s, 2H, D_2O exchangeable, NH_2), 4.22 (q, 2H, J = 6.11 Hz, $O\underline{CH_2}CH_3$), 7.24–7.46 (m, 4H, C_6H_4), 10.30 (s, 1H, D_2O exchangeable, OH). ^{13}C NMR (DMSO-d_6, 75 MHz): δ 16.4 ($OCH_2\underline{CH_3}$), 50.5 ($O\underline{CH_2}CH_3$), 121.6, 122.4, 122.9, 123.1, 123.7, 124.8, 125.6 (C_6H_4), 138.5, 138.2, 140.7, 142.7 (thiophene C), 164.9 (CO), 168.6 (C=N). Anal. Calcd for: $C_{14}H_{12}N_2O_3S_2$ (320.39): C, 52.48; H, 3.78; N, 8.74; S, 20.02. Found: C, 52.56; H, 3.87; N, 8.90; S, 19.91%. EIMS: *m/z* 320 $[M]^+$ (70%).

Ethyl 2-Amino-5-(benzo[*d*]thiazol-2-yl)-4-methylthiophene-3-carboxylate (6f)

Pale brown crystals from ethanol, yield 1.90 g (60%), m.p. 204–206 °C. IR (KBr) ν_{max} (cm^{-1}): 3451–3346 (NH_2), 3058 (CH-aromatic), 2952 (CH-aliphatic), 1689 (CO), 1588 (C=C). ^{1}H NMR (DMSO-d_6, 300 MHz): δ 1.12 (t, 3H, J = 7.11 Hz, $OCH_2\underline{CH_3}$), 2.69 (s, 3H, CH_3), 4.29 (s, 2H, D_2O exchangeable, NH_2), 4.24 (q, 2H, J = 6.11 Hz, $O\underline{CH_2}CH_3$), 7.26–7.49 (m, 4H, C_6H_4). ^{13}C NMR (DMSO-d_6, 75 MHz): δ 16.1 ($OCH_2\underline{CH_3}$), 36.8 (CH_3), 50.1 ($O\underline{CH_2}CH_3$), 121.4, 122.8, 123.4, 123.5, 124.1, 124.8, 125.5 (C_6H_4), 138.5, 138.7, 140.5, 142.9 (thiophene C), 165.3 (CO), 168.3 (C=N). Anal. Calcd for: $C_{15}H_{14}N_2O_2S_2$ (318.41): C, 56.58; H, 4.43; N, 8.80; S, 20.14. Found: C, 56.32; H, 4.62; N, 8.73; S, 19.88%. EIMS: *m/z* 318 $[M]^+$ (66%).

2. 1. 3. General Procedure for the Synthesis of the Arylhydrazone Derivatives 8a–i

To a cold solution (0–5 °C) of either compound **4a** (1.74 g, 0.01 mol), **4b** (2.21 g, 0.01 mol) or **4c** (1.91 g, 0.01 mol) in ethanol (60 mL) containing sodium acetate (3.0 g) either of benzenediazonium chloride (0.01 mol), 4-chlorobenzenediazonium chloride or 4-methoxybenzenediazonium chloride [prepared by the addition of sodium nitrite solution (0.70 g, 0.01 mol) to a cold solution of either aniline (0.93 g, 0.01 mol), 4-chloroaniline (1.27 g, 0.01 mol) or 4-methoxyaniline (1.23 g, 0.01 mol) in concentrated hydrochloric acid (8.0 mL, 18%) with continuous stirring] was added with continuous stirring. The solid product formed upon stirring for 1 h was collected by filtration.

N′-Phenylbenzo[*d*]thiazole-2-carbohydrazonoyl Cyanide (8a)

Yellow crystals from 1,4-dioxane, yield 1.61 g (58%), m.p. 247–249 °C. IR (KBr) ν_{max} (cm^{-1}): 3348–3321 (NH), 3050 (CH-aromatic), 2951 (CH-aliphatic), 2220 (CN), 1587 (C=C). ^{1}H NMR (DMSO-d_6, 300 MHz): δ 7.23–7.42 (m, 9H, C_6H_5, C_6H_4), 8.52 (s, 1H, D_2O exchangeable, NH). ^{13}C NMR (DMSO-d_6, 75 MHz): δ 116.8 (CN), 120.2, 121.5, 122.0, 122.5, 122.8, 123.1, 123.6, 124.7, 124.9, 125.3 (C_6H_5, C_6H_4), 168.5, 170.0 (2×C=N). Anal. Calcd for: $C_{15}H_{10}N_4S$ (278.33): C, 64.73; H, 3.62; N, 20.13; S, 11.52. Found: C, 64.90; H, 3.42; N, 20.07; S, 11.65%. EIMS: *m/z* 278 $[M]^+$ (68%).

N′-(4-Chlorophenyl)benzo[*d*]thiazole-2-carbohydrazonoyl Cyanide (8b)

Orange crystals from ethanol, yield 1.69 g (63%), m.p. 211–213 °C. IR (KBr) ν_{max} (cm^{-1}): 3352–3341 (NH), 3050 (CH-aromatic), 2951 (CH-aliphatic), 2221 (CN), 1587 (C=C). ^{1}H NMR (DMSO-d_6, 300 MHz): δ 7.25–7.58 (m, 8H, 2×C_6H_4), 8.49 (s, 1H, D_2O exchangeable, NH). ^{13}C NMR (DMSO-d_6, 75 MHz): δ 116.9 (CN), 120.0, 120.7, 121.3, 122.5, 122.6, 123.3, 123.8, 124.2, 124.5, 125.9 (2×C_6H_4), 168.7, 170.1 (2×C=N). Anal. Calcd for: $C_{15}H_9ClN_4S$ (312.78): C, 57.60; H, 2.90; N, 17.91; S, 10.25. Found: C, 57.83; H, 3.19; N, 18.21; S, 10.36%. EIMS: *m/z* 312 $[M]^+$ (70%).

N′-(4-Methoxyphenyl)benzo[*d*]thiazole-2-carbohydrazonoyl Cyanide (8c)

Orange crystals from ethanol, yield 1.90 g (62%), m.p. 197–199 °C. IR (KBr) ν_{max} (cm^{-1}): 3362–3336 (NH), 3050 (CH-aromatic), 2951 (CH-aliphatic), 2220 (CN), 1586 (C=C). ^{1}H NMR (DMSO-d_6, 300 MHz): δ 3.69 (s, 3H, OCH_3), 7.23–7.53 (m, 8H, 2×C_6H_4), 8.47 (s, 1H, D_2O exchangeable, NH). ^{13}C NMR (DMSO-d_6, 75 MHz): δ 50.8 (OCH_3), 116.7 (CN), 120.3, 120.9, 121.1, 122.4, 122.8, 123.0, 123.6, 124.5, 124.8, 125.3 (2×C_6H_4), 168.9, 170.3 (2×C=N). Anal. Calcd for: $C_{16}H_{12}N_4OS$ (308.36): C, 62.32; H, 3.92; N, 18.17; S, 10.40. Found: C, 62.49; H, 3.75; N, 18.36; S, 10.42%. EIMS: *m/z* 308 $[M]^+$ (68%).

Ethyl 2-(Benzo[*d*]thiazol-2-yl)-2-(2-phenylhydrazono) acetate (8d)

Red crystals from ethanol, yield 1.78 g (55%), m.p. 215–217 °C. IR (KBr) ν_{max} (cm^{-1}): 3349–3327 (NH), 3050 (CH-aromatic), 2951 (CH-aliphatic), 2220 (CN), 1688 (CO), 1585 (C=C). ^{1}H NMR (DMSO-d_6, 300 MHz): δ 1.15 (t, 3H, *J* = 7.28 Hz, $OCH_2\underline{CH_3}$), 4.25 (q, 2H, *J* = 7.28 Hz, $O\underline{CH_2}CH_3$), 7.27–7.40 (m, 9H, C_6H_5, C_6H_4), 8.47 (s, 1H, D_2O exchangeable, NH). ^{13}C NMR (DMSO-d_6, 75 MHz): δ 16.3 ($O\underline{CH_2}CH_3$), 50.2 ($OCH_2\underline{CH_3}$), 120.1, 120.8, 121.4, 122.6, 122.2, 123.5, 123.8, 124.1, 124.5, 125.1 (C_6H_5, C_6H_4), 165.4 (CO), 168.7, 170.0 (2×C=N). Anal. Calcd for: $C_{17}H_{15}N_3O_2S$ (325.38): C, 62.75; H, 4.65; N, 12.91; S, 9.85. Found: C, 62.88; H, 4.80; N, 13.21; S, 10.16%. EIMS: *m/z* 325 $[M]^+$ (78%).

Ethyl 2-(Benzo[*d*]thiazol-2-yl)-2-(2-(4-chlorophenyl) hydrazono)acetate (8e)

Red crystals from 1,4-dioxane, yield 2.13 g (60%), m.p. 188–190 °C. IR (KBr) ν_{max} (cm^{-1}): 3354–3343 (NH), 3050 (CH-aromatic), 2954 (CH-aliphatic), 1669 (CO), 1585 (C=C). ^{1}H NMR (DMSO-d_6, 300 MHz): δ = 1.13 (t, 3H, *J* = 6.68 Hz, $OCH_2\underline{CH_3}$), 4.22 (q, 2H, *J* = 6.68 Hz, $O\underline{CH_2}CH_3$), 7.23–7.56 (m, 8H, 2 C_6H_4), 8.51 (s, 1H, D_2O exchangeable, NH). ^{13}C NMR (DMSO-d_6, 75 MHz): δ 16.6 ($O\underline{CH_2}CH_3$), 50.3 ($OCH_2\underline{CH_3}$), 120.3, 120.5, 121.6, 122.9, 122.1, 123.7, 123.8, 124.3, 124.8, 125.9 (2×C_6H_4), 165.4 (CO), 168.9, 170.1 (2×C=N). Anal. Calcd for: $C_{17}H_{14}ClN_3O_2S$ (359.83): C, 56.74; H, 3.92; N, 11.68; S, 8.91. Found: C, 56.83; H, 4.15; N, 11.80; S, 9.25%. EIMS: *m/z* 359 $[M]^+$ (86%).

Ethyl 2-(Benzo[*d*]thiazol-2-yl)-2-(2-(4-methoxyphenyl) hydrazono)acetate (8f)

Orange crystals from 1,4-dioxane, yield 2.48 g (70%), m.p. 148–150 °C. IR (KBr) ν_{max} (cm^{-1}): 3369–3353 (NH), 3053 (CH-aromatic), 2954 (CH-aliphatic), 1688 (CO), 1588 (C=C). ^{1}H NMR (DMSO-d_6, 300 MHz): δ 1.16 (t, 3H, *J* = 6.48 Hz, $OCH_2\underline{CH_3}$), 3.80 (s, 3H, OCH_3), 4.25 (q, 2H, *J* = 6.48 Hz, $O\underline{CH_2}CH_3$), 7.23–7.56 (m, 8H, 2×C_6H_4), 8.49 (s, 1H, D_2O exchangeable, NH). ^{13}C NMR (DMSO-d_6, 75 MHz): δ 16.4 ($O\underline{CH_2}CH_3$), 50.1 ($OCH_2\underline{CH_3}$), 50.8 (OCH_3), 120.1, 120.8, 121.3, 122.6, 122.1, 123.9, 124.1, 124.5, 125.2, 125.7 (2×C_6H_4), 165.8 (CO), 168.9, 169.8 (2×C=N). Anal. Calcd for: $C_{18}H_{17}N_3O_3S$ (355.41): C, 60.83; H, 4.82; N, 11.82; S, 9.02. Found: C, 60.77; H, 4.79; N, 11.97; S, 9.28%. EIMS: *m/z* 355 $[M]^+$ (60%).

1-(Benzo[*d*]thiazol-2-yl)-1-(2-phenylhydrazono)propan-2-one (8g)

Orange crystals from 1,4-dioxane, yield 1.79 g (61%), m.p. 208–210 °C. IR (KBr) ν_{max} (cm^{-1}): 3353–3348 (NH), 3053 (CH-aromatic), 2950 (CH-aliphatic), 1688 (CO), 1584 (C=C). ^{1}H NMR (DMSO-d_6, 300 MHz): δ 2.87 (s, 3H, CH_3), 7.26–7.48 (m, 9H, C_6H_5, C_6H_4), 8.46 (s, 1H, D_2O exchangeable, NH). ^{13}C NMR (DM-

SO-d_6, 75 MHz): δ 36.6 (CH_3), 120.0, 120.6, 121.5, 122.8, 123.4, 123.5, 123.6, 124.2, 124.8, 125.6 (C_6H_5, C_6H_4), 165.5 (CO), 168.8 (C=N). Anal. Calcd for: $C_{16}H_{13}N_3OS$ (295.36): C, 65.06; H, 4.44; N, 14.23; S, 10.86. Found: C, 65.15; H, 4.60; N, 14.37; S, 11.07%. EIMS: *m/z* 295 $[M]^+$ (58%).

1-(Benzo[*d*]thiazol-2-yl)-1-(2-(4-chlorophenyl)hydrazono)propan-2-one (8h)

Orange crystals from 1,4-dioxane, yield 2.13 g (64%), m.p. 166–168 °C. IR (KBr) ν_{max} (cm^{-1}): 3372–3350 (NH), 3053 (CH-aromatic), 2950 (CH-aliphatic), 1688 (CO), 1583 (C=C). ^{1}H NMR (DMSO-d_6, 300 MHz): δ 2.93 (s, 3H, CH_3), 7.23–7.49 (m, 8H, 2×C_6H_4), 8.43 (s, 1H, D_2O exchangeable, NH). ^{13}C NMR (DMSO-d_6, 75 MHz): δ 36.3 (CH_3), 120.2, 120.5, 121.1, 122.6, 123.1, 123.4, 124.0, 124.2, 124.5, 125.8 (2×C_6H_4), 165.8 (CO), 168.5, 170.3 (2×C=N). Anal. Calcd for: $C_{16}H_{12}ClN_3OS$ (329.80): C, 58.27; H, 3.67; N, 12.74; S, 9.72. Found: C, 58.31; H, 3.80; N, 12.42; S, 9.59%. EIMS: *m/z* 329 $[M]^+$ (66%).

1-(Benzo[*d*]thiazol-2-yl)-1-(2-(4-methoxyphenyl)hydrazono)propan-2-one (8i)

Orange crystals from 1,4-dioxane, yield 2.17 g (67%), m.p. 177–179 °C. IR (KBr) ν_{max} (cm^{-1}): 3389–3334 (NH), 3058 (CH-aromatic), 2950 (CH-aliphatic), 1689 (CO), 1581 (C=C). ^{1}H NMR (DMSO-d_6, 300 MHz): δ 2.96 (s, 3H, CH_3), 3.80 (s, 3H, OCH_3), 7.22–7.58 (m, 8H, 2×C_6H_4), 8.45 (s, 1H, D_2O exchangeable, NH). ^{13}C NMR (DMSO-d_6, 75 MHz): δ 36.2 (CH_3), 120.3, 120.8, 121.4, 122.8, 123.4, 123.9, 124.2, 124.5, 124.6, 125.2 (2×C_6H_4), 165.7 (CO), 168.9, 170.1 (2×C=N). Anal. Calcd for: $C_{17}H_{15}N_3O_2S$ (325.38): C, 62.75 H, 4.65; N, 12.91; S, 9.85. Found: C, 62.51; H, 4.75; N, 12.72; S, 9.69%. EIMS: *m/z* 325 $[M]^+$ (68%).

2. 1. 4. General Procedure for the Synthesis of the Pyridazine Derivatives 9a–i

To a solution of either **8a** (2.78 g, 0.01 mol), **8b** (3.12 g, 0.01 mol), **8c** (3.08 g, 0.01 mol), **8d** (3.25 g, 0.01 mol), **8e** (3.59 g, 0.01 mol), **8f** (3.55 g, 0.01 mol), **8g** (2.95 g, 0.01 mol), **8h** (3.29 g, 0.01 mol) or **8i** (3.25 g, 0.01 mol) in 1,4-dioxane (40 mL) containing triethylamine (1.0 mL), malononitrile (0.66 g, 0.01 mol) was added. The reaction mixture was heated under reflux for 2 h then poured onto ice/water mixture containing a few drops of hydrochloric acid and the formed solid product was collected by filtration.

5-Amino-6-(benzo[*d*]thiazol-2-yl)-3-imino-2-phenyl-2,3-dihydropyridazine-4-carbonitrile (9a)

Pale yellow crystals from 1,4-dioxane, yield 1.72 g (50%), m.p. 166–168 °C. IR (KBr) ν_{max} (cm^{-1}): 3354–3360 (NH), 3050 (CH-aromatic), 2220 (CN), 1658 (C=N), 1585 (C=C). ^{1}H NMR (DMSO-d_6, 300 MHz): δ 4.96 (s, 2H, D_2O echangeable, NH_2), 7.25–7.43 (m, 9H, C_6H_5, C_6H_4), 8.58 (s, 1H, D_2O exchangeable, NH). ^{13}C NMR (DMSO-d_6, 75 MHz): δ 117.1 (CN), 120.2, 120.4, 121.1, 122.5, 122.9, 123.2, 123.7, 124.7, 125.4, 125.8 (C_6H_5, C_6H_4), 140.1, 142.3 (pyridazine C-3, C-4), 168.6, 170.2, 170.3 (3×C=N). Anal. Calcd for: $C_{18}H_{12}N_6S$ (344.39): C, 62.77; H, 3.51; N, 24.40; S, 9.31. Found: C, 62.82; H, 3.69; N, 24.65; S, 19.52%. EIMS: *m/z* 344 $[M]^+$ (72%).

5-Amino-6-(benzo[*d*]thiazol-2-yl)-2-(4-chlorophenyl)-3-imino-2,3-dihydropyridazine-4-carbonitrile (9b)

Pale yellow crystals from 1,4-dioxane, yield 2.49 g (66%), m.p. 240–243 °C. IR (KBr) ν_{max} (cm^{-1}): 3361–3343 (NH), 3050 (CH-aromatic), 2220 (CN), 1658 (C=N), 1586 (C=C). ^{1}H NMR (DMSO-d_6, 300 MHz): δ 4.85 (s, 2H, D_2O echangeable, NH_2), 7.28–7.52 (m, 8H, 2×C_6H_4), 8.42 (s, 1H, D_2O exchangeable, NH). ^{13}C NMR (DMSO-d_6, 75 MHz): δ 117.3 (CN), 120.3, 120.7, 121.2, 122.6, 122.9, 122.8, 122.5, 124.4, 125.8, 125.9 (C_6H_5, C_6H_4), 140.1, 142.5 (pyridazine C-3, C-4), 168.4, 170.1, 170.6 (3×C=N). Anal. Calcd for: $C_{18}H_{11}ClN_6S$ (378.84): C, 57.07; H, 2.93; N, 22.18; S, 8.46. Found: C, 57.26; H, 3.18; N, 22.31; S, 8.69%. EIMS: *m/z* 378 $[M]^+$ (68%).

5-Amino-6-(benzo[*d*]thiazol-2-yl)-3-imino-2-(4-methoxyphenyl)-2,3-dihydropyridazine-4-carbonitrile (9c)

Pale yellow crystals from 1,4-dioxane, yield 2.20 g (59%), m.p. 196–198 °C. IR (KBr) ν_{max} (cm^{-1}): 3349–3362 (NH), 3050 (CH-aromatic), 2220 (CN), 1662 (C=N), 1587 (C=C). ^{1}H NMR (DMSO-d_6, 300 MHz): δ 3.66 (s, 3H, OCH_3), 4.88 (s, 2H, D_2O echangeable, NH_2), 7.25–7.58 (m, 8H, 2×C_6H_4), 8.46 (s, 1H, D_2O exchangeable, NH). ^{13}C NMR (DMSO-d_6, 75 MHz): δ 50.6 (OCH_3), 116.9 (CN), 120.6, 120.6, 121.4, 122.6, 122.5, 123.8 123.9, 124.1, 125.5, 125.6 (2×C_6H_4), 140.5, 142.3 (pyridazine C-3, C-4), 168.4, 170.3, 170.5 (3×C=N). Anal. Calcd for: $C_{19}H_{14}N_6OS$ (374.42): C, 60.95; H, 3.77; N, 22.45; S, 8.56. Found: C, 61.28; H, 3.86; N, 22.29; S, 8.69%. EIMS: *m/z* 374 $[M]^+$ (58%).

6-(Benzo[*d*]thiazol-2-yl)-5-hydroxy-3-imino-2-phenyl-2,3-dihydropyridazine-4-carbonitrile (9d)

Yelow crystals from 1,4-dioxane, yield 2.07 g (60%), m.p. 188–190 °C. IR (KBr) ν_{max} (cm^{-1}): 3349–3352 (OH, NH), 3050 (CH-aromatic), 2220 (CN), 1663 (C=N), 1585 (C=C). ^{1}H NMR (DMSO-d_6, 300 MHz): δ 7.25–7.43 (m, 9H, C_6H_5, C_6H_4), 8.44 (s, 1H, D_2O exchangeable, NH), 10.30 (s, 1H, D_2O exchangeable, OH). ^{13}C NMR (DMSO-d_6, 75 MHz): δ 116.7 (CN), 120.2, 120.4, 121.8, 122.1, 122.8, 123.2 123.9, 124.1, 125.3, 125.9 (C_6H_5, C_6H_4), 140.1, 142.6 (pyridazine C-3, C-4), 168.8, 170.1, 170.6 (3×C=N). Anal. Calcd for: $C_{18}H_{11}N_5OS$ (345.38): C, 62.60; H, 3.21; N, 20.28; S, 9.28. Found: C, 62.73; H, 3.36; N, 20.42; S, 9.31%. EIMS: *m/z* 345 $[M]^+$ (70%).

6-(Benzo[*d*]thiazol-2-yl)-2-(4-chlorophenyl)-5-hydroxy-3-imino-2,3-dihydropyridazine-4-carbonitrile (9e)

Yellow crystals from 1,4-dioxane, yield 2.41 g (70%), m.p. 155–157 °C. IR (KBr) ν_{max} (cm^{-1}): 3356–3332 (OH, NH), 3050 (CH-aromatic), 2220 (CN), 1661 (C=N), 1584 (C=C). ^{1}H NMR (DMSO-d_6, 300 MHz): δ 7.23–7.56 (m, 8H, 2×C_6H_4), 8.46 (s, 1H, D_2O exchangeable, NH), 10.28 (s, 1H, D_2O exchangeable, OH). ^{13}C NMR (DMSO-d_6, 75 MHz): δ 116.9 (CN), 120.1, 120.5, 121.5, 122.7, 122.8, 123.2 123.9, 124.6, 125.1, 125.6 (2×C_6H_4), 140.1, 142.3 (pyridazine C-3, C-4), 168.9, 170.0, 170.8 (3×C=N). Anal. Calcd for: $C_{18}H_{10}ClN_5OS$ (379.82): C, 56.92; H, 2.65; N, 18.44; S, 8.44. Found: C, 57.13; H, 2.80; N, 18.72; S, 8.24%. EIMS: *m/z* 379 $[M]^+$ (62%).

6-(Benzo[*d*]thiazol-2-yl)-5-hydroxy-3-imino-2-(4-methoxyphenyl)-2,3-dihydropyridazine-4-carbonitrile (9f)

Pale yellow crystals from 1,4-dioxane, yield 2.36 g (63%), m.p. 196–198 °C. IR (KBr) ν_{max} (cm^{-1}): 3358–3337 (OH, NH), 3050 (CH-aromatic), 2220 (CN), 1660 (C=N), 1585 (C=C). ^{1}H NMR (DMSO-d_6, 300 MHz): δ 3.68 (s, 3H, OCH_3), 7.23–7.56 (m, 8H, 2×C_6H_4), 8.45 (s, 1H, D_2O exchangeable, NH), 10.22 (s, 1H, D_2O exchangeable, OH). ^{13}C NMR (DMSO-d_6, 75 MHz): δ 50.3 (OCH_3), 116.7 (CN), 120.2, 120.8, 121.5, 122.1, 122.6, 123.3, 123.5, 124.7, 125.2, 125.5 (2×C_6H_4), 140.1, 142.3 (pyridazine C-3, C-4), 168.6, 170.1, 170.3 (3×C=N). Anal. Calcd for: $C_{19}H_{13}N_5O_2S$ (375.40): C, 60.79; H, 3.49; N, 18.66; S, 8.54. Found: C, 60.59; H, 3.52; N, 18.73; S, 8.72%. EIMS: *m/z* 375 $[M]^+$ (60%).

6-(Benzo[*d*]thiazol-2-yl)-3-imino-5-methyl-2-phenyl-2,3-dihydropyridazine-4-carbonitrile (9g)

Pale yellow crystals from 1,4-dioxane, yield 2.05 g (60%), m.p. 213–215 °C. IR (KBr) ν_{max} x (cm^{-1}): 3349–3353 (NH), 3050 (CH-aromatic), 2220 (CN), 1663 (C=N), 1585 (C=C). ^{1}H NMR (DMSO-d_6, 300 MHz): δ 2.83 (s, 3H, CH_3), 7.27–7.48 (m, 9H, C_6H_5, C_6H_4), 8.43 (s, 1H, D_2O exchangeable, NH). ^{13}C NMR (DMSO-d_6, 75 MHz): δ 37.2 (CH_3), 116.9 (CN), 120.4, 120.6, 121.3, 122.4, 122.8, 123.2, 123.7, 124.7, 125.0, 125.8 (C_6H_5, C_6H_4), 168.8, 170.2, 170.4 (3×C=N). Anal. Calcd for: $C_{19}H_{13}N_5S$ (343.41): C, 66.45; H, 3.82; N, 20.39; S, 9.34. Found: C, 66.53; H, 3.69; N, 20.41; S, 9.55%. EIMS: *m/z* 343 $[M]^+$ (50%).

6-(Benzo[*d*]thiazol-2-yl)-2-(4-chlorophenyl)-3-imino-5-methyl-2,3-dihydropyridazine-4-carbonitrile (9h)

Pale brown crystals from 1,4-dioxane, yield 2.48 g (66%), m.p. 149–151 °C. IR (KBr) ν_{max} (cm^{-1}): 3358–3328 (NH), 3050 (CH-aromatic), 2220 (CN), 1660 (C=N), 1585 (C=C). ^{1}H NMR (DMSO-d_6, 300 MHz): δ 2.85 (s, 3H, CH_3), 7.25–7.52 (m, 8H, 2×C_6H_4), 8.46 (s, 1H, D_2O exchangeable, NH). ^{13}C NMR (DMSO-d_6, 75 MHz): δ 37.8 (CH_3), 117.2 (CN), 120.2, 120.8, 121.1, 122.6, 122.9, 123.1, 123.8, 124.7, 125.4, 125.6 (2×C_6H_4), 140.3, 142.6 (pyridazine C-3, C-4), 168.4, 170.1, 170.2 (3×C=N). Anal. Calcd for: $C_{19}H_{12}ClN_5S$ (377.85): C, 60.40; H, 3.20; N, 18.53; S, 8.49. Found: C, 60.63; H, 3.36; N, 18.70; S, 8.52%. EIMS: *m/z* 377 $[M]^+$ (68%).

6-(Benzo[*d*]thiazol-2-yl)-3-imino-2-(4-methoxyphenyl)-5-methyl-2,3-dihydropyridazine-4-carbonitrile (9i)

Pale brown crystals from 1,4-dioxane, yield 2.16 g (58%), m.p. 201–203 °C. IR (KBr) ν_{max} (cm^{-1}): 3373–3346 (NH), 3050 (CH-aromatic), 2220 (CN), 1660 (C=N), 1586 (C=C). ^{1}H NMR (DMSO-d_6, 300 MHz): δ 2.87 (s, 3H, CH_3), 3.59 (s, 3H, OCH_3), 7.22–7.58 (m, 8H, 2×C_6H_4), 8.44 (s, 1H, D_2O exchangeable, NH). ^{13}C NMR (DMSO-d_6, 75 MHz): δ 37.5 (CH_3), 50.8 (OCH_3), 117.1 (CN), 120.2, 120.6, 121.2, 122.4, 122.9, 123.5, 123.8, 124.4, 125.8, 125.8 (2×C_6H_4), 140.1, 142.2 (pyridazine C-3, C-4), 168.6, 170.3, 170.5 (3×C=N). Anal. Calcd for: $C_{20}H_{15}N_5OS$ (373.43): C, 64.33; H, 4.05; N, 18.75; S, 8.59. Found: C, 64.51; H, 3.87; N, 18.49; S, 8.68%. EIMS: *m/z* 373 $[M]^+$ (85%).

2. 1. 5. General Procedure for the Synthesis of the Pyridazin-6-one Derivatives 10a–i

To a solution of either **8a** (2.78 g, 0.01 mol), **8b** (3.12 g, 0.01 mol), **8c** (3.08 g, 0.01 mol), **8d** (3.25 g, 0.01 mol), **8e** (3.59 g, 0.01 mol), **8f** (3.55 g, 0.01 mol), **8g** (2.95 g, 0.01 mol), **8h** (3.29 g, 0.01 mol) or **8i** (3.25 g, 0.01 mol) in 1,4-dioxane (40 mL) containing triethylamine (1.0 mL), ethyl cyanoacetate (1.07 g, 0.01 mol) was added. The reaction mixture was heated under reflux for 2 h then poured onto ice/water mixture containing a few drops of hydrochloric acid and the formed solid product was collected by filtration.

5-Amino-6-(benzo[*d*]thiazol-2-yl)-3-oxo-2-phenyl-2,3-dihydropyridazine-4-carbonitrile (10a)

Pale brown crystals from acetic acid, yield 2.00 g (58%), m.p. 179–181 °C. IR (KBr) ν_{max} (cm^{-1}): 3368–3343 (NH_2), 3050 (CH-aromatic), 2220 (CN), 1688 (CO), 1658 (C=N), 1585 (C=C). ^{1}H NMR (DMSO-d_6, 300 MHz): δ 4.98 (s, 2H, D_2O echangeable, NH_2), 7.24–7.41 (m, 9H, C_6H_5, C_6H_4). ^{13}C NMR (DMSO-d_6, 75 MHz): δ 117.3 (CN), 120.1, 120.5, 121.4, 122.8, 122.9, 123.5, 123.7, 124.2, 125.4, 125.9 (C_6H_5, C_6H_4), 140.1, 142.3 (pyridazine C-3, C-4), 165.8 (CO), 168.8, 170.2 (2×C=N). Anal. Calcd for: $C_{18}H_{11}N_5OS$ (345.38): C, 62.60; H, 3.21; N, 20.28; S, 9.28. Found: C, 62.87; H, 3.39; N, 20.53; S, 9.42%. EIMS: *m/z* 345 $[M]^+$ (60%).

5-Amino-6-(benzo[*d*]thiazol-2-yl)-2-(4-chlorophenyl)-3-oxo-2,3-dihydropyridazine-4-carbonitrile (10b)

Pale yellow crystals from 1,4-dioxane, yield 1.89 g (50%), m.p. 166–168 °C. IR (KBr) ν_{max} (cm^{-1}): 3378–3323 (NH_2), 3050 (CH-aromatic), 2220 (CN), 1688 (CO), 1658 (C=N), 1585 (C=C). ^{1}H NMR (DMSO-d_6, 300 MHz): δ

4.88 (s, 2H, D_2O echangeable, NH_2), 7.28–7.56 (m, 8H, 2×C_6H_4). ^{13}C NMR (DMSO-d_6, 75 MHz): δ 116.9 (CN), 120.1, 120.5, 121.2, 122.4, 122.7, 123.2, 123.7, 124.4, 125.4, 125.8 (C_6H_5, C_6H_4), 140.3, 142.2 (pyridazine C-3, C-4), 166.4 (CO), 170.1, 170.8 (2×C=N). Anal. Calcd for: $C_{18}H_{10}ClN_5OS$ (379.82): C, 56.92; H, 2.65; N, 18.44; S, 8.44. Found: C, 57.23; H, 2.80; N, 18.58; S, 8.64%. EIMS: *m/z* 379 $[M]^+$ (60%).

5-Amino-6-(benzo[*d*]thiazol-2-yl)-2-(4-methoxyphenyl)-3-oxo-2,3-dihydropyridazine-4-carbonitrile (10c)

Pale yellow crystals from 1,4-dioxane, yield 2.25 g (60%), m.p. 230–233 °C. IR (KBr) ν_{max} (cm^{-1}): 3353–3322 (NH), 3050 (CH-aromatic), 2220 (CN), 1689 (CO), 1660 (C=N), 1587 (C=C). ^{1}H NMR (DMSO-d_6, 300 MHz): δ 3.68 (s, 3H, OCH_3), 4.83 (s, 2H, D_2O echangeable, NH_2), 7.27–7.56 (m, 8H, 2×C_6H_4). ^{13}C NMR (DMSO-d_6, 75 MHz): δ 50.6 (OCH_3), 116.7 (CN), 120.0, 120.1, 121.4, 122.2, 122.5, 123.4 123.9, 124.6, 125.2, 125.9 (2×C_6H_4), 140.1, 142.2 (pyridazine C-3, C-4), 165.3 (CO), 168.5, 170.2 (2×C=N). Anal. Calcd for: $C_{19}H_{13}N_5O_2S$ (375.40): C, 60.79; H, 3.49; N, 18.66; S, 8.54. Found: C, 60.73; H, 3.52; N, 18.73; S, 8.69%. EIMS: *m/z* 375 $[M]^+$ (68%).

6-(Benzo[*d*]thiazol-2-yl)-5-hydroxy-3-oxo-2-phenyl-2,3-dihydropyridazine-4-carbonitrile (10d)

Yellow crystals from 1,4-dioxane, yield 2.00 g (58%), m.p. 168–170 °C. IR (KBr) ν_{max} (cm^{-1}): 3558–3336 (OH, NH), 3050 (CH-aromatic), 2220 (CN), 1688 (CO), 1660 (C=N), 1583 (C=C). ^{1}H NMR (DMSO-d_6, 300 MHz): δ 7.27–7.43 (m, 9H, C_6H_5, C_6H_4), 10.32 (s, 1H, D_2O exchangeable, OH). ^{13}C NMR (DMSO-d_6, 75 MHz): δ 116.8 (CN), 120.1, 120.6, 121.2, 122.3, 122.8, 123.3 123.6, 124.3, 125.6, 125.7 (C_6H_5, C_6H_4), 140.4, 142.3 (pyridazine C-3, C-4), 166.3 (CO), 170.1, 170.4 (2×C=N). Anal. Calcd for: $C_{18}H_{10}N_4O_2S$ (346.36): C, 62.42; H, 2.91; N, 16.18; S, 9.26. Found: C, 62.53; H, 3.11; N, 16.28; S, 9.40%. EIMS: *m/z* 346 $[M]^+$ (80%).

6-(Benzo[*d*]thiazol-2-yl)-2-(4-chlorophenyl)-5-hydroxy-3-oxo-2,3-dihydropyridazine-4-carbonitrile (10e)

Yellow crystals from 1,4-dioxane, yield 2.39 g (63%), m.p. 168–170 °C. IR (KBr) ν_{max} (cm^{-1}): 3359–3340 (OH, NH), 3053 (CH-aromatic), 2220 (CN), 1688 (CO), 1663 (C=N), 1583 (C=C). ^{1}H NMR (DMSO-d_6, 300 MHz): δ 7.23–7.56 (m, 8H, 2×C_6H_4), 10.38 (s, 1H, D_2O exchangeable, OH). ^{13}C NMR (DMSO-d_6, 75 MHz): δ 117.2 (CN), 120.1, 120.6, 121.3, 122.5, 122.8, 123.1 123.4, 124.3, 125.3, 126.53 (C_6H_5, C_6H_4), 140.1, 142.3 (pyridazine C-3, C-4), 166.5 (CO), 170.1, 170.5 (2×C=N). Anal. Calcd for: $C_{18}H_9ClN_4O_2S$ (380.81): C, 56.77; H, 2.38; N, 14.71; S, 8.42. Found: C, 56.53; H, 2.40; N, 14.59; S, 8.63%. EIMS: *m/z* 380 $[M]^+$ (77%).

6-(Benzo[*d*]thiazol-2-yl)-5-hydroxy-2-(4-methoxyphenyl)-3-oxo-2,3-dihydropyridazine-4-carbonitrile (10f)

Pale yellow crystals from 1,4-dioxane, yield 2.36 g (63%), m.p. 196–198 °C. IR (KBr) ν_{max} (cm^{-1}): 3358–3337 (OH, NH), 3050 (CH-aromatic), 2220 (CN), 1688 (CO), 1660 (C=N), 1585 (C=C). ^{1}H NMR (DMSO-d_6, 300 MHz): δ 3.68 (s, 3H, OCH_3), 7.23–7.56 (m, 8H, 2×C_6H_4), 10.22 (s, 1H, D_2O exchangeable, OH). ^{13}C NMR (DMSO-d_6, 75 MHz): δ 50.3 (OCH_3), 116.7 (CN), 120.2, 120.8, 121.5, 122.1, 122.6, 123.5, 123.3, 124.7, 125.2, 125.5 (2×C_6H_4), 168.6, 170.1 (2 X C=N). Anal. Calcd for: $C_{19}H_{12}N_4O_3S$ (376.39): C, 60.63; H, 3.21; N, 14.89; S, 8.52. Found: C, 60.59; H, 3.42; N, 14.73; S, 8.72%. EIMS: *m/z* 376 $[M]^+$ (64%).

6-(Benzo[*d*]thiazol-2-yl)-5-methyl-3-oxo-2-phenyl-2,3-dihydropyridazine-4-carbonitrile (10g)

Pale yellow crystals from 1,4-dioxane, yield 2.23 g (65%), m.p. 244–247 °C. IR (KBr) ν_{max} (cm^{-1}): 3361–3348 (NH), 3050 (CH-aromatic), 2220 (CN), 1689 (CO), 1663 (C=N), 1587 (C=C). ^{1}H NMR (DMSO-d_6, 300 MHz): δ 2.86 (s, 3H, CH_3), 7.23–7.45 (m, 9H, C_6H_5, C_6H_4). ^{13}C NMR (DMSO-d_6, 75 MHz): δ 37.8 (CH_3), 116.7 (CN), 120.1, 120.4, 121.5, 122.9, 123.0, 123.2, 123.6, 124.5, 125.20, 125.4 (C_6H_5, C_6H_4), 140.3, 142.3 (pyridazine C-3, C-4), 166.3 (CO), 168.8, 170.2 (2 X C=N). Anal. Calcd for: $C_{19}H_{12}N_4OS$ (344.39): C, 66.26; H, 3.51; N, 16.27; S, 9.31. Found: C, 66.35; H, 3.68; N, 16.32; S, 9.53%. EIMS: *m/z* 344 $[M]^+$ (67%).

6-(Benzo[*d*]thiazol-2-yl)-2-(4-chlorophenyl)-5-methyl-3-oxo-2,3-dihydropyridazine-4-carbonitrile (10h)

Pale brown crystals from 1,4-dioxane, yield 2.07 g (55%), m.p. 180–183 °C. IR (KBr) ν_{max} (cm^{-1}): 3361–3328 (NH), 3050 (CH-aromatic), 2220 (CN), 1688 (CO), 1660 (C=N), 1583 (C=C). ^{1}H NMR (DMSO-d_6, 300 MHz): δ 2.88 (s, 3H, CH_3), 7.23–7.56 (m, 8H, 2×C_6H_4). ^{13}C NMR (DMSO-d_6, 75 MHz): δ 37.6 (CH_3), 117.0 (CN), 120.1, 120.6, 121.5, 121.8, 122.4, 123.1, 123.4, 124.2, 125.3, 125.6 (2×C_6H_4), 140.1, 142.5 (pyridazine C-3, C-4), 165.3 (CO), 168.4, 170.3 (2 X C=N). Anal. Calcd for: $C_{19}H_{11}ClN_4OS$ (378.83): C, 60.24; H, 2.93; N, 14.79; S, 8.46. Found: C, 60.39; H, 3.16; N, 14.68; S, 8.58%. EIMS: *m/z* 378 $[M]^+$ (80%).

6-(Benzo[*d*]thiazol-2-yl)-2-(4-methoxyphenyl)-5-methyl-3-oxo-2,3-dihydropyridazine-4-carbonitrile (10i)

Pale brown crystals from 1,4-dioxane, yield 2.24 g (60%), m.p. 198–200 °C. IR (KBr) ν_{max} (cm^{-1}): 3380–3326 (NH), 3050 (CH-aromatic), 2220 (CN), 1688 (CO), 1660 (C=N), 1586 (C=C). ^{1}H NMR (DMSO-d_6, 300 MHz): δ 2.89 (s, 3H, CH_3), 3.65 (s, 3H, OCH_3), 7.22–7.58 (m, 8H, 2×C_6H_4). ^{13}C NMR (DMSO-d_6, 75 MHz): δ 37.8 (CH_3), 50.6 (OCH_3), 117.1 (CN), 120.1, 120.4, 120.8, 122.4, 122.7, 123.3, 123.8, 124.4, 125.6, 125.9 (2× C_6H_4), 140.4, 142.3 (pyridazine C-3, C-4), 166.3 (CO), 168.6, 170.3 (2 X C=N). Anal. Calcd for: $C_{20}H_{14}N_4O_2S$ (374.42): C, 64.16; H, 3.77; N, 14.96; S, 8.56. Found: C, 64.28; H, 3.89; N, 15.42; S, 8.73%. EIMS: *m/z* 374 $[M]^+$ (75%).

2. 1. 6. General Method for the Synthesis of the Thiazole Derivatives 12a–i

To a solution of either **9a** (3.45g, 0.01 mol), **9b** (3.79g, 0.01 mol), **9c** (3.75 g, 0.01 mol), **9d** (3.46 g, 0.01 mol), **9e** (3.80 g, 0.01 mol), **9f** (3.76 g, 0.01 mol), **9g** (3.44 g, 0.01 mol), **9h** (3.78 g, 0.01 mol) or **9i** (3.74 g, 0.01 mol) in 1,4-dioxane (40 mL) containing triethylamine (1.0 mL) thioglycolic acid (0.92 g, 0.01 mol) was added. The reaction mixture was heated under reflux for 2 h then was left to cool and the formed solid product was collected by filtration.

2-(5-Amino-6-(benzo[*d*]thiazol-2-yl)-3-imino-2-phenyl-2,3-dihydropyridazin-4-yl)thiazol-4(5*H*)-one (12a)

Pale brown crystals from acetic acid, yield 2.50 g (58%), m.p. 244–246 °C. IR (KBr) ν_{max} (cm^{-1}): 3349–3343 (NH_2, NH), 3050 (CH-aromatic), 1689 (CO), 1658 (C=N), 1585 (C=C). ^{1}H NMR (DMSO-d_6, 300 MHz): δ 4.96 (s, 2H, D_2O echangeable, NH_2), 5.31 (s, 2H, thiazole CH_2), 7.26–7.45 (m, 9H, C_6H_5, C_6H_4), 8.48 (s, 1H, D_2O exchangeable, NH). ^{13}C NMR (DMSO-d_6, 75 MHz): δ 48.8 (thiazole CH_2), 120.2, 120.3, 121.1, 122.5, 122.8, 123.6, 123.9, 124.3, 124.4, 125.6 (C_6H_5, C_6H_4), 140.1, 142.3 (pyridazine C-3, C-4), 165.9 (CO), 168.8, 169.2, 170.0, 170.1 (4×C=N). Anal. Calcd for: $C_{20}H_{14}N_6OS_2$ (418.49): C, 57.40; H, 3.37; N, 20.08; S, 15.32. Found: C, 57.63; H, 3.51; N, 20.25; S, 15.52%. EIMS: *m/z* 418 $[M]^+$ (72%).

2-(5-Amino-6-(benzo[*d*]thiazol-2-yl)-2-(4-chlorophenyl)-3-imino-2,3-dihydropyridazin-4-yl)thiazol-4(5*H*)-one (12b)

Yellow crystals from 1,4-dioxane, yield 2.71 g (60%), m.p. 177–180 °C. IR (KBr) ν_{max} (cm^{-1}): 3369–3343 (NH_2, NH), 3054 (CH-aromatic), 1689 (CO), 1656 (C=N), 1585 (C=C). ^{1}H NMR (DMSO-d_6, 300 MHz): δ 4.85 (s, 2H, D_2O echangeable, NH_2), 5.66 (s, 2H, thaizole CH_2), 7.23–7.56 (m, 8H, 2×C_6H_4), 8.39 (s, 1H, D_2O exchangeable, NH). ^{13}C NMR (DMSO-d_6, 75 MHz): δ 48.6 (thiazole CH_2), 120.3, 120.6, 121.2, 122.6, 122.9, 123.2, 123.8, 124.1, 125.4, 125.6 (2×C_6H_4), 140.1, 142.5 (pyridazine C-3, C-4), 166.6 (CO), 169.0, 169.5, 170.1, 170.9 (4×C=N). Anal. Calcd for: $C_{20}H_{13}ClN_6OS_2$ (452.94): C, 53.03; H, 2.89; N, 18.55; S, 14.16. Found: C, 52.96; H, 2.93; N, 18.68; S, 14.25%. EIMS: *m/z* 452 $[M]^+$ (66%).

2-(5-Amino-6-(benzo[*d*]thiazol-2-yl)-3-imino-2-(4-methoxyphenyl)-2,3-dihydropyridazin-4-yl)thiazol-4(5*H*)-one (12c)

Pale yellow crystals from 1,4-dioxane, yield 2.77 g (62%), m.p. 166–168 °C. IR (KBr) ν_{max} (cm^{-1}): 3368–3341 (NH_2, NH), 3050 (CH-aromatic), 1689 (CO), 1660 (C=N), 1587 (C=C). ^{1}H NMR (DMSO-d_6, 300 MHz): δ 3.68 (s, 3H, OCH_3), 4.83 (s, 2H, D_2O exchangeable, NH_2), 5.26 (s, 2H, thiazole CH_2), 7.25–7.56 (m, 8H, 2×C_6H_4), 8.36 (s, 1H, D_2O exchangeable, NH). ^{13}C NMR (DMSO-d_6, 75 MHz): δ 48.6 (thiazole CH_2), 50.4 (OCH_3), 120.3, 120.2, 121.6, 122.2, 122.5, 123.6, 123.8, 124.2, 125.4, 125.8 (2×C_6H_4), 140.1, 142.5 (pyridazine C-3, C-4), 165.9 (CO), 168.5, 169.3, 170.0, 170.3 (4×C=N). Anal. Calcd for: $C_{21}H_{16}N_6O_2S_2$ (448.52): C, 56.23; H, 3.60; N, 18.74; S, 14.30. Found: C, 56.48; H, 3.58; N, 18.82; S, 14.53%. EIMS: *m/z* 448 $[M]^+$ (60%).

2-(6-(Benzo[*d*]thiazol-2-yl)-5-hydroxy-3-imino-2-phenyl-2,3-dihydropyridazin-4-yl)thiazol-4(5*H*)-one (12d)

Yellow crystals from 1,4-dioxane, yield 2.30 g (55%), m.p. 183–185 °C. IR (KBr) ν_{max} (cm^{-1}): 3528–3338 (OH, NH), 3050 (CH-aromatic), 1689 (CO), 1660 (C=N), 1583 (C=C). ^{1}H NMR (DMSO-d_6, 300 MHz): δ 5.60 (s, 2H, thiazole CH_2), 7.27–7.46 (m, 9H, C_6H_5, C_6H_4), 8.40 (s, 1H, D_2O exchangeable, NH), 10.32 (s, 1H, D_2O exchangeable, OH). ^{13}C NMR (DMSO-d_6, 75 MHz): δ 45.6 (thiazole CH_2), 120.3, 120.4, 121.0, 121.7, 122.5, 123.7, 123.9, 124.1, 125.2, 125.6 (C_6H_5, C_6H_4), 140.4, 142.3 (pyridazine C-3, C-4), 166.1 (CO), 168.9, 169.3, 170.1, 170.3 (4×C=N). Anal. Calcd for: $C_{20}H_{13}N_5O_2S_2$ (419.48): C, 57.26; H, 3.12; N, 16.70; S, 15.29. Found: C, 57.36; H, 3.30; N, 16.59; S, 15.31%. EIMS: *m/z* 419 $[M]^+$ (73%).

2-(6-(Benzo[*d*]thiazol-2-yl)-2-(4-chlorophenyl)-5-hydroxy-3-imino-2,3-dihydropyridazin-4-yl)thiazol-4(5*H*)-one (12e)

Yellow crystals from 1,4-dioxane, yield 2.76 g (61%), m.p. 205–207 °C. IR (KBr) ν_{max} (cm^{-1}): 3541–3329 (OH, NH), 3050 (CH-aromatic), 1689 (CO), 1662 (C=N), 1583 (C=C). ^{1}H NMR (DMSO-d_6, 300 MHz): δ 5.63 (s, 2H, thiazole CH_2), 7.25–7.56 (m, 8H, 2×C_6H_4), 8.43 (s, 1H, D_2O exchangeable, NH), 10.36 (s, 1H, D_2O exchangeable, OH). ^{13}C NMR (DMSO-d_6, 75 MHz): δ 45.8 (thiazole CH_2), 120.1, 120.3, 121.0, 121.6, 122.8, 123.3, 123.9, 124.1, 125.2, 125.6 (2×C_6H_4), 140.1, 142.3 (pyridazine C-3, C-4), 166.3 (CO), 168.9, 169.2, 170.0, 170.2 (4×C=N). Anal. Calcd for: $C_{20}H_{12}ClN_5O_2S_2$ (453.92): C, 52.92; H, 2.66; N, 15.43; S, 14.13. Found: C, 52.88; H, 2.80; N, 15.57; S, 14.08%. EIMS: *m/z* 453 $[M]^+$ (58%).

2-(6-(Benzo[*d*]thiazol-2-yl)-5-hydroxy-3-imino-2-(4-methoxyphenyl)-2,3-dihydropyridazin-4-yl)thiazol-4(5*H*)-one (12f)

Yellow crystals from 1,4-dioxane, yield 2.91 g (65%), m.p. 177–179 °C. IR (KBr) ν_{max} (cm^{-1}): 3521–3349 (OH, NH), 3050 (CH-aromatic), 1689 (CO), 1660 (C=N), 1583 (C=C). ^{1}H NMR (DMSO-d_6, 300 MHz): δ 3.70 (s, 3H, OCH_3), 5.64 (s, 2H, thiazole CH_2), 7.26–7.53 (m, 8H, 2×C_6H_4), 8.45 (s, 1H, D_2O exchangeable, NH), 10.38 (s, 1H, D_2O exchangeable, OH). ^{13}C NMR (DMSO-d_6, 75 MHz): δ 45.8 (thiazole CH_2), 50.8 (OCH_3), 120.1, 120.6, 121.3, 121.9, 122.4, 123.1, 123.5, 124.4, 124.8, 125.2 (2×C_6H_4), 140.1, 142.5 (pyridazine C-3, C-4), 166.8 (CO), 168.5, 169.3, 169.6, 170.0 (4×C=N). Anal. Calcd for: $C_{21}H_{15}N_5O_3S_2$ (449.51): C, 56.11; H, 3.36; N, 15.58; S, 14.27. Found: C, 56.31; H, 3.42; N, 15.63; S, 14.48%. EIMS: *m/z* 449 $[M]^+$ (64%).

2-(6-(Benzo[*d*]thiazol-2-yl)-3-imino-5-methyl-2-phenyl-2,3-dihydropyridazin-4-yl)thiazol-4(5*H*)-one (12g)

Yellow crystals from 1,4-dioxane, yield 2.29 g (55%), m.p. 233–235 °C. IR (KBr) ν_{max} (cm^{-1}): 3436–3319 (NH), 3050 (CH-aromatic), 1689 (CO), 1660 (C=N), 1580 (C=C). ^{1}H NMR (DMSO-d_6, 300 MHz): δ 2.83 (s, 3H, CH_3), 5.65 (s, 2H, thiazole CH_2), 7.24–7.43 (m, 9H, C_6H_5, C_6H_4), 8.46 (s, 1H, D_2O exchangeable, NH). ^{13}C NMR (DMSO-d_6, 75 MHz): δ 38.6 (CH_3), 45.6 (thiazole CH_2), 120.0, 120.4, 121.3, 121.6, 122.4, 123.3, 123.8, 124.4, 124.6, 125.5 (C_6H_5, C_6H_4), 140.1, 142.3 (pyridazine C-3, C-4), 166.5 (CO), 168.7, 169.3, 170.1, 170.3 (4×C=N). Anal. Calcd for: $C_{21}H_{15}N_5OS_2$ (417.51): C, 60.41; H, 3.62; N, 16.77; S, 15.36. Found: C, 60.59; H, 3.52; N, 16.80; S, 15.49%. EIMS: *m/z* 417 $[M]^+$ (70%).

2-(6-(Benzo[*d*]thiazol-2-yl)-2-(4-chlorophenyl)-3-imino-5-methyl-2,3-dihydropyridazin-4-yl)thiazol-4(5*H*)-one (12h)

Yellow crystals from 1,4-dioxane, yield 2.84 g (63%), m.p. 193–195 °C. IR (KBr) ν_{max} (cm^{-1}): 3448–3329 (NH), 3050 (CH-aromatic), 1689 (CO), 1660 (C=N), 1580 (C=C). ^{1}H NMR (DMSO-d_6, 300 MHz): δ 2.86 (s, 3H, CH_3), 5.67 (s, 2H, thiazole CH_2), 7.24–7.46 (m, 8H, 2×C_6H_4), 8.43 (s, 1H, D_2O exchangeable, NH). ^{13}C NMR (DMSO-d_6, 75 MHz): δ 38.4 (CH_3), 45.9 (thiazole CH_2), 120.2, 120.5, 121.1, 121.7, 122.2, 122.8, 123.5, 124.4, 124.7, 125.8 (C_6H_5, C_6H_4), 140.2, 142.3 (pyridazine C-3, C-4), 166.8 (CO), 169.1, 169.5, 169.8, 170.2 (4×C=N). Anal. Calcd for: $C_{21}H_{14}ClN_5OS_2$ (451.95): C, 55.81; H, 3.12; N, 15.50; S, 14.19. Found: C, 55.93; H, 3.42; N, 15.68; S, 13.93%. EIMS: *m/z* 451 $[M]^+$ (80%).

2-(6-(Benzo[*d*]thiazol-2-yl)-3-imino-2-(4-methoxyphenyl)-5-methyl-2,3-dihydropyridazin-4-yl)thiazol-4(5*H*)-one (12i)

Pale brown crystals from 1,4-dioxane, yield 2.68 g (62%), m.p. 155–157 °C. IR (KBr) ν_{max} (cm^{-1}): 3369–3346 (NH), 3050 (CH-aromatic), 1688 (CO), 1662 (C=N), 1584 (C=C). ^{1}H NMR (DMSO-d_6, 300 MHz): δ 2.87 (s, 3H, CH_3), 3.68 (s, 3H, OCH_3), 5.66 (s, 2H, thiazole CH_2), 7.25–7.56 (m, 8H, 2×C_6H_4), 8.44 (s, 1H, D_2O exchangeable, NH). ^{13}C NMR (DMSO-d_6, 75 MHz): δ 37.5 (CH_3), 50.3 (OCH_3), 120.5, 120.6, 120.8, 122.1, 122.7, 123.6, 123.8, 124.7, 124.9, 125.4 (2×C_6H_4), 140.1, 142.5 (pyridazine C-3, C-4), 166.6 (CO), 168.6, 169.2, 169.6, 170.1 (4×C=N). Anal. Calcd for: $C_{22}H_{17}N_5O_2S_2$ (447.53): C, 59.04; H, 3.83; N, 15.65; S, 14.33. Found: C, 58.79; H, 3.69; N, 15.52; S, 14.50%. EIMS: *m/z* 447.53 $[M]^+$ (82%).

2. 1. 7. General Method for the Synthesis of the Thiazole Derivatives 13a–i

To a solution of either **10a** (3.44g, 0.01 mol), **10b** (3.78g, 0.01 mol), **10c** (3.74 g, 0.01 mol), **10d** (3.45 g, 0.01 mol), **10e** (3.79 g, 0.01 mol), **10f** (3.75 g, 0.01 mol), **10g** (3.43 g, 0.01 mol), **10h** (3.77 g, 0.01 mol) or **10i** (3.73 g, 0.01 mol) in 1,4-dioxane (40 mL) containing triethylamine (1.0 mL) thioglycolic acid (0.92 g, 0.01 mol) was added. The reaction mixture was heated under reflux for 2 h then was left to cool and the formed solid product was collected by filtration.

2-(5-Amino-6-(benzo[*d*]thiazol-2-yl)-3-oxo-2-phenyl-2,3-dihydropyridazin-4-yl)thiazol-4(5*H*)-one (13a)

Pale brown crystals from acetic acid, yield 2.51 g (60%), m.p. 210–212 °C. IR (KBr) ν_{max} (cm^{-1}): 3352–3341 (NH_2), 3050 (CH-aromatic), 1689, 1703 (2×CO), 1585 (C=C). ^{1}H NMR (DMSO-d_6, 300 MHz): δ 4.93 (s, 2H, D_2O echangeable, NH_2), 5.30 (s, 2H, thiazole CH_2), 7.26–7.48 (m, 9H, C_6H_5, C_6H_4). ^{3}C NMR (DMSO-d_6, 75 MHz): δ 48.5 (thiazole CH_2), 120.1, 120.4, 121.1, 122.7, 122.9, 123.3, 123.9, 124.1, 124.4, 125.8 (C_6H_5, C_6H_4), 140.1, 142.4 (pyridazine C-3, C-4), 165.8, 166.8 (2×CO), 168.5, 169.3, 170.3 (3×C=N). Anal. Calcd for: $C_{20}H_{13}N_5O_2S_2$ (419.48): C, 57.26; H, 3.12; N, 16.70; S, 15.29. Found: C, 57.31; H, 3.29; N, 16.58; S, 15.36%. EIMS: *m/z* 419 $[M]^+$ (60%).

2-(5-Amino-6-(benzo[*d*]thiazol-2-yl)-2-(4-chlorophenyl)-3-oxo-2,3-dihydropyridazin-4-yl)thiazol-4(5*H*)-one (13b)

Yellow crystals from 1,4-dioxane, yield 2.26 g (50%), m.p. 199–201 °C. IR (KBr) ν_{max} (cm^{-1}): 3371–3346 (NH_2), 3054 (CH-aromatic), 1689, 1701 (2×CO), 1585 (C=C). ^{1}H NMR (DMSO-d_6, 300 MHz): δ 4.86 (s, 2H, D_2O echangeable, NH_2), 5.64 (s, 2H, thaizole CH_2), 7.23–7.59 (m, 8H, 2×C_6H_4). ^{13}C NMR (DMSO-d_6, 75 MHz): δ 48.8 (thiazole CH_2), 120.1, 120.4, 121.2, 122.3, 122.9, 123.6, 124.0, 124.3, 125.4, 125.6 (2×C_6H_4), 140.0, 142.3 (pyridazine C-3, C-4), 168.8, 169.3, 170.1 (3 X C=N). Anal. Calcd for: $C_{20}H_{12}ClN_5O_2S_2$ (453.92): C, 52.92; H, 2.66; N, 15.43; S, 14.13. Found: C, 52.86; H, 2.80; N, 15.57; S, 14.26%. EIMS: *m/z* 453 $[M]^+$ (68%).

2-(5-Amino-6-(benzo[*d*]thiazol-2-yl)-2-(4-methoxyphenyl)-3-oxo-2,3-dihydropyridazin-4-yl)thiazol-4(5*H*)-one (13c)

Pale yellow crystals from 1,4-dioxane, yield 3.14 g (70%), m.p. 210–212 °C. IR (KBr) ν_{max} (cm^{-1}): 3359–3331 (NH), 3050 (CH-aromatic), 1689, 1701 (2×CO), 1587 (C=C). ^{1}H NMR (DMSO-d_6, 300 MHz): δ 3.75 (s, 3H, OCH_3), 4.86 (s, 2H, D_2O echangeable, NH_2), 5.28 (s, 2H, thiazole CH_2), 7.25–7.58 (m, 8H, 2×C_6H_4). ^{13}C NMR (DMSO-d_6, 75 MHz): δ 48.3 (thiazole CH_2), 50.7 (OCH_3), 120.1, 120.5, 121.6, 122.4, 122.8, 123.6 123.8, 124.6, 125.3, 125.5 (2×C_6H_4), 140.5, 142.6 (pyridazine C-3, C-4), 166.1, 166.8 (2×CO), 168.6, 169.31, 170.3 (3×C=N). Anal. Calcd for: $C_{21}H_{15}N_5O_3S_2$ (449.51): C, 56.11; H, 3.36; N, 15.58; S, 14.27. Found: C, 56.26; H, 3.27; N, 15.63; S, 14.39%. EIMS: *m/z* 449 $[M]^+$ (66%).

2-(6-(Benzo[*d*]thiazol-2-yl)-5-hydroxy-3-imino-2-phe-

nyl-2,3-dihydropyridazin-4-yl)thiazol-4(5*H*)-one (13d)

Yellow crystals from 1,4-dioxane, yield 2.47 g (59%), m.p. 158–160 °C. IR (KBr) ν_{max} (cm^{-1}): 3546–3328 (OH, NH), 3054 (CH-aromatic), 1689, 1702 (2×CO), 1586 (C=C). ^{1}H NMR (DMSO-d_6, 300 MHz): δ 5.63 (s, 2H, thiazole CH_2), 7.25–7.46 (m, 9H, C_6H_5, C_6H_4), 10.38 (s, 1H, D_2O exchangeable, OH). ^{13}C NMR (DMSO-d_6, 75 MHz): δ 45.8 (thiazole CH_2), 120.1, 120.4, 121.3, 121.7, 122.8, 123.7, 123.8, 124.6, 125.4, 125.7 (C_6H_5, C_6H_4), 140.1, 142.3 (pyridazine C-3, C-4), 166.1, 166.8 (2×CO), 168.9, 170.1, 170.5 (3×C=N). Anal. Calcd for: $C_{20}H_{12}N_4O_3S_2$ (420.46): C, 57.13; H, 2.88; N, 13.32; S, 15.25. Found: C, 57.38; H, 3.04; N, 13.55; S, 15.36%. EIMS: *m/z* 420 $[M]^+$ (68%).

2-(6-(Benzo[*d*]thiazol-2-yl)-2-(4-chlorophenyl)-5-hydroxy-3-oxo-2,3-dihydropyridazin-4-yl)thiazol-4(5*H*)-one (13e)

Yellow crystals from 1,4-dioxane, yield 2.72 g (60%), m.p. 196–198 °C. IR (KBr) ν_{max} (cm^{-1}): 3528–3339 (OH), NH), 3054 (CH-aromatic), 1689, 1701 (2×CO), 1583 (C=C). ^{1}H NMR (DMSO-d_6, 300 MHz): δ 5.66 (s, 2H, thiazole CH_2), 7.23–7.55 (m, 8H, 2×C_6H_4), 10.36 (s, 1H, D_2O exchangeable, OH). ^{13}C NMR (DMSO-d_6, 75 MHz): δ 45.6 (thiazole CH_2), 120.2, 120.6, 121.2, 121.4, 122.3, 123.3, 123.9, 124.4, 125.1, 125.8 (2×C_6H_4), 140.1, 142.4 (pyridazine C-3, C-4), 166.6, 166.9 (2×CO), 168.9, 170.0, 170.2 (3×C=N). Anal. Calcd for: $C_{20}H_{11}ClN_4O_3S_2$ (454.91): C, 52.80; H, 2.44; N, 12.32; S, 14.10. Found: C, 52.98; H, 2.63; N, 12.57; S, 14.25%. EIMS: *m/z* 454 $[M]^+$ (65%).

2-(6-(Benzo[*d*]thiazol-2-yl)-5-hydroxy-2-(4-methoxyphenyl)-3-oxo-2,3-dihydropyridazin-4-yl)thiazol-4(5*H*)-one (13f)

Yellow crystals from 1,4-dioxane, yield 2.83 g (63%), m.p. 210–212 °C. IR (KBr) ν_{max} (cm^{-1}): 3363-3347 (OH), 3053 (CH-aromatic), 1688, 1702 (2×CO), 1585 (C=C). ^{1}H NMR (DMSO-d_6, 300 MHz): δ 3.72 (s, 3H, OCH_3), 5.65 (s, 2H, thiaazole CH_2), 7.23–7.58 (m, 8H, 2×C_6H_4), 10.22 (s, 1H, D_2Oexchangeable, OH). ^{13}C NMR (DMSO-d_6, 75 MHz): δ 45.8 (thaizole CH_2), 50.3 (OCH_3), 120.4, 120.6, 121.5, 122.5, 122.6, 123.2, 123.6, 124.7, 125.2, 125.8 (2×C_6H_4), 140.1, 142.3 (pyridazine C-3, C-4), 165.8, 166.3 (2×CO), 168.8, 170.1, 170.5 (3×C=N). Anal. Calcd for: $C_{21}H_{14}N_4O_4S_2$ (450.49): C, 55.99; H, 3.13; N, 12.44; S, 14.24. Found: C, 56.15; H, 3.29; N, 12.60; S, 14.40%. EIMS: *m/z* 450 $[M]^+$ (68%).

2-(6-(Benzo[*d*]thiazol-2-yl)-5-methyl-3-oxo-2-phenyl-2,3-dihydropyridazin-4-yl)thiazol-4(5*H*)-one (13g)

Yellow crystals from 1,4-dioxane, yield 2.59 g (62%), m.p. 244–246 °C. IR (KBr) ν_{max} (cm^{-1}): 3050 (CH-aromatic), 1689, 1700 (2×CO), 1580 (C=C). ^{1}H NMR (DMSO-d_6, 300 MHz): δ 2.86 (s, 3H, CH_3), 5.63 (s, 2H, thiazole CH_2), 7.28–7.45 (m, 9H, C_6H_5, C_6H_4). ^{13}C NMR (DMSO-d_6, 75 MHz): δ 38.8 (CH_3), 45.4 (thiazole CH_2), 120.2, 120.7, 121.1, 121.5, 122.2, 123.6, 123.8, 124.2, 124.3, 125.8 (C_6H_5, C_6H_4), 140.1, 142.3 (pyridazine C-3, C-4), 166.8, 167.3 (2×CO), 168.5, 169.3, 170.0 (3×C=N). Anal. Calcd for: $C_{21}H_{14}N_4O_2S_2$ (418.49): C, 60.27; H, 3.37; N, 13.39; S, 15.32. Found: C, 60.41; H, 3.47; N, 13.17; S, 15.50%. EIMS: *m/z* 418 $[M]^+$ (75%).

2-(6-(Benzo[*d*]thiazol-2-yl)-2-(4-chlorophenyl)-5-methyl-3-oxo-2,3-dihydropyridazin-4-yl)thiazol-4(5*H*)-one (13h)

Yellow crystals from 1,4-dioxane, yield 2.48 g (55%), m.p. 230–232 °C. IR (KBr) ν_{max} (cm^{-1}): 3055 (CH-aromatic), 1689, 1703 (2×CO), 1580 (C=C). ^{1}H NMR (DMSO-d_6, 300 MHz): δ 2.88 (s, 3H, CH_3), 5.62 (s, 2H, thiazole CH_2), 7.24–7.59 (m, 8H, 2×C_6H_4). ^{13}C NMR (DMSO-d_6, 75 MHz): δ 38.5 (CH_3), 45.6 (thiazole CH_2), 120.1, 120.4, 121.1, 121.8, 122.0, 123.4, 123.9, 124.2, 124.6, 125.5 (2×C_6H_4), 140.3, 142.3 (pyridazine C-3, C-4), 166.5, 167.6 (2×CO), 168.7, 169.3, 170.2 (3×C=N). Anal. Calcd for: $C_{21}H_{13}ClN_4O_2S_2$ (452.94): C, 55.69; H, 2.89; N, 12.37; S, 14.16. Found: C, 55.72; H, 3.07; N, 12.44; S, 13.96%. EIMS: *m/z* 452 $[M]^+$ (78%).

2-(6-(Benzo[*d*]thiazol-2-yl)-2-(4-methoxyphenyl)-5-methyl-3-oxo-2,3-dihydropyridazin-4-yl)thiazol-4(5*H*)-one (13i)

Yellow crystals from 1,4-dioxane, yield 3.00 g (68%), m.p. 199–202 °C. IR (KBr) ν_{max} (cm^{-1}): 3453–3360 (NH), 3055 (CH-aromatic), 1688, 1703 (2×CO), 1580 (C=C). ^{1}H NMR (DMSO-d_6, 300 MHz): δ 2.89 (s, 3H, CH_3), 3.77 (s, 3H, OCH_3), 5.65 (s, 2H, thiazole CH_2), 7.25–7.56 (m, 8H, 2×C_6H_4). ^{13}C NMR (DMSO-d_6, 75 MHz): δ 38.5 (CH_3), 50.6 (OCH_3), 45.8 (thiazole CH_2), 120.3, 120.6, 121.4, 121.5, 122.0, 123.2, 123.4, 124.0, 124.6, 125.3 (2×C_6H_4), 140.2, 142.3 (pyridazine C-3, C-4), 166.7, 167.5 (2×CO), 168.7, 169.2, 170.2 (3×C=N). Anal. Calcd for: $C_{22}H_{16}N_4O_3S_2$ (448.52): C, 58.91; H, 3.60; N, 12.49; S, 14.30. Found: C, 59.15; H, 3.58; N, 12.37; S, 14.42%. EIMS: *m/z* 448 $[M]^+$ (80%).

2. 1. 8. General Procedure for the Synthesis of the Thiazole Derivatives 15a–c

To a solution of either **4a** (1.74 g, 0.01 mol), **4b** (2.21 g, 0.01 mol) or **4c** (1.91 g, 0.01 mol) in 1,4-dioxane (60 mL) containing triethylamine (1.0 mL) elemental sulfur (0.32 g, 0.01 mol) and phenylisothiocyanate (1.30 g, 0.01 mol) were added. The whole reaction mixture was heated under the reflux conditions for 1 h then was left to cool to room temperature and the obtained solid product was collected by filtration.

4-Amino-5-(benzo[*d*]thiazol-2-yl)-3-phenylthiazole-2(3*H*)-thione (15a)

Orange crystals from 1,4-dioxane, yield 1.97 g (58%), m.p. 202–204 °C. IR (KBr) ν_{max} (cm^{-1}): 3463, 3342 (NH_2), 3055 (CH-aromatic), 1580 (C=C), 1210 (C=S).

^{1}H NMR (DMSO-d_6, 300 MHz): δ 4.93 (s, 2H, D_2O exchangeable, NH_2), 7.27–7.43 (m, 9H, C_6H_5, C_6H_4). ^{13}C NMR (DMSO-d_6, 75 MHz): δ 120.1, 120.4, 121.0, 121.8, 122.0, 123.6, 123.8, 124.0, 124.2, 125.0 (C_6H_5, C_6H_4), 143.2, 144.5 (thiazole C), 168.8 (C=N), 179.8 (C=S). Anal. Calcd for: $C_{16}H_{11}N_3S_3$ (341.46): C, 56.28; H, 3.25; N, 12.31; S, 28.17. Found: C, 56.06; H, 3.35; N, 12.42; S, 28.25%. EIMS: *m/z* 341 $[M]^+$ (70%).

5-(Benzo[*d*]thiazol-2-yl)-4-hydroxy-3-phenylthiazole-2(3*H*)-thione (15b)

Orange crystals from 1,4-dioxane, yield 2.12 g (62%), m.p. 177–179 °C. IR (KBr) ν_{max} (cm^{-1}): 3571–3339 (OH), 3055 (CH-aromatic), 1583 (C=C), 1210 (C=S). ^{1}H NMR (DMSO-d_6, 300 MHz): δ 7.27–7.43 (m, 9H, C_6H_5, C_6H_4), (s, 1H, D_2O exchangeable, OH). ^{13}C NMR (DMSO-d_6, 75 MHz): δ 120.3, 120.6, 121.3, 121.5, 122.3, 122.7, 123.8, 124.0, 124.6, 125.3 (C_6H_5, C_6H_4), 143.4, 144.5 (thiazole C), 168.9 (C=N), 179.6 (C=S). Anal. Calcd for: $C_{16}H_{10}N_2OS_3$ (342.46): C, 56.12; H, 2.94; N, 8.18; S, 28.09. Found: C, 56.31,+; H, 3.16; N, 8.25; S, 28.18%. EIMS: *m/z* 342 $[M]^+$ (68%).

5-(Benzo[*d*]thiazol-2-yl)-4-methyl-3-phenylthiazole-2(3*H*)-thione (15c)

Orange crystals from 1,4-dioxane, yield 1.70 g (50%), m.p. 211–213 °C. IR (KBr) ν_{max} (cm^{-1}): 3055 (CH-aromatic), 1586 (C=C), 1213 (C=S). ^{1}H NMR (DMSO-d_6, 300 MHz): δ 2.78 (s, 3H, CH_3), 7.25–7.48 (m, 9H, C_6H_5, C_6H_4). ^{13}C NMR (DMSO-d_6, 75 MHz): δ 38.4 (CH_3), 120.4, 120.8, 121.2, 121.7, 122.5, 122.6, 123.8, 124.3, 124.8, 125.6 (C_6H_5, C_6H_4), 143.2, 144.1 (thiazole C), 168.6 (C=N), 179.9 (C=S). Anal. Calcd for: $C_{17}H_{12}N_2S_3$ (340.49): C, 59.97; H, 3.55; N, 8.23; S, 28.25. Found: C, 59.83; H, 3.46; N, 8.42; S, 28.30%. EIMS: *m/z* 340 $[M]^+$ (80%).

***N*-(5-(Benzo[*d*]thiazol-2-yl)-3-phenyl-2-thioxo-2,3-dihydrothiazol-4-yl)-2-cyanoacetamide (16)**

To a solution of compound **15a** (3.41 g, 0.01 mol) in dimethylformamide, ethyl cyanoacetate (1.07 g, 0.01 mol) was added. The reaction mixture was heated under the reflux conditions for 1 h then poured onto ice/water and the produced solid product was collected by filtration.

Orange crystals from 1,4-dioxane, yield 2.44 g (60%), m.p. 265–267 °C. IR (KBr) ν_{max} (cm^{-1}): 3055 (CH-aromatic), 2220 (CN), 1688 (CO), 1586 (C=C), 1211 (C=S). ^{1}H NMR (DMSO-d_6, 300 MHz): δ 5.32 (s, 2H, CH_2), 7.27–7.45 (m, 9H, C_6H_5, C_6H_4), 8.28 (s, 1H, D_2O exchangeable, NH). ^{13}C NMR (DMSO-d_6, 75 MHz): δ 48.9 (CH_2), 117.3 (CN), 120.2, 120.6, 121.5, 121.9, 122.2, 122.8, 123.3, 123.6, 124.5, 125.3 (C_6H_5, C_6H_4), 143.3, 144.4 (thiazole C), 166.7 (CO), 168.8 (C=N), 180.2 (C=S). Anal. Calcd for: $C_{19}H_{12}N_4OS_3$ (408.52): C, 55.86; H, 2.96; N, 13.71; S, 23.55. Found: C, 55.74; H, 3.26; N, 13.89; S, 23.72%. EIMS: *m/z* 408 $[M]^+$ (75%).

2. 1. 9. General Procedure for the Synthesis of the Thiophene Derivatives 17a,b

To a solution of **16** (4.08 g, 0.01 mol) in absolute ethanol (40 mL) containing triethylamine (1.0 mL) elemental sulfur and either malononitrile (0.66 g, 0.01 mol) or ethyl cyanoacetate (1.07 g, 0.01 mol) were added. The reaction mixture was heated under the reflux conditions for 2 h then was poured onto ice/water containing a few drops of hydrochloric acid and the produced solid product was collected by filtration.

3,5-Diamino-*N*-(5-(benzo[*d*]thiazol-2-yl)-3-phenyl-2-thioxo-2,3-dihydro-thiazol-4-yl)-4-cyanothiophene-2-carboxamide (17a)

Yellow crystals from 1,4-dioxane, yield 3.03 g (60%), m.p. 177–179 °C. IR (KBr) ν_{max} (cm^{-1}): 3480–3372 (NH_2), 3055 (CH-aromatic), 2220 (CN), 1689 (CO), 1586 (C=C), 1215 (C=S). ^{1}H NMR (DMSO-d_6, 300 MHz): δ 5.21, 5.60 (2×s, 4H, D_2O exchangeable, 2×NH_2), 7.27–7.50 (m, 9H, C_6H_5, C_6H_4), 8.20 (s, 1H, D_2O exchangeable, NH). ^{13}C NMR (DMSO-d_6, 75 MHz): δ 117.0 (CN), 120.2, 120.8, 121.2, 121.4, 122.8, 122.9, 123.5, 124.7, 125.2, 125.4 (C_6H_5, C_6H_4), 139.5, 140.3, 141.5, 143.1, 144.3, 146.5 (thiazole, thiophene C), 166.2 (CO), 168.4 (C=N), 180.3 (C=S). Anal. Calcd for: $C_{22}H_{14}N_6OS_4$ (506.65): C, 52.15; H, 2.79; N, 16.59; S, 25.32. Found: C, 52.37; H, 2.83; N, 16.70; S, 25.49%. EIMS: *m/z* 506 $[M]^+$ (64%).

Ethyl 2,4-Diamino-5-((5-(benzo[*d*]thiazol-2-yl)-3-phenyl-2-thioxo-2,3-dihydrothiazol-4-yl)carbamoyl)thiophene-3-carboxylate (17b)

Yellow crystals from 1,4-dioxane, yield 3.04 g (55%), m.p. 148–150 °C. IR (KBr) ν_{max} (cm^{-1}): 3469–3328 (NH_2), 3055 (CH-aromatic), 2220 (CN), 1688, 1889 (2×CO), 1584 (C=C), 1215 (C=S). ^{1}H NMR (DMSO-d_6, 300 MHz): δ 1.16 (t, 3H, *J* = 7.21 Hz, $OCH_2\underline{CH_3}$), 4.24 (q, 2H, *J* = 7.21 Hz, $O\underline{CH_2}CH_3$), 5.25, 5.39 (2×s, 4H, D_2O exchangeable, 2×NH_2), 7.24–7.53 (m, 9H, C_6H_5, C_6H_4), 8.24 (s, 1H, D_2O exchangeable, NH). ^{13}C NMR (DMSO-d_6, 75 MHz): δ 16.2 ($OCH_2\underline{CH_3}$), 50.6 ($O\underline{CH_2}CH_3$), 117.0 (CN), 120.3, 120.7, 121.0, 121.3, 122.5, 122.8, 123.5, 124.7, 125.1, 125.6 (C_6H_5, C_6H_4), 139.6, 140.1, 141.6, 143.1, 144.2, 146.8 (thiazole, thiophene C), 166.3, 166.7 (2×CO), 168.6 (C=N), 180.1 (C=S). Anal. Calcd for: $C_{24}H_{19}N_5O_3S_4$ (553.70): C, 52.06; H, 3.46; N, 12.65; S, 23.16. Found: C, 52.27; H, 3.59; N, 12.80; S, 23.27%. EIMS: *m/z* 553 $[M]^+$ (80%).

2. 1. 10. 1-(5-(Benzo[*d*]thiazol-2-yl)-3-phenyl-2-thioxo-2,3-dihydrothiazol-4-yl)-3-phenylthiourea (18)

To a solution of **15a** (3.41 g, 0.01 mol) in 1,4-dioxane (40 mL) containing triethylamine (1.0 mL) phenylisothiocyanate (1.30 g, 0.01 mol) was added. The reaction mixture was heated under the reflux conditions for 1 h then poured onto ice/water and the produced solid product was collected by filtration.

Yellow crystals from 1,4-dioxane, yield 2.38 g (50%), m.p. 188–190 °C. IR (KBr) ν_{max} (cm^{-1}): 3480-3341 (NH), 3055 (CH-aromatic), 1584 (C=C), 1211 (C=S). ^{1}H NMR (DMSO-d_6, 300 MHz): δ 7.26–7.57 (m, 14H, 2×C_6H_5, C_6H_4), 8.28, 8.32 (2×s, 2H, D_2O exchangeable, 2×NH). ^{13}C NMR (DMSO-d_6, 75 MHz): δ 120.1, 120.7, 120.9, 121.0, 121.1, 122.3, 122.8, 123.8, 124.6, 124.7, 125.0, 125.1, 125.4, 125.8 (2×C_6H_5, C_6H_4), 140.1, 143.1, 144.2, 146.8 (thiazole C), 168.6 (C=N), 180.1, 182.3 (2×C=S). Anal. Calcd for: $C_{23}H_{16}N_4S_4$ (476.66): C, 57.95; H, 3.38; N, 11.75; S, 26.91. Found: C, 58.13; H, 3.46; N, 11.83; S, 27.27%. EIMS: *m/z* 476 $[M]^+$ (72%).

2. 1. 11. General Procedure for the Synthesis of the 2*H*-[3,4'-Bithiazole]-2'(3'*H*)-thione Derivatives 20a–c

Either of ethyl chloroacetate (1.22 g, 0.01 mol), α-bromoacetone (1.36, 0.01 mol) or ω-bromoacetophenone (2.0 g, 0.01 mol) was added to a solution of compound **18** (4.76 g, 0.01 mol) in absolute ethanol (60 mL). The reaction mixture was heated under the reflux conditions for 2 h then was left to cool and the produced solid product was collected by filtration.

5'-(Benzo[*d*]thiazol-2-yl)-4-hydroxy-3'-phenyl-2-(phenylimino)-2*H*-[3,4'-bithiazole]-2'(3'*H*)-thione (20a)

Yellow crystals from 1,4-dioxane, yield 3.14 g (61%), m.p. 222–225 °C. IR (KBr) ν_{max} (cm^{-1}): 3572–3352 (OH), 3055 (CH-aromatic), 1584 (C=C), 1209 (C=S). ^{1}H NMR (DMSO-d_6, 300 MHz): δ 6.25 (s, 1H, thiazole H-5), 7.26–7.52 (m, 14H, 2×C_6H_5, C_6H_4), 10.24 (s, 1H, D_2O exchangeable, OH). ^{13}C NMR (DMSO-d_6, 75 MHz): δ 120.3, 120.6, 121.1, 121.3, 121.6, 122.3, 122.9, 123.5, 124.4, 124.9, 125.0, 125.3, 125.7, 125.8 (2×C_6H_5, C_6H_4), 142.3, 143.0, 144.1, 146.6 (two thiazole C), 168.8, 172.1 (2×C=N), 180.1 (C=S). Anal. Calcd for: $C_{25}H_{16}N_4OS_4$ (516.68): C, 58.11; H, 3.12; N, 10.84; S, 24.82. Found: C, 58.25; H, 3.31; N, 10.62; S, 24.75%. EIMS: *m/z* 516 $[M]^+$ (70%).

5'-(Benzo[*d*]thiazol-2-yl)-4-methyl-3'-phenyl-2-(phenylimino)-2*H*-[3,4'-bithiazole]-2'(3'*H*)-thione (20b)

Yellow crystals from 1,4-dioxane, yield 3.28 g (64%), m.p. 158–160 °C. IR (KBr) ν_{max} (cm^{-1}): 3055 (CH-aromatic), 1582 (C=C), 1210 (C=S). ^{1}H NMR (DMSO-d_6, 300 MHz): δ 2.83 (s, 3H, CH_3), 6.28 (s, 1H, thiazole H-5), 7.24–7.50 (m, 14H, 2×C_6H_5, C_6H_4). ^{13}C NMR (DMSO-d_6, 75 MHz): δ 36.8 (CH_3), 120.1, 120.4, 121.1, 121.8, 121.9, 122.3, 122.9, 123.3, 124.4, 124.8, 125.0, 125.1, 125.3, 126.5 (2×C_6H_5, C_6H_4), 143.3, 143.6, 144.1, 146.6 (two thiazole C), 168.7, 169.1 (2 X C=N), 180.3 (C=S). Anal. Calcd for: $C_{26}H_{18}N_4S_4$ (514.71): C, 60.67; H, 3.52; N, 10.89; S, 24.92. Found: C, 60.80; H, 3.48; N, 10.66; S, 25.85%. EIMS: *m/z* 514 $[M]^+$ (60%).

5'-(Benzo[*d*]thiazol-2-yl)-3',4-diphenyl-2-(phenylimino)-2*H*-[3,4'-bithiazole]-2'(3'*H*)-thione (20c)

Yellow crystals from 1,4-dioxane, yield 3.74 g (65%), m.p. 177–179 °C. IR (KBr) ν_{max} (cm^{-1}): 3055 (CH-aromatic), 1580 (C=C), 1213 (C=S). ^{1}H NMR (DMSO-d_6, 300 MHz): δ 6.27 (s, 1H, thiazole H-5), 7.22–7.54 (m, 19H, 3×C_6H_5, C_6H_4). ^{13}C NMR (DMSO-d_6, 75 MHz): δ 119.3, 119.6, 120.1, 120.4, 120.4, 120.7, 121.0, 121.6, 121.7, 122.3, 122.6, 123.3, 124.5, 124.9, 125.2, 125.4, 125.5, 126.2 (3C_6H_5, C_6H_4), 143.3, 143.8, 144.5, 146.9 (two thiazole C), 168.6 (C=N), 180.3 (C=S). Anal. Calcd for: $C_{31}H_{20}N_4S_4$ (576.78): C, 64.55; H, 3.50; N, 9.71; S, 22.24. Found: C, 64.49; H, 3.36; N, 9.83; S, 22.40%. EIMS: *m/z* 576 $[M]^+$ (65%).

2. 1. 12. General Procedure for the Synthesis of the Azo Derivatives 21a–c

To a cold solution (0–5 °C) of **20a** (5.16 g, 0.01 mol) in ethanol (60 mL) containing sodium acetate (3.0 g) either of benzenediazonium chloride (0.01 mol), 4-chlorobenzenediazonium chloride or 4-methoxybenzenediazonium chloride [prepared by the addition of sodium nitrite solution (0.70 g, 0.01 mol) to a cold solution of either aniline (0.93 g, 0.01 mol), 4-chloroaniline (1.27 g, 0.01 mol) or 4-methoxyaniline (1.23 g, 0.01 mol) in concentrated hydrochloric acid (8.0 mL, 18%) with continuous stirring] was added with continuous stirring. The solid product formed upon stirring for 1 h was collected by filtration.

5'-(Benzo[*d*]thiazol-2-yl)-4-hydroxy-3'-phenyl-5-((*Z*)-phenyldiazenyl)-2-(phenylimino)-2*H*-[3,4'-bithiazole]-2'(3'*H*)-thione (21a)

Yellow crystals from 1,4-dioxane, yield 3.72 g (60%), m.p. 166–168 °C. IR (KBr) ν_{max} (cm^{-1}): 3561–3339 (OH), 3055 (CH-aromatic), 1584 (C=C), 1212 (C=S). ^{1}H NMR (DMSO-d_6, 300 MHz): δ 7.23–7.54 (m, 19H, 3×C_6H_5, C_6H_4), 10.29 (s, 1H, D_2O exchangeable, OH). ^{13}C NMR (DMSO-d_6, 75 MHz): δ 120.3, 120.7, 121.0, 121.2, 121.3, 121.6, 122.3, 122.5, 122.9, 123.5, 123.7, 123.9, 124.4, 124.6, 125.2, 125.3, 125.7, 125.8 (3×C_6H_5, C_6H_4), 142.3, 143.0, 144.4, 146.9 (thiazole C), 168.6, 170.3 (2×C=N), 180.1 (C=S). Anal. Calcd for: $C_{31}H_{20}N_6OS_4$ (620.79): C, 59.98; H, 3.25; N, 13.54; S, 20.66. Found: C, 59.72; H, 3.41; N, 13.39; S, 20.59%. EIMS: *m/z* 620 $[M]^+$ (65%).

5'-(Benzo[*d*]thiazol-2-yl)-5-((*Z*)-(4-chlorophenyl)diazenyl)-4-hydroxy-3'-phenyl-2-(phenylimino)-2*H*-[3,4'-bithiazole]-2'(3'*H*)-thione (21b)

Yellow crystals from 1,4-dioxane, yield 3.14 g (48%), m.p. 155–157 °C. IR (KBr) ν_{max} (cm^{-1}): 3532–3341 (OH), 3055 (CH-aromatic), 1582 (C=C), 1218 (C=S). ^{1}H NMR (DMSO-d_6, 300 MHz): δ 7.25–7.57 (m, 18H, 2×C_6H_5, 2×C_6H_4), 10.27 (s, 1H, D_2O exchangeable, OH). ^{13}C NMR (DMSO-d_6, 75 MHz): δ 120.1, 120.5, 120.8, 121.2, 121.6, 121.8, 122.1, 122.7, 123.0, 123.5, 123.5, 123.9, 124.4, 124.8, 125.1, 125.2, 125.6, 125.9 (2×C_6H_5, 2×C_6H_4), 142.1, 143.5, 144.4, 146.7 (thiazole C), 168.7, 170.2 (2×C=N), 180.3

(C=S). Anal. Calcd for: $C_{31}H_{19}ClN_6OS_4$ (655.24): C, 56.82; H, 2.92; N, 12.83; S, 19.57. Found: C, 56.72; H, 2.83; N, 12.79; S, 19.42%. EIMS: *m/z* 655 $[M]^+$ (68%).

5'-(Benzo[*d*]thiazol-2-yl)-4-hydroxy-5-((*Z*)-(4-methoxyphenyl)diazenyl)-3'-phenyl-2-(phenylimino)-2*H*-[3,4'-bithiazole]-2'(3'*H*)-thione (21c)

Yellow crystals from 1,4-dioxane, yield 3.90 g (60%), m.p. 132–136 °C. IR (KBr) ν_{max} (cm^{-1}): 3548–3327 (OH), 3055 (CH-aromatic), 1582 (C=C), 1212 (C=S). ^{1}H NMR (DMSO-d_6, 300 MHz): δ 3.77 (s, 3H, OCH_3), 7.28–7.59 (m, 18H, 2×C_6H_5, 2×C_6H_4), 10.29 (s, 1H, D_2O exchangeable, OH). ^{13}C NMR (DMSO-d_6, 75 MHz): δ 50.4 (OCH_3), 120.2, 120.3, 120.5, 121.0, 121.4, 121.7, 122.1, 122.4, 123.2, 123.5, 123.6, 123.8, 124.1, 124.4, 125.0, 125.1, 125.6, 125.7 (2×C_6H_5, 2×C_6H_4), 142.3, 143.7, 144.2, 146.5 (thiazole C), 168.3, 170.3 (2×C=N), 180.1 (C=S). Anal. Calcd for: $C_{32}H_{22}N_6O_2S_4$ (650.82): C, 59.06; H, 3.41; N, 12.91; S, 19.71. Found: C, 58.92; H, 3.29; N, 12.82; S, 19.50%. EIMS: *m/z* 650 $[M]^+$ (58%).

3. Results and Discussion

3. 1. Chemistry

The reaction sequences for the synthesized compounds are depicted in Schemes 1–4 starting with the benzo[*d*]thiazole derivatives **4a**–**c**. The latter compounds were obtained through the reaction of *ortho*-aminothiophenol (**1**) with ethyl cyanoacetate (**2a**), diethylmalonate (**2b**) or ethyl 3-oxobutanoate (**2c**) in an oil bath at 120 °C. The structures of compounds **4a**–**c** were based on the obtained analytical and spectral data (see Experimental section). Compounds **4a**–**c** were used to produce thiophene derivatives through their reactions with elemental sulfur and either malononitrile (**5**) or ethyl cyanoacetate (**2a**) in ethanolic solution containing triethylamine to afford the thiophene derivatives **6a**–**f**, respectively (Scheme 1). Their structures were confirmed on the basis of their spectral data. Thus, the ^{1}H NMR spectrum showed two singlets at δ 3.84 and 4.26 ppm (D_2O exchangeable) indicating the two NH_2 groups and a multiplet at δ 7.27–7.42 ppm corresponding to the phenyl group. Moreover, the ^{13}C NMR spectrum which revealed the presence of a signal at δ 116.7 indicating the presence of the CN group, six signals at δ 121.5, 122.9, 123.5, 123.6, 123.8, and 124.8 corresponding to the C_6H_4 group, four signals at δ 138.3, 138.9, 140.2, 142.6 due to the thiophene moiety, and a signal at δ 168.6 for the C=N moiety.

Compounds **4a**–**c** were appropriate for arylhydrazone production *via* their reactions with aryldiazonium salts. Thus, the reaction of **4a**–**c** with either of the diazonium salts namely benzenediazonium chloride (**7a**), 4-chlorobenzenediazonium chloride (**7b**) or 4-methoxybenzenediazonium chloride (**7c**) gave the arylhydrazono derivatives **8a**–**i**, respectively. The latter compounds reacted with malononitrile in 1,4-dioxane solution containing triethylamine to give the pyridazin-2-imino derivatives **9a**–**i**, respectively (Scheme 2); the reaction took place according to the previously reported work.[27–30]

Similarly, the reaction of **8a**–**i** with ethyl cyanoacetate under the same reaction conditions gave the pyridazin-2-oxo derivatives **10a**–**i**, respectively. Interestingly, all of the pyridazin-2-imino derivatives **9a**–**i** were also converted to the pyridazin-2-oxo derivatives upon heating under the reflux conditions in ethanol containing sodium hydroxide (2.0 g, dissolved in 10 mL water) (confirmed by m.p. and mixed m.p.). All of compounds **9a**–**i** and **10a**–**i** with the α-oxocyano moiety reacted with thioglycolic acid affording the thiazole derivatives **12a**–**i** and **13a**–**i**, respectively (Schemes 3 and 4).

Compounds **4a**–**c** reacted with elemental sulfur and phenylisothiocynate (**14**) in 1,4-dioxane solution containing triethylamine to give the thiazole derivatives **15a**–**c**, respectively. Structures of the latter products were established on the basis of their respective analytical and spectral data. Thus, the ^{1}H NMR spectrum of **15a** showed the presence of a singlet at δ 4.93 ppm (D_2O exchangeable) corresponding to the NH_2 group and a multiplet at δ 7.27–7.43 indicating the two phenyl groups. In addition the ^{13}C NMR which revealed the presence of ten signals at δ 120.1, 120.4, 121.0, 121.8, 122.0, 123.6, 123.8, 124.0, 124.2, 125.0 for the C_6H_5 and C_6H_4 groups, two signals at δ 143.2, 144.5 for the thiazole C-4, C-5, a signal at δ 168.8 due to the C=N moiety and a signal at δ 179.8 due to the C=S group. Compound **15a** underwent acylation reaction through its reaction with ethyl cyanoacetate in dimethylformamide solution to give the *N*-cyanoacetamido derivative **16** (Scheme 4).

Compound **16** reacted with either malononitrile (**5**) or ethyl cyanoacetate (**2a**) and elemental sulfur in ethanol containing triethylamine to produce the thiophene derivatives **17a** and **17b**, respectively. Moreover, the reaction of **15a** with phenylisothiocyanate (**14**) gave the thiourea derivative **18**. Compound **18** reacted with the α-halocarbonyl derivatives namely ethyl chloroacetate (**19a**), α-bromoacetone (**19b**) or ω-bromoacetophenone (**19c**) in absolute ethanol solution under the reflux conditions affording the thiazole derivatives **20a**–**c**, respectively. Compound **20a** was found to be an active compound toward azo formation. Thus, its reaction with benzenediazonium chloride (**7a**), 4-chlorobenzenediazonium chloride (**7b**) or 4-methoxybenzenediazonium chloride (**7c**) produced the arylazo derivatives **21a**–**c**, respectively (Scheme 5).

3. 2. Biology

3. 2. 1. Cell Proliferation Assay

The anti-proliferative activities of the newly synthesized compounds (Table 1) were evaluated against the six cancer cell lines A549, HT-29, MKN-45, U87MG, SMMC-7721, and H460 using the standard MTT assay *in vitro*,

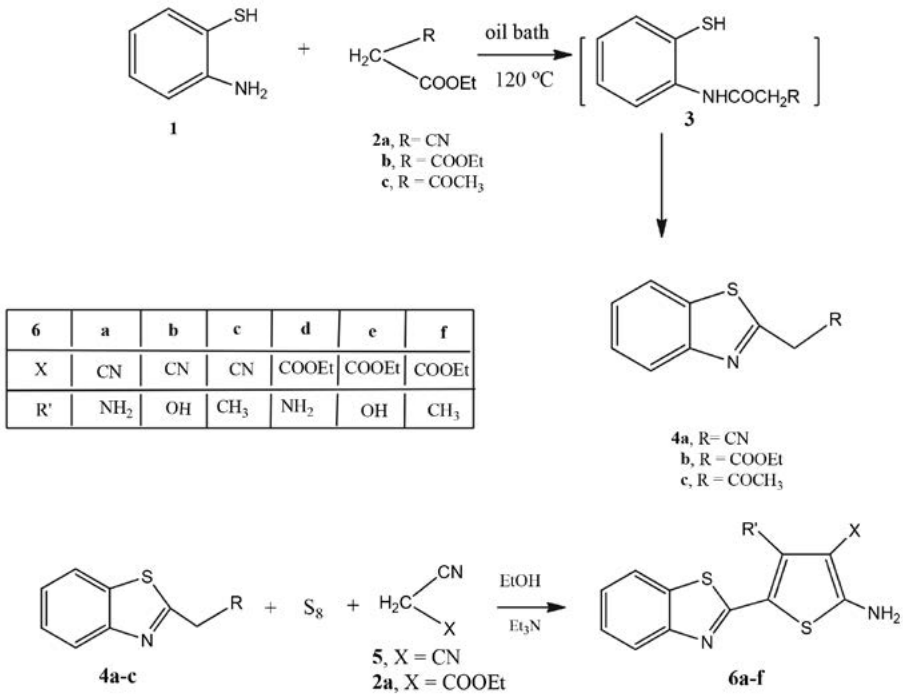

6	a	b	c	d	e	f
X	CN	CN	CN	COOEt	COOEt	COOEt
R'	NH_2	OH	CH_3	NH_2	OH	CH_3

Scheme 1. Synthesis of compounds **4a–c** and **6a–f**.

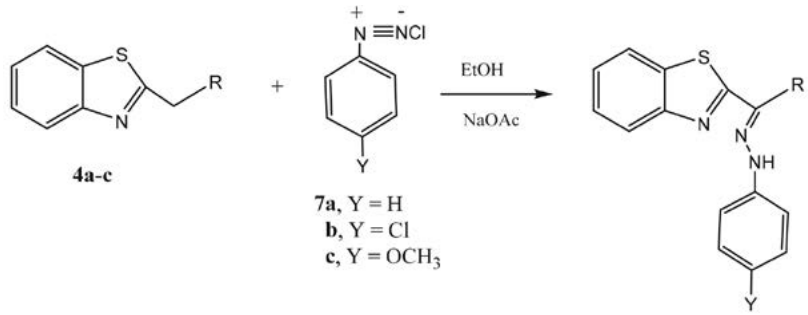

8	a	b	c	d	e	f	g	h	i
R	CN	CN	CN	COOEt	COOEt	COOEt	$COCH_3$	$COCH_3$	$COCH_3$
Y	H	Cl	OCH_3	H	Cl	OCH_3	H	Cl	OCH_3

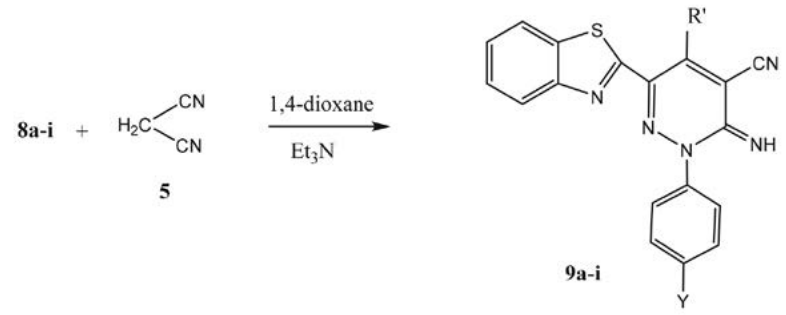

9	a	b	c	d	e	f	g	h	i
R'	NH_2	NH_2	NH_2	OH	OH	OH	CH_3	CH_3	CH_3
Y	H	Cl	OCH_3	H	Cl	OCH_3	H	Cl	OCH_3

Scheme 2. Synthesis of compounds **8a–i** and **9a–i**.

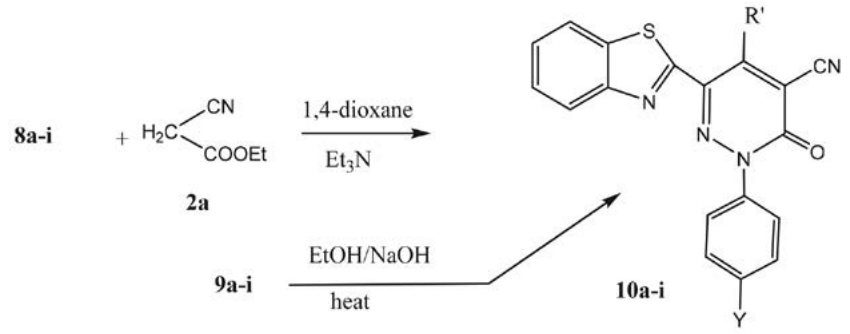

10	a	b	c	d	e	f	g	h	i
R	NH_2	NH_2	NH_2	OH	OH	OH	CH_3	CH_3	CH_3
Y	H	Cl	OCH_3	H	Cl	OCH_3	H	Cl	OCH_3

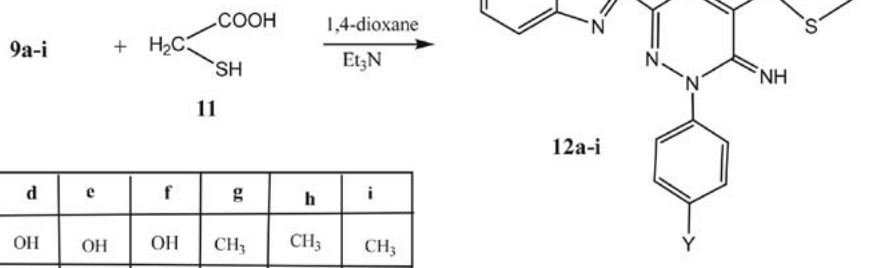

12	a	b	c	d	e	f	g	h	i
R	NH_2	NH_2	NH_2	OH	OH	OH	CH_3	CH_3	CH_3
Y	H	Cl	OCH_3	H	Cl	OCH_3	H	Cl	OCH_3

Scheme 3. Synthesis of compounds **10a–i** and **12a–i**.

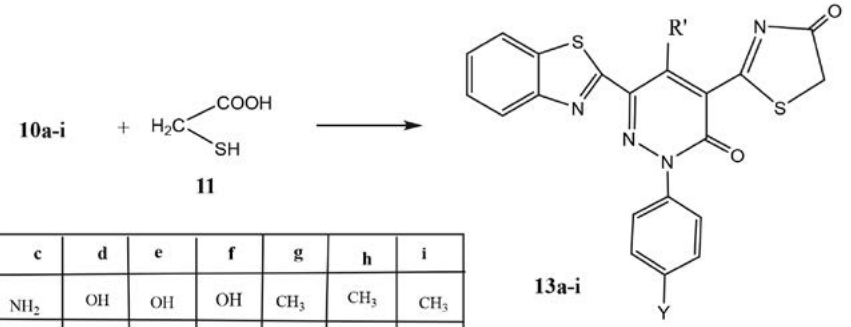

13	a	b	c	d	e	f	g	h	i
R'	NH_2	NH_2	NH_2	OH	OH	OH	CH_3	CH_3	CH_3
Y	H	Cl	OCH_3	H	Cl	OCH_3	H	Cl	OCH_3

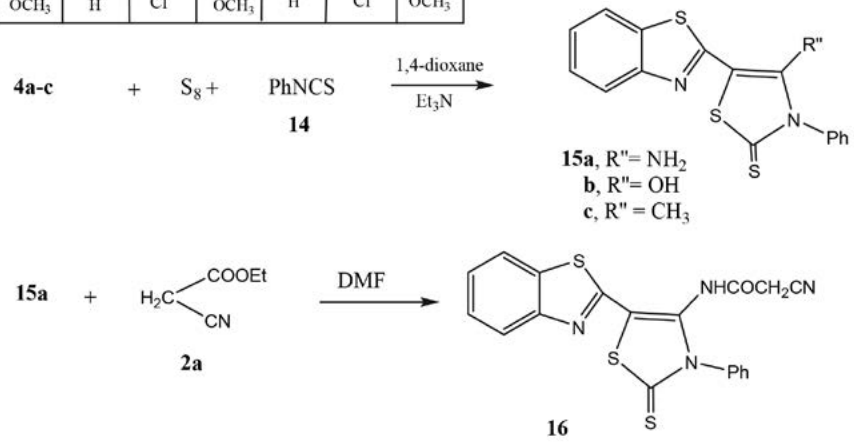

Scheme 4. Synthesis of compounds **13a–i**, **15a–c** and **16**.

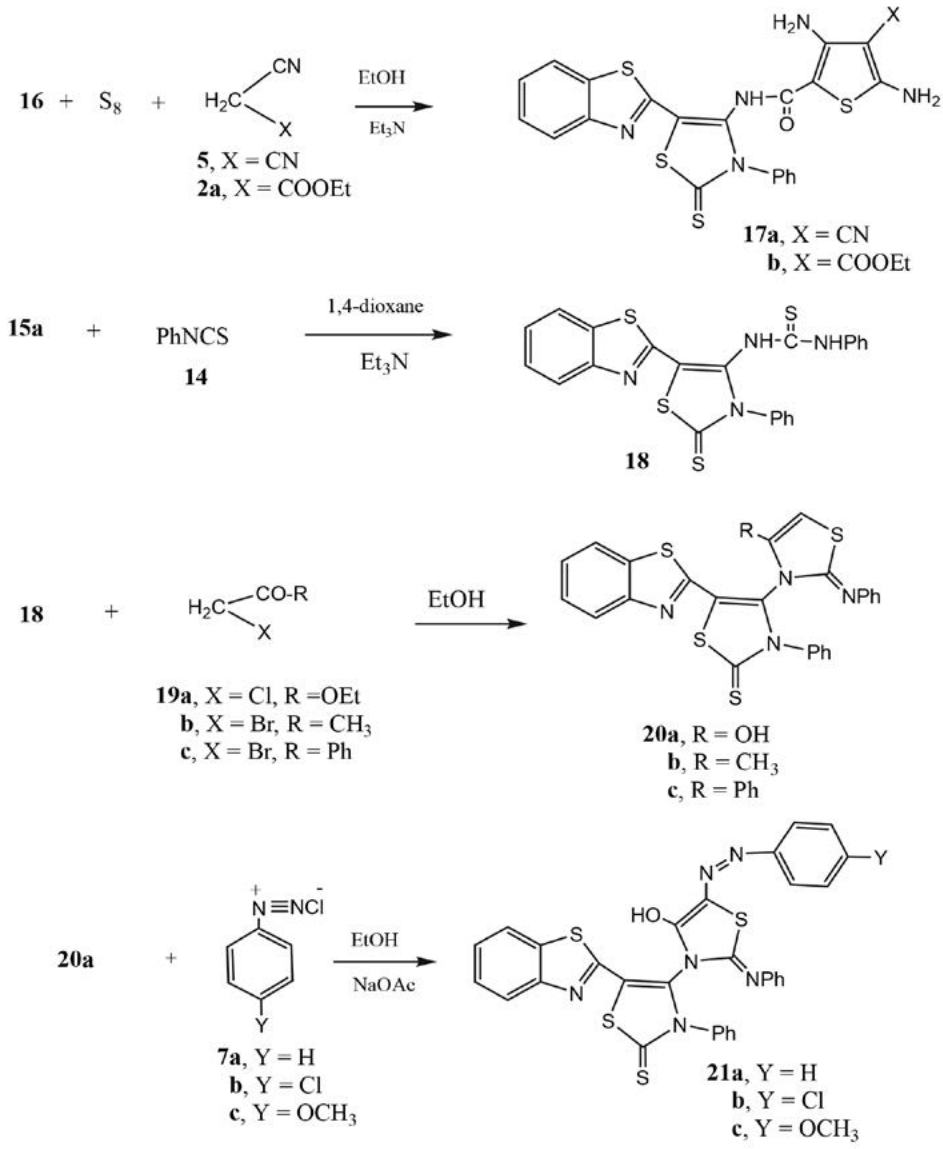

Scheme 5. Synthesis of compounds **17a**,**b**, **18**, **20a**–**c** and **21a**–**c**.

with foretinib as the positive control.[31–33] The cancer cell lines were cultured in minimum essential medium (MEM) supplemented with 10% fetal bovine serum (FBS). Approximately 4×10^3 cells, suspended in MEM medium, were plated onto each well of a 96-well plate and incubated in 5% CO_2 at 37 °C for 24 h. The compounds tested at the indicated final concentrations were added to the culture medium and the cell cultures and were continued for 72 h. Fresh MTT was added to each well at a terminal concentration of 5 μg/mL, and incubated with cells at 37 °C for 4 h. The formazan crystals were dissolved in 100 μL of DMSO in each well, and the absorbance at 492 nM (for absorbance of MTT formazan) and 630 nM (for the reference wavelength) was measured with an ELISA reader. All of the compounds were tested three times in each cell line. The results expressed as IC_{50} (inhibitory concentration 50%) were the averages of three determinations and calculated by using the Bacus Laboratories Incorporated Slide Scanner (Bliss) software.

The mean values of three independent experiments, expressed as IC_{50} values, are presented in Table 1. Most of the synthesized compounds exhibited potent anti-proliferative activity with IC_{50} values less than 30 μM. Generally, the variations of substituents within the aryl moiety together with the heterocycle ring being attached have a notable influence on the anti-proliferative activity.

3. 2. 2. Structure Activity Relationship

Table 1 demonstrates that many of the synthesized compounds revealed high inhibitions toward the used cancer cell lines. It is clear that most of the tested compounds

Table 1. *In vitro* growth inhibitory effects IC_{50} ± SEM (μM) of the newly synthesized compounds against cancer cell lines

Compd No	IC_{50} ± SEM (μM)					
	A549	H460	HT29	MKN-45	U87MG	SMMC-7721
4a	3.31 ± 1.42	2.38 ± 1.16	2.48 ± 1.69	3.30 ± 1.38	2.18 ± 0.98	2.60 ± 1.05
4b	6.12 ± 1.26	4.35 ± 1.42	5.23 ± 1.34	4.62 ± 1.53	5.49 ± 1.29	3.28 ± 1.42
4c	2.58 ± 1.11	2.72 ± 1.15	3.26 ± 1.08	2.52 ± 1.16	2.41 ± 1.16	3.21 ± 1.22
6a	5.31± 1.46	3.16 ± 1.46	4.1 6 ± 1.41	5.19 ± 2.30	4.46 ± 1.23	5.64 ± 1.37
6b	0.46 ± 0.21	0.32 ± 0.19	0.28 ± 0.04	0.32 ± 0.18	0.42 ± 0.26	0.39 ± 0.20
6c	4.31 ± 1.24	3.28 ± 1.13	3.42 ± 1.27	5.36 ± 2.16	3.49 ± 1.16	4.38 ± 1.15
6d	1.36 ± 0.98	2.29 ± 0.87	1.38 ± 0.91	1.36 ± 0.77	3.67 ± 1.27	1.27 ± 0.88
6e	0.31 ± 0.51	0.62 ± 1.63	0.17 ± 0.16	0.43 ± 0.16	0.23 ± 0.06	0.31 ± 0.18
6f	0.41 ± 0.25	0.71 ± 0.57	0.42 ± 0.39	0.42 ± 0.22	0.28 ± 0.23	0.31 ± 0.21
8a	6.42 ± 2.28	5.37 ± 1.45	7.50 ± 1.87	6.65 ± 2.27	5.51 ± 2.39	6.34 ± 2.18
8b	0.22 ± 0.05	0.33 ± 0.21	0.39 ± 0.17	0.22 ± 0.16	0.30 ± 0.21	0.28 ± 0.17
8c	4.29 ± 1.52	3.38 ± 1.48	4.46 ± 2.19	3.85 ± 1.36	4.70 ± 1.39	5.54 ± 1.19
8d	5.31 ± 1.13	4.32 ± 1.26	3.29 ± 1.37	5.26 ± 2.26	4.36 ± 1.85	5.38 ± 1.39
8e	0.23 ± 0.18	0.39 ± 0.15	0.27 ± 0.09	0.23 ± 0.11	0.32 ± 0.13	0.22 ± 0.19
8f	5.86 ± 2.38	4.62 ± 1.64	3.76 ±1.32	4.42 ± 2.15	3.59 ± 1.26	4.68 ± 1.47
8g	1.84 ± 0.84	0.95 ± 0.36	1.58 ± 0.86	2.62 ± 1.07	3.59 ± 1.16	2.68 ± 1.03
8h	0.26 ± 0.15	0.35 ± 0.16	0.27 ± 0.15	0.29 ± 0.09	0.43 ± 0.22	0.39 ± 0.16
8i	4.63 ± 1.17	3.41 ± 1.34	5.33 ± 2.62	5.27 ± 1.29	4.31 ± 1.02	3.84 ± 1.32
9a	4.41 ± 2.08	6.31 ± 1.48	5.50 ± 1.83	4.68 ± 2.14	6.52 ± 2.41	5.38 ± 2.38
9b	0.24 ± 0.08	0.23 ± 0.11	0.29 ± 0.16	0.42 ± 0.19	0.35 ± 0.26	0.42 ± 0.16
9c	3.11 ± 1.37	3.68 ± 1.58	4.52 ± 2.30	4.80 ± 1.49	4.52 ± 1.63	5.26 ± 1.79
9d	0.35 ± 0.259	0.35 ± 0.17	0.26 ± 0.23	0.29 ± 0.17	0.46 ± 0.30	0.40 ± 0.24
9e	0.21 ± 0.15	0.29 ± 0.13	0.36 ± 0.15	0.28 ± 0.15	0.41 ± 0.17	0.24 ± 0.15
9f	3.22 ± 1.13	4.52 ± 1.14	5.60 ± 1.45	4.82 ± 2.31	4.52 ± 1.26	5.13 ± 1.16
9g	0.23 ± 0.14	0.25 ± 0.16	0.53 ± 0.26	0.31± 0.19	0.53 ± 0.16	0.42 ± 0.23
9h	0.23 ± 0.12	0.28 ± 0.15	0.34 ± 0.17	0.22 ± 0.08	0.31 ± 0.20	0.48 ± 0.17
9i	2.83 ± 1.13	2.80 ± 1.64	3.16 ± 1.45	3.87 ± 1.35	3.62 ± 1.12	3.78 ± 1.60
10a	2.81 ± 1.16	2.53 ± 1.25	3.62 ± 1.41	5.23 ± 2.31	2.70 ± 0.91	5.38 ± 2.38
10b	0.24 ± 0.08	0.23 ± 0.11	0.29 ± 0.16	0.42 ± 0.19	0.35 ± 0.26	0.51 ± 0.18
10c	5.34 ± 1.49	3.68 ± 1.32	5.42 ± 2.54	6.71 ± 1.29	6.31 ± 1.52	4.87 ± 1.23
10d	0.35 ± 0.23	0.42 ± 0.18	0.25 ± 0.14	0.29 ± 0.16	0.43 ± 0.21	0.35 ± 0.24
10e	0.21 ± 0.14	0.35 ± 0.16	0.26 ± 0.15	0.28 ± 0.15	0.41 ± 0.17	0.24 ± 0.15
10f	1.26 ± 0.93	2.40 ± 1.12	2.39 ± 0.86	1.53 ± 0.79	1.82 ± 1.43	1.62 ± 0.74
10g	0.25 ± 0.16	0.35 ± 0.14	0.41 ± 0.23	0.62 ± 0.25	0.41 ± 0.13	0.53 ± 0.19
10h	0.24 ± 0.15	0.38 ± 0.16	0.42 ± 0.15	0.35 ± 0.16	0.52 ± 0.23	0.35 ± 0.18
10i	1.62 ± 0.69	2.63 ± 1.14	2.17 ± 1.12	1.32 ± 1.15	2.42 ± 1.12	1.73 ± 0.93
12a	0.80 ± 0.25	0.21 ± 0.11	0.37 ± 0.20	0.42 ± 0.16	0.81 ± 0.20	0.62 ± 0.14
12b	0.38 ± 0.15	0.42 ± 0.27	0.23 ± 0.12	0.57 ± 0.25	0.41 ± 0.23	0.37 ± 0.13
12c	0.15 ± 0.26	0.31 ± 0.25	0.41 ± 0.42	0.72 ± 0.25	0.80 ± 0.36	0.53 ± 0.25
12d	0.35 ± 0.19	0.35 ± 0.17	0.26 ± 0.23	0.29 ± 0.17	0.46 ± 0.30	0.40 ± 0.24
12e	0.21 ± 0.15	0.29 ± 0.13	0.36 ± 0.15	0.28 ± 0.15	0.41 ± 0.17	0.24 ± 0.15
12f	3.22 ± 1.13	4.52 ± 1.14	5.60 ± 1.45	4.82 ± 2.31	4.52 ± 1.26	5.13 ± 1.16
12g	0.23 ± 0.14	0.25 ± 0.16	0.53 ± 0.26	0.31 ± 0.19	0.53 ± 0.16	0.42 ± 0.23
12h	0.23 ± 0.12	0.28 ± 0.15	0.34 ± 0.17	0.22 ± 0.08	0.31 ± 0.20	0.48 ± 0.17
12i	0.83 ± 0.13	0.80 ± 0.64	0.16 ± 0.05	0.87 ± 0.35	0.62 ± 0.12	0.78 ± 0.60
13a	0.80 ± 0.60	0.63 ± 0.26	0.57 ± 0.13	0.53 ± 0.39	0.61 ± 0.44	0.31 ± 0.16
13b	0.28 ± 0.13	0.31 ± 0.17	0.26 ± 0.15	0.32 ± 0.22	0.50 ± 0.24	0.15 ± 0.06
13c	0.16 ± 0.06	0.32 ± 0.15	0.42 ± 0.18	0.52 ± 0.23	0.53 ± 0.21	0.39 ± 0.24
13d	0.25± 0.17	0.32 ± 0.13	0.24 ± 0.15	0.25 ± 0.14	0.32 ± 0.23	0.29 ± 0.15
13e	0.39 ± 0.21	0.27 ± 0.12	0.27 ± 0.13	0.24 ± 0.12	0.30 ± 0.14	0.29 ± 0.11
13f	0.26 ± 0.13	0.32 ± 0.16	0.39 ± 0.25	0.32 ± 0.21	0.39 ± 0.23	0.35 ± 0.15
13g	0.33 ± 0.15	0.25 ± 0.18	0.40 ± 0.28	0.34 ± 0.17	0.29 ± 0.14	0.58 ± 0.24
13h	0.21 ± 0.14	0.27 ± 0.12	0.30 ± 0.19	0.28 ± 0.12	0.35 ± 0.16	0.28 ± 0.15
13i	0.23 ± 0.13	0.73 ± 0.34	0.36 ± 0.25	0.57 ± 0.15	0.36 ± 0.13	0.32 ± 0.21
15a	1.33 ± 1.03	1.62 ± 0.87	1.06 ± 0.85	1.62 ± 0.96	1.02 ± 0.82	1.38 ± 0.49
15b	0.24 ± 0.12	0.37 ± 0.13	0.29 ± 0.13	0.22 ± 0.13	0.32 ± 0.19	0.27 ± 0.14
15c	1.62 ± 0.59	1.13 ± 0.86	1.24 ± 0.83	0.51 ± 0.24	0.32 ± 0.16	0.78 ± 0.26

Compd No	IC_{50} ± SEM (μM)					
	A549	H460	HT29	MKN-45	U87MG	SMMC-7721
16	0.26 ± 0.16	0.27 ± 0.15	0.33 ± 0.27	0.28 ± 0.14	0.35 ± 0.15	0.35 ± 0.17
17a	0.24 ± 0.16	0.23 ± 0.18	0.24 ± 0.16	0.39 ± 0.12	0.38 ± 0.15	0.30 ± 0.17
17b	0.63 ± 0.32	0.51 ± 0.24	0.66 ± 0.29	0.45 ± 0.16	0.56 ± 0.16	0.68 ± 0.31
18	0.23 ± 0.15	0.29 ± 0.16	0.27 ± 0.14	0.26 ± 0.17	0.22 ± 0.17	0.38 ± 0.16
20a	0.22 ± 0.13	0.32 ± 0.27	0.14 ± 0.03	0.54 ± 0.23	0.25 ± 0.12	0.17 ± 0.08
20b	0.23 ± 0.14	0.35 ± 0.16	0.25 ± 0.16	0.27 ± 0.14	0.41 ± 0.16	0.26 ± 0.13
20c	0.68 ± 0.29	0.53 ± 0.26	0.24 ± 0.14	0.42 ± 0.25	0.53 ± 0.18	0.42 ± 0.23
21a	0.12 ± 0.03	0.22 ± 0.16	0.12 ± 0.08	0.32 ± 0.11	0.45 ± 0.22	0.27 ± 0.11
21b	0.25 ± 0.14	0.33 ± 0.14	0.35 ± 0.24	0.35 ± 0.16	0.21 ± 0.11	0.35 ± 0.17
21c	0.66 ± 0.23	0.83 ± 0.22	0.62 ± 0.16	0.50 ± 0.25	0.38 ± 0.15	0.38 ± 0.27
Foretinib	0.08 ± 0.01	0.18 ± 0.03	0.15 ± 0.023	0.03 ± 0.0055	0.90 ± 0.13	0.44 ± 0.062

exhibited high inhibitions toward the six cancer cell lines. Considering the benzo[*d*]thiazole derivatives **4a–c**, it is clear that compound **4c** exhibited the highest cytotoxicity out of these three compounds; this might be attributed to the presence of the acetyl moiety. For the thiophene derivatives **6a–f**, all compounds showed high inhibitions except compounds **6a** (X = CN, R^- = NH_2) and **6c** (X = CN, R^- = CH_3). On the other hand compound **6d** (X = COOEt, R' = NH_2) showed moderate inhibitions toward the six cancer cell lines. Considering the aryl hydrazone derivatives **8a–i** it can be seen that compounds **8a**, **8c**, **8d**, **8f** and **8i** exhibited low inhibitions. However, compounds **8b** (R= CN, Y = Cl), **8e** (R= COOEt, Y = Cl), **8g** (R= $COCH_3$, Y = H) and **8h** ((R= $COCH_3$, Y = Cl), showed moderate to high inhibitions toward the six cancer cell lines. On the other hand, among the pyridazine derivatives **9–i**, all compounds exhibited from high to moderate inhibitions: compounds **9b**, **9d**, **9e**, **9g** and **9h** showed high inhibitions and compounds **9a**, **9c**, **9f** and **9i** exhibited moderate inhibition. In most cases the high inhibitions are attributed to the presence of either OH group at the pyridazine ring or of the Cl group attached to the aryl moiety. Similarly for the pyridazin-2-one derivatives **10a–i**: compounds **10b**, **10d**, **10e**, **10g** and **10h** showed high inhibitions and compounds **10a**, **10f** and **10i** exhibited moderate inhibition while compound **10c** exhibited low inhibitions. Interestingly, among the thiazole derivatives **12a–i** and **13a–i** all compounds exhibited high inhibitions toward the six cancer cell lines except compound **12f** which showed moderate inhibitions. Although some compounds contain electron donating groups like the OCH_3 or electron repealing groups like the CH_3 group it seemed that in these compounds the presence of the second thiazole moiety enhances the inhibitions. For the thiazol-2-thione derivatives **15a–c**, it was obvious that compound **15b** (R" = OH) exhibited the highest inhibitions among the three compounds, although compounds **15a** (R" = NH_2) and **15c** (R" = CH_3) showed moderate inhibitions. Moreover, the *N*-alkylated thiazol-thione derivative **16** exhibited high inhibitions toward the selected cancer cell lines. Compounds **17a** (X = CN), **17b** (X = COOEt) and **18** with the two thiazole rings and the thiophene ring showed high inhibitions toward the six cancer cell lines. Finally, for the trithiazolyl derivatives **20a–c** and **21a–c** it was seen that all compounds exhibited high inhibitions toward the six cancer cell lines. It was obvious that the three thiazole moieties had a strong effect on the activities of such compounds.

3. 2. 3. *In vitro* Evaluation of the Anticancer Activity of compounds 13b–g and 13i

The 2,3-dihydropyridazin-4-yl)thiazol-4(5*H*)-one derivatives **13b**, **13c**, **13d**, **13e**, **13f**, **13g** and **13i** were selected for an advanced assay against a panel of approximately seventeen tumor cell lines at 10-fold dilutions of five concentrations (100 μM, 10 μM, 1.0 μM, 0.1 μM and 0.01 μM).[34,35] The tested compounds exhibited inhibition activity (GI_{50} < 5 μM) against the cancer cell lines that are classified into groups according to the type of disease, the data are shown in Table 2. Throughout our work for compounds **13b**, **13c**, **13d, 13e**, **13f, 13g** and **13i** there are two factors, the substituent at C-4 of the pyridazine ring and the substituent at the position 4 of the aryl group. It is clear from Table 2 that all tested compounds exhibited high inhibitions toward the cell lines categorized according to the type of the disease. From the tested compounds compound **13e** (R" = OH, Y = Cl) exhibited the highest inhibitions among the tested compounds, it was obvious that the presence of the electronegative OH and Cl groups has a strong impact on the activity of this compound. On the other hand, compound **13i** (R" = CH3, Y = OCH_3) exhibited the lowest inhibitions toward the cancer cell lines. Such finding was attributed to the presence of both of the OCH_3 and CH_3 groups within the structure of the compound. Interestingly, compound **13c** (R = NH_2, Y = OCH_3) exhibited highest inhibition toward K-526 cell line with GI_{50} = 0.14 μM although it contains the OCH_3 moiety. On the other hand, compound **13f** (R" = OH, Y = OCH_3) exhibited the highest inhibition toward RPMI-8262 cell line.

Table 2. The influence of compounds **13b**–**g** and **13i** on the growth of individual tumor cell lines (GI_{50} < 5 μM).

Disease	Cell line	13b	13c	13d	13f	13e	13g	13i
Leukemia	CCRF-CEM	0.32	0.29	0.29	0.46	0.22	0.36	0.86
Leukemia	RPMI-8262	0.36	0.27	0.30	0.11	0.37	0.28	0.79
Leukemia	SR 0.44	0.29	0.57	0.41	0.31	0.62	0.97	
Leukemia	HI-60 (TB)	0.36	0.42	0.27	0.32	0.27	0.16	0.63
Leukemia	K-526	0.26	0.14	0.46	0.41	0.12	0.36	0.81
NCS-Lung cancer	HOP-62	0.60	0.51	0.47	0.312	0.16	0.52	1.97
NCS-Lung cancer	NCI-H460	0.37	0.42	0.37	0.26	0.66	0.52	2.18
Colon cancer	HCT-116	0.45	0.36	0.47	0.26	0.26	0.38	3.18
Colon cancer	HCT-15	0.25	0.38	0.29	0.39	0.42	0.31	1.42
Colon cancer	KM12	0.74	0.37	0.28	0.42	0.48	0.37	0.93
CNS cancer	SF-295	0.58	0.26	0.45	0.63	0.39	0.70	0.73
CNS cancer	U251	0.27	0.16	0.34	0.81	0.89	0.37	0.62
Melanoma	LOX IMVI	0.41	0.48	0.58	0.32	0.29	0.44	1.17
Melanoma	MDA-MB-435	0.40	0.27	0.59	0.53	0.40	0.77	1.23
Melanoma	UACC-62	0.38	0.47	0.44	0.46	0.20	0.56	0.79
Ovarian cancer	OVCAR-3	0.52	0.42	0.29	0.28	0.31	0.55	0.80
Renal cancer	786-0	0.53	0.43	0.19	0.28	0.27	0.43	0.99

3. 2. 4. HTRF Kinase Assay

Mesenchymal epithelial transition factor (c-Met) is a multifunctional transmembrane tyrosine kinase and acts as a receptor for hepatocyte growth factor/Scatter factor (HGF/SF).[36] There are multiple oncogenetic characteristics of c-Met that were outlined shortly after its discovery, including cell division and transportation through an extracellular matrix invasion.[37] Moreover, c-Met kinase activity has a high relationship to prostate cancer where c-Met played a key role in the transformation of prostate cancer from the primary androgen-sensitive to androgen-insensitive state along with the increase in radioresistance.[38–41] Based on these reported observations, the c-Met kinase activity of all compounds was evaluated using homogeneous time-resolved fluorescence (HTRF) assay as previously reported.[42] Taking foretinib as the positive control, the results are expressed as IC_{50} and summarized in Table 3. The anti-proliferative activities of all target compounds against the human prostatic cancer PC-3 cell line were measured by MTT assay[43] using anibamine as the reference drug. The mean values of three independent experiments were expressed as IC_{50} values and are presented in Table 3. Generally, the variations of substituents within the aryl moiety together with the heterocyclic ring being attached have a notable influence on the anti-proliferative activity.

As indicated in Table 3, all the tested compounds displayed potent c-Met enzymatic activity with IC_{50} values ranging from 0.12 to 8.93 nM and potent prostate PC-3 cell line inhibitions with IC_{50} values ranging from 0.11 to 12.91 μM. Compared with foretinib (IC_{50} = 1.16 nM), the forty compounds **4a**, **6c**, **6e**, **8b**, **8c**, **8e**, **8g**, **8h, 8i**, **9b**, **9c**, **9e**, **9h**, **9i**, **10b**, **10c**, **10e**, **10h**, **10i**, **12b**, **12c**, **12e**, **12g**, **12h**, **12i**, **13b**, **13c**, **13g**, **13h**, **13i**, **15b**, **15c**, **16**, **17a**, **18**, **20a**, **20c**, **21a**, **21b** and **21c** exhibited highest potency with IC_{50} values less than 1.16 nM. Remarkably, among the synthesized compounds **4a**, **4b**, **4c**, **6b**, **6c**, **6d**, **6e**, **8b**, **8c**, **8e**, **8g**, **8h**, **8i**, **9b**, **9c**, **9h**, **9i**, **10b**, **10c**, **10e**, **10h**, **10i**, **12b**, **12e**, **12h**, **12i**, **13b**, **13c**, **13g**, **13h**, **13i**, **15b**, **16**, **17a**, **17b**, **18**, **20a**, **20c** and **22b** displayed much higher anti-proliferation activities than the standard anibamine (IC_{50} = 3.26 μM). Analyzing the data in Table 3 showed that compound **9e** exhibited the lowest GI_{50} (GI_{50} = 0.17 μM) among the tested compounds. On the other hand, compound **9c** showed the highest inhibition toward PC-3 cell line with IC_{50} = 0.16 μM.

All synthesized compounds were tested against the VERO, Monkey Kidney normal cell line, where they showed low activities against the normal cell line. Interestingly, from Table 3 compounds **4b**, **4c**, **6b** and **6d** showed SI > 15, while the thirty three compounds **4a**, **6c**, **6e**, **8b**, **8c**, **8e**, **8i**, **8h**, **9b**, **9c**, **9h**, **9i**, **10b**, **10c**, **10e**, **10h**, **10i**, **12b**, **12e**, **12h**, **12i**, **13b**, **13c**, **13g**, **13h**, **13i**, **15b**, **16**, **17a**, **17b**, **18**, **20a** and **21b** exhibited SI > 100, while the rest of compounds showed SI < 15.

Table 3. c-Met enzymatic activity and PC-3 inhibition of the newly synthesized compounds

Compound No	IC_{50} (nM) c-Met	IC_{50}(μM) PC-3	VERO[a] (μM)	SI PC-3[b]
4a	0.43 ± 0.21	0.52 ± 0.25	66.23 ± 4.90	> 100
4b	1.13 ± 0.79	1.23 ± 0.93	33.52 ± 3.71	27.25
4c	1.86 ± 0.86	1.24 ± 0.93	34.32 ± 8.37	27.68
6a	2.63 ± 1.02	3.48 ± 1.14	28.92 ± 4.53	8.31
6b	2.42 ± 1.23	2.29 ± 1.31	36.52 ± 3.69	15.94
6c	0.21 ± 0.14	0.39 ± 0.24	69.43 ± 6.52	> 100
6d	1.62 ± 0.87	1.04 ± 0.74	40.58 ± 4.52	39.01
6e	0.26 ± 0.14	0.29 ± 0.13	68.49± 4.26	> 100
6f	8.52 ± 3.53	10.43 ± 3.65	26.31 ± 3.49	2.52
8a	4.83 ± 1.53	5.63 ± 2.73	23.82 ± 5.23	4.23
8b	0.29 ± 0.08	0.33 ± 0.15	60.43 ± 5.34	>100
8c	0.24 ± 0.16	0.38 ± 0.24	68.48 ± 4.51	> 100
8d	1.68 ± 1.12	3.29 ± 1.24	30.58 ± 3.84	1.08

Compound No	IC_{50} (nM) c-Met	IC_{50}(μM) PC-3	VERO[a] (μM)	SI PC-3[b]
8e	0.42 ± 0.25	0.42 ± 0.24	68.52 ± 5.38	> 100
8f	6.51 ± 1.32	7.25 ± 1.37	23.27 ± 2.39	3.21
8g	0.28 ± 0.11	0.33 ± 0.18	22.23 ± 3.45	67.36
8h	0.35 ± 0.15	0.27 ± 0.14	58.90 ± 6.84	> 100
8i	0.24 ± 0.16	0.31 ± 0.19	62.19 ± 4.32	> 100
9a	2.81 ± 1.13	4.68 ± 0.16	20.50 ± 2.33	4.38
9b	0.25 ± 0.14	0.24 ± 0.12	66.58 ± 5.31	> 100
9c	0.31 ± 0.16	0.17 ± 0.09	70.26 ± 4.24	> 100
9d	2.13 ± 1.01	8.62 ± 1.62	44.81 ± 2.16	5.42
9e	0.15 ± 0.02	8.46 ± 2.42	40.61 ± 2.69	4.80
9f	5.26 ± 2.15	10.32 ± 2.31	30.76 ± 4.31	2.98
9g	3.19 ± 2.25	5.68 ± 2.32	28.27 ± 2.63	4.97
9h	0.38 ± 0.13	0.24 ± 0.12	59.12 ± 3.32	> 100
9i	0.37 ± 0.17	0.36 ± 0.27	68.12 ± 4.35	> 100
10a	6.83 ± 1.28	10.63 ± 3.58	25.73 ± 4.61	2.42
10b	0.25 ± 0.13	0.32 ± 0.22	59.68 ± 5.21	> 100
10c	0.23 ± 0.13	0.30 ± 0.15	62.38 ± 4.23	> 100
10d	4.26 ± 1.85	6.65 ± 1.78	25.28 ± 4.80	3.80
10e	0.18 ± 0.06	0.21 ± 0.13	58.76 ± 4.13	> 100
10f	8.11 ± 2.52	12.62 ± 3.16	22.18 ± 4.60	1.75
10g	7.48 ± 2.43	6.82 ± 2.51	30.52 ± 3.62	4.47
10h	0.48 ± 0.16	0.29 ± 0.13	65.16 ± 4.63	>100
10i	0.12 ± 0.08	0.16 ± 0.07	70.58 ± 5.19	> 100
12a	7.38 ± 1.67	8.26 ± 2.17	31.26 ± 3.73	3.78
12b	0.29 ± 0.13	0.43 ± 0.26	59.32 ± 4.62	>100
12c	0.42 ± 0.21	5.29 ± 2.23	48.69 ± 1.62	9.20
12d	8.93 ± 2.53	7.85 ± 3.52	64.90 ± 5.43	8.26
12e	0.25 ± 0.13	0.39 ± 0.17	68.24 ± 6.43	> 100
12f	5.62 ± 1.34	6.36 ± 1.81	35.25 ± 2.79	5.54
12g	0.32 ± 0.18	4.64 ± 0.14	30.17 ± 4.52	6.50
12h	0.17 ± 0.09	0.27 ± 0.15	44.31 ± 4.62	>100
12i	0.32 ± 0.14	0.19 ± 0.08	77.48 ± 4.82	> 100
13a	6.31 ± 2.52	9.39 ± 1.42	26.54 ± 3.42	2.82
13b	0.28 ± 0.15	0.36 ± 0.19	58.37 ± 5.82	>100
13c	0.63 ± 0.26	0.58 ± 0.169	68.32 ± 4.51	> 100
13d	8.96 ± 2.81	9.41 ± 2.82	22.73 ± 3.51	2.41
13e	2.83 ± 1.64	4.58 ± 1.53	23.59 ± 2.71	5.15
13f	4.32 ± 1.54	12.91 ± 3.81	27.24 ± 2.94	2.10
13g	0.34 ± 0.28	0.29 ± 0.18	44.13 ± 4.53	>100
13h	0.15 ± 0.08	0.36 ± 0.14	65.54 ± 5.31	>100
13i	0.41 ± 0.24	0.38 ± 0.15	66.25 ± 3.52	> 100
15a	8.36 ± 2.51	10.61 ± 4.28	27.24 ± 2.94	2.56
15b	0.22 ± 0.14	0.11 ± 0.07	69.34 ± 5.20	> 100
15c	0.31 ± 0.22	8.71 ± 3.53	25.24 ± 3.82	2.89
16	0.29 ± 0.16	0.29 ± 0.08	66.31 ± 4.62	> 100
17a	0.48 ± 0.23	0.62 ± 0.18	69.28 ± 4.63	> 100
17b	1.46 ± 0.91	0.21 ± 0.08	57.28 ± 4.62	> 100
18	0.25 ± 0.13	0.23 ± 0.16	72.38 ± 6.80	> 100
20a	0.12 ± 0.07	0.41 ± 0.23	65.28 ± 5.73	> 100
20b	6.39 ± 2.18	8.25 ± 2.36	36.30 ± 3.52	4.39
20c	1.45 ± 0.88	2.82 ± 0.13	49.20 ± 5.71	5.57
21a	9.98 ± 0.26	8.82 ± 2.37	64.22 ± 4.82	7.28
21b	0.23 ± 0.16	0.25 ± 0.09	67.24 ± 4.81	> 100
21c	0.28 ± 0.16	12.25 ± 4.19	26.24 ± 5.62	2.14
	Foretinib	**Anibamine**		
	1.16 ± 0.17	3.26 ± 0.35	–	–

[a] VERO, Monkey Kidney cell line (Cat No-11095–080).
[b] Selectivity index (SI) were calculated by IC_{50} values in normal cell line divided by IC_{50} values in PC-3 cancer cell line.

3. 2. 5. Determination of Morphological Changes of A549 Cell Line by the Effect of Compounds 13c and 13h

The lung is a unique organ that should be protected against inhaled pathogens and toxins, without imbalanced immune responses or compromising its vital function. For that matter microenvironment of the lung tissue is regulated through complex and refined cell interactions.[44,45] For that reason we studied the effect of compound **13c** (Fig. 2) and **13h** (Fig. 3) toward A549 cell line which was selected for studying the morphological changes. There are many reports concerned with morphological changes of other cell lines.[46,47] To understand the ability of compound **13c** and **13h** in apoptosis induction, various qualitative (morphological) and quantitative assays were performed on the A549 lung cancer cell line. The changes in the morphological features of A549 cells were observed after the treatment with compound **13c** and **13h** at different concentrations along with the untreated control cells. Further, images shown in Fig. 2A and 3A were captured using phase-contrast microscopy after 72 h; revealing the characteristic apoptotic features like changes in morphology (shape, shrinkage) of the cell, reduction in the number of live cells. In the present study, A549 cells after treatment with compound **13c** and **13h** for 72 h exhibited the formation of apoptotic features such as the appearance of membrane blebs and inverse proportion in the number of cells with the concentration of compound tested as indicated in Fig. 2B and 3B, respectively. Compound **13c** and **13h** treated A549 cells after 72 h, on staining with DAPI visualized the chromatin condensation as well as pyknotic (inset of 1.25 μM) and condensed (bright colored: inset of 2.5 μM) nuclei formation as depicted in Fig. 2C and 3C, respectively.

4. Conclusion

Throughout this work we aimed to synthesize a set of novel compounds that were produced from benzo[*d*]thiazole derivatives. The structures of the synthesized compounds were confirmed by multiple techniques and they were screened for cytotoxic activity against six cancer cell lines. In addition, most of the tested compounds exhibited high inhibitions toward c-Met kinase and PC-3 cell lines. The results obtained in this assay indicate that these compounds are good candidates as anti-cancer agents thus encouraging further work in the future.

Human and Animal Rights

No animals/humans were used for studies that are basis of this research.

Consent for Publication

This work is consent for publication through the Journal formats.

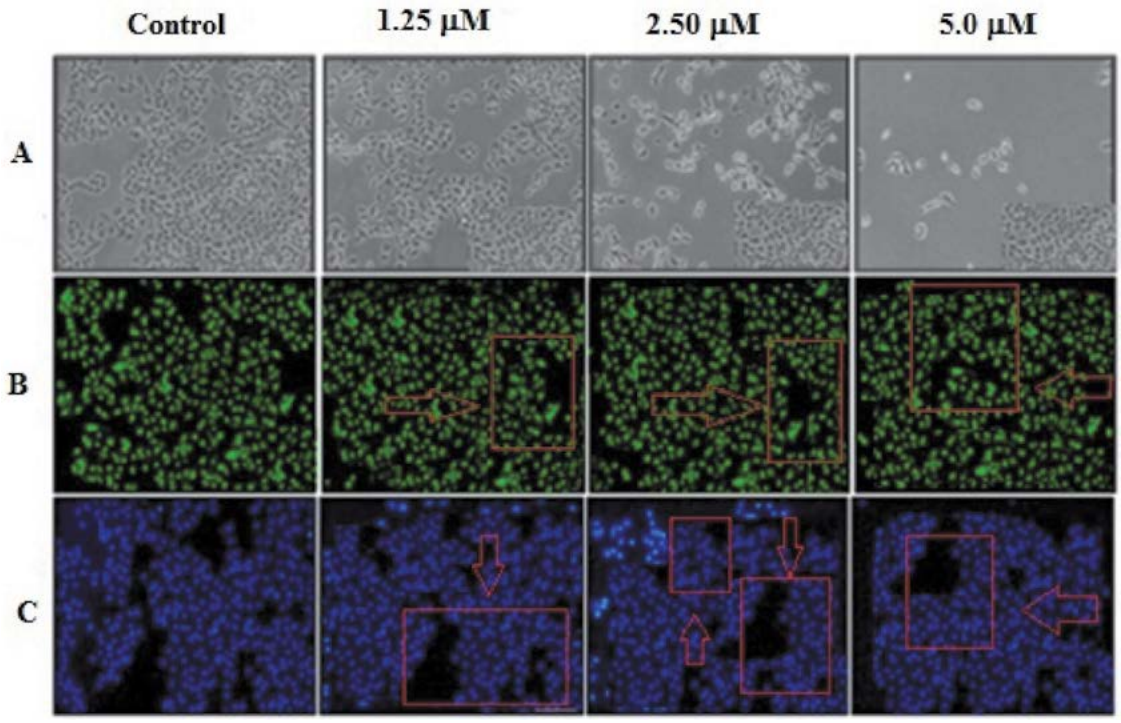

Figure 2. Microscopic observation of the effect of different concentrations (1.25, 2.5, and 5 µM) of compound **13c** in comparison to control (untreated) on A549 cells after 72 h of treatment. (A) Morphological changes were observed through phase-contrast microscopy. (B) Morphological changes such as membrane blebs were visualized through a fluorescence microscopy by performing acridine orange staining. (C) Nuclear changes were observed by DAPI staining using a fluorescence microscopy. Photos at different concentrations of treatment indicate the changes induced by treatment and red-colored arrows specify the area of effect.

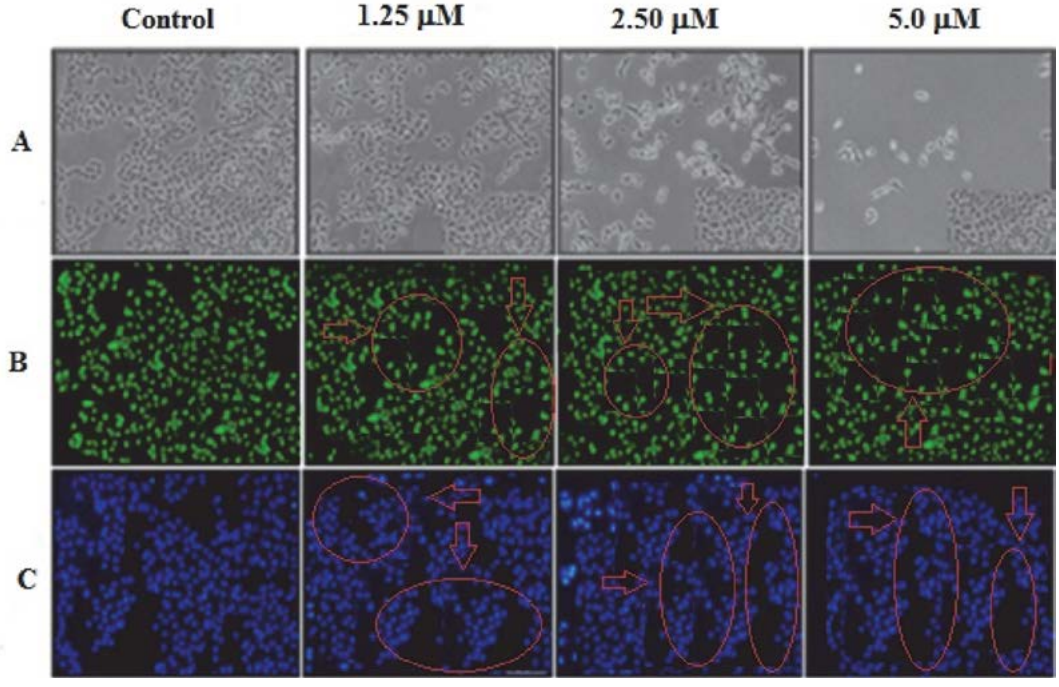

Figure 3. Microscopic observation of the effect of different concentrations (1.25, 2.5, and 5 µM) of compound **13h** in comparison to control (untreated) on A549 cells after 72 h of treatment.

Conflict of Interest

The authors declare no conflict of interest, financial or otherwise.

5. References

1. M. Gjorgjieva, T. Tomašič, D. Kikelj, L. Peterlin Mašič, *Curr. Med. Chem.* **2018**,, *25*, 5218–5236. **DOI:**10.2174/0929867324666171009103327
2. S. Zhao, L. Zhao, X. Zhang, C. Liu, C. Hao, H. Xie, B. Sun, D. Zhao, M. Cheng, *Eur. J. Med. Chem.* **2016**, *123*, 514–522. **DOI:**10.1016/j.ejmech.2016.07.067
3. N.-D. D'Angelo, T.-S. Kim, K. Andrews, S.-K. Booker, S. Caenepeel, K. Chen, D. D. D'Amico, J. Freeman, L. Jiang, J.-D Liu, T. McCarter, E.-L. San Miguel, M. Schrag, R. Subramanian, J. Tang, R.-C. Wahl, L. Wang, D.-A. Whittington, T. Wu, N. Xi, Y. Xu, P. Yakowec, K. Yang, L.-P. Zalameda, N. Zhang, P. Hughes, M.-H. Norman, *J. Med. Chem.* **2011**, *54*, 1789–1811. **DOI:**10.1021/jm1014605
4. A. Ammazzalorso, A. Giancristofaro, A. D'Angelo, B. De Filippis, M. Fantacuzzi, L. Giampietro, C. Maccallini, R. Amoroso, *Bioorg. Med. Chem. Lett.* 2011, *21*, 4869–4872. **DOI:**10.1016/j.bmcl.2011.06.028
5. Ü. D. Özkay, C. Kaya, U. A. Çevik, Ö. Can, *Molecules* **2017**, *22*, 1490. **DOI:**10.3390/molecules22091490
6. D.-C Liu, H.-J. Zhang, C.-M. Jin, Z.-S. Quan, *Molecules* **2016**, *21*, 164. **DOI:**10.3390/molecules21030164
7. C. Prouillac, P. Vicendo, J.-C. Garrigues, R. Poteau, G. Rima, *Free Radical Biol. Med.* **2009**, *46*, 1139–1148. **DOI:**10.1016/j.freeradbiomed.2009.01.016
8. L. Hroch, O. Benek, P. Guest, L. Aitken, O. Soukup, J. Janockova, K. Musil, V. Dohnal, R. Dolezal, K. Kuca, T. K. Smith, F. Gunn-Moore, K. Musilek, *Bioorg. Med. Chem. Lett.* **2016**, *26*, 3675–3678. **DOI:**10.1016/j.bmcl.2016.05.087
9. S. Ilgın, D. Osmaniye, S. Levent, B. Sağlık, U. Acar Çevik, B. Çavuşoğlu, Y. Özkay, Z. Kaplancıklı, *Molecules,* **2017**, *22*, 2187. **DOI:**10.3390/molecules22122187
10. B. Satyanarayana, M. Saravanan, K. Siva Kumari, D.-P. Lokamaheshwari, C. Sridhar, R. Ravishankar, A. Nageswari, P. Reddy, *Arkivoc,* **2008**, (*xiv*), 109. **DOI:**10.3998/ark.5550190.0009.e12
11. A. Doble, *Neurology* **1996**, *47*, 233S–241S. **DOI:**10.1212/WNL.47.6_Suppl_4.233S
12. J. Phukan, N. P. Pender, O. Hardiman, *The Lancet. Neurology* **2007**, *6*, 994–1003. **DOI:**10.1016/S1474-4422(07)70265-X
13. S. Kanie, T. Nishikawa, M. Ojika, Y. Oba, *Sci. Rep.* **2016**, *6*, 24794. **DOI:**10.1038/srep24794
14. V. Hrobáriková, P. Hrobárik, P. Gajdoš, I. Fitilis, M. Fakis, P. Persephonis, P. Zahradník, *J. Org. Chem.* **2010**, *75*, 3053–3068. **DOI:**10.1021/jo100359q
15. N. P. Prajapati, R. H. Vekariya, M. A. Borad, H. D. Patel, *RSC Adv.* **2014**, *4*, 60176–60208. **DOI:**10.1039/C4RA07437H
16. C. Fortenberry, B. Nammalwar, R. A. Bunce, *Org. Prep. Proced. Int.* **2013**, *45*, 57–65. **DOI:**10.1080/00304948.2013.743751
17. Y. Liu, X. Yuan, X. Guo, X. Zhang, B. Chen, *Tetrahedron* **2018**, *74*, 6057–6062. **DOI:**10.1016/j.tet.2018.08.047
18. A. Shaikh, O. Ravi, S. P. Ragini, N. Sadhana, S. R. Bathula, *Tetrahedron Lett.* **2020**, *61*, 151356. **DOI:**10.1016/j.tetlet.2019.151356
19. G. Satish, K. H. V. Reddy, K. Ramesh, K. Karnakar, Y. V. D. Nageswar, *Tetrahedron Lett.* **2012**, *53*, 2518–2521. **DOI:**10.1016/j.tetlet.2012.03.012
20. A. K. Chakraborti, C. Selvam, G. Kaur, S. Bhagat, *Synlett* **2004**, *5*, 851–855. **DOI:**10.1055/s-2004-820012
21. X. Yu, Q. Yin, Z. Zhang, T. Huang, Z. Pu, M. Bao, *Tetrahedron Lett.* **2019**, *60*, 1964–1966. **DOI:**10.1016/j.tetlet.2019.06.039
22. A. Saeed, H. Rafique, A. Hameed, S. Rasheed, *Pharm. Chem. J.* **2008**, *42*, 191. **DOI:**10.1007/s11094-008-0094-x
23. N. Y. M. Abdo, R. M. Mohareb, *Acta Chim. Slov.* **2022**, *69*, 700–713. **DOI:**10.17344/acsi.2021.6886
24. A. E. M. Abdallah, R. M. Mohareb, M. H. E. Helal, G. J. Mofeed, *Acta Chim. Slov.* **2021**, *68*, 604–616. **DOI:**10.17344/acsi.2020.6446
25. R. M. Mohareb, R. A. Ibrahim. E. S. Alwan, *Acta Chim. Slov.* **2021**, *68*, 51–64. **DOI:**10.17344/acsi.2020.6090
26. R. M. Mohareb, P. A. Halim, *Acta Chim. Slov.* **2018**, *65*, 554–568. **DOI:**10.17344/acsi.2017.4146
27. F. M. Abdelrazek, A. M. Salah, E. A. M. Mekky, *Tetrahedron* **2001**, *57*, 1813–1817. **DOI:**10.1016/S0040-4020(00)01153-4
28. S. M. Al-Mousawi, S. M. Moustafa, M. H. Elnagdi, *J. Saudi Chem. Soc.* **2011**, *15*, 309–312. **DOI:**10.1055/s-0030-1261182
29. B. Stanovnik, M. Tišler, *Tetraheron* **1967**, *23*, 387–395. **DOI:**10.1016/S0040-4020(01)83324-X
30. H. A. Mohamed, M. H. M. Abd Elazim, M. G. Assy, I. Atef, *J. Heterocycl. Chem.* **2020**, 57, 1974–1980. **DOI:**10.1002/jhet.3926
31. L. Liu, A. Siegmund, N. Xi, P. Kaplan-Lefko, K. Rex, A. Chen, J. Lin, J. Moriguchi, L. Berry, L. Y. Huang, Y. Teffera, Y. J. Yang, Y. H. Zhang, S. F. Bellon, M. Lee, R. Shimanovich, A. Bak, C. Dominguez, M. H. Norman, J. C. Harmange, I. Dussault, T. S. Kim, *J. Med. Chem.* **2008**, *51*, 3688–3691. **DOI:**10.1021/jm800401t
32. M. L. Peach, N. Tan, S. J. Choyke, A. Giubellino, G. Athauda, T. R. Burke Jr., M. C. Nicklaus, D. P. Bottaro, *J. Med. Chem.* **2009**, *52*, 943–951. **DOI:**10.1021/jm800791f
33. F. D. Bacco, P. Luraghi, E. Medico, G. Reato, F. Girolami, T. Perera, P. Gabriele, P. M. Comoglio, C. Boccaccio, *J. Natl. Cancer Inst.* **2011**, *103*, 645–661. **DOI:**10.1093/jnci/djr093
34. M. R. Boyd, K. D. Paull, *Drug Dev. Res.* **1995**, *34*, 91–109. **DOI:**10.1002/ddr.430340203
35. M. R. Boyd, in: Teicher, B. A. (Ed.), Cancer Drug Discovery and Development, 2, Humana Press, **1997**, pp. 23–43.
36. J. S. Rubin, D. P. Bottaro, S. A. Aaronson, *Biochim. Biophys. Acta* **1993**, *1155*, 357–371. **DOI:**10.1016/0304-419X(93)90015-5
37. S. L. Organ, M. S. Tsao, *Ther. Adv. Med. Oncol.* **2011**, *3*, S7–S19. **DOI:**10.1177/1758834011422556
38. M. Jeffers, S. Rong, G. F. V. Woude, *J. Mol. Med.* **1996**, *74*, 505–513. **DOI:**10.1007/BF00204976
39. B. S. Knudsen, G. A. Gmyrek, J. Inra, D. S. Scherr, E. D. Vaughan, D. M. Nanus, M. W. Kattan, W. L. Gerald, G. F. Vande Woude, *Urology* **2002**, *60*, 1113–1117. **DOI:**10.1016/S0090-4295(02)01954-4
40. P. A. Humphrey, X. Zhu, R. Zarnegar, P. E. Swanson, T. L.

Ratliff, R. T. Vollmer, M. L. Day, *Am. J. Pathol.* **1995**, *147*, 386–396.
41. M. Verras, J. Lee, H. Xue, T. H. Li, Y. Wang, Z. Sun, *Cancer Res.* **2007**, *67*, 967–975. **DOI:**10.1158/0008-5472.CAN-06-3552
42. F. De Bacco, P. Luraghi, E. Medico, G. Reato, F. Girolami, T. Perera, P. Gabriele, P. M. Comoglio, C. Boccaccio, *J. Natl. Cancer Inst.* **2011**, *103,* 645–661. **DOI:**10.1093/jnci/djr093
43. S. Li, Y. Zhao, K. Wang, Y. Gao, J. Han, B. Cui, P. Gong, *Bioorg. Med. Chem.* **2013**, *21***,** 2843–2855. **DOI:**10.1016/j.bmc.2013.04.013
44. X. Han, A. Alu, H. Liu, Y. S. X. Wei, L. Cai, Y. Wei, *Bioactive Materials* **2022**, *17*, 29–48. **DOI:**10.1016/j.bioactmat.2022.01.011
45. I. Mendieta, M. R. Nieto, R. E. Anita, J. Luis, M. Arredondo, G. G. Alcocer, C. L. Berumen, *Acta Histochemica* **2021**, *123*, 151797. **DOI:**10.1016/j.acthis.2021.151797
46. J. Gao, Y. Zhao, C. Wang, H. Ji, J. Yu, C. Liu, A. Liu, *Internat. J. Biol. Macromolec.* **2020**, *158*, 689–697. **DOI:**10.1016/j.ijbiomac.2020.05.016
47. P. Nunhart, E. Konkoľová, L. Janovec, R. Jendželovský, J. Vargová, J. Ševc, M. Matejová, B. Miltáková, P. Fedoročko, M. Kozurkova, *Bioorg. Chem.* **2020**, *94*, 103393. **DOI:**10.1016/j.bioorg.2019.103393

Povzetek

Pripravili smo benzo[*d*]tiazolne derivate **4a**–**c** ter jih uporabili za nadaljnjo sintezo tiofenskih derivatov **6a**–**f**. Iz njih smo pripravili arilhidrazonske derivate **8a**–**i**, ki smo jih lahko pretvorili v piridazinske derivate **9a**–**i** in **10a**–**i**. Te spojine smo reagirali s tioglikolno kislino in tako pripravili tiazolne derivate **12a**–**i** in **13a**–**i**. Iz spojin **4a**–**c** smo z reakcijo z elementarnim žveplom in fenilizotiocianatom sintetizirali še tiazolne derivate **15a**–**c**. Z nadaljnjimi reakcijami heterociklizacij smo spojino **15a** pretvorili v tiofenske derivate. Sintetizirane spojine smo preizkusili na izbranih rakastih celičnih linijah in najbolj aktivne spojine testirali proti razširjenemu setu sedemnajstih rakastih celičnih linij, ki smo jih razvrstili glede na vrsto bolezni, ki jo povzročajo. Morfološke spremembe celične linije A549 kot posledico učinkovanja spojin **13c** in **13h** smo študirali v mikrookolju pljučnega tkiva ter prišli do odličnih rezultatov.

Scientific paper

Microwave-Assisted Synthesis, Characterization, Crystal Structures and Antibacterial Activities of Zinc Complexes Derived from 5–Bromo-2-((cyclohexylimino)methyl)phenol

Wei-Guang Zhang

College of Chemistry and Chemical Engineering, Qiqihar University, Qiqihar 161006, P. R. China

** Corresponding author: E-mail: zhangweiguang1230@163.com*

Received: 03-19-2023

Abstract

A dinuclear zinc complex $[Zn_2L_2]$ (**1**), and four mononuclear zinc complexes $[ZnBr_2(LH)_2]$ (**2**), $[ZnCl_2(LH)_2]$ (**3**), $[Zn(LH)_2(NCS)_2]$ (**4**) and $[ZnI(CH_3OH)L]$ (**5**), have been prepared from the Schiff base 5-bromo-2-((cyclohexylimino) methyl)phenol (HL) by microwave irradiation method. All the zinc complexes were characterized by CHN elemental analyses, infrared and electronic spectra. Structures of the complexes were further studied by single crystal X-ray determination, which reveals that all the zinc atoms in the complexes are in tetrahedral geometry. The halide and pseudohalide anions are preferred co-ligands in the preparation of such complexes with binary ligands. The biological activity of the complexes on the bacterial strains *Bacillus subtilis*, *Staphylococcus aureus*, *Pseudomonas aeruginosa* and *Escherichia coli* was evaluated. The complexes bearing halide and pseudohalide ligands show effective activities on the bacteria strains.

Keywords: Schiff base; zinc complex; crystal structure; antibacterial activity

1. Introduction

Microwave-assisted synthesis of various organic and coordination compounds has received much attention in recent years because it can accelerate their reactions.[1] In addition, this method has obvious advantages in providing a cheap, clean and easy handling heating way in the synthesis of various types of compounds with higher yields and less reaction time by comparing with those heating at reflux in organic solvents or solvothermal method.[2] Schiff bases can be prepared by the reaction of aldehydes and primary amines. They and their complexes have suitable biomimetic properties that can mimic the structural features of active sites, and have been widely used in various fields such as biochemical reactions and biological regulation.[3] The antimicrobial and anticancer activities of Schiff bases and their metal complexes have been widely studied.[4] When bioorganic molecules or drugs are bound to metal ions, there is drastic enhance in their biomimetic properties, therapeutic effects and pharmacological properties.[5] Zinc complexes are reported to be biological active like antimicrobial and cytotoxic.[6] In this study, the synthesis, characterization and antibacterial properties of five new zinc complexes $[Zn_2L_2]$ (**1**), $[ZnBr_2(LH)_2]$ (**2**), $[ZnCl_2(LH)_2]$ (**3**), $[Zn(LH)_2(NCS)_2]$ (**4**), and $[ZnI(CH_3OH)L]$ (**5**), derived from the Schiff base 5-bromo-2-((cyclohexylimino)methyl)phenol (HL), are presented.

2. Experimental

2. 1. Materials and Physical Methods

4-Bromosalicylaldehyde, cyclohexylamine, zinc salts and ammonium thiocyanate were obtained from TCI. The solvents were of AR grade and used as received. The microwave synthesis was carried out with a WX-4000 microwave digestion system. CHN elemental analyses were performed on a Perkin-Elmer 2400 Elemental Analyzer. Infrared spectra were recorded on a Bio-Rad FTS 135 spectrophotometer with KBr pellets. UV-Vis spectra were performed on a Lambda 35 spectrometer. X-ray single crystal structure diffraction was determined with a Bruker Smart 1000 CCD diffractometer.

2. 2. Synthesis of the Complexes

All the complexes were prepared with the same method as described. 4-Bromosalicylaldehyde (0.20 g, 1.0

mmol), cyclohexylamine (0.10 g, 1.0 mmol), methanol (30 mL) and zinc salts (1.0 mmol as follows) were placed in a Teflon-lined autoclave (30 mL). The reaction mixture was maintained at 350 K and 200 W for 10 min at the cavity of the microwave reactor. Then the reaction mixture was cooled to room temperature for about 60 min. The mixture was filtered and with the filtrate to slow evaporate in air for a week. Colorless crystals were formed and collected by filtration and washed with cold methanol.

2. 2. 1. $[Zn_2L_2]$ (1)

Zinc acetate dihydrate (0.22 g, 1.0 mmol). Yield: 0.18 g (58%). Anal. Calcd. for $C_{26}H_{30}Br_2N_2O_2Zn$ (%): C, 49.75; H, 4.82; N, 4.46. Found (%): C, 49.61; H, 4.90; N, 4.52. IR data (KBr, cm^{-1}): 1616, 1587, 1515, 1451, 1427, 1395, 1287, 1170, 1150, 1132, 1065, 927, 896, 866, 845, 800, 779, 733, 620, 603, 569, 497, 454. UV-Vis data in methanol [λ_{max} (nm), ε ($L{\cdot}mol^{-1}{\cdot}cm^{-1}$)]: 225, 19375; 245, 18720; 280, 13010; 356, 5910.

2. 2. 2. $[ZnBr_2(LH)_2]$ (2)

Zinc bromide (0.23 g, 1.0 mmol). Yield: 0.38 g (48%). Anal. Calcd. for $C_{26}H_{32}Br_4N_2O_2Zn$ (%): C, 39.55; H, 4.09; N, 3.55. Found (%): C, 39.73; H, 4.15; N, 3.47. IR data (KBr, cm^{-1}): 1618, 1589, 1518, 1452, 1433, 1413, 1313, 1222, 1178, 1130, 1065, 1019, 930, 835, 778, 749, 661, 618, 550, 454. UV-Vis data in methanol [λ_{max} (nm), ε ($L{\cdot}mol^{-1}{\cdot}cm^{-1}$)]: 227, 18230; 245, 17810; 278, 9315; 360, 5230.

2. 2. 3. $[ZnCl_2(LH)_2]$ (3)

Zinc chloride (0.14 g, 1.0 mmol). Yield: 0.32 g (45%). Anal. Calcd. for $C_{26}H_{32}Br_2Cl_2N_2O_2Zn$ (%): C, 44.57; H, 4.60; N, 4.00. Found (%): C, 44.45; H, 4.54; N, 4.07. IR data (KBr, cm^{-1}): 1618, 1589, 1520, 1450, 1427, 1405, 1314, 1218, 1165, 1130, 1063, 1015, 921, 862, 763, 676, 615, 553, 500, 463. UV-Vis data in methanol [λ_{max} (nm), ε ($L{\cdot}mol^{-1}{\cdot}cm^{-1}$)]: 226, 18325; 245, 16020; 276, 11456; 360, 6020.

2. 2. 4. $[Zn(LH)_2(NCS)_2]$ (4)

Zinc acetate dihydrate (0.22 g, 1.0 mmol) and ammonium thiocyanate (0.15 g, 2.0 mmol). Yield: 0.43 g (57%). Anal. Calcd. for $C_{28}H_{32}Br_2N_4O_2S_2Zn$ (%): C, 45.09; H, 4.32; N, 7.51. Found (%): C, 44.87; H, 4.38; N, 7.38. IR data (KBr, cm^{-1}): 3138, 2093, 1621, 1586, 1523, 1463, 1432, 1393, 1365, 1342, 1287, 1233, 1189, 1143, 1060, 1015, 973, 928, 867, 799, 738, 617, 539, 471. UV-Vis data in methanol [λ_{max} (nm), ε ($L{\cdot}mol^{-1}{\cdot}cm^{-1}$)]: 220, 16850; 262, 10900; 315, 3436; 365, 1602.

2. 2. 5. $[ZnI(CH_3OH)L]$ (5)

Zinc iodide (0.32 g, 1.0 mmol). Yield: 0.27 g (54%). Anal. Calcd. for $C_{14}H_{19}BrINO_2Zn$ (%): C, 33.26; H, 3.79; N, 2.77. Found (%): C, 33.41; H, 3.70; N, 2.65. IR data

Table 1. Crystallographic data for the zinc complexes

Complex	1	2	3	4	5
Formula	$C_{26}H_{30}Br_2N_2O_2Zn$	$C_{26}H_{32}Br_4N_2O_2Zn$	$C_{26}H_{32}Br_2Cl_2N_2O_2Zn$	$C_{28}H_{32}Br_2N_4O_2S_2Zn$	$C_{14}H_{19}BrINO_2Zn$
Formula weight	627.71	789.54	700.62	745.88	505.48
Crystal system	Monoclinic	Triclinic	Triclinic	Triclinic	Triclinic
Space group	$P2_1/c$	P-1	P-1	P-1	P-1
a (Å)	13.6013(3)	9.1058(11)	9.0954(12)	9.5033(15)	9.686(2)
b (Å)	18.5360(2)	13.4278(13)	13.1170(13)	12.1423(16)	9.887(2)
c (Å)	11.0769 (1)	13.4369(13)	13.2710(13)	14.5203(19)	10.448(2)
α (°)	90	105.602(1)	104.636(1)	84.864(2)	69.630(2)
β (°)	109.700(1)	102.410(1)	102.736(1)	72.965(2)	66.647(2)
γ (°)	90	95.859(1)	96.913(1)	72.723(2)	79.268(2)
V (Å^3)	2629.19(7)	1522.9(3)	1468.0(3)	1529.7(4)	859.8(3)
λ (Å)	0.71073	0.71073	0.71073	0.71073	0.71073
ρ_{calcd} (g cm^{-3})	1.586	1.722	1.585	1.619	1.952
Z	4	2	2	2	2
μ (mm^{-1})	3.998	6.078	3.766	3.584	5.547
θ ranges (°)	1.59–25.50	1.60–25.50	1.63–25.50	1.47–25.50	2.20–25.50
Reflections collected	59148	9152	7916	9024	4596
Independent reflections	4903	5660	5410	5665	3171
Observed reflections ($I \geq 2\sigma(I)$)	3693	2999	3608	3335	2650
Restraints	0	0	0	0	1
Parameters	298	316	316	352	184
Goodness-of-fit on F^2	1.021	0.999	1.033	0.979	1.045
Final R indices [$I \geq 2\sigma(I)$]	0.0366, 0.0775	0.0520, 0.1037	0.0399, 0.0836	0.0663, 0.1810	0.0422, 0.1128
R indices (all data)	0.0578, 0.0873	0.1176, 0.1319	0.0747, 0.0952	0.1205, 0.2381	0.0507, 0.1189

Table 2. Selected bond distances (Å) and bond angles (°) for the complexes

		1	
Zn1–O1	1.918(2)	Zn1–O2	1.921(2)
Zn1–N1	2.018(3)	Zn1–N2	1.995(3)
O1–Zn1–O2	121.39(11)	O1–Zn1–N2	112.85(11)
O2–Zn1–N2	96.46(10)	O1–Zn1–N1	95.90(10)
O2–Zn1–N1	108.78(11)	N2–Zn1–N1	123.45(11)
		2	
Zn1–O1	1.955(5)	Zn1–O2	1.956(4)
Zn1–Br3	2.3457(12)	Zn1–Br4	2.3518(11)
O1–Zn1–O2	104.3(2)	O1–Zn1–Br3	114.20(14)
O2–Zn1–Br3	103.86(13)	O1–Zn1–Br4	103.14(14)
O2–Zn1–Br4	112.81(13)	Br3–Zn1–Br4	117.99(5)
		3	
Zn1–O1	1.947(2)	Zn1–O2	1.964(2)
Zn1–Cl1	2.2168(11)	Zn1–Cl2	2.2005(12)
O1–Zn1–O2	102.87(11)	O1–Zn1–Cl2	105.24(8)
O2–Zn1–Cl2	113.03(9)	O1–Zn1–Cl1	113.18(8)
O2–Zn1–Cl1	103.02(8)	Cl2–Zn1–Cl1	118.57(5)
		4	
Zn1–O1	1.953(5)	Zn1–O2	1.933(5)
Zn1–N3	1.934(7)	Zn1–N4	1.900(7)
N4–Zn1–O2	117.4(3)	N4–Zn1–N3	119.1(3)
O2–Zn1–N3	100.8(3)	N4–Zn1–O1	99.1(3)
O2–Zn1–O1	103.3(2)	N3–Zn1–O1	116.9(3)
		5	
Zn1–O1	1.951(3)	Zn1–O2	2.039(4)
Zn1–N1	1.991(4)	Zn1–I1	2.5027(8)
O1–Zn1–N1	96.57(15)	O1–Zn1–O2	97.69(15)
N1–Zn1–O2	107.00(15)	O1–Zn1–I1	118.16(11)
N1–Zn1–I1	123.84(12)	O2–Zn1–I1	109.95(10)

(KBr, cm^{-1}): 1616, 1586, 1528, 1469, 1448, 1392, 1363, 1277, 1259, 1194, 1146, 1132, 1072, 1015, 925, 896, 855, 788, 728, 686, 617, 594, 566, 507, 451. UV-Vis data in methanol [λ_{max} (nm), ε ($L \cdot mol^{-1} \cdot cm^{-1}$)]: 223, 17220; 245, 13645; 275, 7465; 363, 4000.

2. 3. X-Ray Structure Determination

X-ray single crystal diffraction were performed on the diffractometer equipped with a graphite monochromated Mo-Kα radiation (λ = 0.71073 Å) at 298(2) K. The collected data were integrated and reduced with SAINT.[7] Structures of the five complexes were solved by direct methods and refined by full-matrix least-squares based on F^2 with SHELXL.[8] The empirical absorption correction was applied with SADABS.[9] All non-H atoms were anisotropically refined. Selected crystal data for the complexes are summarized in Table 1. Coordinate bond lengths and bond angles are provided in Table 2.

2. 4. Antibacterial Assay

The Schiff base and the five zinc complexes were assayed the *in vitro* antibacterial activities against two Gram-positive bacteria strains *Staphylococcus aureus* and *Bacillus subtilis*, and two Gram-negative bacteria strains *Escherichia coli* and *Pseudomonas aeruginosa* by agar well diffusion method with the literature method.[10] The negative control is DMSO, and the positive control is Ciprofloxacin.

2. 5. Determination of Minimum Inhibitory Concentration (MIC)

MIC values of the compounds was tested through a modified agar well diffusion method.[11] A two-fold serial dilution of each compound was prepared by first reconstituting in DMSO followed by dilution in sterile distilled water to achieve a decreasing concentration range 256 μM. Each dilution (100 μL) was introduced into wells in the agar plates seeded with 100 μL of standardized inoculums

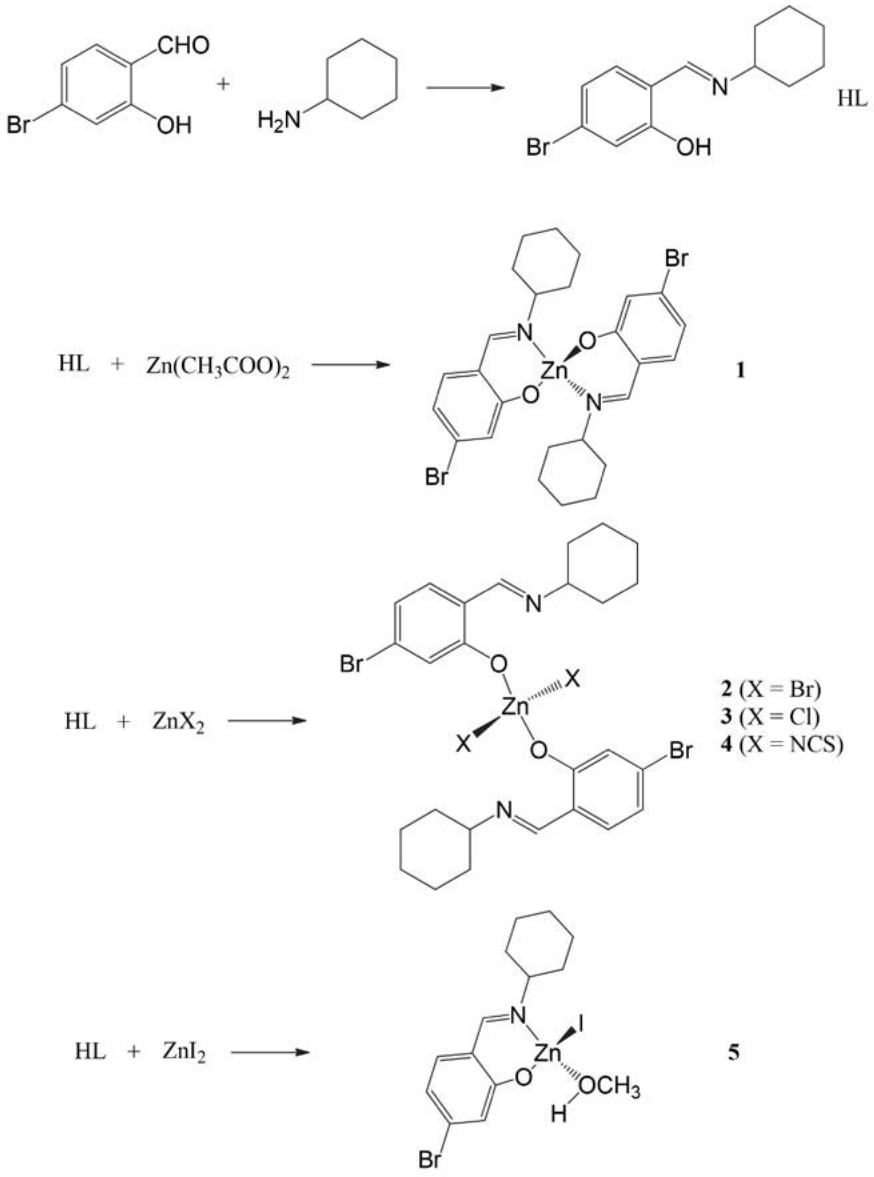

Scheme 1. The synthetic procedure for the Schiff base and the complexes.

(10^6 cfu mL^{-1}) of the microbial strain. All test plates were incubated aerobically at 37 °C for 24 h and observed for the inhibition zones.

3. Results and Discussion

3. 1. Chemistry

Reaction of in situ formed HL with zinc acetate (for **1**), zinc bromide (for **2**), zinc chloride (for **3**), zinc acetate and ammonium thiocyanate (for **4**), and zinc iodide (for **5**), respectively, afforded the complexes (Scheme 1).

3. 2. IR and UV-Vis Spectra

In the IR spectra of the complexes, the characteristic imine stretching is observed at 1616–1621 cm^{-1} as strong signals.[12] The Schiff base ligands coordination is substantiated by the phenolic C–O stretching bands at 1165–1194 cm^{-1} in the complexes.[13] Coordination of the Schiff bases is further confirmed by the appearance of weak bands in the low wave numbers 400–600 cm^{-1}, corresponding to ν(Zn–N) and ν(Zn–O).[14] The intense absorption of the thiocyanate ligands for complex **4** appears at 2093 cm^{-1}.[15]

In the UV-Vis spectra, the bands at 220–245 nm and 262–280 nm can be attributed to π–π^* and n–π^* transitions.[16] The bands at 356–365 nm are attributed to the ligand to metal charge transfer transition (LMCT).[17]

3. 3. Structure Description of Complex 1

The molecular structure of complex **1** is shown in Fig. 1. The Zn atom is coordinated by two phenolate oxygens and two imino nitrogens from two deprotonated

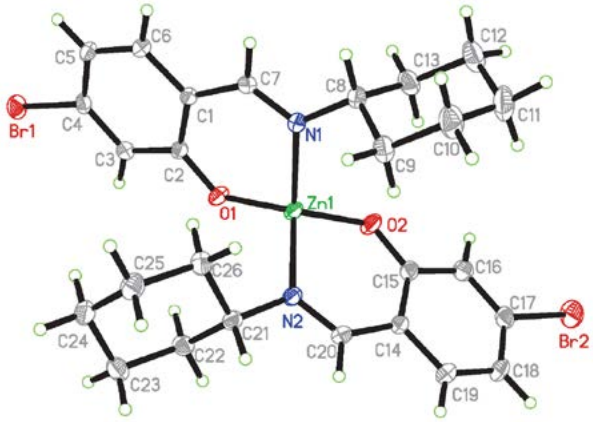

Fig. 1. Molecular structure of complex **1**. Displacement ellipsoids are drawn at the 30% probability level.

Schiff base ligands, forming tetrahedral geometry. The tetrahedral coordination is distorted from the ideal model, which can be evidenced by the bond angles, ranging from 95.90(10) to 123.45(11)°. The lengths of Zn-O bonds (1.918(2) – 1.921(2) Å) and Zn-N bonds (1.995(3) – 2.018(3) Å) are comparable to those observed in Schiff base zinc complexes with tetrahedral coordination.[18] The two six-membered chelate rings Zn1-O1-C2-C1-C7-N1 and Zn1-O2-C15-C14-C20-N2 form a dihedral angle of 80.0(3)°. The dihedral angle between the two benzene rings of the Schiff base ligands is 83.4(3)°. There are no obvious short contacts among the molecules in the crystal structure.

3. 4. Structure Description of Complexes 2, 3 and 4

The molecular structures of complexes **2**, **3** and **4** are shown in Figs. 2, 3 and 4, respectively. All the complexes are mononuclear zinc compounds. The Zn atoms in the complexes are coordinated by two phenolate oxygens from two Schiff base ligands, and two anionic ligands, *viz.* Br for **2**, Cl for **3** and NCS for **4**, forming tetrahedral geometry. The Schiff base ligand is in its zwitterionic form, with the H atom of the phenol group transferred to the N atom of the imine group, and there forms an intramolecular N-H···O hydrogen bond. The tetrahedral coordination is slightly distorted from the ideal model, which can be observed from the bond angles. The coordinate bond angles in complexes **2**, **3** and **4** are in the ranges of 103.14(14) – 117.99(5)°, 102.87(11) – 118.57(5)°, and 96.57(15) – 123.84(12)°, respectively, which are close to the value of 109°28' for a perfect tetrahedral geometry. The Zn-O, Zn-Br, Zn-Cl and Zn-N bond lengths are comparable to those observed in Schiff base zinc complexes with tetrahedral coordination.[19]

In the crystal structures of the three complexes (Figs. 5, 6, 7), the molecules are linked through hydrogen bonds (Table 3). In the packing structure of complex **2**, there is $\pi\cdots\pi$ interaction among the rings C1-C6 and C1-C6 (1 – *x*, 1 – *y*, 1 – *z*) with centroid to centroid distance of 3.904(3) Å. In the packing structure of complex **3**, there is $\pi\cdots\pi$ interaction among the rings C14-C19 and C14-C19 (1 – *x*, 1 – *y*, 1 – *z*) with centroid to centroid distance of 3.898(3) Å. In the packing structure of complex **4**, there is $\pi\cdots\pi$ interaction among the rings C1-C6 and C1-C6 (1 – *x*, 2 – *y*, – *z*) with centroid to centroid distance of 3.825(4) Å.

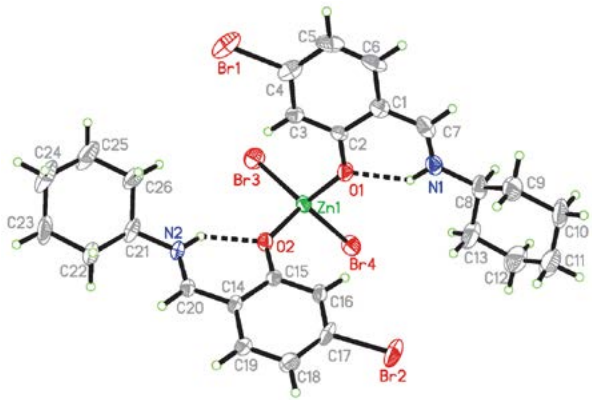

Fig. 2. Molecular structure of complex **2**. Displacement ellipsoids are drawn at the 30% probability level. Hydrogen bonds are shown as dashed lines.

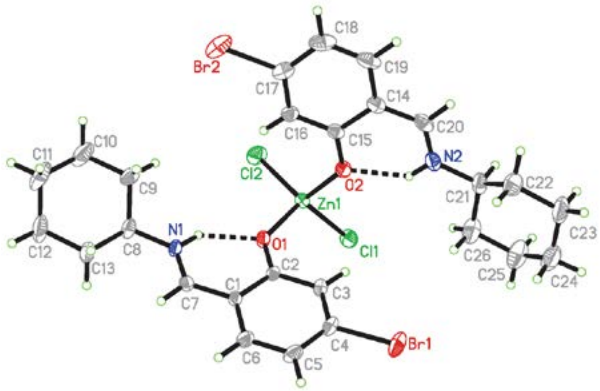

Fig. 3. Molecular structure of complex **3**. Displacement ellipsoids are drawn at the 30% probability level. Hydrogen bonds are shown as dashed lines.

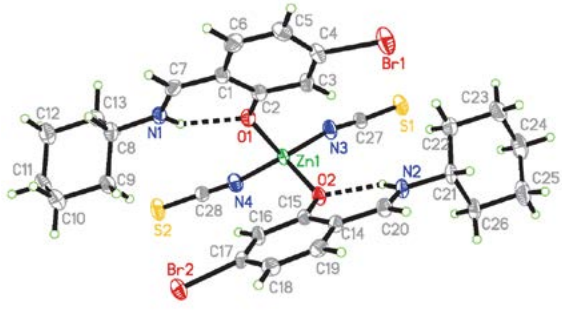

Fig. 4. Molecular structure of complex **4**. Displacement ellipsoids are drawn at the 30% probability level. Hydrogen bonds are shown as dashed lines.

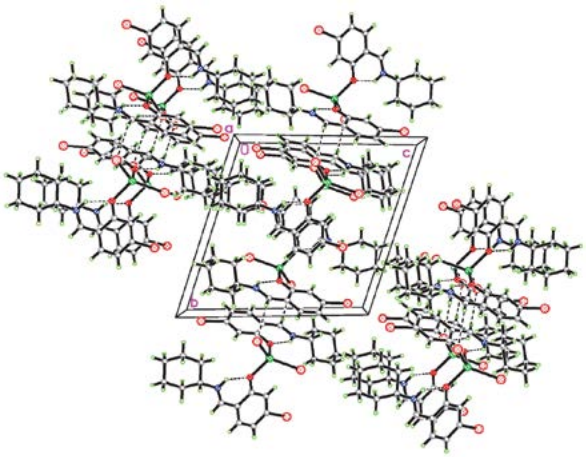

Fig. 5. Molecular packing structure of complex **2**. Hydrogen bonds are drawn as dashed lines.

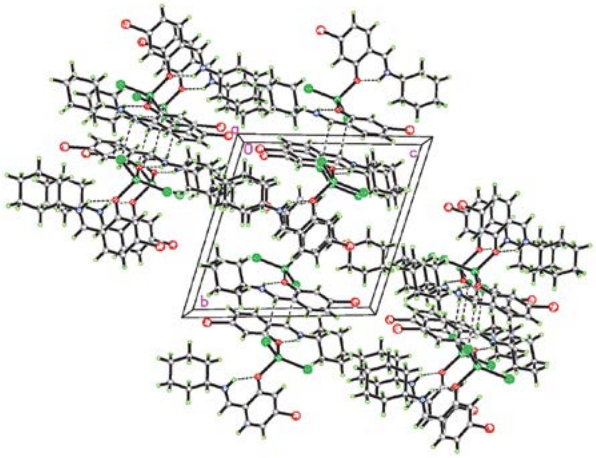

Fig. 6. Molecular packing structure of complex **3**. Hydrogen bonds are drawn as dashed lines.

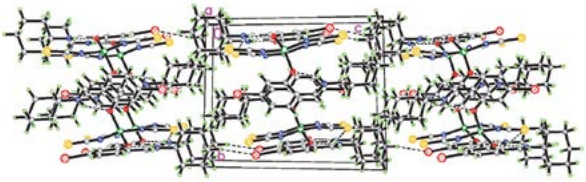

Fig. 7. Molecular packing structure of complex **4**. Hydrogen bonds are drawn as dashed lines.

3. 5. Structure Description of Complex 5

The molecular structure of the mononuclear zinc complex **5** is shown in Fig. 8. The Zn atom in the complex is coordinated by one phenolate oxygen and one imino nitrogen of a Schiff base ligand, one iodide ligand, and one methanol oxygen, forming tetrahedral geometry. The tetrahedral coordination is distorted from ideal model, which can be observed from the bond angles, ranging from 99.1(3) to 119.1(3)°. The Zn-O, Zn-N, and Zn-I bond lengths are comparable to those observed in Schiff base zinc complexes with tetrahedral coordination.[20]

As shown in Fig. 9, adjacent two molecules are linked through two O-H···O hydrogen bonds (Table 3) to form a dimer. In addition, there are $\pi\cdots\pi$ interactions among the rings C1-C6 and C1-C6 ($-x$, $1-y$, $1-z$) with centroid to centroid distance of 4.418(5) Å, and among the rings C1-C6 and C14-C19 with centroid to centroid distance of 4.893(5) Å.

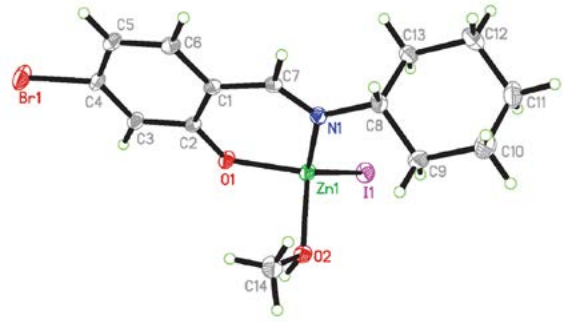

Fig. 8. Molecular structure of complex **5**. Displacement ellipsoids are drawn at the 30% probability level. Hydrogen bonds are shown as dashed lines.

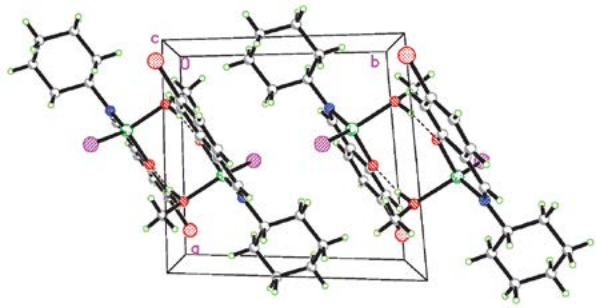

Fig. 9. Molecular packing structure of complex **5**. Hydrogen bonds are drawn as dashed lines.

Table 3. Hydrogen bond distances (Å) and bond angles (°) for the complexes

D–H···*A*	*d*(*D*–H)	*d*(H···*A*)	*d*(*D*···*A*)	Angle (*D*–H···*A*)
2				
N1–H1···O1	0.86	1.89	2.579(7)	136(5)
N2–H2···O2	0.86	1.87	2.562(6)	136(5)
3				
N1–H1···O1	0.86	1.86	2.562(3)	138(4)
N2–H2···O2	0.86	1.88	2.577(4)	136(4)
4				
O2–H2···O1^{ii}	0.85(1)	1.75(2)	2.583(4)	167(6)
5				
N1–H1···O1	0.86	1.96	2.611(8)	138(6)
N2–H2···O2	0.86	1.88	2.577(8)	136(6)

Symmetry codes: i): x, y, $1+z$; ii): $1-x$, $2-y$, $1-z$.

3. 6. Antibacterial Activities

The results of the antibacterial activities are given in Tables 4 and 5. All the complexes showed enhanced antibacterial activities as compared with the free Schiff base HL. Ciprofloxacin produced significantly sized inhibition zones against the bacteria, while DMSO produced no inhibitory effect against any of the tested organisms. HL gave inhibition zones in the range of 2.7–11.3 mm against the bacteria. The MIC results showed that complex **1** has weak activities against *Staphylococcus aureus*, *Escherichia coli* and *Pseudomonas aeruginosa*, and medium activity against *Bacillus subtilis*. Complexes **2**, **3** and **4** have similar activities against the bacterial strains, which are better than complex **1**. Complexes **2**, **3** and **4** have strong activities against *Bacillus subtilis*, *Escherichia coli* and *Pseudomonas aeruginosa*, and medium activity against *Staphylococcus aureus*. Complex **5** has strong activities against all the tested bacteria. The results of this study agree well with those reported previously that metal complexes have higher activities than their precursors.[21] The overtone's concept[22] and Tweedy's chelation theory[23] can explain the enhanced in antibacterial activity of the zinc complexes.

Table 4. Diameter of growth of inhibition zone (mm)

Compounds	*Staphylococcus aureus*	*Bacillus subtilis*	*Escherichia coli*	*Pseudomonas aeruginosa*
HL	5.3	11.3	6.2	2.7
1	8.5	13.8	8.7	6.3
2	9.7	16.9	14.3	13.2
3	10.2	17.3	14.6	12.9
4	9.4	15.5	13.1	10.6
5	13.4	19.7	21.2	16.8
Ciprofloxacin	25.0	21.3	25.2	23.3

Table 5. MIC values (μM)

Compounds	*Staphylococcus aureus*	*Bacillus subtilis*	*Escherichia coli*	*Pseudomonas aeruginosa*
HL	64	32	64	128
1	32	16	64	64
2	16	8	8	8
3	16	8	8	8
4	16	8	8	16
5	8	4	4	8
Ciprofloxacin	16	8	16	16

4. Conclusion

Five new zinc(II) complexes derived from 5-bromo-2-((cyclohexylimino)methyl)phenol have been synthesized with microwave assisted heating method. Structures of the complexes have been confirmed by X-ray single crystal determination. The complexes bearing halide and pesudohalide ligands have effective antibacterial activities on the bacteria strains *Bacillus subtilis*, *Staphylococcus aureus*, *Pseudomonas aeruginosa* and *Escherichia coli*.

Supplementary Materials

The X-ray crystallographic data in the CIF format for the structures of the complexes reported in this paper have been deposited with the Cambridge Crystallographic Data Center, and the supplementary crystallographic data can be obtained free of charge on request at www.ccdc.cam.ac.uk/conts/retrieving.html [or from The Director, Cambridge Crystallographic Data Center, CCDC, 12 Union Road, Cambridge CB2 1EZ, UK; fax: +44(0)1223-336033; email: deposit@ccdc.cam.ac.uk], quoting the CCDC numbers 2249782-2249786.

Acknowledgments

This project was supported by the Qiqihar University.

5. References

1. (a) F. Nouali, J. L. C. Sousa, H. M. T. Albuquerque, R.F. Mendes, F. A. A. Paz, L. Saher, Z. Kibou, N. Choukchou-Braham, O. Talhi, A. M.S. Silva, *J. Mol. Struct.* **2023**, *1275*, 134608; **DOI:**10.1016/j.molstruc.2022.134608
(b) I. Gurgul, O. Mazuryk, D. Rutkowska-Zbik, M. Lomzik, A. Krasowska, P. Pietrzyk, G. Stochel, M. Brindell, *Polyhedron* **2022**, *225*, 116049; **DOI:**10.1016/j.poly.2022.116049
(c) E. Gabano, M. Ravera, *Molecules* **2022**, *27*, 4249; **DOI:**10.3390/molecules27134249
(d) A. J. Winstead, K. Alabrash, B. V. Powell, S. J. Parnell, T. V. Hinton, T. Odebode, J.N. Peng, J. A. Krause, P. Y . Zavalij, S. K. Mandal, *J. Organomet. Chem.* **2021**, *936*, 121718; **DOI:**10.1016/j.jorganchem.2021.121718
(e) R.A. Krishna, R. Dheepika, M. Muralisankar, S. Nagarajan, *J. Coord. Chem.* **2021**, *74*, 838–849. **DOI:**10.1080/00958972.2021.1885650
2. (a) S.-H. Zhang, Y.-L. Zhou, X.-J. Sun, L.-Q. Wei, M.-H. Zeng, H. Liang, *J. Solid State Chem.* **2009**, *182*, 2991–2996; **DOI:**10.1016/j.jssc.2009.08.009
(b) S.-H. Zhang, C. Feng, *J. Mol. Struct.* **2010**, *977*, 62–66. **DOI:**10.1016/j.molstruc.2010.05.010
3. (a) N. Ranjitha, G. Krishnamurthy, H.S.B. Naik, M. Pari, L. Afroz, K.R. Sumadevi, M.N. Manjunatha, *Inorg. Chim. Acta* **2022**, *543*, 121191; **DOI:**10.1016/j.ica.2022.121191
(b) A. Ali, M. Pervaiz, Z. Saeed, U. Younas, R. Bashir, S. Ullah, S.M. Bukhari, F. Ali, S. Jelani, A. Rashid, A. Adnan, *Inorg. Chem. Commun.* **2022**, *145*, 109903; **DOI:**10.1016/j.inoche.2022.109903
(c) C. Maxim, C.D. Ene, I. Nicolau, L.L. Ruta, I.C. Farcasanu, *Dalton Trans.* **2022**, *51*, 18383–18399; **DOI:**10.1039/D2DT02620A

(d) K. Venkateswarlu, A. Rambabu, D.S. Shankar, P.V.A. Lakshmi, Shivaraj, *Chem. Biodivers.* **2022**, *19*, e202100686. **DOI:**10.1002/cbdv.202100686

4. (a) P. Devi, K. Singh, P. Davas, *J. Coord. Chem.* **2022**, *75*, 162–177;
(b) M. Pavlovic, E. Kahrovic, S. Arandelovic, S. Radulovic, P.P. Ilich, S. Grguric-Sipka, N. Ljubijankic, D. Ailic, J. Jurec, *J. Biol. Inorg. Chem.* **2023.**
DOI:10.1007/s00775-023-01989-0
(c) T. Ashraf, B. Ali, H. Qayyum, M.S. Haroone, G. Shabbir, *Inorg. Chem. Commun.* **2023**, *150*, 110449;
DOI:10.1016/j.inoche.2023.110449
(d) M. Yadav, D. Yadav, D.P. Singh, J.K. Kapoor, *Inorg. Chim. Acta* **2022**, *546*, 121300; **DOI:**10.1016/j.ica.2022.121300
(e) S. Esmaielzadeh, K. Shekoohi, M. Sharif-Mohammadi, G. Mashhadiagha, K. Mohammadi, *Acta Chim. Slov.* **2015**, *62*, 805–817; **DOI:**10.17344/acsi.2015.1533
(f) S.H. Sumrra, W. Zafar, S.A. Malik, K. Mahmood, S.S. Shafqat, S. Arif, *Acta Chim. Slov.* **2022**, *69*, 200–216.
5. (a) H. Kargar, *Trans. Met. Chem.* **2014**, *39*, 811–817;
DOI:10.1007/s11243-014-9863-4
(b) A. Sahraei, H. Kargar, M. Hakimi, M. N. Tahir, *J. Mol. Struct.* **2017**, *1149*, 576–584;
DOI:10.1016/j.molstruc.2017.08.022
(c) A. Sahraei, H. Kargar, M. Hakimi, M. N. Tahir, *Trans. Met. Chem.* **2017**, *42*, 483–489; **DOI:**10.1007/s11243-017-0152-x
(d) A. Jamshidvand, M. Sahihi, V. Mirkhani, M. Moghadam, I. Mohammadpoor-Baltork, S. Tangestaninejad, H. A. Rudbari, H. Kargar, R. Keshavarzi, S. Gharaghani, *J. Mol. Liquids* **2018**, *253*, 61–71; **DOI:**10.1016/j.molliq.2018.01.029
(e) H. Kargar, R. Behjatmanesh-Ardakani, V. Torabi, M. Kashani, Z. Chavoshpour-Natanzi, Z. Kazemi, V. Mirkhani, A. Sahraei, M. N. Tahir, M. Ashfaq, K. S. Munawar, *Polyhedron* **2021**, *195*, 114988; **DOI:**10.1016/j.poly.2020.114988
(f) H. Kargar, F. Aghaei-Meybodi, R. Behjatmanesh-Ardakani, M. R. Elahifard, V. Torabi, M. Fallah-Mehrjardi, M. N. Tahir, M. Ashfaq, K. S. Munawar, *J. Mol. Struct.* **2021**, *1230*, 129908; **DOI:**10.1016/j.molstruc.2021.129908
(g) H. Kargar, A. A. Ardakani, M. N. Tahir, M. Ashfaq, K. S. Munawar, *J. Mol. Struct.* **2021**, *1233*, 130112.
DOI:10.1016/j.molstruc.2021.130112
6. (a) N. Farahani, M. Khalaj, *J. Mol. Struct.* **2021**, *1228*, 129747;
DOI:10.1016/j.molstruc.2020.129747
(b) Y.-L. Sang, X.-S. Lin, W.-D. Sun, *Acta Chim. Slov.* **2020**, *67*, 581–585; **DOI:**10.17344/acsi.2019.5595
(c) F.-M. Wang, L.-J. Li, G.-W. Zang, T.-T. Deng, Z.-L. You, *Acta Chim. Slov.* **2020**, *67*, 1155–1162;
DOI:10.17344/acsi.2020.6056
(d) H. Kargar, R. Behjatmanesh-Ardakani, V. Torabi, M. Kashani, Z. Chavoshpour-Natanzi, Z. Kazemi, V. Mirkhani, A. Sahraei, M. N. Tahir, M. Ashfaq, K. S. Munawar, *Polyhedron* **2021**, *195*, 114988; **DOI:**10.1016/j.poly.2020.114988
(e) N. S. Rukk, L. G. Kuzmina, R. S. Shamsiev, G. A. Davydova, E. A. Mironova, A. M. Ermakov, G. A. Buzanov, A. Y. Skryabina, A. N. Streletskii, G. A. Vorobeva, V. M. Retivov, P. A. Volkov, S. K. Belus, E. I. Kozhukhova, V. N. Krasnoperova, *Inorg. Chim. Acta* **2019**, *487*, 184–200.
DOI:10.1016/j.ica.2018.11.036
7. Siemens, SAINT: Area Detector Control and Integration Software, Siemens Analytical X-ray Instruments Inc., Madison, WI, USA, **1996**.
8. G. M. Sheldrick, SHELXL97 and SHELXTL Software Reference Manual, Version 5.1, Brucker AXS Inc., Madison, WI, USA, **1997**.
9. G. M. Sheldrick, SADABS, University of Göttingen, Germany, **1996**.
10. K. Singh, Y. Kumar, P. Puri, C. Sharma, K. R. Aneja, *Med. Chem. Res.* **2012**, *21*, 1708–1716.
DOI:10.1007/s00044-011-9683-4
11. M. I. Okeke, C. U. Iroegbu, E. N. Eze, A. S. Okoli, C. O. Esimone, *J. Ethnopharmacol.* **2001**, *78*, 119–127.
DOI:10.1016/S0378-8741(01)00307-5
12. G. Kastas, C. A. Kastas, A. Tabak, *Spectrochim. Acta A* **2019**, *222*, 117198.
13. S. Daravath, A. Rambabu, N. Vamsikrishna, N. Ganji, S. Raj, *J. Coord. Chem.* **2019**, *72*, 1973–1993.
DOI:10.1080/00958972.2019.1634263
14. A. A. El-Sherif, A. Fetoh, Y. K. Abdulhamed, G. M. Abu El-Reash, *Inorg. Chim. Acta* **2018**, *480*, 1–15.
DOI:10.1016/j.ica.2018.04.038
15. (a) S.S. Massoud, F.A. Mautner, *Inorg. Chim. Acta* **2005**, *358*, 3334–3340; **DOI:**10.1016/j.ica.2005.05.007
(b) S. Basak, S. Sen, S. Banerjee, S. Mitra, G. Rosair, M.T. Garland Rodriguez, *Polyhedron* **2007**, *26*, 5104–5112.
DOI:10.1016/j.poly.2007.07.025
16. A. Jayamani, M. Sethupathi, S. O. Ojwach, N. Sengottuvelan, *Inorg. Chem. Commun.* **2017**, *84*, 144–149.
DOI:10.1016/j.inoche.2017.08.013
17. S. Shit, P. Talukder, J. Chakraborty, G. Pilet, M. S. El Fallah, J. Ribas, S. Mitra, *Polyhedron* **2007**, *26*, 1357–1363.
DOI:10.1016/j.poly.2006.11.013
18. (a) Y.-F. Ji, R. Wang, S. Ding, C.-F. Du, Z.-L. Liu, *Inorg. Chem. Commun.* **2012**, *16*, 47–50;
DOI:10.1016/j.inoche.2011.11.027
(b) O. Kotova, K. Lyssenko, A. Rogachev, S. Eliseeva, I. Fedyanin, L. Lepnev, L. Pandey, A. Garnovskii, A. Vitukhnovsky, M. van der Auweraer, N. Kuzmina, J. Photochem. Photobiol. A: Chem. 2011, 218, 117–129.
DOI:10.1016/j.jphotochem.2010.12.011
19. (a) Y. Luo, J. Wang, X. Ding, R. Ni, M. Li, T. Yang, J. Wang, C. Jing, Z. You, *Inorg. Chim. Acta* **2021**, *516*, 120146;
DOI:10.1016/j.ica.2020.120146
(b) Z.-L. You, Y. Lu, N. Zhang, B.-W. Ding, H. Sun, P. Hou, C. Wang, *Polyhedron* **2011**, *30*, 2186–2194;
DOI:10.1016/j.poly.2011.05.048
(c) W.-G. Zhang, J.-H. Liang, *Acta Chim. Slov.* **2021**, *68*, 921–929. **DOI:**10.17344/acsi.2021.6902
20. (a) J.-N. Li, *Synth. Inorg. Nano-Met. Chem.* **2013**, *43*, 826–831; **DOI:**10.1080/15533174.2012.750343
(b) N. Wang, L.X. Chen, L.J. Yang, Y.M. Wan, *Synth. Inorg. Nano-Met. Chem.* **2014**, *44*, 315–319.
DOI:10.1080/15533174.2013.770763

21. K. Singh, Y. Kumar, P. Puri, M. Kumar, C. Sharma, *Eur. J. Med. Chem.* **2012**, *52*, 313–321.
DOI:10.1016/j.ejmech.2012.02.053
22. N. Raman, A. Kulandaisamy, K. Jayasubramanian, *Polish J. Chem.* **2002**, *76*, 1085–1094.
23. B. G. Tweedy, *Phytopathology* **1964**, *55*, 910–915.

Povzetek

Iz Schiffove baze 5-bromo-2-((cikloheksilimino)metil)fenol (HL) smo z mikrovalovnim obsevanjem pripravili dvojedrni cinkov kompleks $[Zn_2L_2]$ (**1**) in štiri dvojedrne cinkove komplekse $[ZnBr_2(LH)_2]$ (**2**), $[ZnCl_2(LH)_2]$ (**3**), $[Zn(LH)_2(NCS)_2]$ (**4**) in $[ZnI(CH_3OH)L]$ (**5**). Vse komplekse smo karakterizirali s CHN elementno analizo, infrardečo in elektronsko spektroskopijo. Strukture produktov smo določili z monokristalno rentgensko difrakcijo, ki kaže na tetraedrično geometrijo okoli cinkovih atomov v kompleksih. Halogenidni in psevdohalogenidni anioni so pogosti koligandi v pripravi tovrstnih kompleksov z binarnimi ligandi. Preučevali smo protibakterijsko aktivnost kompleksov na bakterijah *Bacillus subtilis*, *Staphylococcus aureus*, *Pseudomonas aeruginosa* in *Escherichia coli*. Kompleksi s halogenidnimi in psevdohalogenidnimi ligandi kažejo dobro delovanje na omenjene bakterije.

DOI: 10.17344/acsi.2023.8121 *Acta Chim. Slov.* **2023,** *70,* 430–439

Scientific paper

Spectrophotometric Measurement of Lithium in Human Saliva Using the Chromogenic Reagent Thorin

Stephen R. Levitt[1,*]

School of Medicine, Case Western Reserve University, Cleveland, Ohio 44106, USA

[1] Current affiliation: Pain Resource Center, Inc., Hillsborough, NC 27278

** Corresponding author: E-mail: stevelevitt@earthlink.net*

Received: 03-07-2023

Abstract

The feasibility of using the chromogenic dye Thorin to spectrophotometrically measure lithium concentration in human saliva was explored. Absorbance wavelength maximum of the Li-Thorin complex was found to be 480 nm. Absorbance at 480 nm was obtained for saliva calibration standards containing 0.00–5.29 mEq/L of lithium. A least-squares fit produced a regression equation y = 0.128x + 1.449, R = 0.997. This was used to predict lithium concentrations in both artificially prepared lithium/saliva test solutions and in hospitalized patients treated with lithium. Results agree well with atomic absorption spectroscopy. Using a reagent blank with an equivalent amount of saliva as the test samples eliminated protein and electrolyte absorbance interference. This study supports the continued exploration of this method as a non-invasive point-of-care testing approach for monitoring saliva lithium in bipolar disorder.

Keywords: Lithium, saliva, Thorin, spectrophotometric, bipolar, colorimetric

1. Introduction

There has been a long and increasing interest over decades in measuring lithium in human biological fluids.[1–7] This is due mainly to lithium's first line use as an important psychopharmacological medicine for the acute and maintenance phase of the psychiatric illness bipolar disorder.[8] Lithium is administered orally as a lithium salt, such as lithium carbonate/sulfate/citrate/chloride. It has been shown to effectively reduce the frequency and intensity of both the mania/hypomania and depressive cycles in bipolar illness, aid in relapse prevention, as well as decrease the incidence of suicide.[9] However, lithium has the potential to be highly toxic and even deadly when its blood level exceeds the safe therapeutic range.[10–13] Therefore, lithium must be monitored frequently which requires repeated venipunctures over long periods of time.

The qualitative and quantitative determination of lithium has presented one of the more difficult problems in analytical chemistry, due mainly to the similarities of lithium to other alkali metals and alkaline earths. Over the years, early analytical techniques for measuring lithium have included gravimetric,[14] fluorometric,[15] colorimetric,[16–18] and separation techniques.[19]

Currently, the most relied-upon methods related to clinical care measure the lithium level in blood serum, and the most commonly accepted gold-standard analytical techniques are atomic absorption spectroscopy,[20] flame emission photometry,[21] and occasionally conventional ion- selective electrodes.[10]

In spite of their accuracy, these techniques present some significant limitations. These include patient scheduling and travel inconvenience, non-compliance with monitoring due to discomfort from venipuncture, time for the blood sample to be sent off to a lab or hospital, expensive equipment that requires professional training, time delays for complex sample preparation and equipment readiness, and substantial overall costs. Current methods also prevent patient self-monitoring by centralizing rather than decentralizing lithium testing.

Point-of-care testing that avoids venipuncture by using a different body fluid than blood such as saliva, urine or sweat, combined with using low-cost and user-friendly techniques with adequate accuracy would allow physicians to test in the office in a timely, non-invasive and inexpensive manner, and allow patients to self-test at home on an as-needed basis.[22]

In spite of much progress exploring many different approaches,[23–29] no point-of-care, minimally invasive, easy-to-use, cost-effective, and acceptably accurate measurement methods combined with a suitable bodily fluid testing medium, has yet been achieved.

Research has indicated the usefulness of saliva as a biological fluid medium for measuring the lithium concentration because it is found to be about 2 times the level in blood, often remains relatively constant over time in an individual, and decreases the need for frequent venipunctures.[6,30–34]

The chromogenic dye Thorin 3-hydroxy-4-[(2-arsonophenyl)diazenyl]naphthalene-2,7-disulfonate disodium salt functions as an optical ligand that combines with lithium to form a Li-Thorin complex.[22] This causes a chelation-induced shift in the absorbance spectra.[22] This organic compound is relatively selective for lithium and forms orange-colored Li-Thorin complexes in a strongly alkaline medium.[35] Thorin was first used with visual comparisons for direct lithium detection in non-biological systems in 1948.[35] This work was refined further in 1951, however using visual comparisons of colors was observed to be limited.[36]

This was followed in 1956 by the development of a spectrophotometric method using Thoron to measure lithium in a non-biological medium.[37] An acetone-water-potassium hydroxide reagent mixture was found to be sensitive and allowed reproducible testing results. The absorbance of the Li-Thoron complex using this reagent mixture was measured at 486 nm in lithium chloride test solutions. This test method was found to have an accuracy of ± 3%. Little interference was encountered by calcium and magnesium in amounts less than 10 times the lithium concentration, or by sodium in amounts 50 times the lithium concentration. Sodium in amounts 100 times that of lithium produced a positive error of 5%.[37]

In 1983 a similar spectrophotometric method using Thoron was used to measure lithium in blood serum and found it necessary to reduce absorbance interference by both removing proteins and adding a synthetic serum electrolyte to the reagent blank.[29] A thorough literature search does not reveal any prior or subsequent use of this spectrophotometric method using Thoron to measure lithium in human saliva. The present research study, conducted twenty years after this method was originally described,[37] explored the feasibility of applying this spectrophotometric method using the Li-Thorin complex to measure lithium in the biological medium, human saliva. A modification of prior methods was employed to avoid the interfering effects of protein and electrolytes in the absorption spectra.

2. Methods

2. 1. Saliva Collection*

Three methods of saliva collection are designated as Method A, Method B and Method C.

Method A: Saliva was collected from subjects not taking lithium for subsequent preparation of calibration standards. Saliva was collected at various times of the day after the subjects were without eating or smoking for two hours. The subjects then stimulated saliva production by chewing on a latex rubber band for fifteen minutes, discarding saliva produced during the first five minutes, and collecting the remainder in a polyethylene bottle. The saliva was frozen until further studies were conducted, including measurement of pH and volume produced. Fifteen mL each, from five males and five females ranging in age from 30–40, were pooled to produce 150 mL of pooled human saliva to be used for calibration standards described below.

Method B: A less time-consuming method for saliva collection, used for controls and for patients treated with lithium, involved a brief rinse of the mouth with water, waiting 15 minutes during which the subject remained without eating or smoking, and then chewing on a latex rubber-band for five minutes. The saliva was collected in two small paper cups, one used for the first two minutes and the second for the remaining three minutes of collection. The saliva specimens were transferred to capped plastic tubes and frozen until needed. Only saliva collected during the latter three minutes were used for the study.

Method C: The saliva of one hospitalized patient was collected periodically during two weeks, with the saliva being collected immediately upon awakening in the morning before placing anything in the mouth, including water or smoking. The patient chewed on a latex rubber band for five minutes, depositing the first two minutes of saliva production in one paper cup and the following three minutes in a second cup which was used for testing. The samples were transferred to capped plastic tubes and frozen until further study.

2. 2. Lithium/Saliva Calibration Sample Preparation

Lithium Chloride (LiCl), reagent grade, was added to deionized water to produce lithium chloride solutions of approximate concentrations 0.0, 5.0, 10.0, 20.0, 25.0, 30.0, 35.0, 40.0 and 50.0 mEq/L. One mL aliquots of each of these solutions were added to 9 mL of the pooled human saliva collected by Method A above, to produce saliva solutions with lithium concentrations of approximately 0.0, 0.5, 1.0, 2.0, 2.5, 3.0, 3.5, 4.0 and 5.0 mEq/L. In this way, the original electrolyte concentration of the pooled human saliva was reduced by approximately 10%, thereby remaining within the normal range, as later analysis revealed, Table 2. The lithium concentrations in each of these calibration standards was measured by atomic absorption spectroscopy described below.

2. 3. Spectrophotometric Testing of Lithium/Saliva Calibration and Test Samples

Reagents (Fisher Scientific) include potassium hydroxide (KOH), reagent grade; acetone, reagent grade;

* Saliva collection was performed in compliance with Department of Psychiatry, Case Western Reserve University

deionized water; and Thorin dye: C16H11AsN2Na-2O10S2, Lot No. 325002, J.T. Baker Chemical Company.**

Thorin, 3-hydroxy-4-[(2-arsonophenyl)diazenyl] naphthalene-2,7-disulfonate disodium salt, belongs to the class of compounds called naphthalenesulfonates which is used as a chromogen dye in the present study. The Thorin molecule, which is an azo compound, consists of a naphthylazo group (naphthalene rings with an azo linkage) and an arsenic acid group. The naphthylazo group contains a hydroxyl group (OH) and two sulfonic acid groups (HSO_3) attached to it. These groups can form hydrogen bonds and participate in various chemical reactions.

When a lithium cation (Li^+) interacts with the Thorin compound, it forms a coordination bond with one of the available oxygen atoms from the hydroxy groups or the arsenic atom to create a Li-Thorin complex. The exact coordination mode will depend on the reaction conditions and the molecular geometry of the complex. For example, a simple Li-Thorin complex could be formed by coordination of a single Thorin molecule with a lithium ion, resulting in a 1:1 complex.

The absorption spectra of Thorin undergoes a shift in frequency and intensity upon formation of the Li-Thorin complex. The absorbance is directly proportional to the concentration of the complex, which in turn reflects the concentration of lithium ions in the test medium.

The overall structure of the complex is determined by the coordination of the lithium ion to the Thorin molecule, which influences the geometry and shape of the complex. The specific arrangement of atoms and bond angles may vary depending on the experimental conditions and the nature of the complex.

The present method applied the chemical reaction protocol of prior studies using the chromogen Thorin to form a Li-Thorin complex to spectrophotometrically determine the lithium concentration in human saliva. A reagent mixture similar to that used in previous findings for lithium chloride solutions,[37] was used in the present study for both calibration standards and patient testing. Lithium/saliva calibration sample (0.1 mL) was pipetted into a 10 mL glass stoppered volumetric flask, to which was added 0.1 mL of 20% reagent grade potassium hydroxide (KOH) solution, 1.2 mL of deionized water, 3.5 mL of reagent grade acetone, and 0.3 mL of 0.2% Thorin solution. Potassium hydroxide (KOH) was used to create the necessary alkaline solution and acetone to increase the sensitivity of the result, as established in prior studies.[29–37]

Lithium/saliva calibration standards prepared in the above manner were measured against a reference blank prepared in an identical manner, including saliva, except replacing the 0.3 mL of 0.2% Thorin solution with 0.3 mL deionized water. This was done to investigate the possibility of using a patient's own saliva for both the test sample and reagent blank, thereby cancelling out interfering effects of protein and electrolyte unique to the patient. This is discussed further in Results and Discussion.

The 10 mL flasks were kept stoppered after the addition of acetone to minimize evaporation. After addition of the Thorin dye, the flasks were carefully inverted a few times for mixing and then allowed to stand for 30 minutes. The solutions were then transferred by pipette from the stoppered volumetric flask to quartz cuvettes with a 1 cm path length and equipped with covers to minimize evaporation.

The maximum absorbance wave length of the Li-Thorin complex was first determined to be 480 nm using two saliva test samples, one with 2.48 mEq/L lithium and the other with 0.00 mEq/L lithium, as measured against a water reference blank and by measuring the difference spectrum between them (see Results and Discussion, Figure 1). All subsequent absorbance measurements of calibration standards and patient test samples were made at 480 nm.

Absorbance spectra were measured utilizing a Gilford Model 2400 automatic recording spectrophotometer set on manual mode. Wavelength scale was calibrated with Holmium oxide glass filters to an accuracy of better than ±2 nm over the range of 400 to 600 nm. Absorbance was calibrated utilizing neutral density filters at 550 nm. A spectral band width of 20 nm per nm slit width at 480 nm was used, with slit widths ranging from 0.025–0.03 nm.

The absorbance intensity of the Li-Thorin complex in the calibration samples containing differing concentrations of lithium were plotted against the actual concentration of lithium in the calibration samples as determined by atomic absorption. A least-squares fit to this data resulted in a regression equation which then allowed the prediction of the concentration of lithium in subsequent studies of patient saliva test samples.

2. 4. Atomic Absorption Testing

A Perkin-Elmer Model 107 Atomic Absorption Spectrophotometer was utilized, at a frequency of 6708 Å and a slit width of 7 Å. An acetylene-air gas mixture producing an oxidizing flame was used. Harleco $LiNO_3$ standards were used for calibration, diluting the original 1000 ppm to a series of solutions between 0.4 to 2.0 ppm. Lithium concentration was recorded in mEq/L with an accuracy of ± 0.05 mEq/L. All samples were diluted ten-fold in deionized water.

3. Results and Discussion

The first goal was to determine at what wavelength does the absorbance maximum for the Li-Thorin complex occur in human saliva. The absorption spectra for the Li-Thorin complex in human saliva are shown in Fig. 1, for A)

** Warning: Thorin is rated as dangerous, acutely toxic if swallowed or inhaled, and a health and environmental (aquatic) hazard. Take all necessary precautions when using! See Supplementary Information.

2.48 mEq/L, and B) 0.00 mEq/L, over the frequency range 400 to 540 nm. The absorbance maximum in B, in the absence of lithium, occurs at 440 nm. There is an increase in absorption and a bathochromic shift to 450 nm in the presence of lithium, Spectrum A. The difference spectrum C, obtained by measuring a saliva test sample containing 2.48 mEq/L lithium against a reference blank containing 0.00 mEq/L lithium in an identical reagent medium shows a broad absorbance maximum peaking at approximately 480 nm. These results in saliva are similar to those obtained previously for pure lithium chloride/water solutions.[37] Therefore, all subsequent absorbance measurements for determination of lithium concentration in saliva were made at 480 nm.

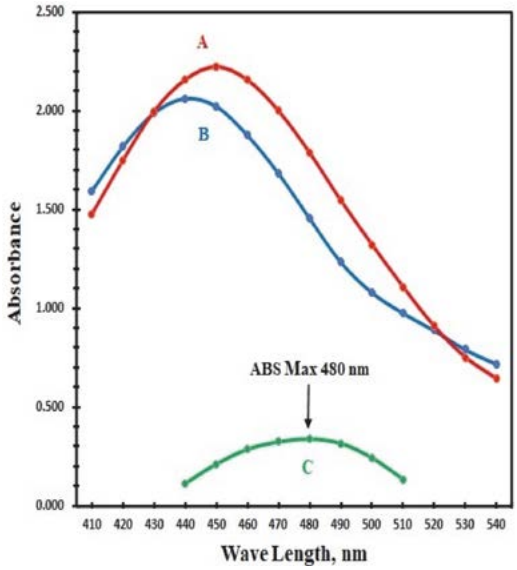

Figure 1: Absorption spectra of Li-Thorin complex in potassium hydroxide-acetone-water medium using human saliva* containing 2.48 mEq/L lithium (Spectrum A) and 0 mEq/L lithium (Spectrum B) and measured against a water reference blank. Spectrum C is the difference spectrum between Spectrum A and B.

* Saliva collected from an adult male by Method A with LiCl solution, 10% by volume, added to produce 2.48 mEq/L of lithium as determined by atomic absorption spectroscopy.

Absorbance of a pooled saliva calibration standard containing 2.42 mEq/L lithium was measured at 480 nm vs time with reference to a saliva calibration reference blank containing 0.00 mEq/L lithium. This saliva lithium concentration is equivalent to the usual maximum desired therapeutic blood level of about 1.2 mEq/L, assuming a saliva/blood ratio often found to be about 2:1.[6,30–34] Figure 2 shows that absorbance is 98% complete at 30 minutes post-reaction start. Therefore, the Li-Thorin reaction is essentially complete, within experimental error, in approximately 30 minutes agreeing with previous findings in LiCl solutions.[37] Therefore, all subsequent measurements were made at 30 minutes post reaction.

Saliva secretion rate and pH of saliva collected for the production of pooled human saliva is shown in Table 1.

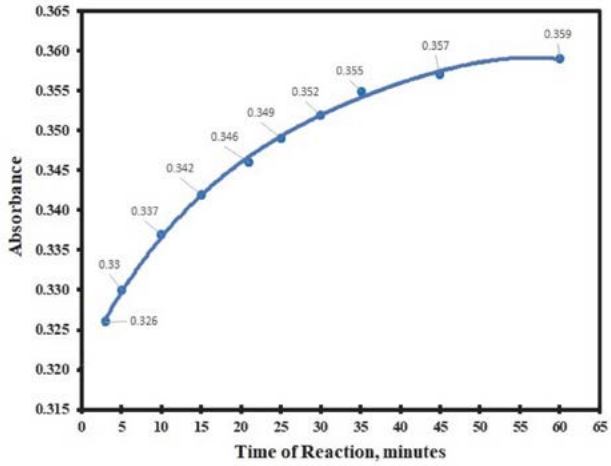

Figure 2: Absorbance vs time at 480 nm for lithium/Thorin complex using pooled saliva with 2.42 mEq/L of lithium.*

*Absorbance measured vs reference blank containing same amounts of constituents, except substituting 0.1 mL pooled human saliva containing 0 mEq/L lithium for 0.1 mL pooled saliva containing 2.42 mEq/L lithium.

Table 1: Saliva Secretion Rate and pH From Non-Patient Adults

Male			Female		
Age (years)	Secretion Rate mL/minute	pH*	Age (years)	Secretion Rate mL/minute	pH*
33	2.3	8	32	1.5	7–8
30	1.5	7–8	30	1.9	7–8
38	1.9	7–8	36	1.7	7–8
39	1.7	7	38	1.5	6–7
31	1.5	6–7	31	1.5	7

* pH measured with indicator papers

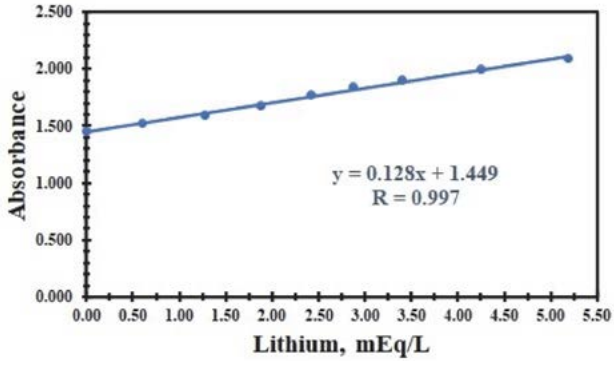

Figure 3: Absorbance at 480 nm for pooled human saliva* calibration standards containing different lithium concentrations in test solution 0.1 mL saliva, 0.1 mL 20% reagent grade KOH, 3.5 mL reagent grade acetone, 1.2 mL deionized H_2O, 0.3 mL 0.2% Thorin solution. Absorbance, 30 minutes post reaction start, measured against a reference reagent blank with same contents as the test solution except replacing 0.3 mL 2% Thorin with 0.3 mL H_2O. The Graph shows the least-squares regression equation and line calculated from absorbance means, along with slope, Y-intercept and correlation coefficient, R.

* Pooled saliva from 10 adults collected by Method A.

Table 2: Absorbance of Pooled Saliva Calibration Standards*

Li** mEg/L	Absorbance vs Reagent Blank***	Absorbance Mean	Absorbance Range	Std Deviation	Std Error of Mean
0.0	1.447				
	1.464				
	1.442				
	1.461				
	1.431	1.449	0.033	0.012	±0.005
0.61	1.524				
	1.538				
	1.514	1.525	0.024	0.010	±0.006
1.27	1.575				
	1.595				
	1.587	1.589	0.020	0.008	±0.005
1.87	1.682				
	1.688				
	1.664	1.678	0.024	0.010	±0.006
2.42	1.773				
	1.782				
	1.780	1.778	0.009	0.004	±0.002
2.88	1.865				
	1.830				
	1.844	1.846	0.035	0.014	±0.008
3.40	1.907				
	1.903				
	1.900	1.903	0.007	0.003	±0.002
4.25	1.979				
	2.008				
	2.001	1.996	0.029	0.012	±0.007
5.19	2.095				
	2.096				
	2.082	2.091	0.014	0.006	±0.004
		Average Values	0.022	0.010	±0.005

* Pooled saliva standards all contain: 16.4±1.1 mEq/L Na^+, 17.5±0.6 mEq/L K^+, 5.2±.04 mg% Ca^{++}, and 0.6±0.5 mg% Mg^{++}. Na and K determined on Corning Flame Photometer, Model 450 using propane gas and automatic dilution. Ca and Mg determined on DuPont Automatic Clinical analyzer.

** Atomic Absorption

*** Reagent blank identical to test solution except 0.3 mL of 0.2% Thorin replaced by 0.3 mL deionized H_2O

Chemical analysis of the calibration standards produced from this pooled saliva is listed at the bottom of Table 2. Three separate absorbance measurements were taken for each lithium concentration calibration standard, except for 0.00 mEq/L which had five measurements, Table 2. The average range of absorbance measurement was 0.022 with an average standard deviation of 0.010 and average standard deviation of the mean of 0.005.

The absorbance mean for each of the lithium concentrations was used in a least squares regression line calculation resulting in the calibration line plotted in Fig. 3, with slope 0.128, y-intercept 1.449 and correlation coefficient 0.997.

Measuring lithium in biological media such as saliva poses the additional problem of interference by saliva proteins and electrolytes. The protein interference can be eliminated by centrifuging the saliva test sample or precipitating out the protein. The electrolyte interference may be avoided by adding synthetic electrolytes with an average concentration of elements to the reagent blank.[29] The latter approach only approximates the electrolytes in the patient's test saliva. Furthermore, centrifuging the saliva or precipitating out the protein would add several additional steps to the measurement which would not be feasible in a point-of-care test.

This study investigated a different approach to this problem. Patient saliva was used in both the test sample and reagent blank. Therefore, the interference of both saliva proteins and electrolytes was avoided by measuring absorbance of each calibration or patient test sample with reference to a

Table 3: Predicted Li Concentration for Artificially Prepared Li-Saliva Solutions*

Li** mEq/L	Absorbance Li/Saliva vs reagent blank	Predicted Li *** mEq/L	Prediction Error mEq/L	Prediction Error %
0.00	1.445	–0.03	–0.30	–
2.05	1.742	2.29	0.24	11.7
2.48	1.777	2.56	0.08	3.2
2.73	1.823	2.92	0.19	7.0
3.58	1.916	3.65	0.07	2.0
4.26	1.984	4.18	–0.08	1.9
5.12	2.079	4.92	–0.20	3.9
		Mean	0.04	
		Standard Deviation	0.14	
		Standard Error of Mean	0.05	

* Saliva collected from one subject my Method A (see Methods)
** Atomic Absorption
*** Calculated from calibration regression equation y= 0.128x + 1.449, Figure 3
Absorbance reagent: 0.1 mL Li/saliva + 0.1 mL 20% KOH + 3.5 mL acetone + 1.2 mL H_2O + 0.3 mL 0.2% Thorin Reagent Blank: same as above except replace 0.3 mL 0.2% Thorin with0.3 mL H_2O

reagent blank which had the same saliva contents as the test sample. Both test sample and reference blank had an equivalent amount of saliva protein and interfering ion effects which were therefore nullified. The use of 0.1 mL of saliva allowed the lithium concentration to fall within the range satisfying Beer's law as found in previous studies.[37]

To be able to detect the lithium-Thorin complex in the calibration or patient test saliva, the 0.3 mL of 0.2% Thorin in the reagent blank was replaced by 0.3 mL water. In the absence of Thorin in the reagent blank, the lithium in the reagent blank saliva is not detected and produces no absorbance. This allows the lithium-Thorin complex in the calibration or patient test saliva to be measured. However, the absorbance of Thorin dye itself in the calibration or patient test sample will now be present, as it is not cancelled-out due to the absence of Thorin in the reagent blank. This means that the absorbance intensity of the calibration or patient saliva will be due to both the lithium-Thorin complex and due to the Thorin dye.

An absorbance value of 1.449 was found for the calibration standard containing 0.0 mEq/L lithium, Figure 3. This absorbance is due to the Thorin dye itself. Therefore, the regression line intercept at 1.449 on the y-axis represents the baseline for other absorbance measurements of calibration or patient test samples containing the lithium-Thorin complex, which will have absorbance value greater than 1.449 based on their lithium concentration.

The first attempt to utilize this calibration curve was made on a series of saliva solutions collected from one subject by saliva collection Method A, to which various

Table 4: Effect of pH on Predicted Lithium Concentration in Saliva*

pH	Absorbance vs Reagent Blank**	Predicted Li*** mEq/L	Prediction Error mEq/L	Prediction Error %
8.5	1.774	2.54	0.06	2.4
7.0	1.788	2.65	0.17	6.9
6.2	1.774	2.54	0.06	2.4
5.5	1.776	2.55	0.07	2.8
		Mean	0.09	
		Standard Deviation	0.05	
		Standard Error of Mean	0.02	

* Saliva from one subject collected by Method A with 2.48 mEq/L of lithium. Saliva Li Concentration maintained at 2.48 mEq/L for all pH values by using concentrated HCL to alter pH.
** Absorbance reagent: 0.1 mL Li/Saliva+0.1 mL 20% KOH+3.5 mL acetone+1.2 mL water+0.3 mL 0.2% Thorin. Reagent blank: same as above except replace 0.3 mL 0.2% Thorin with 0.3 mL water.
*** Calculated from calibration regression equation y = 0.128x + 1.449, Figure 3.

concentrations of lithium chloride solutions were added, Table 3. Lithium concentrations vary from 0.0 mEq/L to well into the toxic blood level range found clinically, assuming a saliva/blood lithium ratio of 2:1.[6,30–34] The mean error was found to be 0.04 mEq/L with standard deviation 0.14 mEq/L, and standard error of mean 0.05 mEq/L. Percent error in Li prediction vs atomic absorption measurements averaged less than 5%.

Using saliva from one subject collected by Method A with 2.48 mEq/L of lithium, the effect of saliva pH on accuracy of this technique is shown in Table 4. The pH was varied from 8.5 to 5.5 while maintaining a constant lithium concentration. The results demonstrate no substantial error introduced over the entire pH range found in human mixed saliva.[20] Average % error for predicted lithium was 3.6%.

Saliva was collected by Method B from nine hospitalized patients, ages 18 to 49, being treated with Li_2CO_3. The patients' duration of lithium therapy varied from one to two days up to five years. No restrictions were placed on time of saliva collection relative to the last lithium dose, time of day, or last meal, diet, or other medications. Predicted lithium levels based on this colorimetric technique and calculated errors from atomic absorption results are shown in Table 5.

Average error was 0.13 mEq/L with a standard deviation of 0.15 mEq/L and a standard error of the mean of 0.05 mEq/L. The overall average error was 6%. The predicted lithium error in mEq/L will result in a higher % error at lower actual concentrations of saliva lithium. The usual target therapeutic lithium level in blood is 0.4–1.2 mEq/L lithium, which roughly corresponds to 0.8–2.4 mEq/L saliva lithium assuming a saliva/blood ratio of about 2:1.[6,30–34] Within this range the average error in the present results is found to be 4%.

Finally, this method was used to monitor the lithium levels of a hospitalized patient (52 year old male) for 13 days starting on day 4 of the initial medication titration phase of treatment with Li_2CO_3. Treatment was initiated on Day 0 with Li_2CO_3 300 mg 1x/day. Saliva lithium monitoring began on Day 4. The Li_2CO_3 dose was increased to 300 mg 2x/day on Day 5, 300 mg 3x/day on Day 7 and 600

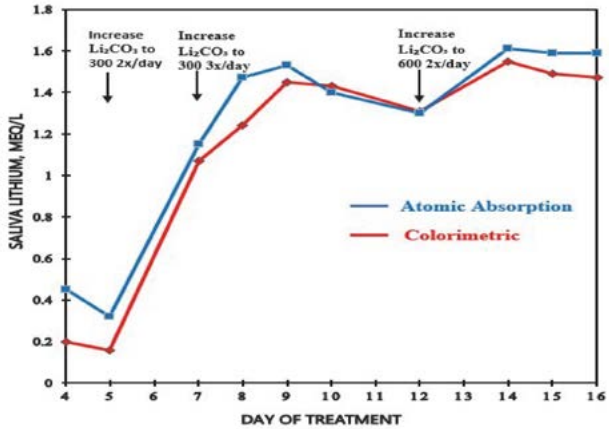

Figure 4: Comparison of Colorimetric vs Atomic Absorption Monitoring of Saliva Lithium in a Hospitalized Patient during Initial Treatment Titration with Lithium Carbonate (Li_2CO_3).*

* Male patient, age 52, admitted with diagnosis of hypomanic episode and therapy initiated with Li_2CO_3 on Day 0. Saliva levels were monitored starting on 4th day of Li therapy. Saliva collected by Method C, without any restrictions on diet or medications.

Table 5: Predicted Saliva Lithium Concentration[a] in Hospitalized Patients on Lithium Therapy[b]

Gender (M/F)	Age (yrs)	Absorbance[c] vs Reagent Blank	Predicted Li[d] (mEq/L)	Actual Li[e] (mEq/L)	Prediction Error (mEq/L)	Prediction Error (%)
M	18	1.836	3.02	3.28	–0.26	7.9
M	49	1.666	1.70	1.79	–0.09	5.0
M	30	1.594	1.13	1.18	–0.05	4.2
M	22	1.792	2.68	2.56	0.12	4.7
M	37	1.703	1.98	2.05	–0.07	3.4
M	31	1.699	1.95	1.90	0.05	2.6
F	35	1.759	2.42	2.74	–0.32	11.7
F	43	1.800	2.74	2.98	–0.24	8.1
F	33	1.811	2.83	3.10	–0.27	8.7
			Mean		0.13	
			Standard Deviation		0.15	
			Standard Error of Mean		0.05	

[a] Saliva collected by Method B
[b] Patients hospitalized at Hanna Pavilion, University Hospitals, CWRU, Cleveland Ohio and St. Lukes Hospital, Psychiatric Division, Cleveland, Ohio
[c] Absorbance test sample: 0.1 mL Saliva/Li + 0.1 mL 20% KOH + 3.5 mL acetone + 1.2 mL water +0.3 mL 0.2% Thorin. Reagent Blank: same as for Absorbance test sample except replace 0.3 mL 0.2% Thorin with 0.3 mL ionized water. Absorbance measured at 480 nm.
[d] Calculated from calibration regression equation y = 0.128x + 1.449, Figure 3.
[e] Atomic Absorption

mg 2x/day on Day 12, after which the lithium level was allowed to stabilize during Days 14–16.

A comparison of lithium concentrations predicted by this colorimetric technique with atomic absorption results is shown graphically in Fig. 4. The mean error was –0.10 mEq/L with standard deviation of 0.09 mEq/L and standard error of the mean of 0.03 mEq/L. The colorimetric results clearly show the expected increases and decreases in saliva lithium levels in response to Li_2CO_3 dosage adjustments. The overall results indicate the ability of this method to monitor saliva levels over time with reasonable accuracy.

This study suggests that several issues need further investigation to improve results. The time it takes for the Li-Thorin reaction to be completed, approximately 30 minutes, does significantly increase the time needed for test results of this method to be obtained and used. This reduces the effectiveness of this method in emergent situations, such as in an emergency room or hospital, where rapid determination of lithium toxicity is critical. Therefore, further studies to explore ways of speeding up the Li-Thorin reaction time would be helpful, such as studying the effect of temperature on the reaction time to completion

Another issue is the volatility of acetone used in the reagent mixture, which might alter test results and present difficulties in handling. The use of closed and sealed cuvettes may help. This needs further investigation for a safe and practical procedure to be developed.

The chromogen dye Thorin contains the element arsenic, and therefore is considered acutely toxic, a health and environmental risk, and a potential hazard. For this method to become practical, safe handling of Thorin containing reagents and safe ways of disposing those substances would have to be developed.

Studies of changes in saliva lithium concentration that occur with variations in how saliva production is stimulated, and with saliva pH and secretion rates, would need further investigation. How these factors might affect the saliva/blood lithium ratio would also need clarification.

Finally, the accuracy and reliability of the results found in the present study would need further improvement for clinical applications. Efforts to further refine and control sample handling and testing techniques would be helpful. Also, much larger studies in multiple venues and by different investigators would be needed to establish the general validity, reliability, and confidence in this testing method, along with developing a practical and convenient method of implementation for point-of-care use.

4. Conclusion

This study finds that a spectrophotometric method employing the chromogenic dye Thorin, in a potassium hydroxide-acetone-water reagent mixture, can be used to measure the concentration of lithium in human saliva. A regression equation for absorbance vs lithium concentration in calibration standards produced reasonably accurate predictions of lithium concentration compared to atomic absorption in both artificially prepared saliva test samples and in saliva from patients treated with lithium. Both saliva protein and electrolyte interfering effects were avoided by using an equivalent amount saliva in both the tested samples and the reagent blank. This non-invasive method of measuring lithium using saliva, instead of blood, may reduce the frequency of needed venipunctures during lithium treatment and be adaptable for point-of-care monitoring. Further refinements in technique to improve accuracy and larger scale studies to reproduce, validate and extend the present findings may now be explored, including adaptability and applicability to different clinical settings including patient self-monitoring.

Data Availability

All data are made available in the main manuscript along with additional background data supporting the reported findings uploaded as Supplementary Materials.

Author Contributions

SRL: conceived the project idea, background literature search, designed and conducted the experiments, saliva collection, calibration and test sample preparation, infrared spectroscopy, data analysis, and writing (original draft, editing and final manuscript).

Conflicts of Interest

There are no conflicts to declare.

Acknowledgments

This research project was approved and sponsored by Douglas D. Bond MD, Full Professor, former Dean School of Medicine and Chairman Department of Psychiatry, Case Western Reserve University, Cleveland, Ohio. Thank you to Robert L. Martin, MD, Department of Pathology, University Hospitals and School of Medicine, Case Western Reserve University for laboratory equipment, supplies and technical support. Thanks to John B. Sawyer, MD, David G. Logan, MD and Gottfried K. Spring, MD, Department of Psychiatry, Case Western Reserve University for allowing patient participation. Thank you to Ronald W. Chen, PhD, VA Medical Center, Cleveland, Ohio for atomic absorption measurements. Grateful appreciation to the patients and non-patient control subjects, whose cooperation made this research study possible.

5. References

1. Lehman, V., Direct determination of lithium in serum by atomic absorption spectroscopy. *Clin. Chim. Acta* **1960,** *20*, 523–525. **DOI:**10.1016/0009-8981(68)90312-4

2. Little, B. R.; Platman, S.R.; Fieve, R. R., The measurement of lithium in biologic samples by atomic absorption spectrophotometry. *Clin. Chem.* **1968,** *14*, 12, 1211–1217. **DOI:**10.1093/clinchem/14.12.1211
3. Robetson, R.; Fritze, K.; Grof, P., On the determination of lithium in blood and urine. *Clin. Chim. Acta* **1973,** *45*, 1, 25–31. **DOI:**10.1016/0009-8981(73)90140-X
4. Grime, J. K.; Vickers, T. J., Determination of lithium in microliter samples of blood serum using flame atomic emission spectrometry with a tantalum filament vaporizer, *Anal. Chem.* **1975,** *47*, 432–435. **DOI:**10.1021/ac60353a031
5. Neu, C.; DiMascio, A.; Williams, D., Saliva levels: Clinical Applications. Am. J. *Psychiatry* **1975,** *132*, 66–68. **DOI:**10.1176/ajp.132.1.66
6. Ravenscroft, P.; Vozeh, S.; Weinstein, M.; Sheiner, L. B., Saliva lithium concentrations in the management of lithium therapy. *Arch. Gen. Psychiatry* **1978,** *35*, 1123–1127. **DOI:**10.1001/archpsyc.1978.01770330097009
7. Evrard, J. L.; Bauman, P.; Pera, R.; Peters-Haefeli, L., Lithium concentrations in saliva, plasma and red blood cells of patients given lithium acetate. *Acta. Psychiatry Scand*. **1978,** *58*, 67–79. **DOI:**10.1111/j.1600-0447.1978.tb06922.x
8. Shorter, E., The history of lithium therapy. *Bipolar Disord*. **2009,** *11*, 4–9. **DOI:**10.1111/j.1399-5618.2009.00706.x
9. deMendiola, X. P.; Hidalgo-Mazzei, D.; Vieta, E.; Gozalez-Pinto, A., Overview of lithium use: A nationwide survey. *Int. J. Bipolar Disord.* **2021,** *9*, 1–8. **DOI:**10.1186/s40345-020-00215-z
10. Gitlin, M., Lithium side effects and toxicity: Prevalence and management strategies. Int. J. *Bipolar Disord*. **2016,** *4*, 1–10. **DOI:**10.1186/s40345-016-0068-y
11. Camus, M.; Baron, G.; Peytavin, G.; Massias, L.; Farinotti, R., Comparison of lithium concentrations in red blood cells and plasma in samples collected for TDM, acute toxicity, or acute-on-chronic toxicity. *Eur. J. Clin. Pharmacol.* **2003,** *59*, 583–587. **DOI:**10.1007/s00228-003-0670-7
12. Couffignal, C.; Chevillard, L.; El Balkhi, S.; Cisterino, S.; Decleves, X., The pharmacokinetics of lithium. in The Science of Practice of Lithium Therapy; Malhi, G.S., Masson, M., Bellivier, F., Eds.; Springer International *Publishing: Cham, Switzerland*, **2017**; pp. 25–53. **DOI:**10.1007/978-3-319-45923-3_2
13. Ohlund, L.; Ott, M.; Oja, S.; Bergqvist, M.; Lundqvist, R.; Sandlund, M.; Renberg, E. S.; Werneke, U., Reasons for lithium discontinuation in men and women with bipolar disorder: A retrospective cohort study, *BMC Psychiatry* **2018,** *18*, 1–10. **DOI:**10.1186/s12888-018-1622-1
14. Fletcher, M. H., Determination of lithium in rocks by distillation. *Anal. Chem.* **1949,** *21*, 1, 173–175. **DOI:**10.1021/ac60025a031
15. White, C.; Fletcher, M.; Parks, J., Determination of lithium in rock. *Anal. Chem*. **1951,** *23*, 3, 478–481. **DOI:**10.1021/ac60051a024
16. Caley, E. R., The detection and estimation of small amounts of lithium. *J. Amer. Chem.* Soc. **1930,** *52*, 7, 2754–2758. **DOI:**10.1021/ja01370a024
17. McMaster, L., A further study of the preparation and properties of the ammonium salts of organic acids. *J. Amer. Chem. Soc.* **1914,** *36*, 9, 1916–1925. **DOI:**10.1021/ja02186a014
18. Nazarenko, V. A.; Filatova, V. Ya., A rapid method of semimicro-colorimetric determination of lithium in minerals and ores. Zhur. *Anal. Khim.* **1950,** *5*, 234–238.
19. Hering, H., Quantitative separation of lithium traces from calcium. *Anal. Chem. Acta* **1952**, *6*, 340–350. **DOI:**10.1016/S0003-2670(00)86954-8
20. Bowman, J., The application of resonance monochromators to the determination of lithium in blood serum by atomic absorption spectrophotometry. *Anal. Chem. Acta* **1967,** *37*, 465–471. **DOI:**10.1016/S0003-2670(01)80708-X
21. Doku, G. N.; Gadzekpo, V. P., Simultaneous determination of lithium, sodium and potassium in blood serum by flame photometric flow-injection analysis. *Talanta* **1996,** *43*, 735–739. **DOI:**10.1016/0039-9140(95)01808-5
22. Sheikh, M.; Qassem, M.; Triantis, I.; Kyriacou, P. A., Advances in the therapeutic monitoring of lithium in the management of bipolar disorder. *Sensors* **2022,** *22*, 3, 736–758. **DOI:**10.3390/s22030736
23. Bertholf, R. L., et. al., Lithium determined in serum with an ion-selective electrode. *Clin. Chem.***1988,** *34*, 1500–1502. **DOI:**10.1093/clinchem/34.7.1500
24. Vroouwe, E. X.; Luttge, R.; Berg, A. V. D., Direct measurement of lithium in whole blood using microchip capillary electrophoresis with integrated conductivity detection. *Electrophoresis* **2004,** *25*, 1660–1667. **DOI:**10.1002/elps.200405885
25. Manfro, I.D. et.al., Determination of lithium in dried blood spots and dried plasma spots by graphite furnace atomic absorption spectrometry: method development, validation and clinical application. *Talanta* **2020,** *216,* 120907–120103. **DOI:**10.1016/j.talanta.2020.120907
26. Eltayib, E. et. al., Hydrogel-forming microneedle arrays: potential for use in minimally-invasive lithium monitoring. *Eur. J. Pharm. Biopharm.* **2016,** *102* 13–131. **DOI:**10.1016/j.ejpb.2016.03.009
27. Obare, S. O.; Hollowell, A. R. E.; Murphy, C. J., Sensing strategy for lithium ion based on gold nanoparticles. *Langmuir* **2002,** *18*, 10407–10410. **DOI:**10.1021/la0260335
28. Obare, S. O.; Murphy, C. J. A., A two -color fluorescent lithium-ion sensor. *Inorg. Chem.* **2001,** *40*, 6080–6082. **DOI:**10.1021/ic010271q
29. Trautman, J. K.; Gadzekpo, V. Y P.; Christian, G. D., Spectrophotometric determination of lithium in blood serum with thoron. *Talanta* **1983,** *8*, 587–591.
30. Shopsin, B.; Gershon, S.; Pinckney, L., The Secretion of lithium in Human Mixed Saliva: Effects of ingested lithium on electrolyte distribution in saliva and serum. *Int. Pharmacopsychiatry* **1969,** *2*, 148–169. **DOI:**10.1159/000468850
31. Khare, C. B.; Sankaranarayanan, A.; Goel, A.; Khandelwal, S. K.; Srinivasa, M. R., Saliva lithium levels for monitoring lithium prophylaxis of manic-depressive psychosis. Int. *J. Clin. Pharmacol Ther. Toxicol.* **1983,** *21,* 9, 451–453.
32. Ben-Aryeh, H., Naon, H., Szargel, R., Gutman, D., Hefetz, A., Salivary lithium concentration-a tool for monitoring psychiatric patients. *Oral Surg. Oral Med. Oral Pathol.* **1980,** *50*, 2,

127–129. **DOI:**10.1016/0030-4220(80)90198-X
33. Bowden C. L.; Houston, J. P.; Shulman, R. S.; Clothier, J. M., Clinical Utility of salivary lithium concentration. *Int. Pharmacopsychiatry* **1982,** *17,* 2, 104–113. **DOI:**10.1159/000468563
34. Verghese, A.; Indrani, N.; Kuruvilla, K.; Hill, P. G., Usefulness of saliva lithium estimation. *Br. J. Psychiatry* **1977,** *130,* 148–150. **DOI:**10.1192/bjp.130.2.148
35. Kuznetsov, V. I., Color reaction for lithium. *Zhur. Anal. Khim.* **1948,** *3,* 295–302.
36. Nikolaev, A. V.; Sorokina, A. A., Colorimetric determination of lithium. *Doklady Akad. Nauk. S.S.S.R.* **1951,** *17*, 427–428.
37. Thomason, P. F. Spectrophotometric determinations of lithium. *Anal. Chem.***1956,** *28*, 1527–1530. **DOI:**10.1021/ac60118a007

Povzetek

Raziskana je bila izvedljivost uporabe kromogenega barvila Thorin za spektrofotometrično merjenje koncentracije litija v človeški slini. Ugotovili smo, da se absorpcijski maksimum kompleksa Li-Thorin nahaja pri 480 nm. Absorbanco pri 480 nm smo pomerili za umeritvene standarde sline, ki so vsebovali 0,00–5,29 mEq/L litija. Prileganje po metodi najmanjših kvadratov je dalo regresijsko enačbo y = 0,128x + 1,449, R = 0,997. To smo uporabili za napovedovanje koncentracij litija tako v umetno pripravljenih testnih raztopinah litija/sline kot pri hospitaliziranih bolnikih, zdravljenih z litijem. Rezultati se dobro ujemajo z rezultati pridobljenimi z atomsko absorpcijsko spektroskopijo. Uporaba slepega reagenta z enako količino sline kot v testnih vzorcih je odpravila motnje absorbance beljakovin in elektrolitov. Ta študija podpira nadaljnje raziskovanje te metode kot neinvazivnega pristopa testiranja na točki oskrbe za spremljanje litija v slini pri osebah z bipolarno motnjo.

DOI: 10.17344/acsi.2023.8155 *Acta Chim. Slov.* **2023,** *70,* 440–448

Scientific paper

Synthesis and Determination of Cerium(IV)-Reducing Antioxidant Capacity (CERAC) Assay of Some New Anthraquinones

Necla Bektas*,[1] and Nihal Onul[2]

[1] *Department of Chemistry, Istanbul Technical University, Maslak, 34469, Istanbul, Turkey*

[2] *Department of Chemistry, Istanbul University-Cerrahpasa, Avcilar, Istanbul, Turkey*

* *Corresponding author: E-mail: bektasn@itu.edu.tr*
Phone: +90 (212) (0212) 285 33 40

Received: 03-24-2023

Abstract

Novel anthraquinone-based cyclic antioxidants containing amino, thio and oxo groups were synthesized and their antioxidant capacity was determined by using the cerium(IV)-reducing antioxidant capacity (CERAC) assay. ^{1}H, ^{13}C NMR, FTIR-spectroscopy and ESI (Electrospray Ionization) mass spectrometry were used for the characterization of anthraquinone derivatives exhibiting CERAC antioxidant capacity. This study is of great importance, because the antioxidant capacity of anthraquinone compounds was analyzed for the first time by the CERAC method and CERAC-Trolox equivalent antioxidant capacity (TEAC) values were higher than that for Trolox. It should also be noted that, since all synthesized anthraquinone derivatives have the potential to find applications in terms of their biological properties due to their sulfur and nitrogen content, they will make an important contribution to the literature.

Keywords: Anthraquinone, Antioxidant, Bioactive compounds.

1. Introduction

Anthraquinones (anthracene-9,10-dione) constitute a very important class of compounds in drug production due to their high biological activities. Antioxidant, antifungal, antiviral, antimicrobial, antidiabetic are among the most interesting pharmacological activities of anthraquinone compounds; thus they have been a focus of a wide range of studies in recent years.[1–5]

In addition to their pharmacological properties, there are many natural and synthetic anthraquinone derivatives that find application for imaging devices, in cosmetics, textile, food and paint industry products.[6–8] In all these areas of use, separation processes of pollutants with redox potential by various chemical and biochemical processes can also be added.[9,10]

Antioxidants are molecules that delay or prevent damage to the cell structure by inhibiting free radical reactions or by promoting their decomposition.[11] Most heart and cancer diseases occur as a result of low antioxidant limit.[12,13] Antioxidants protect against many genetic disorders such as asthma, cancer, eczema, aging and cataracts.[14]

Nitrogen- and sulfur-containing 9,10-anthraquinone derivatives are widely used in chemistry and technology and exhibit a wide range of biological properties such as anticancer, antimicrobial and antioxidant.[15–19]

Nucleophilic substitution reactions of dichloroanthraquinones are a highly preferred type of reaction as they allow their easy functionalization. There are many studies in the literature examining the mono- and/or di-product formation conditions as a result of the selective nucleophilic substitution reaction of 1,5-dichloroanthraquinone with various nucleophiles.[20–22]

Most dichloroanthraquinone compounds have been successfully synthesized via the Buchwald–Hartwig cross-coupling reaction or by the Ullmann coupling reaction.[23–25] For this type of coupling reaction, whether the nucleophile has terminal electron-donating alkylamino groups is important for reaction efficiency. If terminal electron donor groups are absent, the reaction will take place in higher yield. For example, in a published study, the reactions of alkylphenylamine and alkylphenylsulfonamide without terminal electron-donating alkylamino groups occurred smoothly, yielding the corresponding

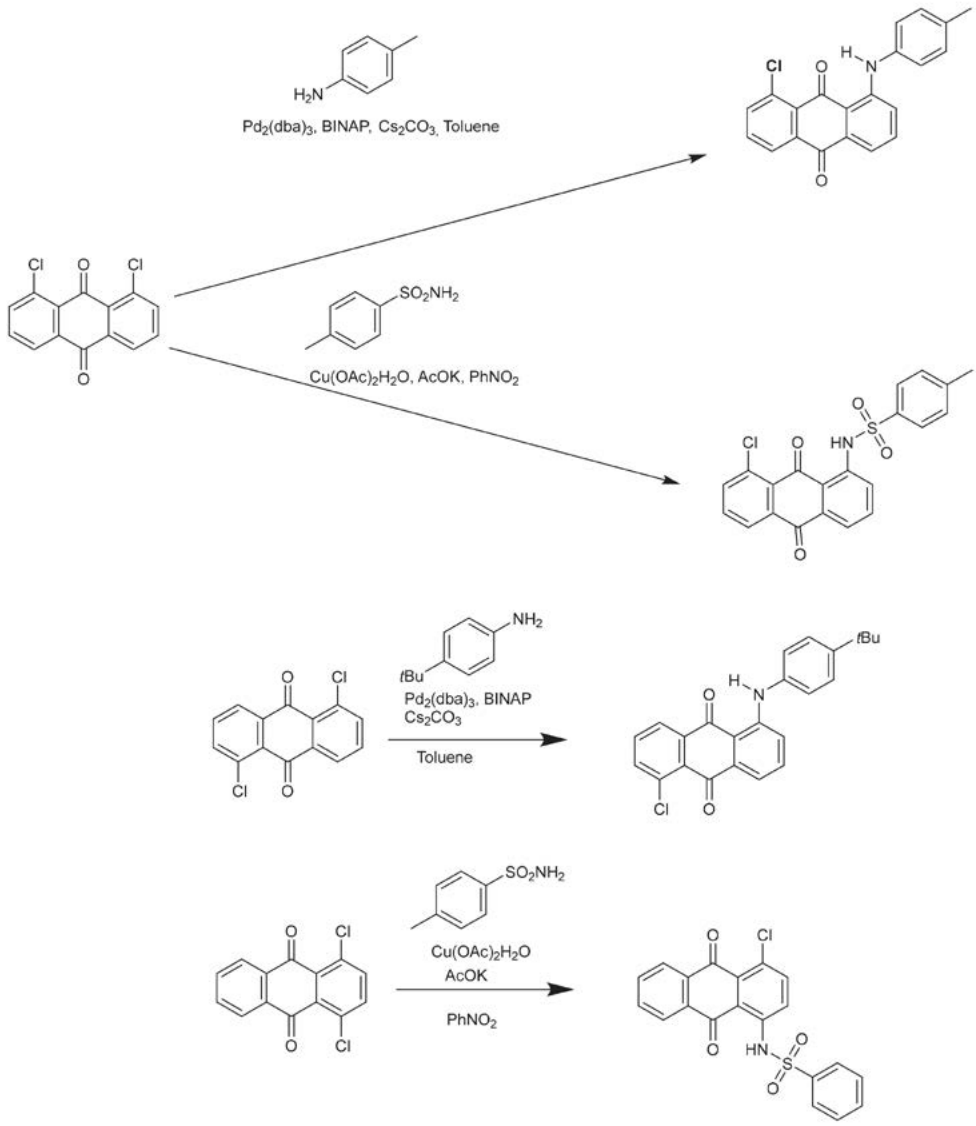

Scheme 1. Nucleophilic substitution reactions of dichloroantraquinones.

arylamino derivatives and arylsulfonamide derivatives in good yields (62–98%) (Scheme 1).[20]

The nucleophiles used can also allow the formation of the disubstituted anthraquinones along with the mono product in the reaction. For example, in the same study, nucleophiles containing a terminal *tert*-butyl group were used to increase solubility and to carry out the reaction to form 1,5-disubstituted anthraquinone derivatives. In the reaction with *N*,*N*-dimethylaminophenylsulfonamide, 1,4- and 1,8-disubstituted anthraquinone derivatives were obtained in reasonable yield, while 1,5-disubstituted product could not be obtained under the same reaction conditions. Considering that the electron donating property of the terminal NH_2 group, which is suitable for the Buchwald–Hartwig cross-coupling reaction, is reduced due to the electron accepting neighboring sulfone unit, it is concluded that this limited reactivity is due to the limited solubility of these derivatives (Scheme 2).[20,26]

Anthraquinone derivatives that can be used as antioxidants are very good electron and hydrogen donors. However, their radical structure is relatively stable due to their resonance delocalization. Interpretation of antioxidant values of anthraquinones is quite difficult due to the existence of different types of molecular radical scavenging mechanisms and their antioxidant properties depending on the structure.[27] Although the antioxidant activity determinations of anthraquinones have been studied with most of the classical methods known before, as far as we know, they have never been investigated with the CERAC assay (Table 1).[28,29]

The basis of the CERAC method is based on electron transfer between Ce(IV) and antioxidant compound in an acidic sulfate-containing medium (i.e., H_2SO_4 and Na_2SO_4). In this redox reaction, antioxidant compounds are oxidized and Ce(IV) ions are reduced to Ce(III) ions. Meanwhile, the absorbance of Ce(IV) decreases after interacting with the antioxidant molecule.[36] The reasons for

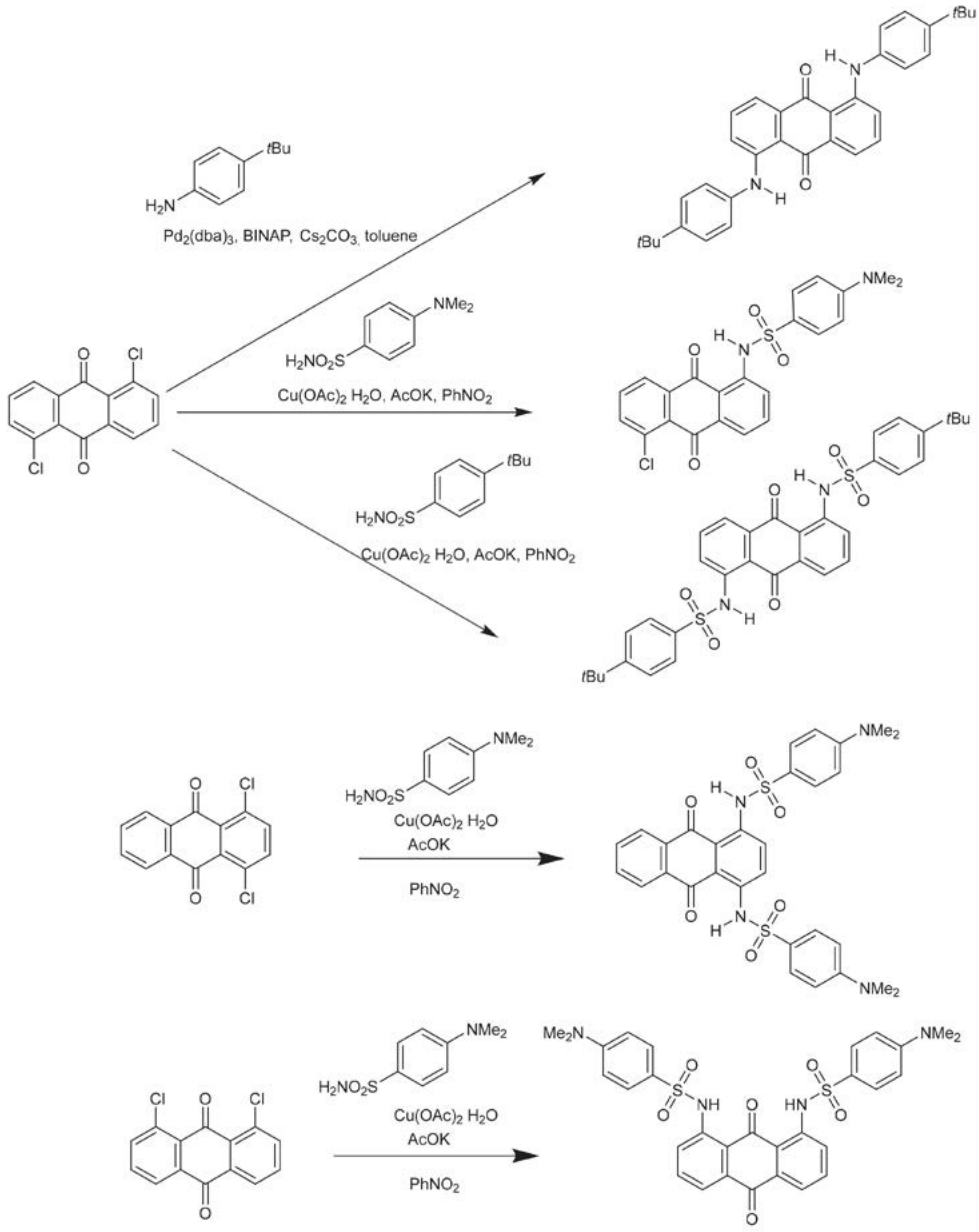

Scheme 2. Synthesis of disubstitue anthraquinones.

using sulphate media in this method are: (i) Ce(IV)/Ce(III) reduction potential is low when sulphate ions are sufficiently present; (ii) the ability of Ce(IV) to complex with organic molecules is reduced; and (iii) Ce(IV) sulphate is of long-term stability in the solutions in the environment containing H_2SO_4.[37–39]

2. Experimental

2. 1. Chemicals and Apparatus

Unless specifically indicated, all chemicals and reagents used in this study were purchased from commercial sources and used without purification. Chemicals used for synthesis and CERAC analysis of anthraquinone derivatives were: 1,5-dichloroanthraquinone, allylamine, 3,3'-diaminodiphenylsulfone, *para*-aminobenzenesulfonamide, 2-(ethylmercapto)ethanol, ethylene glycol, Trolox (Sigma-Aldrich), $Ce(SO_4)_2{\cdot}4H_2O$ and H_2SO_4 (Merck). FTIR, ESI-MS, ^1H and ^{13}C NMR spectra were recorded with Shimadzu IR Spirit Spectrophotometer, Shimadzu LC-MS 8045 Triple Quadrupole Mass Spectrometer and Agilent VNMRS 500 MHz Nuclear Magnetic Resonance Spectrophotometer, respectively. Melting points were recorded by digital melting point equipment Büchi SMP20 (B-540). CERAC antioxidant assay studies were carried out at Istanbul University Plant and Herbal Products Application and Research Center.

Table 1. Antioxidant activities and mechanisms of some anthraquinones

Anthraquinone	Experimental Method	Mechanism
Purpurin	• DPPH (1,1-diphenyl-2-picrylhydrazyl) radical scavenging capacities.	Can be associated with 3 hydroxy groups.[30]
Alizarin	• Trolox (6-Hydroxy-2,5,7,8-tetramethylchroman-2-carboxylic acid) equivalents (measure the free radical scavenging activity).	Can be associated with electron or hydrogen atom transfer.[31]
Emodin Physcion Emodin-8-*O*-β-D-idopyranoside	• DPPH radical scavenging capacities.	Can be associated with intermolecular hydrogen bridges and asidic portion's ability to donate H• and form the oxidized structure.[32]
Asphodeline anatolica *Asphodeline baytopae* *Asphodeline brevicaulis* *Asphodeline cilicica*	• Radical scavenging activities measured using DPPH radical. • Phosphomolybdenum and β-carotene bleaching methods. • ABTS (2,2'-azino-bis(3-ethylbenzthiazoline-6-sulfonic acid) radical cation were expressed as trolox equivalents. • The reducing power measured using cupric ion reducing activity (CUPRAC). • Ferric ion reducing antioxidant power (FRAP). • Metal chelating activity on ferrous ions was expressed as EDTA equivalents.	• Antioxidant molecules interact with DPPH and ABTS radicals via electron or hydrogen atom transfer, converting them to a stable structure or a non-radical species. ABTS activity can be explained as dependent on flavonoid level. • High reducing power may be attributed to high polyphenol and flavonoid content of structure.[33]
Alaternoside Physcion-8-*O*-rutinoside Rhamnocitrin	• DPPH radical scavenging capacity.	May be attributed to the higher number of hydroxyl groups.[34]
Aloe	• AAPH (2,2'-azobis(2-methylpropionamidine) dihydrochloride) were generated peroxyl radicals scavenging capacity. • CUPRAC	Reducing power may be attributed to hydrogen donating ability.[35]

2. 2. 1-Synthesis of Anthraquinone Derivatives 3a–d

Anthraquinone derivatives were synthesized by a similar method to that in the literature (Scheme 3).[40] Based on the application of this method, after adding 25 mL of ethylene glycol to the 3.6 mmole of 1,5-dichloroanthraquinone compound, nucleophile and potassium hydroxide at an equimolar ratio were added to the mixture. Thereafter the mixture was refluxed at 110–120 °C for 48 h, the product was obtained by column chromatography, if necessary, and dried in a vacuum oven at 40 °C.

2. 3. 2-Characterization of Synthesized Compounds

1-Chloro-5-(2-(ethylthio)ethoxy)anthracene-9,10-dione (3a). Obtained by the reaction of 1,5-dichloroanthraquinone (**1**) (1 g, 3.6 mmol) and 2-(ethylmercapto)ethanol (**2a**) (0.38 g, 3.6 mmol). Product is yellow solid, 0.359 g (28.72%), R_f 0.54 (ethyl acetate), m.p. 164–165 °C. FTIR (ATR, cm^{-1}): 3100 (-$CH_{aromatic}$), 2933 (-$CH_{aliphatic}$), 1650, 1583 (C=O), 1260, 1055 (C–O). ^{1}H NMR (500 MHz, DMSO-d_6): δ (ppm) 7.90–7.74 (m, 3H, -$CH_{aromatic}$), 7.60 (t, J = 7.50 Hz, 2H, -$CH_{aromatic}$), 7.27 (d, J = 8.0 Hz, H, -$CH_{aromatic}$), 4.90 (t, J = 5.40 Hz, 2H, -OCH_2), 2.48–2.40 (m, 4H, -SCH_2), 1.30–1.26 (m, 3H, -CH_3). ^{13}C NMR (126 MHz, DMSO-d_6): δ (ppm) 189.0, 182.0, 138.0, 136.0, 122.0, 118.0. ESI+: *m/z* 364.5 $[M+NH_4]^+$, $C_{18}H_{15}ClO_3S$ (M_A = 346.8 g/mol).

1-(Allylamino)-5-chloroanthracene-9,10-dione (3b). Obtained by the reaction of **1** (1 g, 3.6 mmol) and allylamine (**2b**) (0.21 g, 3.6 mmol). Product is orange solid, 0.196 g (18.32%), R_f 0.64 (ethyl acetate), m.p. 155–156 °C. FTIR (ATR, cm^{-1}): 3502 (-NH), 3080 (-$CH_{aromatic}$), 2949 (-$CH_{aliphatic}$), 1648, 1585 (C=O). ^{1}H NMR (500 MHz, DMSO-d_6): δ (ppm) 7.83–7.76 (m, 3H, -$CH_{aromatic}$), 7.62–7.58 (m, 2H, -$CH_{aromatic}$), 7.29 (dd, J_1 = 8.40 Hz, J_2 = 1.1 Hz, H, -$CH_{aromatic}$), 4.88 (bs, H, -NH), 4.17 (m, 3H, =$CH_{allylic}$, =$CH_{2allylic}$), 3.80 (t, J = 4.90 Hz, 2H, -NCH_2). ^{13}C NMR (126 MHz, DMSO-d_6): δ (ppm) 188.0, 180.0, 160.0, 161.0, 138.0, 136.0, 133.0, 122.0. ESI+: *m/z* 298.3 $[M+H]^+$, $C_{17}H_{12}ClNO_2$ (M_A = 297.7 g/mol).

4-((5-Chloro-9,10-dioxo-9,10-dihydroanthracen-1-yl) amino)benzenesulfonamide (3c). Obtained by the reaction of **1** (1 g, 3.6 mmol) and *para*-aminobenzenesulfonamide (**2c**) (0.62 g, 3.6 mmol). Product is yellow oily substance, 0.175 g (11.7%), R_f 0.60 (ethyl acetate). FTIR (ATR, cm^{-1}): 3400, 3300 (-NH), 3091 (-$CH_{aromatic}$), 1640, 1580 (C=O),

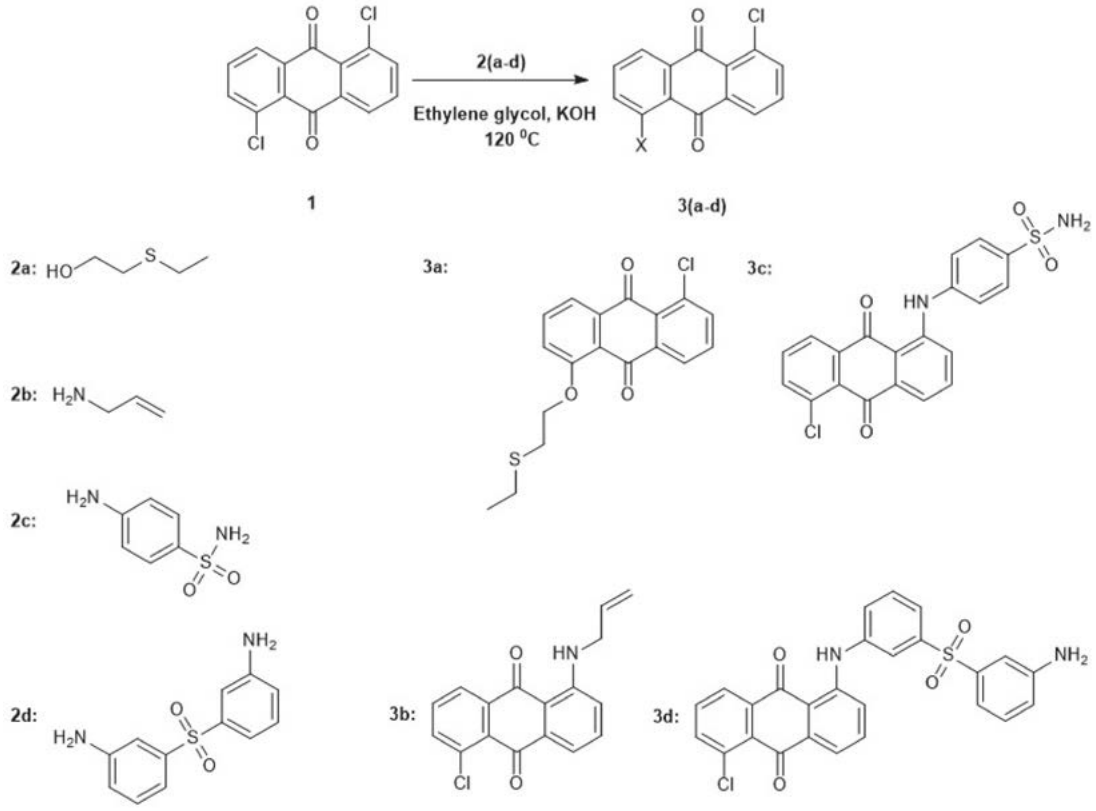

Scheme 3. Synthesized anthraquinone compounds.

1261 (S=O). ^{1}H NMR (500 MHz, DMSO-d_6): δ (ppm) 8.10 (bs, 1H, -NH), 7.85–7.75 (m, 4H, -$CH_{aromatic}$), 7.63–7.58 (m, 4H, -$CH_{aromatic}$), 7.29 (d, J = 8.0 Hz, 2H, -$CH_{aromatic}$), 4.87 (bs, 2H, -NH_2). ^{13}C NMR (126 MHz, DMSO-d_6): δ (ppm) 189.0, 181.0, 160.0, 136.0, 120.0, 118.0. ESI: m/z 414.0 $[M+H]^+$, $C_{20}H_{13}ClN_2O_4S$ (M_A = 412.8 g/mol).

1-((3-((3-Aminophenyl)sulfonyl)phenyl)amino)-5-chloroanthracene-9,10-dione (3d). Obtained by the reaction of **1** (1 g, 3.6 mmol) and 3,3'-diaminodiphenylsulfone (**2d**) (0.89 g, 3.6 mmol). Product is yellow solid, 0.136 g (7.7%), R_f 0.56 (ethyl acetate), m.p. 173–174 °C. FTIR (ATR, cm^{-1}): 3360, 3290 (-NH), 3100 (-$CH_{aromatic}$), 1740, 1680 (C=O), 1295 (S=O). ^{1}H NMR (500 MHz, DMSO-d_6): δ (ppm) 8.10 (bs, H, -NH), 7.80–7.73 (m, 4H, -$CH_{aromatic}$), 7.61–7.56 (m, 5H, -$CH_{aromatic}$), 7.27 (d, J = 8.30 Hz, 5H, -$CH_{aromatic}$), 4.89 (bs, 2H, -NH_2). ^{13}C NMR (126 MHz, DMSO-d_6): δ (ppm) 188.0, 181.0, 162.0, 160.0, 138.0, 136.0, 124.0, 116.0. ESI+: m/z 489.9 $[M+H]^+$, $C_{26}H_{17}ClN_2O_4S$ (M_A = 488.9 g/mol).

2. 4. 3-CERAC (Cerium(IV) Reduction Antioxidant Capacity) Method

The Trolox equivalent antioxidant capacity of an antioxidant molecule is the millimolar (mM) concentration of the Trolox solution, which has the same reducing power as 1 mM antioxidant solution under the same conditions. Furthermore, the measure of total antioxidant capacity (TAC) refers to the cumulative effect of all antioxidants present in the compound.[36,41]

In the laboratory study to determine the CERAC antioxidant activities of anthraquinone compounds, $Ce(SO_4)_2$ solution was added to anthraquinone solution prepared in DMSO at certain concentrations in an acidic sulfate-containing medium. After the reaction mixture was left for 30 min at room temperature, absorbance measurements were made at 320 nm, which is the maximum absorption wavelength of Ce(IV). Since the initial absorption of Ce(IV) decreases after interacting with antioxidant molecules, the ratio of the antioxidant molar absorptivity coefficient obtained from the measured absorbance values to the molar absorptivity coefficient obtained from the concentration–absorbance plot of Trolox gives the TEAC (Trolox equivalent antioxidant capacity) value.

3. Results and Discussion

In this study, we prepared systematically a series of arylaminoanthraquinone derivatives containing electron accepting sulfone units and electron donating dialkylami-

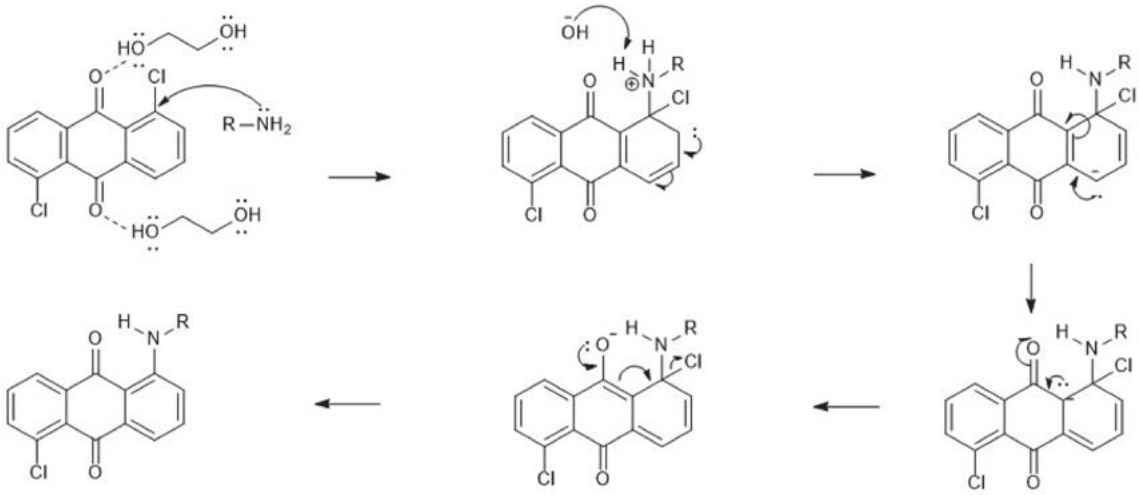

Scheme 4. Possible mechanism of nucleophilic substitution reaction.

no or oxo units, by refluxing 1,5-dichloroanthraquinone compound with amino, thio and oxo nucleophile in basic KOH medium in ethylene glycol at 110–120 °C. This synthesis method, besides being economical and practical, is a one-step (one pot synthesis) reaction and makes it possible to obtain pure products without the need for hard-to-find and expensive catalysts.[40]

Reaction between nucleophiles and 1,5-dichloroanthraquinones is driven by the S_NAr mechanism (aromatic nucleophilic substitution reaction). The hydrogen bond between the ethylene glycol and the oxygen of the carbonyl group increases the electrophilicity of the anthraquinone, facilitating the attack of the nucleophile (Scheme 4.)

Amino- and sulfur-containing derivatives of 9,10-anthraquinones have received great attention for their beneficial antioxidant properties.[16] In this context, based on this bioactivity, we preferred amino-, sulpho- and sulfur-containing nucleophiles, which can significantly affect the antioxidant properties of anthraquinones, in order to develop new and powerful biological agents of synthetic origin.

FTIR spectra of compounds **3b–d** showed clear absorption bands at 3500–3290 cm^{-1}, 1740–1580 cm^{-1} and 1583–1520 cm^{-1} belonging to υ(NH) amine, υ(C=O) and υ(C=C) aromatic, respectively. Furthermore, υ(C–O) band of **3a** and υ(S=O) bands of compound **3c–d** appeared at 1055 cm^{-1} and 1261–1295 cm^{-1}, respectively.

For compounds **3a–d**, the aromatic protons of the anthraquinone moiety gave resonance signals in ^1H NMR spectra between 7.90–7.27 ppm as multiplets, doublets and triplets. The $-OCH_2$ and $-SCH_2$ protons of compound **3a** showed resonance signals at 4.90 and 2.48–2.40 ppm, respectively. The signal of the -NH proton for compound **3b** was observed at 4.88 ppm, while it was around 8.10 ppm for both **3c** and **3d**. In addition, the $-NH_2$ proton signals for compounds **3c** and **3d** were observed at about 4.87 ppm. The carbon atom resonance signal of the carbonyl group of anthraquinone derivatives **3a–d** in ^{13}C NMR was observed in the range of 189.0–180.0 ppm. The ^1H, ^{13}C NMR and FTIR spectroscopic data of the obtained compounds are in agreement with similar anthraquinone derivatives described in the literature.[19,20,42]

The presence of an electron accepting sulpho unit between amino and aryl units, the terminal group containing an electron donating amino unit, the number and position of nitrogen and sulfur atoms in the structure contributed significantly to the decrease of yield and antioxidant activity. Since mercaptoethanol and allylamine nucleophiles do not contain terminal electron-donating alkyl amino groups, their reactions proceeded more smoothly, producing the corresponding **3a** and **3b** anthraquinone derivatives in higher yields than **3c** and **3d**. Because of the fact that, 3,3'-diaminodiphenylsulfone and *para*-aminobenzenesulfonamide contain strong electron donating alkylamino terminal groups, their reactions with 1,5-dichloroanthraquinone have not progressed completely. On the other hand, during the synthesis of **3b** not only the monoproduct (**3b**), but also the disubstituted anthraquinone derivative was formed with the removal of both chlorines as a result of the nucleophilic substitution reaction. When the synthesis of **3b** was terminated, it was observed that the amount of 1,5-dichloroanthraquinone compound still present in the reaction medium was higher than the amount of unreacted anthraquinone in the synthesis of **3c** and **3d**.

In the nucleophilic substitution reactions of **2a** and **2c** as nucleophiles reacting with 1,5-dichloroanthraquinone, it can be thought that further reactivity of the monoproduct is more suppressed due to the fact that the electron withdrawing properties of the monochloroanthraquinone derivatives (**3a** and **3c**) formed in the reaction are more reduced compared to **3b** and **3d** by the addition of electron donating nucleophiles to the anthraquinone.[20]

TEAC and TAC values of compound **1** and its syn-

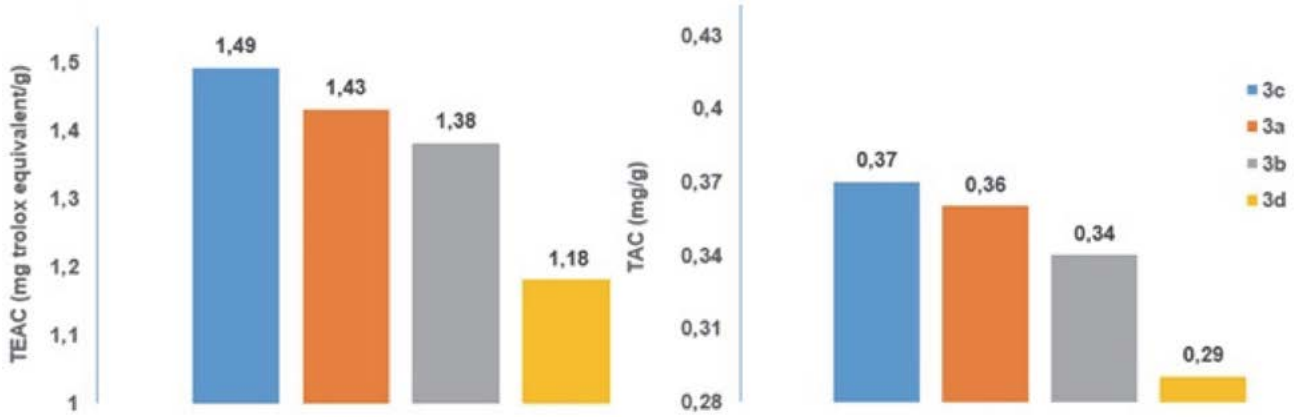

Figure 1. TEAC and TAC values of synthesized anthraquinones: blue (**3c**), orange (**3a**), grey (**3b**) and yellow (**3d**).

thesized derivatives **3a**–**d** determined by CERAC method are shown in the Figure 1.

It is difficult to interpret the antioxidant activity properties of anthraquinone compounds. Because the antioxidant effect, the radical capture molecule mechanism, may differ in terms of structure-dependent characteristics and environmental effects.[43]

Anthraquinones are good electron and proton donors. In addition, radical structures show relative stability due to the resonance delocalization.[44] In the CERAC method, electron transfer takes place.[36] According to the results of the CERAC analysis, starting 1,5-anthraquinone compound (**1**) did not exhibit antioxidant activity unlike its derivatives; this can be explained by the fact that it does not contain nitrogen and sulfur atoms in its structure.

Among the analyzed samples, compound **3c** showed the highest TEAC and TAC values determined by CERAC assay. It can be interpreted that it originates from the sulpho (O=S=O) group and -N atom in its structure. In addition, the increased stability as a result of the increase in electron density on the carbon atom to which the sulpho group is attached, through delocalization caused by the unshared electron pair in the -NH atom in this compound, may have affected the activity. Considering the free structure effects of atoms on the antioxidant activity, it can be commented that the low number of bonds of the sulfur atom in compound **3a** may have contributed to high antioxidant activity compared to **3d**.

4. Conclusıons

A simple metal-free alternative procedure for Ullmann type C–N coupling reactions has been carried out by allowing dichloroanthraquinones to react with a variety of nucleophiles in the presence of ethylene glycol. In conclusion, we have successfully developed a simple, moderate, economical and environmentally friendly procedure for the synthesis of N- and O-aryl anthraquinone derivatives under metal-free conditions.[40] The fact that the derivatives of 1,5-anthraquinone containing similar groups to those introduced by our nucleophiles have not been studied much, increases the importance of the study.[20,45,46]

In addition to what we said, the reason why the CERAC method was preferred for the determination of antioxidant activity is that it is easy, does not require a very high level of equipment, and as far as we know, the antioxidant activities of anthraquinones have never been studied with this method before. According to the results of the analysis, while the 1,5-dichloroanthraquinone starting compound (**1**) did not exhibit CERAC antioxidant activity, all the synthesized derivatives responded to the CERAC method.

Acknowledgements

We would like to thank Istanbul University Plant and Herbal Products Application and Research Center for their CERAC assay studies.

5. References

1 H. Li, J. Wei, S. Y. Pan, J. M. Gao, J. M. Tian, *Nat Prod Res.* **2014**, *28*, 2358–2361. **DOI:**10.1080/14786419.2014.940586

2 M. Masi, P. Nocera, M. C. Zonno, A. Tuzi, G. Pescitelli, A. Cimmino, A. Boari, A. Infantino, M. Vurro, A. Evidente, *J. Nat. Prod.* **2018**, *81*, 2700–2709. **DOI:**10.1021/acs.jnatprod.8b00556

3 N. Khan, F. Afroz, M. N. Begum, S.R. Rony, S. Sharmin, F. Moni, C. M. Hasan, K. Shaha, M. H. Sohrab, *Toxicol. Rep.* **2018**, *5*, 970–976. **DOI:**10.1016/j.toxrep.2018.08.016

4 A. Arvindekar, T. More, P. V. Payghan, K. Laddha, N. Ghoshal, A. Arvindekar, *Food Funct.* **2015**, *6*, 2693–2700. **DOI:**10.1039/C5FO00519A

5 X. Zhang, P.T. Thuong, W. Jin, N. D. Su, D. E. Sok, K. Bae, S.

S. Kang, *Arch. Pharm. Res.* **2005**, *28*, 22–27. **DOI:**10.1007/BF02975130
6 E. M. Malik, Y. Baqi, C. E. Müller, *Beilstein J. Org. Chem.* **2015**, *11*, 2326–2333. **DOI:**10.3762/bjoc.11.253
7 S. Patnaik, A. Swami, D. Sethi, A. Pathak, B. S. Garg, K. C. Gupta, P. Kumar, *Bioconjug. Chem.* **2007**, *18*, 8–12. **DOI:**10.1021/bc0602634
8 Y. Caro, L. Anamale, M. Fouillaud, P. Laurent, T. Petit, L. Dufosse, *Nat. Prod. Bioprospect.* **2012**, 2, 174–193. **DOI:**10.1007/s13659-012-0086-0
9 M. Uchimiya, A. T. Stone, *Chemosphere* **2009**, 77, 451–458. **DOI:**10.1016/j.chemosphere.2009.07.025
10 J. C. Forti, R. S. Rocha, M. R. V. Lanza, R. Bertazzoli, *J. Electroanal. Chem.* **2007**, *601*, 63–67. **DOI:**10.1016/j.jelechem.2006.10.023
11 I. Young, J. Woodside, *J. Clin. Pathol.* **2001**, *54*, 176–186 **DOI:**10.1136/jcp.54.3.176
12 P. M. Kris-Etherton, K. D. Hecker, A. Bonanome, S. M. Coval, A. E. Binkoski, K. F. Hilpert, A. E. Griel, T. D. Etherton, *Am. J. Med*. **2002**, *113*, 71–88. **DOI:**10.1016/S0002-9343(01)00995-0
13 D. Pal, S. Banerjee, A. K. Ghosh, *J. Adv. Pharm. Technol. Res*. **2012**, *3*, 16–24.
14 E. Lissi, M. Salim-Hanna, C. Pascual, M. D. Castillo, *Free Radic. Biol. Med*. **1995**, *18*, 153–158. **DOI:**10.1016/0891-5849(94)00117-3
15 Y. Baqi, K. Atzler, M. Köse, M. Glänzel, C. E. Müller, *J. Med. Chem*. **2009**, *52*, 3784–3793. **DOI:**10.1021/jm9003297
16 V. Zvarych, M. Stasevych, V. Lunin, N. G. Deniz, C. Sayil, M. Ozyurek, K. Guclu, M. Vovk, V. Novikov, *Monatsh. Chem.* **2016**, *147*, 2093–2101. **DOI:**10.1007/s00706-016-1839-y
17 V. Zvarych, M. Stasevych, V. Novikov, E. Rusanov, M. Vovk, P. Szweda, K. Grecka, S. Milewski, *Molecules* **2019**, *24*, 4581. **DOI:**10.3390/molecules24244581
18 M. Stasevych, V. Zvarych, V. Lunin, N. G. Deniz, Z. Gokmen, O. Akgun, E. Ulukaya, V. Poroikov, T. Gloriozova, V. Novikov, *SAR QSAR Environ. Res*. **2017**, *28*, 355–366. **DOI:**10.1080/1062936X.2017.1323796
19 A. K. Khan, J. Essa, S. M. H. Al-Majidi, *ANJS* **2016**, *19*, 25–35. **DOI:**10.1111/dome.12065
20 T. Takeda, Y. Kasahara, T. Akutagawa, *RSC Adv.* **2021**, *11*, 24217–24231. **DOI:**10.1039/D1RA03985G
21 E. H. Ruediger, M. L. Kaldas, S. S. Gandhi, C. Fedryna, M. S. Gibson, *J. Org. Chem.* **1980**, *45*, 1974–1978. **DOI:**10.1021/jo01298a044
22 I. P. Beletskaya, A. G. Bessmertnykh, A. D. Averin, F. Denat, R. Guilard, *Eur. J. Org. Chem.* **2005**, 281–305. **DOI:**10.1002/ejoc.200400456
23 J. F. Hartwig, *Synlett* **2006**, *9*, 1283–1294. **DOI:**10.1055/s-2006-939728
24 D. S. Surry, S. L. Buchwald, *Chem. Sci*. **2011**, *2*, 27–50. **DOI:**10.1039/C0SC00331J
25 S. V. Ley, A. W. Thomas, *Angew. Chem. Int. Ed.* **2003**, *42*, 5400–5449. **DOI:**10.1002/anie.200300594
26 C. Binisti, L. Assogba, E. Touboul, C. Mounier, J. Huet, J. E. Ombetta, C. Z. Dong, C. Redeuilh, F. Heymans, J. J. Godfroid, *Eur. J. Med. Chem.* **2001**, *36*, 809–828.
27 N. Boonnak, C. Karalai, S. Chantrapromma, C. Ponglimanont, H. K. Fun, A. Kanjana-Opas, S. Laphookhieo, *Tetrahedron* **2006**, *62*, 8850–8859. **DOI:**10.1016/j.tet.2006.06.003
28 Y. Li, J. G. Jiang, *Food Funct.* **2018**, *9*, 6063–6080. **DOI:**10.1039/C8FO01569D
29 B. Pongnaravane, M. Goto, M. Sasaki, T. Anekpankul, P. Pavasant, A. Shotipruk, *J. Supercrit. Fluids* **2006**, *37*, 390–396. **DOI:**10.1016/j.supflu.2005.12.013
30 W. Nam, S. P. Kim, S. H. Nam, M. Friedman, J. M. Sabatier, *Molecules* **2017**, *22*, 265. **DOI:**10.3390/molecules22020265
31 Y. Cai, M. Sun, J. Xing, H. Corke, *J. Agric. Food Chem.* **2004**, *52*, 7884–7890. **DOI:**10.1021/jf0489116
32 M. Mellado, A. Madrid, H. Peña-Cortés, R. López, C. Jara, L. Espinoza, *J. Chil. Chem. Soc.* **2013**, 58 (2). **DOI:**10.4067/S0717-97072013000200028
33 G. Zengin, M. Locatelli, R. Ceylan, A. Aktumsek, *J. Enzyme Inhib. Med. Chem.* **2016**, *31*, 754–759. **DOI:**10.3109/14756366.2015.1063623
34 R. B. Ammar, T. Miyamoto, L. Chekir-Ghedira, K. Ghedira, M. A. Lacaille-Dubois, *Nat Prod Res.* **2019**, *33*, 280–286. **DOI:**10.1080/14786419.2018.1446135
35 Y. N. Sun, W. Li, S. H. Lee, H. D. Jang, J. Y. Ma, Y. H. Kim, *Nat. Prod. Res.* **2017**, *31*, 2810–2813. **DOI:**10.1080/14786419.2017.1295238
36 D. Ozyurt, B. Demirata, R. Apak, *J. Fluoresc.* **2011**, *21*, 2069–2076. **DOI:**10.1007/s10895-011-0905-4
37 D. J. Czappa, *The Institute of Paper Chemistry* Appleton, Wisconsin, 1974.
38 B. Fang, S. Iwasa, Y. Wei, T. Arai, M. Kumagai, *Electrochim. Acta* **2002**, *47*, 3971–3976. **DOI:**10.1016/S0013-4686(02)00370-5
39 D. Ozyurt, B. Demirata, R. Apak, *Talanta* **2007**, *71*, 1155–1165. **DOI:**10.1016/j.talanta.2006.06.015
40 F. Ozkok, Y. M. Sahin, *Biyoaktif Antrakinon Anologlarının Sentezine Yönelik Özgün Metot Geliştirilmesi, TR Patent No 19610 B*, December **2016**. **DOI:**10.1016/S0891-5849(00)00394-4
41 A. Ghiselli, M. Serafini, F. Natella, C. Scaccini, *Free Radic. Biol. Med.* **2000**, *29*, 1106–1114.
42 P. L. Pant, R. K. Sonune, G. S. Shankarling, *ChemistrySelect* **2018**, *3*, 5249–5253. **DOI:**10.1002/slct.201800546
43 S. R. Jeremić, S. F. Šehović, N. T. Manojlović, Z. S. Marković, *Monatsh. Chem.* **2012**, *143*, 427–435. **DOI:**10.1007/s00706-011-0695-z
44 A. M. Shaikh, S. Chacko, R. M. Kamble, *ChemistrySelect* **2017**, *2*, 7620–7629. **DOI:**10.1002/slct.201701475
45 M. Koc, N. Kabay, *J. Porphyr. Phthalocyanines* **2022**, *26*, 19–30. **DOI:**10.1142/S1088424621500814
46 M. Kadarkaraisamy, E. Dufek, D. L. Elk, A. G. Sykes, *Tetrahedron* **2005**, *61*, 479–484. **DOI:**10.1016/j.tet.2004.10.047

Povzetek

Povzetek. Sintetizirali smo nove ciklične antioksidante, ki temeljijo na antrakinonu, in vsebujejo aminsko, tiolno in okso skupine ter določili njihovo antioksidativno kapaciteto s pomočjo CERAC testa (antioksidativna kapaciteta glede na redukcijo cerijevih(IV) ionov). Za karakterizacijo pripravljenih antrakinonskih derivatov, ki so izkazovali CERAC antioksidativno kapaciteto, smo uporabili ^{1}H, ^{13}C NMR in FTIR spektroskopijo ter ESI (ionizacija z razprševanjem v električnem polju) masno spektrometrijo. Ta študija je pomembna, saj je bila antioksidativna kapaciteta antrakinonskih derivatov prvič določena s pomočjo CERAC metode in na osnovi vrednosti CERAC-Trolox ekvivalentne antioksidativne kapacitete (TEAC); poleg tega so bile vrednosti za preučevane spojine večje kot za sam Trolox. Pomembno je tudi poudariti, da imajo pripravljene spojine potencialno biološko uporabnost, saj vsebujejo žveplove in dušikove atome, vse skupaj pa se odslikuje v pomembnosti te objave v literaturi.

Scientific paper

Novel Thiazolactone Derivatives: Synthesis and Quantum Chemical Study

Behzad Khalili* and Niloofar Bakhshi Boroon

Department of Chemistry, Faculty of Sciences, University of Guilan, P.O. Box 41335-1914, Rasht, Iran

** Corresponding author: E-mail: b.khalili@guilan.ac.ir*
Tel.:+981333367262 and fax: +981333367262

Received: 12-03-2022

Abstract

In this research, 15 novel derivatives of the thiazolactone skeleton were synthesized using the Erlenmeyer–Plöchl reaction procedure. Glycine, alanine and leucine amino acids were used to make dithiocarbamate precursor by reacting amino acids with carbon disulfide and benzyl chloride. Obtained benzyl dithiocarbamate underwent thiazolactone formation in the presence of acetic anhydride and then condensed with arylglyoxals as condensing carbonyl group source. Products were characterized using their spectroscopic IR, ^{1}H NMR, and ^{13}C NMR data. In continuation, computational chemistry methods were used to get some information about the products such as structural characteristics, charge distribution, ^{1}H NMR and UV-visible spectra. Results showed that the calculated chemical shifts are in good agreement with experimentally recorded ones. The B3LYP density functional method in conjunction with the 6-311++G(d,p) basis set was used for all calculations.

Keywords: Thiazolactone; Erlenmeyer–Plöchl reaction; Amino acids; DFT study

1. Introduction

Azlactones were synthesized for the first time in 1893 by Erlenmeyer and Plöchl by the condensation reaction between benzaldehyde and *N*-acetylglycine in the presence of acetic anhydride and sodium acetate in the manner that cyclization of the *N*-acetylglycine followed by the Perkin condensation yields the products that are called Erlenmeyer azlactones (Scheme 1).[1] Erlenmeyer azlactones have been used as precursors for many important biological and industrial compounds such as peptides, drugs, pesticides, herbicides, fungicides and agrochemical intermediates. Azlactones also show an inhibition activity against tyrosinase enzyme. Some of their diaryl derivatives show inhibition of cyclooxygenase-2 (COX-2), *in vivo* anti-inflammatory and excellent activities against of arthritis and hyperalgesia.[2–4]

Different sources of carbonyl functional group containing compounds are used to synthesize various Erlenmeyer products.[5–8] In addition modifications other than using different carbonyl compounds such as using other reagents than acetic anhydride such as triphenylphosphine[9] are used for the Erlenmeyer reaction. Preparation of oxazolones[10–12] using acetic anhydride and α-(α-haloacyl)amino acids as starting materials was reported by Bergmann and Stern.[13] *N*-Chloroacetylphenylalanine with acetic anhydride were refluxed according to the Bergmann and Stern procedure to give 4-benzylidene-2-methyl-2-oxazolin-5-one (Scheme 2).

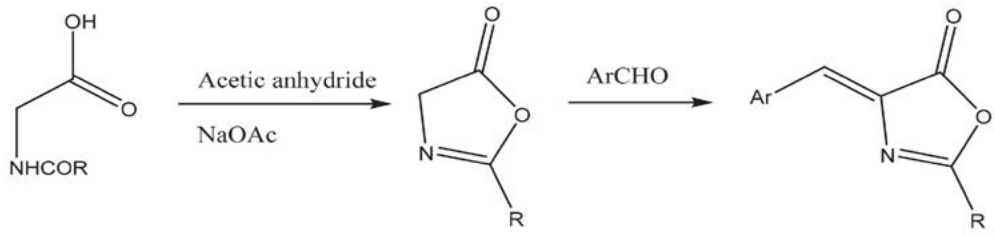

Scheme 1. Erlenmeyer–Plöchl reaction

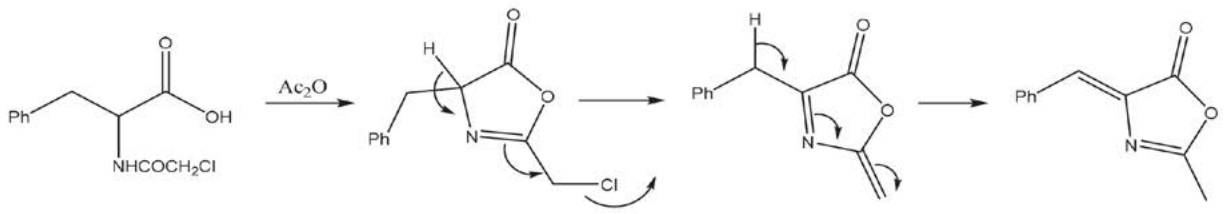

Scheme 2. Bergman reaction

Using amino acid-derived dithiocarbamates as precursors for the Erlenmeyer reaction is one of the recent modifications for acquiring different analogs of azlactones, as reported by Ziyaei *et al.*[14] In this protocol at first dithiocarbamates were synthesized using the reaction of the carbon disulfide, amino acids and an alkyl or benzyl halide. The product of the first step (alkyl/benzyl dithiocarbamate) undergoes azlactonization according to the Erlenmeyer procedure in the presence of acetic anhydride and sodium acetate followed by the reaction with an aromatic aldehyde to give corresponding products, which are thiazolones instead of oxazolones (Scheme 3). Oxazolones undergo various reactions to give important products with a variety of applications.

In this study we try to synthesize new derivatives of thiazolactones based on amino acid-derived dithiocarbamates. Arylglyoxals are used instead of simple aromatic aldehydes at the Perkin condensation step, therefor the products are conjugated enone derivatives of thiazolactones instead of their ethenyl derivatives. This modification leads to thiazolactones with broader reaction scope than the previous methods used before, because of the existence of two carbonyl compounds nearby the new carbon–carbon double bond is generated. The newly inserted carbonyl function lets the thiazolactone to undergo cyclization with an amine source such as ammonia and hydrazine to make new five and six membered heterocycles, this being the aim of our next study. Arylglyoxals are

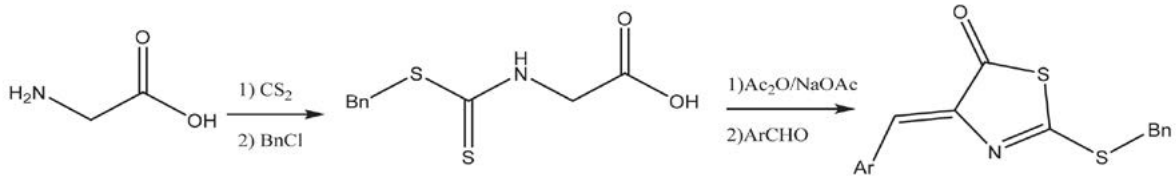

Scheme 3. Thiazolone synthesis

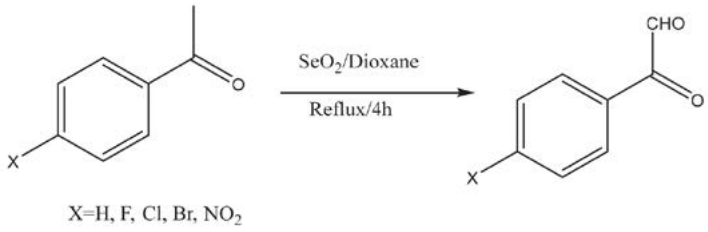

Scheme 4. Synthesis of arylglyoxals

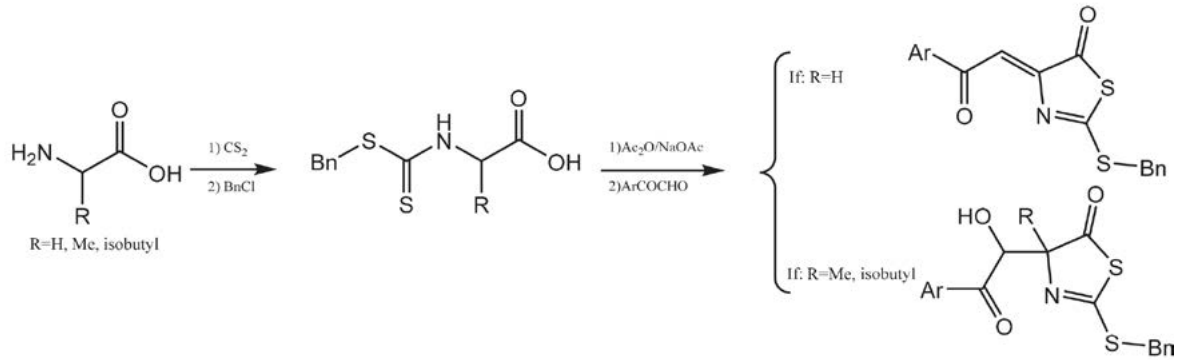

Scheme 5. Overall reaction studied here

oxidation products of the acetophenones in the presence of the selenium dioxide in dioxane as the solvent. They are used as very applicable precursors in heterocyclic synthetic chemistry.[15–22] The general reaction scheme for transforming acetophenones to glyoxals is shown in Scheme 4.

From the available acetophenones we made corresponding arylglyoxal derivatives and made use of them in the second step of the Erlenmeyer reaction of amino acid-based dithiocarbamates. The overall reaction is shown in Scheme 5.

2. Result and Discussion

In continuation of our research toward the synthesis of novel heterocyclic compounds,[16–27] herein we report an efficient synthesis of a novel class of azlactone derivatives via a one-pot reaction of amino acids, carbon disulfide, aryl or alkyl halides and arylglyoxals as outlined in Scheme 5.

Our literature survey revealed that the glyoxals have not been yet used in the Erlenmeyer reaction, therefore we used them to produce new azlactone derivatives with two carbonyl functional groups that could be promising candidates as precursors for five membered heterocycles obtained via Paal–Knorr method which makes use of 1,4-dicarbonyl compounds as the main starting material. They also can be used for the synthesis of new pyridazine derivatives if they react with hydrazine or its derivatives.

For this purpose, we investigated a one-pot reaction between arylglyoxals and the azlactone intermediates which are made during the reaction of amino acids, CS_2 and aryl/alkyl halides. At first, glycine was used as the amino acid source and its reaction with CS_2 and benzyl chloride and then phenylglyoxal in the presence of acetic anhydride and sodium acetate gave the desired products that were named as 4X-Gly where X = H, F, Cl, Br and NO_2 in this article. The reaction is performed under solvent-free conditions due to the simplicity and to improve the reaction rate.

Replacing glycine with alanine and also leucine as an amino acid source in this reaction gives products named as 4X-Ala and 4X-Leu where X = H, F, Cl, Br and NO_2, respectively. In the case of the latter two ones, elimination of the water molecule from the last product does not occur as we expected because of lacking of a hydrogen atom nearby the hydroxyl group containing carbon atom. Therefore, using alanine and leucine as amino acids gave different products than the glycine in which the hydroxyl group is present instead of a conjugated carbon-carbon double bond. Because of such differences in the product structures we may expect that the former ones incorporate substitution reactions via OH group and the latter ones incorporate an addition and also a conjugated addition reactions to make diverse derivatives with different applications. All these reveal that the described products could be very useful for discovering new organic compounds with various applications.

The reaction was carried out using the classical method in the presence of acetic anhydride and sodium acetate. Arylglyoxals including Ph, 4F-C_6H_4-, 4Cl-C_6H_4-,

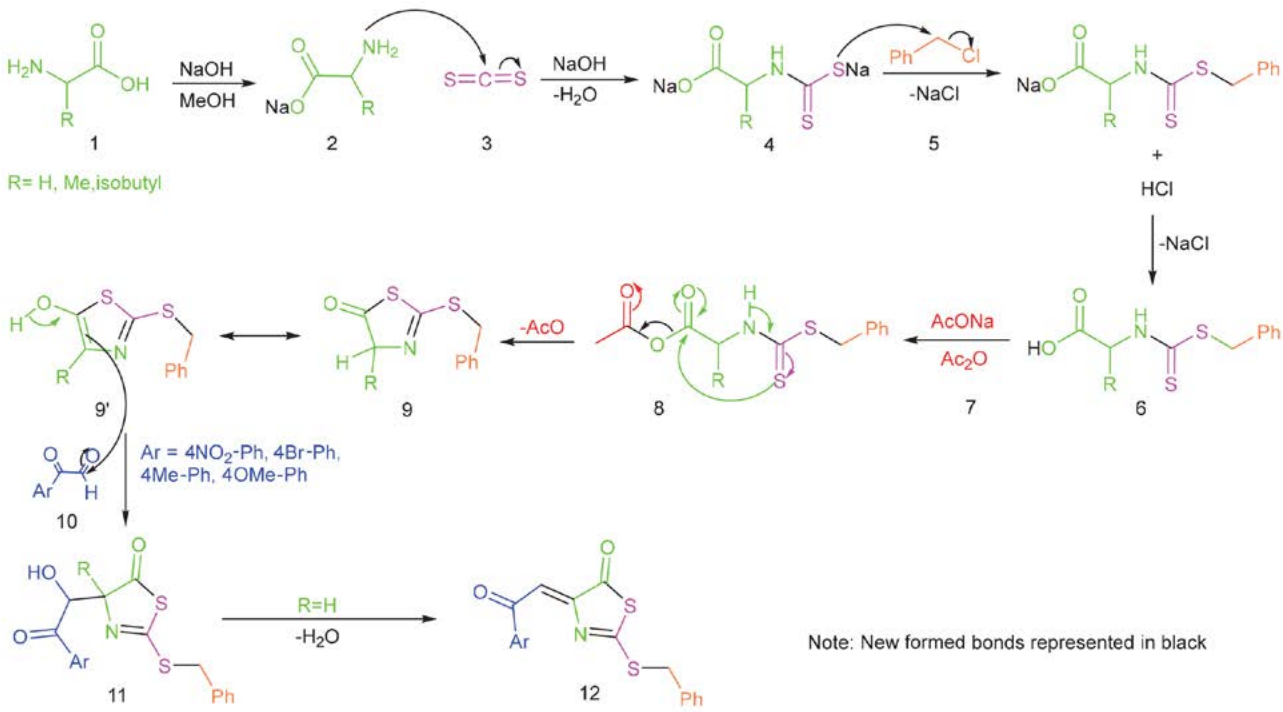

Scheme 6. Proposed mechanism

Table 1. Synthesized new thiazolactones. Optimized structure of the products are also included.

Comp.	Optimized Structure	Intramolecular Hydrogen Bond Distance (Å) & Angle (°)	Yield (%) m.p. (°C)
4H-Gly	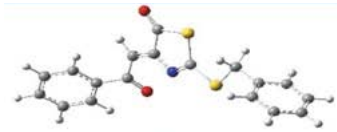	—	64 93–97
4F-Gly	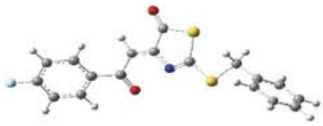	—	68 104–106
4Cl-Gly	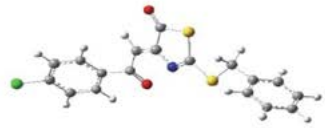	—	72 98–101
4Br-Gly		—	87 124–125
4NO_2-Gly	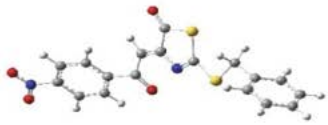	—	81 117–119
4H-Ala	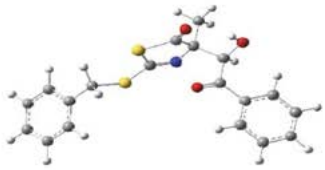	2.191 133.05	74 101–103
4F-Ala	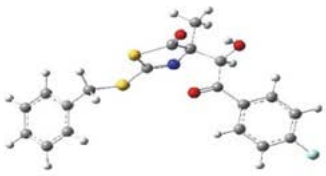	2.179 133.39	84 163–166
4Cl-Ala	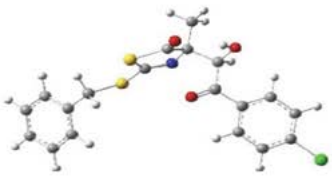	2.179 133.46	81 152–155
4Br-Ala	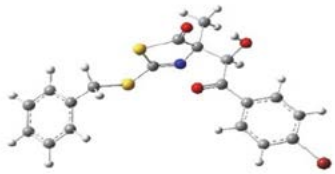	2.185 133.34	79 147–150
4NO_2-Ala	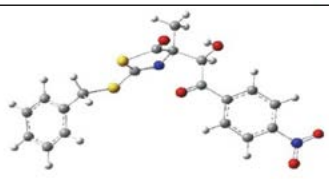	2.162 134.23	86 113–114

Comp.	Optimized Structure	Intramolecular Hydrogen Bond Distance (Å) & Angle (°)	Yield (%) m.p. (°C)
4H-Leu	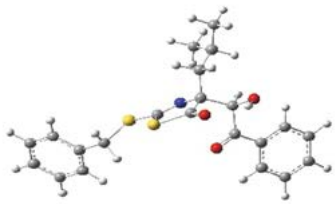	2.190 133.53	69 113–117
4F-Leu	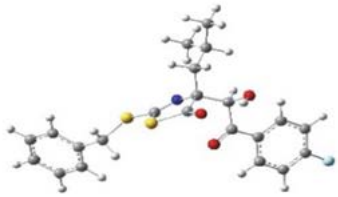	2.195 133.29	67 149–153
4Cl-Leu	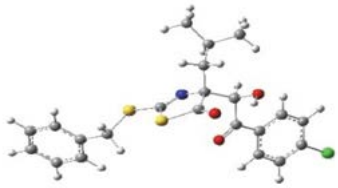	2.154 134.54	64 176–178
4Br-Leu	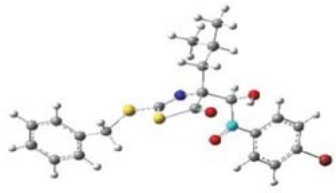	2.186 133.62	73 141–144
$4NO_2$-Leu	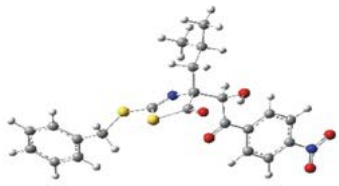	2.162 134.50	58 121–125

$4Br\text{-}C_6H_4$-, and $4NO_2\text{-}C_6H_4$- rings were prepared from the corresponding acetophenones and used in this reaction. Three amino acids including glycine, alanine and leucine were selected as amino acid sources and finally benzyl chloride was used as aryl halide substrate.

In all cases, the reaction proceeds through the known reaction mechanism. The only difference is that in the case of using of alanine and leucine the final step (dehydration) does not occur because of lacking of a hydrogen atom at the adjacent carbon atom to the one bearing hydroxyl group. All of the reactions are completed in almost 4 hours and led to the desired products in high yields. The results are presented in Table 1.

A proposed mechanism for this reaction is given in Scheme 6. It is proposed that at first the reaction of amino acid **1** with carbon disulfide **3** in the presence of sodium hydroxide in methanol as the solvent produced the corresponding dithiocarbamic acid anion **4** which then attacks the benzyl chloride **5** in a S_N2 mechanism to afford benzyl dithiocarbamic acid **6** after workup with hydrochloric acid. Benzyl dithiocarbamic acid **6** in the presence of acetic anhydride and sodium acetate undergoes intramolecular cyclization via attacking a nucleophilic sulfur atom to the most electrophilic carbon atom to produce thiazolactone **9** after eliminating one acetate anion. Thiazolactone **9** can be tautomerized to the second form of **9'** which is the enol form of the thiazolactone **9**. Then thiazolactone **9'** as a nucleophile attacks the aldehyde carbonyl group as the most electrophilic moiety of arylglyoxal **10** to produce compound **11**, which could undergo dehydration to afford compound **12** where the R group is hydrogen atom.[14,28]

3. Experimental

3. 1. General

All reagents and solvents were purchased from Merck or Fluka chemical companies and used without further purification. Melting points were measured on an Electro thermal apparatus. IR spectra were recorded on a

VERTEX 70 Bruker spectrometer. ^{1}H and ^{13}C NMR spectra of isolated products were recorded on a Bruker DRX-400 Avance (measuring frequency: ^{1}H NMR 400 MHz, ^{13}C NMR 100 MHz) in $CDCl_3$ solution. Elemental analyses were performed using a Leco Analyzer 932.

3. 2. Typical Procedure for the Synthesis of Dithiocarbamates

In a test tube equipped with a magnetic stir bar, amino acid (5 mmol (equals about 0.38 g of Gly, 0.45 g of Ala and 0.66 g of Leu)) and sodium hydroxide (10 mmol, 0.40 g) were dissolved in methanol (10 mL). The mixture was cooled in an ice bath (–5 °C) and then carbon disulfide (6 mmol, 0.46 g) was added and the mixture was stirred for 1 h. Then benzyl chloride (5.5 mmol, 0.70 g) was added and let the reaction mixture reach the room temperature and stirring was continued for 15 h at room temperature. Progress of the reaction was checked using TLC (ethyl acetate : *n*-hexane 3 : 1). After completion of the reaction 0.1 M aqueous HCl was added until the reaction media pH reached 5. At this point the crude product solidified. The crude product was filtered and washed twice with distilled water (20 mL). In continuation it was dried and recrystallized from ethanol to get pure product.[14] The known 6-Gly and 6-Ala dithiocarbamic acid products (in the case of using glycine and alanine as the amino acid, respectively) were verified by comparing melting points and the new 6-Leu dithiocarbamic acid product (in the case of using leucine as the amino acid) was characterized by its IR, ^{1}H and ^{13}C NMR spectra and CHN analysis (See section 3. 5).

3. 3. Typical Procedure for the Synthesis of Arylglyoxals

Arylglyoxals were prepared by oxidation of the acetophenone derivatives with selenium dioxide in dioxan/water solvent mixture under reflux condition according to the full detailed reported procedure.[29] The crude product could be recrystallized from boiling water to get its hydrated form.

3. 4. Typical Procedure for the Synthesis of Thiazolactones

In a test tube equipped with a magnetic stir bar, dithiocarbamic acid (1 mmol, (0.241 g of 6-Gly, 0.255 g of 6-Ala or 0.297 g of 6-Leu)), acetic anhydride (2.5 mmol, 0.255 g) and anhydrous sodium acetate (0.75 mmol, 0.061 g) were mixed and kept at 80 °C for 1 h with stirring. In continuing to this dark brown mixture the arylglyoxal (1.2 mmol, 0.182 g) was added. The reaction continued under the same conditions for the next 1 h. Progress of the reaction was monitored using TLC (ethyl acetate : *n*-hexane 10 : 1). Then the reaction mixture was cooled and kept in a refrigerator (2–4 °C) for 24 h. Thereafter, distilled water (15 mL) was added to the reaction mixture and stirred vigorously. The resulting solid crude product was filtered and washed first with distilled water (2 × 15 mL) and then with *n*-hexane (2 × 15 mL) to get the pure product.

3. 5. Characterization Data of the New Products

((Benzylthio)carbonothioyl)leucine (6-Leu). Yield 71%, m.p. 127–130 °C, FT-IR (KBr): *ν* (cm^{-1}) 3264, 3021, 2927, 1651, 1492, 695. ^{1}H NMR (400 MHz, $CDCl_3$): δ (ppm) 0.91 (d, 6H, CH_3), 1.51 (m, 1H, CH), 1.72 (m, 2H, CH_2), 4.13 (s, 2H, CH_2), 4.17 (m, 1H, CH), 7.25–7.28 (m, 5H, ArH); ^{13}C NMR (100 MHz, $CDCl_3$: δ (ppm) 22.7, 27.1, 36.9, 43.4, 64.3, 80.3, 128.9, 129.3, 136.4, 175.4, 196.5. Anal. calcd. for $C_{14}H_{19}NO_2S_2$: C, 56.54: H, 6.44; N, 4.71; S, 21.56. Found: C, 56.34; H, 6.74; N, 4.60; S, 21.50.

(*Z*)-2-(Benzylthio)-4-(2-oxo-2-phenylethylidene)thiazol-5(4*H*)-one (4H-Gly). Yield 64%, m.p. 93–97 °C, FT-IR (KBr): ν (cm^{-1}) 3026, 2926, 1727, 1456, 1392, 1277, 1126, 699. ^{1}H NMR (400 MHz, $CDCl_3$): δ (ppm) 4.67 (s, 2H), 7.13 (s, 1H, CH), 7.46 (m, 5H, ArH), 7.85 (m, 5H, ArH); ^{13}C NMR (100 MHz, $CDCl_3$): δ (ppm) 37.8, 49.3, 103.1, 127.6, 128.5, 128.8, 128.9, 129.0, 134.4, 136.1, 137.6, 162.8, 185.8, 193.5. Anal. calcd. For $C_{18}H_{13}NO_2S_2$: C, 63.69; H, 3.86; N, 4.13. Found: C, 63.45; H, 3.74; N, 4.26.

(*Z*)-2-(Benzylthio)-4-(2-(4-fluorophenyl)-2-oxoethylidene)thiazol-5(4*H*)-one (4F-Gly). Yield 68%, m.p. 104–106 °C, FT-IR (KBr): ν (cm^{-1}) 3078, 2957, 1696, 1601, 1510, 1443, 1230, 1126, 1029, 603. ^{1}H NMR (400 MHz, $CDCl_3$): δ (ppm) 4.44 (s, 2H, CH_2), 6.87 (s, 1H, CH), 7.19 (m, 1H, ArH), 7.27 (m, 2H, ArH), 7.39 (m, 2H, ArH), 7.68 (d, 2H, *J* = 8.8 Hz), 7.80 (d, 2H, *J* = 8.6 Hz); ^{13}C NMR (100 MHz, $CDCl_3$): δ (ppm) 37.7, 103.6, 115.3, 115.6, 128.7, 128.8, 128.9, 129.8, 129.9, 131.3, 131.76, 134.5, 134.9, 137.7, 162.1, 163.5, 186.5, 194.1. Anal. calcd. for $C_{18}H_{12}FNO_2S_2$: C, 60.49; H, 3.38; N, 3.92. Found: C, 60.63; H, 3.21; N, 3.64.

(*Z*)-2-(Benzylthio)-4-(2-(4-chlorophenyl)-2-oxoethylidene)thiazol-5(4*H*)-one (4Cl-Gly). Yield 72%, m.p. 101–98 °C, FT-IR (KBr): ν (cm^{-1}) 3048, 2924, 1792, 1643, 1549, 1384, 1227, 694. ^{1}H NMR (400 MHz, $CDCl_3$): δ (ppm) 4.43 (s, 2H), 6.88 (s, 1H, CH), 7.51 (m, 5H, ArH), 7.72 (d, 2H, *J* = 8.4 Hz), 7.89 (d, 2H, *J* = 8.4 Hz); ^{13}C NMR (100 MHz, $CDCl_3$): δ (ppm) 37.2, 103.6, 128.2, 128.7, 128.7, 129.5, 129.6, 129.7, 129.8, 129.9, 129.9, 134.9, 135.7, 136.7, 137.5, 162.2, 186.5, 193.5. Anal. calcd. for $C_{18}H_{12}ClNO_2S_2$: C, 57.83; H, 3.24; N, 3.75. Found: C, 58.05; H, 3.43; N, 3.52.

(*Z*)-2-(Benzylthio)-4-(2-(4-bromophenyl)-2-oxoethylidene)thiazol-5(4*H*)-one (4Br-Gly). Yield 78%, m.p. 124–125 °C, FT-IR (KBr): ν (cm^{-1}) 3035, 2924, 1722, 1621,

1440, 1383, 1268, 1070, 619. ^{1}H NMR (400 MHz, $CDCl_3$): δ (ppm) 4.42 (s, 2H, CH_2), 6.89 (s, 1H, CH), 7.19 (m, 1H, ArH), 7.27 (m, 2H, ArH), 7.65 (m, 2H, ArH), 7.96 (d, 2H, *J* = 8.4 Hz), 7.79 (d, 2H, *J* = 8.4 Hz); ^{13}C NMR (100 MHz, $CDCl_3$): δ (ppm) 36.9, 101.3, 124.5, 128.7, 128.7, 128.8, 129.1, 129.2, 130.3, 130.6, 132.3, 132.4, 134.9, 136.7, 137.5, 162.2, 187.3, 193.8. Anal. calcd. for $C_{18}H_{12}BrNO_2S_2$: C, 51.68; H, 2.89; N, 3.35. Found: C, 51.45; H, 3.10; N, 3.55.

(*Z*)-2-(Benzylthio)-4-(2-(4-nitrophenyl)-2-oxoethylidene)thiazol-5(4*H*)-one (4NO_2-Gly). Yield 81%, m.p. 117–119 °C, FT-IR (KBr): ν (cm^{-1}) 3066, 2860, 1692, 1603, 1533, 1348, 1220, 1010, 1013, 724. ^{1}H NMR (400 MHz, $CDCl_3$): δ (ppm) 4.44 (s, 2H, CH_2), 7.18 (s, 1H, CH), 7.24 (m, 3H, ArH), 7.27 (m, 2H, ArH), 7.94 (d, 2H, *J* = 8.4 Hz), 8.10 (d, 2H, *J* = 8.4 Hz); ^{13}C NMR (100 MHz, $CDCl_3$): δ (ppm) 37.8, 103.6, 117.3, 117.3, 128.8, 128.8, 129.8, 129.9, 134.4, 134.4, 134.8, 136.0, 137.1, 140.7, 162.1, 186.5, 193.6. Anal. calcd. for $C_{18}H_{12}N_2O_4S_2$: C, 56.24; H, 3.15; N; 7.29. Found: C, 56.51; H, 3.37; N, 6.95.

2-(Benzylthio)-4-(1-hydroxy-2-oxo-2-phenylethyl)-4-methylthiazol-5(4*H*)-one (4H-Ala). Yield 74%, m.p. 101–103 °C, FT-IR (KBr): ν (cm^{-1}) 3416, 3018, 2926, 2859, 1728, 1629, 1384, 1275, 1126, 702, 619. ^{1}H NMR (400 MHz, $CDCl_3$): *δ* (ppm) 1.57 (s, 3H, CH_3), 4.22 (s, 2H, CH_2), 5.43 (d, 1H, *J* = 3.2 Hz), 7.27 (m, 5H, ArH), 7.96 (m, 5H, ArH); ^{13}C NMR (100 MHz, $CDCl_3$): δ (ppm) 27.6, 37.8, 63.4, 79.0, 128.4, 128.5, 128.6, 128.7, 128.7, 128.9, 129.3, 129.3, 129.6, 129.6, 131.8, 134.8, 161.7, 193.8, 196.6. Anal. calcd. for $C_{19}H_{17}NO_3S_2$: C, 61.43; H, 4.61; N, 3.77. Found: C, 61.27; H, 4.46; N, 3.60.

2-(Benzylthio)-4-(2-(4-fluorophenyl)-1-hydroxy-2-oxoethyl)-4-methylthiazol-5(4*H*)-one (4F-Ala). Yield 84%, m.p. 163–166 °C, FT-IR (KBr): ν (cm^{-1}) 3457, 3064, 2982, 1698, 1578, 1388, 1221, 1114, 634. ^{1}H NMR (400 MHz, $CDCl_3$): δ (ppm) 1.55 (s, 3H, CH_3), 4.22 (s, 2H, CH_2), 5.43 (s, 1H, CH), 7.24 (m, 1H, ArH), 7.25 (m, 2H, ArH), 7.27 (m, 2H, ArH), 7.44 (d, 2H, *J* = 8.4 Hz), 7.91 (d, 2H, *J* = 8.4 Hz); ^{13}C NMR (100 MHz, $CDCl_3$): δ (ppm) 28.3, 36.1, 64.0, 76.1, 114.5, 114.6, 128.7, 128.8, 128.9, 129.4, 129.7, 131.4, 131.5, 131.7, 134.9, 162.6, 163.7, 193.6, 197.6. Anal. calcd. for $C_{19}H_{16}FNO_3S_2$: C, 58.60; H, 4.14; N, 3.60. Found: C, 58.46; H, 4.39; N, 3.75.

2-(Benzylthio)-4-(2-(4-chlorophenyl)-1-hydroxy-2-oxoethyl)-4-methylthiazol-5(4*H*)-one (4Cl-Ala). Yield 81%, m.p. 152–155 °C, FT-IR (KBr): ν (cm^{-1}) 3377, 3038, 2972, 1695, 1589, 1398, 1226, 1130, 1097, 611. ^{1}H NMR (400 MHz, $CDCl_3$): δ (ppm) 1.62 (s, 3H, CH_3), 4.24 (s, 2H, CH_2), 5.46 (s, 1H, CH), 7.27 (m, 5H, ArH), 7.53 (d, 2H, *J* = 8.8 Hz), 7.89 (d, 2H, *J* = 8.7 Hz); ^{13}C NMR (100 MHz, $CDCl_3$): δ (ppm) 28.5, 36.4, 64.3, 77.3, 128.3, 128.5, 128.6, 129.4, 129.7, 129.8, 129.9, 130.0, 130.3, 131.9, 134.7, 136.5, 163.2, 194.1, 196.6. Anal. calcd. for $C_{19}H_{16}ClNO_3S_2$: C, 56.22; H, 3.97; N, 3.45. Found: C, 56.41; H, 4.021; N, 3.15.

2-(Benzylthio)-4-(2-(4-bromophenyl)-1-hydroxy-2-oxoethyl)-4-methylthiazol-5(4*H*)-one (4Br-Ala). Yield 79%, m.p. 147–150 °C, FT-IR (KBr): ν (cm^{-1}) 3423, 3035, 2920, 1732, 1618, 1375, 1256, 1062, 631. ^{1}H NMR (400 MHz, $CDCl_3$): δ (ppm) 1.52 (s, 3H, CH_3), 4.24 (s, 2H, CH_2), 5.42 (s, 1H, CH), 7.27 (m, 5H, ArH), 7.66 (d, 2H, *J* = 8.6 Hz), 7.96 (d, 2H, *J* = 8.7 Hz); ^{13}C NMR (100 MHz, $CDCl_3$): δ (ppm) 27.0, 38.7, 63.3, 79.6, 124.9, 128.3, 128.3, 128.8, 129.3, 129.6, 130.3, 130.7, 131.3, 132.1, 132.4, 134.9, 162.6, 193.2, 196.9. Anal. calcd. for $C_{19}H_{16}BrNO_3S_2$: C, 50.67; H, 3.58; N, 3.11. Found: C, 50.40; H, 4.25; N, 3.36.

2-(Benzylthio)-4-(1-hydroxy-2-(4-nitrophenyl)-2-oxoethyl)-4-methylthiazol-5(4*H*)-one (4NO_2-Ala). Yield 86%, m.p. 113–114 °C, FT-IR (KBr): ν (cm^{-1}) 3415, 3052, 2923, 1721, 1622, 1384, 1269, 1115, 619. ^{1}H NMR (400 MHz, $CDCl_3$): δ (ppm) 1.59 (s, 3H, CH_3), 4.21 (s, 2H, CH_2), 5.59 (s, 1H, CH), 7.24 (m, 1H, ArH), 7.93 (m, 2H, ArH), 7.95 (m, 2H, ArH), 8.18 (d, 2H, *J* = 8 Hz), 8.22 (d, 2H, *J* = 8.1 Hz); ^{13}C NMR (100 MHz, $CDCl_3$): δ (ppm) 26.4, 37.7, 62.6, 79.0, 117.3, 117.5, 128.6, 128.8, 128.9, 129.4, 129.7, 130.4, 130.4, 131.7, 134.9, 140.5, 162.2, 193.6, 196.8. Anal. calcd. for $C_{19}H_{16}N_2O_5S_2$: C, 54.80; H, 3.87; N, 6.73. Found: C, 54.64; H, 3.71; N, 6.82.

2-(Benzylthio)-4-(1-hydroxy-2-oxo-2-phenylethyl)-4-isobutylthiazol-5(4*H*)-one (4H-Leu). Yield 69%, m.p. 113–117 °C, FT-IR (KBr): ν (cm^{-1}) 3405, 3020, 2928, 2862, 1714, 1627, 1453, 1375, 1273, 1238, 1119, 706. ^{1}H NMR (400 MHz, $CDCl_3$): *δ (ppm)* 0.91 (d, 6H, *J* = 6.8 Hz), 1.52 (m, 1H, CH), 1.74 (d, 2H, *J* = 8.4 Hz), 4.28 (s, 2H, CH_2), 5.56 (s, 1H, CH), 7.28 (m, 5H, ArH), 7.96 (m, 5H, ArH); ^{13}C NMR (100 MHz, $CDCl_3$): δ (ppm) 22.6, 22.6, 26.1, 36.9, 43.4, 64.3, 80.3, 127.8, 127.8, 128.3, 128.4, 129.2, 129.3, 130.1, 130.1, 132.5, 135.2, 163.7, 195.3, 198.8. Anal. calcd. for $C_{22}H_{23}NO_3S_2$: C, 63.90; H, 5.61; N, 3.39 Found: C, 64.12; H, 5.78; N, 3.19.

2-(Benzylthio)-4-(2-(4-fluorophenyl)-1-hydroxy-2-oxoethyl)-4-isobutylthiazol-5(4*H*)-one (4F-Leu). Yield 67%, m.p. 149–153 °C, FT-IR (KBr): ν (cm^{-1}) 3462, 3055, 2973, 1688, 1568, 1448, 1382, 1209, 1231, 1109, 641. ^{1}H NMR (400 MHz, $CDCl_3$): δ (ppm) 0.91 (d, 6H, *J* = 6.6 Hz), 1.52 (m, 1H, CH), 1.73 (d, 2H, *J* = 8.06 Hz), 4.21 (s, 2H, CH_2), 5.44 (s, 1H, CH), 7.32 (m, 5H, ArH), 7.36 (m, 5H, ArH), 7.46 (d, 2H, *J* = 8.7 Hz), 7.91 (d, 2H, *J* = 8.8 Hz); ^{13}C NMR (100 MHz, $CDCl_3$): *δ* (ppm) 22.5, 22.6, 27.0, 37.9, 42.4, 63.5, 78.3, 128.3, 128.4, 129.7, 129.8, 130.1, 131.5, 131.6, 132.4, 132.6, 133.1, 135.2, 136.6, 165.2, 195.3, 198.1. Anal. calcd. for $C_{22}H_{22}FNO_3S_2$: C, 61.23; H, 5.14; N, 3.25. Found: C, 61.55; H, 5.32; N, 3.37.

2-(Benzylthio)-4-(2-(4-chlorophenyl)-1-hydroxy-2-oxoethyl)-4-isobutylthiazol-5(4*H*)-one (4Cl-Leu). Yield

64%, m.p. 176–178 °C, FT-IR (KBr): ν (cm^{-1}) 3365, 3033, 2969, 1681, 1588, 1429, 1384, 1221, 1132, 1085, 613. ^{1}H NMR (400 MHz, $CDCl_3$): δ (ppm) 0.91 (d, 6H, *J* = 6.8 Hz), 1.53 (m, 1H, CH), 1.72 (d, 2H, *J* = 8.4 Hz), 4.21 (s, 2H, CH_2), 5.39 (s, 1H, CH), 7.27 (m, 5H, ArH), 7.33 (m, 5H, ArH), 7.73 (d, 2H, *J* = 12.8 Hz), 7.87 (d, 2H, *J* = 8.8 Hz); ^{13}C NMR (100 MHz, $CDCl_3$): δ (ppm) 21.8, 21.9, 25.7, 34.8, 40.6, 61.38, 77.8, 126.3, 126.5, 127.6, 128.1, 128.2, 129.6, 129.8, 130.5, 130.7, 131.9, 136.3, 163.1, 194.9, 197.3. Anal. calcd. for $C_{22}H_{22}ClNO_3S_2$: C, 58.98; H, 4.95; N, 3.13. Found: C, 59.26; H, 5.15; N, 3.34.

2-(Benzylthio)-4-(2-(4-bromophenyl)-1-hydroxy-2-oxoethyl)-4-isobutylthiazol-5(4*H*)-one (4Br-Leu). Yield 73%, m.p. 141–144 °C, FT-IR (KBr): ν (cm^{-1}) 3431, 3039, 2910, 1727, 1624, 1453, 1432, 1365, 1247, 1106, 1062, 623. ^{1}H NMR (400 MHz, $CDCl_3$): δ (ppm) 0.93 (d, 6H, *J* = 6.8 Hz), 1.54 (m, 1H, CH), 1.64 (d, 2H, *J* = 8.4 Hz), 4.31 (s, 2H, CH_2), 5.38 (s, 1H, CH), 7.34 (m, 5H, ArH), 7.36 (m, 5H, ArH), 7.66 (d, 2H, *J* = 8.21 Hz), 7.97 (d, 2H, *J* = 7.56 Hz); ^{13}C NMR (100 MHz, $CDCl_3$): δ (ppm) 21.5, 21.6, 26.7, 26.8, 42.6, 62.6, 75.1, 124.9, 126.5, 126.6, 127.3, 131.2, 131.3, 132.4, 132.5, 133.4, 133.6, 134.1, 136.8, 164.7, 195.7, 195.3, 194.5. Anal. calcd. for $C_{22}H_{22}BrNO_3S_2$: C, 53.66; H, 4.50; N, 2.84. Found: C, 53.85; H, 4.40; N, 3.12.

2-(Benzylthio)-4-(1-hydroxy-2-(4-nitrophenyl)-2-oxoethyl)-4-isobutylthiazol-5(4*H*)-one (4NO_2-Leu). Yield 58%, m.p. 121–125 °C, FT-IR (KBr): ν (cm^{-1}) 3418, 3052, 2929, 1725, 1628, 1441, 1369, 1274, 1171, 611. ^{1}H NMR (400 MHz, $CDCl_3$): 1.01 (d, 6H, *J* = 6.65 Hz), 1.63 (m, 1H, CH), 1.82 (d, 2H, *J* = 8 Hz), 4.38 (s, 2H, CH_2), 5.36 (s, 1H, CH), 7.20 (m, 5H, ArH), 7.23 (m, 5H, ArH), 7.97 (d, 2H, *J* = 8.8 Hz), 8.21 (d, 2H, *J* = 8.4 Hz); ^{13}C NMR (100 MHz, $CDCl_3$): δ (ppm) 23.9, 24.1, 28.3, 38.7, 44.1, 65.8, 79.6, 117.2, 117.3, 126.5, 126.7, 128.3, 128.4, 129.2, 131.4, 131.5, 133.4, 137.6, 140.6, 164.7, 191.8, 194.6. Anal. calcd. for $C_{22}H_{23}N_2O_5S_2$: C, 57.63; H, 4.84; N, 6.11. Found: C, 57.50; H, 4.64; N, 6.37.

4. Computational Study of the Products

4. 1. Method

All computations were carried out with the Gaussian 09 program package.[30] The energies and geometries were calculated with B3LYP method[31,32] and 6-311++G(d,p) basis set. Harmonic vibrational frequencies were computed to confirm an optimized geometry corresponding to the local minimum that has only real frequencies. NMR spectra have been calculated at B3LYP/6–311++G(d,p) level of theory in $CDCl_3$ solvent using the gauge-independent atomic orbital (GIAO) method.[33] UV-visible spectra were calculated theoretically in $CDCl_3$ solvent as well as gas phase using time-dependent (TD) DFT method with B3LYP level of theory and 6–311++G(d,p) basis set based on the previously optimized ground state geometry of the products.[34,35]

4. 2. Geometrical Analysis

First of all, to find the most stable geometries of the compounds we done optimization calculations on the molecular structures of the synthesized compounds which are verified with IR and NMR spectroscopic techniques. Then for verifying that the optimized structures are true minima we calculated the vibrational frequencies of them. The results showed that all of the calculated frequencies for all compounds have positive values verifying that all structures are true minima. The optimized structures of the products are shown in column 2 of Table 1. In addition, some selected most important geometrical data of all products are collected in Tables 2a, 2b, and 2c. The atom numbered model structure of each of the 4X-Gly, 4X-Ala, and 4X-Leu products are included in Tables 2a, 2b and 2c, respectively.

The results of the geometry optimization of 4X-Gly derivatives proved our proposed (*Z*) stereochemistry of the conjugated C=C double bond. This stereochemistry let the conjugation spread longer through the whole molecule from the X substituted phenyl ring to the thiazolone carbonyl double bond and enabled the products to absorb UV-visible light in the visible area as we will discuss later. The results also revealed that there are no significant differences in the geometrical characteristics of the products with different X substituents and almost all of them have nearly the same geometrical structures with some small differences in bond lengths and/or angles. Calculated dihedral angles also revealed that the whole molecular structure of the products is not planar but the un-planarity is not too large to prevent conjugation.

The 4X-Ala and 4X-Leu products have the same optimized geometrical structures because they both have hydroxyl functional groups attached to the carbon atoms between carbonyl groups instead of a C=C double bond; therefore in these cases we do not have a longer conjugation system as we see in 4X-Gly products. These structural differences make some differences from the structural and chemical reactivity point of view between the 4X-Ala and 4X-Leu with 4X-Gly products.

Unlike the 4X-Gly products the optimization calculations revealed that the 4X-Ala and 4X-Leu products have one intramolecular hydrogen bond which is located between the hydroxyl group and the oxygen atom of the carbonyl group. Hydrogen bond characterization data of these two groups are included in Table 1. This intramolecular hydrogen bond makes the products more stable and also more rigid than that of 4X-Gly products. Observed intramolecular hydrogen bond lengths and angles varied from 2.154 to 2.195 Å and 133.05° to 134.50° which is in accordance with nearly strong hydrogen bonds. As

Tables 2a. Optimized geometrical data of 4X-Gly products.

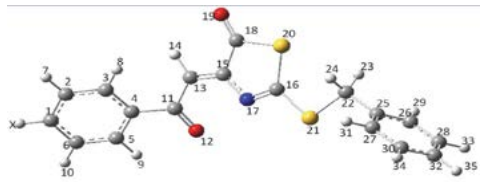

X	H	F	Cl	Br	NO_2
Bond length/(Å)					
C_4–C_{11}	1.500	1.499	1.501	1.501	1.509
C11–C13	1.490	1.489	1.487	1.487	1.482
C11–O12	1.218	1.218	1.218	1.218	1.217
C13–C15	1.351	1.351	1.352	1.352	1.354
C13–H14	1.084	1.084	1.084	1.084	1.083
C15–C18	1.513	1.513	1.514	1.515	1.517
C15–N17	1.376	1.376	1.375	1.374	1.370
N17–C16	1.286	1.286	1.287	1.287	1.289
C16–S20	1.799	1.799	1.798	1.798	1.797
C18–S20	1.833	1.833	1.833	1.833	1.832
C18–O19	1.196	1.196	1.196	1.196	1.195
C16–S21	1.751	1.750	1.745	1.745	1.746
S21–C22	1.858	1.858	1.858	1.858	1.859
Angle/(°)					
C4–C11–O12	121.23	121.03	120.81	120.76	120.05
C4–C11–C13	117.42	117.47	117.46	117.46	117.33
C11–C13–C15	125.58	125.58	125.68	125.72	125.78
C13–C15–N17	127.15	127.25	127.37	127.41	127.61
H14–C13–C15	116.20	116.09	115.97	115.92	115.87
C15–C18–C19	118.59	128.68	128.67	128.67	128.53
C15–C18–S20	106.78	106.79	106.81	106.80	106.83
N17–C16–S20	117.86	117.87	117.89	117.90	117.94
N17–C16–S21	119.52	119.51	119.48	119.47	119.37
C16–S21–C22	103.64	103.67	103.62	103.68	103.76
Dihedral/(°)					
C3–C4–C11–C13	–13.22	–12.49	–13.02	–13.42	–17.95
C4–C11–C13–C15	147.88	149.30	152.09	153.32	158.11
O12–C11–C13–C15	–33.94	–32.45	–29.66	–28.46	–23.56
C13–C15–C18–S20	–179.38	–179.17	–179.10	–178.81	–179.47
S20–C16–S21–C22	0.820	0.207	–0.002	–0.448	0.291

we discussed about 4X-Gly products in the case of 4X-Ala and 4X-Leu products also structural characteristics such as bond length, angles and dihedral angles do not show obvious differences within the products of each type with various X substituents. As the dihedral angles showed both of the 4X-Ala and 4X-Leu products are not planar same as the 4X-Gly ones. Another structural feature of 4X-Ala and 4X-Leu products is that the carbonyl functional group is directed to the center of the thiazolactone ring at all of the X substituted derivatives of them.

4. 3. UV-Visible Spectra Prediction

In this part, we get help from chemical computational methods to get information about the UV-visible light absorption capability of the products. Therefore, the optimized ground state geometry of the synthesized products have been submitted to the calculation of the UV-visible spectra using the time-dependent (TD) DFT method at B3LYP/6–311++G(d,p) computational level in both gas and solution phase. "Time-dependent density functional theory (TD-DFT)[36] has recently emerged as a powerful tool for investigating the static and dynamic properties of the molecules in their excited states, allowing for the best compromise between accuracy and computational cost."[37] The calculated absorption maxima (λ_{max}) are a function of the electron availability for the synthesized compounds and their corresponding oscillator strengths are listed in Table 3.

Figure 1 shows the resulting absorption spectra for each type of the synthesized compounds over the wave-

Tables 2b. Optimized geometrical data of 4X-Ala products.

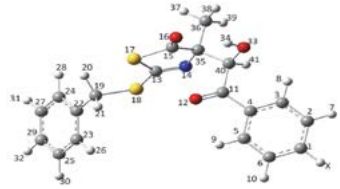

X	H	F	Cl	Br	NO_2
Bond length/(Å)					
C4–C11	1.492	1.490	1.491	1.492	1.500
C11–O12	1.217	1.217	1.217	1.217	1.214
C11–C40	1.545	1.545	1.545	1.545	1.543
C40–O33	1.422	1.422	1.422	1.422	1.422
C40–C35	1.553	1.552	1.552	1.552	1.551
C35–C15	1.542	1.542	1.542	1.542	1.542
C15–O16	1.201	1.201	1.201	1.201	1.201
C35–N14	1.448	1.448	1.449	1.448	1.448
C35–C36	1.545	1.545	1.545	1.545	1.545
N14–C13	1.270	1.270	1.270	1.270	1.271
C13–S17	1.805	1.806	1.806	1.806	1.806
C13–S18	1.768	1.768	1.768	1.767	1.766
S17–C15	1.817	1.815	1.815	1.815	1.814
S18–C19	1.858	1.858	1.859	1.858	1.858
Angle/(°)					
C5–C4–C11	118.01	118.04	118.06	118.09	122.58
C4–C11–O12	121.61	121.54	121.43	121.39	120.97
C4–C11–C40	118.55	118.40	118.44	118.46	118.31
C40–C35–C15	110.96	110.84	110.81	110.85	110.88
C35–C15–O16	126.27	126.17	126.12	126.15	126.07
C35–C40–O33	112.70	112.63	112.69	112.71	112.96
C15–C35–N14	109.64	109.64	109.65	109.65	109.66
C15–C35–C36	107.54	107.59	107.62	107.59	107.59
C15–S17–C13	87.97	87.98	87.99	87.99	87.99
S17–C13–S18	121.60	121.51	121.49	121.56	121.65
C13–S18–C19	103.58	103.52	103.46	103.58	103.74
Dihedral/(°)					
C4–C11–C40–O33	–73.66	–71.73	–71.80	–71.55	–72.79
C11–C40–C35–C15	60.29	60.20	60.12	59.94	60.81
C40–C35–C15–O16	50.44	49.99	50.15	50.05	49.71
C36–C35–C40–O33	55.34	55.11	55.15	54.95	56.05
S17–C13–S18–C19	–8.81	–10.13	–13.24	–12.12	–5.46

length range of 200–800 nm in both the gas and solution phases which are obtained using the above-mentioned calculation methods. Analysis of the obtained plots for each class of the synthesized compounds from the absorption maxima (λ_{max}) and intensity points of view clearly point to the following results:

1. All of the products have absorption bands in the range of 250–350 nm because of the presence of a phenyl ring in all structures.
2. The absorption spectra of 4X-Gly products show the two absorption bands in which the absorption maxima are located in visible light range as expected because of the long conjugated π system present in their structure.
3. The absorption spectra of 4X-Ala and 4X-Leu products do not have an absorption band in the range of visible light because they lack a long conjugated π system and show only one absorption band in the ultraviolet region.
4. The calculated UV-visible spectrum for each product in the solution phase has a higher intensity than that of its gas phase for all compounds.
5. Absorption maxima for 4X-Gly, 4X-Ala, and 4X-Leu compounds in solution phase range from 481–494, 262–297, and 260–293 nm, respectively.
6. The absorption maxima order in the case of 4X-Gly products is: $4NO_2 > 4Br > 4Cl > 4F > 4H$.
7. Substituting the F, Cl, Br and NO_2 groups instead of a hydrogen atom at the *para* position of the phenyl ring

Tables 2c. Optimized geometrical data of 4X-Leu products.

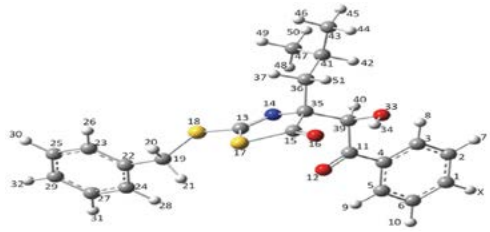

X	H	F	Cl	Br	NO_2
Bond length/(Å)					
C4–C11	1.493	1.491	1.492	1.493	1.501
C11–O12	1.217	1.217	1.217	1.216	1.214
C11–C39	1.546	1.546	1.545	1.545	1.544
C39–O33	1.422	1.422	1.422	1.422	1.422
C39–C35	1.552	1.552	1.551	1.552	1.551
C35–N14	1.448	1.448	1.449	1.448	1.448
N14–C13	1.269	1.269	1.270	1.270	1.270
C13–S17	1.804	1.804	1.805	1.805	1.806
C13–S18	1.768	1.768	1.768	1.768	1.767
S18–C19	1.858	1.858	1.858	1.858	1.859
S17–C15	1.815	1.815	1.815	1.815	1.812
C15–O16	1.201	1.201	1.201	1.201	1.202
C15–C35	1.546	1.546	1.542	1.546	1.546
C35–C36	1.563	1.563	1.561	1.564	1.564
Angle/(°)					
C5–C4–C11	117.99	117.98	118.08	118.04	122.71
C4–C11–O12	121.48	121.40	121.34	121.30	120.82
C11–C39–O33	109.16	109.14	108.67	109.09	108.68
O12–C11–C39	120.05	120.23	120.24	120.33	120.94
C11–C39–C35	112.53	112.64	112.55	112.64	112.85
C39–C35–C15	110.25	110.23	110.33	110.26	110.16
C35–C15–O16	126.11	126.07	126.14	126.06	125.92
C15–C35–N14	109.17	109.17	109.41	109.18	109.18
C36–C35–C39	111.24	111.20	111.95	111.14	111.18
C35–C15–S17	108.75	108.74	108.72	108.76	108.80
N14–C13–S17	118.25	118.24	118.23	118.21	118.14
C13–S18–C19	103.57	103.63	103.61	103.60	103.66
S17–C13–S18	121.59	121.59	121.57	121.60	121.58
Dihedral/(°)					
C4–C11–C39–O33	–72.01	–70.47	–72.16	–70.89	–70.30
C4–C11–C39–C35	162.26	163.66	162.28	163.26	163.89
C11–C39–C35–C15	58.67	58.40	59.88	58.76	50.01
O33–C39–C35–C36	51.23	50.81	54.48	51.27	51.78
O16–C15–C35–C36	–68.98	–69.37	–70.96	–69.48	–69.97
S17–C13–S18–C19	–10.64	–8.93	–10.17	–7.28	–8.33

Table 3. Calculated absorption maxima (λ_{max}) and corresponding oscillator strength of the products.

Comp.	**4X-Gly**				**4X-Ala**				**4X-Leu**			
phase	**Gas**		**CH_3CN**		**Gas**		**CH_3CN**		**Gas**		**CH_3CN**	
X	**λ/nm**	***f***	**λ/nm**	***f***	**λ/nm**	***f***	**λ/nm**	***f***	**λ/nm**	***f***	**λ/nm**	***f***
H	457.79	0.3795	481.89	0.4854	291.41	0.0542	274.05	0.0945	253.99	0.1721	260.93	0.3160
F	462.32	0.3856	484.43	0.4916	257.02	0.3040	262.10	0.2732	257.24	0.3096	262.82	0.2906
Cl	467.38	0.4223	488.76	0.5470	288.52	0.2724	287.65	0.2960	270.64	0.2140	277.82	0.2619
Br	471.95	0.4229	488.87	0.5707	295.09	0.4917	297.15	0.3445	277.18	0.3763	283.56	0.4633
NO_2	465.84	0.4002	494.26	0.5086	302.93	0.0187	292.66	0.5185	303.31	0.0182	293.52	0.5116

resulted in redshift effects at UV-visible absorption behavior of the 4X-Gly products and the $4NO_2$ group showed the highest redshift value among all of the substituting groups.

The lower wavelength absorption band appeared for the 4X-Gly products and also the only absorption band of the 4X-Ala and 4X-Leu products correspond to the electronic transitions among the aromatic rings which are mainly derived from the contribution of π–π* bands. And the visible absorption maxima of the 4X-Gly products correspond to the electron transition from the highest occupied molecular orbital (HOMO) to the lowest unoccupied molecular orbital (LUMO).

4. 4. NMR Spectra

The most powerful analytical tool for structural elucidation of organic compounds is Nuclear magnetic resonance (NMR) spectroscopy.[38] In addition to the recording of the experimental ^{1}H NMR spectra for the products in chloroform ($CDCl_3$) using Bruker AMX 400 MHz spectrometer we have employed the gauge-independent atomic orbital (GIAO) method[33,39] at B3LYP/6–311++G(d,p) level of theory in $CDCl_3$ solvent to calculate the chemical shielding of each atom in the ground state optimized geometry of the products. The theoretical ^{1}H NMR chemical shift values for the products in $CDCl_3$ solvent are listed in Table 4. We also includ some of the experimental ^{1}H NMR chemical shift values for comparison.

To get ^{1}H NMR chemical shift of the products on the TMS scale we first calculated the isotropic shielding values for tetramethylsilane (TMS) protons using the same model which was used in the case of the products in chloroform ($CDCl_3$) solvent and 31.9707 ppm was determined as the ^{1}H NMR chemical shift of the 12 equivalent protons of TMS. With the absolute chemical shift of the TMS protons in hand, the real chemical shift of each proton of the products was obtained using $\delta_{rel}(Hx) = \delta(TMS) - \delta(Hx)$ equation where

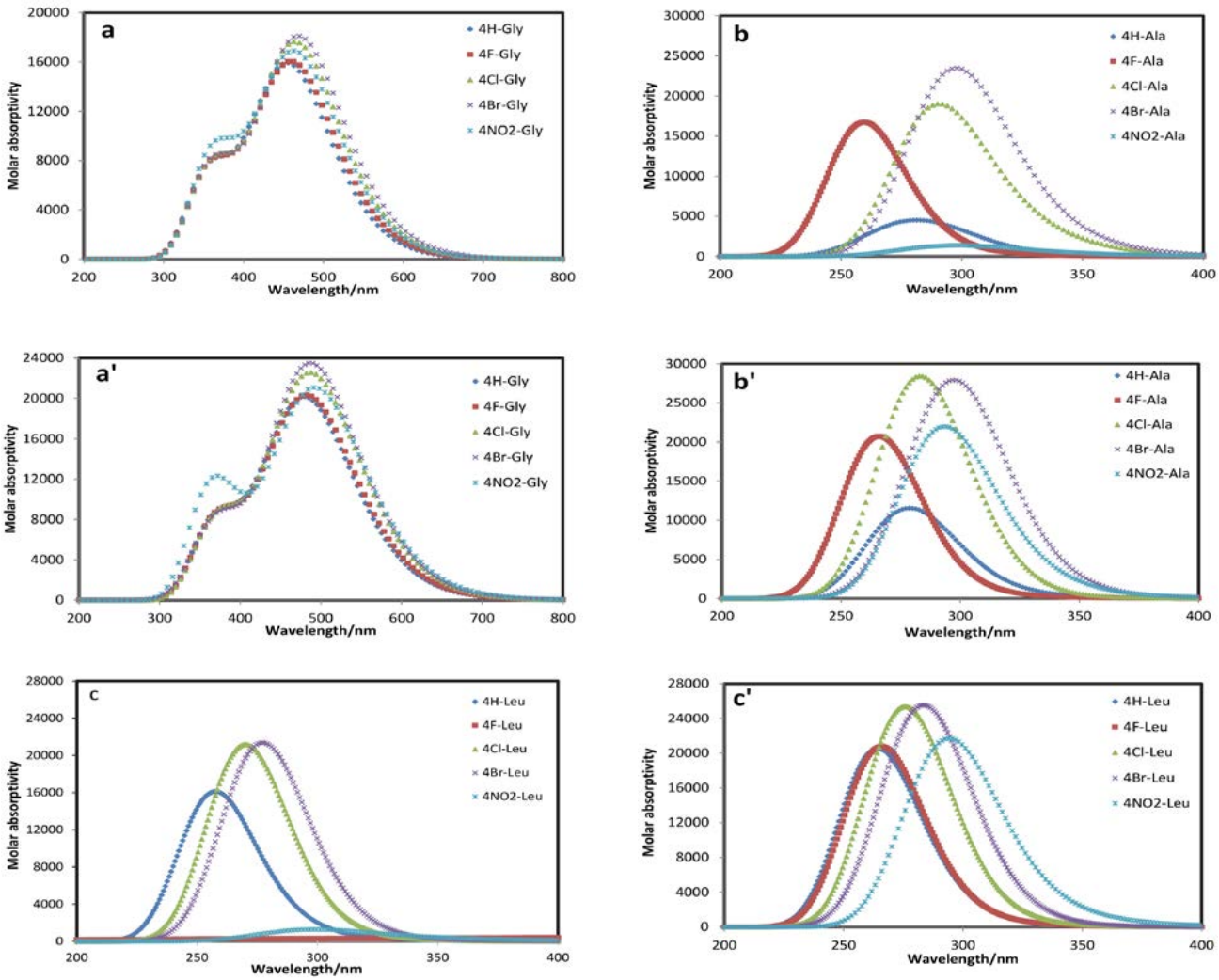

Figure 1. Calculated UV-visible spectra for the synthesized products. 4X-Gly (a: gas; a': CH_3CN), 4X-Ala (b: gas; b': CH_3CN) and 4X-Leu (c: gas; c': CH_3CN).

δ_{rel}(Hx) is the real chemical shift of the proton x, δ(Hx) is the absolute shielding of the proton x and δ(TMS) is the absolute shielding of the TMS equivalent protons. From the results collected in Table 4, it is clear that there is a good agreement between theoretically calculated chemical shifts and the experimental data for protons of the products. Figure 2 presents this correlation, showing the calculated chemical shifts versus computed ones for some protons of $4NO_2$-Gly, $4NO_2$-Ala, and $4NO_2$-Leu derivatives of the synthesized products.

The same correlation as depicted on Figure 2 could be found in the case of the other derivatives of all three classes of the products which are not shown here.

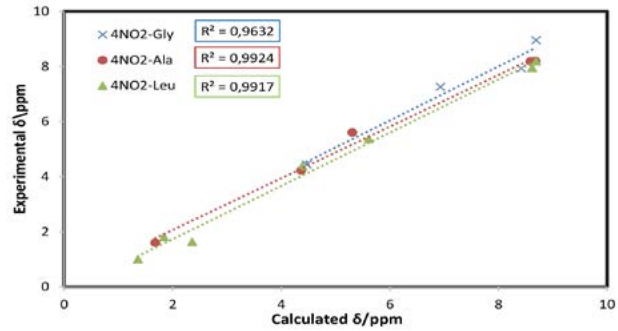

Figure 2. Correlation between calculated and experimental chemical shifts.

Table 4. Theoretical ^{1}H isotropic chemical shifts (with respect to TMS, all values in ppm) for the products obtained at B3LYP/6–311++G(d,p) level of theory (some experimental data are shown in *italic* for comparison).

Atom number	**4H-Gly**	**4F-Gly**	**4Cl-Gly**	**4Br-Gly**	**$4NO_2$-Gly**
H7, H10	7.80	7.42	7.74	7.81	8.69
H8, H9	8.37	8.37	8.29	8.26	8.42
H(X)	7.91	—	—	—	—
H14	7.42	7.34	7.32	7.31	7.26
H14	*7.13*	*6.87*	*6.89*	*6.89*	*6.93*
H23, H24	4.42	4.42	4.43	4.44	4.47
H23, H24	*4.68*	*4.44*	*4.44*	*4.42*	*4.44*
H29, H31	7.81	7.80	7.81	7.81	7.81
H33, H34	7.73	7.73	7.73	7.74	7.75
H35	7.68	7.68	7.69	7.69	7.70
Atom number	**4H-Ala**	**4F-Ala**	**4Cl-Ala**	**4Br-Ala**	**$4NO_2$-Ala**
H8, H9	8.17	8.53	8.44	8.40	8.59
H7, H10	8.20	7.42	7.74	7.81	8.68
H(X)	7.91	—	—	—	—
H41	5.39	5.34	5.33	5.32	5.31
H41	*5.44*	*5.44*	*5.46*	*5.42*	*5.60*
H34	3.35	3.41	3.40	3.37	3.57
H37, H38, H39	1.67	1.66	1.65	1.65	1.68
H37, H38, H39	*1.57*	*1.55*	*1.63*	*1.52*	*1.60*
H20, H21	4.36	4.38	4.36	4.36	4.37
H20, H21	*4.23*	*4.22*	*4.24*	*4.24*	*4.22*
H26, H28	7.76	7.78	7.76	7.76	7.76
H30, H31	7.68	7.70	7.68	7.68	7.69
H32	7.63	7.65	7.63	7.63	7.64
Atom number	**4H-Leu**	**4F-Leu**	**4Cl-Leu**	**4Br-Leu**	**$4NO_2$-Leu**
H8, H9	8.54	8.54	8.44	8.41	8.62
H7, H10	7.81	7.42	7.76	7.82	8.69
H(X)	7.95	—	—	—	—
H40	5.69	5.61	5.56	5.59	5.61
H40	*5.57*	*5.44*	*5.40*	*5.39*	*5.37*
H34	3.41	3.38	3.62	3.44	3.62
H37, H51	1.76	1.76	1.72	1.76	1.84
H37, H51	*1.73*	*1.72*	*1.71*	*1.63*	*1.81*
H42	2.38	2.35	2.16	2.36	2.36
H42	*1.52*	*1.52*	*1.53*	*1.50*	*1.63*
H44–46, H48–50	1.07	1.38	1.13	1.07	1.36
H44–46, H48–50	*0.90*	*0.90*	*0.91*	*0.92*	*1.00*
H20, H21	4.38	4.37	4.37	4.37	4.39
H20, H21	*4.29*	*4.22*	*4.21*	*4.32*	*4.39*
H26, H28	7.78	7.78	7.78	7.78	7.78
H30, H31	7.70	7.70	7.70	7.70	7.70
H32	7.65	7.65	7.65	7.65	7.65

4. 5. Atomic Net Charges

One of the most important and useful concepts which describe how the electron density is distributed within a molecule is atomic charges. Many theories, which could be applied to understand the structural characteristics of the molecules, make use of atomic charges as fundamental properties.[40] In addition, atomic charges of the molecules can be correlated with many observable characteristics of the molecules, such as electric potentials, dipole moments, polarizability, nuclear magnetic resonance chemical shifts,

Table 5. Mulliken and natural bond orbital (NBO) atomic charge distribution of the products calculated using B3LYP/6–311++G(d,p) level in gas phase.

Atom number	4H-Gly		4F-Gly		4Cl-Gly		4Br-Gly		$4NO_2$-Gly	
	Mulliken	NBO	Mulliken	NBO	Mulliken	NBO	Mulliken	NBO	Mulliken	NBO
C4	1.450	–0.140	1.469	–0.153	1.488	–0.141	1.453	–0.139	1.483	–0.102
C11	–0.641	0.509	–0.620	0.507	–1.125	0.505	–0.717	0.504	–1.006	0.501
O12	–0.192	–0.521	–0.193	–0.523	–0.194	–0.521	–0.184	–0.521	–0.177	–0.511
C13	–0.065	–0.204	–0.093	–0.209	0.002	–0.212	0.030	–0.213	0.098	–0.228
C15	0.450	0.709	0.478	0.083	0.545	0.086	0.483	0.087	0.608	0.099
C18	0.030	0.406	0.034	0.406	0.017	0.406	0.018	0.406	–0.030	0.405
O19	–0.241	–0.514	–0.240	–0.513	–0.237	–0.512	–0.237	–0.512	–0.230	–0.507
S20	0.200	0.215	0.197	0.218	–0.200	0.218	–0.197	0.218	–0.190	0.225
N17	0.250	–0.499	0.250	–0.499	0.250	–0.498	0.251	–0.498	0.252	–0.499
C16	–0.183	–0.055	–0.185	–0.055	–0.218	–0.055	–0.194	–0.055	–0.255	–0.055
S21	0.205	0.378	0.206	0.381	0.229	0.383	0.212	0.384	0.245	0.394
C22	–0.729	–0.502	–0.736	–0.502	–0.717	0.502	–0.739	–0.502	–0.729	–0.501
C25	0.659	–0.070	0.661	–0.071	0.663	–0.071	0.660	–0.071	0.660	–0.072
Atom number	**4H-Ala**		**4F-Ala**		**4Cl-Ala**		**4Br-Ala**		**$4NO_2$-Ala**	
	Mulliken	NBO	Mulliken	NBO	Mulliken	NBO	Mulliken	NBO	Mulliken	NBO
C4	1.191	–0.154	1.253	–0.168	0.524	–0.151	1.446	–0.148	1.044	–0.115
C11	–0.475	0.558	–0.469	0.556	–0.367	0.554	–0.750	0.554	–0.260	0.556
O12	–0.102	–0.552	–0.100	–0.553	–0.106	–0.552	–0.085	–0.551	–0.081	–0.537
C40	–0.273	0.066	–0.301	0.065	0.255	0.065	0.286	0.065	–0.133	0.063
O33	–0.086	–0.725	–0.088	–0.726	–0.087	–0.726	–0.086	–0.726	–0.078	–0.725
C35	0.421	0.003	0.413	0.003	0.440	0.003	0.423	0.003	0.423	0.003
C15	–0.293	0.445	–0.310	0.443	–0.300	0.443	–0.295	0.443	–0.291	0.441
O16	–0.217	–0.563	–0.217	–0.563	–0.214	–0.563	–0.214	–0.563	–0.208	–0.562
S17	0.145	0.237	0.154	0.239	0.135	0.240	0.157	0.239	0.176	0.243
C13	–0.408	–0.036	–0.397	–0.036	–0.395	–0.036	–0.393	–0.036	–0.401	–0.037
N14	0.098	–0.520	0.103	–0.523	0.100	–0.522	0.103	–0.523	0.111	–0.527
S18	–0.086	0.324	–0.087	0.325	–0.097	0.324	–0.104	0.324	–0.095	0.329
C19	–0.655	–0.500	–0.646	–0.499	–0.642	–0.499	–0.691	–0.499	–0.633	–0.499
C22	0.606	–0.066	0.603	–0.067	0.621	–0.007	0.663	–0.067	0.554	–0.068
Atom number	**4H-Leu**		**4F-Leu**		**4Cl-Leu**		**4Br-Leu**		**$4NO_2$-Leu**	
	Mulliken	NBO	Mulliken	NBO	Mulliken	NBO	Mulliken	NBO	Mulliken	NBO
C4	0.972	–0.154	1.031	–0.169	0.170	–0.170	0.520	–0.193	0.787	–0.164
C11	–0.578	0.560	–0.582	0.530	–0.504	0.290	–0.477	0.297	–0.365	0.296
O12	–0.077	–0.551	–0.075	–0.554	–0.095	–0.569	–0.083	–0.571	–0.060	–0.558
C39	–0.373	0.059	–0.404	0.159	–0.162	0.241	–0.179	0.452	–0.134	0.442
O33	–0.024	–0.725	–0.027	–0.741	–0.029	–0.862	0.027	–0.895	–0.016	0.897
C35	0.920	0.016	0.920	–0.012	0.511	–0.128	1.004	–0.180	1.033	–0.184
C36	–0.436	–0.365	–0.376	–0.368	0.225	–0.386	–0.378	–0.406	–0.441	–0.406
C15	–0.261	0.447	–0.286	0.445	–0.442	0.441	–0.270	0.425	–0.271	0.423
O16	–0.185	–0.565	–0.185	–0.565	–0.178	–0.562	–0.182	–0.571	–0.177	–0.571
S17	0.183	0.239	0.203	0.240	0.168	0.242	0.187	0.230	0.204	0.236
C13	–0.581	–0.034	–0.576	–0.034	–0.395	–0.034	–0.591	–0.041	–0.564	–0.042
N14	0.282	–0.529	0.281	–0.532	0.280	–0.538	0.278	–0.550	0.285	–0.559
S18	–0.134	0.322	–0.128	0.323	–0.097	0.324	–0.136	0.321	–0.146	0.323
C19	–0.674	–0.499	–0.665	–0.499	–0.631	–0.499	–0.678	–0.501	–0.678	–0.500
C22	0.570	–0.065	0.543	–0.066	0.509	–0.067	0.525	–0.067	0.532	–0.068

electromagnetic spectra, vibrational spectra, and chemical reactivities.[40]

Making help of the atomic charges of the molecules to analyze and better understand their experimental data in favor of computational chemistry methods is usual and popular. Because the net charge of the whole molecule but not the atomic charges are accessible using experimental methods, determination of them by using computational chemistry methods could be so useful for many researchers to better understand the electron density distribution related property results of the interested molecules.[40]

Many methods to determine atomic charges exist; here we report the atomic charges on some important atoms of the studied molecules, which are obtained by the use of Milliken and natural bond orbital (NBO) analysis.

Both the Mullikan[41–43] and NBO[44] atomic charges are defined based on orbitals. The former one uses the sum of the electronic charge contributions of centered orbitals at each atom and half of the electronic overlap clouds between two atoms for each atom. But the latter one, uses electronic charge contributions of the orbitals which are orthogonalized and localized to form one or two center orbitals, so-called natural bond orbitals. Therefore, from the viewpoint of chemistry, natural bond orbital charge is more meaningful than the Mulliken charge.[40]

Some atomic charges for the products which were obtained using the B3LYP/6–311++G(d,p) method in the gas phase according to the natural bond orbital (NBO) analysis and also the Mulliken population are listed in Table 5.

Using NBO charges, C11 and C13 carbon atoms in 4X-Gly products have positive and negative charges, respectively. The amount of the positive charge on C11 increased with the increasing of the electron-withdrawing effect and also the polarizability of the substituent X from X = H to X = NO_2, therefore, the 4NO_2-Gly compound has the most positive C11 atom whereas the 4H-Gly compound has the lowest positive C11 atom.

The negative charge on the C13 atom is increased from X = H to X = NO_2 because the electron-withdrawing effect and polarizability of the substituent X diminished the electron-withdrawing effect of the benzoyl group and consequently on the C13 atom as well.

The NBO analysis revealed that the C4 atom of the 4X-Ala products shows the highest difference in its negative charge among the five products of that type. As evident for the C4 atom, the 4NO_2-Ala compound has the most negatively charged C4 atom.

Finally, NBO results showed that the charge on the C11 atom of the 4X-Leu products decreased with the increasing withdrawing effect and polarizability of the substituent X because of balancing of the electron-withdrawing effect of the oxygen atom due to its electronegativity with the withdrawing effect and polarizability of the substituent X attached to the phenyl ring.

4. 6. Electrostatic Potential Map

"Molecular electrostatic potential (MEP), *V*(r) at a given point r(x, y, z) in the vicinity of a molecule, is defined in terms of the interaction energy between the electrical charge generated from the molecule's electrons and nuclei and a positive test charge (a proton) located at (r)".[37] In this section, the molecular electrostatic potential (MEP) for the 4H-Gly, 4H-Ala and 4H-Leu products at the B3LYP/6–311++G(d,p) level are depicted in Figure 3. The electron-rich, neutral and electron-deficient regions around the specified molecule are presented by red, green and blue colors, respectively. Light blue and yellow colors represent the slightly electron-deficient and slightly electron-rich regions, respectively. Where the interaction energy between the electrical charges results in the strongest attractions, the surface appeared in blue; in contrast where it results in the strongest repulsion the surface appeared in red. Therefore, the electrostatic potential increases in the red < orange < yellow < green < blue order.[37]

Since molecular electrostatic potential was obtained based on the electronic density it could be applicable as a tool for evaluation of the electrophilic sites of the molecule and nucleophilic reactivity. In addition it is a useful descriptor for investigation of the non-covalent interactions such as hydrogen-bonding interactions.[37,45,46]

As seen from the Figure 3, the red regions of all three titled products are mainly localized around the oxygen atom of the carbonyl groups, therefore those are the most favorable sites for electrophilic attack. On the other hand, posi-

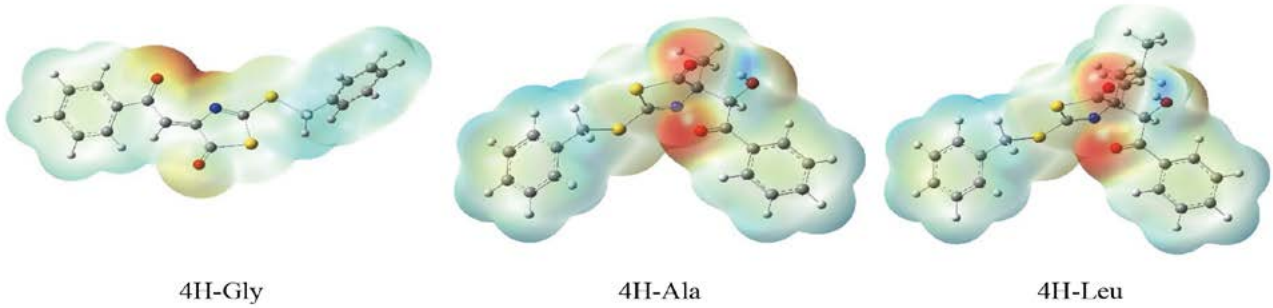

Figure 3. Electrostatic potential map for 4H-Gly, 4H-Ala and 4H-Leu products.

tive regions of the electrostatic potential are localized mainly around the hydrogen atoms attached to the phenyl rings.

To obtain more information about the sites which are more probable to be involved in nucleophilic attack, the maximum potential electrostatic values were determined and some of them are listed in Table 6. Data in Table 6 indicate that in the case of 4H-Gly the C18 is more nucleophilic than the C11. C15 is more nucleophilic than C13 indicating that the Michael addition occurred on C15 and then the structure of the main regioisomer could be predicted. In the case of the 4H-Ala and 4H-Leu products, the C15 and C11 are determined as the most nucleophilic sites.

Table 6. Maximum electrostatic potentials in kcal/mol for some selected atoms of 4H-Gly, 4H-Ala and 4H-Leu products.

4H-Gly		4H-Ala		4H-Leu	
Atom	***Vs*(Max)**	**Atom**	***Vs*(Max)**	**Atom**	***Vs*(Max)**
C11	9.30	C11	6.48	C11	7.62
C13	5.55	C13	6.74	C13	5.88
C15	15.67	C15	8.06	C15	5.48
C16	6.30	C19	0.00	C19	0.00
C18	15.67	C40	0.00	C39	0.00

5. Conclusion

In conclusion, we have shown that the dithiocarbamates prepared with natural amino acids can be simply used in the Erlenmeyer–Plöchl reaction. We also have presented an efficient procedure for the synthesis of 15 novel derivatives of the thiazolactone skeleton via Erlenmeyer–Plöchl reaction without using any catalyst and harsh conditions in good to high yields. Thereafter, quantum chemical calculations were used to deeply investigate the structural characteristics and charge distribution analysis of the newly prepared products. ^{1}H NMR spectra of the products were computed and compared with the experimental ones. The results revealed that there is a good agreement between calculated and experimentally obtained ^{1}H NMR chemical shifts.

Conflict of interest

The authors declare no conflict of interest.

Acknowledgements

Support of this work from the Research Council of the University of Guilan is gratefully appreciated.

6. References

1. E. Erlenmeyer, *Ann.,* **1893**, 275, 1–8. **DOI:**10.1002/jlac.18932750103
2. D. Benedlt, V. Daniel, *J. Med. Chem.,* **1994**, *37*, 710–712. **DOI:**10.1021/jm00031a023
3. E. R. Pereira, M. Sancelme, A. Voldoire, M. Prudhomme, *Bioorganic Med. Chem. Lett.,* **1997**, *7*, 2503–2506. **DOI:**10.1016/S0960-894X(97)10007-5
4. A. El-Mekabaty, *I. J. Org. Chem.*, **2013**, *2*, 40–66.
5. M. A. F. El-Kaschef, F. M. E. Abdel-Megeid, S. M. A. Yassin, *Ann. Chem.,* **1974**, *1,* 37–43. **DOI:**10.1002/jlac.197419740106
6. E. Erlenmeyer, *Ber.,* **1889**, *22*, 792–795. **DOI:**10.1002/cber.188902201174
7. J. L. Diaz, B. Villacampa, F. Lopez-Calahorra, D. Velasco, *Tetrahedron Lett.*, **2002**, *43,* 4333–4337. **DOI:**10.1016/S0040-4039(02)00806-7
8. G. Koczan, G. Csik, A. Csampai, E. Balog, S. Bosze, P. Sohar, F. Hudecz, *Tetrahedron*, **2001**, *57*, 4589–4598. **DOI:**10.1016/S0040-4020(01)00332-5
9. S. Fozooni, A. M. Tikdari, H. Hamidian, H. Khabazzadeh, *Arkivoc,* **2008**, *xiv*, 115–123. **DOI:**10.3998/ark.5550190.0009.e13
10. N. Illy, E. Mongkhoun, *Polym. Chem.*, **2022**, *13*, 4592–4614. **DOI:**10.1039/D2PY00731B
11. C. Gündoğdu, D. Topkaya, G. Öztürk, S. Alp, Y. Ergün, *J. Heterocycl. Chem.*, **2010**, *47*, 1450–1453. **DOI:**10.1002/jhet.499
12. D. S. A. Haneen, W. S. I. Abou-Elmagd, A. S. A. Youssef, *Synth. Commun.*, **2021**, *51*, 215–233. **DOI:**10.1080/00397911.2020.1825746
13. M. Bergmann, F. Stern, *Ann.* **1926**, *448,* 20–31. **DOI:**10.1002/jlac.19264480103
14. A. Ziyaei Halimehjani, P. Aghabozorg Naneva, Y. Lotfi Nosod, B. Khalili, *NSMSI (In Persian)*, **2016**, *35*, 43–55.
15. B. Eftekhari-Sis, M. Zirak, A. Akbari, *Chem. Rev.*, **2013**, *113*, 2958–3043. **DOI:**10.1021/cr300176g
16. B. Khalili, P. Jajarmi, B. Eftekhari-Sis, M. M. Hashemi, *J. Org. Chem.*, **2008**, *73,* 2090–2095. **DOI:**10.1021/jo702385n
17. B. Khalili, T. Tondro, M. M. Hashemi, *Tetrahedron*, **2009**, *65,* 6882–6887. **DOI:**10.1016/j.tet.2009.06.082
18. M. Rimaz, H. Mousavi, L. Nikpey, B. Khalili, *Res. Chem. Intermed.,* **2017**, *43*, 3925–3937. **DOI:**10.1007/s11164-016-2848-5
19. M. Rimaz, P. Pourhossein, B. Khalili, *Turk. J. Chem.*, **2015**, *39*, 244–254. **DOI:**10.3906/kim-1408-32
20. M. Rimaz, H. Rabiei, B. Khalili, R. H. Prager, *Aust. J. Chem.*, **2014,** *67*, 283–288.
21. M. Rimaz, F. Aali, B. Khalili, R. H. Prager, *Aust. J. Chem.*, **2016**, *70*, 660–668. **DOI:**10.1071/CH16364
22. M. Rimaz, H. Mousavi, B. Khalili, F. Aali, *J. Chin. Chem. Soc.*, **2018**, *65*, 1389–1397. **DOI:**10.1002/jccs.201700470
23. M. Rimaz, B. Khalili, G. Khatyal, H. Mousavi, F. Aali, *Aust. J. Chem.*, **2017**, *70*, 1274–1284. **DOI:**10.1071/CH17146
24. M. Rimaz, H. Mousavi, L. Ozzar, B. Khalili, *Res. Chem. Intermed.*, **2019**, *45*, 2673–2694. **DOI:**10.1007/s11164-019-03757-9
25. M. Rimaz, J. Khalafy, H. Mousavi, S. Bohlooli, B. Khalili, *J. Heterocycl. Chem.,* **2017,** *54*, 3174–3186. **DOI:**10.1002/jhet.2932
26. N. O. Mahmoodi, B. Khalili, O. Rezaeianzade, A. Ghavidast,

Res. Chem. Intermed., **2016**, *42*, 6531–6542. **DOI:**10.1007/s11164-016-2478-y
27. B. Khalili, F. Sadeghzadeh Darabi, B. Eftekhari-Sis, M. Rimaz, *Monatsh. Chem.,* **2013**, *144*, 1569–1572. **DOI:**10.1007/s00706-013-1038-z
28. S. J. Ahmadi, S. Sadjadi, M. Hosseinpour, *Ultrason Sonochem.,* **2013**, *20*, 408–412. **DOI:**10.1016/j.ultsonch.2012.07.008
29. H. A. Riley, A. R. Gray, *Org. Synth.*, **1935**, *Coll. 15*, 67–69. **DOI:**10.15227/orgsyn.015.0067
30. M. J. Frisch, G. W. Trucks, H. B. Schlegel, G. E. Scuseria, M. A. Robb, J. R. Cheeseman, G. Scalmani, V. Barone, B. Mennucci, G. A. Petersson, H. Nakatsuji, M. Caricato, X. Li, H. P. Hratchian, A. F. Izmaylov, J. Bloino, G. Zheng, J. L. Sonnenberg, M. Hada, M. Ehara, K. Toyota, R. Fukuda, J. Hasegawa, M. Ishida, T. Nakajima, Y. Honda, O. Kitao, H. Nakai, T. Vreven, J. A. Montgomery, Jr., J. E. Peralta, F. Ogliaro, M. Bearpark, J. J. Heyd, E. Brothers, K. N. Kudin, V. N. Staroverov, R. Kobayashi, J. Normand, K. Raghavachari, A. Rendell, J. C. Burant, S. S. Iyengar, J. Tomasi, M. Cossi, N. Rega, J. M. Millam, M. Klene, J. E. Knox, J. B. Cross, V. Bakken, C. Adamo, J. Jaramillo, R. Gomperts, R. E. Stratmann, O. Yazyev, A. J. Austin, R. Cammi, C. Pomelli, J. W. Ochterski, R. L. Martin, K. Morokuma, V. G. Zakrzewski, G. A. Voth, P. Salvador, J. J. Dannenberg, S. Dapprich, A. D. Daniels, Ö. Farkas, J. B. Foresman, J. V. Ortiz, J. Cioslowski, D. J. Fox, *Gaussian 09, Revision A.11.4*, **2009**, Gaussian Inc., Wallingford CT.
31. A. D. Becke, *J. Chem. Phys.,* **1993**, *98*, 5648–5652. **DOI:**10.1063/1.464913
32. C. T. Lee, W. T. Yang, R. G. Parr, *Phys. Rev. B* **1988**, *37*, 785–789. **DOI:**10.1103/PhysRevB.37.785
33. M. J. Frisch, J. A. Pople, J. S. Binkley, *J. Chem. Phys.,* **1984,** *80*, 3265–3269. **DOI:**10.1063/1.447079
34. P. C. Chen, Y. C. Chieh, J. C. Wu, *J. Mol. Struct.,* **2005**, *715*, 183–189. **DOI:**10.1016/j.theochem.2004.10.012
35. E. K. U. Gross, W. Kohn, *Adv. Quantum Chem.*, **1990**, *21*, 255–291.
36. A. Streitwieser, *Molecular Orbital Theory for Organic Chemists*, **1961,** Wiley, New York. **DOI:**10.1149/1.2425396
37. A. Eşme, S. Güneşdoğdu Sağdınç, *Spectrochim. Acta A,* **2018**, *188*, 443–455. **DOI:**10.1016/j.saa.2017.07.034
38. J. K. M. Sanders, B. K. Hunter, *Modern NMR Spectroscopy. A Guide for Chemists, Magnetic Resonance in Chemistry*, Oxford University Press, Oxford, **1987**, *25*, 1092. **DOI:**10.1002/mrc.1260251217
39. J. R. Cheeseman, G. W. Trucks, T. A. Keith, and M. J. Frisch, *J. Chem. Phys.*, **1996**, *104*, 5497–5509. **DOI:**10.1063/1.471789
40. J. X. Mao, *JPR*, **2014**, *2*, 15–18.
41. R. S. Mulliken, *J. Chem. Phys.,* **1955,** *23*, 1833–1840. **DOI:**10.1063/1.1740588
42. R. S. Mulliken, *J. Chem. Phys.,* **1955**, *23*, 1841–1846. **DOI:**10.1063/1.1740589
43. R. S. Mulliken, *J. Chem. Phys.,* **1955**, *23*, 2338–2342. **DOI:**10.1063/1.1741876
44. A. E. Reed, R. B. Weinstock, F. Weinhold, *J. Chem. Phys.,* **1985**, *83*, 735–746. **DOI:**10.1063/1.449486
45. P. Politzer, J. Murray, *Theor. Chem. Acc.*, 2002, *108*, 134–142. **DOI:**10.1007/s00214-002-0363-9
46. P. Politzer, J. S. Murray, *Theoretical Biochemistry and Molecular Biophysics: A Comprehensive Survey,* **1991**, Adenine Press, New York.

Povzetek

V okviru te raziskave smo s pomočjo Erlenmeyer–Plöchlove reakcije sintetizirali 15 derivatov s tiazolaktonskim skeletom. Kot prekurzorje ditiokarbamata smo uporabili aminokisline glicin, alanin in levcin tako, da smo jih reagirali z ogljikovim disulfidom in benzil kloridom. Dobljene benzil ditiokarbamate smo v prisotnosti acetanhidrida pretvorili v ustrezne tiazolaktone ter jih v nadaljevanju kondenzirali z arilglioksali kot viri karbonilne skupine. Produkte smo karakterizirali s spektroskopskimi metodami IR, ^{1}H NMR in ^{13}C NMR. V nadaljevanju smo s pomočjo računskih metod pridobili dodatne informacije o produktih, vključno z njihovimi strukturnimi značilnostmi, razporeditvijo nabojev ter ^{1}H NMR in UV-VIS spektri. Rezultati so pokazali, da se izračunane vrednosti kemijskih premikov dobro ujemajo z eksperimentalno izmerjenimi. Za vse izračune smo uporabili B3LYP DFT metodo skupaj s 6-311++G(d,p) baznim setom.

DRUŠTVENE VESTI IN DRUGE AKTIVNOSTI
SOCIETY NEWS, ANNOUNCEMENTS, ACTIVITIES

Vsebina

Contents

70 let izhajanja revije *Acta Chimica Slovenica*: pozdravne besede in čestitke ob jubileju

dr. Peter Venturini

predsednik Slovenskega kemijskega društva

Kot predsednik Slovenskega kemijskega društva sem ponosen, da *Acta Chimica Slovenica*, naša ugledna znanstvena revija, igra pomembno vlogo pri spodbujanju znanstvenega dialoga in izmenjavi znanja znotraj slovenske in globalne kemijske skupnosti že sedem desetletij. Je izraz skrbnega dela in odličnosti vseh sodelujočih pri reviji, tako preteklih kot sedanjih. Hkrati je neprecenljiva platforma za raziskovalce, ki omogoča širjenje odkritij in poglobljenih študij.

Kemija velja za eno od osrednjih znanosti in nam, znanstvenikom, na več načinov omogoča interakcijo z drugimi disciplinami. V reviji *Acta Chimica Slovenica* so dobrodošle tako teoretične kot eksperimentalne študije. Strog postopek ocenjevanja prispelih člankov, ki temelji na visokih standardih strokovne uredniške ekipe, je prispeval k stalnemu večanju ugleda revije. Verjamem, da visoko kvalitetne raziskave zaslužijo veliko odmevnost, saj s tem dosežejo širše občinstvo. *Acta Chimica Slovenica* pomembno prispeva k širjenju prodornih znanstvenih del z vseh področij kemije tudi z brezplačnim izvodom skrbno pripravljene revije.

V vseh teh letih je *Acta Chimica Slovenica* v tiskani ali v digitalni obliki pomembno prispevala k obogatitvi znanstvene literature. Ob visoki obletnici je potrebno poudariti veliko opravljeno delo uredniškega odbora, recenzentov, avtorjev in vseh tistih, ki skrbijo za visoko kakovost revije. Prav zavezanost k zasledovanju znanstvenega znanja in širjenju vrhunskih raziskav je bila tista, ki je vplivala na prestiž revije in utrditev njenega ugleda v znanstveni skupnosti.

Ob tej priložnosti se zahvaljujem vsem ustvarjalcem revije, dolgoletnim podpornikom ter oglaševalcem, ki so pripomogli k rednemu izdajanju in rasti revije *Acta Chimica Slovenica* že sedem desetletij.

prof. dr. Franc Perdih

glavni in odgovorni urednik revije Acta Chimica Slovenica

Fakulteta za kemijo in kemijsko tehnologijo Univerze v Ljubljani

Sedemdeset let izhajanja revije *Acta Chimica Slovenica*, sprva pod imenom *Vestnik Slovenskega kemijskega društva*, predstavlja obdobje, ki si zasluži podrobnejšo osvetlitev ene od pomembnih dejavnosti Slovenskega kemijskega društva. Če je delovanje društva v osnovi namenjeno povezovanju slovenskih kemičark in kemikov, so glavne aktivnosti, kot so Slovenski kemijski dnevi ter izdajanje revije *Acta Chimica Slovenica*, namenjene povezovanju znanstvene in strokovne skupnosti, ki znatno presega nacionalne meje. Ob tej priložnosti smo pripravili pregled dosedanjega dela pri izdajanju revije *Acta Chimica Slovenica* z željo omogočiti vpogled v aktivnosti, ki so potrebne za delovanje znanstvene revije, ter izpostaviti entuziazem, požrtvovalnost in trud številnih posameznikov, ki so in še skrbijo za delovanje in uveljavljanje revije v mednarodnem prostoru. Odpiranje svetovni znanstveni javnosti je bila ena od osrednjih točk uredniške aktivnosti v preteklih desetletjih, saj so bili že v prvi številki revije *Vestnik Slovenskega kemijskega društva* leta 1954 članki objavljeni v angleščini in nemščini, med avtorji pa so bili tudi tuji raziskovalci. Sodobne informacijske tehnologije so omogočile prehod iz tiskane na elektronsko obliko člankov, kar je znatno olajšalo dostopnost revije in s tem povečalo mednarodno vpetost revije in seveda s tem tudi znatno povečalo vpliv znanstvenih objav v reviji *Acta Chimica Slovenica* na razvoj kemije, kemijskega inženirstva, biokemije, kemijskega izobraževanja in drugih sorodni ved. Široka mednarodna vpetost revije tako s prostim dostopom člankov na spletu kakor tudi z vključitvijo v različne znanstvene baze, kot so na primer Web of Science, PubMed, CrossRef in druge, ter z dodelitvijo DOI številk člankom, je omogočila uveljavljanje revije *Acta Chimica Slovenica* v znanstveni skupnosti. Na kakovost objav v reviji pa kaže tudi to, da imajo najbolj citirani članki več kakor 200 citatov. Dolgoletno požrtvovalno delo urednikov in uredniških odborov, trdna podpora Slovenskega kemijskega društva ter njegovih predsednikov in tajnic, podpora tako društvu kakor tudi reviji s strani univerz oziroma fakultet ter inštitutov, kvalitetno delo avtorjev in konstruktivna kritika recenzentov ter podpora s strani državnih inštitucij, so omogočili 70 let razvoja in napredka na področju izdajanja slovenske znanstvene revije *Acta Chimica Slovenica*. S tem je dana reviji odlična popotnica za nadaljnje delovanje.

prof. dr. Venčeslav Kaučič

častni predsednik Slovenskega kemijskega društva

Kemijski inštitut, Ljubljana

Spoštovane članice in člani Slovenskega kemijskega društva in drugi bralci revije *Acta Chimica Slovenica*!

Letos mineva 50 let odkar sem postal član Slovenskega kemijskega društva (od leta 1973), v letih od 1986 do 1996 sem bil tajnik društva in od leta 1996 do 2017 njegov predsednik. V vseh teh letih sem spremljal razvoj društvenega glasila, ki je že zelo kmalu preraslo v ugledno znanstveno in strokovno revijo, ki je objavljala in objavlja znanstvene in strokovne prispevke iz vseh področij kemije in je pridobila sorazmerno visok faktor vpliva.

Tako kot so se glavni, področni in tehnični uredniki ter ves uredniški odbor *Acta* trudili zagotoviti kvaliteto revije v vseh pogledih, tako sem se dolga leta z drugimi kolegi trudil zagotavljati finančna sredstva za njeno izhajanje. Zahvala za vsestransko podporo društvu in izhajanju *Acta* gre pomembnim industrijskim partnerjem, fakultetam, znanstvenim in strokovnim inštitutom ter ministrstvu oz. RSS in ARRS, zdaj ARIS.

Objavljeni članki v *Acta* pokrivajo aktualna področja anorganske, organske, fizikalne in analizne kemije, kemije materialov, kemijskega, biokemijskega in okoljskega inženirstva ter splošne, uporabne in biomedicinske kemije. Pisani so v angleškem jeziku s slovenskim povzetkom. V slovenskem delu revije – Društvenih vesteh, so bila objavljena poročila sekcij in podružnic ter seznami diplomskih, magistrskih in doktorskih del na širšem področju kemije v vsakem letu na slovenskih univerzah. Posebej radi smo brali posvečene številke revije, ki so izšle ob posebnih priložnostih. Na internetu objavljamo elektronsko verzijo revije, kar povečuje branost in mednarodno odmevnost revije.

Veliko truda je bilo vloženega v pripravo kvalitetnih vsebin naše revije, ki izhaja že 70 let. Slovenskemu kemijskemu društvu čestitam in želim mnogo uspehov v bodoče.

prof. dr. Andreja Žgajnar Gotvajn

dekanja

Fakulteta za kemijo in kemijsko tehnologijo Univerze v Ljubljani

Ob tej svečani priložnosti, ko revija *Acta Chimica Slovenica* praznuje svojo sedemdesetletnico izhajanja, imam čast in veselje, da kot dekanja Fakultete za kemijo in kemijsko tehnologijo UL napišem nekaj besed. Ta pomemben mejnik odraža ne le dolgotrajno zavezanost revije kemijski znanosti, ampak tudi njen vpliv na razvoj kemije in s tem povezanih ved v Sloveniji in širše. Revija je od samega začetka predstavljala pomembno platformo za objavo visokokakovostnih znanstvenih prispevkov s področja kemije. Njena vloga pri spodbujanju raziskovalne dejavnosti ter izmenjavi znanja med raziskovalci in akademiki je neprecenljiva. Revija je postala ugleden vir informacij za kemijsko skupnost, ki ji omogoča, da sledi razvoju stroke v mednarodnem okolju in k njemu tudi pomembno prispeva. Njena vsebina, ki obsega širok spekter tematik, od bazičnih raziskav do predstavitev bolj aplikativnih in industrijskih dosežkov, je prispevala k bogatitvi znanja in razumevanju kemije in njenih vedno bolj interdisciplinarnih uporab v praksi. Številni avtorji, recenzenti in uredniki, ki so sodelovali pri reviji, so neprecenljivo prispevali k njeni odličnosti in ugledu.

V tem obdobje sedemdesetih let so se ljudje in svet okoli revije bliskovito spreminjali. Tehnološke spremembe, ki so nas vodile od klicev s stacionarnih telefonov do video klicev z mobilnimi telefonu, od tiskanih in magnetnih medijev za zapis podatkov do virtualnih oblakov, od enostavnih avtomobilov do samovozečih hibridov in električnih vozil, od enostavnih do kompleksnih bioloških zdravil, od naravnih materialov do domala neuničljivih trajnostnih kompozitov, so neločljivo povezane s kemijo v vseh njenih pestrih oblikah. Tudi samo razumevanje znanja, raziskovanja ter njune predstavitve in pomena v javnosti v preteklih desetletjih se je z zavedanjem pomena etike raziskovanja ter odprte znanosti popolnoma spremenilo. V ospredje smo stopile tudi ženske, ki se moramo za svoje mesto v znanosti ter akademskem okolju še vedno velikokrat in neprestano dokazovati. Živimo v trenutku, v katerem imajo slike ter besede, kot so trajnost, interdisciplinarnost, mednarodnost, odmevnost, veliko moč. Pred revijo in vsemi nami se neprestano odpirajo nova vprašanja, novi izzivi. Nekaj, kar nas v tem trenutku po eni strani navdušuje in po drugi strani straši, je tudi razvoj umetne inteligence, njene sposobnosti, avtonomnost ter s tem povezana vprašanja. Klepetalni roboti so tisti, ki bodo nedvomno spremenili svet okoli nas in njegovo dojemanje. Tudi prvi odstavek tega uvodnika je brez napak z le nekaj vnesenimi ključnimi besedami sestavil ChatGPT in kot raziskovalka se zavedam priložnosti, ki jih tak digitalen svet s svojimi orodji ponuja, a nelagodje in previdnost ostajata. Ko sem sestavek prvič prebrala, me je osupnila njegova popolnost, pri ponovnem branju pa me je zbodla njegova površinskost, praznost in brezosebnost. Tisto »nekaj« manjka, da bi se bralca dotaknilo, da bi mu karkoli od prebranega sploh ostalo v spominu. Zato smo raziskovalci lahko pomirjeni, saj bo raziskovalno delo, z vsemi velikimi prebojnimi odkritji, uspehi, pa tudi skepso, zgrešenimi hipotezami, napačnimi meritvami ter napakami ostalo v domeni ljudi. Ljudje s svojo energijo, razmišljanjem in empatijo smo tisti, ki s skupnimi močmi zagotavljamo napredek in vodimo ter usmerjamo razvoj, kot je bilo in je pri reviji *Acta Chimica Slovenica*. Ne glede na tehnični in vsebinski napredek njenega delovanja so avtorji, uredniki ter recenzenti tisti, ki prepoznajo aktualnost ter kvaliteto objavljenih prispevkov in na ta način zagotavljajo njen preboj ter obstoj med globalno prepoznanimi pomembnimi znanstvenimi revijami s faktorjem vpliva. Zato lahko mirno sprejmem pomoč klepetalnika pri zaključnem odstavku tega uvodnika, saj vem, da mi znanje in izkušnje zagotavljajo, da bom znala preceniti smiselnost, vrednost in primernost napisanega.

Veselim se prihodnosti revije in njenega nadaljnjega prispevka k raziskovalnemu in akademskemu okolju. Verjamem, da bo revija ostala ključen vir informacij na področju kemijskih znanosti in neločljiv del širokega področja delovanja naše fakultete ter stroke!

akad. prof. dr. Gregor Anderluh

direktor

Kemijski inštitut, Ljubljana

Kemijski inštitut z vrhunskimi raziskovalnimi dosežki, raznovrstnimi razvojnimi projekti, prenosom inovacij v gospodarstvo in z vzgojo vrhunskega kadra sooblikuje raziskovalne in razvojne trende prihodnosti. Vsak dan znova želimo biti tudi odprt učni prostor za mlade znanstvenice in znanstvenike, s čimer smo tesno vpeti v izobraževalne procese na različnih univerzitetnih ravneh. Na ta način skrbimo za razvoj in vpetost stroke v življenja prihodnjih generacij. Podobno poslanstvo ima tudi Slovensko kemijsko društvo, ki kot organizacija strokovnjakov s področja kemije, kemijske tehnologije in kemijskega inženirstva skrbi za napredek stroke in strokovnega znanja članic in članov ter zainteresirane javnosti. Z izdajanjem društvene revije *Acta Chimica Slovenica* pa v svetovnem merilu izpolnjuje tudi namen širjenja znanstvenih in strokovnih spoznanj ter dosežkov širši mednarodni kemijski stroki. Na Kemijskem inštitutu kot donatorji že vrsto let podpiramo prizadevanja in napore stanovskih kolegic in kolegov in uredniškega odbora za nemoteno izdajanje revije, kot tudi za njen razvoj v vsebinskem in tehničnem smislu. Na tem mestu želim poudariti, da so oziroma pri soustvarjanju revije še sodelujejo naslednje raziskovalke in raziskovalci s Kemijskega inštituta: prof. Igor Belič (kot urednik), dr. Marko Razinger (kot tehnični urednik), dr. Johannes T. Van Elteren, dr. Michael Beeston, dr. Jernej Stare, dr. Irena Vovk in dr. Alen Albreht (kot področni uredniki), prof. dr. Blaž Likozar in prof. dr. Janez Mavri (kot člana uredniškega odbora). Veseli me dejstvo, da se revija pri izdajanju številk, posvečenih uglednim slovenskim znanstvenikom, osredotoča ne samo na področje kemije, temveč tudi širše na področji farmacije in biokemije. Reviji *Acta Chimica Slovenica* in uredniškemu odboru ter vsem soustvarjalcem želim uspešno delo in neumorno izdajanje številk tudi v prihodnje, predvsem pa uspešno spopadanje z vse bolj zahtevnimi izzivi na področju publicistične dejavnosti.

prof. dr. Boštjan Zalar

direktor

Institut »Jožef Stefan«, Ljubljana

Veseli nas, da Acta Chimica Slovenica praznuje tako častitljivo obletnico. 70 let je v tem hitro se spreminjajočem svetu prav zavidanja vredna številka in na to smo lahko slovenski raziskovalci zelo ponosni.

Revija, ki jo izdaja Slovensko kemijsko društvo, združuje raziskovalke in raziskovalce z različnih področij, v veliki meri pa je namenjena kemikom. Raziskovalke in raziskovalci z Instituta »Jožef Stefan«, ki v največji meri sodelujejo z *Acto Chimico Slovenico,* prihajajo predvsem s področij kemije, znanosti o materialih, biokemije in znanosti o okolju. Raziskovalci z Instituta pri njenem sooblikovanju sodelujejo kot avtorji, recenzenti, uredniki področij in člani uredniškega odbora. Še posebej bi izpostavil urednice in urednike področij, ki so nekoč in še vedno prispevajo k razvoju revije. Zavedam se, da uredniško delo prav gotovo ni lahko in veseli me, da ga z vso zavzetostjo opravljajo ob svojem raziskovalnem delu.

Prav z zanimanjem sem prebrskal bazo Web of Science in glede na podatke so sodelavci Instituta »Jožef Stefan« v preteklih 25 letih prispevali več kot 150 prispevkov, večinoma znanstvenih člankov, in kar 13 preglednih člankov. Pomembno se nam zdi, da revija že vsa leta ohranja svoj status »odprte« revije in tako sledi načelom odprte znanosti; dandanašnji je prosta dostopnost objavljenih člankov in prispevkov dragocena.

Revija *Acta Chimica Slovenica* se je sprva imenovala *Vestnik slovenskega kemijskega društva* in je zdajšnje ime prevzela leta 1993. V treh desetletjih je postala priznana mednarodna znanstvena revija, v kateri objavljajo tako domači kot tuji raziskovalci in raziskovalke.

Acti Chimici Slovenici želim še vrsto uspešnih let. Revija je pomemben del slovenske raziskovalne sfere, raziskovalke in raziskovalci Instituta »Jožef Stefan« pa bomo gotovo po svojih najboljših močeh prispevali k njenemu nadaljnjemu razvoju.

prof. dr.
Zoran Novak

dekan

Fakulteta za kemijo in kemijsko tehnologijo Univerze v Mariboru

70-letnica *Acta Chimica Slovenica* kaže na častitljivo starost in trajnost revije tako v slovenskem kakor tudi v mednarodnem prostoru. Obeleževanje 70-letnice revije pomeni, da so njeni ustanovitelji, uredniški odbori, uredniki, avtorji in ocenjevalci prispevkov v celotni zgodovini predano in odgovorno utrjevali in razvijali njeno vsebinsko zasnovo, sporočilnost in kvaliteto. Le tako je bilo mogoče reviji na dolgi rok preživeti in se utrditi v mednarodnem prostoru kvalitetnih revij s področij kemije, kemijskega inženirstva in sorodnih ved.

Prav to poslanstvo revije je Fakulteta za kemijo in kemijsko tehnologijo Univerze v Mariboru ves čas vzpodbujala, kot sponzorica sofinancirala in z univerzitetnimi učitelji in raziskovalci soizvajala. Delovanje članov fakultete je skladno z njeno vizijo, namreč da fakulteta postane mednarodno prepoznavno središče inovativnih znanj za izzive 21. stoletja s področij kemije, kemijskega in biokemijskega inženirstva ter sorodnih ved, da postane privlačna za motivirane študente, ustvarjalne univerzitetne učitelje in raziskovalce, prav tako pa vse zanimivejša za domače in mednarodne znanstvene mreže ter kemično in procesne industrije. Fakulteta za kemijo in kemijsko tehnologijo Univerze v Mariboru spada po svojem bistvu delovanja med znanstvene fakultete, kar pomeni, da je znanstvena dejavnost integrirana v študijski proces in da so vsebine študijskih programov prežete z rezultati raziskovalnega dela. Raziskave so pretežno odprtega značaja, kar univerzitetnim učiteljem omogoča, da najnovejša znanja neposredno prenašajo študirajoči generaciji, da svoje rezultate sprotno predstavljajo na domačih in mednarodnih konferencah ter objavljajo v kvalitetnih revijah. Še posebej so pri tem pomembne revije odprtega dostopa. Zelo naju veseli, da je revija *Acta Chimica Slovenica* ena od revij odprtega dostopa in da ima podeljen status platinskega odprtega dostopa, torej trajnega dostopa, kar lahko dosežejo le zanesljive revije - in *Acta Chimica Slovenica* je prav to. Še več, z leti ji raste mednarodni rang po različnih kazalnikih – trenutno je njen faktor vpliva 1,524.

Acta Chimica Slovenica je nekoliko starejša od visokošolske kemije v Mariboru, ki je predlani beležila 60-letnico svojega obstoja. Vendar so kasnejši sodelavci Fakultete za kemijo in kemijsko tehnologijo Univerze v Mariboru objavljali ali sodelovali pri reviji že od njene ustanovitve. Tako je mogoče iz arhiva *Acta Chimica Slovenica* ugotoviti, da je V. Ozim, ki je bil kasneje dolgoletni univerzitetni predavatelj v Mariboru, že leta 1958 v 5. volumnu takratnega *Vestnika Slovenskega kemijskega društva* kot soavtor s S. Kotnikom in V. Sorškom objavil prilogo "S. Kotnik, V. Ozim, V. Soršak: Professional workman in the Yugoslav chemical industry". Nekoliko kasneje leta 1961 je prof. Mirko Čeh objavil "M. Čeh: Das Jodsorptionsvermögen der durch die Salzsäure hydrolysierten und gealterten Amylose aus Kartoffelstärke". Razen znanstvenih prispevkov so posamezniki v reviji objavljali tudi poročila, npr. prof. Peter Glavič je leta 1978 objavil "P. Glavič: International system of units". Večja prisotnost avtorjev s Fakultete za kemijo in kemijsko tehnologijo Univerze v Mariboru se je pričela z letom 1984. Kot zanimivost velja omeniti, da je bila v 42. volumnu leta 1995 z uvodom prof. Petra Glaviča in prof. Zdravka Kravanje objavljena posebna številka znanstvenih prispevkov, predstavljenih na evropskem simpoziju ESCAPE 5, Bled. V naslednjih letih je vse več sodelavcev fakultete objavljalo v *Acta Chimica Slovenica*, ki se je na fakulteti uveljavila kot kvalitetna revija, še posebej po pridobitvi faktorja vpliva, kar jo je uvrstilo med revije, v katerih so lahko doktorski študenti objavljali rezultate svojih disertacij, saj so za pripravo disertacije potrebovali minimalno dva do tri članke s faktorjem vpliva.

Ob visokem jubileju *Acta Chimica Slovenica* Slovenskemu kemijskemu društvu in uredniškemu odboru revije čestitava ter v imenu vseh sodelavcev Fakultete za kemijo in kemijsko tehnologijo Univerze v Mariboru želiva nadaljnji razvoj revije po kvaliteti, vsebinskem obsegu in mednarodni odzivnosti. (Besedilo pripravila Z. Kravanja in Z. Novak)

prof. dr.
Matjaž Valant

prorektor

Univerza
v Novi Gorici

Acta Chimica Slovenica je bila ustanovljena leta 1953 in je od takrat napredovala in se razvila v zelo ugledno znanstveno revijo na področju kemijskih znanosti. Svojo kakovost je utrdila z izjemno selekcijo člankov, ki so objavljeni po strogem recenzijskem postopku. Revija je vselej sledila najvišjim standardom objavljanja in znanstvene integritete, kar se danes kaže tudi v uspešnem prodoru na mednarodno sceno. *Acta Chimica Slovenica* je s svojim bogatim izborom člankov prispevala k razvoju različnih področij kemije, kot so organska, anorganska, fizikalna kemija, biokemija in kemija materialov ter tudi na področju kemijskega izobraževanja. Objavila je številne pomembne študije, ki so prispevale k širjenju znanja in razumevanju kemije ter so imele vpliv na druge znanstvenike po vsem svetu.

Pomembno je omeniti tudi vlogo revije pri izobraževanju in mentorstvu mlajših generacij kemikov. Mnogi mladi raziskovalci so svoje prve znanstvene članke objavili prav v reviji *Acta Chimica Slovenica*, kar jim je omogočilo pridobiti izkušnje v znanstvenem pisanju, izpostavljenost v akademski skupnosti ter gradnjo njihove kariere. S tega stališča je revija pomembna za vzpostavitev in negovanje naslednje generacije kemijskih strokovnjakov. Osebno me zelo veseli, da sem tudi sam del skupnosti kemikov, ki objavlja svoja znanstvena dela v tej naši slovenski reviji. Zavezujem se temu, da bom v prihodnje kot mentor k temu intenzivno prigovarjal mlajše sodelavce.

Obletnica izdajanja revije *Acta Chimica Slovenica* je priložnost za refleksijo in ponos na dosežke, v tem dolgem obdobju sedemdesetih let. Obenem pa je to tudi priložnost za pogled v prihodnost. Revija se bo zagotovo soočila z novimi izzivi, ki jih prinaša hitro spreminjajoče se znanstveno okolje, vendar bo z močno temeljno strukturo in predanimi ljudmi, ki sodelujejo pri njenem delovanju, zagotovo ohranila svoj vpliv in ugled.

Ob 70. letnici izdajanja revije *Acta Chimica Slovenica* je torej treba čestitati vsem, ki so soustvarjali to izjemno znanstveno revijo. Njihova predanost, strokovnost in strast do kemije so omogočili njen uspeh in trajno prisotnost v akademski skupnosti. Prepričan sem, da bo revija še naprej ostala pomembno stičišče za izmenjavo idej, spodbujanje inovacij ter promocijo kemijskih dosežkov.

prof. dr.
Irena
Mlinarič-Raščan

dekanja

Fakulteta za farmacijo
Univerze v Ljubljani

V imenu Fakultete za farmacijo Univerze v Ljubljani izrekam čestitke Slovenskemu kemijskemu društvu ob 70-letnici izhajanja revije *Acta Chimica Slovenica* in se zahvaljujem urednikom, recenzentom in avtorjem revije, da s predanim delom širijo meje znanja v dobrobit slovenske in globalne znanosti na področju kemije in sorodnih področjih.

Acta Chimica Slovenica je renome vplivne znanstvene revije pridobila in obdržala z zagotavljanjem kriterijev odličnosti, ki temeljijo na objavah izvirnih znanstvenih člankov z ustreznim konceptualnim in tehničnim napredkom obravnavanega področja.

Acta Chimica Slovenica sledi načelom odprtega dostopa, brez stroškov objave člankov, kar ji podeljuje platinasto odprtokodno oznako. Revija na ta način omogoča hitrejše širjenje znanstvenih izsledkov in večjo vidnost rezultatov raziskovalnega dela.

Acta Chimica Slovenica nudi raziskovalkam in raziskovalcem Fakultete za farmacijo dragoceno priložnost za objavo znanstvenih dosežkov, ki z objavami svojih znanstvenih ugotovitev doprinašajo k interdisciplinarnosti revije in jo s tem bogatijo.

Fakulteta za farmacijo bo tudi v prihodnje aktiven partner pri oblikovanju revije.

prof. dr. Janez Vogrinc

dekan

Pedagoška fakulteta
Univerze v Ljubljani

V imenu raziskovalk in raziskovalcev fakultete izrekam iskrene čestitke ob 70-letnici izhajanja revije *Acta Chimica Slovenica* Slovenskemu kemijskemu društvu, ki podpira in skrbi za redno izdajanje revije, ter vsem dosedanjim urednikom, katerih zasluga je mednarodna prepoznavnost revije in umeščenost revije med najkakovostnejše revije, ki objavljajo izvirne znanstvene dosežke s področja kemije ter sorodnih ved. Za sodelavce Pedagoške fakultete Univerze v Ljubljani so še posebej pomembne znanstvene objave s področja kemijskega izobraževanja, kjer sodelujemo v vlogi avtorjev prispevkov in recenzentov. Sistematični pregled raziskovanja v kemijskem izobraževanju v Sloveniji po letu 1991 avtorjev Devetak in Ferk Savec (2020), je razkril, da so ključna raziskovalna področja slovenskih raziskovalcev na področju kemijskega izobraževanja predvsem: raziskave uporabe submikroreprezentacij, modelov in animacij pri poučevanju in učenju kemije; raziskave povezane z izobraževanjem učiteljev kemije; preučevanje vloge različnih oblik eksperimentalnega dela v kemijskem izobraževanju in preučevanje razumevanja osnovnih kemijskih pojmov. Skupno so raziskovalci Pedagoške fakultete od leta 1984 pa do danes v reviji *Acta Chimica Slovenica* objavili več kot 45 prispevkov. Glede na citate v Web of Science in Scopus so prispevki objavljeni s področja submikroreprezentacij najbolj pomemben prispevek slovenskih raziskovalcev v mednarodnem raziskovalnem prostoru. Poleg navedenega pa je bistven tudi prenos znanstveno-raziskovalnih spoznanj kemijskega izobraževanja v pedagoško prakso v celotni vzgojno-izobraževalni vertikali. Z objavljanjem izvirnih znanstvenih prispevkov s področja kemijskega izobraževanja ima revija *Acta Chimica Slovenica* ključno vlogo pri seznanjanju strokovne javnosti o najnovejših spoznanjih, ki prispevajo k razvijanju kakovostnega znanja kemije pri učečih v celotni šolski vertikali. Srečno, *Acta Chimica Slovenica,* tudi v prihodnje!

izr. prof. dr. Blaž Nardin

dekan

Fakulteta za tehnologijo polimerov,
Slovenj Gradec

Bogatenje zakladnice znanja, tako slovenske kot tudi svetovne, je ena od nalog nas raziskovalcev. Znanstveni področji kemije in kemijskega inženirstva sta med seboj neločljivo povezani. Če v ta zbor dodamo še znanstveno disciplino strojništva, pridemo na področje polimernih tehnologij, eno najhitreje razvijajočih se panog. Danes se na svetu letno predela 350 milijonov ton polimernih materialov, do leta 2035 pa naj bi se povečala na 650 milijonov ton. To pomeni praktično podvojitev proizvodnje in ponovne uporabe materialov, razvoj novih tehnologij in orodij. Nesluten razvoj se dogaja na področju zbiranja, reciklaže in ponovne uporabe izdelkov iz polimernih materialov. Predvsem pa to pomeni izjemen izziv za varovanje našega planeta, kot zelenega doma, ki nam je bil podarjen od naših staršev in ga moramo ohraniti za naše otroke. Zato smo odgovorni vsi, ki se ukvarjamo s tem področjem. Na Fakulteti za tehnologijo polimerov se, tako izobraževalno kot raziskovalno, ukvarjamo s polimeri, od sinteze do predelave v končne izdelke. V ta namen spremljamo tudi objave v reviji *Acta Chimica Slovenica*, ne le polimerne, pač pa tudi članke o organski sintezni kemiji.

Acta Chimica Slovenica je znanstvena revija, ki omogoča raziskovalcem objavljanje doseženih raziskovalnih rezultatov in jih postavlja ob rob ostalim svetovnim znanstvenim revijam iz področja. S svojim Open Access statusom omogoča objavljanje raziskovalnih rezultatov tudi iz vseh Horizon Europe projektov. To daje reviji potencial in dodaten zagon za privabljanje raziskovalcev. Posebej pa bi pohvalil dolgoletno prakso, da je na koncu vsakega članka ustrezen povzetek v slovenščini, saj se na ta način tudi razvija in ohranja slovenski strokovni jezik oziroma izrazoslovje.

Vemo, da je revija močna toliko, kot so močni avtorji, ki v njej objavljajo. Zato pozivam vse raziskovalce, da še bolj aktivno sodelujejo pri objavljanju različnih znanstvenih in tudi industrijskih dosežkov. Reviji *Acta Chimica Slovenica* želim ob njeni 70. obletnici, da še naprej proaktivno deluje na tem perspektivnem znanstvenem področju, vsem soustvarjalcem pa čestitam za izjemni jubilej.

prof. dr.
Blaž Zmazek

dekan

Fakulteta za naravoslovje in matematiko Univerze v Mariboru

Revija *Acta Chimica Slovenica* je nepogrešljiv del slovenske znanstvene skupnosti. Od ustanovitve Slovenskega kemijskega društva leta 1951 je ta prestižna revija služila kot most, ki povezuje slovensko znanstveno skupnost z mednarodnimi raziskovalci, obenem pa tudi kot ključno orodje za napredek in razvoj kemije in sorodnih znanstvenih področij v Sloveniji ter po svetu. Z objavo izvirnih znanstvenih raziskav in preglednih člankov iz široke palete področij kemije revija aktivno prispeva k širitvi in poglabljanju znanstvenega znanja in razumevanja.

Zgodovina *Acta Chimica Slovenica* je tesno prepletena z zgodovino kemije v Sloveniji. Vsak izid revije je kot kamenček v mozaiku razvoja in napredka kemije v državi, ki dokumentira pomembne dosežke, odkritja in inovacije slovenskih kemikov. Prav tako je *Acta Chimica Slovenica* pomemben del slovenske znanstvene dediščine in služi kot pomemben medij za dialog in sodelovanje med slovenskimi kemiki in njihovimi kolegi po vsem svetu.

Teme, ki jih revija pokriva, so široke in segajo od organske, anorganske, analizne in fizikalne kemije do molekularne biologije, biokemije, kemije materialov, kemijskega, biokemijskega in okoljskega inženiringa. Prav tako revija aktivno podpira kemijsko izobraževanje, kar je odraz njenega interdisciplinarnega pristopa in poudarka na povezovanju različnih znanstvenih področij.

Acta Chimica Slovenica je znana po svoji zavezanosti visokim standardom znanstvenega objavljanja, znanstveni integriteti in nenehnemu iskanju napredka. Prav tako ima s svojo odločenostjo za izobraževanje in usposabljanje prihodnjih generacij kemikov ključno vlogo pri razvijanju naravoslovne pismenosti med študenti in širšo javnostjo.

Fakulteta za naravoslovje in matematiko Univerze v Mariboru med drugim izobražuje tudi bodoče učitelje kemije. Zaradi podajanja aktualnih kemijskih vsebin, ki jih bogatijo objave domačih in tujih avtorjev, je revija dolgoletna spremljevalka tako zaposlenih kot študentov naše fakultete. Ponosni smo, da z revijo aktivno sodelujejo tudi nekateri naši zaposleni in kot avtorji ali recenzenti prispevajo k obstoju revije. Zato se na tem mestu iskreno zahvaljujem kolegicama doc. dr. Janji Majer Kovačič in doc. dr. Brini Dojer za prehojeno pot z revijo in za prehojeno pot z bodočimi učitelji kemije, tj. na področju kemijskega izobraževanja, ki je v slovenskem prostoru izjemnega pomena.

Ob 70-letnici revije *Acta Chimica Slovenica* izrekamo iskrene čestitke. Ta pomemben mejnik ni samo priznanje za dosedanje dosežke revije, temveč tudi priložnost za priznanje njene vloge pri spodbujanju razvoja znanosti, izobraževanja in družbenega napredka.

Želimo si, da bi revija še naprej igrala ključno vlogo v kemiji in širši znanstveni skupnosti ter da bi se njeno pomembno delo nadaljevalo še mnogo let. Čestitamo za njeno vlogo, njen vpliv in prispevek, ki ga je imela na slovensko in globalno znanstveno skupnost!

Sedemdeset let prehojene poti od *Vestnika slovenskega kemijskega društva* do *Acta Chimica Slovenica*

akad. prof. dr. Branko Stanovnik

Fakulteta za kemijo in kemijsko tehnologijo Univerze v Ljubljani

predsednik uredniškega odbora v obdobju 1977–2003
predsednik programskega sveta od leta 2004

V začetku septembra 1945 (2. 9. 1945) je bil Maks Samec odstranjen z univerze. Njegovo nadaljnje delovanje je povezano z gradnjo instituta za kemijo, ki je bil ustanovljen hkrati s fizikalnim institutom Jožef Stefan in elektroinstitutom Milana Vidmarja v okviru Slovenske akademije znanosti in umetnosti. Od 1. 10. 1946 do 1959 je bil upravnik kemijskega laboratorija Akademije znanosti in umetnosti (pozneje Slovenske akademije znanosti in umetnosti), ki se je 12. 6. 1953 preimenoval v Kemični institut Borisa Kidriča. Maks Samec je odigral pionirsko vlogo na področju organiziranja Slovenskega kemijskega društva, ki je bilo ustanovljeno 15. 2. 1951. Bil je njegov prvi predsednik v obdobju 1951–1962 in častni predsednik 1963/64.

Maks Samec je odigral pionirsko vlogo tudi na področju organiziranja slovenskih kemikov v okviru Slovenskega kemijskega društva. Samec je kot predstojnik Kemijskega instituta preko Akademije znanosti in umetnosti naslovil leta 1948 Komiteju za šole in znanost Federativne narodne republike Jugoslavije v Beogradu prošnjo za soglasje, da bi smeli objaviti dve znanstveni deli v tujini. Komite iz Beograda je Akademiji sporočil, da naj se znanstvena spoznanja jugoslovanskih znanstvenikov najprej objavijo v domačih strokovnih revijah, šele nato pa v tujih.

Tako je nastal najprej *Kemijski zbornik*, ki ga je izdalo Slovensko kemijsko društvo leta 1951 z Igorjem Beličem kot urednikom in Rajkom Kavčičem, Dušanom Štucinom in Vinkom Kramaršičem kot člani uredniškega odbora. V uvodni besedi so zapisali: »V tem zborniku so zbrani članki iz področja čiste in uporabne kemijske znanosti ter rezultati osnovnega in uporabnega raziskovanja. Zbrani so sadovi raziskovalnega dela, izvršenega od osvoboditve Jugoslavije dalje.« Kemijskemu zborniku je sledil *Vestnik slovenskega kemijskega društva*, ki naj bi po Samčevih besedah predstavljal primerno osebno izkaznico slovenskih kemikov v mednarodnem prostoru, za slovensko kemijsko skupnost pa »urbar slovenske kemijske kulture«.

Slika 1: Naslovnica *Kemijskega zbornika*

Vestnik Slovenskega kemijskega društva **1** (1954) je začel izhajati leta 1954. Izdajatelji so bili Ladislav Guzelj, Anton Peterlin, Ciril Rekar in Maks Samec. Prvo številko so pripravili za tisk Igor Belič, Rajko Kavčič, A. Nučič, Črtomir Nučič in Marcel Žorga, odgovorni urednik pa je bil Marcel Žorga. Uvodoma je Maks Samec zapisal: »Slovensko kemijsko društvo se je odločilo pričeti z izdajanjem lastnega glasila *Vestnika slovenskega kemijskega društva* predvsem iz razloga, da omogoči slovenskim kemikom podajati kolegom v domovini in po širnem svetu obračun o svojem delu … Izdajatelji in uredniki *Vestnika slovenskega kemijskega društva* so prepričani, da bo novi kemijski časopis izdatna pomoč Slovenskemu kemijskemu društvu pri izpolnjevanju ene najosnovnejših nalog, to je razširjanje in poglabljanje kemijske znanosti in njene uporabe ter da bo z združenim naporom vseh kmalu tudi primerna mednarodna legitimacija slovenskih kemikov.«

Z drugim letnikom **II** (1955) je postal urednik Rajko Kavčič, odgovorni urednik pa Marcel Žorga. S tretjim letnikom **III** (1956) je bil ustanovljen tudi uredniški odbor v sestavi: Rajko Kavčič (predsednik) in člani Davorin Dolar, Dušan Hadži, Franjo Kočevar, Lado Kosta, Črtomir Nučič, Dušan Stucin in Marcel Žorga. V naslednjih letih so se uredniškemu odboru pridružili še Bogdan Zega (1957), Janko Kavčič, Srečko Kotnik, Drago Leskovšek, Roman Modic in Marija Perpar (1961), Igor Belič, Branko Brčić, Mirko Čeh, Tita Kovač in Miha Tišler (1962), Jernej Jernejčič in Bogdan Volavšek (1969), Jože Šiftar in Andrej Šmalc (1977). Drago Kolar pa je postal urednik (1969). *Vestnik slovenskega kemijskega društva* je nato do konca leta 1977 izhajal, večinoma kot dve dvojni številki letno, včasih vse štiri številke skupaj, včasih celo za dve leti skupaj.

Leta 1976 me je prof. Dušan Hadži kot predsednik SKD zaprosil, da bi z letom 1977 prevzel vodenje uredništva *Vestnika*, ki je do takrat zelo neredno izhajal. Kot novi predsednik uredniškega odbora sem si zadal dve nalogi: 1. da bo *Vestnik* izhajal redno štirikrat na leto in 2. predlagal sem, da bi *Vestnik* preimenovali v *Acta Chimica Slovenica*. Glede rednega izhajanja mi je stvar uspela ob izdatni pomoči Draga Kolarja kot urednika, Marka Razingerja kot tehničnega urednika oziroma kasneje pomočnika urednika in uredniškega odbora, ki sem ga redno skliceval za vsako številko posebej. In tako nam je s precejšnimi napori, ob optimizmu nekaterih in skepsi drugih, uspelo s 25. letnikom (1978) začeti izdajati novo obliko *Vestnika slovenskega kemijskega društva* po novem konceptu. Uvedli smo posebne številke, na eni strani jubilejne številke, ki so bile posvečene starejšim profesorjem ob njihovem jubileju, npr. profesorjem Mariji Perpar, Davorinu Dolarju, Romanu Modicu, Mihu Tišlerju in drugim, na drugi strani pa posebne številke s plenarnimi predavanji s kongresov in simpozijev, ki so bili organizirani pod okriljem Slovenskega kemijskega društva. Prav te posebne številke so bistveno pripomogle, da je bil *Vestniku SKD* kmalu priznan faktor vpliva. Glede preimenovanja pa je moj predlog leta 1976 popolnoma pogorel. Eksplicitno sta bila proti prof. Hadži in prof. Dolar. Nisem se hotel prepirati, sklenil sem počakati na ugodnejše čase. Čakal sem šestnajst let. Počakal sem do razglasitve samostojne države. Potem, ko sem kot član Sveta Federacije evropskih kemijskih društev uspel, da je bilo Slovensko kemijsko društvo leta 1992 sprejeto v Federacijo evropskih kemijskih društev, sem kot urednik *Vestnika* ponovno predlagal spremembo naslova. Tokrat je bil predlog brez pripomb soglasno sprejet in leta 1993 je začel izhajati s spremenjeno naslovnico kot *Acta Chimica Slovenica* in je nato sicer v nespremenjeni obliki izhajal do konca leta 2004. V času mojega vodenja uredniškega odbora je kot urednik do leta 1996 sodeloval Drago


ZVEZEK I JANUAR-FEBRUAR 1954 ŠT. 1

VESTNIK SLOVENSKEGA KEMIJSKEGA DRUŠTVA

VSEBINA

CONTENTS

LJUBLJANA 1954

SLOVENSKO KEMIJSKO DRUŠTVO

Slika 2: Naslovnica *Vestnika slovenskega kemijskega društva* iz leta 1954.

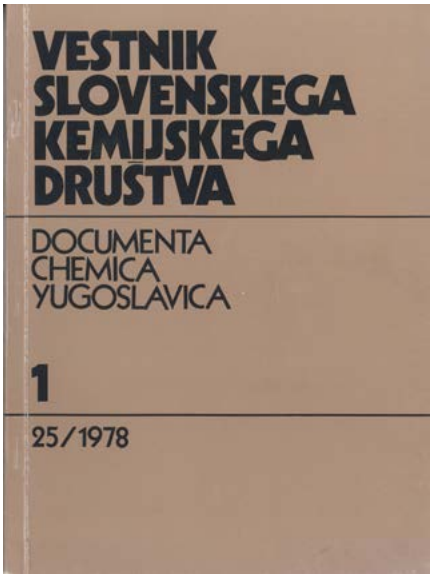

Slika 3: Naslovnica *Vestnika slovenskega kemijskega društva* leta 1978.

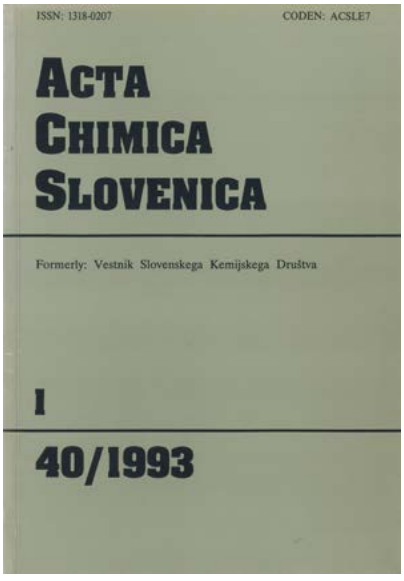

Slika 4: Naslovnica revije *Acta Chimica Slovenica* leta 1993.

Kolar, Marko Razinger je bil v obdobju 1978–1982 tehnični urednik in nato v obdobju 1983–1996 pomočnik urednika. Za krajši čas je v letih 1997–1998 postal urednik Ljubo Golič, nato v letih 1999–2002 Andrej Petrič in leta 2003 Janez Košmrlj. V letu 2004 je bila izvedena reorganizacija uredniškega odbora, glavni in odgovorni urednik je postal Janez Košmrlj z ekipo petih področnih urednikov, sam pa sem prevzel vodenje uredniškega sveta. Z 52. letnikom (2005) so revijo *Acta Chimica Slovenica* ustrezno preoblikovali in nadaljevali z digitalizacijo in že v nekaj letih so *Acta Chimica Slovenica* postala mednarodno prepoznaven časopis.

Glede na to, da je preimenovanje *Vestnika SKD* v *Acta Chimica Slovenica* povezano s sprejemom Slovenskega kemijskega društva v Federacijo evropskih kemijskih društev je prav, da povem še nekaj o tem. Sprejem Slovenskega kemijskega društva v Federacijo evropskih kemijskih društev je namreč prvo mednarodno priznanje strokovnega društva v neki mednarodni organizaciji v samostojni Sloveniji.

V osemdesetih in devetdesetih letih prejšnjega stoletja sem bil najprej kot predstavnik Unije jugoslovanskih kemijskih društev pozneje pa kot predstavnik Slovenskega kemijskega društva član Sveta Federacije evropskih kemijskih društev. Seja Sveta Federacije EKD je bila v Londonu 24. in 25. junija 1991. Ker je bilo takrat že jasno, kakšna bo usoda Jugoslavije, sem situacijo pojasnil in se dogovoril s predsednikom Sveta Federacije evropskih kemijskih društev dr. Gowom, generalnim sekretarjem Royal Society of Chemistry in drugimi člani Sveta za sprejem Slovenskega kemijskega društva v Federacijo evropskih kemijskih društev. To ustno soglasje je bilo sprejeto nekaj ur pred razglasitvijo samostojne Slovenije. Ko sem zgodaj popoldne prišel na letališče v Londonu in sem se hotel prijaviti za let v Ljubljano, mi povedo, da je Adrijin let odpovedan, namesto tega pa leti letalo Air France. Izkazalo se je, da je Adrijino letalo letelo pod francosko zastavo in tako smo varno pristali v Ljubljani na predvečer razglasitve samostojne Slovenije. To je bilo zadnje letalo, ki je pristalo v Ljubljani pred desetdnevno vojno za Slovenijo. Tisto noč so tanki odpeljali iz vrhniške kasarne proti Brniku. Letališče je bilo nato nekaj mesecev zaprto. Glede na to, da sem prinesel iz Londona ustno zagotovilo o priznanju, je prof. Ljubo Golič, tedanji predsednik Slovenskega kemijskega društva pripravil pisno vlogo, ki je bila obravnavana na seji Sveta Federacije evropskih kemijskih društev v Varšavi na sedežu Poljske akademije znanosti 22. junija 1992. Slovenija je bila sprejeta z aklamacijo brez kakršne koli pripombe ali komentarja. To je prvo mednarodno priznanje nekega slovenskega strokovnega društva v mednarodni asociaciji.

Acta Chimica Slovenica od papirja do svetovnega spleta in faktorja vpliva po SCI

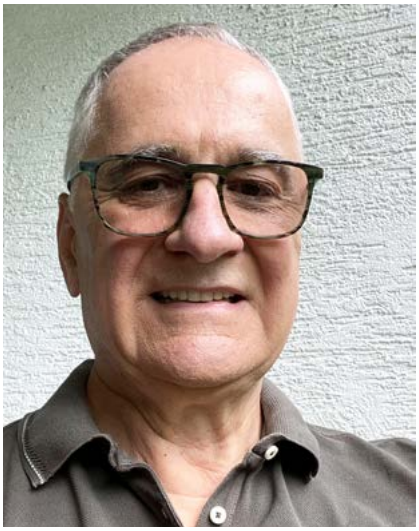

prof. dr. Andrej Petrič

Fakulteta za kemijo in kemijsko tehnologijo Univerze v Ljubljani

glavni urednik v obdobju 1999–2002

Prvih štiriinštirideset let izhajanja strokovne revije Slovenskega kemijskega društva *Vestnik slovenskega kemijskega društva*, kasneje *Acta Chimica Slovenica* (*ACSi*), v tiskani obliki je zaznamovalo več pomanjkljivosti: sorazmerno nizko število v objavo prejetih prispevkov, počasna komunikacija z avtorji in recenzijski postopek, zamudno oblikovanje in tisk, včasih neredno izhajanje in posledično šibka mednarodna opaznost revije.

V letih okoli 1997, ko sem bil ob profesorju Ljubu Goliču sourednik revije, so osebni računalniki z urejevalniki besedil, svetovnim spletom in elektronsko pošto postajali stalnica v vseh pisarnah. Ob prevzemu uredništva leta 1999 se mi je zdelo primerno izkoristiti prednosti informacijske tehnologije za posodobitev celotnega postopka pridobivanja prispevkov, recenzij, oblikovanja in objavljanja prispevkov v *ACSi* ter zelo pomembno povečanje vidnosti revije v mednarodnem okolju.

Posodobitev je imela svojo ceno. Poleg stalnega napora pridobivanja dovolj velikega števila primernih prispevkov, je bilo potrebno prispevke, ki so ustrezali kriterijem za objavo, pripraviti za tisk. Na srečo se mi je kot sourednik pridružil Sašo Pavko, s katerim sva si razdelila delo. Ko razmišljam o teh časih, skoraj ne morem verjeti, da je najinemu »two men band« ob polni zaposlitvi na fakulteti uspelo spraviti *ACSi* na naslednji nivo.

V prvem koraku smo z novimi, podrobnejšimi navodili avtorjem nadomestili način posredovanja prispevkov v natisnjeni obliki s posredovanjem le-teh v digitalni obliki v formatu urejevalnika besedil Word na takrat dostopnih nosilcih disketah in zgoščenkah. To je sicer nekoliko poenostavilo pripravo prispevkov za tisk, a komunikacija z avtorji je bila še vedno dokaj počasna, saj je potekala preko poštnih pošiljk. S Sašom Pavkom sva s skupnimi močmi sorazmerno majhnem številu prejetih prispevkov uspela sestaviti in pravočasno za tisk pripraviti štiri številke 46. zvezka (letnik 1999).

Revijo je ves čas pestilo pomanjkanje kvalitetnih znanstvenih prispevkov, tako slovenskih kot tujih. Avtorji so pogosto kot glavni razlog za omahovanje pri objavljanju rezultatov kvalitetnih raziskav v *ACSi* navajali, da revija nima faktorja vpliva po SCI in s tem, da rezultati ne dosežejo znanstvenikov po svetu. To sicer ni bilo popolnoma res, saj so povzetki v *ACSi* objavljenih člankov našli svoje mesto tudi v najbolj razširjeni bazi Chemical Abstracts Service. Je pa res, da je bila mednarodna vidnost revije skromna, saj knjižnice v tujini v veliki večini niso imele sklenjenih naročniških razmerij in s tem se izvodi *ACSi* niso znašli na njihovih knjižnih policah. Raziskovalci so bili v primeru potrebe po nekem celem prispevku v *ACSi* in ne samo kratkem povzetku v Chemical Abstracts, prisiljeni ubrati mnogokrat časovno zahtevno pot medknjižnične izposoje ali naročila natisnjenega članka.

V dogovoru z vodstvom Slovenskega kemijskega društva smo se odločili širši svetovni strokovni javnosti ponuditi brezplačen dostop do vsebin, objavljenih v *ACSi*. Kot alternativo pošiljanju brezplačnih izvodov revije v knjižnice po svetu, ki bi pomenilo precejšnje finančno breme društvu, smo se odločili ponuditi brezplačen dostop do

vsebin na svetovnem spletu. Posodobili smo oblikovanje strani in uvedli grafične povzetke. S tem smo *ACSi* po vsebini in obliki približali revijam tujih založnikov.

Pokazalo se je, da smo z rednim četrtletnim izdajanjem številk, z objavo prispevkov v angleščini, urejenim recenzijskim procesom in s široko dostopnostjo na spletu vzbudili pozornost v mednarodni strokovni srenji. V uredništvu smo prejeli pismo iz Science Citation Index Expanded z obvestilom, da so uvrstili *Acta Chimica Slovenica* v svojo bazo podatkov. Prvi izračunani faktor vpliva je bil 0,12. Počakati smo morali do leta 2000, ko je bil prvič javno v lestvici SCI Expanded objavljen dvoletni faktor vpliva 0,239.

Revija *Acta Chimica Slovenica* je postala mednarodno priznana revija na področju kemijskih znanosti z objavljenim faktorjem vpliva. Po letu 2002 in objavljenem 49. zvezku revije je prišel čas za predajo štafetne uredniške palice mlajšim kolegom in kolegicam. Tako, kot sem jaz gradil na prizadevanjih svojih predhodnikov in poskusil prispevati kamenček v mozaik uspešnega razvoja revije *Acta Chimica Slovenica*, revije, na katero moramo biti vsi ponosni, sem Janezu Košmrlju predal uredništvo v prepričanju, da bo revijo popeljal na še višji nivo. Zgodovina pove, da je njemu s sodelavci in njihovim naslednicam in naslednikom to zelo dobro uspelo. Več naj povedo sami.

Čas velikih sprememb

prof. dr. Janez Košmrlj

Fakulteta za kemijo in kemijsko tehnologijo Univerze v Ljubljani

glavni in odgovorni urednik v obdobju 2003–2005

Acta Chimica Slovenica je kot nacionalna znanstvena revija sicer maloštevilnega naroda po zaslugi entuziazma in požrtvovalnega dela urednikov pred mojim nastopom funkcije dosegla osupljiv uspeh (Slika 1). Konec leta 2002, na začetku svoje znanstvene in pedagoške kariere, sem na željo, pobudo in spodbudo profesorja Andreja Petriča sprejel dela in naloge urednika revije. Kot sourednik se mi je pridružil profesor Aleksander Pavko, ki je že prej pomagal prof. Petriču, kot tehnični urednik pa g. Vinko Volk. G. Volk, ki je z neverjetnim občutkom za tehniko takrat skrbel za nemoteno delovanje rentgenskih difraktometrov na fakulteti, je na enak način sprva neformalno pomagal pri nastajanju revije in urejanju spletne strani ter nekoliko pozneje postal tehnični urednik. Prof. Pavko in g. Volk sta bila polna dobre volje in energije in bili smo sanjska ekipa, ki lahko premika gore.

Acta Chimica Slovenica je leta 2000 dosegla faktor vpliva 0,161, ki se je v letu 2002 dvignil na 0,538. Število rokopisov znanstvenih in strokovnih prispevkov, poslanih v objavo, je takrat zaradi vse večje prepoznavnosti revije hitro naraščalo. Dva odstavka obveznega poročila za leto 2003, ki sem ga pripravil za Oddelek za informacijsko infrastrukturo Ministrstva za šolstvo, znanost in šport, sta se glasila:

»V letniku revije *Acta Chimica Slovenica* **2003**, 50 so izšle štiri številke s skupno 69 originalnimi znanstvenimi in strokovnimi prispevki na skupno 814 straneh. Od tega je bilo 46 znanstvenih člankov, 12 kratkih in 11 strokovnih prispevkov, ena predstavitev knjige in dva komentarja.« in »Na internetu na strani *http://acta.chem-soc.si* objavljamo elektronsko obliko revije, kar povečuje branost in mednarodno odmevnost revije. Članke, objavljene v reviji, so v kratkem času po izidu elektronske oblike povzeli ISI Science Citation Index Expanded (Web of Science), Current Contents (Physical, Chemical and Earth Sciences), ISI Alerting Services in Chemical Abstracts. Na spletni strani http://acta.chem-soc.si je mogoče zaslediti več kot 950 povezav predvsem iz tujih knjižnic, univerz in drugih znanstvenih ustanov. Tiskano izdajo revije izmenjujemo s približno 30 knjižnicami po svetu. Poleg znanstvenih in strokovnih člankov ter predstavitev knjig smo objavili tudi društvene vesti in seznam diplomskih, magistrskih in doktorskih del v letu 2003 v Sloveniji.«

V tem letu, 2003, je v uredništvo prispelo 110 rokopisov, že na začetku leta pa je postalo jasno, da bo število rokopisov kar hitro naraščalo. To je zahtevalo takojšnje spremembe v delovanju uredništva. Ena od številnih je bila povezana s postopno digitalizacijo postopkov, kar je omočilo boljši pregled nad stanjem rokopisov. Predhodni način nadzora je namreč temeljil na kratkih beležkah o rokopisu na papirju, ki so vsebovale ime avtorja in recenzenta, predvsem pa na dobrem spominu urednika.

Naraščajoče število rokopisov, prispelih v uredništvo, pa je poleg izdatnejšega dela za malo uredniško ekipo ponujalo enkratno priložnost za selekcijo objavljenih člankov in s tem dvig standarda in kakovosti revije tako na strokovni kot na oblikovni ravni. Za izboljšanje predvsem slednjega smo se s sourednikom in tehničnim urednikom lotili izdatnega stilskega urejanja in poenotenja člankov pred objavo, da so

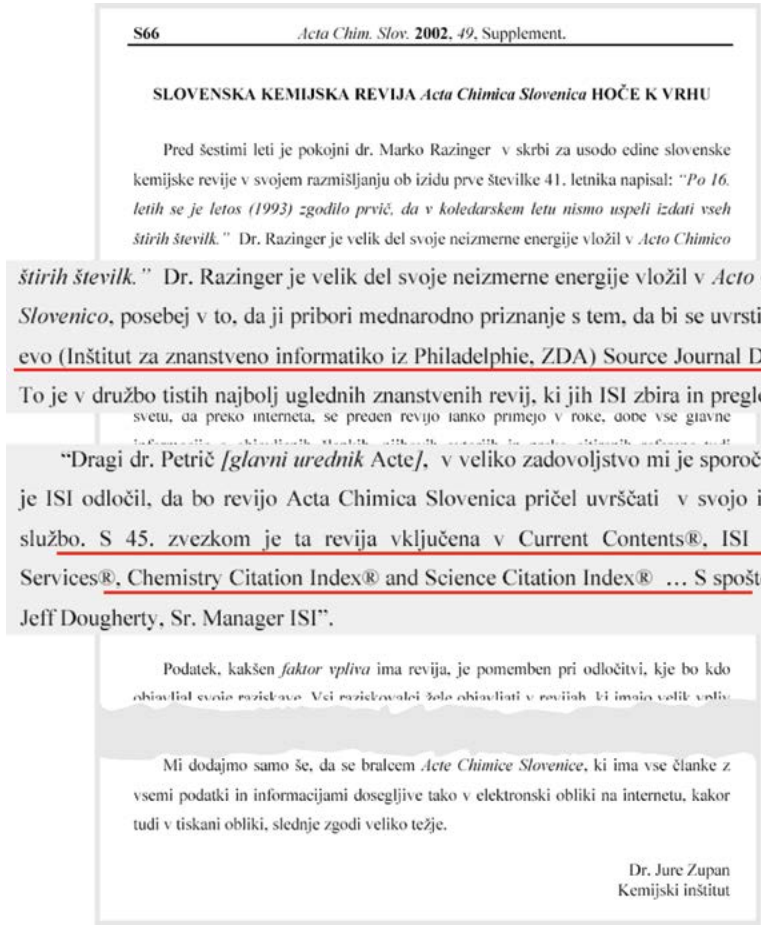

S66 *Acta Chim. Slov.* **2002**, *49*, Supplement.

SLOVENSKA KEMIJSKA REVIJA *Acta Chimica Slovenica* HOČE K VRHU

Pred šestimi leti je pokojni dr. Marko Razinger v skrbi za usodo edine slovenske kemijske revije v svojem razmišljanju ob izidu prve številke 41. letnika napisal: *"Po 16. letih se je letos (1993) zgodilo prvič, da v koledarskem letu nismo uspeli izdati vseh štirih številk."* Dr. Razinger je velik del svoje neizmerne energije vložil v *Acto Chimico Slovenico*, posebej v to, da ji pribori mednarodno priznanje s tem, da bi se uvrstila v ISI-evo (Inštitut za znanstveno informatiko iz Philadelphie, ZDA) Source Journal Database. To je v družbo tistih najbolj uglednih znanstvenih revij, ki jih ISI zbira in pregleduje ter

"Dragi dr. Petrič *[glavni urednik* Acte*]*, v veliko zadovoljstvo mi je sporočiti, da se je ISI odločil, da bo revijo Acta Chimica Slovenica pričel uvrščati v svojo indeksno službo. S 45. zvezkom je ta revija vključena v Current Contents®, ISI Alerting Services®, Chemistry Citation Index® and Science Citation Index® ... S spoštovanjem Jeff Dougherty, Sr. Manager ISI".

Podatek, kakšen *faktor vpliva* ima revija, je pomemben pri odločitvi, kje bo kdo

Mi dodajmo samo še, da se bralcem *Acte Chimice Slovenice*, ki ima vse članke z vsemi podatki in informacijami dosegljive tako v elektronski obliki na internetu, kakor tudi v tiskani obliki, slednje zgodi veliko težje.

Dr. Jure Zupan
Kemijski inštitut

Slika 1. Del besedila dr. Jureta Zupana v *Acta Chim. Slov.* **2002**, *49*, S66.

dobivali čedalje bolj enotno podobo. Avtorje smo prosili, da za svoje članke pripravijo grafične povzetke, ki so od druge številke *Acta Chimica Slovenica* **2003**, *50*, naprej obvezno spremljali objavo (Slika 2). No, na začetku smo zaradi slabe odzivnosti avtorjev grafične povzetke pripravljali kar sami v uredništvu. Da bi bilo v objavljenih člankih čim manj napak, smo takrat vpeljali »krtačne odtise«, ki smo jih pred končno postavitvijo revije avtorjem poslali v pregled in popravo. Skupaj s kolegoma v uredništvu smo potem vnašali popravke napak, ki so jih predlagali avtorji, pa še mnogo drugih, ki smo jih med pozornim prebiranjem besedil našli tudi sami. Proces izboljšanja je bil seveda počasen, vendar je vloženo delo vodilo do povečanega zanimanja do objavljanja v reviji *Acta Chimica Slovenica*; s tem pa spet do povečanja dela majhne uredniške ekipe … Tako smo po vzoru uveljavljenih založniških hiš čedalje več tega dela prelagali na avtorje z neprestanim posodabljanjem navodil za pripravo rokopisov in pa z vztrajanjem, da se avtorji navodil držijo, kar je bilo večinoma daleč od samoumevnega.

Osnovni pogoj za priznanje nacionalne strokovne revije v mednarodnem prostoru je njena cena v očeh domače znanstvene srenje. Presenečen sem bil, kako neverjetno nizka je bila takrat cena naše revije s tega vidika. To se je odražalo v pogosto neverjetno dolgih, površnih, nekritič-

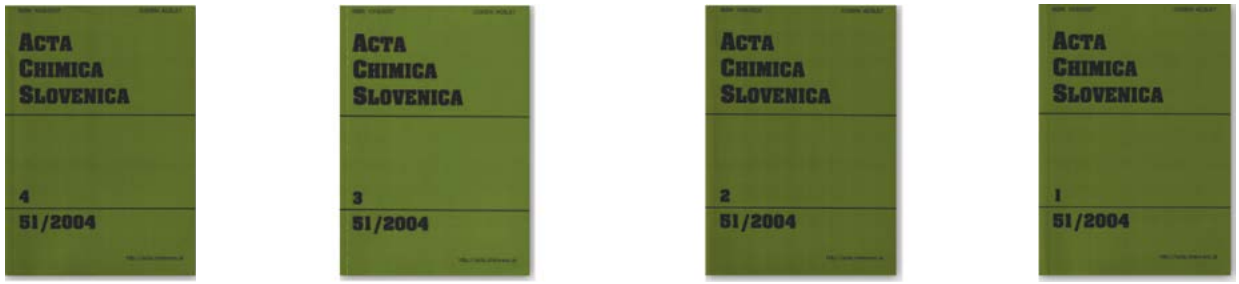

Slika 2. Zunanja podoba revije *Acta Chimica Slovenica* leta 2003 in 2004.

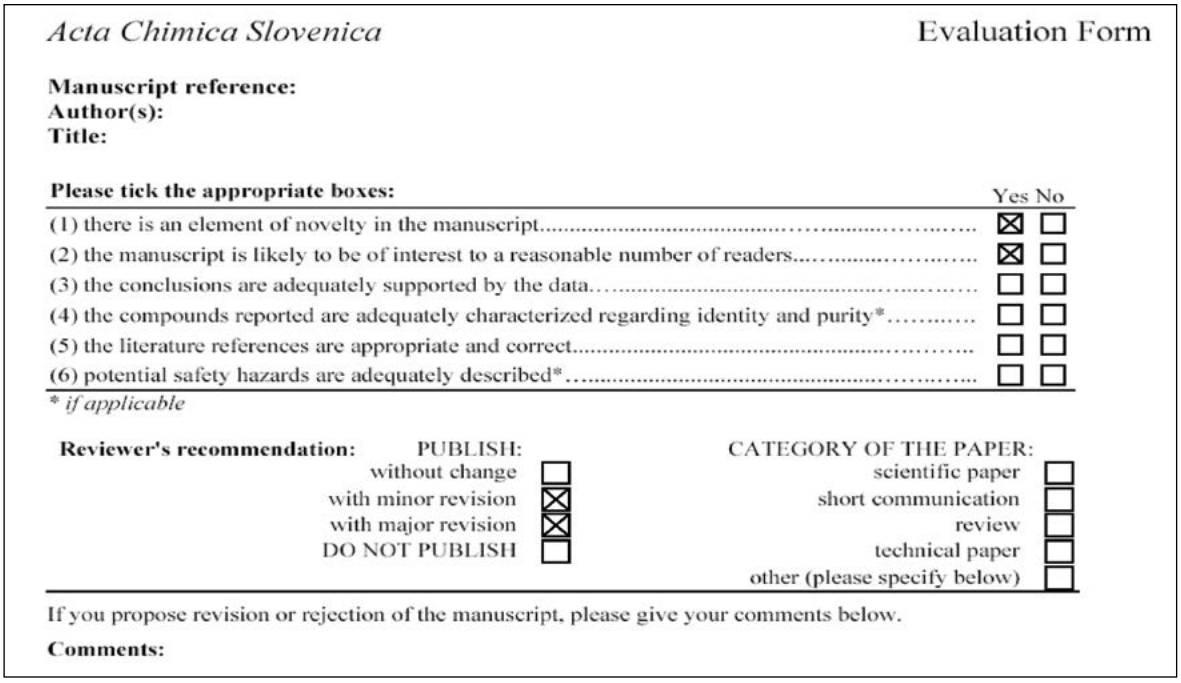

Acta Chimica Slovenica — Evaluation Form

Manuscript reference:
Author(s):
Title:

Please tick the appropriate boxes:	Yes	No
(1) there is an element of novelty in the manuscript	☒	☐
(2) the manuscript is likely to be of interest to a reasonable number of readers	☒	☐
(3) the conclusions are adequately supported by the data	☐	☐
(4) the compounds reported are adequately characterized regarding identity and purity*	☐	☐
(5) the literature references are appropriate and correct	☐	☐
(6) potential safety hazards are adequately described*	☐	☐

* *if applicable*

Reviewer's recommendation:

PUBLISH:
without change ☐
with minor revision ☒
with major revision ☒
DO NOT PUBLISH ☐

CATEGORY OF THE PAPER:
scientific paper ☐
short communication ☐
review ☐
technical paper ☐
other (please specify below) ☐

If you propose revision or rejection of the manuscript, please give your comments below.

Comments:

Slika 3. Ocenjevalni list iz tistega obdobja.

nih recenzijah številnih domačih strokovnjakov, ki smo jih prosili za recenzije v stilu: 'saj za Acto je dobro'. No, pa tudi marsikateri rokopis, poslan v objavo, je bil v tem kakovostnem razredu. Po vzoru uveljavljenih mednarodnih revij smo pripravili »ocenjevalni list« in dodatna navodila, ki naj bi recenzentom pomagala pri pripravi strokovnih ocen rokopisov (Slika 3). Rekordni čas, ki ga je neki rokopis preživel pri recenzentu leta 2002, je bil 12 mesecev. V naslednjem letu nam je ta čas uspelo skrajšati na pol, kar je bilo še vedno daleč od sprejemljivega. Za dvig kakovosti sem se s sourednikom odločil, da je čas, da vsak rokopis ocenita dva strokovnjaka s področja in da je vsaj en recenzent iz tujine. Razumljivo, za slabe rokopise, poslane v objavo, so bili avtorji pripravljeni čakati na recenzijo dolgo, kakovostnejše prispevke pa so ob dolgi, pa tudi nekakovostni recenziji radi umikali iz uredništva in jih poslali v objavo drugam. Seveda je bilo takšno pravilo lahko postaviti, težje pa realizirati, saj sva sourednik in jaz za vse prispele rokopise sama iskala recenzente, povabilu pa se jih navadno ni odzvalo veliko niti iz domačih niti iz tujih krogov.

Ni skrivnost niti to, da k vidnosti revije pripomorejo pregledni članki. Sourednik in jaz sva bila aktivna tudi na tem področju, čeprav na začetku prav posebnega uspeha ni bilo. Medtem ko mi je od nekaterih tujih znanstvenikov uspelo izvabiti vsaj obljubo, da bodo prispevali, sem imel precej manj sreče pri domačih. Na prošnjo za pregledni članek je poveden eden od odgovorov, citiram: »Objava preglednega članka v Acti bi škodila mojemu ugledu v mednarodni javnosti.«

Požrtvovalno delo s sourednikom in tehničnim urednikom je ob izdatni podpori takratnega predsednika Slovenskega kemijskega društva profesorja Venčeslava Kaučiča v treh letih mojega urednikovanja vodilo do velikih sprememb. Skupaj smo preoblikovali uredniški odbor in končno odprli možnost, da v vlogi sourednikov (Associate Editors) s posameznih področij sodelujejo izjemni slovenski znanstveniki. Tako je profesorica Marija Bešter Rogač prijazno sprejela funkcijo urednice za področje fizikalne kemije, profesorja Matija Strlič in Mladen Franko pa za področje analizne kemije, za katero je bilo takrat največ prispevkov. Profesor Alojz Demšar je skrbel za prispevke iz anorganske kemije, profesorju Andreju Petriču pa sem bil hvaležen, da je prevzel organsko kemijo (Slika 4). S sourednikom sem se trudil pokriti vsa druga področja. Prof. Petriča je kmalu za tem, ko je leta 2004 postal prodekan na Fakulteti za kemijo in kemijsko tehnologijo, med področnimi uredniki zamenjal profesor Bert U. W. Maes z Univerze v Antwerpnu. Tako smo našo revijo počasi, a vztrajno internacionalizirali, ustanovili pa smo tudi mednarodni uredniški odbor (Editorial Board), ki je bil takrat zelo aktiven, predvsem v privabljanju tujih piscev znanstvenih in preglednih člankov. Na moje vabilo so se prijazno odzvali in sprejeli vlogo v uredniškem odboru profesorji Mahesh K. Lakshman (The City College and The City University of New York), Janez Mavri (Kemijski inštitut), Jiři Pinkas (Masaryk University Brno), Wolfgang Buchberger (Johannes Kepler University), leta 2005 pa so se pridružili še profesor Günter Grampp (Graz University of Technology), profesor Danijel Kikelj (Fakulteta za farmacijo) in profesor Friedrich Srienc (University of Minnesota). In oblikoval se je svetovalni uredniški odbor (Advisory Editorial Board).

In čas je bil, da je *Acta Chimica Slovenica* dobila tudi novo, privlačnejšo podobo. Na sestanek sem povabil akademskega slikarja, gospoda Simona Kajtno, in skupaj s so-

Slika 4. Kolofon revije v začetku leta 2005.

urednikom in tehničnim urednikom sem mu hitel razlagati naše želje in ideje ter mu pokazal nekaj naslovnic drugih mednarodnih revij. Po približno enem mesecu smo se ponovno dobili. Prof. Pavko in jaz se spomniva, kako je g. Kajtna pod pazduho prinesel zvitek papirja z osnutkom, in ko ga je odvil, smo vsi trije uredniki enoglasno vzdihnili: »To je to!« *Acta Chimica Slovenica* je leta 2005 dobila novo celostno podobo (Slike 5–8), med drugim večji format in dvokolonsko postavitev besedila. Privlačne naslovnice so z vsakič novo naslovno grafiko oglaševale enega od objavljenih člankov (Slika 8), zadnja stran pa je bila namenjena reklami katerega od sponzorjev revije. Dobila je tudi novo obliko internetne strani (Slika 7). G. Volk se je moral nato naučiti še uporabljati program InDesign, ki je zamenjal MS Word pri postavitvi sprejetih člankov za objavo.

Tisk revije je bil dogovorjen v Tiskarni Skušek v Ljubljani, tam sem se s sourednikom in tehničnim urednikom z veseljem oglasil pri gospe Darji Koderman – ta nam je v pregled in odobritev pokazala prvo natisnjeno platnico, ki je privrela iz stroja.

Za prvo številko v novi podobi je z velikim veseljem prispeval pregledni članek na temo napredka kemije divodikovega trioksida (HOOOH) profesor Božo Plesničar (*Acta Chim. Slov.* **2005**, *52*, 1–12, Slika 6 desno). Ne, to ni zmanjšalo njegovega ugleda v mednarodni javnosti, o tej temi je pozneje objavil številna znanstvena dela, pa tudi pregledni članek v prestižni reviji *Chemical Reviews*.

To leto so pregledne članke prispevali še profesorji Jeffrey B. Arterburn (New Mexico State University), Andreas Taubert (University of Basel) in Bhanu P. S. Chauhan

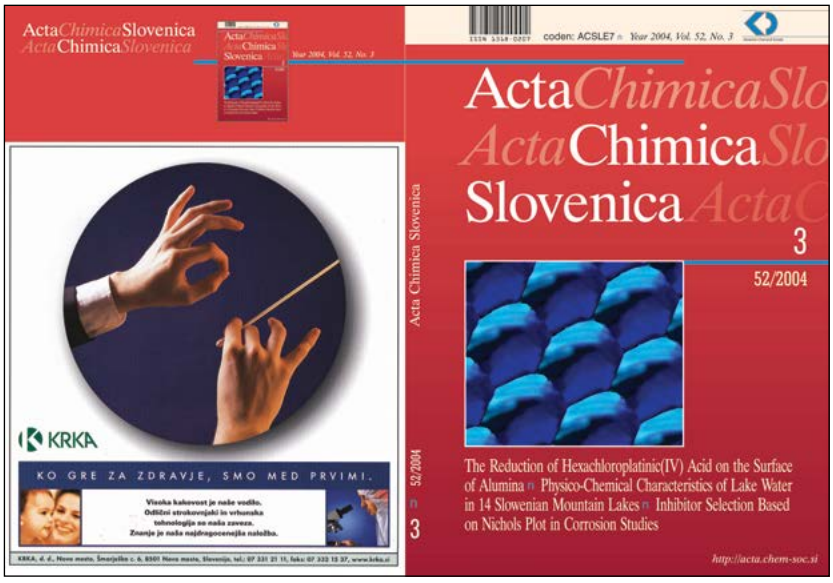

Slika 5. Vzorčna platnica nove podobe revije *Acta Chimica Slovenica*.

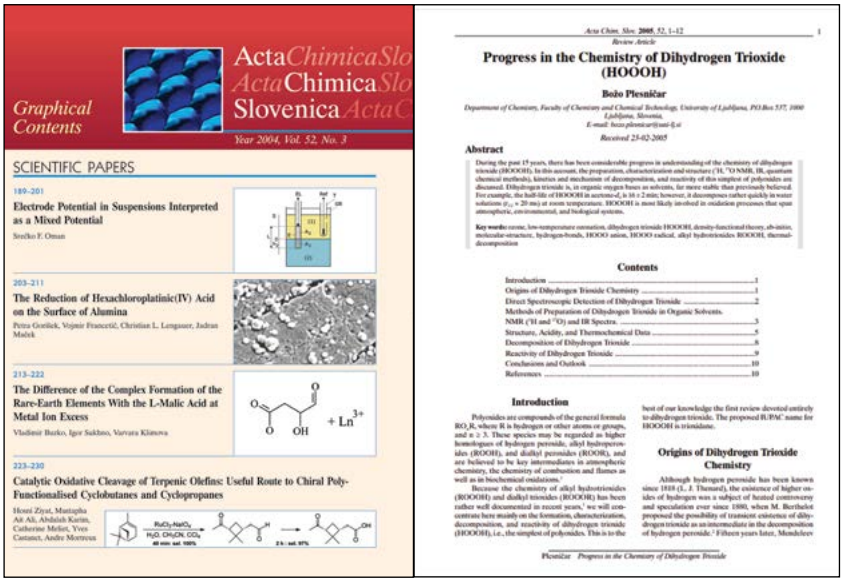

Slika 6. Vzorčna stran z grafičnimi povzetki in dvokolonska postavitev prvega članka v l. 2005.

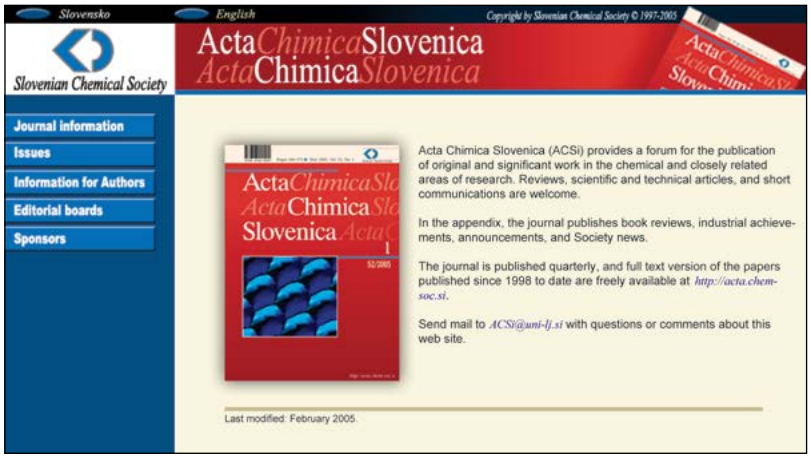

Slika 7. Vstopna internetna stran ACSi leta 2005.

Slika 8. Zunanja podoba revije *Acta Chimica Slovenica* leta 2005.

(City University of New York at The College of Staten Island). Na osnovi moje izbire in idejne zasnove je g. Kajtna izdelal naslovne slike vseh številk revije. Spomnim se priprave naslovnice za četrto številko v letu 2005, za katero je prof. Chauhan prispeval pregledni članek na temo strategije »meatball-spaghetti«, pri kateri silikonski nanoreaktorji (špageti) generirajo in stabilizirajo nanoobjekte (mesne kroglice). To se mi je zdela izvrstna iztočnica za nekoliko bolj kulinarično obarvano naslovno grafiko, ki bo zagotovo pritegnila oko bralca. Zamislil sem si fotografijo trenutka, ko čisto prave mesne kroglice v paradižnikovi omaki, pomešane s pravimi špageti, padajo iz lonca na krožnik. G. Kajtni sem natančno razložil scenarij in ga prosil, da to upodobi. Čez kakšen teden mi je sporočil, da so doma za realizacijo projekta ves teden kuhali mesne kroglice s špageti in eksperimentirali s fotoaparatom, vendar z rezultati ni bil zadovoljen. In ker se je družina naveličala omenjene jedi (da ni šlo vse skupaj v nič, so jo seveda vsakič pojedli), se je odločil za nekoliko drugačno upodobitev (Slika 8 desno). G. Kajtna ni obupal, mogoče so bili moji nasledniki manj zahtevni glede naslovnic, in z revijo *Acta Chimica Slovenica* in Slovenskim kemijskim društvom uspešno sodeluje še danes. Tudi midva še danes sodelujeva, ko mi pomaga pri moji strasti do grafične, bolje rečeno, umetniške upodobitve naslovnic znanstvenih člankov moje raziskovalne skupine. Ne morem se bolj strinjati z mislijo, ki sem jo nekje slišal: »V znanosti je umetnost in v umetnosti je znanost.«

14.3.2005

ZAPISNIK

14. seje Senata Fakultete za kemijo in kemijsko tehnologijo, **ki je bila v petek, 25.2.2005 ob 12. uri v predavalnici M/4 v četrtem nadstropju,** Fakultete za kemijo in kemijsko tehnologijo, Aškerčeva 5, Ljubljana.

Dnevni red:

1. **Poročilo dekana in prodekanov**
2. **Predstavitev Acta Chimica Slovenica**

Ad. 2 Predstavitev Acta Chimica Slovenica

Doc. dr. Janez Košmrlj, je podal poročilo o spremembah in dosežkih revije v zadnjih dveh letih, ko vodi Acta Chimica Slovenica, kot glavni in odgovorni urednik. V tem času je, da bi dvignil strokovno raven revije, oblikoval odbor pridruženih urednikov in nov uredniški odbor. Pridruženi uredniki urejajo posamezna strokovna področja, ki jih revija pokriva. Oba odbora imata člane tudi iz tujih univerz. K dvigu kvalitete in vidnosti revije v mednarodnem prostoru so usmerjene aktivnosti pridobivanja preglednih člankov avtorjev, priznanih na svojih področjih. Prav tako je bil v dvig kvalitete usmerjen projekt prenove celostne podobe revije. Kot rezultat tega projekta bo s prvo letošnjo številko Acta Chimica Slovenica, tako v printani kot ektronski verziji, začela izhajati v novi sodobni obliki. Urednik poziva slovenske kemike, da s kvalitetnimi članki in recenzijami pomagajo pri prizadevanjih uredništva in prispevajo k ugledu edine slovenske kemijske revije, doma in svetu. Člani senata so spremembe pri reviji pozitivno sprejeli.

Slika 9. Del zapisnika 14. seje Senata Fakultete za kemijo in kemijsko tehnologijo (25. 2. 2005).

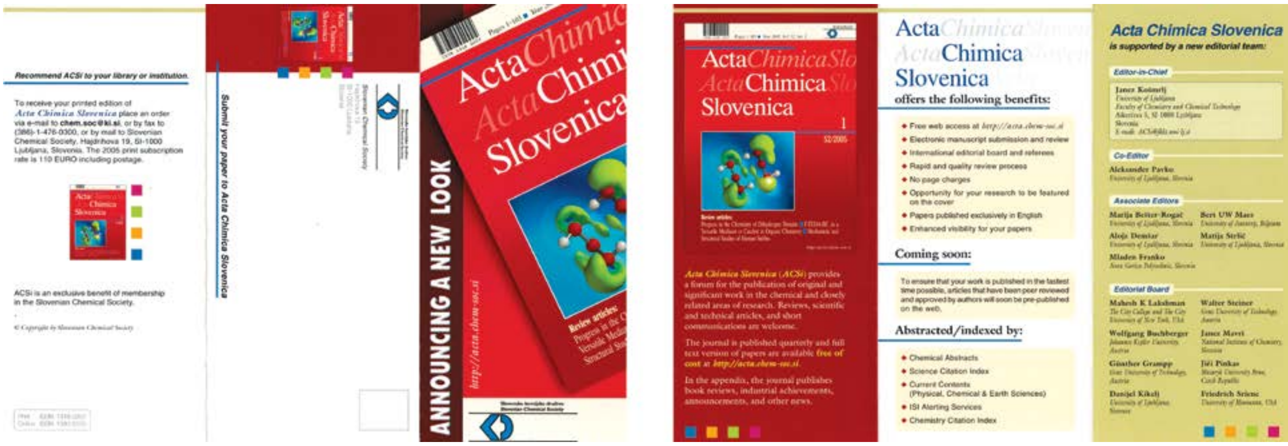

Slika 10. Zloženka.

Dosežke in spremembe revije sem imel čast predstaviti na 14. seji Senata Fakultete za kemijo in kemijsko tehnologijo – »Člani senata so spremembe pri reviji pozitivno sprejeli« (Slika 9).

In nikoli ni zmanjkalo novih idej. Da bi revijo *Acta Chimica Slovenica* ponesli v svet, smo s pomočjo g. Kajtne pripravili zloženko, reklamni pamflet, ki smo ga »goreči privrženci Acte« delili npr. na konferencah, ki smo se jih udeležili (Slika 10). Sam sem jih zajeten šop septembra 2005 odnesel v Brno, kjer sem jih s prijaznim dovoljenjem profesorja Milana Potáčka, organizatorja simpozija 11th Blue Danube Symposium on Heterocyclic Compounds, delil med udeleženci konference.

Tako je tista tri leta nastajala *Acta Chimica Slovenica*. Teh neverjetnih let ne bi bilo brez številnih oseb, ki jih v tem kratkem »potopisu« omenjam, niti brez avtorjev in recenzentov, ki so v zgodbo verjeli. Še posebej in še enkrat naj omenim profesorje Andreja Petriča, Aleksandra Pavka in Venčeslava Kaučiča, gospoda Vinka Volka in gospoda Simona Kajtno. Prav tako sem hvaležen ekipam, ki so po mojem odhodu to pot nadaljevale in revijo dvignile na še višjo raven, da je postala slovenska znanstvena revija z najvišjim faktorjem vpliva (Slika 11). Po izidu zadnje številke revije v letu 2005 sem se od uredništva poslovil, da sem se lahko posvetil raziskovalnemu in pedagoškemu delu.


12 DELO petek 26. junija 2009 znanost@delo.si

ZNANOST

Acta Chimica Slovenica

Slovenska znanstvena revija z največjim faktorjem vpliva

V Sloveniji imamo samo štiri revije s faktorjem vpliva (Acta Chimica Slovenica, Informacije MIDEM, Strojniški vestnik in Javnost), od katerih je daleč najvišjo vrednost v zadnjih letih dosegla Acta Chimica Slovenica (ACSi). Prvič je bila ocenjena za leto 2002 (IF = 0,12), vrednost IF se je povečevala in za leto 2007 dosegla za nacionalno revijo zavidljivih 1,093 (druge tri med 0,088 in 0,151).

MARIJA BEŠTER - ROGAČ
ALEKSANDER PAVKO
VENČESLAV KAUČIČ
Slovensko kemijsko društvo

Zadnjih nekaj let Agencija za raziskave in razvoj (ARRS) ocenjuje raziskovalno uspešnost posameznikov in raziskovalnih (programskih) skupin. Eden izmed glavnih kriterijev ocenjevanja je točkovanje bibliografskih enot oziroma znanstvenih publikacij. Pri znanstvenih člankih je glavno merilo vrednotenja kakovost revije, ki je članek objavila. Mednarodna bibliografska baza podatkov Web of Science revije razvršča po faktorju vpliva (impact factor, IF), ki se izračuna kot razmerje med številom citatov in številom objavljenih člankov v reviji za določeno leto.

Čeprav mnogi, predvsem evropski avtorji, nasprotujejo faktorju IF, saj privilegira angleško govoreče narode na škodo manjših in ameriško potrošniško kulturo postavlja nad manjše, a zgodovinsko bogatejše evropske kulture, ga danes široko uporabljajo pri ocenjevanju. Vsekakor pa se je nacionalnim revijam na to lestvico težko uvrstiti.

Izdajanje kakovostne revije, seveda, zahteva veliko denarja. Glavni del stroškov sta tisk in tehnično urejanje. Revijo *ACSi* ob finančni podpori ARRS in sponzorjev (fakultete, inštituti, podjetja) izdaja Slovensko kemijsko društvo. Sredstva ARRS so največji delež prihodkov, sicer na podlagi razpisov za triletno financiranje, vendar glede na dolgoletno prakso in naraščajočo znanstveno kakovost revije upamo, da ta vir ne bo usahnil. Vendar ne bi bilo nič narobe, če bi se pri financiranju upoštevala tudi višina faktorja IF. Del prihodkov prinaša tudi članarina. Svoje finančne prispevke že vsa leta dajejo vse tri slovenske »kemijske« fakultete v Ljubljani, Mariboru in Novi Gorici, Fakulteta za farmacijo Univerze v Ljubljani ter Kemijski inštitut in Institut Jožefa Stefana. Ti prispevki so predmet vsakoletnih dogovorov in upamo, da bodo še poslej na dosedanji ravni. Seveda pa je zaželeno, da se zagotovi dolgoročen in stabilen vir financiranja, ki bi zagotovil tudi varno prihodnost in nadaljnji razvoj naše revije. To je ne nazadnje edini razlog, zakaj še ni sodelovanja s tujo ugledno založbo. Precejšen del prihodkov pa smo vsaj pred leti dobili z oglaševanjem. A žal pogled na oglase v številkah pred tremi leti in letos priča, da so naša kemijska industrija in podjetja močno priprli denarnice – edina svetla izjema je tovarna Krka. Recesija ali morda kaj drugega? Kar ne moremo si predstavljati, da je uglednemu podjetju težko dati 500 evrov za oglas ...

Ostaja tudi glasilo SKD

Acta Chimica Slovenica je razdeljena na dva dela: v prvem, strokovnem, ki je napisan v angleškem jeziku, so zbrani znanstveni in strokovni članki z aktualnih področij kemije (s slovenskim povzetkom). Prispevki so strogo recenzirani. Pri tem se preverjata znanstvena kakovost in primernost predstavitve, ki morata ustrezati normativom mednarodnih kemijskih publikacij. Vsebine vseh člankov so sprotno povzete v publikaciji Ameriškega kemijskega društva *Chemical Abstracts, Science Citation Index Expanded, Current Contents: Physical, Chemical and Earth Sciences, Chemistry Citation Index, ISI Alerting Services*, prizadevamo pa si tudi za indeksiranje v *Medline*. Prav tako so vsi članki sproti ustrezno katalogizirani v sistemu COBISS.

V drugem delu, ki je večinoma napisan v slovenščini, so objavljene društvene vesti. Gre za sezname diplom, magisterijev in doktoratov s slovenskih univerz s študijskimi programi na področju kemije, biokemije, kemijske tehnike in materialov, poročila o delovanju sekcij slovenskega kemijskega društva ter strokovne članke in recenzije knjig. Objavljamo tudi obvestila o konferencah, simpozijih in drugih srečanjih.

Revijo v nakladi 1200 izvodov dobivajo člani Slovenskega kemijskega društva; v elektronski obliki je prosto dostopna na spletni strani društva http://acta.chem-soc.si. Približno 200 tiskanih izvodov dobijo knjižnice in raziskovalne institucije po vsem svetu. Približno eno tretjino prispevkov napišejo domači znanstveniki, tako da je tuja znanstvena javnost dobro obveščena o raziskavah v Sloveniji.

NASLOVNICE REVIJE ACSI V LETU 2008

Čedalje zahtevnejše urejanje

Vsekakor je visoka ocena IF za nacionalno revijo izreden uspeh, ki pa ga lahko pripišemo predvsem dobri uredniški politiki. Vedno večji ugled revije je plod dolgoletnega dela in truda številnih ljudi. *Acta Chimica Slovenica* izhaja že 56 let. Uredniški odbor od leta 1977 vodi **prof. dr. Branko Stanovnik**, na mestu glavnega urednika pa se je do leta 2004 zvrstilo več sodelavcev (**prof. dr. Drago Kolar, prof. dr. Ljubo Golič, prof. dr. Andrej Petrič**). Leta 2005 je to mesto prevzel **prof. dr. Janez Košmrlj** in poskrbel za temeljito preobrazbo revije: nadel ji je popolnoma novo, svežo obliko in uredniški odbor okrepil s področnimi uredniki.

Na pobudo **prof. dr. Aleksandra Pavka**, ki je postal glavni urednik leta 2006, smo se področni uredniki ob izidu vsake številke začeli srečevati, si izmenjevati izkušnje in načrtovati vsebine naslednjih številk. Pred desetimi leti je v uredništvo prvič v enem letu prispelo več kot sto prispevkov, od katerih jih je bila dobra polovica objavljenih. V zadnjih treh letih pa dobimo več kot 200 prispevkov, izmed katerih dobro tretjino zavrnemo. S povečevanjem faktorja vpliva in s tem kakovosti revije namreč dobivamo v objavo vedno več člankov z vsega sveta. Za vse področni uredniki pridobijo dve neodvisni oceni večinoma uglednih tujih strokovnjakov in šele na podlagi pozitivnih mnenj se začne postopek za objavo. Uredniško delo, ki ga področni uredniki (univerzitetni profesorji in sodelavci inštitutov) opravljajo volontersko, je tako tudi časovno čedalje zahtevnejše, saj uredniki komunicirajo s številnimi avtorji in recenzenti iz vsega sveta. ARRS priznava in ugodno ocenjuje publikacije, ki jih avtorji objavljajo v *ACSi*, a uredniško delo žal ni primerno vrednoteno: bibliografski kazalci raziskovalne uspešnosti po metodologiji ARRS tega ne upoštevajo, v univerzitetnih habilitacijskih postopkih pa je dolgoletno uredništvo enakovredno avtorstvu enega članka v srednje kakovostni reviji.

Razpotje

In kako naprej? Nedvomno je listanje novega izvoda revije poseben izziv. Vendar se informacijska tehnologija nezadržno razvija in naklada tiskanih revij se v svetu hitro zmanjšuje na račun revij, dostopnih na spletu v elektronski obliki. Tudi naša *Acta* je na razpotju. Zaradi dobre kakovosti se zanjo zanima ugledna svetovna založba. Skupaj z drugimi revijami, ki jih izdaja, ponuja distribucijo v ugledne svetovne knjižnice in institucije, kar bi povečalo branost revije ter potencialno kakovost in število avtorjev iz zahodnega sveta, kar si vsekakor želimo. Vendar bi to potekalo v elektronski obliki, tako da bi se tiskana naklada revije žal bistveno zmanjšala, s tem pa bi počasi šli v pozabo tudi »papirni« užitki. Poleg tega bi bilo treba urediti zadevo s slovenskim delom revije – *Acta* je ne nazadnje glasilo Slovenskega kemijskega društva, ki med drugim skrbi za kulturo našega znanstvenega in tehničnega izrazoslovja. V kratkem bo potrebna odločitev: vztrajati pri klasiki ali na račun razvoja plačati globalizacijski davek.

Slika 11. Objava v Delu 26. junija 2009.

Ob 70 letnici izhajanja revije *Acta Chimica Slovenica*

prof. dr. Aleksander Pavko

Fakulteta za kemijo in kemijsko tehnologijo Univerze v Ljubljani

glavni in odgovorni urednik v obdobju 2006–2017

Uredniški ekipi revije *Acta Chimica Slovenica* (*ACSi*) sem se na pobudo prof. dr. Ljuba Goliča pridružil leta 1999, ko je bil glavni urednik prof. dr. Andrej Petrič. Takrat je revija izhajala v manjšem formatu od sedanjega, prepoznavna je bila po vojaško zelenih platnicah in napisih v črni barvi. Leta 2003 je glavni urednik postal prof. dr. Janez Košmrlj, glavni krivec za novo, sodobno, privlačno podobo *ACSi*, ki jo je pripravil akademski slikar Simon Kajtna. Košmrlj je uvedel tudi dvokolonski tisk in sodobne tehnične standarde. Tehnični urednik je bil naš kolega Vinko Volk, ki je do leta 2008 tehnično urejal revijo, do leta 2013 pa tudi njeno spletno stran. Nanjo je nalagal nove številke in skrbel za pravočasne spletne izdaje in posodabljanje navodil. Leta 2008 je tehnično urejanje revije prevzel profesionalni urednik Stanislav Oražem, ki od takrat skrbi za pripravo prelomov strani revije za objavo v tiskani in spletni izdaji z uporabo vseh sodobnih informacijskih orodij. Aktivno sodeluje tudi pri komunikaciji med glavnim urednikom in Simonom Kajtno pri pripravi naslovnice.

Po nekaj letih souredniške prakse sem leta 2006 prevzel mesto glavnega urednika. Na tem mestu bi rad izrazil spoštovanje in zahvalo vsem tistim, ki so s številnimi idejami in navdušenim pristopom k delu že od samega začetka prispevali k razvoju in priljubljenosti naše revije. Še posebej bi se rad zahvalil obema glavnima in tehničnemu uredniku, ki so mi nesebično pomagali in me vpeljali v skrivnosti tega nadvse zanimivega, ustvarjalnega dela.

Zaradi velikega števila prispelih rokopisov sem dopolnil znanstvena področja in uredniško ekipo. Tako so uredniki pokrivali znanstvena področja fizikalne kemije (prof. dr. Marija Bešter Rogač), organske kemije (prof. dr. Janez Cerkovnik, doc. dr. Krištof Kranjc), analizne kemije (prof. dr. Matija Strlič, prof. dr. Mladen Franko, prof. dr. Boris Pihlar, dr. Johannes T. van Elteren, dr. Irena Vovk, prof. dr. Helena Prosen), splošne in anorganske kemije (prof. dr. Alojz Demšar, prof. dr. Primož Šegedin, prof. dr. Franc Perdih), znanosti o materialih (prof. dr. Barbara Malič, dr. Melita Tramšek), biokemije, molekularne biologije in biomedicinskih aplikacij (prof. dr. Damjana Rozman) ter kemijskega, biokemijskega in okoljskega inženirstva (prof. dr. Aleksander Pavko). Našteti uredniki so se v času mojega uredništva menjali.

V obdobju 2006–2017 je bilo letno objavljenih približno 130 del na okoli 1000 straneh, v glavnem znanstvenih člankov, medtem ko so bili pregledni in tehnični članki redki. Večino so jih napisali slovenski avtorji. Morda zanimiv podatek: v času najvišje naklade 1200 izvodov je bilo za tisk *ACSi* letno porabljenega 3,5 tone papirja. V tem času smo z vabljenimi uredniki ob različnih priložnostih, posvečenih izbranim znanstvenim področjem, pripravili 21 številk, prikazanih v preglednici. Najbolj citiran članek je dosegel skoraj 100 citatov, medtem ko je kar nekaj člankov preseglo 40 citatov.

Obremenitev glavnega urednika je bila velika. Za uredništvo ni bilo posebnega zanimanja, vodenje ekipe prostovoljnih urednikov pa ni bilo enostavno, saj je zahtevalo kompleksen diplomatski pristop. Odgovoren sem bil, da za vsako številko dobim približno 30 prispevkov, ki so

Preglednica posvečenih in tematskih številk *ACSi* v letih 2006-2017

Številka *ACSi*	Posvečeno	Priložnost	Vabljen urednik
53/1 (2006)	mednarodni simpozij o spektroskopiji	tematska številka	prof. dr. Mladen Franko
53/2 (2006)	izbrana dela iz anorganske kemije	tematska številka	prof. dr. Alojz Demšar
53/3 (2006)	prof. dr. Davorin Dolar	spominska številka	prof. dr. Marija Bešter Rogač, prof. dr. Jože Škerjanc
54/3 (2007)	Prof. dr. Jože Škerjanc	70 let	prof. dr. Marija Bešter Rogač
55/4 (2008)	prof. dr. Ljubo Golič	spominska številka	prof. dr. Ivan Leban
56/1 (2009)	prof. dr. Josef Barthel	80 let	prof. dr. Marija Bešter Rogač, prof. dr. Roland Neueder
56/3 (2009)	prof. dr. Branko Stanovnik	70 let	prof. dr. Jurij Svete
57/1 (2010)	prof. dr. Valentin Koloini	spominska številka	prof. dr. Aleksander Pavko
57/3 (2010)	prof. dr. Milan Randić	80 let	prof. dr. Marjana Novič
58/2 (2011)	mednarodno leto kemije, 60 let SKD	tematska številka	prof. dr. Slavko Kaučič, prof. dr. Aleksander Pavko
58/3 (2011)	prof. dr. Dušan Hadži	90 let	prof. dr. Janez Mavri, dr. Jurka Kidrič
58/4 (2011)	prof. dr. Franc Gubenšek	spominska številka	prof. dr. Igor Križaj
59/3 (2012)	prof. dr. Gorazd Vesnaver	70 let	prof. dr. Jurij Lah
60/1 (2013)	60 let *ACSi*		prof. dr. Branko Stanovnik
60/3 (2013)	prof. dr. Boris Žemva	spominska številka	prof. dr. Barbara Malič, dr. Melita Tramšek
61/2 (2014)	simpozij elektrokemije v JV Evropi	tematska številka	prof. dr. Ingrid Milošev, prof. dr. Miran Gaberšček
61/3 (2014)	prof. dr. Marija Kosec	spominska številka	prof. dr. Barbara Malič
62/2 (2015)	prof. dr. Jurij Vinko Brenčič	spominska številka	prof. dr. Barbara Modec
62/3 (2015)	prof. dr. Jože Koller	70 let	prof. dr. Tomaž Urbič
63/3 (2016)	prof. dr. Janko Jamnik	spominska številka	prof. dr. Boštjan Genorio, prof. dr. Robert Dominko, prof. dr. Stane Pejovnik
64/4 (2017)	prof. dr. Miha Tišler	90 let	prof. dr. Janez Cerkovnik

preživeli recenzentski postopek in so jih avtorji že primerno popravili. Za dosego tega cilja sem moral skupaj s svojo uredniško ekipo imeti uredniško politiko, ki bi reviji zagotovila dovolj visok faktor vpliva IF in s tem privabila čim več bralcev in posledično tudi avtorjev z vsega sveta. Prvi korak sta bili nedvomno že nova podoba in tehnična urejenost revije skupaj s spletno stranjo. Ustrezna znanstvena raven, novost in izvirnost že objavljenih člankov ter uvajanje novih področij objav, kot so biokemija, molekularna biologija in biomedicinske aplikacije, pa so delovali kot dodatna reklama in spodbujali znanstvenike k poročanju o svojih raziskovalnih dosežkih. Na osnovi vzorcev uglednih mednarodnih revij smo v pomoč avtorjem, recenzentom in urednikom pripravili natančna navodila. V velikem deležu prispelih prispevkov so namreč avtorji posamezna poglavja, predvsem pa grafični material in navajanje literature, pripravili po svoje in s tem tehnično urejanje precej otežili.

Za prispevke smo prosili tudi mednarodno priznane slovenske znanstvenike, delujoče na področjih, ki jih pokriva tudi njihova domača revija, pa se jih žal velika večina ni odzvala naši prošnji. Očitno zaradi prenizkega faktorja vpliva, čeprav bi ga lahko s svojimi prispevki izboljšali. Na obisku pri enem od njih sem opazil, da je na polici v njegovi pisarni ležal kup številk *ACSi* v še neodprtih plastičnih kuvertah, kar kaže na odnos do naše nacionalne znanstvene revije

Izdajatelj *ACSi* je Slovensko kemijsko društvo (SKD), njegove tajnice, polne pozitivne energije, pa so pomagale tudi pri administrativnem delu za *ACSi*. Pisarna SKD je bila najprej pod stopniščem v avli v prvem nadstropju Kemijskega inštituta (KI) na Hajdrihovi ulici 19 v Ljubljani,

kjer je sredi knjižnih omar in polic ter cigaretnega dima delala Jana Tepina. Leta 2010 se je sedež SKD preselil v nove, adaptirane prostore na podstrešju KI, Jano je zamenjala Olga Gorše, njo pa čez tri leta Marjana Gantar. V prizidku KI je gostovala tudi Katedra za kemijsko inženirstvo ljubljanske Fakultete za kemijo in kemijsko tehnologijo (FKKT), kjer sem bil zaposlen. Tako sem kot sourednik praktično tedensko prenašal material in hodil na sestanke v prostore FKKT na Aškerčevi ulici 5, kjer so imeli svoje pisarne glavna urednika prof. dr. Andrej Petrič, prof. dr. Janez Košmrlj in tehnični urednik Vinko Volk. Vsi našteti skupaj s predsednikom SKD prof. dr. Slavkom Kaučičem so izrazito pripomogli k rednemu izhajanju *ACSi*. Kolegi uredniki, sicer učitelji in raziskovalci, smo svoje urednikovanje ob rednem pedagoškem in znanstvenoraziskovalnem delu opravljali amatersko na profesionalen način.

S pomočjo Olge sem uvedel tako imenovani »mavrični seznam«, na katerem je bila usoda oddanih člankov označena z različnimi barvami. Zelena je na primer pomenila, da so recenzije pri avtorjih, rumena, da so recenzije poslane avtorjem, in rdeča, da recenziranje že predolgo traja in da je treba opomniti in/ali zamenjati recenzente. Z Olgo sem uvedel tudi »simetriranje«. Ob izidu nove številke sva si včasih ob kavi št. 62 iz avtomata privoščila energijski dodatek iz bombonjere: bombone sva iz nje jemala tako, da je v njej ostal simetrični vzorec. Po Olgini upokojitvi je februarja 2013 prišla Marjana Gantar. S svojo mladostno energijo in računalniško spretnostjo je v sodelovanju z zunanjimi izvajalci poskrbela za posodobitev in urejanje spletne strani SKD in naše revije.

Postali smo zanimivi tudi za eno izmed tujih mednarodnih založb, ki bi z naročnino zase naredila dober posel. Ponujali so nam prispevke priznanih mednarodnih avtorjev ter s tem boljšo mednarodno razpoznavnost in povišanje faktorja vpliva *ACSi*, pa tudi tehnično urejanje in tisk. Uredniška ekipa naj bi ostala ista. Kljub nekaterim ugodnostim smo želeli ostali zvesti svojemu izdajatelju SKD in njegovim članom, ki so tiskano revijo dobivali v okviru društvene članarine. Tako smo ohranili svojo uredniško neodvisnost in svobodo ter ostali prosto dostopna revija v okviru OJS.

Vsi oddani rokopisi so najprej pristali v mojem e-poštnem nabiralniku, nato pa sem ocenil, ali se ujemajo z znanstvenim področjem revije, pa tudi, ali so bili pripravljeni v skladu z navodili za avtorje. Pozitivno ocenjeni prispevki so bili nato dodeljeni uredniku ustreznega področja, ki je začel postopek recenzije. Pri komuniciranju z avtorji in recenzenti smo se uredniki ob svojih študijskih in raziskovalnih obveznostih trudili po svojih najboljših močeh. Na srečo smo imeli v postopku recenzije vedno več kot 60 rokopisov, zato je bilo za naslednjo številko teoretično dovolj gradiva. Pridobiti smo morali dve neodvisni recenziji za posamezen članek, kar pomeni več sto recenzij na leto. Recenzentom, večinoma iz mednarodnega prostora, smo za lažje delo sicer pripravili formular, na katerem so lahko hitro in enostavno izpolnili vprašalnik, vendar smo za dobro recenzijo pričakovali tudi konstruktivne komentarje. Aktivne, kakovostne recenzente, ki bi svoje delo opravili pravočasno, smo zelo težko našli; večina izbranih ni imela časa za branje rokopisov ali celo za odgovor na vljudno prošnjo urednikov. Na srečo smo kljub temu imeli veliko skupino komunikativnih recenzentov, ki so opravljali delo na različnih ravneh kakovosti in hitrosti. Posledično je postopek recenzije trajal približno 3–6 mesecev, zelo odvisno od dobre volje in hitrosti recenzenta. Upoštevajoč »mavrični seznam«, sem moral nekatere urednike področij pogosto prositi, da čim prej zaključijo postopek recenzije in sprejmejo ustrezne odločitve. To ni bilo prijetno opravilo, še posebej ker sem ga moral več let ponavljati mesečno ali celo tedensko.

Ko je bil postopek recenziranja končan, so uredniki poslali dokumentacijo s sklepom avtorjem. Če so bile recenzije pozitivne, so avtorji svoj rokopis popravili v skladu s komentarji recenzentov in ga vrnili uredniku. Če je bilo vse narejeno pravilno, je bil rokopis sprejet in poslan tehničnemu uredniku.

Približno mesec dni pred izdajo številke se je komunikacija med menoj in tehničnim urednikom okrepila, da bi preverila krtačne odtise, uredila prispevke in pripravila grafično vsebino. Posebna izziv in zadovoljstvo sta zame bila, da sem skupaj s tehničnim urednikom iz grafičnega materiala prispevkov izbral sliko, iz katere je potem Simon Kajtna pripravil naslovnico. Ta je pripovedovala zanimivo zgodbo s širokega področja kemije. Navajam dva primera.

V zadnji številki *ACSi* letnika 2014 je objavljen pogovor z akademikom prof. dr. Dušanom Hadžijem o spominu vode in na naslovnici sem želel na neki način predstaviti vodo. V svoji modelarski delavnici sem plastično folijo za prekrivanje letalskih modelov najprej premazal s tekočino za impregniranje čevljev in oblačil ter nato površino z modelarsko pršilko za nanašanje barv rahlo poškropil z

Slika na naslovnici *ACSi* 2014/4

vodo. Nastale so drobne kapljice. S finim čopičem sem napisal kemijsko formulo vode in kapljice so se združile v njen simbol. Fotografijo je potem za naslovnico privlačno obdelal Simon Kajtna.

Druga številka letnika 2015 je posvečena prof. dr. Juretu Brenčiču. Bil je univerzitetni učitelj in raziskovalec. Skupaj s prof. dr. Francem Lazarinijem je napisal srednješolski in univerzitetni učbenik na področjih splošne in anorganske kemije, raziskoval pa je koordinacijske spojine kroma, molibdena in volframa, med drugim tudi spojine s četvernimi vezmi, in njihove kristalne strukture. Njegovo učiteljsko vlogo predstavljata tabla in naslovnica učbenika, področje raziskav pa ustrezne kemijske formule in strukture anorganskih spojin.

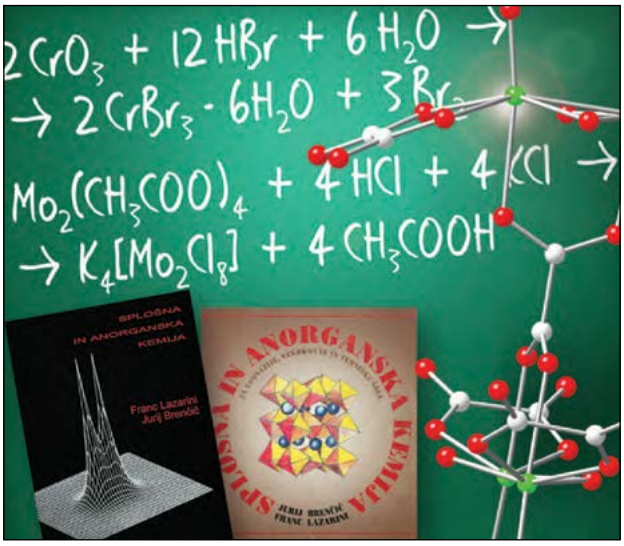

Slika na naslovnici *ACSi* 2015/2

Po izdaji številke sem sklical uredniški sestanek, na katerem smo razpravljali o rezultatih našega dela in načrtovali prihodnje številke. Verjamem namreč, da sta poleg že vzpostavljene komunikacije po e-pošti in telefonu osebni stik s pozitivno energijo in prijetno vzdušje nujna za plodno uredniško delo. Kot nagrado za svoj trud smo dvakrat letno imeli delovno kosilo, običajno v gostilni Pod vrbo v Trnovem. Posebna zahvala gre predsedniku SKD prof. dr. Slavku Kaučiču. Je eden redkih, ki je razumel in cenil vrednost in obseg uredniškega dela ter nas spodbujal s svojim prijaznim odnosom in konstruktivnim pristopom. Z nekaterimi uredniki slovenskih mednarodnih naravoslovnih in tehničnih revij s faktorjem vpliva smo pri Javni agenciji za raziskovalno dejavnost RS (ARRS) in Javni agenciji za knjigo RS poskušali doseči precej boljše finančno ovrednotenje dela urednikov, pa smo žal naleteli na nerazumevanje. Uredniki teh revij smo med seboj izmenjevali strokovne izkušnje in si pomagali. Posebna zahvala za konstruktivne debate gre prof. dr. Tomažu Pisanskemu, takratnemu glavnemu uredniku matematične revije *ARS Mathematica Contemporanea*.

Varčevanje in znatne finančne omejitve na znanstveno raziskovalnem področju v Sloveniji so dosegli tudi *ACSi*. Večino stroškov revije je desetletja krila ARRS, vendar se je pod mojim uredništvom ta finančna podpora, ne po naši krivdi, močno zmanjšala. Pomoč slovenskih podjetij z oglaševanjem se je z leti zelo skrčila. Na srečo so Kemijski inštitut ter Institut Jožef Stefan, ljubljanska in mariborska Fakulteta za kemijo in kemijsko tehnologijo, Fakulteta za znanosti o okolju iz Nove Gorice in nekaj let Fakulteta za farmacijo UL pomagali kriti stroške izdajanja revije. Na žalost je to omogočilo predvsem preživetje naše revije in ne njenega bistvenega napredka. Morali smo zmanjšati število natisnjenih izvodov posamezne številke s 1200 na 200. Kljub temu smo se potrudili narediti vse, kar je bilo v naši moči, da smo sledili trendom na področju informacijske tehnologije in povečali vrednost naše revije v znanstvenem svetu. *ACSi* je od leta 2013 indeksirana v podatkovni zbirki PubMed. Po približno šestih mesecih priprav smo januarja 2014 začeli uporabljati dobro znani sistem prosto dostopnih revij (Open Journal System, OJS) – za našo revijo ga je skupaj s podjetjem Abelium uvedel dr. Alen Orbanić, ki je zaslužen tudi za uvedbo drugih sodobnih informacijskih orodij. Leta 2015 smo uvedli sistem Digital Object Identifier (DOI), malo pozneje pa smo začeli preverjati rokopise z učinkovitim programom za odkrivanje plagiatorstva iThenticate. Z uporabo teh sistemov smo začeli objavljati elektronske različice rokopisov takoj po njihovem sprejetju in tako povečali znanstveni ugled naše revije. *ACSi* je od 1998 revija s prostim dostopom, od januarja 2017 pa je objavljena pod licenco Creative Commons Attribution 3.0, kasneje pa pod licenco Creative Commons Attribution 4.0.

Našo revijo sem rad urejal. Delo je bilo pestro in zanimivo in ni potekalo po nekem ustaljenem urniku. Druženje in pogovori s sodelavci pri *ACSi* so bili ustvarjalni in prijetni, komunikacija z avtorji in recenzenti je bila vselej zanimiva. Z vznemirjenjem sem vsake tri mesece pričakoval izid našega odgovornega dela in si vsakokrat oddahnil, ker je bilo vedno vse v redu. Ko se ozrem nazaj, z zadovoljstvom ugotavljam, da je v času mojega urejanja napredek opazen in da smo ustvarili nekaj dobrega. Po dobrem desetletju pa je prišel čas, da prepustim krmilo novemu, mlajšemu glavnemu uredniku s svežimi idejami in ustvarjalno energijo. Ta izziv je sprejela prof. dr. Ksenija Kogej z dragocenimi znanstvenimi in vodstvenimi izkušnjami ter ustvarjalnim pristopom do dela in konstruktivnim odnosom do kolegov. Vesel sem, da je to nalogo pet let več kot uspešno opravljala. Prav tako želim novemu uredniku prof. dr. Francu Perdihu in njegovi uredniški ekipi, da uživajo v uredniškem delu in povečajo ali vsaj ohranijo zanimanje bralcev in znanstveno vrednost revije *Acta Chimica Slovenica* na mednarodnem odru.

70-letnica revije *Acta Chimica Slovenica:* mednarodno prepoznavna znanstvena revija na področju kemije

prof. dr. Ksenija Kogej

Fakulteta za kemijo in kemijsko tehnologijo, Univerza v Ljubljani

glavna in odgovorna urednica v obdobju 2018–2022

Leta 2018 sem od dolgoletnega glavnega in odgovornega urednika profesorja Aleksandra Pavka prevzela vlogo glavne in odgovorne urednice revije *Acta Chimica Slovenica* (*ACSi*). Ob prevzemu te funkcije nisem imela izkušenj z uredniškim delom, a sem se dela lotila z veliko volje in entuziazma, pri čemer mi je bil v veliko pomoč Sašo. S svojimi bogatimi izkušnjami mi je pomagal narediti prve korake pri uredniškim delom. Revija je imela tedaj že oblikovano znanstveno prepoznavnost s stabilnim faktorjem vpliva, za kar gre zahvala vsem urednikom in ostalemu osebju, ki so skrbeli za njeno izhajanje in posodabljanje pred menoj. Postaviti si je bilo treba nove izzive, ki smo se jih lotili z izkušeno ekipo področnih urednikov in tehničnega osebja, administratorke gospe Marjane Gantar Albreht, tehničnega urednika revije gospoda Stanislava Oražma, skrbnika sistema za oddajanje in sprejemanje člankov (*Open Journal System*, OJS) gospoda Alena Orbanića, podjetje Abelium, ter neprecenljivi pomoči osebja Centralne in tehniške knjižnice Univerze v Ljubljani, gospe Maje Vihar in gospoda Mitje Vovk-Iskrića. Vsi ti so mi bili pri spoznavanju z uredniškim delom v neizmerno pomoč.

Največji spremembi v prvem letu mojega mandata (2018) sta bili opustitev izdajanja tiskanih izvodov *ACSi* in prenova spletne strani revije. Tiskanje revije je predstavljalo ogromne stroške in je postalo v obdobju digitalizacije vse manj smiselno. Mnogi prejemniki revije so povedali, da tiskanega izvoda revije skorajda ne odprejo, še več, da takoj roma v koš za smeti, zato je bila ta odločitev edina smiselna. Odločili smo se, da bodo v tiskani obliki, v omejenem številu izvodov, izhajale le še posvečene številke. V času mojega mandata je bila taka le ena številka, ki je bila posvečena prof. dr. Igorju Kregarju (leto 2019, volumen 66, številka 1). Lotili smo se tudi prenove spletne strani revije v bolj sodobno in interaktivno obliko, nadgradnje navodil za avtorje in odprave določenih pomanjkljivosti v delovanju OJS. Tako je v sredini leta 2018 zaživela nova sodobna spletna stran *ACSi* (slika 1), ki smo jo predstavili tudi na srečanju Slovenski kemijski dnevi septembra leta 2018 v Portorožu.

Naslednja novost, katere namen je bil predvsem dvig faktorja vpliva revije, je bila uvedba nove kategorije člankov, to je Tematskih člankov (*Feature Articles*, FA). Ta kategorija naj bi predstavljala dopolnitev k tedaj že obstoječim Preglednim člankom (*Review Articles*, RA). Poudarek pri FA je bil na aktualnih raziskavah avtorjev s poudarkom na smernicah za nadaljnje raziskave. K pisanju FA smo najprej vabili priznane slovenske znanstvenike z odmevnimi objavami s področja kemije, v nadaljevanju pa tudi tuje avtorje. Spisek FA in RA, ki so bili objavljeni v letih 2018–2022, je podan v Tabeli 1. Prvi Tematski članek je bil objavljen že v 2. številki *ACSi* leta 2018, napisali pa so ga kolegi iz skupine profesorice Damjane Rozman, tedaj tudi urednice pri *ACSi* za področje biokemije, molekularne biologije in biomedicinskih aplikacij. V naslednjih letih so Tematske članke prispevale raziskovalne skupine iz mnogih raziskovalnih skupin v Sloveniji in tudi iz tujine, vse do konca leta 2022 pa je v *ACSi* izšlo 15 FA in 5 RA. Trudili

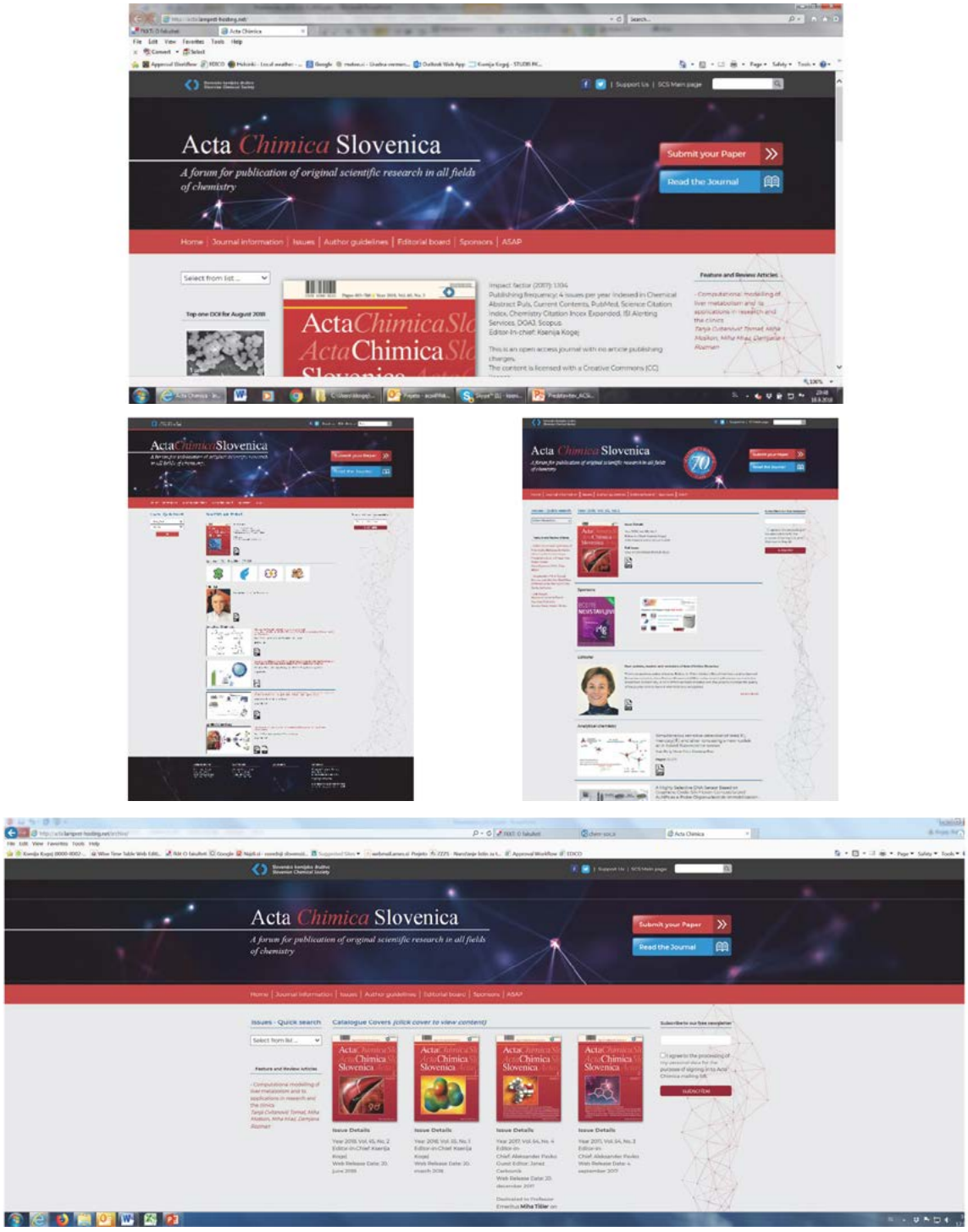

Slika 1. Podoba prenovljene spletne strani revije *Acta Chimica Slovenica*.

smo se, da bi bile pri tem zastopane vse večje raziskovalne ustanove v Sloveniji, vendar pri tem nismo bili popolnoma uspešni. Pokazalo se je, da objavljanje v *ACSi* pri marsikaterem slovenskem znanstveniku ni prav privlačno, saj je faktor vpliva (*Impact Factor*, IF) revije, ki tekmuje na področju splošne kemije z mnogo bolj prepoznavnimi in finančno podprtimi mednarodnimi revijami, kljub velikim naporom uredniških odborov revije nizek. Zato smo še toliko bolj cenili prispevke vseh, ki so se opogumili in napisali članke za našo revijo. Izredno veseli smo bili tudi prispevkov slovenskih znanstvenikov, ki delujejo v tujini (glej članek J. Petrovčič, C. N. Ungarean, D. Šarlah *Acta Chim. Slov.* **2021**, *68*, 247–267) in priznanih tujih raziskovalcev (glej članka J. Siirilä, H. Tenhu *Acta Chim. Slov.*

Tabela 1. Objavljeni prispevki v kategoriji Tematskih (*Feature Articles*, FA) in Preglednih člankov (*Review Articles*, RA) v *Acta Chimica Slovenica* v letih 2018–2022 (kronološki seznam) in naslovnica revije, oblikovana na osnovi FA ali RA.

avtor(ji) in institucija	Naslov prispevka	številka *ACSi* in naslovnica
T. Cvitanović Tomaš, M. Moškon, M. Mraz, D. Rozman *Univerza v Ljubljani, Medicinska fakulteta, Ljubljana*	**Computational modelling of liver metabolism and its applications in research and the clinics**	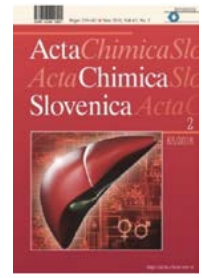 FA: **2018**, *65* (2), 253–265
J. Gašperšič, M. Kastelic, U. Novak, B. Likozar *Kemijski Inštitut Slovenije, Ljubljana*	**Metabolic network modelling of chinese hamster ovary (CHO) culture bioreactors operated as microbial cell factories**	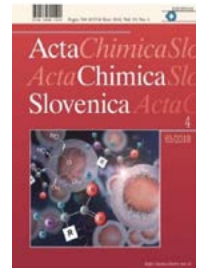 FA: **2018**, *65* (4), 769–786
V. Turk, D. Turk, I. Dolenc, V. Stoka *Inštitut Jožef Stefan, Ljubljana*	**Characteristics, structure, and biological role of stefins (type-1 cystatins) of human, other mammals, and parasite origin**	 RA: **2019**, *66* (1), 5–17
D. Štepec, M. Ponikvar-Svet *Inštitut Jožef Stefan, Ljubljana*	**Fluorine in human health and nutrition**	 FA: **2019**, *66* (2), 255–275
I. Milošev *Inštitut Jožef Stefan, Ljubljana*	**Contemporary modes of corrosion protection and functionalization of materials**	 RA: **2019**, *66* (3), 511–533

avtor(ji) in institucija	Naslov prispevka	številka *ACSi* in naslovnica
A. Iglič, E. Gongadze, V. Kralj-Iglič *Univerza v Ljubljani, Fakulteta za elektrotehniko, Ljubljana*	**Differential capacitance of electric double layer – influence of asymmetric size of ions, thickness of Stern layer and orientational ordering of water dipoles**	 FA: **2019**, *66* (3), 534–541
M. Knez Hrnčič, D. Cör, P. Kotnik, Ž. Knez *Univerza v Mariboru, Fakulteta za kemijo in kemijsko tehnologijo, Maribor*	**Extracts of white and red grape skin and rosehip fruit: phenolic compounds and their antioxidative activity**	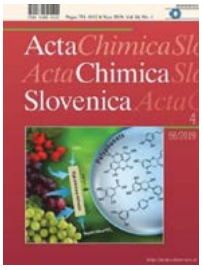 FA: **2019**, *66* (4), 751–761
T. Dodevska, Y. Lazarova, I. Shterev *University of Food Technology, Plovdid, Bolgarija*	**Amperometric biosensors for glucose and lactate with applications in food analysis: a brief review**	RA: **2019**, *66* (4), 762–776
M. Bešter-Rogač *Univerza v Ljubljani, Fakulteta za kemijo in kemijsko tehnologijo, Ljubljana*	**Ionic liquids: simple or complex electrolytes?**	 FA: **2020**, *67* (1), 1–14
A. Koler, I. Pulko, P. Krajnc *Univerza v Mariboru, Fakulteta za kemijo in kemijsko tehnologijo, Maribor*	**Post polymerisation hypercrosslinking with emulsion templating for hierarchical and multi-level porous polymers**	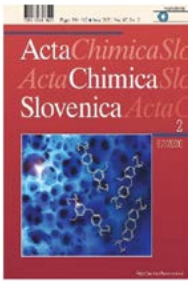 FA: **2020**, 67 (2), 349–360
P. M. Mitrašinović *Belgrade Institute of Science and Technology, Belgrade, Serbia*	**G-quadruplexes: emerging targets for the structure-based design of potential anti-cancer and antiviral therapies**	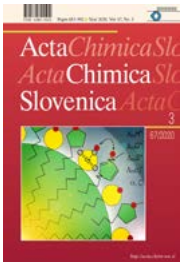 RA: **2020**, *67* (3), 683–700

avtor(ji) in institucija	Naslov prispevka	številka *ACSi* in naslovnica
T. Rijavec, M. Strlič, I. Kralj Cigić *Univerza v Ljubljani, Fakulteta za kemijo in kemijsko tehnologijo, in University College London, Velika Britanija*	**Plastics in heritage collections: review of poly(vinyl chloride) degradation and characterization**	 FA: **2020**, *67* (4), 993–1013
P. Žnidaršič-Plazl *Univerza v Ljubljani, Fakulteta za kemijo in kemijsko tehnologijo, Ljubljana*	**Let the biocatalyst flow**	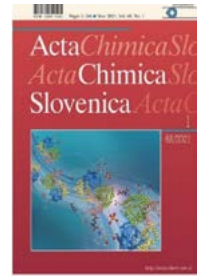 FA: **2021**, *68* (1), 1–16
J. Petrovčič, C. N. Ungarean, D. Šarlah *University of Illinois, Združene države Amerike*	**Recent chemical methodology advances i n the total synthesis of meroterpenoids**	 FA: **2021**, *68* (2), 247–267
B. Furlani, K. Kouter, D. Rozman, A. Videtič Paska *Univerza v Ljubljani, Medicinska fakulteta, Ljubljana*	**Sequencing of nucleic acids: from the first human genome to next generation sequencing in COVID-19 pandemic**	RA: **2021**, *68* (2), 268–278
T. Urbič *Univerza v Ljubljani, Fakulteta za kemijo in kemijsko tehnologijo, Ljubljana*	**Analytical modeling of thermodynamic and transport anomalies of water**	 FA: **2021**, *68* (3), 505–520
K. Balantič, D. Miklavčič, I. Križaj, P. Kramar	**The good and the bad of cell membrane electroporation**	 FA: **2021**, *68* (4), 753–764

avtor(ji) in institucija	Naslov prispevka	številka *ACSi* in naslovnica
J. Siirilä, H. Tenhu *Department of Chemistry, University of Helsinki, Finland*	**Soft poly(N-vinylcaprolactam) based aqueous particles**	 FA: **2022**, *69* (2), 251–260
N. Popovics-Tóth, E. Bálint *Department of Organic Chemistry and Technology, Budapest University of Technology and Economics, Hungary*	**Multicomponent synthesis of potentially biologically active heterocycles containing a phosphonate or a phosphine oxide moiety**	 FA: **2022**, *69* (4), 735–755
D. Makovec *Inštitut Jožef Stefan, Ljubljana*	**Adaptation of the crystal structure to the confined size of mixed-oxide nanoparticles**	FA: **2022**, *69* (4), 756–771

2022, *69*, 251–260 in N. Popovics-Tóth, E. Bálint *Acta Chim. Slov.* **2022**, *69*, 735–755). Med drugim se je tudi po zaslugi Tematskih in Preglednih člankov IF revije v letu 2020 dvignil do rekordne vrednosti 1,735.

Dokaj logično je tudi bilo, da smo naslovnico revije dali oblikovati na osnovi FA ali RA, ki je bil objavljen v dani številki reviji. Avtorji so pri tem zelo tvorno sodelovali in včasih tudi sami izživeli svojo umetniško žilico (glej na primer naslovnico za članek P. Žnidaršič-Plazl *Acta Chim. Slov.* **2021**, *68*, 1–16). Objavljene naslovnice, oblikovane na osnovi FA ali RA, so prikazane v zadnjem stolpcu Tabele 1.

V letu 2019 smo dosegli, da je bila naša revija uvrščena v najvišjo, to je zeleno kategorijo člankov v bazi podatkov *Sherpa Romeo*. Na osnovi tega smo potem pridobili pečat za OAP (*Open Access Platinum*) revije v *Directory of Open Acces Journals* (DOAJ), tako imenovani *DOAJ Seal*. Poudariti velja, da je takrat le okrog 1300 znanstvenih revij, zavedenih v DOAJ, imelo oznako OAP, *ACSi* pa je tako postala prva slovenska znanstvena revija s tem pečatom. Le-ta je namenjen revijam, ki se držijo najboljših praks pri objavljanju v odprtem dostopu. Pogoj za dodelitev pečata so funkcije, povezane z dostopnostjo, odprtostjo, ponovno uporabo in pravicami avtorjev. Avtorji prispevkov v *ACSi* namreč za svoje objave ohranijo avtorske pravice in članki so odprto dostopni na spletu, brez plačila za avtorje ali bralce. S tem je *ACSi* izpolnila pogoje nacionalne strategije Republike Slovenije 2015–2020 o odprtem dostopu do znanstvenih objav in raziskovalnih podatkov. Ob tej priložnosti smo dopolnili še opis licence *Creative Commons Attribution* (CC BY) in logotipe za vse navedeno dodali na spletno stran in na prve strani vsakega članka. Za dosego vsega navedenega je bilo potrebno kar nekaj tehnično-računalniškega dela in poznavanja raznih baz podatkov, pri čemer so bili uredniškemu odboru *ACSi* v veliko pomoč gospa Maja Vihar in gospod Mitja Vovk-Iskrić iz Centralne in tehniške knjižnice Univerze v Ljubljani ter skrbnik sistema OJS gospod Alen Orbanić. Brez njih bi to težko izpeljali.

Slika 2. Logotip revij OAP, kamor se je leta 2019 uvrstila revija *Acta Chimica Slovenica*.

V sklopu promocije *ACSi* smo leta 2021 izdelali grafično pasico spletne strani in zgibanko *ACSi* (slika 3), kasneje, ob 70-letnici Slovenskega kemijskega društva (SKD), pa je bil izdelan še promocijski video (https://acta.chem-soc.si/, https://www.youtube.com/watch?v=vMGcWpStUPk).

A) Grafična pasica spletne strani

B) Zgibanka

Slika 3. A) Grafična pasica spletne strani in B) zgibanka revije *Acta Chimica Slovenica*.

Z letom 2019 sta delo v uredniškem odboru *ACSi* zaključili dolgoletni urednici Damjana Rozman (področje Biokemija, molekularna biologija in biomedicinska aplikacija) in Melita Tramšek (področji Anorganska kemija in Materiali). Nadomestili so ju Aleš Berlec, Mirela Dragomir (oba iz Inštituta Jožef Stefan) in Matjaž Kristl (Fakulteta za kemijo in kemijsko tehnologijo, Univerza v Mariboru). Hkrati smo uredniško okrepili še področje Analizna kemija, kjer se je urednicama Heleni Prosen in Ireni Vovk pridružil Alen Albreht (Kemijski inštitut Slovenije). Leta 2021 pa je uredniški odbor zapustil še Aleš Podgornik, ki je skrbel za področje Kemijsko, biokemijsko in okoljsko inženirstvo; nasledil ga je Aleš Ručigaj. Leta 2022 je z delom tajnice SKD in tudi administratorke pri reviji *ACSi*

prenehala gospa Marjana Gantar Albreht. »Štafetno palico« je predala gospej Evi Mihalinec.

V vseh letih mojega mandata, kot verjamem pa tudi že prej, je bil poglavitni cilj dela urednikov *ACSi* visoka kvaliteta člankov in mednarodni ugled revije. Za dosego tega cilja je bilo potrebno ogromno uredniškega dela. Prvo sito je bil moj pregled oddanih člankov in na tej prvi stopnji je odpadlo okrog 70 % oddanih člankov, bodisi zaradi tehnične ali tematske neprimernosti ali pa tudi zaradi očitnega prenizkega znanstvenega nivoja. Šele potem sem članke dodelila področnim urednikom. Tudi od preostalih 30 % člankov niso bili vsi sprejet v objavo; groba ocena je, da je bilo na koncu objavljenih okrog 15 % oddanih člankov. Uredniki smo vedno vlagali velike napore v to, da so bile končne objave kvalitetne. Zelo pomembna stopnja v procesu sprejemanja člankov je delo recenzentov. Ta stopnja je bila za nas urednike vedno najtežja, predvsem kadar odziva potencialnih recenzentov na vabilo k recenziji ni bilo. Sama sem poleg dela glavne in odgovorne urednice opravljala še delo urednice za področje Fizikalna kemija. Za kakšen članek se je zgodilo, da je bilo potrebno povabiti tudi 20 ali več recenzentov, da sta končno 2 od njih sprejela vabilo in opravila recenzijo. Kljub temu pa smo vedno izdali 4 številke na letnik, ki so bile ustrezno zapolnjene, kar pomeni, da so vsebovale 250 strani ali več. V času mojega mandata težav pri zapolnitvi številk ni bilo, vedno je ostala varna zaloga člankov za naslednjo številko, in izhajanje revije je bilo redno. Lahko smo bili celo nekoliko »izbirčni« pri izbiri člankov. Vse to je na koncu privedlo tudi do dvigovanja IF. Verjetno je tudi zato obstajal interes tujih izdajateljskih družb (na primer *Andewandte Chemie*), da bi pod svoje okrilje dobile *ACSi*. Seveda pa vsega tega ne bi bilo, če ne bi že vsi uredniki pred nami pripravili odličnih podlag za nadaljnjo rast revije.

Izredno me veseli, da je delo odgovornega urednika *ACSi* sprejel prof. dr. Franc Perdih. S svojimi bogatimi uredniškimi izkušnjami bo zagotovo revijo *ACSi* popeljal k novim dosežkom. Njemu in vsem področnim urednikom in tehničnemu osebju želim uspešno delo še naprej.

Mednarodna vpetost in odmevnost revije *Acta Chimica Slovenica* v obdobju 1998–2022

prof. dr. Franc Perdih

Fakulteta za kemijo in kemijsko tehnologijo Univerze v Ljubljani

glavni in odgovorni urednik od leta 2023

Znanstvene revije si vedno želijo doseči čim širši krog raziskovalcev, ki objavljajo svoje izsledke, ter krog raziskovalcev in strokovnjakov, ki sledijo najnovejšim odkritjem znanstvenikov. V ta namen skušajo revije presegati meje med državami in tako povezujejo raziskovalce iz različnih delov sveta. Želja po preseganju domačega okolja je opazna že od začetka izhajanja znanstvene revije, ki jo je začelo izdajati Slovensko kemijsko društvo leta 1954, takrat še pod imenom *Vestnik Slovenskega kemijskega društva*. Že pri pregledu prvega letnika lahko opazimo, da so prispevki objavljeni v angleščini ali nemščini, med avtorji pa so tudi tuji raziskovalci. Široka dostopnost do mednarodne skupnosti raziskovalcev pa je seveda občutno lažja, odkar lahko s pridom izkoriščamo svetovni splet. Mednarodno

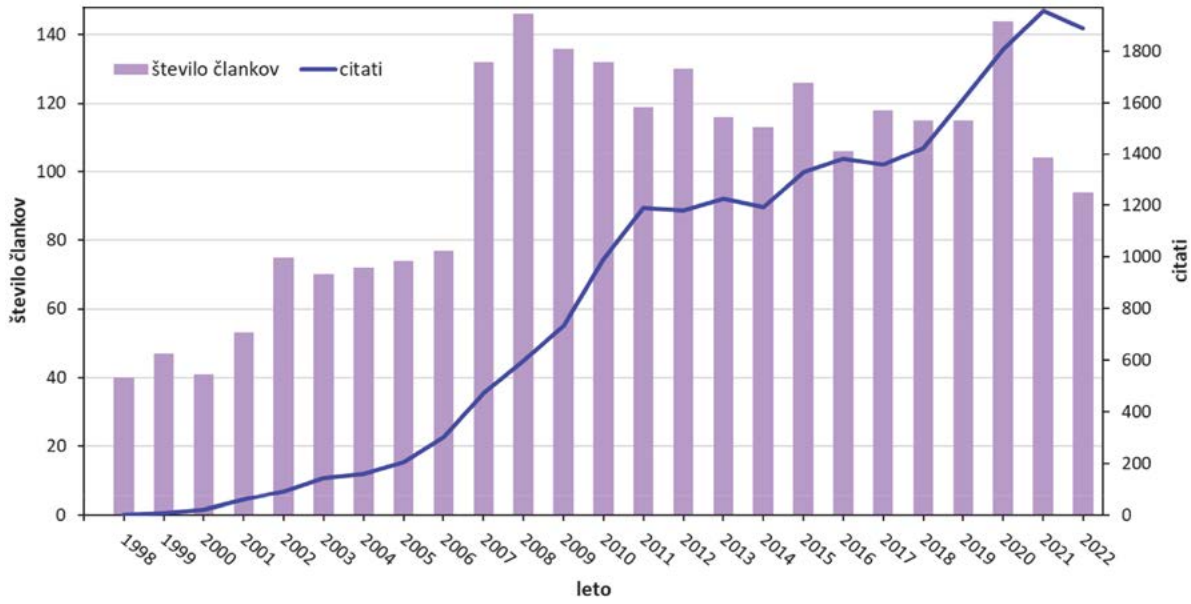

Slika 1: Število prispevkov v reviji *Acta Chimica Slovenica* in število vseh citatov v posameznem koledarskem letu.

uveljavljanje revije je danes tako znatno lažje, kot je bilo še v časih, ko je *Acta Chimica Slovenica* izhajala samo v tiskani obliki. Odpiranje svetovni znanstveni javnosti je bila ena od osrednjih točk uredniške aktivnosti v preteklih desetletjih, kar je opazno tudi v razvoju revije *Acta Chimica Slovenica*. Vpogled v mednarodno vpetost in odmevnost revije omogoča na primer Web of Science (WoS) od leta 1998 dalje, ko je bila revija uvrščena v to bazo; faktor vpliva (IF) pa je na voljo od leta 2000 dalje, zato se ta prispevek nanaša predvsem na obdobje 1998–2022.

V obdobju 1998–2001 je bilo v *ACSi* objavljenih med 40 in 50 prispevkov letno (v statistiki WoS so zajeti znanstveni in strokovni članki), z letom 2002 pa se je število člankov skoraj podvojilo (Slika 1). Ponoven dvig števila objavljenih člankov je sledil leta 2007, ko je bilo objavljenih 132 prispevkov, torej približno trikrat toliko objav kot leta 1998. Število prispevkov od leta 2007 dalje sicer niha okoli številke 120, s tem, da je bilo največ člankov objavljenih v letu 2008 (146 člankov) in najmanj v lanskem letu, ko je bilo objavljenih 94 prispevkov. Od leta 1998 do danes se je izrazito povečalo tudi število citatov, kar potrjuje mednarodno vpetost in aktualnost znanstvenih objav v reviji (Slika 1). V obravnavanem obdobju 1998–2022 sta opazna dva izrazita porasta citiranosti in sicer v obdobju 2006–2011 in v obdobju 2018–2021.

Mednarodno odmevnost revije največkrat podajamo s faktorjem vpliva (IF), seveda pa obstajajo tudi drugi bibliometrični podatki, ki omogočajo (delno) ovrednotenje vpliva revije na razvoj znanosti. Uradni faktor vpliva za revijo *Acta Chimica Slovenica* je na voljo od leta 2000 in kaže na relativno stabilen faktor vpliva. Faktor vpliva revije *Acta Chimica Slovenica* lahko primerjamo z revijami *Helvetica Chimica Acta*, *Bulletin of Korean Chemical Society*, *Australian Journal of Chemistry* in *Canadian Journal of Chemistry* (Slika 2) in z revijami, ki izhajajo v naši bližini, kot so *Monatshefte für Chemie*, *Journal of Serbian Chemical Society*, *Macedonian Journal of Chemistry and Chemical Engineering* in *Croatica Chemica Acta* (Slika 3). Naša revija je do leta 2010 že dosegla faktor vpliva podoben večini naštetih revij, v zadnjem obdobju pa je prehitela vse te

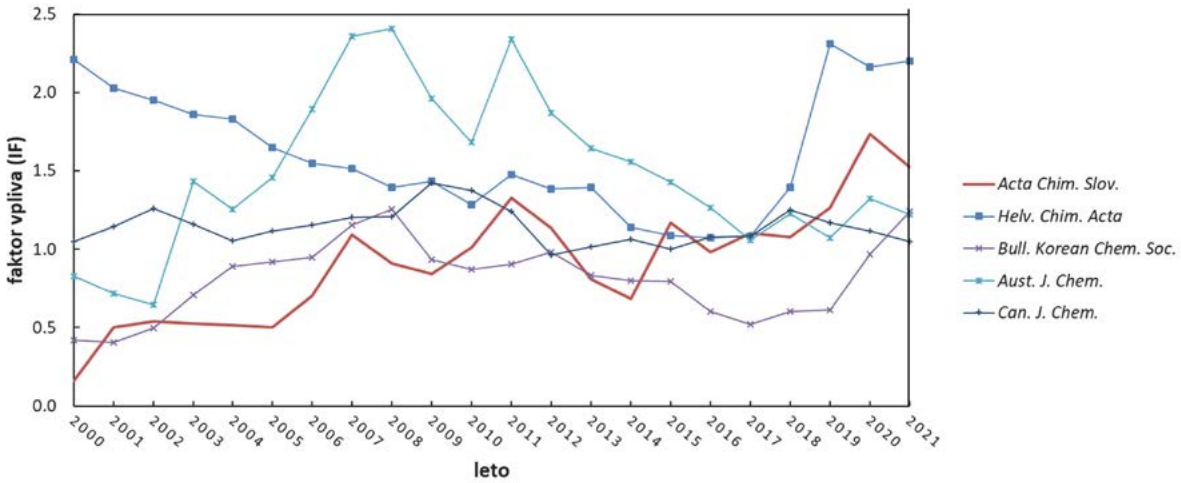

Slika 2: Faktor vpliva (IF) revije *Acta Chimica Slovenica* v obdobju 2000–2021 in primerjava z nekaterimi revijami.

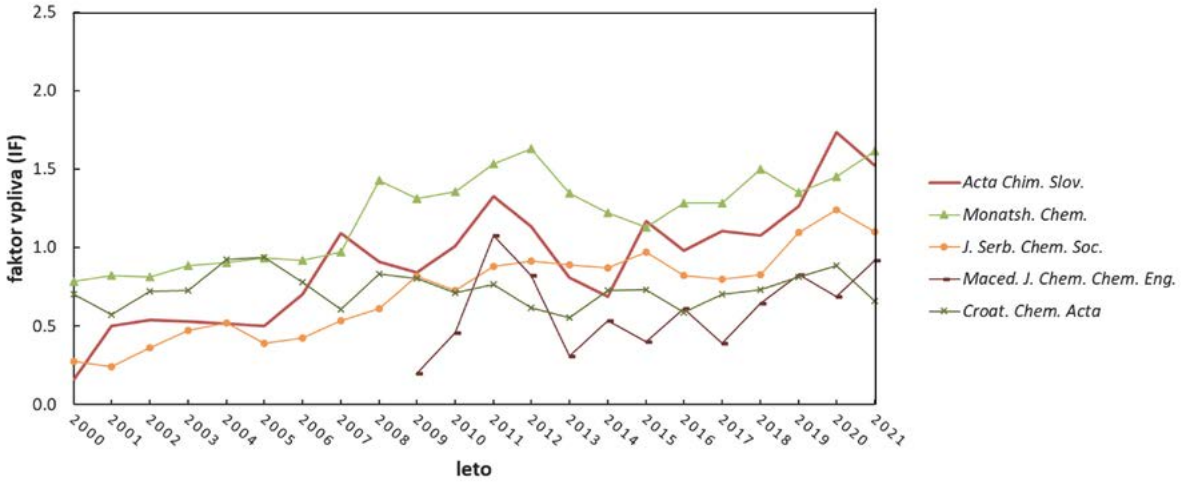

Slika 3: Faktor vpliva (IF) revije *Acta Chimica Slovenica* v obdobju 2000–2021 in primerjava z nekaterimi revijami, ki izhajajo v naši bližini.

revije razen revije *Helvetica Chimica Acta*, ki je v zadnjih nekaj letih vidno izboljšala faktor vpliva po sicer daljšem obdobju, ko ji je faktor vpliva vztrajno padal. Zelo blizu smo z revijo *Monatshefte für Chemie*, ki ima večinoma nekoliko višji faktor vpliva kakor *ACSi*. Revijo *Croatica Chemica Acta* smo prehiteli leta 2006, leta 2010 pa jo je prehitela tudi revija *Journal of Serbian Chemical Society*, sedaj pa se ji je že zelo približala tudi revija *Macedonian Journal of Chemistry and Chemical Engineering*. Najvišji faktor vpliva je *Acta Chimica Slovenica* dosegla leta 2020 in sicer 1,735.

Mednarodno vpetost lahko spremljamo tudi na podlagi deleža objav tujih avtorjev. V obdobju 1998–2022 so bili v reviji objavljeni prispevki iz 89 držav oz. regij (WoS obravnava Anglijo, Wales, Škotsko in Severno Irsko kot ločene entitete). Največ člankov v *ACSi* v tem obdobju so prispevali slovenski avtorji in sicer 35,3 %, sledili so avtorji iz Irana (11,2 %), Kitajske (6,8 %), Indije (6,7 %), Turčije (6,4 %) in Hrvaške (4,1 %) (Slika 4). Med 2 in 4 % na državo so prispevali avtorji iz Egipta, Romunije, Srbije, Češke republike, ZDA in Nemčije. Med 1 in 2 % na državo pa so prispevali raziskovalci iz Poljske, Bolgarije, Francije, Pakistana, Ukrajine, Italije, Slovaške, Madžarske in Avstrije. Pod 1 % prispevkov na državo je prišlo iz 68 držav, njihov skupni delež predstavlja 17,3 %.

Pregled po celinah kaže, da so v obravnavanem obdobju 1998–2022 prevladovali prispevki iz Evrope (69,3 %), sledijo Azija (37,6 %), Afrika (5,9 %), Severna in Južna Amerika (4,8 %), ter Avstralija in Oceanija (0,7 %) (Slika 5).

Slika 4: Prikaz deležev člankov v *ACSi* po državah.

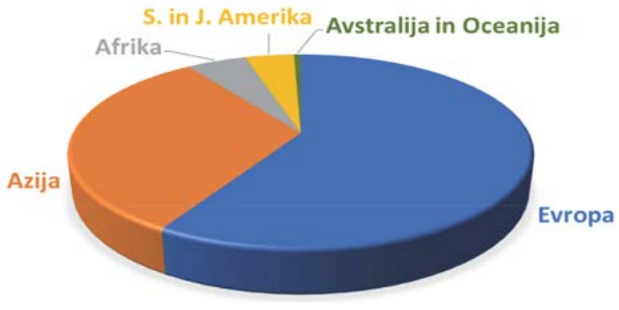

Slika 5: Prikaz deležev člankov v *ACSi* po kontinentih.

Podrobnejši pregled obdobja 1998–2022 pokaže spreminjanje deleža objav po državah. Te spremembe so pričakovane glede na izrazito željo v uredniški politiki od leta 1998 dalje po internacionalizaciji revije, čim širšem dostopu tako do avtorjev kakor tudi do bralcev. Široko mednarodno vpetost je revija dosegla predvsem s prostim dostopom člankov na spletu, z vključitvijo v WoS, PubMed, CrossRef in druge baze ter z dodelitvijo DOI številk člankom. S širšo mednarodno vpetostjo se je večal delež prispevkov tujih avtorjev in s tem se je seveda pričakovano zmanjševal delež slovenskih avtorjev, se pa je hkrati tudi znatno povečalo število prispevkov v reviji s 40–50 člankov na leto v letih 1998–2001 na 100–140 na leto od leta 2007 dalje. Če primerjamo posamezna petletna obdobja, postane ta trend izrazitejši. Za primerjavo si lahko pogledamo tri izmed petih petletnih obdobij in sicer prvo petletno obdobje 1998–2002, tretje petletno obdobje 2008–2012 in zadnje, peto petletno obdobje 2018–2022.

V prvem petletnem obdobju 1998–2002, ki ga že lahko analiziramo s pomočjo podatkov v WoS, so v *ACSi* objavljali avtorji iz 30 držav. Pričakovano je delež slovenskih člankov prevladujoč in znaša 71,9 % (184 prispevkov), kar ni presenetljivo glede na izrazito slovenski značaj revije pred letom 1998 (Slika 6). Z znatno manjšimi deleži sledijo Romunija (7,0 %), ZDA (5,5 %), Iran (3,1 %), med 2 in 3 % na državo pa Egipt in Anglija, med 2 in 1,6 % na državo pa Belgija, Hrvaška, Nemčija, Madžarska, Jordanija in Turčija. Pod 1,2 % na državo (do tri članke na državo) so prispevali raziskovalci iz 18 držav, njihov skupni delež predstavlja 13,7 %.

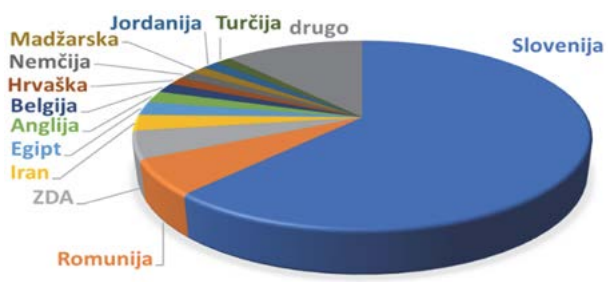

Slika 6: Prikaz deležev člankov v *ACSi* po državah v obdobju 1998–2002.

V tretjem petletnem obdobju 2008–2012 so prispevali članke raziskovalci že iz 59 držav, kar predstavlja podvojitev števila držav glede na obdobje 1998–2002. Delež prispevkov slovenskih avtorjev se je skoraj razpolovil glede na obdobje 1998–2002 in je znašal samo še 35,6 % (236 prispevkov) (Slika 7). Sledili so raziskovalci iz Irana (9,8 %), Indije (9,5 %), Hrvaške (6,2 %), Češke republike (5,9 %), Turčije (5,1 %), Srbije in ZDA (obe po 4,1 %). Med 2 in 4 % na državo so prispevali raziskovalci iz Nemčije, Egipta, Kitajske, Romunije, Francije in Poljske. Pod 2 % na državo (manj kot 12 člankov na državo) so

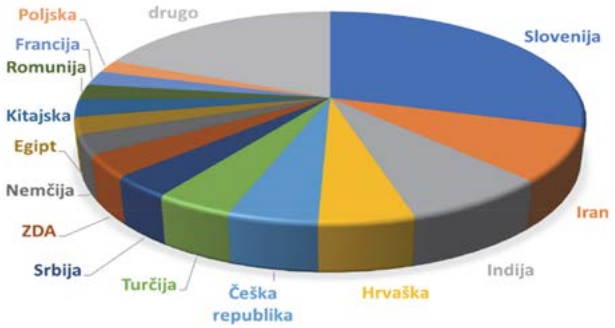

Slika 7: Prikaz deležev člankov v *ACSi* po državah v obdobju 2008–2012.

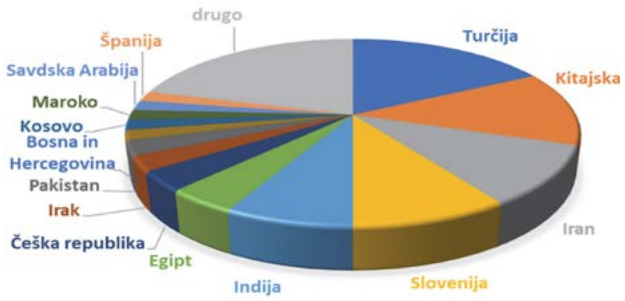

Slika 9: Prikaz deležev člankov v *ACSi* po državah v letu 2022.

prispevali raziskovalci iz 45 držav, njihov skupni delež predstavlja 22,6 %.

V zadnjem, petem petletnem obdobju 2018–2022 so prispevali članke raziskovalci iz 64 držav, kar predstavlja nekolikšno povečanje glede na obdobje 2008–2012 (59 držav). Delež prispevkov slovenskih avtorjev se je več kot razpolovil glede na obdobje 2008–2012 in je znašal le še 15,9 % (91 prispevkov), a še vedno so slovenski avtorji prispevali največji delež člankov v *ACSi*, čeprav je samo število prispevkov (91) najmanjše v vseh petih petletnih obdobjih od leta 1998 dalje (Slika 8). Tesno za Slovenijo sledijo deleži raziskovalcev iz Kitajske (14,9 %), Irana (12,4 %), Turčije (12,1 %), Indije (8,7 %), Egipta (4,5 %) in Srbije (3,8 %). Med 2 in 3 % na državo predstavljajo prispevki iz Bolgarije, Pakistana, Ukrajine, Hrvaške in Češke republike. Pod 2 % na državo (manj kot 11 člankov na državo) so prispevali raziskovalci iz 52 držav, njihov skupni delež predstavlja 33,6 %. Razlog za izreden padec v številu objav slovenskih avtorjev (za primerjavo: 184 prispevkov v obdobju 1998–2002, 236 prispevkov v obdobju 2008–2012 in samo 91 prispevkov v obdobju 2018–2022) je predvsem v manjšem številu posvečenih številk revije, saj so bile te številke praviloma posvečene slovenskim raziskovalcem, zato so bili tudi avtorji člankov v posvečenih številkah večinoma slovenski raziskovalci.

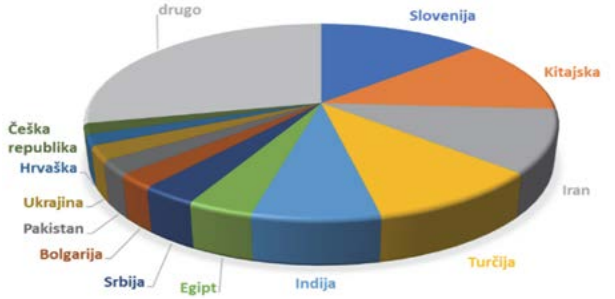

Slika 8: Prikaz deležev člankov v *ACSi* po državah v obdobju 2018–2022.

Trend upadanja deleža člankov slovenskih avtorje se še nadaljuje, kar je razvidno tudi iz deležev člankov v *ACSi* po državah za posamezni leti 2021 in 2022. V letu 2021 je delež prispevkov slovenskih avtorjev znašal 20,2 %, sledili so raziskovalci iz Kitajske (18,3 %), Turčije (14,4 %) in Indije (11,5 %). V letu 2022 pa je že prišlo do spremembe vrstnega reda držav, tako je prvo mesto po deležu člankov zasedla Turčija (21,3 %), sledila je Kitajska (16,0 %), Iran (12,8 %) in na četrtem mestu Slovenija z 11,7 % (Slika 9).

Če primerjamo deleže objav iz Slovenije, Irana, Turčije, Indije in Kitajske v petih petletnih obdobjih od leta 1998 do 2022, je opazen trend zmanjšanja deleža objav iz Slovenije ter postopno večanja deleža objav iz Irana, Turčije, Indije in Kitajske (Slika 10). Pri Kitajski lahko pričakujemo nadaljnjo rast deleža objav predvsem zaradi izrednega razvoja v zadnjih tridesetih letih tako v ekonomskem oziru kakor tudi na področju znanosti.

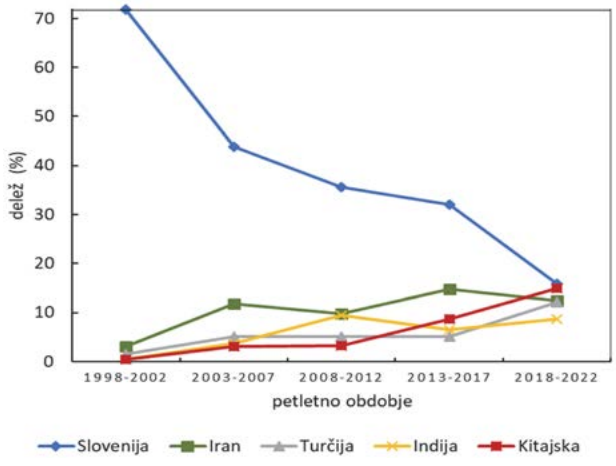

Slika 10: Spreminjanje deleža objav po državah v petletnih obdobjih od 1998 do 2022 za Slovenijo, Iran, Turčijo, Indijo in Kitajsko.

Prosta dostopnost člankov na spletu in vključenost revije v najpomembnejše baze podatkov predstavljata temelje mednarodne dostopnosti in s tem dosegljivosti vsem raziskovalcem na svetu. S tem so ustvarjene tudi možnosti za odmevnost objavljenih raziskav. *ACSi* izpolnjuje vse te pogoje in s tem omogoča avtorjem raz-

Preglednica 1: Seznam člankov v *ACSi*, ki imajo 70 ali več citatov (Web of Science Core Collection).

Avtorji in naslov članka	Leto objave	Število citatov	Povp. št. citatov/leto
G. Parshetti, S. Kalme, G. Saratale, S. Govindwar: *Biodegradation of malachite green by Kocuria rosea MTCC 1532*	2006	**230**	12.78
I. Poljanšek, M. Krajnc: *Characterization of phenol-formaldehyde prepolymer resins by in line FT-IR spectroscopy*	2005	**227**	11.95
M. Horsfall, A. I. Spiff: *Equilibrium sorption study of Al^{3+}, Co^{2+} and Ag^{+} in aqueous solutions by fluted pumpkin (Telfairia occidentalis HOOK f) waste biomass*	2005	**150**	7.89
A. Telke, D. Kalyani, J. Jadhav, S. Govindwar: *Kinetics and mechanism of reactive red 141 degradation by a bacterial isolate Rhizobium radiobacter MTCC 8161*	2008	**139**	8.69
R. Gabrovšek, T. Vuk, V. Kaučič: *Evaluation of the hydration of Portland cement containing various carbonates by means of thermal analysis*	2006	**130**	7.22
M. Strlič, J. Kolar, V.-S. Šelih, D. Kočar, B. Pihlar: *A comparative study of several transition metals in Fenton-like reaction systems at circum-neutral pH*	2003	**128**	6.10
R. Ansari: *Application of polyaniline and its composites for adsorption/recovery of chromium(VI) from aqueous solutions*	2006	**120**	6.67
R. Cerc Korošec, P. Bukovec: *Sol-gel prepared NiO thin films for electrochromic applications*	2006	**118**	6.56
O. Hamdaoui, M. Chiha: *Removal of methylene blue from aqueous solutions by wheat bran*	2007	**99**	5.82
S. Farhadi, M. Javanmard, G. Nadri: *Characterization of Cobalt Oxide Nanoparticles Prepared by the Thermal Decomposition of $[Co(NH_3)_5(H_2O)](NO_3)_3$ Complex and Study of Their Photocatalytic Activity*	2016	**96**	12.00
A. Mobinikhaledi, M. A. B. Fard: *Tetrabutylammonium Bromide in Water as a Green Media for the Synthesis of Pyrano[2,3-d]pyrimidinone and Tetrahydrobenzo[b]pyran Derivatives*	2010	**96**	6.86
M. R. Ganjali, H. A. Zamani, P. Norouzi, M. Adib, M. Accedy: *Novel calcium sensor based on [2-(2-hydroxyphenyl)imino]-1,2-diphenylethanone*	2005	**95**	5.00
M. Randić: *On generalization of Wiener index for cyclic structures*	2002	**95**	4.32
N. Logar Zabukovec, V. Kaučič: *Nanoporous materials: From catalysis and hydrogen storage to wastewater treatment*	2006	**89**	4.94
P. V. Khadikar, S. Karmarkar, R. G. Varma: *On the estimation of PI index of polyacenes*	2002	**88**	4.00
H. Abramovič, C. Klofutar: *The temperature dependence of dynamic viscosity for some vegetable oils*	1998	**85**	3.27
A. Taubert: *Inorganic materials synthesis - a bright future for ionic liquids?*	2005	**84**	4.42
M. M. Aleksić, V. Kapetanović: *An Overview of the Optical and Electrochemical Methods for Detection of DNA - Drug Interactions*	2014	**83**	8.30
N. M. Shamhari, B. S. Wee, S. F. Chin, K. Y. Kok: *Synthesis and Characterization of Zinc Oxide Nanoparticles with Small Particle Size Distribution*	2018	**79**	13.17
J. Grdadolnik: *ATR-FTIR spectroscopy: Its advantages and limitations*	2002	**78**	3.55
D. Vukičević, A. Graovac: *Note on the Comparison of the First and Second Normalized Zagreb Eccentricity Indices*	2010	**77**	5.50
M. Bešter-Rogač, D. Habe: *Modern advances in electrical conductivity measurements of solutions*	2006	**77**	4.28
B. Lomonte, J. M. Gutierrez: *Phospholipases A_2 From Viperidae Snake Venoms: How do They Induce Skeletal Muscle Damage?*	2011	**75**	5.77
Y. Marcus: *Preferential Solvation of Ibuprofen and Naproxen in Aqueous 1,2-Propanediol*	2009	**72**	4.80
C. Spinu, A. Kriza: *Co(II), Ni(II) and Cu(II) complexes of bidentate Schiff bases*	2000	**72**	3.00
M. Randić: *On characterization of molecular attributes*	1998	**71**	2.73
E. Makrlik, P. Vanura, P. Selucky, V. A. Babain, I. V. Smirnov: *Extractive Properties of Synergistic Mixture of Hydrogen Dicarbollylcobaltate and N,N,N′,N′-Tetraisobutyl-2,6-Dipicolinamide in the Water-Nitrobenzene System with Regard to Eu^{3+} and Am^{3+}*	2009	**70**	4.67

širjanje svojih raziskav. Da lahko tudi članki, objavljeni v reviji *Acta Chimica Slovenica*, dosežejo mednarodno odzivnost v znanstveni skupnosti, kažejo najbolj citirani članki v naši reviji. Ker obeležujemo 70 let izhajanja revije, so, v skladu s simbolično številko 70, v Preglednici 1 navedeni članki, objavljeni v *ACSi*, ki so prejeli 70 ali več citatov glede na podatke v Web of Science Core Collection. Člankov z vsaj 70 citati je 27 z različnih področij kemije, kemijskega inženirstva in biokemije (zajem podatkov 4. 8. 2023). Članki so bili objavljeni v obdobju med letoma 1998 in 2018. Med 27 članki v Preglednici 1 jih je 8, ki so prejeli več kot 100 citatov. Teh osem člankov je bilo objavljenih v letih 2003 in 2008 in so na kratko predstavljeni.

Največ citatov izmed člankov objavljenih v reviji *Acta Chimica Slovenica*, in sicer 230, ima prispevek z naslovom *Biodegradation of malachite green by Kocuria rosea MTCC 1532* indijskih avtorjev G. Parshetti, S. Kalme, G. Saratale in S. Govindwar. Članek je prejel največ citatov v revijah založnika Elsevier (84), Springer Nature (63), Wiley (16) in drugih založnikov. Največkrat so ga citirali raziskovalci iz Indije (117), Kitajske (29), Severne Koreje (16), Malezije (15), Tajvana (13) in drugih držav. <u>*Povzetek v slovenščini:*</u> Bakterija *Kocuria Rosea* MTCC 1532 je pod anoksičnimi pogoji popolnoma razbarvala malahitno zeleno (MG) v petih urah, medtem ko v stresanih kulturah razbarvanje ni poteklo. Maksimalna učinkovitost je bila dosežena pri koncentraciji 50 mg/L. Ista bakterija je razbarvala tudi nekatera azo, trifenilmetanska in industrijska barvila, ki so v polsintetskih medijih z melaso, sečnino in saharozo izginevala najhitreje. Razbarvanje, ki ga povzročajo inducirane aktivnosti MG reduktaz in DCIP reduktaz, je posledica razgradnje MG, kar dokazujejo UV-VIS spektri ter HPLC in FTIR analiza. Produkti razgradnje niso toksični.

Drugi najodmevnejši prispevek v reviji *Acta Chimica Slovenica* z 227 citati je članek z naslovom *Characterization of phenol-formaldehyde prepolymer resins by in line FT-IR spectroscopy* slovenskih avtorjev Ide Poljanšek in Matjaža Krajnca. Članek je prejel največ citatov v revijah založnika Elsevier (69), Wiley (26), Springer Nature (22), American Chemical Society in Taylor & Francis (vsak po 14 citatov) in drugih založnikov. Največkrat so ga citirali raziskovalci s Kitajske (52), Indije (30), ZDA (17), Malezije (16) in drugih držav, od tega iz evropskih držav skupaj 70-krat. <u>*Povzetek v slovenščini:*</u> Sintetizirali smo različne fenol-formaldehidne prepolimere s spreminjanjem razmerja med formaldehidom in fenolom. Sestava fenolne smole je odvisna od začetnega razmerja monomerov, vrste katalizatorja, reakcijskih pogojev in koncentracije prostih monomerov na koncu reakcije. Pomemben vpliv na značilnosti sintetizirane smole imata tudi temperatura in pH vrednost pod katerimi poteka reakcija fenola s formaldehidom. Upoštevati moramo tri zaporedne reakcije: adicijo formaldehida na fenol, rast verige ali tvorbo prepolimera in končno zamreževanje ali reakcijo utrjevanja. Glede na pH vrednost dobimo dve vrsti prepolimera, novolak v kislem območju pH vrednosti, medtem ko dobimo rezol pod alkalnimi reakcijskimi pogoji. Rezolno smolo sintetiziramo z molarnim prebitkom formaldehida (1<F/P<3). Produkti so mono- ali polijedrski hidroksimetil fenoli, ki so stabilni pri sobni temperaturi, vendar se pri povišani temperaturi zamrežijo v tridimenzionalen, netopen in netaljiv polimer. Potek sinteze fenol-formaldehidnega prepolimera smo spremljali s pomočjo "in-line" ATR-FTIR spektroskopske analitske tehnike (ReactIR 4000), ki je opremljena z optičnim vodnikom in diamantnim kompozitnim senzorjem. Ta tehnika se je izkazala kot idealna za določanje prostega fenola in formaldehida, kot tudi njunih konverzij, prav tako pa tudi sprememb v sestavi prepolimera v odvisnosti od reakcijskega časa kondenzacije. Kinetični podatki, ki smo jih dobili s pomočjo ReactIR 4000 "in-line" reakcijskega analiznega sistema se dobro ujemajo s podatki določenimi s tradicionalnimi titracijskimi metodami. ReactIR tehnologija nadomešča časovno potratno in nenatančno "off-line" metodologijo.

Tretji najodmevnejši prispevek s 150 citati je članek z naslovom *Equilibrium sorption study of Al^{3+}, Co^{2+} and Ag^{+} in aqueous solutions by fluted pumpkin (Telfairia occidentalis HOOK f) waste biomass* nigerijskih avtorjev M. Horsfall in A. I. Spiff. Članek je prejel največ citatov v revijah založnika Elsevier (65), Springer Nature (13) in drugih založnikov. Največkrat so ga citirali raziskovalci iz Indije (25), Nigerije (15), Kitajske (13), Turčije (13) in drugih držav. <u>*Povzetek v slovenščini:*</u> Z različnimi metodami smo raziskovali vpliv ionskih radijev na sorpcijo Al^{3+}, Co^{2+} in Ag^{+} ionov na odpadni biomasi iz buč. Eksperimentalne rezultate smo analizirali s pomočjo petih dvoparametrskih enačb: Langmuirjeve, Freundlichove, Temkinove, Dubinin-Radushkevicheve in Flory-Hugginsove izoterme. Dobljena kapaciteta monoplastne adsorpcije znaša po Langmuirjevi adsorpcijski izotermi 16.98 mg/g, 10.34 mg/g in 8.03 mg/g za Al^{3+}, Co^{2+} in Ag^{+} ion. Ugotovili smo, da Freundlichova in Langmuirjeva izoterma process adsorpcije opišeta bolje kot Temkinova, Dubinin-Radushkevicheva in Flory-Hugginsova izoterma. Rezultati kažejo, da ionski radij vpliva na hitrost migracije kovinskega iona k površini biomase ter s tem na intenziteto adsosrpcije ter, da so bučni odpadki uporabni za odstranjevanje Al^{3+}, Co^{2+} in Ag^{+} ionov iz odpadnih vod.

Četrti najbolj citirani članek s 139 citati je od istega vodilnega avtorja kakor najbolj citirani članek v *ACSi*. Prispevek *Kinetics and mechanism of reactive red 141 degradation by a bacterial isolate Rhizobium radiobacter MTCC 8161* so objavili indijski avtorji A. Telke, D. Kalyani, J. Jadhav in S. Govindwar, področje raziskave pa je sorodno najbolj citiranemu članku. Članek je prejel največ citatov v revijah založnika Elsevier (57), Springer Nature (23), Wiley (8) in drugih založnikov. Največkrat so ga citirali raziskovalci iz Indije (79), Kitajske (18), Tajvana (11), Južne Koreje (9) in drugih držav. <u>*Povzetek v slovenščini:*</u> Iz odpadne vode tekstilne industrije v

Ichalkaranji, Indija, je bila izolirana bakterija *Rhizobium radiobacter* MTCC 8161. Ta bakterija je sposobna razbarvanja različnih azo, trifenilmetanskih, disperznih in reaktivnih barvil pri statičnih anoksičnih pogojih ter pri optimalni pH vrednosti 7,0 in temperature 30 °C do 80–95 % stopnje z 83,33 % redukcijo KPK. Poskusi so bili izvedeni z različnimi viri ogljika in dušika od katerih sta kvasni ekstrakt in sečnina dala najboljše rezultate. Razbarvanje lahko pripišemo različnim induciranim oksidativnim in reduktivnim encimom. Toksikološke študije so pokazale manj toksično naravo razgradnega produkta.

Peti najbolj citirani članek v reviji *Acta Chimica Slovenica* s 130 citati je prispevek z naslovom *Evaluation of the hydration of Portland cement containing various carbonates by means of thermal analysis*, ki so ga objavili slovenski avtorji Roman Gabrovšek, Tomaž Vuk in Venčeslav Kaučič. Članek je prejel največ citatov v revijah založnika Elsevier (65), Springer Nature (17), MDPI (10) in drugih založnikov. Največkrat so ga citirali raziskovalci s Kitajske (27), Indije (14), ZDA (12), Kanade (10), Brazilije (9) in drugih držav, od tega iz evropskih držav skupaj 45-krat. Povzetek v slovenščini: Portland cement s konstantno vsebnostjo mineralnih dodatkov (kalcit, dolomit in magnezit) smo hidratizirali 7 in 28 dni v suspenziji pri 60 °C. Fazne sestave hidratiziranih produktov smo ovrednotili s termogravimetrično analizo in s praškovno rentgensko difrakcijo, razvoj hidratizirane mikrostrukture pa smo ugotavljali z merjenjem specifične površine. Z detajlno analizo DTG profilov termičnega razpada portlandita in karbonata smo ugotovili določene vplive mineralnih primesi na nastanek portlandita. V procesu hidratacije smo ovrednotili tudi specifično obnašanje posameznih prisotnih karbonatov.

Šesti najbolj citirani članek s 128 citati je prispevek z naslovom *A comparative study of several transition metals in Fenton-like reaction systems at circum-neutral pH*, ki so ga objavili slovenski avtorji Matija Strlič, Jana Kolar, Vid-Simon Šelih, Drago Kočar in Boris Pihlar. Članek je prejel največ citatov v revijah založnika Elsevier (45), Springer Nature (13), American Chemical Society (9), Royal Society of Chemistry (8) in drugih založnikov. Največkrat so ga citirali raziskovalci s Kitajske (32), ZDA (20), Slovenije (16), Italije (11), Nemčije (8) in drugih držav, od tega iz evropskih držav skupaj 80-krat. Povzetek v slovenščini: V reakcijskih sistemih podobnih Fentonovemu, s Cd(II), Co(II), Cr(III), Cu(II), Fe(III), Mn(II), Ni(II) ali Zn(II), smo za določitev hitrosti nastajanja oksidirajoče zvrsti uporabili spektrofotometrično metodo hidroksilacije *N*,*N*'-(5-nitro-1,3-fenilen)bisglutaramida. Zanimalo nas je območje pH 5.5–9.5, kar smo uravnavali z dodatkom fosfatnega pufra, in območje temperature 25–80 °C. Hitrosti nastajanja oksidirajoče zvrsti pri pH 7 padajo v naslednjem zaporedju Cu(II) > Cr(III) > Co(II) > Fe(III) > Mn(II) > Ni(II), medtem ko Cd(II) in Zn(II) ne kažeta katalitske sposobnosti, Ni(II) pa le v območju pH > 7.5. V reakcijskih mešanicah z Cu(II) in Fe(III) lahko hitrost nastajanja oksidirajoče zvrsti obravnavamo kot vsoto prispevkov posameznih kovin. Drugačne lastnosti imajo mešanice, ki vsebujejo Zn(II), Co(II) ali Mn(II). Zadnja dva izkazujeta močno prooksidativno aktivnost, medtem ko ima Zn(II) antioksidativen učinek. Navidezne aktivacijske energije za nastajanje oksidirajoče zvrsti so v intervalu 75–110 kJ mol^{-1} in padajo v naslednjem zaporedju: Cu(II) > Ni(II) > Mn(II) > Fe(III) > Co(II).

Sledi članek s 120 citati z naslovom *Application of polyaniline and its composites for adsorption/recovery of chromium(VI) from aqueous solutions* iranskega avtorja R. Ansari. Članek je prejel največ citatov v revijah založnika Elsevier (35), Springer Nature (17), Wiley (10) in drugih založnikov. Največkrat so ga citirali raziskovalci iz Indije (33), Kitajske (20), Irana (17), Egipta (14) in drugih držav. Povzetek v slovenščini: Proučevali smo adsorpcijo Cr(VI) iz vodnih raztopin na žagovini, prevlečeni s polianilinom in polianilinskimi kompoziti z najlonom 66 in poliuretanom. Ugotovili smo, da polianilin v kislinski obliki lahko uporabljamo za adsorpcijo Cr(VI) ionov iz kislih raztopin (pH ≤ 2). Z višanjem pH-ja se adsorpcija bistveno poslabša. Predpostavili smo, da adsorpcijski mehanizem poteka v glavnem na osnovi ionske izmenjave. Izvedba tega procesa v koloni s predstavljenim adsorpcijskim materialom je enostavna in učinkovita v primerjavi z materiali, ki so jih proučevali drugi avtorji.

Osmi najbolj citirani članek v reviji *Acta Chimica Slovenica* s 118 citati je prispevek z naslovom *Sol-gel prepared NiO thin films for electrochromic applications*, ki sta ga objavila slovenska avtorja Romana Cerc Korošec in Peter Bukovec. Članek je prejel največ citatov v revijah založnika Elsevier (47), Springer Nature (15), American Chemical Society (9), Royal Society of Chemistry (6) in drugih založnikov. Največkrat so ga citirali raziskovalci iz Indije (23), Kitajske (16), Južne Koreje (14), Slovenije (14) in drugih držav, od tega iz evropskih držav skupaj 41-krat. Povzetek v slovenščini: Elektrokromni materiali pri določenem potencialu spremenijo svoje optične lastnosti v vidnem delu spektra. Sprememba je reverzibilna in materialu se povrnejo prvotne lastnosti v nasprotnem električnem polju. Elektrokromne lastnosti materialov uporabljamo v elektrokromnih sklopih, kjer v večplastnemu, bateriji podobnemu sestavu s pomočjo električne napetosti reguliramo količino sončnega sevanja skozi okno in ga zato imenujemo pametno okno. V prvem delu članka so jedrnato predstavljene teoretične osnove elektrokromizma ter princip delovanja pametnega okna. Nikljev oksid so v zadnjem desetletju veliko preučevali kot hranilnik ionov v elektrokromnih sklopih, zato so v nadaljevanju podane nekatere njegove lastnosti. Termična obdelava tankih plasti nikljevega oksida v veliki meri določa elektrokromni odziv (stopnjo obarvanja, reverzibilnost med preklapljanem napetosti) teh plasti. Kadar tanke plasti pripravljamo s kemijskimi postopki nanašanja, lahko iz rezultatov termične analize

dobimo koristne informacije o primerni temperaturi in času toplotne obdelave. Termična analiza tankih plasti, nanesenih na podlago, ne spada med klasične analizne tehnike, zato so v članku zbrani osnovni pristopi k tem meritvam. Po teoretičnem uvodu je v članku prestavljena metoda optimizacije elektrokromnega odziva nikelj-oksidnih tankih plasti, pripravljenih po sol-gel postopku. Elektrokromne lastnosti termično različno obdelanih tankih plasti smo testirali s pomočjo spektroelektrokemijskih meritev, z IR, TEM, AFM in EXAFS pa smo spremljali strukturne in morfološke spremembe med segrevanjem.

Število citatov daje le delen vpogled v odmevnost članka, saj so lahko starejši članki v prednosti pred novejšimi članki zaradi daljšega obdobja, ko so lahko citirani. Drug možen vpogled na citiranost daje povprečno število citatov na leto (Preglednica 2). V Preglednici 2 je zbranih 10 člankov z najvišjim povprečnim številom citatov na leto glede na Web of Science Core Collection. Devet izmed desetih člankov v tej preglednici lahko najdemo med 27 članki v Preglednici 1. Vrstni red prvih desetih člankov, razporejenih glede na povprečno število citatov na leto, je nekoliko spremenjen glede na Preglednico 1 in tudi delež člankov, objavljenih po letu 2010, je seveda pričakovano večji. Pričakujemo lahko, da bodo nekateri novejši članki lahko kmalu prehiteli članke iz obdobja 1998–2010 po celokupnem številu citatov.

Naj zaključim s pogledom na svojo prehojeno pot z revijo *Acta Chimica Slovenica*. K sodelovanju v uredništvu revije me je jeseni 2012 pritegnil prof. dr. Primož Šegedin, ki je iskal zamenjavo za svoje mesto sourednika za področje anorganske kemije in kemijskega izobraževanja in tako sem se z letom 2013 pridružil uredniškemu odboru pod vodstvom prof. dr. Aleksandra Pavka. V tistem obdobju je vsa komunikacija z avtorji in recenzenti potekala še po elektronski pošti, že v naslednjem letu pa smo prešli na Open Journal System (OJS), ki je znatno olajšal uredniško delo, saj platforma omogoča vse na enem mestu. Delo sourednika mi je tudi omogočilo vpogled v uredniško delo in v uredniške odločitve, kar je neprecenljiva izkušnja, saj je objavljanje raziskovalnih rezultatov pomemben vidik znanstveno-raziskovalnega dela. V uredniškem odboru sem pridobil številne izkušnje; izmenjava idej, konstruktivne debate ter razmišljana v širšem kontekstu delovanja akademske sfere širijo naša obzorja in prispevajo tudi k uspešnosti revije. Za vse to sem hvaležen obema nekdanjima glavnima in odgovornima urednikoma prof. dr. Aleksandru Pavku in prof. dr. Kseniji Kogej, vsem nekdanjim sourednicam in sourednikom prof. dr. Mariji Bešter-Rogač, prof. dr. Damjani Rozman, viš. znan. sod. Meliti Tramšek, prof. dr. Alešu Podgorniku in izr. prof. dr. Alešu Ručigaju ter seveda sedanjim sourednicam in sourednikom znan. sod. dr. Alenu Albrehtu, izr. prof. dr. Alešu Berlecu, izr. prof. dr. Janezu Cerkovniku, doc. dr.

Preglednica 2: Seznam desetih člankov v *ACSi* z najvišjim povprečnim številom citatov na leto (Web of Science Core Collection).

Avtorji in naslov članka	Leto objave	Število citatov	Povp. št. citatov/leto
N. M. Shamhari, B. S. Wee, S. F. Chin, K. Y. Kok: *Synthesis and Characterization of Zinc Oxide Nanoparticles with Small Particle Size Distribution*	2018	79	**13.17**
G. Parshetti, S. Kalme, G. Saratale, S. Govindwar: *Biodegradation of malachite green by Kocuria rosea MTCC 1532*	2006	230	**12.78**
S. Farhadi, M. Javanmard, G. Nadri: *Characterization of Cobalt Oxide Nanoparticles Prepared by the Thermal Decomposition of $[Co(NH_3)_5(H_2O)](NO_3)_3$ Complex and Study of Their Photocatalytic Activity*	2016	96	**12.00**
I. Poljanšek, M. Krajnc: *Characterization of phenol-formaldehyde prepolymer resins by in line FT-IR spectroscopy*	2005	227	**11.95**
A. Telke, D. Kalyani, J. Jadhav, S. Govindwar: *Kinetics and mechanism of reactive red 141 degradation by a bacterial isolate Rhizobium radiobacter MTCC 8161*	2008	139	**8.69**
M. M. Aleksić, V. Kapetanović: *An Overview of the Optical and Electrochemical Methods for Detection of DNA - Drug Interactions*	2014	83	**8.30**
M. Horsfall, A. I. Spiff: *Equilibrium sorption study of Al^{3+}, Co^{2+} and Ag^{+} in aqueous solutions by fluted pumpkin (Telfairia occidentalis HOOK f) waste biomass*	2005	150	**7.89**
T. I. Chaban, V. V. Ogurtsov, V. S. Matiychuk, I. G. Chaban, I. L. Demchuk, I. A. Nektegayev: *Synthesis, Anti-Inflammatory and Antioxidant Activities of Novel 3H-Thiazolo[4,5-b]pyridines*	2019	39	**7.80**
R. Gabrovšek, T. Vuk, V. Kaučič: *Evaluation of the hydration of Portland cement containing various carbonates by means of thermal analysis*	2006	130	**7.22**
A. Mobinikhaledi, M. A. B. Fard: *Tetrabutylammonium Bromide in Water as a Green Media for the Synthesis of Pyrano[2,3-d]pyrimidinone and Tetrahydrobenzo[b]pyran Derivatives*	2010	96	**6.86**

Mireli Dragomir, doc. dr. Krištofu Kranjcu, izr. prof. dr. Matjažu Kristlu, prof. dr. Maji Leitgeb, prof. dr. Heleni Prosen, izr. prof. dr. Jerneju Staretu in viš. znan. sod. dr. Ireni Vovk ter tehničnemu uredniku Stanislavu Oražmu. Za podporo se zahvaljujem tudi administratorkama Evi Mihalinec in Marjani Gantar Albreht. Delovanje revije pa ne bi bilo mogoče brez močne zaslombe v Slovenskem kemijskem društvu ter zanesljive podpore nekdanjih predsednikov društva prof. dr. Venčeslava Kaučiča in znan. svet. dr. Albina Pintarja ter sedanjega predsednika dr. Petra Venturinija.

Častitljivih 70 let izhajanja znanstvene revije *Acta Chimica Slovenica* je odlična priložnost za pogled na prehojeno pot in hkrati priložnost za nove pobude in korake v smeri nadaljnjega uveljavljanja revije v svetovni znanstveni skupnosti. Z entuziazmom in skupnimi močmi se bo revija še naprej uspešno razvijala in sledila izzivom v sodobnem založniškem svetu.

Spomini, vtisi in pogledi področnih urednic in urednikov ob 70-letnici izhajanja revije *Acta Chimica Slovenica*

prof. dr. Marija Bešter-Rogač

Fakulteta za kemijo in kemijsko tehnologijo Univerze v Ljubljani

področna urednica za fizikalno kemijo v letih 2004–2017

Kako v 2000 znakih s presledki zajeti štirinajst let, ki sem jih kot področna urednica za fizikalno kemijo pustila, podarila, žrtvovala ali karkoli že hočete uredniškemu delu pri *ACSi*?

Še vedno imam zelo lep spomin na prvo srečanje s prof. dr. Janezom Košmrljem in njegovo povabilo, da naj se pridružim uredniškemu odboru leta 2004, ker se do tedaj nisva poznala. Takrat je postal glavni in odgovorni urednik in je skupaj s temeljito prenovo oblike *ACSi* postavil tudi novo uredniško shemo z imenovanjem področnih urednikov. Bilo mi je v veliko čast, veselje in priznanje, da je nekdo moje delo opazil in prepoznal do te mere, da mi je zaupal tako odgovorno delo. Vsakoletna druženja uredniškega odbora so mi dajala tudi pogled v svet izven ozkih okvirov katedre, širino in zavest, da znanje in sodelovanje ne pozna meja, družbenih in drugih razprtij ter vrtičkarstva. Ali bolje – tudi tu sem spoznala, da pošteno delo lahko vse to obide in – po principu Le Chateliera – ubere drugačno, nevajeno, a (naj)boljšo možno pot. Hvaležna sem za vso to mrežo niti, ki smo jo stkali v štirinajstih letih.

Seveda je imelo uredniško delo tudi svoje »temne« strani – pogosto so se članki nabirali in je bilo težko najti čas za njihov pregled. Najtežje od vsega pa je bilo iskanje recenzentov. Na vabila za recenzijo pogosto ni bilo odgovora, recenzenti so pogosto zamujali in pisali površne in nedosledne recenzije in celo poskušali recenzije izkoristiti sebi v prid tako, da so zahtevali citiranje lastnih del. Celo avtorji, ki so objavljali v *ACSi*, niso sprejemali recenzij člankov, sami pa so zase pričakovali hiter postopek.

Kvaliteta neke znanstvene revije je izjemno odvisna od zanesljivega in poštenega dela recenzentov – končno recenzenti povsod po svetu odločilno vplivajo tudi na izbor projektov in so torej neke vrste »gonilna sila« smeri razvoja znanosti. Želim si, da bi se tega zavedali vsi raziskovalci tudi takrat, ko dobijo vabilo za oceno znanstvenega članka – tudi od *ACSi*.

Foto: Andrej Križ

izr. prof. dr. Janez Cerkovnik

Fakulteta za kemijo in kemijsko tehnologijo Univerze v Ljubljani

področni urednik za organsko kemijo od leta 2006

doc. dr. Krištof Kranjc

Fakulteta za kemijo in kemijsko tehnologijo Univerze v Ljubljani

področni urednik za organsko kemijo od leta 2007

Leta 2006 sta me glavni urednik prof. dr. Aleksander Pavko in predsednik Slovenskega kemijskega društva prof. dr. Venčeslav Kaučič povabila, da prevzamem mesto področnega urednika za organsko kemijo. Zahvaljujoč zavzetosti in prizadevnemu delu prejšnjih urednikov, profesorjev Kolarja, Petriča in Košmrlja, je naraščajoč ugled naše revije pritegnil veliko avtorjev, zato je število prejetih rokopisov zelo naraslo. Posledično so pri reviji uvedli področne urednike, ki pokrivajo različna temeljna področja kemijskih znanosti, vključno z znanostjo o materialih, s kemijskim, biokemijskim in okoljskim inženiringom, splošno kemijo, uporabno kemijo in biomedicinskimi aplikacijami. Po številu prispelih in tudi objavljenih člankov je bilo najbolj priljubljeno področje organska kemija. Zato je kolega Krištof Kranjc kasneje prevzel del uredniškega dela za področje organske kemije in me s tem razbremenil. Kljub temu moramo pridobiti vsaj dve neodvisni recenziji za prispeli rokopis, pri čemer je vedno težje najti aktivne in kompetentne recenzente, ki tudi pravočasno opravijo svoje delo. Zaradi tega je recenzentski postopek močno odvisen od dobre volje in hitrosti recenzentov. Če izpostavim prijetne trenutke uredniškega dela, mi je bilo v veliko čast, ko sem leta 2017 urejal številko revije posvečene prof. Mihi Tišlerju in se z njim osebno srečal ob praznovanju njegove 90. obletnice in izjemne kariere v organski kemiji. S svojim znanstvenim delom je Laboratorij za organsko kemijo v Ljubljani postal mednarodno znan kot šola heterociklične kemije, kot človek in profesor pa se je vtisnil v trajen spomin številnim generacijam kemikov.

Acta Chimica Slovenica na nek način odraža entuziazem, ustvarjalnost in vitalnost slovenske znanstvene skupnosti. Zato reviji želim, da ohranja in razvija visoke uredniške standarde in mednarodni ugled.

Moje sodelovanje z revijo *Acta Chimica Slovenica* se je začelo že pred več kot petnajstimi leti na povabilo tedaj glavnega urednika prof. dr. Aleksandra Pavka. Vendar me ni povabil neposredno on (saj se v bistvu nisva niti poznala, pa še obe katedri sta bili prostorsko precej ločeni, ena na Hajdrihovi, druga pa na Aškerčevi cesti), ampak je prišlo povabilo posredno, preko Katedre za anorgansko kemijo, ki je bila le eno etažo nad Katedro za organsko kemijo, kjer sem imel delovni prostor (zelo majhen, seveda, saj je bila precejšnja prostorska stiska).

Ob tem prvem povabilu si seveda nisem čisto predstavljal, kako izgleda uredniško delo pri znanstveni reviji, čeprav sem seveda že imel nekaj izkušenj z objavljanjem znanstvenih rezultatov v različnih tujih revijah, z njihovimi zahtevami (tudi čisto tehničnimi) in različnimi pravili... ter seveda tudi nekaj izkušenj s tem, kako izgleda, če urednik rokopis zavrne in kaj kot avtor storim v takem primeru. Sem se pa seveda prvič srečal z obratno situacijo, kjer sem moral sam najprej izbrati primerne recenzente in pridobiti ustrezne ocene ter nato sprejeti končno odločitev. Vendar pa se nikoli nisem zanašal samo na mnenje recenzentov, ampak sem vedno (in danes tudi) vsak članek temeljito prebral, pregledal tudi vse eksperimentalne podatke, si zamislil, če bi znal ponoviti sintezne postopke, preveril literaturne navedbe itd. poleg tega pa sem običajno dal članke v branje tudi kolegicam in kolegom v laboratoriju 424 (na Aškerčevi), ki so pogosto našli še kakšno dodatno pomanjkljivost v rokopisu. Na ta način sem dobil dovolj trdno osnovo, da sem prispevek lahko zavrnil ali pa avtorje prosil za dopolnitev.

Malo sem pobrskal po mojem prvem arhivu člankov, ki ga imam še vedno shranjenega, saj je tedaj vse uredniško delo potekalo izključno preko neposrednih e-mailov s priponkami... ugotovil sem, da sem v prvem letu mojega urednikovanja (torej 2007) dobil 29 člankov v pregled in jih od tega 15 sprejel v objavo (seveda po ustreznih popravkih oz. dopolnitvah; nikoli se ni zgodilo, da bi bila prvotna verzija že tudi dokončna in primerna za objavo). Leta 2008 sem dobil že 44 člankov (in jih 19 sprejel), leta 2009 pa 58 člankov (in jih sprejel le 12). Od tedaj naprej pa moj arhiv ni več popoln, saj smo pri *ACSi* začeli uporabljati

OJS sistem, ki je delo seveda močno olajšal, vendar pa zato osebni arhiv člankov ni bil več potreben. Poleg tega je taka, sodobnejša interakcija z avtorji povečala ugled in profesionalnost revije. Ob tem moram še dodati, da sva (kot še vedno) področje organske kemije pokrivala dva področna urednika - prof. dr. Janez Cerkovnik je imel očitno pred mojim prihodom še več dela...

Če se ozrem še malo bolj v preteklost, lahko rečem, da je bilo moje prvo srečanje z *ACSi* oz. s SKD še nekaj let starejše... žal se ne spomnim, kdo mi je le malo po letu 2000 prinesel natisnjeno prijavnico za včlanitev v SKD (morda je bil to moj mentor prof. dr. Marijan Kočevar), se pa spomnim, da z včlanitvijo nisem nič odlašal, saj sem izvedel, da bom "v zameno" dobival natisnjene izvode revije *Acta Chimica Slovenica*... čeprav je bila tedaj oblikovalsko nekoliko manj privlačna, sem se vsakega sivo-zelenega izvoda velikosti A5 posebej razveselil in ga z navdušenjem pregledal... enako kot tudi kasneje, ko je bila revija formata A4 s privlačno in barvito naslovnico ter še bolj obsežno in kvalitetno vsebino... in enako še danes, čeprav izvodi niso več v klasični obliki na tistem težkem, gladkem, bleščečem papirju s posebnim vonjem po barvi in lepilu, ki se je razširil po prostoru, ko sem pretrgal tanko, prozorno zaščitno folijo, v katero so bili zvezki zaprti med poštno dostavo. Ti lepi časi so sicer minili, vendar zakaj ne bi bila tudi prihodnost lepa, zanimiva, prijetna in polna novih odkritij? Še mnogo dobrih in uspešnih let za *ACSi* in SKD!

Foto: Bor Kolar Bačnik

imenom revije v svetlih odtenkih in slika, ki je povezana z vsebino.

Delo področne urednice za (keramične) materiale je bila zame prva tovrstna izkušnja in če pomislim, česa se najbolj spomnim iz nekajletnega obdobja pri reviji *Acta Chimica Slovenica*, mi pride na misel iskanje primernih recenzentov. Potekalo je po elektronski pošti in tudi brez spletnega orodja, ki bi ponudilo vrsto potencialnih recenzentov. Tako sem večinoma pisala bližnjim in daljnim znancem in znankam, kajti avtorji, ki sem jih poznala le po člankih, mi pogosto niti odgovorili niso. Spomnim se, da sem nekemu kolegu pisala, če bi prevzel recenzijo rokopisa, poslanega v *ACSi*, in je sprejel, po prejemu rokopisa pa takoj komentiral, da je prehitro sklepal, da gre za recenzijo rokopisa, poslanega v revijo v okviru ACS (American Chemical Society). Prijazno je vendarle opravil recenzijo, od takrat dalje pa sem se, v izogib nesporazumom, uporabi kratice v dopisih možnim recenzentkam in recenzentom izogibala. Seveda sem kot urednica delala napake in jih, če sem jih opazila, skušala popraviti. Vedno mi zanesljivo ni uspelo. Ampak tako je, na napakah se učimo.

Upam, da sem zaradi uredniških izkušenj postala boljša recenzentka. Uredniško delo me je naučilo, da se spodobi, če sprejmem rokopis v recenzijo, slednjo tudi napisati in to po možnosti v predvidenem roku, saj nekdo računa, da bom svojo obljubo izpolnila. Naučila sem se, da je slab rokopis bolje z ustrezno utemeljitvijo zavrniti, kot preložiti odgovornost za zavrnitev na urednico ali urednika.

prof. dr. Barbara Malič, znan. svet.

Institut »Jožef Stefan« in Mednarodna podiplomska šola Jožefa Stefana

področna urednica za znanosti o materialih v obdobju 2006–2013

Revijo *Acta Chimica Slovenica* sem spoznala v študentskih letih, ko se je imenovala še Vestnik slovenskega kemijskega društva in imela platnice olivno zelene barve. Ko me je vrsto let kasneje takratni glavni urednik profesor Aleksander Pavko povabil, naj se pridružim ekipi urednic in urednikov, je revija že spremenila ime in podobo. Še danes, ko se je branje člankov večinoma preselilo v virtualni svet in revij v papirni obliki ne listamo več, se mi ob misli na revijo *Acta Chimica Slovenica* prikaže opečno rdeča podlaga naslovnice z

zasl. prof. dr. Boris Pihlar

Fakulteta za kemijo in kemijsko tehnologijo Univerze v Ljubljani

področni urednik za analizno kemijo leta 2010

Moj prvi stik s slovensko kemijsko periodiko je bil članek o konstrukciji in lastnostih potenciostata,[1] ki se uporablja v elektrokemijski sintezi in v analitiki za določanje kovin z elektrolizo s kontroliranim potencialom. Tematika je bila predmet mojega raziskovalnega dela pod mentorstvom prof. Koste na Univerzi v Ljubljani. Urednі-

1 B. Pihlar, L. Kosta: A versatile and inexpensive solid-state potentiostat for controlled potential electrolysis. *Vestnik Slovenskega kemijskega društva* 1977, *24*, 31–39.

ništvo *Vestnika slovenskega kemijskega društva* (*VSKD*) pa je z njegovo objavo pokazalo, da je dovzetno za novitete tudi na področjih, sorodnih kemiji. Poleg tega je v takratni državi primanjkovalo domače instrumentacije, ki je bila pogoj za razvoj sodobnih instrumentalnih analiznih tehnik. Prispevek je vzpodbudil sodelovanje med kemiki in elektrotehniki in je kasneje vodil v uspešno sodelovanje med panogami, ki je rezultiralo v konstrukciji številnih elektronskih instrumentov (pH metri, konduktometri, polarografi, spektrofotometri, cianidni analizator…), značilnih za visoko tehnično razvita okolja. Ker se je kemija ob koncu prejšnjega stoletja hitro razvijala in napredovala na številnih specifičnih področjih, me je uredništvo povabilo v uredniški odbor (področni urednik leta 2010, član uredniškega sveta od leta 1998), kjer sem se srečal s svetovno znanimi raziskovalci, in ob številnih recenzijah domačih in tujih znanstvenikov izpopolnjeval svoje znanje predvsem na področju analizne kemije s poudarkom na elektrokemiji, ki je bila moja specialnost.

Ker so v uredniškem odboru že od ustanovitve vodstvo in člani stremeli predvsem h kvaliteti objavljenih del in k znanstvenemu ugledu revije, je v uredniškem odboru dozorela misel o spremembi imena revije, ki po osamosvojitvi Slovenije ni več odražal prave identitete. S tem je uredništvo naredilo velik korak k prepoznavanju revije na mednarodnem nivoju. *Acta Chimica Slovenica* (*ACSi*) je postala vodilna v slovenskem znanstvenem prostoru, z rednim izhajanjem, s širokim izborom tematik, s korektnimi in hitrimi recenzijami prispelih znanstvenih prispevkov domačih in tujih avtorjev pa je pridobila ugled tudi v mednarodnem okolju. K ugledu revije je po mojem mnenju močno prispevala odločitev uredništva o digitalizaciji prispevkov in digitalni obravnavi dosežkov avtorjev, prostem dostopu do člankov ter vztrajanje na zagotavljanju visoke kvalitete objavljenih raziskovalnih dosežkov.

V svoji znanstveni karieri sem objavil vrsto znanstvenih člankov, večino iz področja kemijske analize, mnogi med njimi so bili objavljeni tudi v naši reviji *Acta Chimica Slovenica*. Večino teh del obsega okoljske raziskave, raziskave materialov ter razvoj novih analiznih metod. Tako smo v preteklosti natančno analizirali in identificirali tudi številne okoljske onesnaževalce v Sloveniji in okoljske parametre, saj imamo v našem okolju številne potencialne industrijske onesnaževalce, ki imajo lahko ob neprevidni proizvodnji in uporabi zelo negativne okoljske vplive (npr. rudnik živega srebra v Idriji, Cinkarna Celje, rudnik svinca v Mežici ipd.).

Med svoje zadnje novejše raziskave, objavljene v naši *ACSi*, spada tudi članek, ki obsega potenciometrično določanje fitatov v prisotnosti kovinskih ionov kot kompleksantov.[2] Ta raziskava je med drugim pokazala, da je klasična potenciometrija primerna tudi za precizijske analize. Članek je, tako kot številni drugi, odmeven v mednarodni literaturi, kar nakazuje, da se kvaliteta člankov, objavljenih v *ACSi*, ohranja.

Sam lahko z veseljem poudarim, da sem kariero pričel in končal tudi z objavami v reviji *Acta Chimica Slovenica*, ki v tem letu praznuje 70-letni jubilej uspešnega delovanja.

Ob jubileju vsem članom uredništva čestitam ter želim vsem avtorjem publikacij v *ACSi*, še mnoga leta uspešnega raziskovanja in novih odkritij.

2 G. Marolt, B. Pihlar: Potentiometric determination of phytic acid and investigations of phytate interactions with some metal ions. *Acta Chimica Slovenica* 2015, *62*, 319–327.

prof. dr.
Helena Prosen

Fakulteta za kemijo in kemijsko tehnologijo
Univerze v Ljubljani

področna urednica
za analizno kemijo
od leta 2012

Zbrati skupaj spomine na leta urednikovanja pri reviji *Acta Chimica Slovenica* sicer ni težko, jih je pa težko posredovati občinstvu kot neko zaokroženo besedilo. Vendar bom poskusila.

Pri *Acti* sem področna urednica že nekaj časa, prav letos mineva enajst let. Leta 2012 me je poklical takratni glavni urednik prof. dr. Aleksander Pavko, ki je iskal nove področne urednike za analizno kemijo. Bil je zelo prepričljiv; mogoče pa je na tistem uvodnem sestanku tudi zamolčal kako manj prijetno podrobnost. Vsekakor ni skrival, da biti urednik pri *Acti* pomeni dobiti dodatno delo in redno obveznost, ki je niti med dopustom ne smeš (preveč) zanemariti...

Poleg prepričljivosti prof. dr. Pavka je k moji odločitvi, da postanem področna urednica, gotovo prispeval tudi nek občutek dolžnosti, da moram podpreti slovensko srenjo kemikov, biokemikov, kemijskih inženirjev in tehnologov ter ostalih sorodnih poklicev.

Takrat, ko sem delo prevzela, in še nekaj let zatem je vsa komunikacija za *Acto* tako z recenzenti kot avtorji potekala samo preko elektronske pošte in priponk. Tu se je pogosto zataknilo, saj so taki e-dopisi zaradi priponk včasih končali v predalu za neželeno pošto. Zato je bilo vedno treba preverjati, ali je recenzent sploh dobil gradivo.

Ko je bil uveden OJS sistem za urednikovanje, so zgornje komunikacijske težave izginile. Postal je zanesljiv partner za drugo polovico moje uredniške službe; le-

tos spomladi pa ga je zamenjala nova različica, ki je sicer mlajša in lepša, se pa z njo še ne razumeva preveč dobro. Pošteno povedano, kakih prednosti razen lepote zaenkrat ne vidim. Je bila pa zato pomembna pridobitev že nekaj let nazaj dostop do antiplagiatorskega sistema. Ta je omogočil odkrivanje avtorjev, ki pošljejo v *Acto* svoj že objavljen članek z nekaj spremenjenimi podatki, kako novo sliko... Žal sem na tako neetično prakso že večkrat naletela.

Z dobrim delom glavnega urednika prof. dr. Aleksandra Pavka, kasneje pa glavne urednice prof. dr. Ksenije Kogej, ter seveda trudom vseh nas področnih urednikov ima *Acta* večji faktor vpliva, ki je že nekaj let stabilno krepko nad 1,0 in se občasno približa 2,0. Poleg očitnih prednosti ima to dejstvo tudi nekaj slabosti, zlasti to, da je naša revija postala zanimiva za vse mogoče tuje avtorje, ki bi radi v slabi angleščini objavili nekaj ne posebej kvalitetnega v neplačljivi reviji z znatnim faktorjem vpliva. Tako je glavni izziv nas področnih urednikov, da preverjamo podobnost avtorjevih drugih člankov, pa celo podobnost z deli drugih avtorjev – celo na take prakse »prepisovanja« sem že naletela. Avtorji včasih želijo objaviti kako delo, ki bi bilo po naših standardih komaj diplomska naloga, pri čemer jim uvrstitev pod »tehnični članek« nič ne diši in so se tudi pripravljeni prerekati o tem. Daleč največji izziv, s katerim se čedalje bolj soočajo tudi višje kotirajoče revije, pa je najti kakovostne recenzente.

Kljub vsem tem izzivom pa uredniško delo za *Acto* ostaja izpolnjujoče poslanstvo, ki ga rada opravljam. Naša revija je ena redkih slovenskih »stanovskih« strokovnih revij s faktorjem vpliva in mednarodnim avtorstvom. To, da lahko prispevam k njeni kvaliteti, je največje zadovoljstvo urednikovanja, ki ga pri tujih revijah ni mogoče dobiti. Prepričana sem, da bomo z novim urednikom prof. dr. Francem Perdihom postali samo še boljši, zato se splača ostati.

prof. dr. Damjana Rozman

Medicinska fakulteta Univerze v Ljubljani

področna urednica za biokemijo v obdobju od 2008–2019

Biokemija je ena od mlajših vej interdisciplinarne kemije. Združuje izsledke večih področij, kjer vsako področje prispeva edinstveni vpogled v skrivnosti življenja na molekulski ravni. Čeprav lahko začetke biokemije zaslutimo že v 17. stoletju, predvsem pri iskanjih vpliva zelišč na zdravje in razumevanju anatomije človeškega telesa, pa so že stare civilizacije, kot so Egipčani in Grki, proučevali učinek različnih naravnih substanc na človeško telo in na zdravje. Začetki molekulske biokemije, kot jo poznamo danes, se prepletajo z organsko kemijo. Zanimivo je, da je bil koncept "vitalizma" živih bitij (18.–19. stoletje) sprva izpodbijan prav z izsledki organske kemije, saj je bilo mnoge telesu lastne snovi možno sintetizirati tudi v laboratoriju. Šele odkritje encimov kot naravnih katalizatorjev in dognanja Louis Pasteurja, ki je prepoznal, da glive kvasovke lahko katalizirajo reakcije, je zakoličilo biokemijo kot samostojno vedo oziroma kot novo vejo interdiciplinarne kemije.

Študentje kemije, ki nas je bolj zanimal biološki del kemije, smo se zbirali na katedri za organsko kemijo, kjer nas je akad. prof. dr. Branko Stanovnik, dolgoletni član uredniškega odbora *ACSi*, nekoč vprašal: "Ali vi sploh veste, kaj pomeni *biokemik*"? Še preden je vsak od nas pričel navajati svojo razlago, je profesor naznanil: "*Biokemik pomeni (nekad) bio kemik*"! Ker je bilo to še v času nekdanje Jugoslavije, smo srbohrvaščino seveda vsi razumeli. Če pogledam nazaj, je imel prof. Stanovnik prav. Tako kot smo tedanji biokemiki izhajali iz kemikov, je tudi pobuda za biokemijsko vejo *ACSi* nastala na podoben način. Ko sem kot *"bio kemik"* leta 2007 organizirala velik mednarodni kongres s področja biokemije o naddružini proteinov, ki jim rečemo citokromi P450 (oznaka naddružine je CYP), sem se spomnila, da bi vrhunske mednarodne strokovnjake s tega področja lahko zaprosili, da pripravijo članke. Smiselno se mi je zdelo, da bi podprli eno od slovenskih znanstvenih revij, ki bi jih biokemijska tematika zanimala. Obrnila sem se na tedanjega urednika prof. Aleksandra Pavka z vprašanjem, če bi bil zainteresiran, da v *ACSi* objavimo posebno številko o citokromih P450. To so proteini, ki so prisotni v vseh bioloških kraljestvih, od bakterij, gliv, rastlin in živali, vključno s človekom. Pri ljudeh sodelujejo pri presnovi predvsem lipidotopnih endobiotikov (snovi, ki jih proizvede telo) in jih z dodajanjem hidroksilnih ali drugih skupin naredijo bolj topne in tako primernejše za nadaljnjo presnovo. Ključni pa so tudi za presnovo lipidotopnih ksenobiotikov, telesu tujih snovi, kot so na primer zdravila in druge kemijske spojine, ki jih zanesemo v telo. Tako sem kot gostujoča urednica sodelovala pri pripravi posebne številke *ACSi*, ki je bila posvečena 15. mednarodni konferenci o citokromih P450 in je potekala junija 2007 na Bledu. Tematska številka *Acta Chim. Slov.* 2008, *55,* je vsebovala 14 recenziranih biokemijskih člankov, znanstvenih in revijskih, s področja CYP, članki so bili kasneje tudi dobro citirani. Ker je bila izkušnja s sodelovanjem dobra in me je uredniško delo veselilo, sem predlagala, da bi poizkusili biokemijske tematike redno vključevati v *ACSi*. Imenovana sem bila za področno urednico *ACSi* za biokemijo. Od leta 2008 dalje smo v vsaki številki *ACSi* objavljali tudi biokemijske članke, tako s področja proteinske biokemije, encimatike, začetkov sin-

tezne biologije, kasneje pa je bilo vse več tudi prispevkov s področja molekularne biologije in genomike, ki se z biokemijo tesno prepletata. Tako letos poleg 70-letnice *ACSi* letos obeležujemo tudi 15-letnico biokemijskih prispevkov v tej reviji.

Ena izmed zadreg, ki sem jo kot področna urednica opazila, je bila, da *ACSi* ni bila vključena v zbirko PubMed, ki predstavlja osnovno bibliografsko zbirko za iskanje in pridobivanje biomedicinske in biokemijske literature. Baza podatkov PubMed danes vsebuje več kot 35 milijonov citatov in povzetkov biomedicinske literature in je dostopna na spletu od leta 1996 dalje, vzdržuje pa jo Nacionalni center za biotehnološke informacije (NCBI) pri Nacionalni medicinski knjižnici ZDA (NLM) na Nacionalnem inštitutu za zdravje (NIH). Prvič smo poizkušali z vključitvijo *ACSi* v PubMed že leta 2009, a žal revija še ni izpolnjevala vseh pogojev – eden od pogojev je bil prav povečanje števila objav s področij interdisciplinarne kemije, kamor spada tudi biokemija. Z vključitvijo *ACSi* v PubMed smo uspeli marca 2013. To je bil pomemben korak, saj je *ACSi* tako postala privlačnejša tudi za mednarodne avtorje člankov s področja biokemije, številni od teh člankov pa so pomembno prispevali tudi k boljši citiranosti revije in k povečanemu in stabilnemu faktorju vpliva.

Vesela sem, da je tudi po koncu mojega urednikovanja biokemija ostala sestavni del revije *ACSi*. Pri uredniškem delu mi je bilo v veliko veselje sodelovati z vsemi glavnimi uredniki (profesorji Aleksander Pavko, Ksenija Kogej, Franc Perdih), kot tudi z dolgoletnim bivšim predsednikom Slovenskega kemijskega društva prof. Venčeslavom Kavčičem. Brez njih *ACSi* ne bi bila to, kar je.

viš. znan. sod. dr. Melita Tramšek

Institut »Jožef Stefan«

področna urednica za znanosti o materialih v obdobju 2013–2019

Z uredniškim delom pri reviji *Acta Chimica Slovenica* sem se kot gostujoča urednica prvič srečala ob pripravi številke, ki je bila posvečena prof. dr. Borisu Žemvi in je izšla leta 2013. Urejati članke z ožjega raziskovalnega področja kemije fluora je bilo prijetno in razmeroma enostavno. V tem letu sem prevzela tudi delo urednice na področju materialov (*angl.* Material science) in ga opravljala do konca leta 2019. Ker je področje materialov izjemno raznoliko, mi je bilo v začetku težko prepoznati kakovost prispevka. Delo področne urednice je hkrati lepo in težko. V tem obdobju sem imela priložnost spoznavanja novih raziskovalnih področij ter možnost dopisnega spoznavanja pestre množice avtorjev. Osebno sem se zavedala, da lahko tudi sama z uredniškim delom doprinesem svoj delček k napredku znanosti še zlasti pri reviji, kjer so vsi članki prosto dostopni.

Delo področne urednice pa je bilo tudi težko, saj je zahtevalo veliko časa, truda in veliko mero odgovornosti. Kot področna urednica sem morala skrbeti za hitro in učinkovito obravnavo prispevkov ter za izbiro primernih recenzentov, ki bodo ocenili njihovo kakovost in ustreznost. Nenazadnje sem morala sprejeti tudi odločitev, ali je prispeli prispevek primeren za končno objavo. Mukotrpen in v nekaterih primerih tudi dolgotrajen postopek mi je predstavljalo predvsem iskanje kompetentnih recenzentov, ki bi bili pripravljeni oceniti oddani prispevek.

V mozaiku prijetnih spominov na to obdobje mi bodo prav gotovo ostali uredniški sestanki in srečanja. Slednji so potekali v sproščenem vzdušju, za kar sta v prvi vrsti zaslužna glavni urednik in urednica tega obdobja. Iskrena hvala prof. dr. Aleksandru Pavku in prof. dr. Kseniji Kogej za vso spodbudo in uspešno urednikovanje revije *Acta Chimica Slovenica*, na katero smo kemiki v slovenskem prostoru lahko upravičeno ponosni.

Foto: Marjan Verč

Srebrna in bronasta medalja ter dve častni priznanji na kemijski olimpijadi 2023

Andrej Godec, UL, FKKT

Slovenska ekipa se je vrnila iz Züricha, kjer je od 16. 7. do 24. 7. 2023 potekala 55. mednarodna kemijska olimpijada.

Tega tekmovanja se je udeležilo 348 dijakinj in dijakov iz 89 držav, potekalo pa je na Univerzi ETH v Švici (https://www.icho2023.ch/). Dijaki imajo dva tekmovalna dneva: najprej je na vrsti eksperimentalni del v laboratorijih ETH, in potem še teoretični. Vsak od obeh traja 5 ur, naloge pa so zelo težke in dostopne na spletni strani.

Našo državo so zastopali štirje dijaki: Matej Nastran in Nejc Mohorič iz gimnazije Škofja Loka, ter Gabriel Žnidaršič in Jakob Starec Oman iz gimnazije Vič. Matej je osvojil srebrno medaljo, Jakob bronasto, Nejc in Gabriel pa sta dobila častni priznanji. ČESTITKE celi ekipi!

Mentorja ekipe sva bila dr. Berta Košmrlj in dr. Andrej Godec, oba FKKT.

Strokovne priprave na olimpijado izvajamo na Fakulteti za kemijo in kemijsko tehnologijo v Ljubljani, organizacija pa poteka v sodelovanju z Zvezo za tehniško kulturo Slovenije Zotks.

Letos je priprave izvajala naslednja ekipa FKKT: dr. Marta Počkaj, dr. Berta Košmrlj, dr. Darko Dolenc, mag. Jernej Imperl ter dr. Andrej Godec. Pri prevajanju je pomagal še dr. Miha Lukšič.

Vsem navedenim, kot tudi Zotks, se najlepše zahvaljujemo za sodelovanje.

Letošnja olimpijada je po treh dogodkih na daljavo končno potekala v živo. Vse skupaj se je začelo 16. julija, ko smo pripotovali v Švico. Organizator nas loči; dijaki so nastanjeni posebej, že kar na začetku pa jim poberejo tudi vse naprave za komuniciranje, to je telefone, tablice, laptope in podobno.

Gostiteljica letošnje olimpijade je bila ETH s sedežem v Zürichu. Na tej Univerzi je študiralo in delovalo kar nekaj Nobelovcev, naprimer Albert Einstein, Peter Debye in Vladimir Prelog, zato smo nekako pričakovali, da bo ta olimpijada nekaj posebnega. Tako je tudi bilo.

Otvoritvena slovesnost je bila v ponedeljek dopoldne. Povezovala jo je odlična prof. Helma Wennemers, ki je poleg znanstvenih pokazala tudi veliko sposobnost vodenja prireditev. Na otvoritvi organizator predstavi državo in ustanovo, kjer se bo vse skupaj dogajalo, ter zatem še vse ekipe držav. Takoj zatem smo mentorji odšli na pregled laboratorijev na ETH Hönggerberg, kjer je fakulteta za kemijo in še nekatere druge.

Z leve smo Berta, Matej, Nejc, Gabriel, Jakob in Andrej.

Laboratoriji na ETH.

Pregledati moramo namreč laboratorijske pulte naših dijakov, preveriti, če je za vsakega dovolj opreme, in če imajo pripravljene vse raztopine. Ta del nam vzame kar nekaj časa, saj je predvsem veliko razne steklovine.

ETH je sicer javna univerza, ki je trenutno rangirana kot osma najboljša na svetu; glavna zgradba je locirana na robu starega dela Züricha.

Ko preverimo opremo, podrobneje pregledamo še eksperimentalne naloge, in jih po potrebi tudi prediskutiramo z avtorji. Naslednji dan sledi prevajanje: tukaj se zahteva precizno delo, saj je od dobrega in natančnega prevoda odvisen rezultat. V nadaljevanju bom na kratko predstavil naloge; celoten tekst najdete na spletnih straneh olimpijade.

Letošnje eksperimentalne naloge so bile tri: najprej so morali dijaki narediti analizo vzorca na ione. Z mešanjem dobljenih raztopin ter opazovanjem barv in oborin so morali dokazati, katere ione imajo v vzorcu, ter napisati ionske reakcije, ki potekajo. Za ta del so imeli na voljo 1 uro časa.

Druga eksperimentalna naloga je bila sinteza: iz p-metoksiacetofenona so morali najprej sintetizirati p-metoksibenzojsko kislino (levo na sliki), in potem še 1-(3-kloro-4-metoksifeli)etan-1-on (desno na sliki). Uporabili so natrijev hipoklorit, variirali pa so pogoje, pri katerij je bila izvedena reakcija.

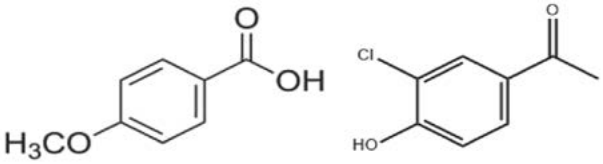

Pri tej sintezi so morali med drugim sestaviti napravo za nučiranje, ter destilacijsko napravo. Izvesti so morali tudi tankoplastno kromatografijo, in na koncu odgovoriti še na kopico vprašanj, povezanih z nalogo.

Tretja eksperimentalna naloga je bila analitska: dobili so vzorec zmesi $FeCl_3$ and $CaCl_2$, ki je bila raztopljena v vodni raztopini HCl. Takšna zmes sicer ponazarja realni vzorec železove rude. Nato pa so morali s kompleksometričnimi titracijami določiti koncentracijo železa ter ostalih sestavin v vzorcu.

Za te tri naloge imajo 5 ura časa; računati je treba, da so laboratoriji vedno vroči, da je gneča, ter da je v vsem tem hrupu težko ostati zbran. Vendar pa so naši dijaki naloge vseeno uspešno opravili; njihov povprečni dosežek je okrog 75 % na praktičnem delu tekmovanja, vsak pa seveda tekmuje zase.

Na dan, ko dijaki tekmujejo v laboratoriju, imamo mentorji dopoldne prosto; obiskali smo raziskovalna inštituta Empa in Eawag, kjer se ukvarjajo z materiali in tehnologijami prihodnosti. Glavni poudarki raziskav so konstrukcijski in varnostni inženiring, površinska tehnologija, kovinski in kompozitni materiali, kemijske analize, analiza izpušnih plinov in zunanjega zraka, stanovanjska tehnologija, gradbena fizika, akustika in nadzor hrupa. Videli smo lahko nekatere laboratorije, panelno predstavitev raziskav, ter sodelovali v diskusiji o vlogi izobraževanja v svetu, ki nas čaka.

Prevajanje nalog.

Laboratoriji Empa

Že popoldne ta dan pa smo mentorji dobili teoretične naloge, ki jih bodo dijaki reševali drugi tekmovalni dan. Letos so te obsegale 10 nalog; 3 so bile iz organske kemije, in 7 iz pretežno fizikalne kemije ter nekaj anorganske. Ponovno najprej sledi diskusija z avtorji, zvečer pa na sestanku vseh držav besedila usklajujemo in na koncu potrdimo.

Naslednji dan sledi prevajanje teoretičnih nalog; to je še bolj zahtevno, saj je besedila precej več, zato sva s sodelavko mentorico imela nekaj pomoči tudi od doma. To je bila letos novost, ki so jo vse države izkoristile.

Naloge so bile res raznovrstne, in po mnenju vseh jih je bilo preveč. Vse so tudi dostopne na spletnih straneh organizatorja.

Prva naloga je bila na temo diagnostike v medicini z radioaktivnimi izotopi, v tem primeru ^{99}Tc. Dijaki so morali ugotoviti izhodni nuklid za nastanek tega izotopa, zatem pa še oksidacijska stanja izotopa v različnih spojinah, ki se uporabljajo pri slikanju srca, možgan in kosti. Izračunati so morali med drugim še aktivnost tega izotopa, ter koliko časa mora pacient po vbrizganju počakati, da se aktivnost zmanjša pod 1%.

Druga naloga je bila katalizirana elektrokemična redukcija CO_2, ki jo je možno izvesti z obnovljivimi viri. Dijaki so morali napisati enačbe za redukcijska procesa pretvorbe ogljikovega dioksida v etanol, in v n-propanol. Sestaviti so morali tudi galvanski člen, kjer bi takšna reakcija eventuelno lahko potekala. Nato so se posvetili katalizatorjem: sistemi CuAg so odlični katalizatorji za elektrosintezo alkoholov iz CO_2.

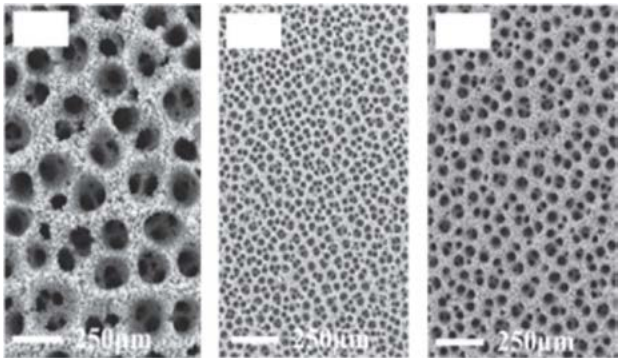

Cu »pene«, dobljene z galvanostatsko elektrodepozicijo Cu pri gostoti toka j = 3 A cm^{-2}. Nanašanje je bilo v vsakem od primerov prekinjeno po različno dolgem času trajanja: 5 s, 20 s, in 80 s.

Okarakterizirali so nanašanje tankih plasti takšnega katalizatorja na nosilec, izračunali izkoristek tega procesa, ter na koncu še gostoto toka, ki je potrebna za nastanek etanola in n-propanola iz CO_2 v prisotnosti takšnega katalizatorja.

Tretja naloga je bila na temo umetne fotosinteze. Raziskave na tem področju so usmerjene v shranjevanje Sončeve energije v kemijskih vezeh. Najprej so morali s pomočjo termodinamskih podatkov izračunati spremembo standardne entalpije in entropije pri reakciji razklopa vode, in nato raziskati še vlogo potencialnih katalizatorjev,

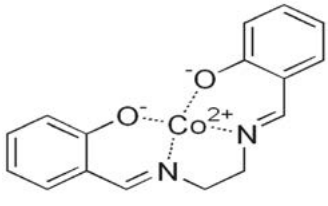

Salkomin

naprimer kompleksov tipa kobalt-salen (salkomin), in reakcije nastanka H_2 iz protonov in elektronov.

Tvorba H_2 poteka izključno na kobaltovem centru. Reakcijo lahko opišemo s 4-stopenjskim katalitičnim ciklom, ki se začne tako, da Co^{2+} porabi 2 H^+ in 2 elektrona. Dijaki so morali najprej predlagati dva možna drugačna cikla, in nato z uporabo redoks potencialov kobaltovih kompleksov oceniti, kateri je najbolj primeren za oksidacijo ali redukcijo vode pri različnih pH.

Četrta naloga je bila povezana s fluorom. Fluor tvori spojine - ki so stabilne ali pa se jih da vsaj izolirati - s praktično vsemi elementi, vključno z žlahtnima plinoma Kr in Xe. Molekule, ki vsebujejo fluor, imajo pogosto neobičajne strukture. Tako fluor dostikrat sodeluje pri tvorbi spojin z elementi skupin 14-18, ki so opredeljeni kot hipervalentni. V tej nalogi so morali dijaki pokazati prostorsko predstavo in določiti osnovne celice ter kote med atomi v različnih kompleksih fluora.

Proizvodnja goriv brez žvepla je splošni trend k zmanjševanju emisij žveplovih spojin, strupenih za okolje. Za odstranjevanje žvepla se v rafinerijah uporablja postopek razžvepljevanja s pomočjo vodika. Peta naloga je bila na to temo; dijaki so morali najprej narisati strukture produktov od A do E, ki nastanejo pri razžvepljevanju tiofena na sliki spodaj; dobili so še informacijo, da sta A in B ciklična regioizomera, C pa je ciklična spojina.

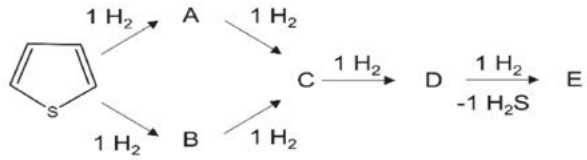

Razžveplanje je katalitski proces, ki se običajno izvaja s katalizatorjem MoS_2 na nosilcu iz SiO_2 (MoS_2/SiO_2). Za preučevanje površine katalizatorja se lahko uporabijo metode izmenjave izotopov, naprimer $H_2{}^{34}S$ v zmesi z Ar. Dijaki so morali ob poznavanju pretokov in drugih pogojev izračunati, koliko žveplovih atomov se izmenja na površini katalizatorja, in kolikšen je njihov difuzijski koeficient.

Šesta naloga je bila na temo direktne pretvorbe metana v metanol. Metan je široko dostopen naravni plin in zato atraktivna surovina za procese v kemijski industriji, kot je na primer proizvodnja metanola. Kontrola tega procesa predstavlja velik izziv, saj se metanol dosti lažje oksidira od metana. Prekomerni oksidaciji se lahko izognemo z uporabo zeolitnih katalizatorjev z vgrajenimi bakrovimi atomi v strukturi (naprimer S1 in S2 na sliki spodaj), ki zagotavljajo zgolj posamezen kisikov atom, potreben za

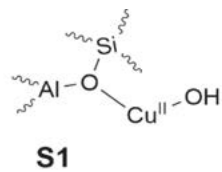

S1

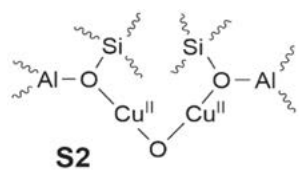

S2

oksidacijo do metanola, nakar katalizator regeneriramo s kisikom v odsotnosti metana.

Dijaki so morali določiti število mest S1 in S2, potrebnih za oksidacijo metana. Izračunati so morali še odstotek bakra, ki je zreagiral, ter iz grafičnih podatkov red reakcije oksidacije CH_4. Izračunati so morali še, ali metan reagira hitreje v primeru S1 ali S2. Metanol lahko nadalje pretvorimo v koristne olefine z drugimi zeolitnimi katalizatorji. S pomočjo podatkov za elementno analizo in ^{1}H NMR spektrov so morali na koncu določiti še strukture vmesnih produktov pri takšni reakcij.

Sedma naloga je bila encimska kinetika. Po mnenju dijakov je bila to najtežja naloga na olimpijadi, in tudi uspeh je bil pičel. Michaelis–Mentenin (MM) mehanizem je bil vpeljan leta 1913; z njim so opisali kinetiko encimskih reakcij. Po tem mehanizmu encim **E** katalizira pretvorbo substrata **S** v produkt **P**.

$$\mathbf{E} + \mathbf{S} \underset{k_2}{\overset{k_1}{\rightleftarrows}} \mathbf{ES} \overset{k_3}{\rightarrow} \mathbf{E} + \mathbf{P}$$

Začetna hitrost encimske reakcije, ki poteka po MM mehanizmu, je običajno podana z:

$$v_0 = \frac{v_{\max}[\mathbf{S}]_0}{[\mathbf{S}]_0 + K_M}$$

kjer je začetna koncentracija **E** veliko manjša od začetne koncentracije **S** ([**E**]0 ≪ [**S**]0). Michaelisova konstanta je definirana kot $K_M = (k_2 + k_3)/k_1$. Dijaki so morali najprej iz alternativnih oblik zapisa teh enačb izbrati pravilne, ter izbrati in narisati takšen graf, da bo odvisnost linearna.

Številni encimi katalizirajo transformacije več substratov namesto enega samega substrata. Če pa je koncentracija enega od substratov veliko višja od koncentracije drugega substrata ali če ostane konstantna, tudi velja mehanizem MM. Dijaki so morali izpeljati hitrostne zakone za dva neodvisna encimska sistema, ki sledita kinetiki MM. Enega predstavljamo za primer tukaj, slika spodaj: encim **E** ima pet aktivnih mest, od katerih je vsako specifično za enega od substratov $\mathbf{S_A}$, $\mathbf{S_B}$, ali $\mathbf{S_C}$, ki se selektivno pretvorijo v ustrezne produkte $\mathbf{P_A}$, $\mathbf{P_B}$, ali $\mathbf{P_C}$. Za vsak substrat obstaja vsaj eno aktivno mesto. Vsako aktivno mesto je neodvisno od ostalih.

Dijaki so morali s pomočjo nekaj podatkov izračunati število aktivnih mest, nato vse konstante reakcijskih hitrosti in na koncu še Michaelisovo konstanto za ta encimski sistem.

Zadnje tri naloge so bile iz organske kemije: tema osme naloge je bila Nazarova reakcija. Ta reakcija se pogosto uporablja za sintezo ciklopentenonov iz divinilketonov. Poteka lahko fotokemično ali katalizirano s kislino. Reakcija je elektrociklizacija, ki ji sledi prenos protona.

Dijaki so morali narisati pi molekulske orbitale, in napovedati pogoje, ko bo reakcija potekala disrotatorno ali konrotatorno. Razen tega so morali dopolniti še reakcijsko shemo sinteze kapnelena, ter narisati strukture intermediatov s prikazano stereokemijo.

Deveta naloga je bila uporaba elektrolize v organski sintezi. Kolbejeva elektroliza je dekarboksilativna dimerizacija karboksilnih kislin, ki poteka le z deprotonirano obliko kisline. Neurejena enačba za reakcijo je prikazana spodaj, base pomeni baza.

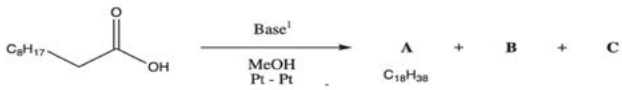

Dijaki so morali z uporabo dodatnih informacij narisati strukturne formule A, B in C, napisati polreakcije in celokupno reakcijo, ter narisati še nekatere intermediate pri oksidativni dekarboksilaciji in tvorbi produkta. Nato so okarakterizirali še elektrolizo neke karboksilne kisline, ki v prisotnosti prebitne količine druge kisline daje dva glavna produkta, ki ju ne moremo ločiti s kromatografijo na silikagelu. Njuni spektroskopski podatki so skoraj identični, v ^{1}H NMR spektru pa ju lahko razlikujemo le po dveh signalih z nizkim kemijskim premikom. Na osnovi podatkov o teh signalih so morali narisati strukturo obeh produktov.

Izbira elektrodnega materiala lahko vpliva na selektivnost organske elektrosintezne reakcije. Reduktivna ele-

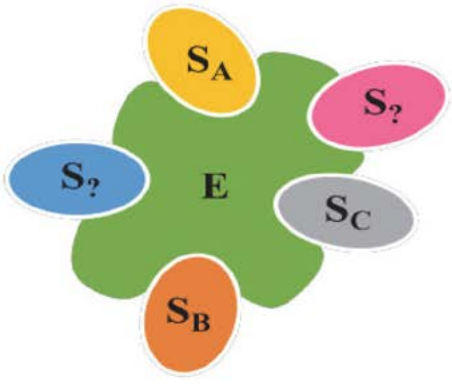

$$\mathbf{E} + \mathbf{S_A} \underset{k_{a2}}{\overset{k_{a1}}{\rightleftarrows}} \mathbf{ES_A} \overset{k_{a3}}{\rightarrow} \mathbf{E} + \mathbf{P_A}$$

$$\mathbf{E} + \mathbf{S_B} \underset{k_{b2}}{\overset{k_{b1}}{\rightleftarrows}} \mathbf{ES_B} \overset{k_{b3}}{\rightarrow} \mathbf{E} + \mathbf{P_B}$$

$$\mathbf{E} + \mathbf{S_C} \underset{k_{c2}}{\overset{k_{c1}}{\rightleftarrows}} \mathbf{ES_C} \overset{k_{c3}}{\rightarrow} \mathbf{E} + \mathbf{P_C}$$

ktroliza benzaldehida (M, 16 mM v 1 M KOH(aq), Pt anoda, -1.3 V proti Ag/AgO) daje različne produkte, odvisno od materiala katode. Močna vezava na površino elektrode daje prednost intermolekulskim reakcijam. Spodnja slika kaže porazdelitev produktov za različne katodne materiale in masna spektra produktov.

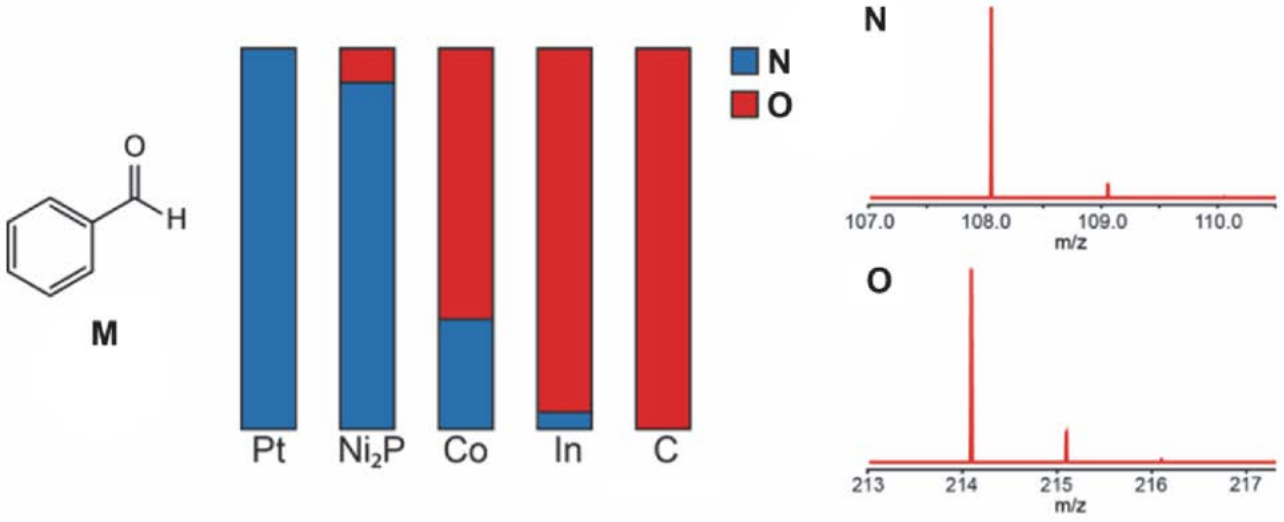

Na osnovi teh podatkov so morali dijaki narisati strukturi N in O.

Zadnja, deseta naloga, je bila seveda posvečena Švici, deželi zdravil in farmacevtskih podjetij. Pasireotid (1) je zdravilo na osnovi peptidov, ki ga je razvilo švicarsko farmacevtsko podjetje Novartis za zdravljenje Cushingove bolezni, ko se v telesu izloča preveč kortizola.

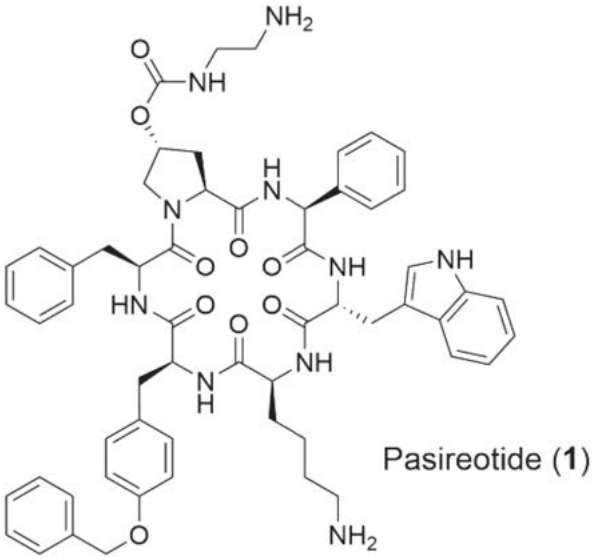

Dijaki so morali določiti število stereogenih centrov (*n*) v pasireotidu (1) in izračunati število vseh možnih stereoizomerov pasireotida (1). Nato so morali narisati intermediate v sintezi te snovi, ki je zelo obsežna, in poteka preko mnogih vmesnih stopenj.

Šesti dan, ko dijaki rešujejo teoretični test, se mentorji ponavadi odpravimo na celodnevni izlet; letos je to bila spektakularna gora Säntis, 2502 m. Po obisku gore smo se mimogrede ustavili še v Metrohm AG, Herisau, kjer smo si ogledali proizvodnjo. Metrohm je bil tudi eden od glavnih sponzorjev olimpijade.

Pogled na švicarske Alpe iz gore Säntis Z

Zvečer ta dan sledi srečanje z dijaki, ki jih nismo videli že cel teden. To srečanje je bilo letos na Univerzi Zürich, še eni znameniti izobraževalni ustanovi v Švici. Tega se mentorji vedno veselimo, saj cel teden pripravljamo in prevajamo naloge, in nas zanima, kako je kaj šlo na testih.

Naslednji dan sledi popravljanje testov naših dijakov; reči je treba, da tega nikoli ne moremo narediti v celoti, saj za praktični del naprimer nimamo vseh podatkov in njihovih izdelkov. Teste oceniva mentorja, in seveda tudi organizator; sledi arbitraža, kjer se usklajujejo ocene obeh.

Nikoli pa ne vemo vnaprej, kaj določen odstotek pomeni; to izvemo šele na zaključni slovesnosti, ki je bila v čudoviti koncertni dvorani Tonhalle. Ta je pred kratkim dobila obnovljene orgle, narejene iz 4800 cevi. Imeli smo čast, da smo lahko slišali, kako zvenijo; med podelitvijo

Zaključna slovesnost v Tonhalle

nagrad je namreč vsakič sledila glasbena pavza, dvakrat klasična, tretjič pa We are the champions, katere avtor je Freddy Mercury in skupina The Queen.

Na zaključni slovesnosti je vedno veliko veselja, in tudi nekaj razočaranja, če ni nagrad. Kemijska olimpijada je sicer tekmovanje, a tudi priložnost, da dijaki dobijo nove znanke in znance, s katerimi bodo sodelovali morda vse življenje. Sodelovanje na tem dogodku je res vsakič nekaj posebnega.

Vabljene in vabljeni na naslednjo olimpijado!

Foto: Andrej Godec

KOLEDAR VAŽNEJŠIH ZNANSTVENIH SREČANJ S PODROČJA KEMIJE IN KEMIJSKE TEHNOLOGIJE

SCIENTIFIC MEETINGS – CHEMISTRY AND CHEMICAL ENGINEERING

2023

October 2023

15 – 19	31ST INTERNATIONAL SYMPOSIUM ON THE CHEMISTRY OF NATURAL PRODUCTS AND 11TH INTERNATIONAL CONGRESS ON BIODIVERSITY Naples, Italy
Information:	https://www.iscnp31-icob11.org/
15 – 19	STEM-CPD SUMMER SCHOOL Aveiro, Portugal
Information:	https://ectn.eu/stem-cpd-summer-school/
22 – 25	2nd INTERNATIONAL CONFERENCE ON ENERGY, ENVIRONMENT & DIGITAL TRANSITION Palermo, Italy
Information:	https://www.aidic.it/e2dt2023/

November 2023

22 – 24	13TH INTERNATIONAL VANADIUM SYMPOSIUM (V13) Lisboa, Portugal
Information:	https://vanadium13.events.chemistry.pt/

December 2023

12 – 14	INTERNATIONAL CONFERENCE ON BIOINSPIRED AND BIOBASED CHEMISTRY & MATERIALS – NICE WINTER 2023 Nice, France
Information:	https://www.nice-conference.com

2024

January 2024

24 – 26	SCF CHEMICAL BIOLOGY SYMPOSIUM 2024 Orsay, France
Information:	https://scf-chembio2024.com/

Acta Chimica Slovenica

Author Guidelines

Submissions

Submission to ACSi is made with the implicit understanding that neither the manuscript nor the essence of its content has been published in whole or in part and that it is not being considered for publication elsewhere. All the listed authors should have agreed on the content and the corresponding (submitting) author is responsible for having ensured that this agreement has been reached. The acceptance of an article is based entirely on its scientific merit, as judged by peer review. There are no page charges for publishing articles in ACSi. The authors are asked to read the Author Guidelines carefully to gain an overview and assess if their manuscript is suitable for ACSi.

Additional information

- Citing spectral and analytical data
- Depositing X-ray data

Submission material

Typical submission consists of:

- full manuscript (PDF file, with title, authors, abstract, keywords, figures and tables embedded, and references)
- supplementary files
  - ***Full manuscript*** (original Word file)
  - ***Statement of novelty*** (Word file)
  - ***List of suggested reviewers*** (Word file)
  - ***ZIP file containing graphics*** (figures, illustrations, images, photographs)
  - ***Graphical abstract*** (single graphics file)
  - ***Proposed cover picture*** (optional, single graphics file)
  - ***Appendices*** (optional, Word files, graphics files)

Incomplete or not properly prepared submissions will be rejected.

Submission process

Before submission, authors should go through the checklist at the bottom of the page and prepare for submission.

Submission process consists of 5 steps.

Step 1: Starting the submission

- Choose one of the journal sections.
- Confirm all the requirements of the ***checklist.***
- Additional plain text comments for the editor can be provided in the relevant text field.

Step 2: Upload submission

- Upload full manuscript in the form of a Word file (with title, authors, abstract, keywords, figures and tables embedded, and references).

Step 3: Enter metadata

- First name, last name, contact email and affiliation for all authors, in relevant order, must be provided. Corresponding author has to be selected. Full postal address and phone number of the corresponding author has to be provided.
- ***Title and abstract*** must be provided in plain text.
- Keywords must be provided (max. 6, separated by semicolons).
- Data about contributors and supporting agencies may be entered.
- ***References*** in plain text must be provided in the relevant text filed.

Step 4: Upload supplementary files

- Original Word file (original of the PDF uploaded in the step 2)
- ***List of suggested reviewers*** with at least five reviewers with two recent references from the field of submitted manuscript must be uploaded as a Word file. At the same time, authors should declare (i) that they have no conflict of interest with suggested reviewers and (ii) that suggested reviewers are experts in the field of the submitted manuscript.
- All ***graphics*** have to be uploaded in a single ZIP file. Graphics should be named Figure 1.jpg, Figure 2.eps, etc.
- ***Graphical abstract image*** must be uploaded separately
- ***Proposed cover picture*** (optional) should be uploaded separately.
- Any additional ***appendices*** (optional) to the paper may be uploaded. Appendices may be published as a supplementary material to the paper, if accepted.
- For each uploaded file the author is asked for additional metadata which may be provided. Depending of the type of the file please provide the relevant title (Statement of novelty, List of suggested reviewers, Figures, Graphical abstract, Proposed cover picture, Appendix).

Step 5: Confirmation

- Final confirmation is required.

Article Types

Feature Articles are contributions that are written on Editor's invitation. They should be clear and concise summaries of the author's most recent work written with the broad scope of ACSi in mind. They are intended to be general overviews of the authors' subfield of research but should be written in a way that engages and informs scientists in other areas. They should contain the following (see also general guidelines for article structure below): (1) an introduction that acquaints readers with the authors' research field and outlines the important questions for which answers are being sought; (2) interesting, novel, and recent contributions of the author(s) to the field; and (3) a summary that presents possible future directions. Manuscripts should normally not exceed 40 pages of one column format (font size 12, 33 lines per page). Generally, experts who have made an important contribution to a specific field in recent years will be invited by the Editor to contribute a **Feature Article**. Individuals may, however, send a proposal (of no more than one page) for a **Feature Article** to the Editor-in-Chief for consideration.

Scientific articles should report significant and innovative achievements in chemistry and related sciences and should exhibit a high level of originality. They should have the following structure:

1. Title (max. 150 characters),
2. Authors and affiliations,
3. Abstract (max. 1000 characters),
4. Keywords (max. 6),
5. Introduction,
6. Experimental,
7. Results and Discussion,
8. Conclusions,
9. Acknowledgements,
10. References.

The sections should be arranged in the sequence generally accepted for publications in the respective fields and should be successively numbered.

Short communications generally follow the same order of sections as Scientific articles, but should be short (max. 2500 words) and report a significant aspect of research work meriting separate publication. Editors may decide that a Scientific paper is categorized as a Short Communication if its length is short.

Technical articles report applications of an already described innovation. Typically, technical articles are not based on new experiments.

Preparation of Submissions

Text of the submitted articles must be prepared with Microsoft Word. Normal style set to single column, 1.5 line spacing, and 12 pt Times New Roman font is recommended. Line numbering (continuous, for the whole document) must be enabled to simplify the reviewing process. For any other format, please consult the editor. Articles should be written in English. Correct spelling and grammar are the sole responsibility of the author(s). Papers should be written in a concise and succinct manner. The authors shall respect the ISO 80000 standard [1], and IUPAC Green Book [2] rules on the names and symbols of quantities and units. The Système International d'Unités (SI) must be used for all dimensional quantities.

Graphics (figures, graphs, illustrations, digital images, photographs) should be inserted in the text where appropriate. The captions should be self-explanatory. Lettering should be readable (suggested 8 point Arial font) with equal size in all figures. Use common programs such as MS Excel or similar to prepare figures (graphs) and ChemDraw to prepare structures in their final size. Width of graphs in the manuscript should be 8 cm. Only in special cases (in case of numerous data, visibility issues) graphs can be 17 cm wide. All graphs in the manuscript should be inserted in relevant places and **aligned left**. The same graphs should be provided separately as images of appropriate resolution (see below) and submitted together in a ZIP file (Graphics ZIP). Please do not submit figures as a Word file. In **graphs**, only the graph area determined by both axes should be in the frame, while a frame around the whole graph should be omitted. The graph area should be white. The legend should be inside the graph area. The style of all graphs should be the same. **Figures and illustrations** should be of sufficient quality for the printed version, i.e. 300 dpi minimum. **Digital images and photographs** should be of high quality (minimum 250 dpi resolution). On submission, figures should be of good enough resolution to be assessed by the referees, ideally as JPEGs. High-resolution figures (in JPEG, TIFF, or EPS format) might be required if the paper is accepted for publication.

Tables should be prepared in the Word file of the paper as usual Word tables. The captions should appear above the table and should be self-explanatory.

References should be numbered and ordered sequentially as they appear in the text, likewise methods, tables, figure captions. When cited in the text, reference numbers should be superscripted, following punctuation marks. It is the sole responsibility of authors to cite articles that have been submitted to a journal or were in print at the time of submission to ACSi. Formatting of references to published work should follow the journal style; please also consult a recent issue:

1. J. W. Smith, A. G. White, *Acta Chim. Slov.* **2008**, *55*, 1055–1059.
2. M. F. Kemmere, T. F. Keurentjes, in: S. P. Nunes, K. V. Peinemann (Ed.): Membrane Technology in the Chemical Industry, Wiley-VCH, Weinheim, Germany, **2008**, pp. 229–255.
3. J. Levec, Arrangement and process for oxidizing an aqueous medium, US Patent Number 5,928,521, date of patent July 27, **1999**.
4. L. A. Bursill, J. M. Thomas, in: R. Sersale, C. Collela, R. Aiello (Eds.), Recent Progress Report and Discussions: 5th International Zeolite Conference, Naples, Italy, 1980, Gianini, Naples, **1981**, pp. 25–30.
5. J. Szegezdi, F. Csizmadia, Prediction of dissociation constant using microconstants, http://www. chemaxon.com/conf/Prediction_of_dissociation _constant_using_microco nstants.pdf, (assessed: March 31, 2008)

Titles of journals should be abbreviated according to Chemical Abstracts Service Source Index (CASSI).

Special Notes

- Complete characterization, **including crystal structure**, should be given when the synthesis of new compounds in crystal form is reported.
- Numerical **data should be reported with the number of significant digits corresponding to the magnitude** of experimental uncertainty.
- **The SI system of units and IUPAC recommendations** for nomenclature, symbols and abbreviations should be followed closely. Additionally, the authors should follow the general guidelines when citing spectral and analytical data, and depositing crystallographic data.
- **Characters** should be correctly represented throughout the manuscript: for example, 1 (one) and l (ell), 0 (zero) and O (oh), x (ex), D7 (times sign), B0 (degree sign). Use Symbol font for all Greek letters and mathematical symbols.
- The rules and recommendations of the **IUBMB** and the **International Union of Pure and Applied Chemistry (IUPAC)** should be used for abbreviation of chemical names, nomenclature of chemical compounds, enzyme nomenclature, isotopic compounds, optically active isomers, and spectroscopic data.
- **A conflict of interest** occurs when an individual (author, reviewer, editor) or its organization is in-

volved in multiple interests, one of which could possibly corrupt the motivation for an act in the other. Financial relationships are the most easily identifiable conflicts of interest, while conflicts can occur also as personal relationships, academic competition, etc. **The Editors** will make effort to ensure that conflicts of interest will not compromise the evaluation process; potential editors and reviewers will be asked to exempt themselves from review process when such conflict of interest exists. When the manuscript is submitted for publication, **the authors** are expected to disclose any relationships that might pose potential conflict of interest with respect to results reported in that manuscript. In the Acknowledgement section the source of funding support should be mentioned. The statement of disclosure must be provided as Comments to Editor during the submission process.

- **Published statement of Informed Consent.** Research described in papers submitted to ACSi must adhere to the principles of the Declaration of Helsinki (***http://www.wma.net/e/policy/b3.htm***). These studies must be approved by an appropriate institutional review board or committee, and informed consent must be obtained from subjects. The Methods section of the paper must include: 1) a statement of protocol approval from an institutional review board or committee and 2), a statement that informed consent was obtained from the human subjects or their representatives.
- **Published Statement of Human and Animal Rights.**When reporting experiments on human subjects, authors should indicate whether the procedures followed were in accordance with the ethical standards of the responsible committee on human experimentation (institutional and national) and with the Helsinki Declaration of 1975, as revised in 2008. If doubt exists whether the research was conducted in accordance with the Helsinki Declaration, the authors must explain the rationale for their approach and demonstrate that the institutional review body explicitly approved the doubtful aspects of the study. When reporting experiments on animals, authors should indicate whether the institutional and national guide for the care and use of laboratory animals was followed.
- To avoid conflict of interest between authors and referees we expect that not more than one referee is from the same country as the corresponding author(s), however, not from the same institution.
- Contributions authored by **Slovenian scientists** are evaluated by non-Slovenian referees.
- Papers describing **microwave-assisted reactions** performed in domestic microwave ovens are not considered for publication in *Acta Chimica Slovenica.*
- *Manuscripts that are **not prepared and submitted** in accord with the instructions for authors are not considered for publication.*

Appendices

Authors are encouraged to make use of supporting information for publication, which is supplementary material (appendices) that is submitted at the same time as the manuscript. It is made available on the Journal's web site and is linked to the article in the Journal's Web edition. The use of supporting information is particularly appropriate for presenting additional graphs, spectra, tables and discussion and is more likely to be of interest to specialists than to general readers. When preparing supporting information, authors should keep in mind that the supporting information files will not be edited by the editorial staff. In addition, the files should be not too large (upper limit 10 MB) and should be provided in common widely known file formats to be accessible to readers without difficulty. All files of supplementary materials are loaded separately during the submission process as supplementary files.

Proposed Cover Picture and Graphical Abstract Image

Graphical content: an ideally full-colour illustration of resolution 300 dpi from the manuscript must be proposed with the submission. Graphical abstract pictures are printed in size 6.5 x 4 cm (hence minimal resolution of 770 x 470 pixels). Cover picture is printed in size 11 x 9.5 cm (hence minimal resolution of 1300 x 1130 pixels)

Authors are encouraged to submit illustrations as candidates for the journal Cover Picture*. The illustration must be related to the subject matter of the paper. Usually both proposed cover picture and graphical abstract are the same, but authors may provide different pictures as well.

* The authors will be asked to contribute to the costs of the cover picture production.

Statement of novelty

Statement of novelty is provided in a Word file and submitted as a supplementary file in step 4 of submission process. Authors should in no more than 100 words emphasize the scientific novelty of the presented research. Do not repeat for this purpose the content of your abstract.

List of suggested reviewers

List of suggested reviewers is a Word file submitted as a supplementary file in step 4 of submission process. Authors should propose the names, full affiliation (department, institution, city and country) and e-mail addresses of five potential referees. Field of expertise and at least two references relevant to the scientific field of the submitted manuscript must be provided for each of the suggested reviewers. The referees should be knowledgeable about the subject but have no close connection with any of the authors. In addition, referees should be from institutions other than (and countries other than) those of any of the authors. Authors declare no conflict of interest with suggested reviewers. Authors declare that suggested reviewers are experts in the field of submitted manuscript.

How to Submit

Users registered in the role of author can start submission by choosing USER HOME link on the top of the page, then choosing the role of the Author and follow the relevant link for starting the submission process.

Prior to submission we strongly recommend that you familiarize yourself with the ACSi style by browsing the journal, particularly if you have not submitted to the ACSi before or recently.

Correspondence

All correspondence with the ACSi editor regarding the paper goes through this web site and emails. Emails are sent and recorded in the web site database. In the correspondence with the editorial office please provide ID number of your manuscript. All emails you receive from the system contain relevant links. **Please do not answer the emails directly but use the embedded links in the emails for carrying out relevant actions.** Alternatively, you can carry out all the actions and correspondence through the online system by logging in and selecting relevant options.

Proofs

Proofs will be dispatched via e-mail and corrections should be returned to the editor by e-mail as quickly as possible, normally within 48 hours of receipt. Typing errors should be corrected; other changes of contents will be treated as new submissions.

Submission Preparation Checklist

As part of the submission process, authors are required to check off their submission's compliance with all of the following items, and submissions may be returned to authors that do not adhere to these guidelines.

1. The submission has not been previously published, nor is it under consideration for publication in any other journal (or an explanation has been provided in Comments to the Editor).
2. All the listed authors have agreed on the content and the corresponding (submitting) author is responsible for having ensured that this agreement has been reached.
3. The submission files are in the correct format: manuscript is created in MS Word but will be **submitted in PDF** (for reviewers) as well as in original MS Word format (as a supplementary file for technical editing); diagrams and graphs are created in Excel and saved in one of the file formats: TIFF, EPS or JPG; illustrations are also saved in one of these formats. The preferred position of graphic files in a document is to embed them close to the place where they are mentioned in the text (See ***Author guidelines*** for details).
4. The manuscript has been examined for spelling and grammar (spell checked).
5. The ***title*** (maximum 150 characters) briefly explains the contents of the manuscript.
6. Full names (first and last) of all authors together with the affiliation address are provided. Name of author(s) denoted as the corresponding author(s), together with their e-mail address, full postal address and telephone/fax numbers are given.
7. The ***abstract*** states the objective and conclusions of the research concisely in no more than 150 words.
8. Keywords (minimum three, maximum six) are provided.
9. ***Statement of novelty*** (maximum 100 words) clearly explaining new findings reported in the manuscript should be prepared as a separate Word file.
10. The text adheres to the stylistic and bibliographic requirements outlined in the ***Author guidelines***.
11. Text in normal style is set to single column, 1.5 line spacing, and 12 pt. Times New Roman font is recommended. All tables, figures and illustrations have appropriate captions and are placed within the text at the appropriate points.
12. Mathematical and chemical equations are provided in separate lines and numbered (Arabic numbers) consecutively in parenthesis at the end of the line. All equation numbers are (if necessary) appropriately included in the text. Corresponding numbers are checked.
13. Tables, Figures, illustrations, are prepared in correct format and resolution (see ***Author guidelines***).
14. The lettering used in the figures and graphs do not vary greatly in size. The recommended lettering size is 8 point Arial.
15. Separate files for each figure and illustration are prepared. The names (numbers) of the separate files are the same as they appear in the text. All the figure files are packed for uploading in a single ZIP file.
16. Authors have read ***special notes*** and have accordingly prepared their manuscript (if necessary).
17. References in the text and in the References are correctly cited. (see ***Author guidelines***). All references mentioned in the Reference list are cited in the text, and vice versa.
18. Permission has been obtained for use of copyrighted material from other sources (including the Web).
19. The names, full affiliation (department, institution, city and country), e-mail addresses and references of five potential referees from institutions other than (and countries other than) those of any of the authors are prepared in the word file. At least two relevant references (important recent papers with high impact factor, head positions of departments, labs, research groups, etc.) for each suggested reviewer must be provided. Authors declare no conflict of interest with suggested reviewers. Authors declare that suggested reviewers are experts in the field of submitted manuscript.
20. Full-colour illustration or graph from the manuscript is proposed for graphical abstract.
21. ***Appendices*** (if appropriate) as supplementary material are prepared and will be submitted at the same time as the manuscript.

Privacy Statement

The names and email addresses entered in this journal site will be used exclusively for the stated purposes of this journal and will not be made available for any other purpose or to any other party.

ISSN: 1580-3155

Koristni naslovi

Slovensko kemijsko društvo
www.chem-soc.si
e-mail: chem.soc@ki.si

Wessex Institute of Technology
www.wessex.ac.uk

SETAC
www.setac.org

European Water Association
http://www.ewa-online.eu/

European Science Foundation
www.esf.org

European Federation of Chemical Engineering
https://efce.info/

International Union of Pure and Applied Chemistry
https://iupac.org/

Novice europske zveze kemijskih društev EuChemS najdete na:

Brussels News Updates
http://www.euchems.eu/newsletters/

DONAU LAB Ljubljana
Member of LPPgroup

BÜCHI
SWITZERLAND

SEPIATEC SFC Supercritical Fluid Chromatography

The green standard for fast compound isolation

Donau Lab d.o.o., Ljubljana
Tbilisijska 85
SI-1000 Ljubljana
www.donaulab.si
office-si@donaulab.com

Razvojna usmerjenost

- Nove formulacije na bazi vodikovega peroksida
- Širjenje uporab vodikovega peroksida na različnih področjih

V svoje vrste vabimo mlade raziskovalce, diplomante in post diplomante, ki bodo skupaj z nami reševali nove izzive.

belinka perkemija

Belinka Perkemija, d. o. o., Zasavska cesta 95, Ljubljana
perkemija@belinka.si, www.belinka-perkemija.com
Contact person: mag. Ivan Grčar: igc@belinka.si

Member of KANSAI HELIOS. Part of KANSAI PAINT.

Razvoj in inovacije za globalno uspešnost

Znanje, kreativnost zaposlenih in inovacije so ključnega pomena v okolju, kjer nastajajo pametni premazi skupine KANSAI HELIOS. Z rešitvami, ki zadostijo široki paleti potreb, kontinuiranim razvojem ter s kakovostnimi izdelki, Helios predstavlja evropski center za inovacije in poslovni razvoj skupine Kansai Paint.

Part of KANSAI PAINT

www.helios-group.eu

KANSAI HELIOS
Designing Excellence

Hitro opravi z bolečino.

Učinkuje v **15 minutah.**(1)

Nalgesin S vsebuje natrijev naproksenat.

Ali ste vedeli, da deluje do **12 ur**?

www.nalgesin.si

1. Sevelius H et al. Bioavailability of Naproxen Sodium and Its Relationship to Clinical Analgesic Effects. Br J Clin Pharmacol 1980; 10: 259–63.

KRKA

Pred uporabo natančno preberite navodilo!
O tveganju in neželenih učinkih se posvetujte z zdravnikom ali s farmacevtom.

Acta Chimica Slovenica
Acta Chimica Slovenica

A series of papers in Slovenian language are dedicated to highlight seventy years of the *Acta Chimica Slovenica* issued by Slovenian Chemical Society. More details are presented in the Society news (page S57).

Year 2023, Vol. 70, No. 3